



UNIVERSITÉ DE STRASBOURG



École doctorale de physique et chimie physique ED182

Institut de Physique et de Chimie des Matériaux de
Strasbourg **UMR 7504**

THÈSE

présentée par :

Georges DAHM

Soutenue le 9 décembre 2014

pour obtenir le grade de : **Docteur de l'université de Strasbourg**

Discipline Chimie

Métallobarbènes pour des applications thérapeutiques

Membres du jury :

Dr. BELLEMIN-LAPONNAZ Stéphane	Directeur de thèse	Université de Strasbourg
Dr. CRASSOUS Jeanne	Rapporteur	Université de Rennes
Prof. GASSER Gilles	Rapporteur	Université de Zürich
Prof. FOURNEL Sylvie	Président du jury	Université de Strasbourg
Dr. GUICHARD Gilles	Examineur	Université de Bordeaux
Dr. DAGORNE Samuel	Examineur	Université de Strasbourg

Remerciements

Le travail de thèse nécessite de nombreuses personnes qui y ont contribué d'une façon ou d'une autre que je veux remercier à cette occasion.

Je voulais d'abord remercier le Dr. Stéphane Bellemin-Laponnaz pour son soutien, ses nombreux conseils et la liberté qu'il m'a laissée au cours de cette thèse.

Je tiens à remercier les membres du jury de thèse le Dr. Jeanne Crassous, le Prof. Gilles Gasser, le Prof. Sylvie Fournel, le Dr. Gilles Guichard et le Dr. Samuel Dagorne de me faire l'honneur de juger sur ce travail.

Je voudrais également remercier mes collègues qui ont travaillé avec moi sur le platine. Tout d'abord le Dr. Edith Chardon qui a entamé cette thématique et m'a initié à la chimie organométallique. Ses riches résultats m'ont permis de commencer sur une solide base bien établie. Ensuite mes collègues le Dr. Gian Luigi Puleo et le Dr. Etienne Borré qui ont grandement contribué à ces travaux. Des résultats intéressants ont été obtenus par nos stagiaires. Je remercie Mathilde Bouché non-seulement pour son travail efficace, mais aussi de continuer nos recherches en thèse. Bon courage ! Fu Changkan a largement contribué à développer nos ligands tridentates. Un grand merci revient à Shu Tsuge qui s'est énormément intéressé à la chimie du Pt. Finalement, je tiens à remercier Gilles Backes et Alexandre Desthèves pour leur aide au laboratoire. Je voudrais remercier le Dr. Thierry Achard pour ses conseils pour la rédaction de ce manuscrit et encore Mathilde pour la correction scrupuleuse de mes erreurs d'anglais.

Sans nos nombreux collaborateurs, ce travail ne serait pas complet. Je remercie donc le Pr. Sylvie Fournel et le Dr. Neila Chekkat pour tous les tests biologiques effectués et les discussions intéressantes sur les problèmes biologiques. Un grand merci revient aussi au Dr. Matteo Mauro et Alessandro Aliprandi pour les mesures photophysiques et les calculs DFT entreprises sur nos complexes ainsi que le Dr. Anthony Clotagatide and C. Darcissac de la Radiopharmacie du CHU de Saint Etienne pour l'étude d'introduction d'iode radioactif. Je souhaite également remercier le Dr. Lydia Brelot pour les nombreuses mesures de diffraction des rayons X sur monocristal ainsi que Hélène Nierengarten et Mélanie Lebreton pour les mesures de spectrométrie de masse. Aussi, je voudrais dire merci à Catalina Bordeianu pour son assistance à la synthèse de ligands phosphonates. Pour finir, je remercie le Dr. Sébastien Harlepp qui a commencé une étude mécanistique de nos composés par pince optique.

Je voudrais remercier le Dr. Vincent César de m'avoir accueilli dans son laboratoire et de me m'avoir fait partager son savoir sur les carbenes.

Je souhaiterais exprimer ma reconnaissance envers toute l'équipe du DMO et remercier tout particulièrement le Dr. Benoît Heinrich et Nicolas Beyer pour leur dévouement remarquable.

Je remercie mes collègues de laboratoire pour la bonne ambiance et leur sympathie. Plus particulièrement, je souhaite exprimer ma gratitude envers Geoffrey Hautecouverture d'avoir toujours partagé sa culture chimique phénoménale. Dr. Senthil Kumar Kuppusamy thanks for all our interesting discussions! Ich erinnere mich mit Freude an die gemeinsame Zeit mit Robert Heinrich, besonders unsere verschiedenen Lösungsmitteltestversuche bleiben in Erinnerung. Que serait la vie au bureau sans la présence d'Anis Amokrane et les histoires du Dr. Tamil Selvi Selvam. Thanks! Le Dr. Marco Baron a enrichi non seulement la vie au laboratoire, mais a aussi contribué à certaines soirées inoubliables. Gracias ! Le Dr. Antonio Garofalo reste toujours le champion des blagues bizarres. Merci petit, d'avoir apporté ton humeur au laboratoire ! Je tiens aussi à remercier mes collègues de labo : Catalina Bordeianu, le Dr. Anatolie Gavriluta, le Dr. Hanna Dib, Martin Kärgell et Weiguang Chen pour tout le temps passé ensemble. De plus, je remercie mes anciens collègues le Dr. Carlos Diaz, le Dr. Cristina Domínguez, le Dr. Pierre-Olivier Schwarz, le Dr. Audrey Parat et les collègues du DCMi le Dr. Aurélie Walter et le Dr. Delphine Toulemon.

Les cours de TP et de TD ont été une expérience très enrichissante. Merci donc au Dr. Aline Maise-François, au Prof. Laurent Douce, au Dr. Lucie Routaboul et à Matthieu Jouffroy.

E grouse Merci fir meng gutt Frënn Paul, Daniel, Myriam, Stéphanie, Joe, Mich, Fränzy, Carine, Phil, Anne, fir all di flott Momenter di mer zesumme verbruecht hunn. Zum Schluss well ech awer menger Mamm Merci soen fir hier grouss Léift an Ënnerstëtzung.

Abstract: N-Heterocyclic Carbene Complexes for anticancer applications

Since the serendipitous discovery of the antitumor properties of cisplatin by Rosenberg in 1965, it remains one of the world's best-selling anticancer drugs. However, regardless of this achievement, platinum-based complexes are only efficient on a limited range of cancers and drug resistance may occur upon treatment. In addition, severe side effects still have to be overcome to access more convenient therapy. In this context, need of new and more efficient derivatives is required to circumvent these drawbacks. While screening hundreds of new metal-based anticancer molecules, platinum *N*-Heterocyclic Carbene complexes (NHC) were found to be very promising candidates with similar or higher *in vitro* activities than cisplatin.

In this work, we focused on two strategies to access functionalized [(NHC)Pt(X)₂(L)]-type complexes: i) complexation of prefunctionalized azolium ligands, and ii) post-complexation modification following three strategies:

- Ligand exchange of a labile pyridine ligand by various neutral ligands
- Conjugation between a benzaldehyde featured [Pt(NHC)] complex and various amines, hydrazines and hydroxylamines
- Halogen ligand exchange

Various families of functionalized complexes could be obtained, including:

- *N*-functionalized NHC complexes with various functional groups (alkanes, aryls, alcohols, nitriles, carboxylic acids, phosphonates, aldehydes)
- Complexes functionalized with amines, polyethylenimine (PEI) or pnictogen based ligands (phosphines, arsines, stibines)
- Functionalized carbenes by oxime conjugation of fluorescent anthracene moieties or a PSMA targeting moiety
- Introduction of iodide isotopes

Cytotoxicity of these compounds against different cancer and non-cancer cell lines has been evaluated to determine the best candidates for further *in vivo* investigations. Herein, we demonstrated that most lipophilic compounds present IC₅₀ values in the micromolar range whereas polar and charged complexes had lower activity.

Oxime conjugation and functionalization by ligand exchange do not affect their cytotoxic properties. Introduction of PEI to the complex resulted in cationic water-soluble species. Depending on the PEI chain length and platinum charge, the best combination could be found and studied *in vivo*. Activities of these compounds are comparable to oxaliplatin along with no apparent side effects.

Beside [(NHC)Pt(X)₂(L)] complexes, coordination of tridentate (O[^]N[^]O) and (O[^]C[^]O)-type ligands with group 10 metals have been investigated as well as the luminescent properties of these complexes. While complexes containing the (O[^]C[^]O) ligand only showed luminescence at low temperature, high emission was observed for complexes that contain the (O[^]N[^]O)-type ligand. Photophysical measurements and DFT calculations of selected complexes were undertaken revealing the importance of the (O[^]N[^]O) ligand substituents.

Résumé : Métallocarbènes pour des applications thérapeutiques

Depuis la découverte fortuite des activités antitumorales du cisplatine par Rosenberg en 1965, ce composé reste l'anticancéreux le plus vendu au monde. Malgré tous les efforts entrepris depuis lors, l'application de ces dérivés du platine n'est efficace que sur un nombre limité de cancers, et des phénomènes de résistance apparaissent souvent lors du traitement. A cela s'ajoutent de sévères effets secondaires qui doivent être dépassés pour rendre la thérapie moins contraignante. Ainsi, de nouveaux dérivés capables de supplanter ces effets indésirables sont nécessaires. Alors que des centaines de composés organométalliques ont été testé pour des applications anticancéreuses, les complexes de Carbènes *N*-Hétérocycliques (NHC) de platine (II) sont apparus comme des candidats prometteurs, montrant des activités *in vitro* similaires ou supérieures au cisplatine.

Dans ce manuscrit, nous nous sommes intéressés à deux stratégies pour obtenir des complexes fonctionnalisés de type $[(\text{NHC})\text{Pt}(\text{X})_2(\text{L})]$: i) complexation de sels d'azolium préfonctionnalisés et ii) postmodification de complexes par trois méthodes :

- Echange d'un ligand pyridine labile par une multitude de ligands neutres
- Conjugaison d'un complexe métallique NHC portant un groupement benzaldehyde à différentes amines, hydrazines et hydroxylamines
- Echange de ligands halogénés

Différentes familles de complexes fonctionnalisés ont ainsi pu être obtenues, dont :

- Des complexes de NHC *N*-fonctionnalisés avec différentes fonctions (alcanes, aryles, alcools, nitriles, acides carboxyliques, phosphonates, benzaldehyde)
- Des complexes fonctionnalisés par des amines, du polyéthylèneimine (PEI) ou différents ligands de la famille des pnictogènes (phosphines, arsines, stibines)
- Des carbènes fonctionnalisés par formation d'oxime avec un groupement fluorescent d'anthracène ou un agent de ciblage du PSMA
- Introduction d'isotopes de l'iode

La cytotoxicité de ces composés a été testée sur différentes lignées cellulaires cancéreuses et non-cancéreuses afin de déterminer les meilleurs candidats pour de futurs tests *in vivo*. Nous avons démontré que la plupart des complexes lipophiles ont des valeurs d'IC₅₀ de l'ordre du micromolaire, alors que les dérivés plus polaires ou chargés présentent des activités amoindries.

La formation d'oxime ou la fonctionnalisation par échange de ligand n'influence généralement pas les propriétés cytotoxiques des composés. L'introduction de PEI donne accès à des espèces cationiques hydrosolubles. En fonction de la longueur de chaîne du PEI et de la charge en platine, la combinaison optimale a pu être trouvée et étudiée *in vivo*. Cette espèce présente des activités comparables à l'oxaliplatine, et aucun de ses effets secondaires.

En plus des complexes de type [(NHC)Pt(X)₂(L)], la coordination de ligands tridentates (O^{^-}N^{^+}O^{^-}) et (O^{^-}C^{^+}O^{^-}) avec des métaux du groupe 10 a été étudiée ainsi que les propriétés en luminescence de ces complexes. Alors que les complexes portant des ligands (O^{^-}C^{^+}O^{^-}) ne sont luminescents qu'à basse température, de fortes émissions ont été mesurées pour les composés [(O^{^-}N^{^+}O^{^-})Pt(pyr)]. Des mesures photophysiques ainsi que des calculs DFT ont été entrepris sur plusieurs complexes afin d'évaluer l'influence des substituants portés par le ligand (O^{^-}N^{^+}O^{^-}).

Table of Contents

1	Cancer, the challenge of developing new drugs.....	15
1.1	Cisplatin, first inorganic anticancer drug	16
1.2	<i>N</i> -Heterocyclic Carbenes: a promising class of ligands for various applications.....	20
1.2.1	Historical introduction: the discovery of <i>N</i> -Heterocyclic Carbenes.....	20
1.2.2	Properties and applications of NHC carbenes and their metal complexes	22
1.2.3	Biological applications of NHC complexes	26
1.3	Post-synthetic modification of transition metal complexes for molecular diversity	28
1.3.1	Post-synthetic modification switches of metal complexes by external stimuli	29
1.3.2	Post-complexation modifications of cyclometalated NHC complexes by insertion reaction.....	34
1.3.3	Nucleophilic substitution and cross-coupling reactions	35
1.3.4	Functionalization by cycloaddition reactions	36
1.3.5	Introducing diversity by ligand exchange	42
1.4	Conclusion and aim of this work.....	44
2	Introducing diversity: synthesis of prefunctionalized Pt-NHC complexes.....	45
2.1	Synthesis of azolium precursors and complexation to Pt metal: general synthesis.....	45
2.2	Pt-NHC complexes bearing various <i>N</i> -substituents	47
2.2.1	Pt-NHC complexes bearing innocent <i>N</i> -substituents: alkanes, aromatic rings, alkenes and fluoroalkanes	47
2.2.2	Pt-NHC complexes <i>N</i> -functionalized by hydroxyl groups and amines.....	52

2.2.3	Pt-NHC complexes <i>N</i> -functionalized by nitriles, carboxylic acids and their derivatives	56
2.2.4	Pt-NHC complexes functionalized by aldehydes and acetals	63
2.2.5	Polynuclear platinum NHC complexes	77
2.3	Variation of the alkene substituents of the NHC-backbone	80
2.4	Conclusion: diversity introduction by prefunctionalized azolium precursors	84
3	Synthesis of Pt complexes containing tridentate ligands	85
3.1	Tridentate (O ⁺ C ⁺ O) ligand based complexes	86
3.2	Tridentate (O ⁺ N ⁺ O) ligand based complexes	89
3.3	Conclusion on Pt complexes containing tridentate ligands	102
4	Introducing diversity in NHC-Platinum complexes: Post-synthetic derivatization	103
4.1	Ligand exchange reaction on a pyridine platinum NHC complex	103
4.1.1	Introducing nitrogen based ligands by ligand exchange	105
4.1.2	Reactivity of platinum NHC complexes towards polyamines	114
4.1.3	Introduction of pnictogen based ligands: Phosphines, arsines and stibines	123
4.2	Post-synthetic modification of NHC-Pt complexes featuring benzaldehyde	146
4.2.1	Functionalization of NHC complexes featuring benzaldehyde by oxime formation	147
4.2.2	Post-synthetic modification of NHC complexes by imine formation	150
4.2.3	Post-synthetic modification of NHC complexes by hydrazone and oxime formation	157
4.2.4	Post-synthetic modification of NHC complexes by imine reduction	167
4.2.5	Conjugation of Pt-NHC complexes with a PSMA targeting urea	168
4.2.6	Introduction of fullerenes (C ₆₀) to NHC-Pt complexes	170
4.3	Halide exchange reactions	172
4.3.1	Introducing radioactivity to organometallic complexes	172

4.3.2	Introduction of iodine to NHC-Pt complexes by ligand exchange.....	174
4.3.3	Introduction of ^{123}I	180
4.4	Conclusion: diversity introduction by post-synthetic modifications....	180
5	Biological studies of NHC-Pt complexes	181
5.1	<i>In vitro</i> studies of platinum NHC complexes	181
5.1.1	State of the art: anticancer properties of platinum NHC complexes	182
5.1.2	Cytotoxicity of prefunctionalized [(NHC)PtI ₂ (amine)] complexes.....	183
5.1.3	Preliminary conclusion on <i>in vitro</i> results of functionalized NHC complexes	194
5.1.4	Platinum complexes bearing tridentate ligands	195
5.1.5	Biological properties of post-synthetic modified complexes by ligand exchange and imine condensation	196
5.1.6	Cytotoxicity of platinum complexes containing pnictogen ligands	200
5.1.7	<i>In vitro</i> studies of polyethylenimine platinum complexes.....	202
5.1.8	Conclusions on <i>in vitro</i> biological activities of NHC Pt complexes	205
5.2	Preliminary <i>in vivo</i> studies of PEI platinum NHC conjugates	206
6	General conclusion	209
7	Experimental part	211
7.1	General considerations.....	211
7.2	Synthesis of azolium salts.....	212
7.3	Synthesis of platinum NHC complexes.....	230
7.3.1	Synthesis of prefunctionalized [(NHC)PtI ₂ (L)] complexes.....	230
7.3.2	Synthesis of complexes containing tridentate ligands	280
7.3.3	Post-functionalization of NHC complexes	304
7.4	Biological studies: General descriptions	348
8	Résumé détaillée en français	349

8.1	I Introduction	349
8.2	Complexes NHC de platine synthétisés et étudiés	352
1.1	Fonctionnalisation des complexes NHC	354
8.2.1	Fonctionnalisation par condensation d'hydroxylamines, hydrazines ou amines.....	354
8.2.2	Introduction de ligands pnictogènes (phosphine, arsine, stibine).....	359
8.2.3	Introduction de PEI (polyéthylène imine)	359
8.3	Etude de la chimie de coordination avec des ligands de type (O ⁺ C ⁺ O)Pt(L) et (O ⁺ N ⁺ O)Pt(L)	361
8.4	Introduction d'isotopes radioactives de iode	362
8.5	Résultats biologiques	363
8.6	Conclusions.....	364

1 Cancer, the challenge of developing new drugs

Nowadays, cancer represents one of the major health problems in developed countries.^{1,2} For example, 1.6 million of new cancer cases are projected for 2014 in the United States resulting in 587 000 deaths.³ Cancer (from Greek word *καρκίνοϛ*: crab, cancer) can be defined as a disease of uncontrolled proliferation of abnormal cells. By invasion of adjacent organs and spreading to parts of the body (metastases), cancer cells finally cause death of affected patient. It is provoked by mutations of normal cells (caused by chemicals, radiations, diet, infections or inherited genetic defect) which are not corrected by the DNA repairing system.⁴ Usually, serious DNA damage leads to cellular suicide (apoptosis). This organism protecting mechanism, as well as tumour suppressor genes and division control are damaged in the cancer cells. Moreover, to insure nutriment supply, cancer cells induce blood vessels growth (angiogenesis) by releasing different growth factors.

Cancer treatment includes surgery and radiation therapy (for localised cancers) as well as hormonal, immuno-, hyperthermia therapies and chemotherapy. In chemotherapy, cytotoxic agents induce apoptosis (programmed cell death) or necrosis (cell death by autolysis) of cancer cells.

Beginning in the 1940s with mustard derivatives,⁵ development of new and innovative anticancer drugs constitutes a high challenge for the scientific community.⁶ Most chemotherapeutic drugs act through mitosis disturbance by:

- Blockage of microtubule assembly (*Vinblastine*, *Vincristine*) or disassembly (*Paclitaxel*, *Ixabepilone*)
- Photosensitizers (*Methyl aminolevulinate*, *Porfimer sodium*)
- Inhibitors and antagonists (*Bortezomib*, *Testolactone*)
- DNA targeting: antimetabolites (*Methotrexate*, *Pentostatin*, *Cytarabine*), intercalating agent (*Doxorubicin*), DNA breaking (*Bleomycin*), alkylation agents (Mustards like *chlormethine* or *cyclophosphamide*, nitrosoureas like *carmustine*, sulfonates like *busulfan*) or platinum derivatives (*Cisplatin*)

Noteworthy, while transition metals⁷ represent nearly half of chemical elements on the periodic table, yet only one element⁸ (platinum) found application in anticancer drugs by the FDA.⁹ Obviously, our

¹ Hanahan, D.; Weinberg, R. A. *Cell* **2000**, *100*, 57.

² For detailed definitions of cancer types, diagnosis and treatments, see: Longe, J. L. *The Gale Encyclopaedia of Cancer*, 2nd edition **2005**, Cengage Gale.

³ Siegel, R.; Ma, J.; Zou, Z.; Jemal, A. *CA-Cancer J. Clin.* **2014**, *64*, 9.

⁴ Croce, C. M. *N. Engl. J. Med.* **2008**, *358*, 502.

⁵ For a review of chemotherapy history, see: Hajdu, S. I. *Cancer* **2005**, *103*, 1097; Chabner, B. A.; Roberts, T. G. *Nature Reviews Cancer* **2005**, *5*, 65; Papac, R. J. *Yale J. Biol. Med.* **2001**, *74*, 391.

⁶ Atta-ur-Rahman; Choudhary, I.; *Frontiers in Anti-Cancer Drug Discovery* **2010**, Bentham Science Publishers.

attention as organometallic chemists naturally turned to these platinum derivatives. The first platinum complex used in chemotherapy, cisplatin, will be exposed in more details in the next section.

1.1 Cisplatin, first inorganic anticancer drug

The cisplatin molecule (*cis*-diamminedichloroplatinum (II) or *cis*-PtCl₂(NH₃)₂) was first reported in 1844 by Michele Peyrone.¹⁰ The structure of the complex, known under the name of Peyrone's chloride,¹¹ was elucidated in 1893 by Alfred Werner.¹² The *d*⁸ platinum adopts a square planar geometry with both chlorides located in a *cis* position. This molecule regains attention only in the 60s.¹³ At that time, Barnett Rosenberg, a bio-physicist from Michigan University, worked on the influence of electrical currents on cell division.¹⁴ While studying growth of *Escherichia coli* in ammonium chloride buffer solution, he noticed an inhibition of cell division of the cells as well as abnormal cell elongation. Scrupulous investigations showed that it was not due to electrical field but to the formation of platinum species from platinum electrode reacting with the solution. The most potent of these compounds proved to be cisplatin.¹⁵ The *trans* isomer, transplatin (Reiset's second chloride),¹⁶ revealed to be ineffective. After proving excellent properties on animal model,¹⁷ cisplatin was finally approved by the FDA in 1978 under trade name of *Platinol*. Nevertheless, clinical use clearly shows scope and limitations of cisplatin. Indeed, it is highly active especially against testicular cancer (90% of cure) but less active against ovarian or bladder cancer.¹⁸ Since then, despite thousands of compounds tested,^{19,20} less than 30 entered clinical trials²¹ and only two platinum derivatives attained

⁷ The potential of transition metal complexes for biomedical applications has been highlighted by several authors: Gasser, G.; Metzler-Nolte, N. *Curr. Opin. Chem. Biol.* **2012**, *16*, 84; Cohen, S. M. *Curr. Opin. Chem. Biol.* **2007**, *11*, 115; Ronconi, L.; Sadler, P. J. *Coord. Chem. Rev.* **2007**, *251*, 1633; Zhang, C. X.; Lippard, S. J. *Curr. Opin. Chem. Biol.* **2003**, *7*, 481; especially for anticancer applications: v. Rijt, S. H.; Sadler, P. J. *Drug Discov. Today* **2009**, *14*, 1089; Bruijninx, P. C. A.; Sadler, P. J. *Curr. Opin. Chem. Biol.* **2008**, *12*, 197.

⁸ Auranofin (*Ridaura*), a gold (I) complex, is used to treat rheumatoid arthritis: Suarez-Almazor, M. E.; Spooner, C.; Belseck, E.; Shea, B. *Cochrane Database Syst. Rev.* **2000**, DOI: 10.1002/14651858.CD002048; Gadolinium (*Dotarem*) and technetium (*Cardiolite*) based drugs served for diagnostic medical imaging.

⁹ Bonetti, A.; Leone, R.; Muggia, F.; Howell, S. B. *Platinum and Other Heavy Metal Compounds in Cancer Chemotherapy* **2009**, Totowa, NJ: Humana Press, Springer Science+Business Media, LLC.

¹⁰ Peyrone, M. *Justus Liebigs Ann. Chem.* **1844**, *51*, 1.

¹¹ Kauffman, G. B. *Platinum Metals Rev.* **2010**, *54*, 250.

¹² Werner, A. Z. *Anorg. Chem.* **1893**, *3*, 267.

¹³ For an overview of the discovery of cisplatin, see: Alderdeen, R. A.; Hall, M. D.; Hambley, T. W. *J. Chem. Educ.* **2006**, *83*, 728.

¹⁴ Rosenberg, B.; Van Camp, L.; Krigas, T. *Nature* **1965**, *205*, 698.

¹⁵ Rosenberg, B. *Platinum Metals Rev.* **1971**, *15*, 42.

¹⁶ Reiset, J. *Ann. Chim. Phys., Sér. 3*, **1844**, *11*, 417.

¹⁷ Rosenberg, B.; Van Camp, L.; Trosko, J. E.; Mansour, V. H. *Nature* **1969**, *222*, 385; Rosenberg, B.; Van Camp, L. *Cancer Res.* **1970**, *30*, 1799.

¹⁸ Wang, D. Lippard, S. J. *Nat. Rev. Drug Discov.* **2005**, *4*, 307.

¹⁹ Wilson and Lippard recently reviewed synthetic strategies to access *cis* and *trans* Pt (II) and Pt (IV) complexes: Wilson, J. J.; Lippard, S. J. *Chem. Rev.* **2014**, *114*, 4470.

²⁰ For a review of platinum complexes as antitumor agents: Hambley, T. W. *Coord. Chem. Rev.* **1997**, *166*, 181; Kostova, I. *Recent Pat Anticancer Drug Discov.* **2006**, *1*, 1. Ott, I.; Gust, R. *Anticancer Agents Med. Chem.* **2007**, *7*, 95; Bouliskas, T.;

worldwide marked admission: the second-generation compound carboplatin²² (*Paraplatin*) and third-generation derivative oxaliplatin²¹ (*Eloxatin*) (**Figure 1**).²³ Heptaplatin (*Sunpla*), Lobaplatin and Nedaplatin (*Aqupla*) have been approved in very few countries (South Korea, China and Japan respectively). All these complexes contain two labile X-type ligands and two more coordinating amines.

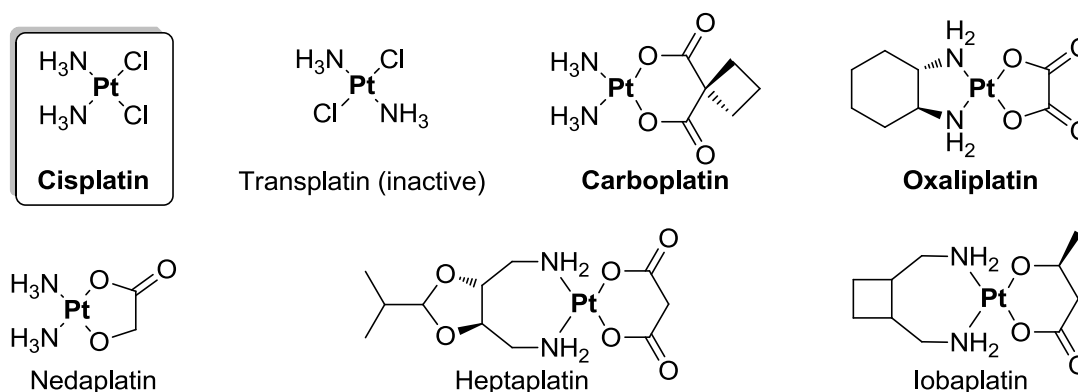


Figure 1: Commonly used platinum anticancer drugs and transplatin

The biological mechanism of cisplatin has been partly elucidated.²⁴ Caused by its limited stability in solution, cisplatin solutions are injected intravenously directly after solubilisation. The complex performs cellular uptake²⁵ by diffusion, endocytosis, organic cation transporter or copper transporters (**Figure 2**).²⁶ Compared to blood ($[Cl^-] = 100 \text{ mM}$), chloride concentration is negligible in the cell resulting in a replacement of chloride ligands of the cisplatin *prodrug* by water molecules. This aquated cationic complex is the active species and reacts with various nucleophiles (proteins, glutathione, DNA). The platinum usually reacts with DNA to form monofunctional adducts, which can further react to form bifunctional lesions, especially 1,2-intrastrand crosslinks, inhibiting DNA replication.²⁷ Preferred position remains *N7* position of the purine bases, which has higher pK_a than pyrimidine bases. Guanine (G) is preferred to adenine because the formed adduct is stabilized by an additional $NH_3^- \cdots O$ hydrogen bond.²⁸ Platinum adduct causes distortion of DNA helix and recognition of the damage by repair proteins conducting to a cascade of cellular responses finishing

Pantos, A.; Bellis, E.; Christofis, P. *Cancer Therapy* **2007**, 5, 537; For cyclometalated complexes, see: Cutillas, N.; Yellol, G. S.; de Haro, C.; Vicente, C.; Rodríguez, V.; Ruiz, J. *Coord. Chem. Rev.* **2013**, 257, 2784.

²¹ Kelland, L. *Nat. Rev. Cancer* **2007**, 8, 573.

²² Laurie, S. A.; Siu, L. L.; Winquist, E.; Maksymiuk, A.; Harnett, E. L.; Walsh, W.; Tu, D.; Parkulekar, W. R. *Cancer* **2010**, 116, 362.

²³ Wheate, N. J.; Walker, S.; Craig, G. E.; Oun, R. *Dalton Trans.* **2010**, 39, 8113.

²⁴ Siddik, Z. H. *Oncogene* **2003**, 22, 7265.

²⁵ Gately, D. P.; Howell, S. B. *Br. J. Cancer* **1993**, 67, 1171.

²⁶ Calandrini, V.; Nguyen, T. H.; Arnesano, F.; Galliani, A.; Ippoliti, E.; Carloni, P.; Natile, G. *Chem. Eur. J.* **2014**, 20, 11719; Calandrini, V.; Arnesano, F.; Galliani, A.; Nguyen, T. H.; Ippoliti, E.; Carloni, P.; Natile, G. *Dalton Trans.* **2014**, 43, 12085.

²⁷ Reißner, T.; Schneider, S.; Schorr, S.; Carell, T. *Angew. Chem. Int. Ed.* **2010**, 49, 3077; Reißner, T.; Schneider, S.; Schorr, S.; Carell, T. *Angew. Chem.* **2010**, 122, 3142; Hambley, T. W. *J. Chem. Soc., Dalton Trans.* **2001**, 2711.

²⁸ Costa, L. A. S.; Hambley, T. W.; Rocha, W. R.; De Almeida, W. B.; Dos Santos, H. F. *Int. J. Quant. Chem.* **2006**, 106, 2129.

with apoptosis.^{29,30} Mechanism of action of oxaliplatin³¹ and carboplatin³² are similar to cisplatin. The latter conducts to ototoxicity, peripheral neuropathy and nephrotoxicity, side effects of carboplatin are myelosuppression while oxaliplatin generally provokes peripheral neuropathy.³³

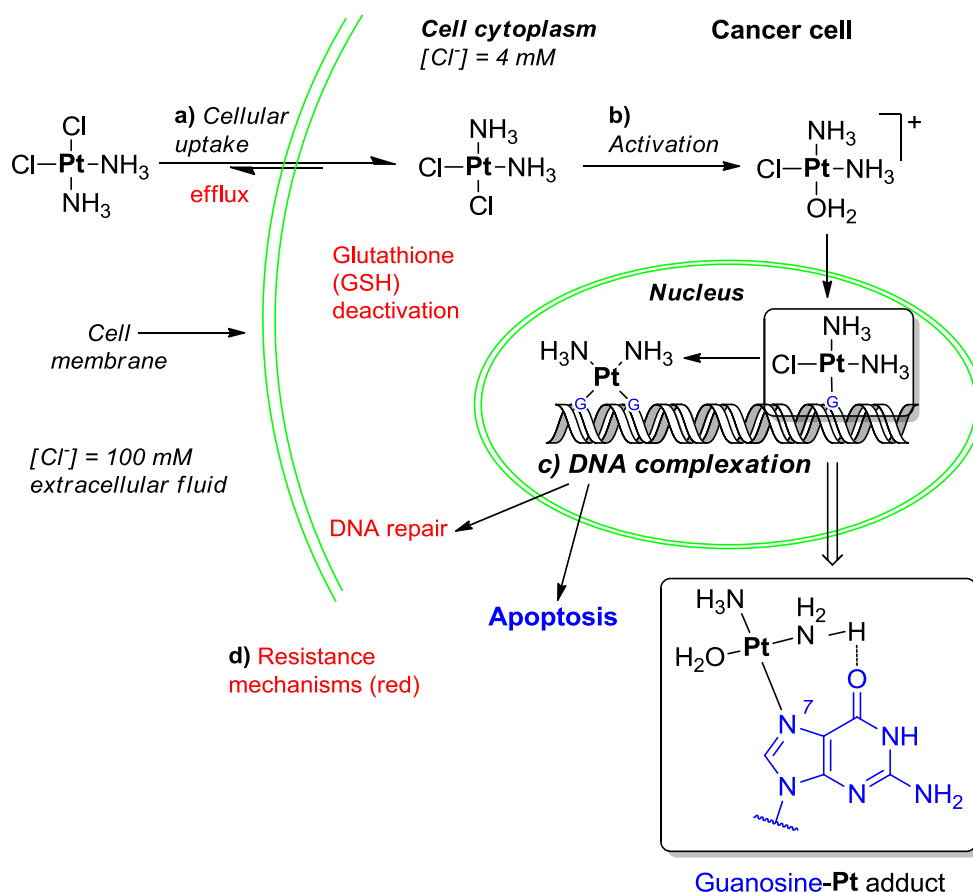


Figure 2: a) Commonly proposed molecular mechanism of cisplatin: a) cellular uptake, b) activation by aquation, c) DNA coordination conducting to apoptosis d) resistance mechanisms

In practical, only 1% of platinum ends up on DNA, mainly due to the presence of other molecules³⁴ (proteins³⁵ for the most) involved in platinum activity.³⁶ Several possible resistance mechanisms of platinum drugs have been postulated.³⁷ The first drawback is due to blood proteins, which are able to

²⁹ Folkman, J. *Semin. Cancer Biol.* **2003**, 13, 159.

³⁰ Jung, Y.; Lippard, S. J. *Chem. Rev.* **2007**, 107, 1387.

³¹ Kasparkova, J.; Vojtiskova, M.; Natile, G.; Brabec, V. *Chem. Eur. J.* **2008**, 14, 1330.

³² For ligand exchange kinetics on platinum, see: Reedijk, J. *Platinum Metals Rev.* **2008**, 52, 2.

³³ Rabik, C. A.; Dolan, M. E. *Cancer Treat. Rev.* **2007**, 33, 9.

³⁴ Messori, L.; Marzo, T.; Merloni, A. *Chem. Comm.* **2014**, 50, 8360.

³⁵ In this context, see: Cubo, L.; Groessl, M.; Dyson, P. J.; Quiroga, A. G.; Navarro-Ranninger, C.; Casini, A. *ChemMedChem* **2010**, 5, 1335; Casini, A.; Reedijk, J. *Chem. Sci.* **2012**, 3, 3135; Pinato, O.; Musetti, C.; Sissi, C. *Metallomics* **2014**, 6, 380.

³⁶ Wesselblatt, E.; Yavin, E.; Gibson, D. *Inorg. Chim. Acta* **2012**, 393, 75.

³⁷ Fuertes, M. A.; Alonso, C.; Pérez, J. M. *Chem. Rev.* **2003**, 103, 645.

interfere with platinum derivatives and decrease their cellular uptake. Molecules containing sulphur, especially glutathione, condense on platinum and conduct to its elimination.³⁸ Once the cisplatin fixed on DNA, DNA repair pathways³⁹ can remove the metal either by nucleotide excision repair (NER), recombinational repair of DNA or mismatch repair (MMR). Reduced apoptotic response and apoptosis inhibitors may explain most of additional resistances. Fortunately, cisplatin resistance can be partly circumvented by its combination with other anticancer products.⁴⁰

The therapeutic inefficiency of transplatin led to the general assumption of the absence of activity for all *trans* configured platinum complexes. However, several *trans* platinum complexes recently depicted similar activities as *cis* compounds.⁴¹ Replacement of ammonia ligands by aromatic heterocycles (pyridine, (iso)quinolone, thiazole, ...), aliphatic amines (piperazine, isopropylamine, ...), iminoether or acetanimine⁴² resulted in cytotoxic complexes.⁴³ *Trans* complexes also need to be aquated to be active.⁴⁴ Transplatin forms monoadducts with DNA, which cannot further react to the active bi-coordinate species. Although the first chloride substitution of transplatin is relatively easy due to *trans* effect of chloride in *trans*, the second aquation is less favoured. Replacement of NH₃ by other ligands may result in stable DNA monoadducts and ternary DNA-Protein cross-links. In order to regulate activity of the platinum core, structurally different ligands would allow circumventing cisplatin drawbacks.⁴⁵ We focused our investigations on *N*-Heterocyclic Carbenes (NHC), a family of neutral ligands, which appeared only 40 years ago. In the next section, we will discuss their properties and their potential anticancer applications.

Brabec, V.; Kasparkova, J. *Drug Resist. Updates* **2002**, 5, 147; Stewart, D. J. *Crit. Rev. Oncol. Hematol.* **2007**, 63, 12; Stordal, B.; Davey, M. *IUBMB Life* **2007**, 59, 696.

³⁸ Wang, X.; Guo, Z. *Anticancer Agents Med. Chem.* **2007**, 7, 19.

³⁹ Zamble, D. B.; Lippard, S. J. *Trends Biochem Sci.* **1995**, 10, 435.

⁴⁰ Dasari, S. D.; Tchounwou, P. B. *Eur. J. Pharmacol.* **2014**, 740, 364.

⁴¹ Natile, G.; Coluccia, M. *Coord. Chem. Rev.* **2001**, 216-217, 383; Coluccia, M.; Natile, G. *Anticancer Agents Med. Chem.* **2007**, 7, 111; Kalinowska-Lis, U.; Ochocki, J.; Matlawska-Wasowska, K. *Coord. Chem. Rev.* **2008**, 252, 1328; Frybortova, M.; Novakova, O.; Stepankova, J.; Novohradsky, V.; Gibson, D.; Kasparkova, J.; Brabec, V. *J. Inorg. Biochem.* **2013**, 126, 46.

⁴² Boccarelli, A.; Intini, F. P.; Sasanelli, R.; Sivo, M. F.; Coluccia, M.; Natile, G. *J. Med. Chem.* **2006**, 49, 829.

⁴³ Aris, S. M.; Farrell, N. P. *Eur. J. Inorg. Chem.* **2009**, 2009, 1293.

⁴⁴ Burda, J. V.; Zeizinger, M.; Leszczynski, J. *J. Comput. Chem.* **2005**, 26, 907.

⁴⁵ For an excellent review on platinum (II) derivatives (dendrimers, liposomes, targeting agents) and Pt(IV) complexes, see: Harper, B. W.; Krause-Heuer, A. M.; Grant, M. P.; Manohar, M.; Garbutcheon-Singh, K. B.; Aldrich-Wright, J. R. *Chem. Eur. J.* **2010**, 16, 7064.

1.2 N-Heterocyclic Carbenes: a promising class of ligands for various applications

1.2.1 Historical introduction: the discovery of N-Heterocyclic Carbenes

Carbenes are moieties containing a bivalent carbon bearing six valence electrons in its valence shell. The simplest example is methylene ($\text{H}_2\text{C}:$). First attempt to its synthesis goes back to 1835 when Dumas tried to dehydrate methanol and form the free methylene.⁴⁶

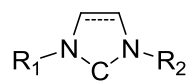


Figure 3: N-Heterocyclic Carbene (NHC)

Early works on N-Heterocyclic Carbenes (NHC) started in the 1960s (**Figure 3**).⁴⁷ At this time, Wanzlick and co-workers studied the reactivity of imidazolidinyldene derivatives. The free carbene was generated by thermolysis and the intermediate was trapped with different electrophiles.⁴⁸ Molecular weight determinations led to the postulation of equilibrium between the free carbene and its subsequent dimer (**Figure 4**). Starting from imidazolium salts, Schönherr and Wanzlick trapped the carbenes by mercurium chloride forming the corresponding mercurium carbene complex. In this study, no evidence for dimeric product was noticed.⁴⁹ In the same period, Öfele synthesized a chromium NHC complex by heating imidazolium $[\text{HCr}(\text{CO})_5]^-$ salt.⁵⁰

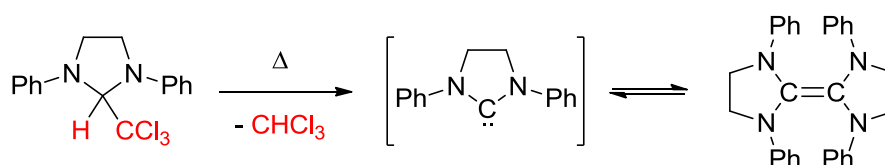


Figure 4: Thermolytic synthesis of NHC carbenes and Wanzlick equilibrium

Nevertheless, this hypothesis of Wanzlick equilibrium was refuted after first dimer crossover experiments of Lemal⁵¹ and Winberg.⁵² In 1999, Denk and co-workers found evidence for crossover⁵³

⁴⁶ Dumas, J. B.; Péligot, *Ann. Chim. Phys.* **1835**, 58, 5.

⁴⁷ For a review of state of art in beginning of the 60^s, see: Wanzlick, H. W. *Angew. Chem. Int. Ed. Engl.* **1962**, 1, 75.

⁴⁸ Wanzlick, H.-W.; Schikora, E. *Angew. Chem.* **1960**, 72, 494; Wanzlick, H.-W.; Schikora, E. *Chem. Ber.* **1961**, 94, 2389.

⁴⁹ Schönherr, H.-J.; Wanzlick, H.-W. *Angew. Chem.* **1968**, 80, 154; Schönherr, H.-J.; Wanzlick, H.-W. *Chem. Ber.* **1970**, 103, 1037.

⁵⁰ Öfele, K. *J. Organomet. Chem.* **1968**, 12, 42.

⁵¹ Lemal, D. L.; Lovald, R. A.; Kawano, K. I. *J. Am. Chem. Soc.* **1964**, 86, 2518.

⁵² Winberg, H. E.; Carnahan, J. E.; Coffman, D. D.; Brown, M. *J. Am. Chem. Soc.* **1965**, 87, 2055.

⁵³ An alternative to Wanzlick equilibrium might be a cycloaddition-cycloreversion pathway.

products,⁵⁴ following an electrophilic attack mechanism of the tetraamin postulated by Lemal.⁵⁵ Paolini and co-workers report proton catalysed dimerization of free carbenes.⁵⁶ Finally, cleavage of tetraaminoethylene into carbenes was proved by ¹³C-NMR studies by Lemal⁵⁷ ascertained by trapping experiments by Hahn and Fröhlich.⁵⁸ These results led Herrmann and collaborators to conclude the effective existence of *Wanzlick* equilibrium shifted to carbene species in case of steric hindered nitrogen substituents.⁵⁹ Theoretical calculations of Cheng *et al.* also indicated that equilibrium is faster attained for benzimidazol-2-ylidenes than imidazolidin-2-ylidenes.⁶⁰ With increasing aromatic character, dimerization of NHC is less favoured.⁶¹

Carbene chemistry is an emerging field that started only 25 years ago with isolation of the first free carbenes.⁶² Pioneer work of NHC isolation was realized by Arduengo.^{63,64,65,66} Subsequently a first singlet carbene-like product⁶⁷ was isolated by the group of Guy Bertrand thanks to its stabilization by adjacent phosphorous atom (**Figure 5**).⁶⁸ Both compounds are extremely stable: Bertrand's phosphine carbene can be distilled under reduced pressure at 85 °C, and the free NHC of Arduengo melts at 241 °C without decomposition. This NHC is stable in absence of air and moisture and its unique structure could be elucidated by single crystal X-ray diffraction studies.

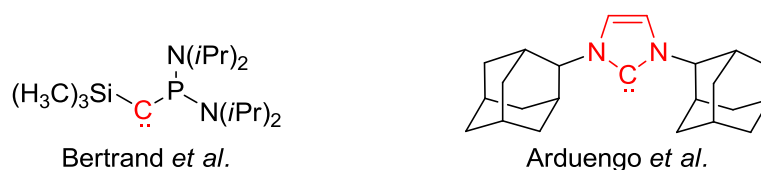


Figure 5: First isolated carbene (left) and first isolated NHC (right)

⁵⁴ Denk, M. K.; Hatano, K.; Ma, M. *Tetrahedron Lett.* **1999**, 40, 2057.

⁵⁵ Liu, Y.; Lemal, D. M. *Tetrahedron Lett.* **2000**, 41, 599.

⁵⁶ Alder, R. W.; Chaker, L.; Paolini, F. P. V. *Chem. Commun.* **2004**, 2172.

⁵⁷ Liu, Y.; Lindner, P. E.; Lemal, D. M. *J. Am. Chem. Soc.* **1999**, 121, 10626.

⁵⁸ Hahn, F. E.; Wittenbecher, L.; Le Van, D.; Fröhlich, R. *Angew. Chem. Int. Ed.* **2000**, 39, 541.

⁵⁹ Böhm, V. P. W.; Herrmann, W. A. *Angew. Chem. Int. Ed.* **2000**, 39, 4036.

⁶⁰ Cheng, M.-J.; Lai, C.-L.; Hu, C.-H. *Mol. Physics* **2004**, 102, 2617.

⁶¹ While dimerization is favoured for imidazolidin-2-ylidene, benzimidazol-2-ylidene give equilibria and imidazol-2-ylidene is not favoured thermodynamically.

⁶² For a review of the history of stable carbenes, see: Arduengo, A. J., III; Krczyk, R. *Chem. unserer Zeit.* **1998**, 32, 6.

⁶³ Arduengo, A. J., III; Harlow, R. L.; Kline, M. *J. Am. Chem. Soc.* **1991**, 113, 361.

⁶⁴ Arduengo, A. J., III; Rasika Dias, H. V.; Harlow, R. L.; Kline, M. *J. Am. Chem. Soc.* **1992**, 114, 5530.

⁶⁵ Arduengo, A. J., III; Kline, M.; Galabrese, J. C.; Davidson, F. *J. Am. Chem. Soc.* **1991**, 113, 9704; Dixon, D. A.; Arduengo, A. J., III. *J. Phys. Chem.* **1991**, 95, 4180; Arduengo, A. J., III; Bock, H.; Chen, H.; Denk, M.; Dixon, D. A.; Green, J. C.; Herrman, W. A.; Jones, N. L.; Wagner, M.; West, R. *J. Am. Chem. Soc.* **1994**, 116, 6641.

⁶⁶ Arduengo, A. J., III; Rasika Dias, H. V.; Dixon, D. A.; Harlow, R. L.; Klooster, W. T.; Koetzle, T. F. *J. Am. Chem. Soc.* **1994**, 116, 6812.

⁶⁷ The special reactivity of this compound conducted to further investigations on its real nature. An ylide structure seems more accordant to X-ray diffractions of an analogue as well as to theoretical calculations: Kirmse, W. *Angew. Chem. Int. Ed.* **2004**, 43, 1767.

⁶⁸ Igau, A.; Grützmacher, H.; Baceiredo, A.; Bertrand, M. *J. Am. Chem. Soc.* **1988**, 110, 6463; Igau, A.; Baceiredo, A.; Trinqueir, G.; Bertrand, G. *Angew. Chem., Int. Ed. Engl.* **1989**, 28, 621; Gilette, G. R.; Baceiredo, A.; Bertrand, G. *Angew. Chem., Int. Ed. Engl.* **1990**, 29, 1429; Dixon, D. A.; Dobbs, K. D.; Arduengo, A. J., III; Bertrand, G. *J. Am. Chem. Soc.* **1991**, 113, 8782; Soleilhavoup, M.; Baceiredo, A.; Treutler, O.; Ahlrichs, R.; Nieger, M.; Bertrand, G. *J. Am. Chem. Soc.* **1992**, 114, 10959.

Despite the five-membered imidazol-2-ylidene remains the most used, its saturated analogue imidazolidin-2-ylidene, benzimidazol-2-ylidene or triazol-2-ylidene (**Figure 6**), 4 to 8 membered cyclic carbenes are nowadays reported with an aim to vary donor capacity of these ligands.⁶⁹

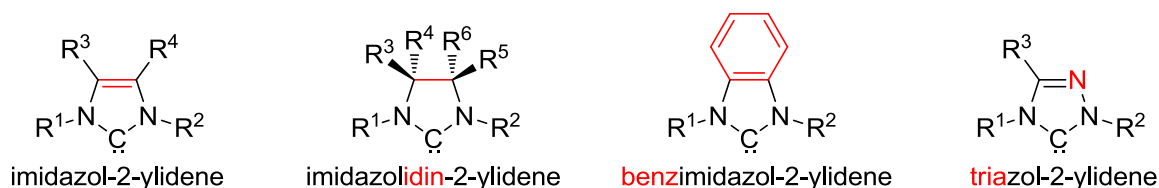


Figure 6: Commonly used five-membered NHC structures

1.2.2 Properties and applications of NHC carbenes and their metal complexes



Figure 7: Electronic configuration of triplet and singlet carbenes

NHCs^{70,71} are cyclic compounds containing one singlet divalent carbon (oxidation state II) atom with 6 electrons in outer shell and bond to two neighbouring nitrogens.⁷² The electronic configuration of the carbonic carbon represents the main difference between NHC and triplet carbenes. In the triplet state, the electrons are located in two different non-bonding orbitals (2 p orbitals) and have parallel spin ($\uparrow\uparrow$), contributing to a linear structure around the sp hybridized carbene carbon. In NHC's (singlet carbenes), a gap of 65-85 kcal/mol between sp^2 and p_π orbitals forces electrons to occupy both the same sp^2 orbital with antiparallel spin ($\uparrow\downarrow$). The carbene carbon geometry is bended in this case.⁷³ NHC stabilization⁷⁴ is attributed mostly to electronic effects.⁶⁴ Both its neighbouring nitrogens act in same time as π -donor (lone pair) as well as σ -acceptors (electronegativity of the nitrogen) (**Figure 8**). The free lone pair of the carbenic carbon is stabilized by electron-withdrawing inductive effect from the nitrogen atoms. Delocalisation of the nitrogen lone pair into empty p orbital of the carbon stabilizes this orbital.⁷⁵ This *push-pull* effect stabilizes the singlet state of the carbene.⁷⁶ Arduengo⁷⁷ showed that steric hindrance does not contribute largely to the stability of NHC.⁷⁸

⁶⁹ Dröge, T.; Glorius, F. *Angew. Chem. Int. Ed.* **2010**, 49, 6940.

⁷⁰ For comprehensive overview, see: Nolan, S. P. *N-Heterocyclic Carbenes in Synthesis* **2006**, Wiley-VCH Verlag GmbH & Co. KGaA, Weinheim, Germany; Nolan, S. P. *N-Heterocyclic Carbenes: Effective Tools for Organometallic Synthesis* **2014**, Wiley-VCH Verlag GmbH & Co. KGaA, Weinheim, Germany.

⁷¹ For a review of NHC complex applications, see: Mercks, L.; Albrecht, M. *Chem. Soc. Rev.* **2010**, 39, 1903.

⁷² Herrmann, W. A.; Köcher, C. *Angew. Chem.* **1997**, 109, 2256.

⁷³ Kirmse, W. *Carbene Chemistry*, **1971**, Academic Press, New York.

⁷⁴ Bourissou, D.; Guerret, O.; Gabbai, F. P.; Bertrand, G. *Chem. Rev.* **2000**, 100, 39.

⁷⁵ Heinemann, C.; Müller, T.; Apeloig, Y.; Schwarz, H. *J. Am. Chem. Soc.* **1996**, 118, 2023.

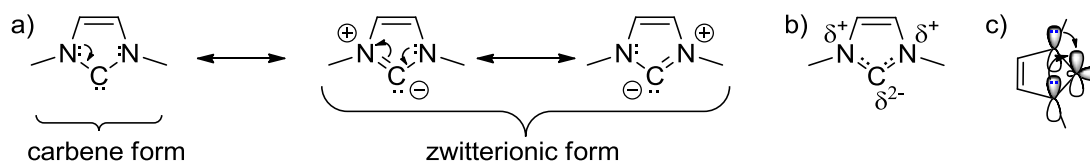


Figure 8: a) b) Resonance structures of NHC and c) orbitals representation of NHC

Coordinated to transition metals,⁷⁹ NHC carbenes are L-type ligands and form complexes by donation of their free lone pair⁸⁰ to the metal centre.⁸¹ Some amount of π -back donation⁸² from the metal to the NHC also contributes to carbene-metal bond.⁸³ The electronic and steric properties of the metal can be easily modulated by changing the NHC backbone and the *N*-substituents. The steric factor can be quantified using the buried volume parameter ($\%V_{\text{bur}}$)⁸⁴ and electronic factor is obtained by the Tolman electronic parameter (TEP).⁸⁵ **Figure 9** represents most common schematic representations of NHC-metal complexes. While d) perhaps best represents the electronic nature of NHC-metal bond, representations a-c are easier to utilize. Representation b) was chosen across the whole manuscript to depict NHC metal complexes.

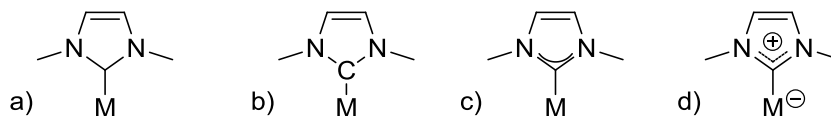


Figure 9: Most common representations of NHC-metal complexes

Compared to phosphines (R_3P), NHC generally present much stronger σ -donation property⁸⁶ and form stronger metal bond. While phosphines ligands always form an equilibrium of coordination-decoordination ($\text{M-PR}_3 \rightleftharpoons \text{M} + \text{PR}_3$), the NHC-metal bond usually do not dissociate.⁸⁷ So no excess

⁷⁶ Herrmann and co-workers oxidize the alkene of several NHC complexes with OsO_4 (classical alkene chemistry) and form the corresponding adducts without touching rest of the molecule: Herrmann, W. A.; Roesky, P. W.; Elison, M.; Artus, G.; Öfele, K. *Organometallics* **1995**, 14, 1085.

⁷⁷ Kinetic stability was also suggested by Arduengo erroneously finding that a NHC is: “true carbene with negligible ylidic character”.⁶⁶

⁷⁸ Arduengo, A. J., III. *Acc. Chem. Res.* **1999**, 32, 913.

⁷⁹ For NHC complex synthesis, see: Peris, E. Top. *Organomet. Chem.* **2007**, 21, 83.

⁸⁰ The $\text{p}K_a$ of common NHC is around 20-24 making them strong bases: Amyes, T. L.; Diver, S. T.; Richard, J. P.; Rivas, F. M.; Toth, K. *J. Am. Chem. Soc.* **2004**, 126, 4366; Magill, A. M.; Cavell, K. J.; Yates, B. F. *J. Am. Chem. Soc.* **2004**, 126, 8717; Chu, Y.; Deng, H.; Cheng, J.-P. *J. Org. Chem.* **2007**, 72, 7790.

⁸¹ Hahn, F. E.; Jahnke, M. C. *Angew. Chem.* **2008**, 120, 3166; Hahn, F. E.; Jahnke, M. C. *Angew. Chem. Int. Ed.* **2008**, 47, 3122; Marchione, D.; Belpassi, L.; Bistoni, G.; Macchioni, A.; Tarantelli, F.; Zuccaccia, D. *Organometallics* **2014**, 33, 4200.

⁸² Back, O.; Henry-Ellinger, M.; Martin, C. D.; Martin, D.; Bertrand, G. *Angew. Chem. Int. Ed.* **2013**, 52, 2939.

⁸³ Salvi, N.; Belpassi, L.; Tarantelli, F. *Chem. Eur. J.* **2010**, 16, 7231.

⁸⁴ Hillier, A. C.; Somer, W. J. Yong, B. S.; Petersen, J. L.; Cavallo, L.; Nolan, S. P. *Organometallics* **2003**, 22, 4322.

⁸⁵ Tolman, C. A. *Chem. Rev.* **1977**, 77, 313.

⁸⁶ For a detailed review about electronic properties of NHC carbenes, see Nelson, D. J.; Nolan, S. P. *Chem. Soc. Rev.* **2013**, 42, 6723; and for their donor properties: Gusev, D. G. *Organometallics* **2009**, 28, 763.

⁸⁷ Jacobsen, H.; Correa, A.; Poater, A.; Costabile, C.; Cavallo, L. *Coord. Chem. Rev.* **2009**, 253, 687.

of this ligand is needed to form stable⁸⁸ and oxidation resistant complexes. NHC precursors (which are azolium salts) are readily and easily available on large scale. For this reason, the NHC are ancillary ligands of choice for organometallic catalysis. Their electronic parameters can easily be tuned by varying the nitrogen's substituents or the backbone itself.⁸⁹

Three main synthetic strategies are employed to generate free NHCs (**Figure 10**):

- Deprotonation of the corresponding azolium salt $[(\text{NHC-H})^+\text{X}^-]$
- Reduction of cyclic thiocarbamides (such as imidazole-2(3H)-thiones),⁹⁰
- Thermolysis^{91,92}

Deprotonation remains the most employed strategy, as it only requires either strong bases (hydrides, steric hindered amidures like LiHMDS) or weak bases with displacement of the acid/base equilibrium by trapping of the generated NHC with metals. NHC complexes can also be obtained under mild conditions starting from metals with internal base.⁵⁰

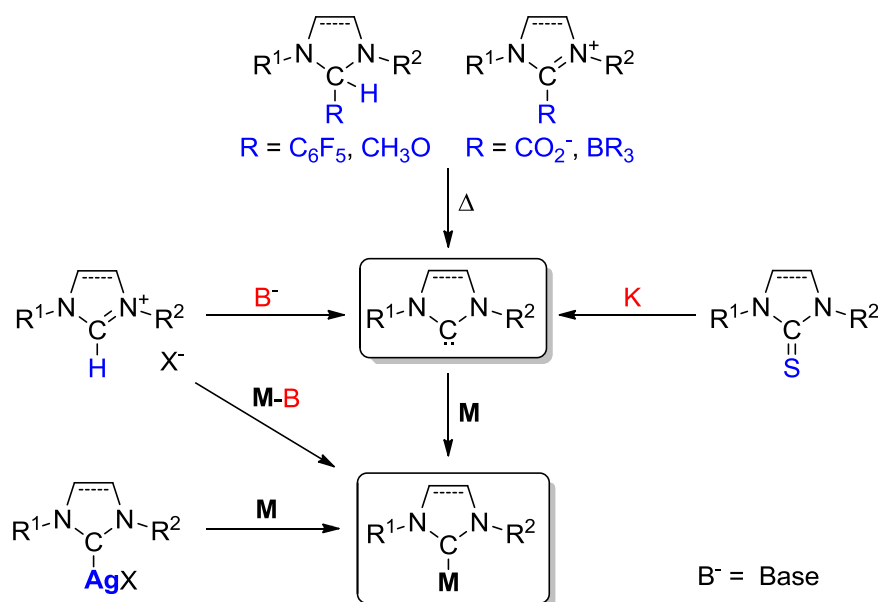


Figure 10: Strategies of generation of NHC carbenes and NHC metal complexes

⁸⁸ Although decomposition pathways of NHC complexes exist: Crudden, C. M.; Allen, D. P. *Coord. Chem. Rev.* **2004**, 248, 2247.

⁸⁹ César, V.; Bellemin-Lapponnaz, S. *Actualité Chimique* **2009**, 326, 10; Blake, G. A.; Moerdyk, J. P.; Bielawski, C. W. *Organometallics* **2012**, 31, 3373; Hopkinson, M. N.; Richter, C.; Schedler, M.; Glorius, F. *Nature* **2014**, 510, 485.

⁹⁰ Kuhn, N.; Kratz, T. *Synthesis* **1993**, 1993, 561.

⁹¹ Wanzlick, H. W.; Esser, F.; Kleiner, H. J. *Chem. Ber.* **1963**, 96, 1208.

⁹² Different NHC-adducts are reported permitting thermolytic NHC release: chloroform: Trnka, T. M.; Morgan, J. P.; Sanford, M. S.; Wilhelm, T. E.; Scholl, M.; Choi, T. L.; Ding, S.; Day, M. W. Grubbs, R.H. *J. Am. Chem. Soc.* **2003**, 125, 2546; methoxy: Enders, D.; Breuer, K.; Raabe, G.; Runsink, J.; Teles, H.; Melder, J.P.; Ebel, K.; Brode, S. *Angew. Chem.* **1995**, 107, 1119; Enders, D.; Breuer, K.; Raabe, G.; Runsink, J.; Teles, J. H.; Melder, J.-P.; Ebel, K.; Brode, S. *Angew. Chem. Int. Ed. Engl.* **1995**, 34, 1021; pentafluorophenyl: Blum, A. P.; Ritter, T. Grubbs, R. H. *Organometallics* **2007**, 26, 2122; Nyce, G. W.; Csihony, S.; Waymouth, R. M.; Hedrick, J. L. *Chem. Eur. J.* **2004**, 10, 4073; boran: Yamaguchi, Y.; Kashiwabara, T.; Ogata, K.; Miura, Y.; Nakamura, Y.; Kobayashi, K.; Ito, T. *Chem. Comm.* **2004**, 19, 2160; or carboxylates: Voutchkova, W. M.; Appelhans, L. N.; Chianese, A. R.; Crabtree, R. H. *J. Am. Chem. Soc.* **2005**, 127, 17624.

NHC have been highlighted as organic catalysts⁹³ as well as ligands for stabilization and reactivity modulation of transition metal complexes.⁹⁴ NHC are strong bases, but also present nucleophilic properties.⁹⁵ Thus, nature uses catalytic properties of thiazolium in thiamine pyrophosphate (TPP) (Vitamin B₁),^{96,97} which is the first discovered vitamin.⁹⁸ This coenzyme is necessary for decarboxylation of pyruvate⁹⁹ or transketolase¹⁰⁰ in sugar and amino acids metabolism.¹⁰¹

Most prominent example of NHC complex as catalyst is the so-called second-generation Grubbs ruthenium catalyst for olefin metathesis (**Figure 11**).¹⁰² Replacement of one phosphine ligand (Grubbs I)¹⁰³ by a NHC (Grubbs II) results in a significant increase of turnover. Their amelioration was further achieved when Hoveyda replaced a second phosphine by styrenyl ether. Grubbs I, II and Grubbs-Hoveyda II catalysts are commercially available and Nobel Prize was discerned to this field proving their grooving importance.¹⁰⁴ NHC palladium complexes are reported as highly stable and modular catalysts for C-C coupling or Buchwald-Hartwig amination reactions.¹⁰⁵

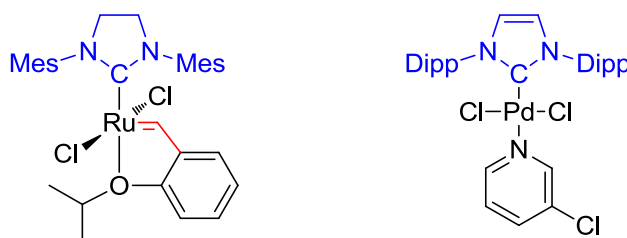


Figure 11: Grubbs/Hoveyda olefin metathesis catalyst and an example of palladium-NHC cross coupling complex

⁹³ For example, see: Jone, W. D. *J. Am. Chem. Soc.* **2009**, *131*, 15075.

⁹⁴ NHC as organocatalysts have recently been reviewed by Nolan and Glorius: Marion, N.; Díez-González, S.; Nolan, S. P. *Angew. Chem. Int. Ed.* **2007**, *46*, 2988; Biju, A. T.; Kuhl, N.; Glorius, F. *Acc. Chem. Res.* **2011**, *44*, 1182.

⁹⁵ Alder, R. W.; Allen, P. R.; Williams, S. J. *J. Chem. Soc., Chem. Commun.* **1995**, 1267.

⁹⁶ Shortcomings of this vitamin lead to Beriberi disease.

⁹⁷ Breslow, R. *J. Am. Chem. Soc.* **1958**, *80*, 3719.

⁹⁸ Williams, R. R.; Cline, J. K. *J. Am. Chem. Soc.* **1936**, *58*, 1504.

⁹⁹ Lohmann, K.; Schuster, P. *Biochem. Z.* **1937**, *294*, 188.

¹⁰⁰ Nilsson, U.; Meshalkina, L.; Lindqvist, Y.; Schneider, G. *J. Biol. Chem.* **1997**, *272*, 1864.

¹⁰¹ Pohl, M.; Sprenger, G. A.; Müller, M. *Curr. Opin. Biotechnol.* **2004**, *15*, 335.

¹⁰² Scholl, M.; Ding, S.; Lee, C. W.; Grubbs, R. H. *Org. Lett.* **1999**, *1*, 953; Boydston, A. J.; Xia, Y.; Kornfield, J. A.; Gorodetskaya, I. A.; Grubbs, R. H. *J. Am. Chem. Soc.* **2008**, *130*, 12775.

¹⁰³ Schwab, P.; Grubbs, R. H.; Ziller, J. W. *J. Am. Chem. Soc.* **1996**, *118*, 100.

¹⁰⁴ Vougioukalakis, G. C.; Grubbs, R. H. *Chem. Rev.* **2010**, *110*, 1746

¹⁰⁵ For a review of NHC-Pd catalysts for C-C coupling, see: Fortman, G. C.; Nolan, S. P. *Chem. Soc. Rev.* **2011**, *40*, 5151.

1.2.3 Biological applications of NHC complexes

Besides their interest as catalysts, NHC complexes also proved promising biological activities.^{106,107,108} Depending on the metal and the structure of the NHC employed, different cellular targets can be attacked making them promising as antimicrobial¹⁰⁹ or antitumor¹¹⁰ agents. Antimicrobial¹¹¹ activities have been highlighted for rhodium and ruthenium¹¹², gold¹¹³ and silver¹¹⁴ NHC complexes. First reported anticancer activities of NHC complexes date from 10 years ago when Berners-Price and co-workers studied cationic NHC complexes.¹¹⁵ Gold NHC complexes¹¹⁶ were reported for their

¹⁰⁶ Imidazole derivatives as well as imidazolium salts, the protonated precursors of NHC carbenes are known for their antitumor and antimicrobial activities: Riduan, S. N.; Zhang, Y. *Chem. Soc. Rev.* **2013**, *42*, 9055; Zhang, L.; Peng, X.-M.; Damu, G. L. V.; Geng, R.-X.; Zhou, C.-H. *Med. Res. Rev.* **2014**, *34*, 340.

¹⁰⁷ Several interesting reviews of biological applications of NHC complexes were recently published, see: Liu, W.; Gust, R. *Chem. Soc. Rev.* **2013**, *42*, 755; Oehninger, L.; Rubbiani, R.; Ott, I. *Dalton Trans.* **2013**, *42*, 3269; Gautier, A.; Cisnetti, F. *Metallomics* **2012**, *4*, 23; Hindi, K. M.; Panzner, M. J.; Tessier, C. A.; Cannon, C. L.; Youngs, W. J. *Chem. Rev.* **2009**, *109*, 3859; Teyssot, M.-L.; Jarrousse, A.-S.; Manin, M.; Chevy, A.; Roche, S.; Norre, F.; Beaudoin, C.; Morel, L.; Boyer, D.; Mahiou, R.; Gautier, A. *Dalton Trans.* **2009**, 6893; Cisnetti, F.; Gautier, A. *Angew. Chem. Int. Ed.* **2013**, *52*, 11976.

¹⁰⁸ Beside NHC, other organometallic complexes (metallocenes, arenes or carbonyl complexes) present anticancer properties: Patra, M.; Gasser, G. *ChemBioChem* **2012**, *13*, 1232; Organometallic approach present an interesting approach for conjugation of transition metals and biological moieties: Monney, A.; Albrecht, M. *Coord. Chem. Rev.* **2013**, *257*, 2420; Hartinger, C. G.; Metzler-Nolte, N.; Dyson, P. J. *Organometallics* **2012**, *31*, 5677; Gasser, G.; Ott, I.; Metzler-Nolte, N. J. *Med. Chem.* **2011**, *54*, 3.

¹⁰⁹ E.g. see: Hindi, K. M.; Siciliano, T. J.; Durmus, S.; Panzner, M. J.; Medvetz, D. A.; Reddy, D. V.; Hogue, L. A.; Hovis, C. E.; Hilliard, J. K.; Mallett, R. J.; Tessier, C. A.; Cannon, C. L.; Youngs, W. J. *J. Med. Chem.* **2008**, *51*, 1577; Kascatan-Nebioglu, A.; Melaiye, A.; Hindi, K.; Durmus, S.; Panzner, M. J.; Hogue, L. A.; Mallett, R. J.; Hovis, C. E.; Coughenour, M.; Crosby, S. D.; Milsted, A.; Ely, D. L.; Tessier, C. A.; Cannon, C. L.; Youngs, W. J. *J. Med. Chem.* **2006**, *49*, 6811; Kascatan-Nebioglu, A.; Panzner, M. J.; Tessier, C. A.; Cannon, C. L.; Youngs, W. J. *Coord. Chem. Rev.* **2007**, *251*, 884; Melaiye, A.; Simons, R. S.; Milsted, A.; Pingitore, F.; Wesdemiotis, C.; Tessier, C. A.; Youngs, W. J. *J. Med. Chem.* **2004**, *47*, 973.

¹¹⁰ For a recent review, see: Aher, S. B.; Muskawar, P. N.; Thenmozhi, K.; Bhagat, P. R. *Eur. J. Med. Chem.* **2014**, *81*, 408.

¹¹¹ For a review, see: Bernardi, T.; Badel, S.; Mayer, P.; Groelly, J.; de Frémont, P.; Jacques, B.; Braunstein, P.; Teyssot, M.-L.; Gaulier, C.; Cisnetti, F.; Gautier, A.; Roland, S. *ChemMedChem* **2014**, *9*, 1140.

¹¹² Çetinkaya, B.; Özdemir, Y.; Binbaşıoğlu, B.; Durmaz, R.; Günel, S. *Arzneim.-Forsch.* **1996**, *46*, 821; Çetinkaya, B.; Özdemir, Y.; Binbaşıoğlu, B.; Durmaz, R.; Günel, S. *Arzneim.-Forsch.* **1999**, *49*, 538.

¹¹³ Özdemir, Y.; Denizci, A.; Öztürk, H. T.; Çetinkaya, B. *Appl. Organomet. Chem.* **2004**, *18*, 318; Ray, S.; Mohan, R.; Singh, J. K.; Samantaray, M. K.; Shaikh, M. M.; Panda, D.; Ghosh, P. *J. Am. Chem. Soc.* **2007**, *129*, 15042.

¹¹⁴ Panzner, M. J.; Hindi, K. M.; Wright, B. D.; Tayloer, J. B.; Han, D. S.; Youngs, W. J.; Cannon, C. L. *Dalton Trans.* **2009**, 7308; Patil, S.; Claffey, J.; Deally, A.; Hogan, M.; Gleeson, B.; Menendez, L. M.; Müller-Bunz, H.; Paradisi, F.; Tacke, M. *Eur. J. Inorg. Chem.* **2010**, 1020; Roland, S.; Jolival, C.; Cresteil, T.; Eloy, L.; Bouhours, P.; Hequet, A.; Mansuy, V.; Vanucci, C.; Paris, J.-M. *Chem. Eur. J.* **2010**, *17*, 1442; Akkoç, S.; Gök, Y.; Özdemir, I.; Günel, S. *J. Chin. Adv. Mat. Soc.* **2014**, DOI: 10.1080/22243682.2014.882795; Panzner, M. J.; Deeraksa, A.; Smith, A.; Wright, B. D.; Hindi, K. M.; Kascatan-Nebioglu, A.; Torres, A. G.; Judy, B. M.; Hovis, C. E.; Hilliard, J. K.; Mallett, R. J.; Cope, E.; Estes, D. M.; Cannon, C. L.; Leid, J. G.; Youngs, W. J. *Eur. J. Inorg. Chem.* **2009**, 2009, 1739.

¹¹⁵ Jellicoe, M. M.; Nichols, S. J.; Callus, B. A.; Baker, M. V.; Barnard, P. J.; Berners-Price, S. J.; Whelan, J.; Yeoh, G. C.; Filipovska, A. *Carcinogenesis* **2008**, *29*, 1124; Baker, M. V.; Barnard, P. J.; Berners-Price, S. J.; Brayshaw, S. K.; Hickey, J. L.; Skelton, B. W.; White, A. H. *Dalton Trans.* **2006**, 3708; Barnard, P. J.; Wedlock, L. E.; Baker, M. V.; Berners-Price, S. J.; Joyce, D. A.; Skelton, B. W.; Steer, J. H. *Angew. Chem., Int. Ed.* **2006**, *45*, 5966; Barnard, P. J.; Baker, M. V.; Berners-Price, S. J.; Day, D. A. *J. Inorg. Biochem.* **2004**, *98*, 1642.

¹¹⁶ Bertrand, B.; Stefan, L.; Pirrotta, M.; Monchaud, D.; Bodio, E.; Richard, P.; Le Gendre, P.; Warmerdam, E.; de Jager, M. H.; Groothuis, G. M. M.; Picquet, M.; Casini, A. *Inorg. Chem.* **2014**, *53*, 2296; Weaver, J.; Gaillard, S.; Yoye, C.; Macpherson, S.; Nolan, S. P.; Riches, A. *Chem. Eur. J.* **2011**, *17*, 6620.

antimitochondrial activities¹¹⁷ and copper complexes for DNA cleavage leading to cell cycle stop and finally apoptosis.¹¹⁸

Later studies of anticancer activity of NHC complexes of group 10 metals have been undertaken by Ghosh and co-workers in 2007.¹¹⁹ *Trans*-[(NHC)PdCl₂(L)] (L = Pyr or NHC) complexes prove to have high cytotoxic activity by arresting cell cycle at G₂ phase (**Figure 12**). Li and co-workers reported a moderately active heteroleptic (NHC)Pd(π -allyl) complex.¹²⁰ Haque *et al.* reported enhanced activity of *trans*-bis(NHC) palladium (II) complexes compared to their *cis* analogues.¹²¹ First proof of activity of platinum NHC derivatives has been reported by the group of Marinetti in 2010.¹²² These easy tuneable *trans*-[(NHC)Pt^{II}(amine)] complexes present higher cytotoxic activities compared to benchmark cisplatin. Preliminary mechanistic investigations indicate that these compounds form monoadducts on DNA inducing DNA fragmentation and apoptosis.¹²³ In contrast to cisplatin, NHC platinum complexes do not stop cell cycle and are caspase 3 and 7 independent, but seem to provoke cellular death by apoptosis-inducing factor (AIF) and caspase 12 translocation. This different biochemical mechanism is extremely important to circumvent cisplatin resistance. In addition, dimeric analogues show similar activity. In our group, we also developed [(NHC)PtI₂(L)] type complexes, with L = nitrogen base ligands (amines, amino acids) and post-functionalized them by ligand exchange and click chemistry.^{124,125,126,127,128} These compounds also present cytotoxicity activities superior to cisplatin. The group of Che extended the range of anticancer platinum NHC complexes to cationic [(C[^]N[^]N)Pt(NHC)] derivatives.¹²⁹ The potential of these compounds have been positively evaluated both *in vitro* and *in vivo* (nude mice). Preferential accumulation of the complexes in cytoplasm could be determined by luminescence due to (C[^]N[^]N) pattern. These compounds inhibit *survivin* protein, an apoptosis suppresser. The dissimilar mechanism may be attributed to their unique structure different to cisplatin or [(NHC)PtI₂(L)] complexes.

¹¹⁷ E.g. see: Barnard, P. J.; Baker, M. V.; Berners-Price, S. J.; Day, D. A. *J. Inorg. Biochem.* **2004**, 98, 1642.

¹¹⁸ Teyssot, M.-L.; Jarrousse, A.-S.; Chevy, A.; De Haze, A.; Beaudoin, C.; Manin, M.; Nolan, S. P.; Diez-Gonzales, S.; Morel, L.; Gautier, A. *Chem. Eur. J.* **2009**, 15, 314.

¹¹⁹ Ray, S.; Mohan, R.; Singh, J. K.; Samantaray, M. K.; Shaikh, M. M.; Panda, D.; Ghosh, P. *J. Am. Chem. Soc.* **2007**, 129, 15042.

¹²⁰ Wang, C.-H.; Shih, W.-C.; Chang, H. C.; Kuo, Y.-Y.; Hung, W.-C.; Ong, T.-G.; Li, W.-S. *J. Med. Chem.* **2011**, 54, 5245.

¹²¹ Haque, R.A.; Salman, A.W.; Budagumpi, S.; Abdullah, A. A. A.; Majid, A. M. S. A. *Metallomics*, **2013**, 5, 760.

¹²² Skander, M.; Retailleau, P.; Bourrie, B.; Schio, L.; Mailliet, P.; Marinetti, A. *J. Med. Chem.* **2010**, 53, 2146; Mailliet, P.; Marinetti, A.; Skander, M. *US Patent 8481522 B2* **2010** CNRS / Sanofi.

¹²³ Chtchigrovsky, M.; Eloy, L.; Jullien, H.; Saker, L.; Ségal-Bendirdjian, E.; Poupon, J.; Bombard, S.; Cresteil, T.; Retailleau, P.; Marinetti, A. *J. Med. Chem.* **2013**, 56, 2074.

¹²⁴ Chardon, E.; Dahm, G.; Guichard, G.; Bellemin-Lapponnaz, S. *Chem. Asian J.* **2013**, 8, 1232.

¹²⁵ Chardon, E.; Dahm, G.; Guichard, G.; Bellemin-Lapponnaz, S.; *Organometallics* **2012**, 31, 7618.

¹²⁶ Chardon, E.; Puleo, G. L.; Dahm, G.; Fournel, S.; Guichard, G.; Bellemin-Lapponnaz, S. *ChemPlusChem* **2012**, 77, 1028.

¹²⁷ Chardon, E.; Puleo, G. L.; Dahm, G.; Guichard, G.; Bellemin-Lapponnaz, S. *Chem. Commun.* **2011**, 47, 5864.

¹²⁸ Chardon, E. *PhD Thesis* **2011**, University of Strasbourg.

¹²⁹ Sun, R. W.-Y.; Chow, A. L.-F.; Li, X.-H.; Yan, J. J.; Chui, S. S.-Y.; Che, C.-M. *Chem. Sci.* **2011**, 2, 728.

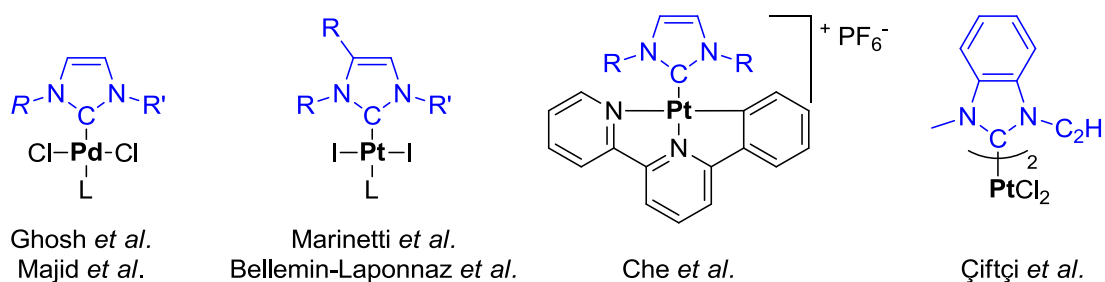


Figure 12: Group 10 metal NHC complexes studied for anticancer applications

Recent studies from Çiftçi and co-workers claim a higher cardio-¹³⁰ and male reproduction toxicity¹³¹ of NHC complexes compared to cisplatin.¹³² The reported values differ globally less than 10% making a general conclusion on toxicity of the bis-NHC Pt^{II} complex difficult. Especially as the authors limited their investigation on this special kind of bis-benzimidazolylidene complexes, extrapolation on other NHC platinum complexes is rendered difficult. Despite these negative side effects, tremendous possibilities of variation of carbene structures combined with other ligands on the metal centre let a wide-open non-explored field for research. Main challenge resides in rapid and easy access to libraries of complexes. Post-synthetic modification of simple preformed complexes, a strategy to access readily various transition metal complexes, will be discussed in next section.

1.3 Post-synthetic modification of transition metal complexes for molecular diversity

In synthetic chemistry, different strategies are possible to reach a target molecule.¹³³ Traditionally, chemists would prefer to use a convergent synthesis. Linear multi-step synthesis requires many steps resulting generally in poor overall yields. Thus, linear strategy is often avoided in total synthesis. As organometallic and coordination synthesis usually include sophisticated ligands, the classical strategy consists in introducing the metal at the last stage of the synthesis with the pre-functionalized ligand (**Figure 13, left**). Unfortunately, this approach presents several disadvantages and constraints such as:

- Generally low overall yield, especially for highly functionalized ligands
- Low modularity (each modification implies to redesign the whole synthesis)
- Incompatibility with large number of chemical functions (due notably to their coordinating ability or sometimes harsh complexation conditions)

¹³⁰ Çiftçi, O.; Özdemir, I.; Vardi, N.; Gurbuz, N. *Hum. Exp. Toxicol.* **2011**, 30, 1342.

¹³¹¹³¹ Çiftçi, O.; Beytur, A.; Cakir, O.; Gurbuz, N.; Vardi, N. *Basic Clin. Pharmacol. Toxicol.* **2011**, 109, 328.

¹³² The group also compared effects of Ru and Au NHC complexes on male reproductivity and their cardiotoxicity: Çiftçi, O.; Beytur, A.; Vardi, N.; Odemir, I. *Drug. Dev. Ind. Pharm.* **2012**, 38, 40; Çiftçi, O.; Özdemir, I.; Cakir, O.; Demir, S. *Toxicol. Ind. Health* **2011**, 27, 735.

¹³³ Corey, E. J. *Chem. Soc. Rev.* **1988**, 17, 111.

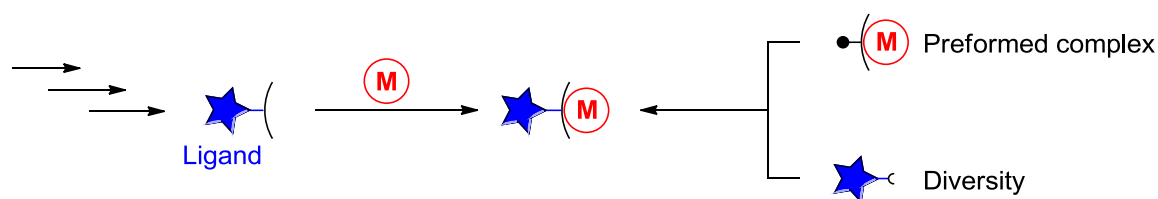


Figure 13: Classical linear strategy of organometallic synthesis (left), versus post-functionalization of a preformed metal complex (right)

Post-synthetic modification of readily synthesized metal complexes remains a strong and attractive challenge (**Figure 13, right**). Convergent strategy involving parallel synthesis can be applied, but only on non-reactive metal complexes that would allow several functionalization. One of the most suitable approaches is the concept of click chemistry^{134,135} to generate a large library of compounds. Two main scenarios can be envisaged using a convergent strategy, i) Post-functionalization of the ligand bound to the metal by reaction on its functional group; ii) Functionalization at the metal centre by adequate ligand substitution. In this chapter, we will present selected examples of post-complexation modifications of transition metal complexes to highlight the potential of this strategy. In a first part, we will discuss complexes controlled by external stimuli interesting e.g. in catalysis, for memory storage devices or cytotoxicity modulation. In a second part, we will present examples of diversity by derivatization of preformed complexes by different strategies: cycloaddition reactions, nucleophilic substitution reactions or ligand exchange.

1.3.1 Post-synthetic modification switches of metal complexes by external stimuli

Three main strategies are reported in the literature using the switch ability of the ligand bound to the metal centre: redox, chemo and photochromism activation (**Figure 14**).

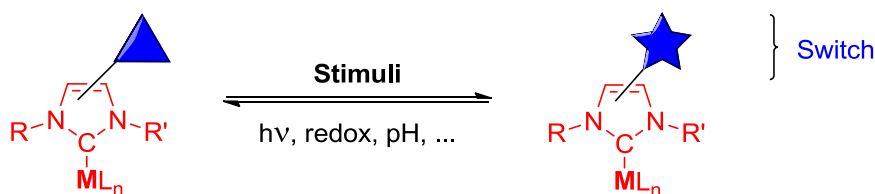


Figure 14: Post-complexation switches of metal complexes by external stimuli

¹³⁴ Selected reviews on click reactions, especially in context of biomolecules: Tiefenbrunn, T. K.; Dawson, P. E. *Biopolymers* **2010**, *94*, 95; Hackenberger, C. P. R.; Schwarzer, D. *Angew. Chem. Int. Ed.* **2008**, *47*, 10030.

¹³⁵ Kolb, H. C.; Finn, M. G.; Sharpless, K. B. *Angew. Chem. Int. Ed.* **2001**, *40*, 2004.

1.3.1.1 Redox-active complexes

Classical ligands can modulate the steric and geometric properties of transition metals. In contrast, redox active ligands¹³⁶ will allow an electrochemical control in several transformations. Consequently, a redox active group can control the electron richness/deficiency of a ligand through electrochemical oxidation or reduction processes. In this context, the ligand would control and modulate the electronic properties of the metal centre.

Most of the time, the redox groups involved in such control are metallocene moieties (ferrocene^{137,138} or cobaltocene¹³⁹). Several variations involving redox active ferrocene-based ligands and metal carbene (Ag, Hg, Pd or W) have been made.¹³⁷ More recently, Bielawski and co-workers reported combinations of redox-active ferrocene diaminocarbene (*FcDAC*) backbone to form several bimetallic complexes incorporating Mo, Rh, Ir, Pd and Ni (**Figure 15, a**).¹⁴⁰ As example, the Fe/Pd couple was found to be a good catalyst for the Mizoroki-Heck cross coupling reaction.

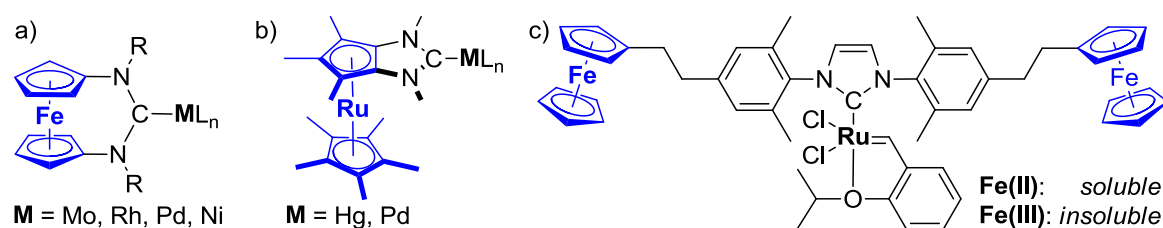


Figure 15: Redox-active a) ferrocene diaminocarbene, b) ruthenocene based complexes and c) Grubbs-Hoveyda catalyst

¹³⁶ For a review of redox active ligands and their complexes, see: Allgeier, A. M.; Mirkin, C. A. *Angew. Chem. Int. Ed.* **1998**, 37, 894; First example of oxidation reaction done directly on a NHC ligand was reported by Herrmann and co-workers.⁷⁶ Selected examples of redox active complexes include: Ringenberg, M. R.; Kokatam, S. L.; Heiden, Z. M.; Rauchfuss, T. B. *J. Am. Chem. Soc.* **2008**, 130, 788; González-Gallardo, S.; Kuzu, I.; Oña-Burgos, P.; Wolfer, T.; Wang, C.; Klinkhammer, K. W.; Kloppe, W.; Bräse, S.; Breher, F. *Organometallics* **2014**, 33, 941; Trapp, I.; González-Gallardo, S.; Hohnstein, S.; Garnier, D.; Oña-Burgos, P.; Breher, F. *Dalton Trans.* **2014**, 43, 4313.

¹³⁷ Bildstein, B.; Malaun, M.; Kopacka, H.; Ongania, K.-H.; Wurst, K. *J. Organomet. Chem.* **1998**, 552, 45; Bildstein, B.; Malaun, M.; Kopacka, H.; Ongania, K.-H.; Wurst, K. *J. Organomet. Chem.* **1999**, 572, 177; Bildstein, B.; Malaun, M.; Kopacka, H.; Wurst, K.; Mitterböck, M.; Ongania, K.-H.; Opromolla, G.; Zanello, P. *Organometallics* **1999**, 18, 4325; Siemeling, U.; Schrock, R. R.; Stammler, A.; Stammler, H.-G.; Kuhnert, O. *Z. Anorg. Allg. Chem.* **2001**, 627, 925; Gregson, C. K. A.; Gibson, V. C.; Long, N. L.; Marshall, E. L.; Oxford, P. J.; Coleman, K. S.; Turberville, S.; Pasco, S. I.; Green, M. L. *J. Organomet. Chem.* **2005**, 690, 653; White, A. J. P. *J. Am. Chem. Soc.* **2006**, 128, 7410; Dallas, A.; Kuhtz, H.; Farrell, A.; Quilty, B.; Nolan, K. *Tetrahedron Lett.* **2007**, 48, 1017; Atkinson, R. C. J.; Long, N. J. *Monodentate Ferrocene Donor Ligands, in Ferrocenes: Ligands, Materials and Biomolecules* (ed P. Štěpnička) **2008**, John Wiley & Sons, Ltd, Chichester, UK; Nyamori, V. O.; Onyancha, D.; McClelland, C. W.; Imrie, C.; Gerber, T. I. A. *J. Organomet. Chem.* **2009**, 694, 1407; Siemeling, U.; Färber, C.; Bruhn, C. *Chem. Commun.* **2009**, 98; Siemeling, U.; Färber, C.; Leibold, M.; Bruhn, C.; Mücke, P.; Winter, R. F.; Sarkar, B.; von Hopffgarten, M.; Frenking, G. *Eur. J. Inorg. Chem.* **2009**, 4607; Siemeling, U.; Färber, C.; Bruhn, C.; Fürmeier, S.; Schulz, T.; Kurlemann, M.; Tripp, S. *Eur. J. Inorg. Chem.* **2012**, 2012, 1413; Rittinghaus, S.; Färber, C.; Bruhn, C.; Siemeling, U. *Dalton Trans.* **2014**, 43, 3508.

¹³⁸ For an early review of carbenes with ferrocenyl substituents, see: Bildstein, B. *J. Organomet. Chem.* **2001**, 617, 28.

¹³⁹ Lorkovic, I. M.; Duff, R. R., Jr.; Wrigton, M. S. *J. Am. Chem. Soc.* **1995**, 117, 3617.

¹⁴⁰ Varnado, C. D., Jr.; Lynch, V. M.; Bielawski, C. W. *Dalton Trans.* **2009**, 7253; Khranov, D. M.; Rosen, E. L.; Lynch, V. M.; Bielawski, C. W. *Angew. Chem., Int. Ed.* **2008**, 47, 2267.

It is noteworthy that other metallocene such as ruthenocene can be used as redox-active ligand as nicely shown by Arduengo in 2005 (b).¹⁴¹ Süßner and Plenio reported a combination of Ferrocene/Grubbs-Hoveyda type complex, applied to redox switchable catalysis¹⁴² (solubility control by redox potential) (c).¹⁴³ Other systems using a combination of quinone moiety (as redox active ligand) and NHC transition metal complex¹⁴⁴ were found promising¹⁴⁵ in Kumada cross-coupling catalysis (**Figure 16**).

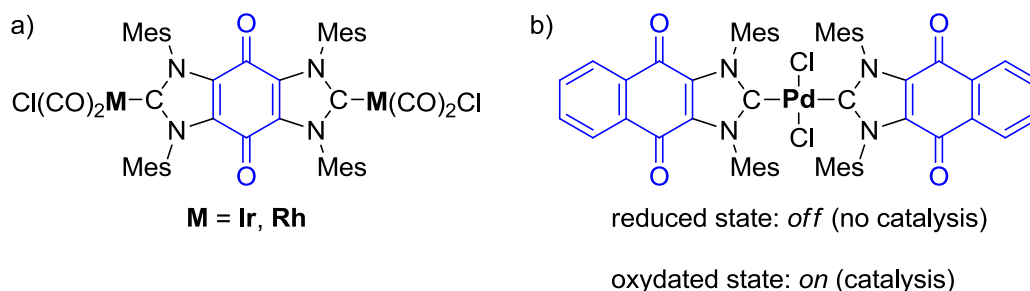


Figure 16: Examples of redox-active quinone-annulated a) Janus-type NHC and b) bis-NHC complexes

1.3.1.2 Photo-active ligands: photochromism

The most explored ligand modification by external stimuli is represented by complexes bearing photochromic ligands.^{146,147} Photochromic molecules changes reversibly under electromagnetic irradiation (generally in UV-visible area) between two chemical forms having different absorption spectra and different chemico-physico properties. These molecular photo-switches are of interest as either memory storage devices or switchable catalysts. Pt complexes with photochromic 1,2-diarylethene featured ligands have been described by the groups of Ko¹⁴⁸ and Yam¹⁴⁹. Ko, Zhu and co-

¹⁴¹ Arduengo, A. J., III; Tapu, D.; Marshall, W. J. *J. Am. Chem. Soc.* **2005**, *127*, 16400; Arduengo, A. J., III; Tapu, D.; Marshall, W. J. *Angew. Chem. Int. Ed.* **2005**, *44*, 7240.

¹⁴² For non-NHC redox-switchable “on/off” catalysts, see e.g.: Lorkovic, I. M.; Wrighton, M. S.; Davis, W. M. *J. Am. Chem. Soc.* **1994**, *116*, 6220.

¹⁴³ Süßner, M.; Plenio, H. *Angew. Chem., Int. Ed.* **2005**, *44*, 6885.

¹⁴⁴ Sanderson, M.; Kamplain, J. W.; Bielawski, C. W. *J. Am. Chem. Soc.* **2006**, *128*, 16514; Rosen, E. L.; Varnado, C. D., Jr.; Tennyson, A. G.; Khramov, D. M.; Kamplain, J. W.; Sung, D. H.; Cresswell, P. T.; Lynch, V. M.; Bielawski, C. W. *Organometallics* **2009**, *28*, 6695; Tennyson, A. G.; Ono, R. J.; Hudnall, T. W.; Khramov, D. M.; Er, J. A. V.; Kamplain, J. W.; Lynch, V. M.; Sessler, J. L.; Bielawski, C. W. *Chem.-Eur. J.* **2010**, *16*, 304.

¹⁴⁵ Tennyson, A. G.; Lynch, V. M.; Bielawski, C. W. *J. Am. Chem. Soc.* **2010**, *132*, 9420.

¹⁴⁶ For an overview about organometallic photochromic complexes, see: Guerchais, V.; Le Bozec, H. *Top. Organomet. Chem.* **2010**, *28*, 171; Ko, C.-C.; Yam, V. W.-W. *J. Mater. Chem.* **2010**, *20*, 2063.

¹⁴⁷ Classical examples are Ru and Os DMSO complexes entering an excited state after irradiation with a S→O isomerization of the DMSO: Rack, J. J. *Coord. Chem. Rev.* **2009**, *258*, 78; McClure, B. A.; Rack, J. J. *Eur. J. Inorg. Chem.* **2010**, *2010*, 3895.

¹⁴⁸ Jung, I.; Choi, H.; Kim, E.; Lee, C.-H.; Kang, S. O.; Ko, J. *Tetrahedron* **2005**, *61*, 12256.

¹⁴⁹ Lee, J. K.-W.; Ko, C.-C.; Wong, K. M.-C.; Zhu, N.; Yam, V. W.-W. *Organometallics* **2007**, *26*, 12.

workers synthesized diarylethene featured NHC silver, gold (I), and palladium complexes (**Figure 17**).¹⁵⁰ The same ligand coordinated to iridium (I) di-carbonyl undergoes same photochemical processes and a decrease of donor strength from *open* to the *closed* form was noticed.¹⁵¹

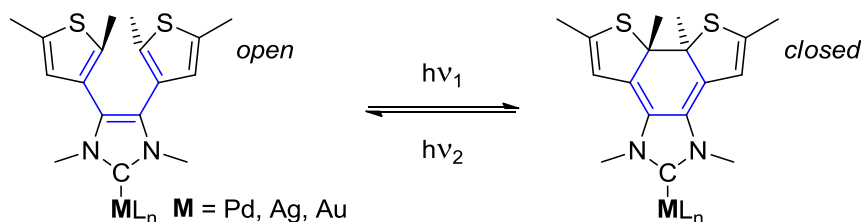


Figure 17: Photochromic change of NHC complexes¹⁵¹

1.3.1.3 Chemo active ligands

Classically, electronic and steric modulation of NHC ligands is achieved by modifying the nitrogen substituents or the backbone of the NHC. These architectural changes are generally introduced during ligand synthesis and therefore cannot be varied after complexation. In the last five years, NHCs bearing a reactive backbone have been designed. In contrast to photochromism strategy (only two possible states), chemical post-synthetic modification allows introduction of various functionalities. The group of Glorius first developed NHC ligands with a pH sensible¹⁵² keto/enol backbone coordinated to iridium (II) dicarbonyl.¹⁵³ CO stretching frequencies in IR confirmed the electron enrichment of the anionic complex (**Figure 18, a**). César and Lavigne probed post-functionalized of rhodium complexes bearing similar ligands by substitution reactions with various electrophiles (*O*-functionalization with oxophile TBDMS-Cl; *C*-functionalization by formaldehyde) (**Figure 18, b**).¹⁵⁴ 4-electron oxidation of the enamine-backbone of an Rh (I) complex is also reported by this group.¹⁵⁵

¹⁵⁰ Yam, V. W.-W.; Lee, J. K.-W.; Ko, C.-C.; Zhu, N. *J. Am. Chem. Soc.* **2009**, *131*, 912.

¹⁵¹ Neilson, B. M.; Lynch, V. M.; Bielawski, C. W. *Angew. Chem. Int. Ed.* **2011**, *50*, 10322.

¹⁵² Non-NHC example of a pH sensible metal catalyst: Zhong, S.; Fu, Z.; Tan, Y.; Xie, Q.; Xie, F.; Zhou, X.; Ye, Z.; Peng, G.; Yin, D. *Adv. Synth. Catal.* **2008**, *350*, 802.

¹⁵³ Biju, A. T.; Hirano, K.; Fröhlich, R.; Glorius, F. *Chem. Asian J.* **2009**, *4*, 1786.

¹⁵⁴ Benhamou, L.; César, V.; Gornitzka, H.; Lugan, N.; Lavigne, G. *Chem. Commun.* **2009**, 4720; Benhamou, L.; Vujkovic, N.; César, V.; Gornitzka, H.; Lugan, N.; Lavigne, G. *Organometallics* **2010**, *29*, 2616.

¹⁵⁵ César, V.; Tourneux, J.-C.; Vujkovic, N.; Brousses, R.; Lugan, N.; Lavigne, G. *Chem. Commun.* **2012**, *48*, 2349.

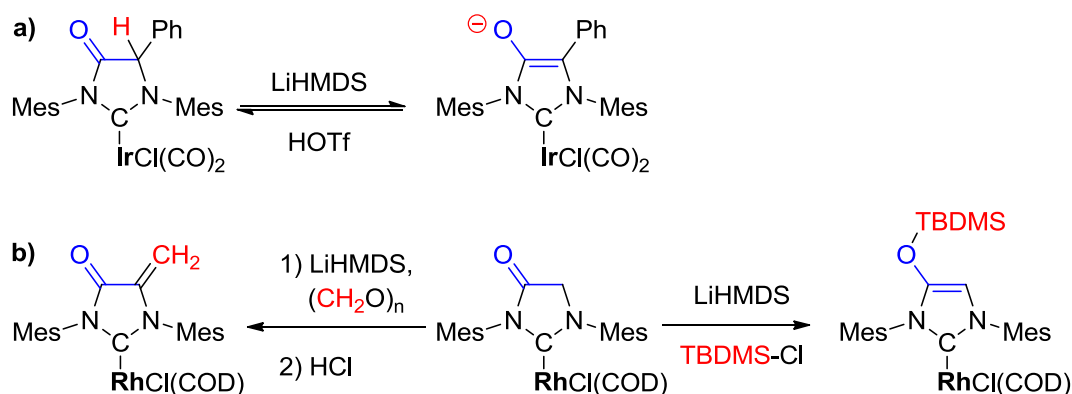


Figure 18: (a) pH sensitive NHC Ir complex, (b) O- and C-functionalization of an Rh complex

In contrast to previous reported multi-step synthesis, Hashmi *et al.* developed a modular and one-pot synthesis of Au, Pd and Pt complexes from a simple metal precursor. In a second step, functionalization with a large variety of electrophiles was achieved (**Figure 19**).¹⁵⁶ The electrophilic substitution methodology is also applicable to six-membered carbenes with a malonate backbone.¹⁵⁷ Modulation with various electrophiles allows easy catalyst optimization for different reactions (phenylacetylene polymerization and styrene hydroboration). Rh, Ag, Au or Fe complexes with comparable imidato backbone ligand were also synthesized. These compounds were subjected to either reversible protonation/deprotonation or coordination on transition metals resulting in polymetallic compounds.¹⁵⁸

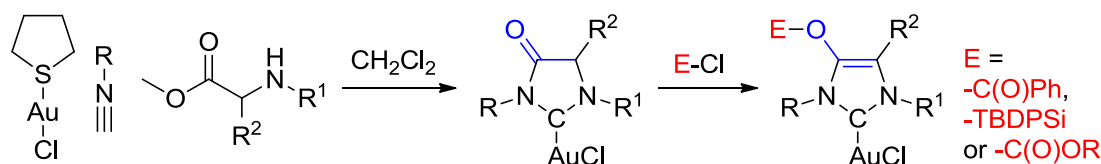


Figure 19: Modular one-step synthesis of gold carbenes followed by subsequent post-functionalization¹⁵⁸

As a conclusion, chemo-active NHC ligands can switch between two distinguish forms as a function of pH. Furthermore, these ligands undergo derivatization with several simple electrophiles changing drastically the donor strength of the concerned carbene. Unfortunately, no introduction of challenging biological moiety by this strategy has been reported yet.

¹⁵⁶ Hashmi, A. S. K.; Lothschütz, C.; Graf, K.; Häffner, T.; Schuster, A.; Rominger, F. *Adv. Synth. Catal.* **2011**, 353, 1407.

¹⁵⁷ César, V.; Lugan, N.; Lavigne, G. *Chem. Eur. J.* **2010**, 16, 11432.

¹⁵⁸ Vujkovic, N.; César, V.; Lugan, N.; Lavigne, G. *Chem. Eur. J.* **2011**, 17, 13151; César, V.; Misal Castro, L. C.; Dombray, T.; Sortais, J.-B.; Darcel, C.; Labat, S.; Miqueu, K.; Sotiropoulos, J.-M.; Brousses, R.; Lugan, N.; Lavigne, G. *Organometallics* **2013**, 32, 4643.

1.3.2 Post-complexation modifications of cyclometalated NHC complexes by insertion reaction

Cyclometalated mono-NHC complexes present enhanced stability and interesting possibilities for steric and electronic tuning. The CH_2 -metal bond is a possible target for insertion reactions enabling introduction of different donor groups (BH_3 , PhCCH , X_2 , RCHN_2 , CO) to the metal. The scope of this post-complexation modification of cyclometalated mono-NHC iridium, platinum or cobalt complexes and their catalytic activities has recently been reviewed by Mo and Deng.¹⁵⁹ To illustrate the concept, the reaction on cyclometalated platinum (II) complex with Br_2 is represented in **Figure 20**.¹⁶⁰ Conejero and co-workers revealed the formation of rare platinum (III) complex by addition of one Br to the metal, followed by a second addition of Br to the metal centre to form platinum (IV) complex. In the last step, reductive insertion of one bromine atoms led to the desired modified complex.

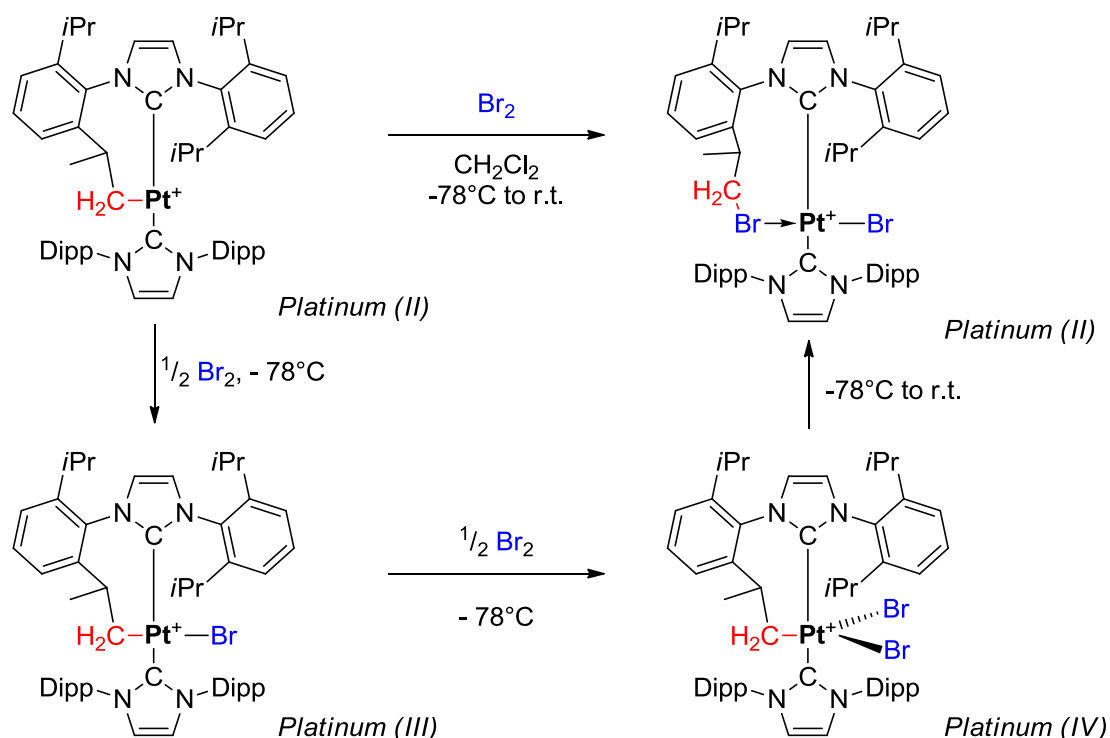


Figure 20: Post-synthetic modification by bromine insertion into a cyclometalated platinum complex, passing by isolated Pt (III) and Pt (IV) intermediates¹⁶⁰

¹⁵⁹ Mo, Z.; Deng, L. *Synlett* **2014**, 25, 1045.

¹⁶⁰ Rivada-Wheelaghan, O.; Ortunño, M. A.; Díez, J.; García-Garrido, S. E.; Maya, C.; Lledós, A.; Conejero, S. *J. Am. Chem. Soc.* **2012**; 134, 15261.

1.3.3 Nucleophilic substitution and cross-coupling reactions

Bimolecular nucleophilic substitutions (S_N2) are one of the basic reactions in organic chemistry allowing substitution of a leaving group by various nucleophiles.¹⁶¹ Huynh, Teng and co-workers derived a bromoalkyl NHC palladium (II) complex by substitution of the bromine with different nucleophiles (**Figure 21**).¹⁶² First-generation tertiary amines were further derivatized to second generation of quarterly amines. The introduced iodine itself was replaced by further nucleophiles to other second-generation products. The authors also reported successful exchange of the bromide ligands by various nucleophiles. Depending of the nucleophiles, the bromide ligands also were exchanged. Third generation complex was finally obtained by reduction of palladium (II) complexes to the corresponding palladium (0) derivative.

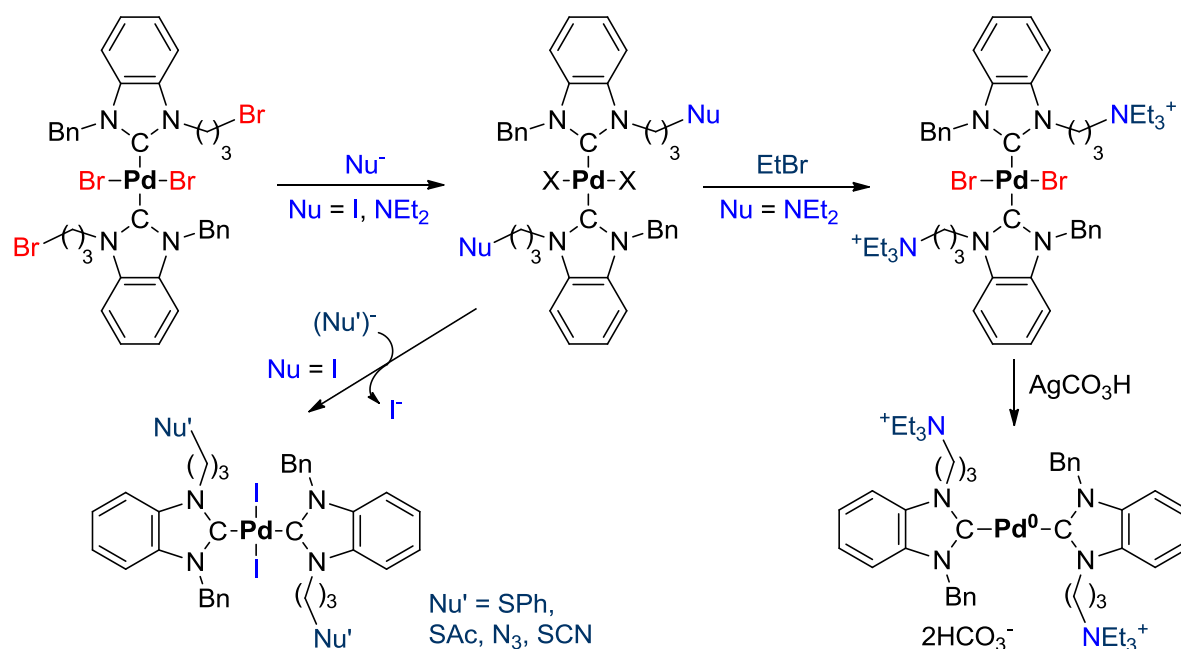


Figure 21: Post-synthetic modification of a palladium NHC complex by nucleophile substitution reaction¹⁶²

This elegant strategy resulted in a large variety of compounds, which are usually not accessible by classical linear complex synthesis. In continuation, this strategy allowed double introduction of amines to bromo-alkane substituted abnormal NHC palladium acetonitrile complex by combined nucleophilic substitution and ligand displacement (**Figure 22**).¹⁶³

¹⁶¹ Clayden, J.; Greeves, N.; Warren, S.; Wothers, P. *Organic Chemistry* **2012**, Oxford University Press.

¹⁶² Huynh, H. V.; Teng, Q. *Chem. Commun.* **2013**, 49, 4244; Teng, Q.; Upmann, D.; Wijaya, S. A. Z. N; Huynh, H. V. *Organometallics* **2014**, 33, 3373.

¹⁶³ Bernhammer, J. C.; Singh, H.; Huynh, H. V. *Organometallics* **2014**, 33, 4295.

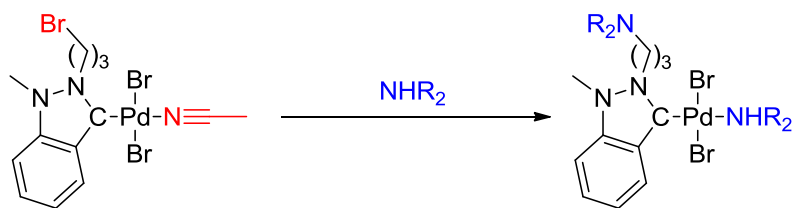


Figure 22: Post-coordinative modification of a bromoalkyl Pd complex with different amines¹⁶³

Suzuki-Miyaura Palladium catalysed cross-coupling reactions¹⁶⁴ are suitable for post-synthetic modification of stable complexes. One example is reported by Williams and co-workers.¹⁶⁵ Sequential cross-coupling-bromination allowed functionalization of an iridium complex along its principal axis and modulate luminescence properties

1.3.4 Functionalization by cycloaddition reactions

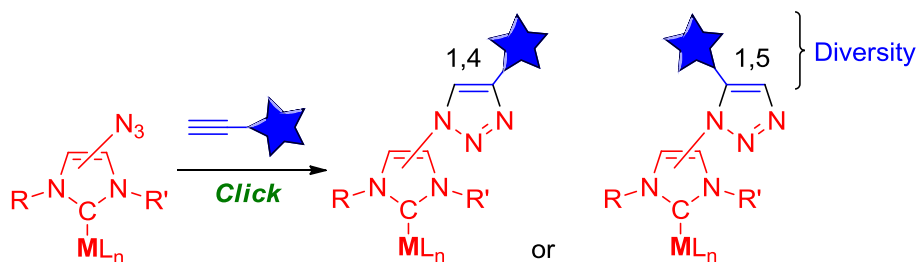


Figure 23: Functionalization of transition metal complexes by cycloaddition reactions

Azide-Alkyne Huisgen Cycloaddition,¹⁶⁶ a 1,3-dipolar cycloaddition between an alkyne and an azide to form a stable 1,2,3-triazole is nowadays the “cream of the crop”¹³⁵ of click reactions.¹⁶⁷ While thermal Huisgen cycloaddition is resulting in a mixture of the two isomers, copper (I) catalysed cycloaddition (Copper (I)-catalysed Azide-Alkyne Cycloaddition or CuAAC)¹⁶⁸ provides selectively 1,4-regioisomer and ruthenium catalysed cycloaddition (Ruthenium-catalysed 1,3-dipolar azide-alkyne cycloaddition or RuAAC)¹⁶⁹ the 1,5-regioisomer. Strain-Promoted 1,3-Dipolar Azide-Alkyne

¹⁶⁴ Miyaura, N.; Suzuki, A. *Chem. Rev.* **1995**, 95, 2457.

¹⁶⁵ Whittle, V. L.; Williams, J. A. G. *Inorg. Chem.* **2008**, 47, 6596.

¹⁶⁶ This reaction was first widely explored by Rolf Huisgen: Huisgen, R. *Proc. Chem. Soc.* **1961**, 357. For mechanistic considerations, see: Huisgen, R. *Angew. Chem. Int. Ed. Engl.* **1963**, 2, 633; Huisgen, R.; Szeimies, G.; Möbius, L. *Chem. Ber.* **1967**, 100, 2494.

¹⁶⁷ Moses, J. E.; Moorhouse, A. D. *Chem. Soc. Rev.* **2007**, 36, 1249.

¹⁶⁸ CuAAC was independently discovered by Meldal and Sharpless: Tornøe, C. W.; Christensen, C.; Meldal, M. *J. Org. Chem.* **2002**, 67, 3057; Rostovtsev, V. V.; Green, L. G.; Fokin, V. V.; Sharpless, K. B. *Angew. Chem. Int. Ed.* **2002**, 41, 2596

¹⁶⁹ Zhang, L.; Chen, X.; Xue, P.; Sun, H. H. Y.; Williams, I. D.; Sharpless, K. B.; Fokin, V. V.; Jia, G. *J. Am. Chem. Soc.* **2005**, 127, 15998; Boren, B. C.; Narayan, S.; Rasmussen, L. K.; Zhang, L.; Zhao, H.; Lin, Z.; Jia, G.; Fokin, V. V. *J. Am. Chem. Soc.* **2008**, 130, 8923.

Cycloadditions (SPAAC) allows catalyst-free coupling under mild conditions between an azide (or tetrazine) and BCN (bicycle[6.1.0]nonyne).¹⁷⁰ This versatile two-moieties coupling strategy (**Figure 23**) is not limited by the nature of neither the ligand nor the metal. It needs only the presence of an azide or an alkyne on the complex. We describe the methodology using examples of highly stable ferrocenes and various transition metal complexes. After one, the most pertinent examples of postmodification of divers platinum complexes and NHC complexes are summarized. We complete this overlook by mentioning derivatization of M-N₃ and M-alkyne derivatives.

1.3.4.1 Post-functionalization of different transition metal complexes by cycloaddition reactions

Ferrocene, whose high stability allows easy further derivatization, is the first complex that has been functionalized by reaction with various electrophiles or by lithiation.¹⁷¹ The first examples of cycloaddition functionalization of self-assembled monolayers (SAMs) with ferrocenes go back to 2004.¹⁷² The scope of cycloaddition reactions with ferrocenes is extremely large. So, Santoyo-González and his collaborators reported CuAAC conjugation of mono and di-azide or alkyne featured ferrocene with mono- and disaccharides alkynes and azides respectively (**Figure 24**).¹⁷³ Ferrocenes were introduced onto dendrimers,¹⁷⁴ boron-doped diamond surfaces¹⁷⁵, SnO₂ nanoparticles¹⁷⁶ and self-assembled monolayers.¹⁷⁷ CuAAC facilitates the obtaining of chiral ferrocenyl phosphine ligands (*ClickFerrophos*) (**Figure 24**).¹⁷⁸

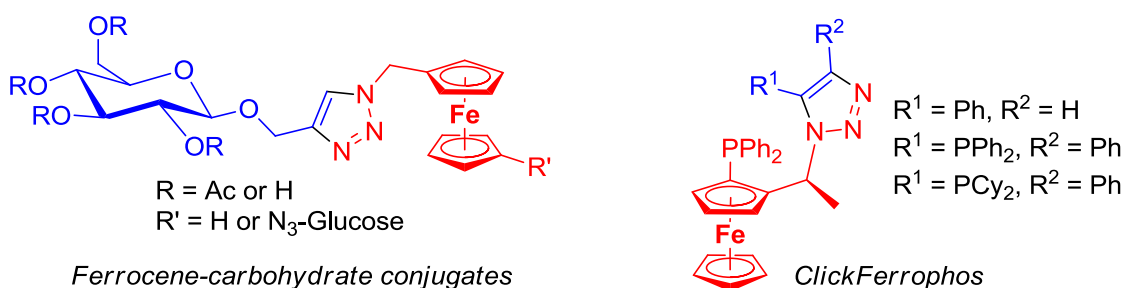


Figure 24: Examples of ferrocenes functionalized by cycloaddition reaction^{173,178}

¹⁷⁰ Sletten, E. M.; Bertozzi, C. R. *Acc. Chem. Res.* **2011**, 44, 666.

¹⁷¹ Togni, A.; Hayashi, T. *Ferrocenes: Homogeneous Catalysis, Organic Synthesis, Materials Science* **2007**, Wiley-VCH Verlag GmbH, Weinheim, Germany.

¹⁷² Collman, J. P.; Devaraj, N. K.; Chidsey, C. E. D. *Langmuir* **2004**, 20, 1051.

¹⁷³ Casas-Solvas, J. M.; Vargas-Berenguel, A.; Capitán-Vallvey, L. F.; Santoyo-González, F. *Org. Lett.* **2004**, 6, 3687.

¹⁷⁴ Ornelas, C.; Ruiz Aranzaes, J.; Cloutet, E.; Alves, S.; Astruc, D. *Angew. Chem. Int. Ed.* **2007**, 46, 872.

¹⁷⁵ Das, M. R.; Wang, M.; Szunerits, S.; Gengembre, L.; Boukherroub, R. *Chem. Commun.* **2009**, 2753.

¹⁷⁶ Benson, M. C.; Ruther, R. E.; Gerken, J. B.; Rigsby, M. L.; Bishop, L. M.; Tan, Y.; Stahl, S. S.; Hamers, R. J. *ACS Appl. Mater. Interfaces* **2011**, 3, 3110.

¹⁷⁷ Siemeling, U.; Rother, D. *J. Organomet. Chem.* **2009**, 694, 1055.

¹⁷⁸ Fukuzawa, S.; Oki, H.; Hosaka, M.; Sugasawa, J.; Kikuchi, S. *Org. Lett.* **2007**, 9, 5557.

The potential of CuAAC to conjugate ferrocene with complex biological interesting moieties has been demonstrated by successful introduction of peptide nucleic acids (PNA)¹⁷⁹ or peptides.¹⁸⁰ Click reaction allows labelling of ruthenocene with biomolecules.¹⁸¹ Beside ferrocenes, porphyrin transition metal complexes are known for both their stability and versatility. The ease of manipulation allows the post-functionalization of preformed complexes of Mn,¹⁸² Ni¹⁸³ or Zn.¹⁸⁴ CuAAC is especially interesting for biological conjugates. In this context, introduction of neuropeptide *enkephaline* (penty-ENK-OH)¹⁸⁵ or PEG-N₃ groups¹⁸⁶ is reported. Coupling of an alkynyl europium (III) chelate with dansyl azide catalysed by copper glutathione in biological media afforded a complex presenting FRET (Förster Resonance Energy Transfer) property. This system could be employed as a sensor for micromolar concentration of copper glutathione.¹⁸⁷ Several groups studied Mn complexes functionalized by a post-formation strategy as CO releasing molecules (CORMs).¹⁸⁸ Gautier applied SPAAC reaction¹⁸⁹ for modulation of luminescence of lanthanide (III) (Eu, Tb, Y) complexes for protein labelling.¹⁹⁰ Graham, Gasser and co-workers attached a [Re(CO)₃(bipy)(py-alkyne)](BF₄) complex to the myristoylated HIV-1 Tat peptide to increase cell permeability.¹⁹¹ By SPAAC reaction, Dyson and co-workers coupled two non-toxic RAPTA-type Ru (II) complexes featured with pending BCN (bicycle[6.1.0]nonyne) group to one binuclear but toxic species using a bis-tetrazine linker.¹⁹² In addition to biological applications, the click methodology is employed to develop new materials with electrochemical and magnetic,¹⁹³ luminescent¹⁹⁴ and catalytic properties.¹⁹⁵

¹⁷⁹ Gasser, G.; Hüskén, N.; Köster, S. D.; Metzler-Nolte, N. *Chem. Commun.* **2008**, 3675; Hüskén, N.; Gasser, G.; Köster, S. D.; Metzler-Nolte, N. *Bioconjugate Chem.* **2009**, *20*, 1578.

¹⁸⁰ Köster, S.D.; Dittrich, J.; Gasser, G.; Hüskén, N.; Henao Castaneda, I.C.; Jios, J.L.; Della Vedova, C.O.; Metzler-Nolte, N. *Organometallics* **2008**, *27*, 6326.

¹⁸¹ Patra, M.; Metzler-Nolte, N. *Chem. Commun.* **2011**, *47*, 11444.

¹⁸² Collman, J. P.; Zeng, L.; Wang, H. J. H.; Lei, A.; Brauman, J. I. *Eur. J. Org. Chem.* **2006**, *2006*, 2707.

¹⁸³ Shen, D.-M.; Liu, C.; Chen, Q.-Y. *Eur. J. Org. Chem.* **2007**, 1419.

¹⁸⁴ Campidelli, S.; Ballesteros, B.; Filoramo, A.; Díaz D. D.; de la Torre, G.; Torres, T.; Rahman, G. M. A.; Ehli, C.; Kiessling, D.; Werner, F.; Sgobba, V.; Guldi, D. M.; Cioffi, C.; Prato, M. Bourgoïn, J.-P. *J. Am. Chem. Soc.* **2008**, *130*, 11503; Palacin, T.; Khanh, H. L.; Jousselmé, B.; Jegou, P.; Filoramo, A.; Ehli, C.; Guldi, D. M.; Campidelli, S. *J. Am. Chem. Soc.* **2009**, *131*, 15394.

¹⁸⁵ Zagermann, J.; Klein, K.; Merz, K.; Molon, M.; Metzler-Nolte, N. *Eur. J. Inorg. Chem.* **2011**, *2011*, 4212.

¹⁸⁶ Yang, H.; Li, L.; Wan, L.; Zhou, Z.; Yang, S. *Inorg. Chem. Commun.* **2010**, *13*, 1387.

¹⁸⁷ Viguer, R. F. H.; Hulme, A. N. *J. Am. Chem. Soc.* **2006**, *128*, 11370.

¹⁸⁸ Pfeiffer, H.; Rojas, A.; Niesel, J.; Schatzschneider, U. *Dalton Trans.* **2009**, 4292.

¹⁸⁹ Other example of SPAAC has been reported by Prokop *et al.*: Gansäuer, A.; Okkel, A.; Schwach, L.; Wagner, L.; Selig, A.; Prokop, A. *Beilstein J. Org. Chem.* **2014**, *10*, 1630.

¹⁹⁰ Candelon, N.; Hädäde, N. D.; Matache, M.; Canet, J.-L.; Cisnetti, F.; Funeriu, D. P.; Nauton, L.; Gautier, A. *Chem. Commun.* **2013**, *49*, 9206.

¹⁹¹ Leonidova, A.; Pierroz, V.; Adams, L. A.; Barlow, N.; Ferrari, S.; Graham, B. Gasser, G. *ACS Med. Chem. Lett.* **2014**, *5*, 809.

¹⁹² Murray, B. S.; Crot, S.; Siankevich, S.; Dyson, P. J. *Inorg. Chem.* **2014**, *53*, 9315.

¹⁹³ Chen, W.-Z.; Fanwick, P. E.; Ren, T. *Inorg. Chem.* **2007**, *46*, 3429; Xu, G.-L.; Ren, T. *Organometallics* **2005**, *24*, 2564.

¹⁹⁴ Sun, Y.; Chen, Z.; Puodziukynaite, E.; Jenkins, D. M.; Reynolds, J. R.; Schanze, K. S. *Macromolecules* **2012**, *45*, 2632; Wang, X.-Y.; Kimyonok, A.; Weck, M. *Chem. Commun.* **2006**, 3933.

¹⁹⁵ Baeza, B.; Casarrubios, L.; Ramírez-López, P.; Gómez-Gallego, M.; Sierra, M. A. *Organometallics* **2009**, *28*, 956; Sawoo, S.; Dutta, P.; Chakraborty, A.; Mukhopadhyay, R.; Bouloussa, O.; Sarkar, A. *Chem. Commun.* **2008**, 5957; Cabrera, D. G.; Koivisto, B. D.; Leigh, D. A. *Chem. Commun.* **2007**, 4218.

The massive clinical success of cisplatin and its derivatives resulted in an increased interest for Pt complexes in the last decades. In addition, their luminescent properties are of interest. First example of post-synthetic modification of a Pt complex was reported by Gladysz.¹⁹⁶ The group took profit of CuAAC to trap labile Pt-poly-ynes with BnN_3 giving stable triazole derivatives (**Figure 25, a**).¹⁹⁷

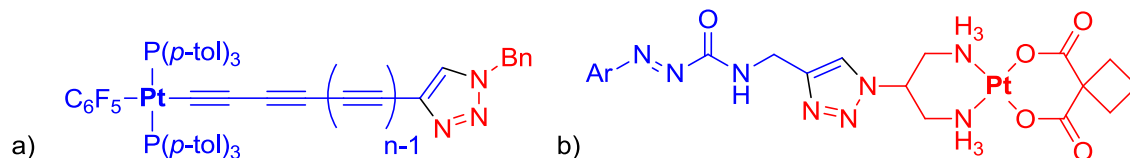


Figure 25: Examples of post-synthetic modification of Pt complexes by CuAAC^{196,198}

In 2010, Urankar and Košmrlj combined platinum (II) complexes with diazenecarboxamide, a modulator of intracellular glutathione (**Figure 25, b**).¹⁹⁸ Attempts to afford these products by classical linear synthesis failed, highlighting the superiority of the post-functionalization pathway. De Cola and Bäuerle reported maintain of bright luminescence of 2,2'-bipyridine Pt^{II} bisacetylide complexes after azide conjugation by [3+2] cycloaddition.¹⁹⁹ Steric and solubility parameters may be tuned by introduction of azides in order to develop best candidates for OLED's materials. This group also studied binuclear Pt^{II} complexes obtained by click reaction between two 2,2'-bipyridine Pt^{II} bisacetylides and different di-azide linkers.²⁰⁰ The group of DeRose develop Picazoplatin, an azide derivative of picoplatin.²⁰¹ Binding of this platinum complex to DNA and RNA oligonucleotides was proved by CuAAC mediated post-labelling reaction to fluorescent dansyl alkyne (**Figure 26**).

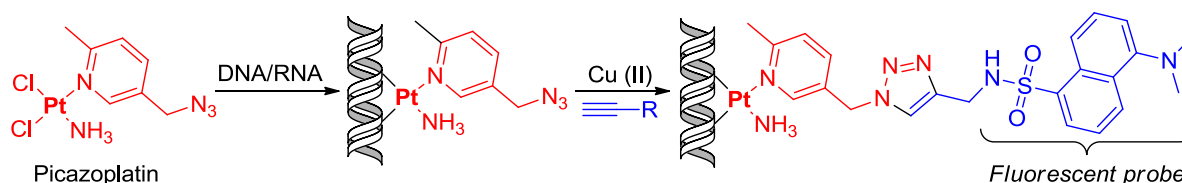


Figure 26: Application of CuAAC for platinum drug target analysis²⁰¹

¹⁹⁶ Mohr, W.; Stahl, J.; Hampel, F.; Gladysz, J. A. *Chem.-Eur. J.* **2003**, 9, 3324; Zheng, Q.; Bohling, J. C.; Peters, T. B.; Frisch, A. C.; Hampel, F.; Gladysz, J. A. *Chem.-Eur. J.* **2006**, 12, 6486.

¹⁹⁷ Gauthier, S.; Weisbach, N.; Bhuvanesh, N.; Gladysz, J. A. *Organometallics* **2009**, 28, 5597.

¹⁹⁸ Urankar, D.; Košmrlj, J. *Inorg. Chim. Acta.* **2010**, 363, 3817.

¹⁹⁹ Stengel, I.; Strassert, C. A.; Plummer, E. A.; Chien, C.-H.; De Cola, L.; Bäuerle, P. *Eur. J. Inorg. Chem.* **2012**, 2012, 1795; Stengel, I.; Pootrakulchote, N.; Dykeman, R. R.; Mishra, A.; Zakeeruddin, S. M.; Dyson, P. J.; Grätzel, M.; Bäuerle, P. *Adv. Energy Mater.* **2012**, 2, 1004.

²⁰⁰ Stengel, I.; Strassert, C. A.; De Cola, L.; Bäuerle, P. *Organometallics* **2014**, 33, 1345; For an whole overview of this chemistry, see: Stengel, I. *PhD Thesis* **2011**, University of Ulm.

²⁰¹ White, J. D.; Osborn, M. F.; Moghaddam, A. D.; Guzman, L. E.; Haley, M. M.; DeRose, V. J. *J. Am. Chem. Soc.* **2013**, 135, 11680.

1.3.4.2 Post-functionalization of NHC complexes by click chemistry

First example of NHC complex derivatization by cycloaddition reaction was reported by Elsevier.²⁰² A bidentate triazolyl-NHC palladium complex was obtained a) from the corresponding pre-functionalized imidazolium salt, b) from an alkyne bearing palladium complex post-modified with adamantyl-azide (**Figure 27**). The nitrogen of triazole group chelates the cationic Pd (II) complex.

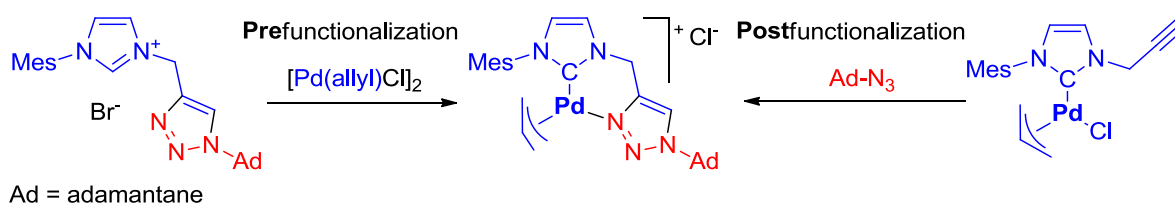


Figure 27: Synthesis of a bidentate triazolyl-NHC Pd complex by pre- and post-functionalization²⁰²

Gautier and co-workers studied pre- and post-functionalization of gold complexes.²⁰³ NHC precursors with azide groups, which in contrast to alkynes do not need protection during complexation, were chosen. Pre-functionalization of these ligands followed by transmetalation reaction from silver NHC precursor gave the functionalized gold complexes. Its post-functionalization by thermal Huisgen reaction with non-activated diphenylacetylene showed no reaction, whereas activated dimethyl but-2-ynedioate reacts in good yield (**Figure 28**). SPAAC with BCN (bicycle[6.1.0]nonyne) afforded the product instantaneously in an exothermic copper-free reaction. Copper complexes with azide featured NHC ligands were post-functionalized auto-catalytically²⁰⁴ with propargyl alcohol.²⁰⁵ For steric reasons, the catalysis proceeds in an intermolecular fashion. This *auto-click* strategy allows introduction of biologically more relevant moieties as unprotected glucose or a fluorescent coumarin.²⁰⁶ Additionally, these copper complexes act as carbene transfer agents to form the corresponding gold (I) complexes.

²⁰² Warsink, S.; Drost, R. M.; Lutz, M.; Spek, A. L.; Elsevier, C. J. *Organometallics* **2010**, 29, 3109.

²⁰³ Hospital, A.; Gibard, C.; Gaulier, C.; Nauton, L.; Théry, V.; El-Ghozzi, M.; Avignant, D.; Cisnetti, F.; Gautier, A. *Dalton Trans.* **2012**, 41, 6803.

²⁰⁴ Auto-catalysed CuAAC is also reported by Bräse *et al.* for cross-link a luminescent copper (I) butynyl-PyrPHOS complex to a polymeric backbone in aim to develop new organic light-emitting diodes, see: Volz, D.; Baumann, T.; Flügge, H.; Mydlak, M.; Grab, T.; Bächle, M.; Barner-Kowollik, C.; Bräse, S. *J. Mater. Chem.* **2012**, 22, 20786.

²⁰⁵ Gibard, C.; Avignant, D.; Cisnetti, F.; Gautier, A. *Organometallics* **2012**, 31, 7902.

²⁰⁶ Ibrahim, H.; Gibard, C.; Hesling, C.; Guillot, R.; Morel, L.; Gautier, A.; Cisnetti, F. *Dalton Trans.* **2014**, 43, 6981.

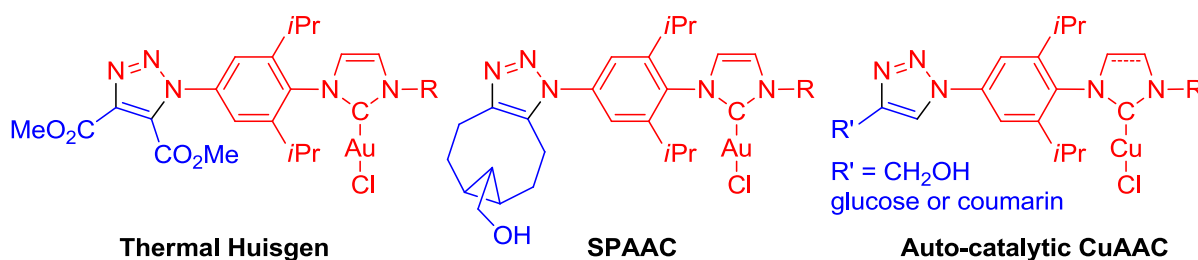


Figure 28: Post-synthetic modification of NHC-azide complexes by thermal Huisgen, SPAAC and autocatalytic CuAAC²⁰⁶

In our group, we developed functionalization of platinum and palladium NHC-alkyne complexes with potentially biologically active azides. Thus, PEG for enhanced water solubility, amino acids and oestrogen derivative for targeting specifically hormone-dependent cancer cell lines were tested (**Figure 29**).^{126,127,207} Complexation of NHC needs protection of the alkyne by TMS, which is easily removable by either fluoride on a macroporous polymer support or potassium carbonate in methanol. While CuAAC led to degradation and polynuclear palladium species, RuAAC (Ruthenium-catalysed 1,3-dipolar azide-alkyne cycloaddition) yields successful conjugated products whose cytotoxicity revealed to be enhanced compared to cisplatin.

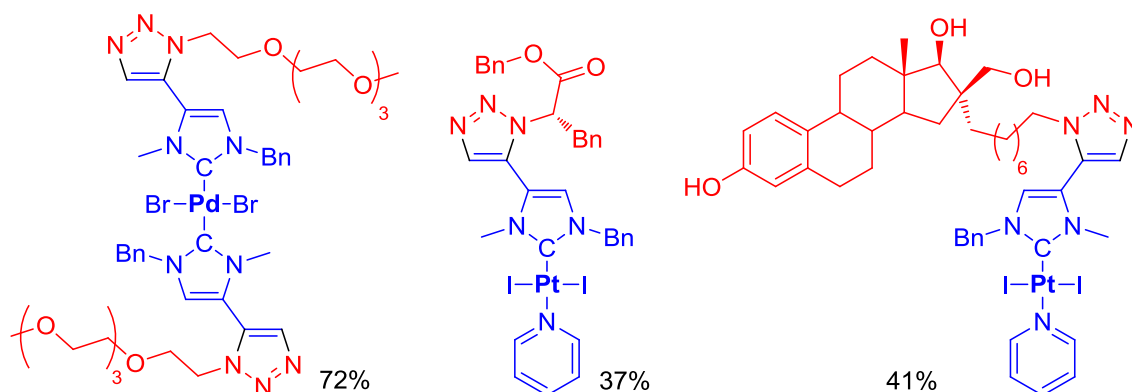


Figure 29: PEG, amino acid and oestrogen derivatives functionalized Pd and Pt NHC complexes¹²⁷

1.3.4.3 Reactivity of metal azide and metal alkyne complexes

Metal azide and metal alkyne complexes are intermediates in the catalytic cycles of CuAAC and RuAAC. Starting from $M-N_3$ or M -alkyne, the use of copper or ruthenium catalyst could be avoided. Ruthenium azido complexes react with alkynes to a triazole remained coordinated to the autocatalytic

²⁰⁷Dahm, G. *Master Thesis* **2011**, University of Strasbourg.

metal centre.²⁰⁸ Gray and co-workers examined copper-free cycloaddition reactions of $[(PPh_3)Au(N_3)]$ and $[(PPh_3)Au(alkyne)]$ complexes with alkynes and azides moieties respectively, resulting in same triazole product where gold is coordinated by carbon atom (**Figure 30**).²⁰⁹ The reaction allows them to create a whole collection of complexes.²¹⁰ $[(PPh_3)Au(N_3)]$ and $[(PPh_3)Au(alkyne)]$ together react to a binuclear complex in a reaction called by Veigh and co-workers as inorganic click (*iClick*).²¹¹

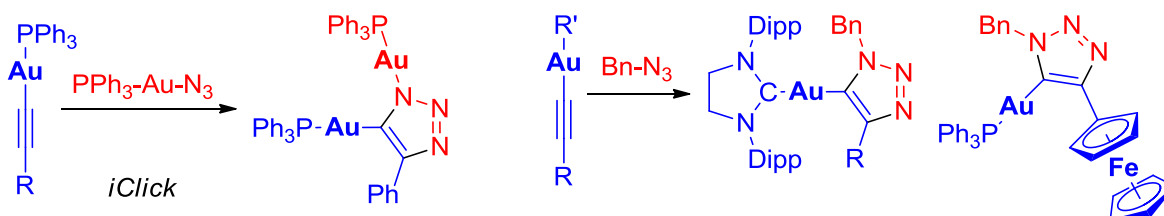


Figure 30: Examples of alkyne respectively azide complexes functionalized by *iClick*^{209,211}

To conclude, Huisgen cycloaddition represents the best-explored post-synthetic modification of the ligand beard by preformed complexes. Its versatility, the ease of access of alkynes and azides allows the straightforward introduction of biological moieties of greatest interest.

1.3.5 Introducing diversity by ligand exchange

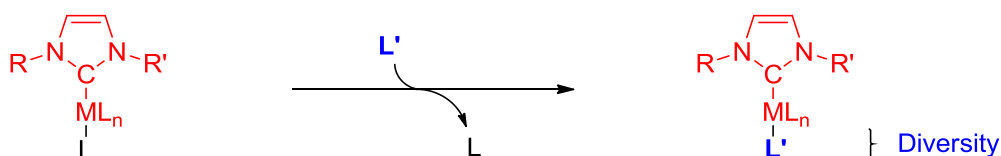


Figure 31: Derivatization of NHC-transition metal complexes by ligand exchange

Perhaps the most obvious post-synthetic modification of a complex is ligand exchange, which constitutes one of the basic reactivity of transition metal complexes.²¹² Although *stricto sensu* any ligand exchange even with small inorganic ligands (H_2O , Cl^- , NO_3^- , ...) could be classified as post-synthetic modification, in our context we will focus here on the introduction of “sophisticated” organic ligands and on post-complexation modifications of an organometallic ligand in the context of NHC complexes.

²⁰⁸ Chen, C.-K.; Tong, H.-C.; Hsu, C.-Y. C.; Lee, C.-Y.; Fong, Y. H.; Chuang, Y.-S.; Lo, Y.-H.; Lin, Y.-C.; Wang, Y. *Organometallics* **2009**, 28, 3358; Chang, C. C.; Lee, G. H. *Organometallics* **2003**, 22, 3107.

²⁰⁹ Partyka, D. V.; Updegraff III, J. B.; Zeller, M.; Hunter, A. D.; Gray, T. G. *Organometallics* **2007**, 26, 183.

²¹⁰ Partyka, D. V.; Gao, L.; Teets, T. S.; Updegraff, III, J. B.; Deligonul, N.; Gray, T. G. *Organometallics* **2009**, 28, 6171.

²¹¹ Del Castillo, T. J.; Sarkar, S.; Abboud, K. A.; Veige, A. S. *Dalton Trans.* **2011**, 40, 8140.

²¹² Langford, C. H.; Gray, H. B. *Ligand Substitution Processes*. **1966**, W. A. Benjamin, Inc., New York.

In 2005, White, Berners-Price and co-workers synthesized a linear gold (I) NHC-chloride complex and subsequently derived a cationic phosphine complex by chloride replacement.²¹³ A neutral glucopyranosyl-thiolate NHC gold complex, the NHC analogue of *Auranofin* (anti-rheumatic agent), is obtained by the same synthetic pathway (**Figure 32**). These compounds show anti-mitochondrial activity. Starting from a similar NHC-Au-Cl complex, introduction of glucopyranosyl-thiol was attempted by the group of Nolan.²¹⁴ On contrary, sodium saccharin salt appeared to be not aurophilic enough to displace the Cl ligand. The authors obtained NHC-Au-saccharin complex starting from the more reactive $[(\text{NHC})\text{Au}(\text{MeCN})]^+\text{PF}_6^-$ complex. Transmetalation reaction of $\text{PPh}_3\text{-Au-Br}$ analogue with aryl-boronic acids gave rise to a series of 15 different $\text{PPh}_3\text{-Au(I)-aryl}$ complexes.²¹⁵



Figure 32: Post-synthetic modification of NHC complexes with glucopyranosyl-thiolate or saccharin moieties^{214,215}

On a Grubbs second generation-type ruthenium $\text{IMes-RuCl}(\text{alkene})\text{-(pyridine)}_2$ complex, Emrick and co-workers substituted both pyridine ligands by click-functionalized water-soluble (PEG or phosphorylcholine) azide-pyridines (**Figure 33**).²¹⁶ The exchange equilibrium was displaced by repeated freeze pump-thaw and re-dissolution cycles of remove pyridine.

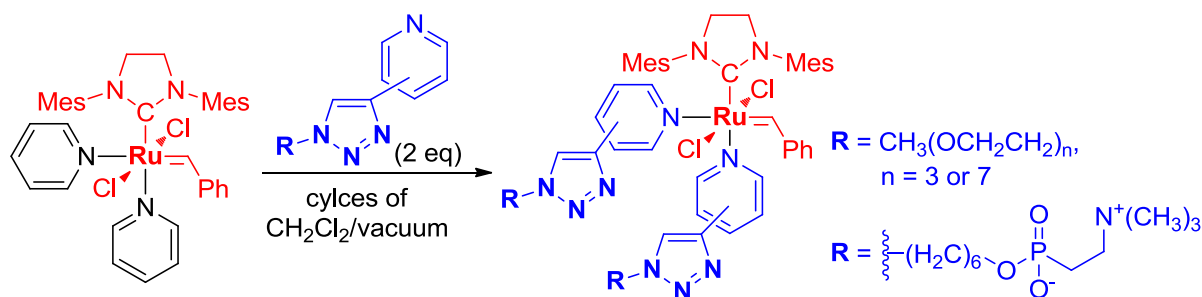


Figure 33: Grubbs-type Ru complex di-functionalization with click functionalized pyridines²¹⁶

²¹³ Hickey, J. L.; Berners-Price, S. J.; Skelton, B. W.; White, A. H.; Barnard, P. J.; Baker, M. V.; Brayshaw, S. K. *J. Organomet. Chem.* **2005**, 690, 5625.

²¹⁴ De Frémont, P.; Stevens, E. D.; Eelman, M. D.; Fogg, D. E.; Nolan, S. P. *J. Organomet. Chem.* **2006**, 25, 5824.

²¹⁵ Partyka, D. V.; Zeller, M.; Hunter, A. D.; Gray, T. G. *Angew. Chem. Int. Ed.* **2006**, 45, 8188.

²¹⁶ Samanta, D.; Kratz, K.; Zhang, X.; Emrick, T. *Macromolecules* **2008**, 41, 530.

In our laboratory, functionalization of NHC-platinum complexes by displacement of the labile pyridine ligand with various primary and secondary amines afforded a family of highly cytotoxic platinum complexes.^{124,125} During present work, this methodology will be further explored.²¹⁷

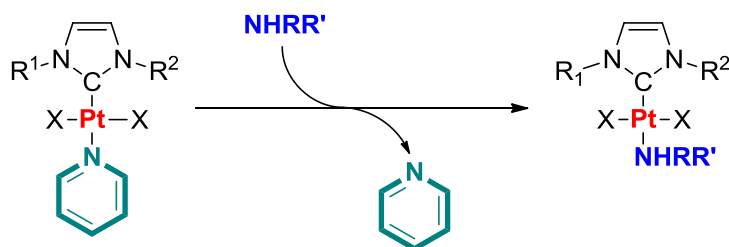


Figure 34: Derivatization of Platinum NHC complexes by ligand displacement

1.4 Conclusion and aim of this work

The clinical success of cisplatin still remains a driving force for the development of new platinum complexes with reduced side effects or (acquired) resistance. As such, platinum NHC complexes are highly promising candidates to develop new drugs. Their versatile nature and relative ease of obtaining allows high modulation of their steric and electronic properties. Post-synthetic modification approach, introduced in the last years, remains a rational strategy to accede an even bigger diversity. In previous section, we reported the most pertinent examples of NHC complex post-synthetic functionalization. The aim of this work will be the synthesis of divers NHC platinum complexes and their subsequent postmodification. This post-functionalization should combine mild conditions, enhanced versatility, high yields, inertness *vis-à-vis* different chemical functionalities and avoid metal-based catalyst. These conditions were fulfilled for post-synthetic modification by ester or peptide bond²¹⁸ and oxime formation as well as ligand exchange. We choose to extend the ligand exchange strategy to various nitrogen and other pnictogen-based ligands. In a second part, we will focus on complexes derivatization by oxime formation. In the third part of this work, biological results of the new complexes will be presented.

²¹⁷ Functionalization of NHC-platinum complexes by ligand exchange is detailed in the chapter 4.1. *Ligand exchange*.

²¹⁸ Several groups report post-modification of complexes by this strategy, e.g.: Raszeja, L.; Maghnouj, A.; Hahn, S.; Metzler-Nolte, N. *ChemBioChem* **2011**, *12*, 371; Kuil, J.; Steunenberg, P.; Chin, P. T. K.; Oldenburg, J.; Jalink, K.; Velders, A. H.; van Leeuwen, F. *ChemBioChem* **2011**, *12*, 1897; Chanawanno, K.; Caporoso, J.; Kondeti, V.; Paruchuri, S.; Leeper, T. C.; Herrick, R. S.; Ziegler, C. J. *Dalton Trans.* **2014**, *43*, 11452; Ravera, M.; Gabano, E.; Pelosi, G.; Fregonese, F.; Tinello, S.; Osellan D. *Inorg. Chem.* **2014**, *53*, 9326.

2 Introducing diversity: synthesis of prefunctionalized Pt-NHC complexes

So far, in medicinal chemistry, only few modifications have been introduced on NHC backbone of the platinum complexes. Thus, we decided to investigate this parameter in order to introduce chemical diversity. In this chapter, we describe the synthesis of simple platinum-NHC complexes bearing various chemical functional groups. The platinum PtI_2 fragment has been kept unchanged (**Figure 35**). A higher cytotoxicity of iodide complexes compared to their bromide or nitrato analogues was reported.¹²² For this reason, we choose iodides as X-type ligand. These two iodide ligands usually coordinate to the platinum (II) centre in *trans* position to each other. Diversity will also be introduced by varying the neutral nitrogen-based ligand (L = pyridine, cyclohexylamine, morpholine or amino acid) located *trans* to the carbene as well as the backbone substituents of the ylidene. Starting from lipophilic alkane groups, we tried to introduce more polar alcohols, amines, carbonyls, esters or hydrophilic carboxylic acids.²¹⁹ These backbone modifications will be introduced before the complexation onto the metal centre following a linear strategy. Several of these complexes will be post-synthetically modified to increase further the chemical diversity.

Variations:

Y (C or N)

R¹-R⁴

L (Neutral ligand)

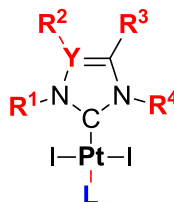


Figure 35: General structure of NHC platinum (II) complexes studied

2.1 Synthesis of azolium precursors and complexation to Pt metal: general synthesis

Access to NHC metal complexes requires the synthesis of azolium precursors.²²⁰ We used well-known strategies to access imidazolium salts with various functionalities: symmetrical imidazolium salts were obtained by three different strategies: i) Arduengo's classic multicomponent cyclization,^{221,63} ii) the

²¹⁹ For functionalized *N*-Heterocyclic Carbenes, see: Kühl, O. *Chem. Soc. Rev.* **2007**, 36, 592; Normand, A. T.; Cavell, K. J. *Eur. J. Inorg. Chem.* **2008**, 2008, 2781.

²²⁰ For a review of the synthesis of imidazolium precursors, see: Benhamou, L.; Chardon, E.; Lavigne, G.; Bellemin-Laponnaz, S.; César, V. *Chem. Rev.* **2011**, 111, 2705.

²²¹ Arduengo III, A. J. US Pat. 5,077,414, **1991**.

reaction between (trimethylsilyl)imidazole and two equivalents of halogenoalkane²²² or iii) reaction of imidazole derivatives²²³ with excess of halogenoalkane.²²⁴ Unsymmetrical imidazolium salts were obtained by alkylation of imidazole derivatives with halogenoalkanes. Further synthetic explanations will be given in experimental part. All imidazolium precursors were purified by recrystallization and characterized by standard technics.

The proposed synthetic pathway to access the NHC-platinum complexes requires a strategy already developed in our group:^{124,125,126,127} after sonication, a suspension of respectively one equivalent of imidazolium salt and platinum dichloride as well as an excess of sodium iodide and potassium carbonate, were heated at 100 °C overnight in pyridine to afford the desired complexes (**Figure 36**). The compounds were characterised by standard ¹H, ¹³C (¹⁹F and ³¹P when possible) NMR techniques, electrospray ionization mass spectrometry (ESI-MS) and single crystals X-ray diffraction analysis. Disappearance of the NCHN signal of imidazolium (8-10 ppm) in ¹H-NMR is the most evident indication for carbene formation. Upon coordination, L ligand signals are usually downfield in NMR (e.g. pyridine: ¹H: from 8.6 to 9.0 ppm; ¹³C: from 150 to 153 ppm). The signal of the carbenic carbon in ¹³C-NMR depends of the donating strength of the ylidene and the geometry (*cis/trans*) of the metal. We observed an ionization of the complexes by loss of an iodide ligand or capture of an H⁺ or Na⁺ during mass spectrometry by electrospray ionization (MS-ESI). X-ray diffraction studies allowed us to determine the geometry of the platinum centre (*cis* or *trans*). The labile pyridine ligand can be relatively displaced by various amines (cyclohexylamine or morpholine), a point that will be discussed in detail in chapter 4.1. *Ligand exchange reaction on a pyridine platinum NHC complex.*

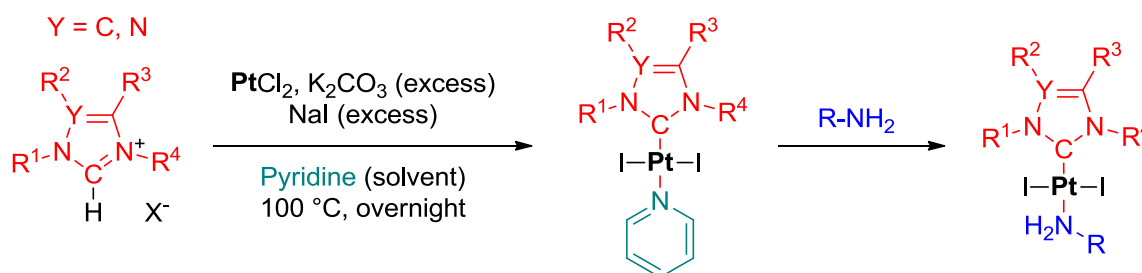


Figure 36: General synthesis of the platinum NHC complexes

²²² Selected examples: Fei, Z.; Zhao, D.; Scopelliti, R.; Dyson, P. J. *Organometallics* **2004**, *23*, 1622; Haque, R. A.; Iqbal, M. A.; Asekunowo, P.; Majid, A. M. S. A.; Ahamed, M. B. K.; Umar, M. I.; Al-Rawi, S. S.; Al-Suede, F. S. R. *Med. Chem. Res.* **2013**, *33*, 4663.

²²³ Reiter, L. A. *J. Org. Chem.* **1987**, *52*, 2714; Jayaram, P. N.; Roy, G.; Muges, G. *J. Chem. Sci.* **2008**, *120*, 143; Salvio, R.; Cacciapaglia, R.; Mandolini, L. *J. Org. Chem.* **2011**, *76*, 5438.

²²⁴ Vlahakis, J.; Lazar, C.; Crandall, I. E.; Szarek, W. A. *Bioorg. Med. Chem.* **2010**, *18*, 6184.

2.2 Pt-NHC complexes bearing various *N*-substituents

2.2.1 Pt-NHC complexes bearing innocent *N*-substituents: alkanes, aromatic rings, alkenes and fluoroalkanes

Alkane chains or aryl groups can be introduced quite easily as *N*-substituents to azolium precursors. As electronic and steric parameters of the metal remain unchanged, we can reasonably assume that variation of alkane chain length may not influence the intrinsic toxicity of the platinum centre. Since efficient cellular uptake is necessary for biological activity, increased lipophilicity of metal complexes may favour cellular uptake through the cellular membrane.²²⁵

Thus, various NHC-Pt-pyridine complexes (**1-11**) have been synthesized following the synthesis depicted in **Figure 36**, and amine complexes were produced by ligand exchange starting from these pyridine complexes. **Figure 37** displays examples of such complexes, with alkanes (**1-5**), cycloalkanes (**6-9**) or fluoroalkanes (**10-11**) substituents, the yields are ranging from 43 to 93%. Ligand exchange with cyclohexylamine also gave the corresponding complexes.

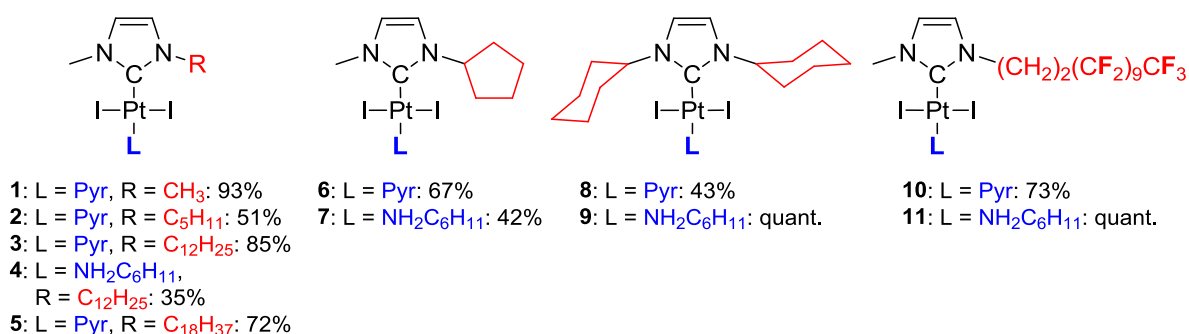


Figure 37: Examples of diversity: *n*-alkanes, cycloalkanes, or fluoroalkanes NHC-Pt complexes
 (The yields refer to complexation step (pyridine complexes), respectively to ligand exchange reaction with cyclohexylamine (NH₂C₆H₁₁))

Different aromatic groups could be introduced as *N*-substituents on the NHC (**Figure 38, a**). Aryl groups (**12-13**) or benzyl substitutions are possible. Thus, phenyl (**14-15**) can be compared with bromo (**16**), cyano (**17**) or nitro groups (**18-21**) (b), bis-*para*-nitrotoluene *N*-substituents on the NHC (**22-23**) (c) or *para*-nitrobenzyl fixed by a formaldehyde *O*-ethyl oxime linker on the NHC (**24-25**) (d).

²²⁵ Gasser suggests that an increase of cytotoxicity of Rhenium complexes may be correlated to lipophilicity: Kitanovic, I.; Can, S.; Alborzinia, H.; Kitanovic, A.; Pierroz, V.; Leonidova, A.; Pinto, A.; Spingler, B.; Ferrari, S.; Molteni, R.; Steffen, A.; Metzler-Nolte, N.; Wölfl, S.; Gasser, G. *Chem. Eur. J.* **2014**, 20, 2496.

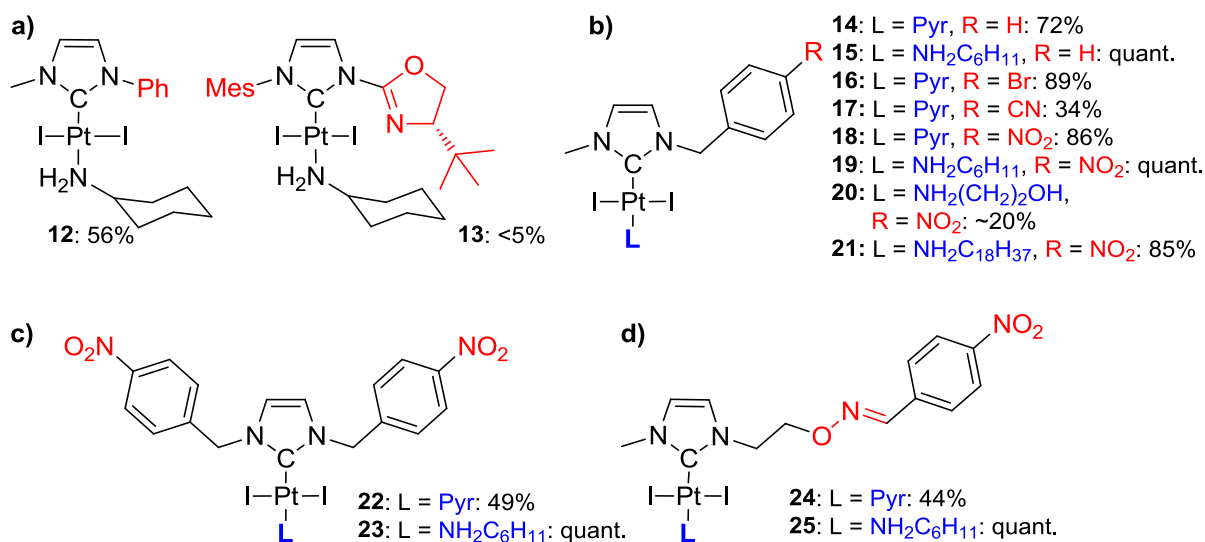


Figure 38: Examples of diversity: modifications of aryl *N*-substituents for NHC platinum complexes (The yields refer to complexation step (pyridine complexes), respectively to ligand exchange reaction with cyclohexylamine)

Introduction of polycyclic aromatic hydrocarbon (PAH) groups (naphthalene, pyrene or anthracene) was also achieved. These fragments should display DNA intercalation properties to the complexes **26-31** (Figure 39).

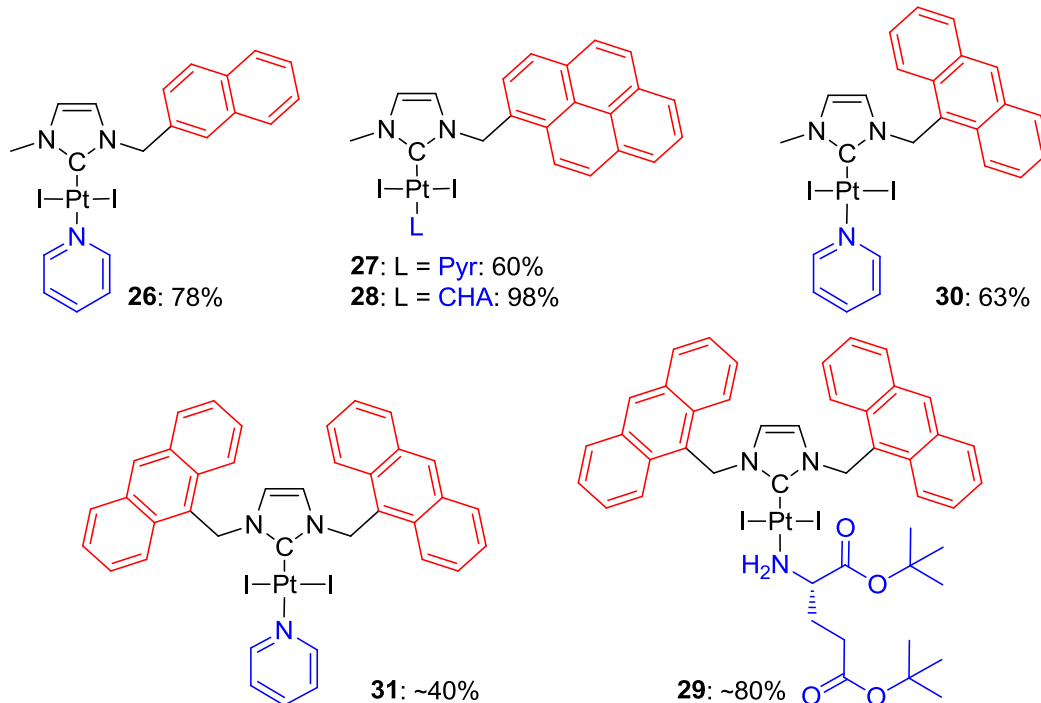


Figure 39: Examples of diversity: intercalation *N*-substituents on NHC platinum complexes (The yields refer to complexation step (pyridine complexes), respectively to ligand exchange reaction with an amine)

One of the most promising and highly developed drug carriers currently investigated are liposomes (phospholipid bilayer vesicles) and derivatives. Several liposomal formulations of platinum drugs have been explored with success. For example, *Lipoplatin* is a cisplatin-liposome formulation of dipalmitoyl phosphatidyl glycerol, soy phosphatidyl choline, cholesterol and methoxy-polyethylene glycol-diastearoyl phosphatidyl-ethanolamine acting as bilayer.²²⁶ The liposomes display higher tumour uptake compared to surrounding non-cancerous tissues due to EPR effect (Enhanced Permeability and Retention effect, due to abnormal molecular transport dynamics).

Synthesis of NHC-Pt complexes with good lipophilicity was thus attempted in order to obtain molecular candidates suitable for liposome delivery application. For this reason, complexes with different chain lengths were synthesized to modulate their lipophilicity (**Figure 40**). Imidazolium proligands were synthesized according to reported procedure,²²⁷ affording a series of complexes bearing different NHC backbones and different L ligands. The biological activities of the complexes **14** and **15** containing simple phenyl substituents will be compared with C₁₂ complexes **32-34**, C₈ complexes **35** and **36** or two chains featured complexes **37** and **38**. The influence of the different L ligands (pyridine, cyclohexylamine and morpholine) can also be evaluated. Complex **12** is the reference for complexes **39** and **40** having no CH₂-bridge between the NHC and the phenyl groups. On the other hand, polyethylene glycol (PEG) chains²²⁸ increased the polarity of the resulting complex **41**²²⁹ and made it soluble in ethanol/water solution.

The stability of [(NHC)PtI₂(cyclohexylamine)] **33** in wet DMSO solution was studied. It remains stable in deuterated DMSO solution up to 100 °C. After heating a solution of the complex in DMSO at 110 °C overnight and purification by silica gel chromatography, 68 % of initial complex was recovered. These experiments show the stability of our NHC complexes *vis-à-vis* ligand exchange by DMSO or decomposition.

²²⁶ Stathopoulos, G. P.; Boulikas, T.; Vougiouka, M.; Deliconstantinos, G.; Rigatos, S.; Darli, E.; Viliotou, V.; Stathopoulos, J. G. *Oncol. Rep.* 2005, 13, 589

²²⁷ Dobbs, W.; Douce, L.; Allouche, L.; Louati, A.; Malbosc, F.; Welter, R. *New J. Chem.* 2006, 30, 528.

²²⁸ The starting material (3,4,5-tris(2,5,8,11-tetraoxatridecan-13-yloxy)phenyl)methanol (obtained from Dr. A. Garofalo) was brominated by thionyl bromide. Alkylation of methylimidazole gave imidazolium precursor.

²²⁹ For water-soluble PEG featured complexes, see e.g.: Gallivan, J. P.; Jordan, J. P.; Grubbs, R. H. *Tetrahedron Letters* 2005, 46, 2577; Meise, M.; Haag, R. *ChemSusChem* 2008, 1, 637.

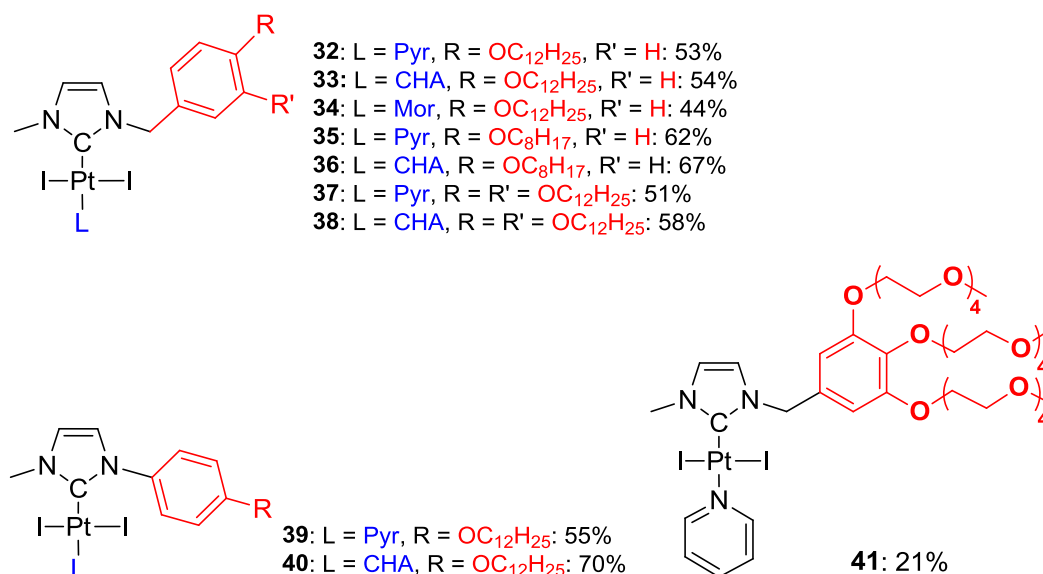


Figure 40: Introduction of fatty chains or PEG to NHC-Pt complexes (%: yield of complexation step)²³⁰

We have also investigated the possibility to functionalize the complexes with substituents containing alkene moieties. A propene derivative was successfully synthesized starting from 3-allyl-1-methyl-1H-imidazol-3-ium iodide (**Figure 41**, a). Ethene derivative was obtained from 3-(2-chloroethyl)-1-methyl-1H-imidazol-3-ium chloride (b). In basic conditions, the chloroethane group is subject of elimination reaction. For both complexes, NMR analysis ascertain that double bond does not coordinate.

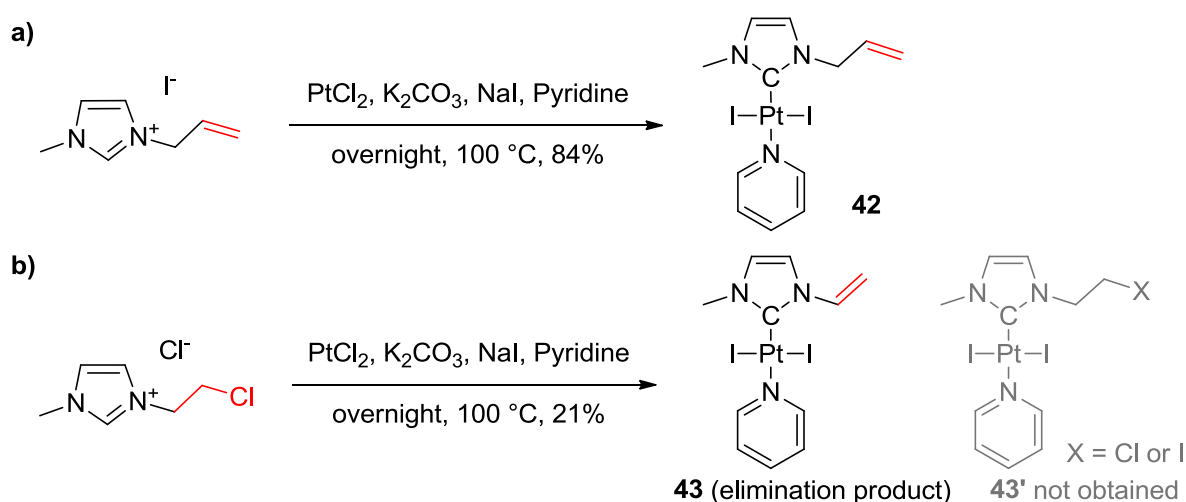


Figure 41: Synthesis of NHC-alkene complexes

²³⁰ Complexes 35, 36, 38, 39 and 40 were synthesized in collaboration with Dr. Giangi Puleo.

Several complexes have been characterized by single crystal X-ray diffraction studies (**Figure 42**).²³¹ All complexes adopt a square planar geometry around platinum, and nitrogen ligands are located in *trans* to the NHC ligand.

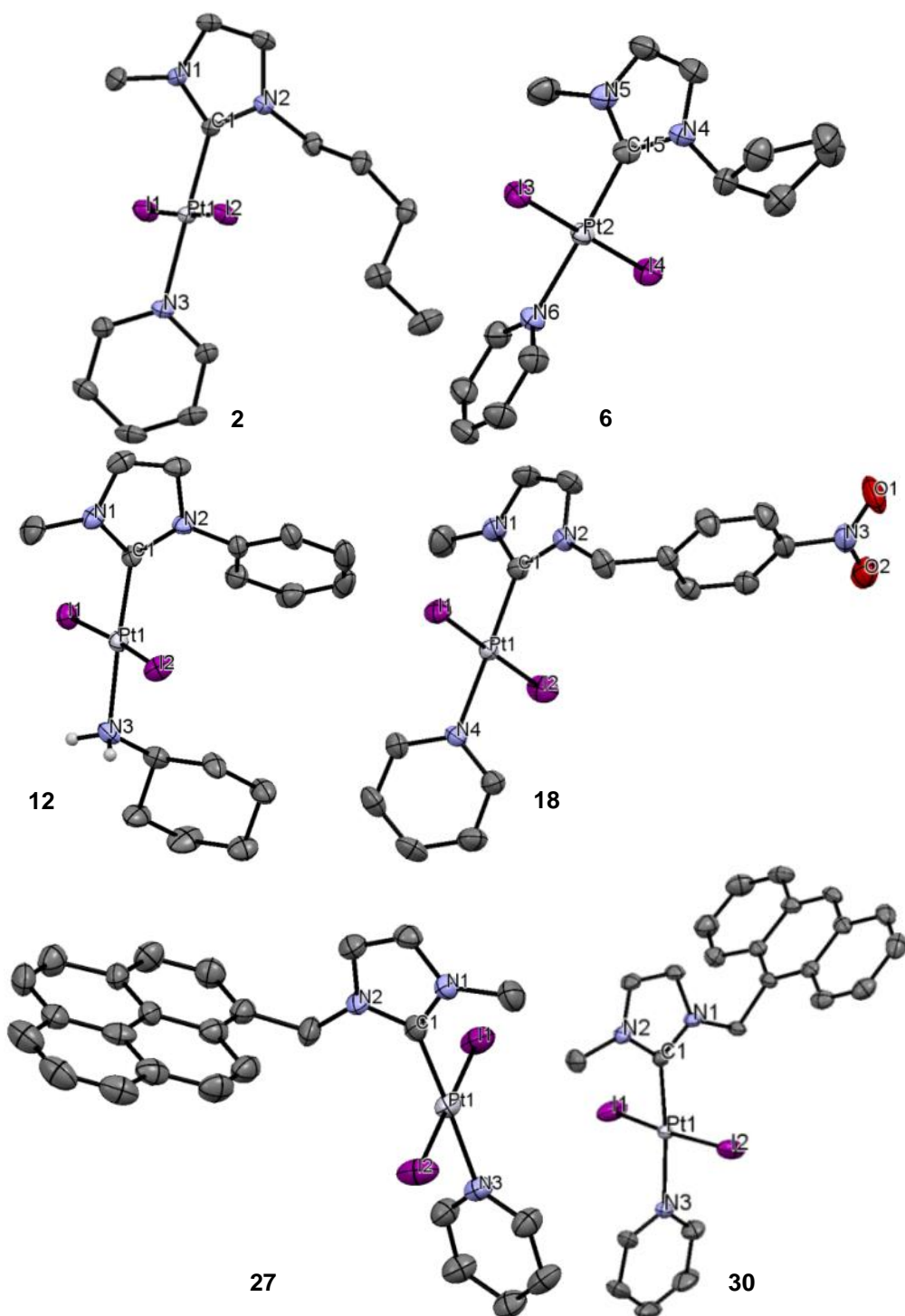


Figure 42: X-ray structures of platinum complexes 2, 6, 12, 18, 27 and 30

²³¹ For a discussion of monocrystall growth technics, see: Spingler, B.; Schnidrig, S.; Todorova, T.; Wild, F. *CrystEngComm* **2012**, *14*, 751.

	Complex	2	6	12	18	27	30
1	Pt-C _{NHC}	1.968	1.965	1.973	1.974	1.969	1.961
2	Pt-N _{Ligand}	2.098	2.091	2.112	2.089	2.090	2.088
3	Pt-I	2.597, 2.610	2.598, 2.601	2.5999, 2.616	2.589, 2.598	2.587, 2.593	2.573, 2.601
4	I-Pt-I	177.08	179.49	174.58	178.43	179.45	172.40
5	C-Pt-I	87.92, 90.29	87.99, 91.50	89.28, 92.08	89.73, 89.90	89.21, 91.22	87.72, 92.02
6	N-C-N	105.57	104.93	105.33	105.15	104.55	105.21

Table 1: Selected bond lengths (Å) and angles (°) of Pt complexes 2, 6, 12, 18, 27 and 30

Selected bond lengths of various NHC complexes are summarized in **Table 1**. Platinum N_{Ligand} bond lengths are longer in the case of cyclohexylamine (2.112 Å) than pyridine complexes (2.089-2.098 Å). The similar bond length of all Pt-pyr complexes indicates similar bond strength. No general trend could be attributed to platinum-C_{NHC} bond length (1.961-1.974 Å). No correlation could be found between this bond length and aromatic/aliphatic substituents or L ligand.

As a conclusion, we afforded a whole series of complexes featured with different alkyne and aryl groups. Their biological activity will be evaluated in this work (chapter 5.1.2.1. *Influence on cytotoxicity of alkyl chains and aryls as N-substituents of NHC complexes*).

2.2.2 Pt-NHC complexes N-functionalized by hydroxyl groups and amines

Hydroxyl functional group is of ubiquitous use in organic chemistry. However, examples of hydroxylated NHC complexes are rare. The first reported example is a *cis*-dicarbene palladium (II) complex prepared by Herrmann and co-workers.²³² By etherification, the alcohol function is immobilized on a polystyrene resin to create a recyclable catalyst for Heck reaction. Since then, only few new palladium,^{233,234} ruthenium,²³⁵ rhodium,²³⁶ gold,²³⁷ silver,²³⁸ nickel,²³⁹ copper,²⁴⁰ or

²³² Schwarz, J.; Böhm, V. P. W.; Gardiner, M. G.; Grosche, M.; Herrmann, W. A.; Hieringer, W.; Raudaschl-Sieber, G. *Chem. Eur. J.* **2000**, *6*, 1773.

²³³ Glas, H.; Herdtweck, E.; Spiegler, M.; Pleier, A.-K.; Thiel, W. R. *J. Organomet. Chem.* **2001**, *626*, 100; Ray, L.; Shaikh, M. M.; Ghosh, P. *Dalton Trans.* **2007**, 4546; Arnold, P. L.; Sandford, M. S.; Pearson, S. M. *J. Am. Chem. Soc.* **2009**, *131*, 13912; Jokić, N. B.; Straubinger, C. S.; Goh, S. L. M.; Herdtweck, E.; Herrmann, W. A.; Kühn, F. E. *Inorg. Chim. Acta* **2010**, *363*, 4181; Peñafiel, I.; Pastor, I. M.; Yus, M.; Esteruelas, M. A.; Oliván, M.; Oñate, E. *Eur. J. Org. Chem.* **2011**, *2011*, 7174.

²³⁴ Hameury, S.; De Frémont, P.; Breuil, P.-A. R.; Olivier-Bourbigou, H.; Braunstein, P. *Inorg. Chem.* **2014**, *53*, 5189.

²³⁵ Prühs, S.; Lehmann, C. W.; Fürstner, A. *Organometallics* **2004**, *23*, 280.

²³⁶ Zarka, M. T.; Bortenschlager, M.; Wurst, K.; Nuyken, O.; Weberskirch, R. *Organometallics* **2004**, *23*, 4817; Straubinger, C. S.; Jokić, N. B.; Högerl, M. P.; Herdtweck, E.; Herrmann, W. A.; Kühn, F. E. *J. Organomet. Chem.* **2011**, *696*, 687; Jokić, N. B.; Zhang-Presse, M.; Goh, S. L. M.; Straubinger, C. S.; Bechlars, B.; Herrmann, W. A.; Kühn, F. E. *J. Organomet. Chem.* **2011**, *696*, 3900; Peñafiel, I.; Pastor, I. M.; Yus, M.; Esteruelas, M. A.; Oliván, M. *Organometallics* **2012**, *31*, 6154

iridium^{241,242} NHC hydroxyl or alkoxy^{243,244} complexes have been described. Alcohol substituted silver NHC complexes developed by Youngs and co-workers contain bactericidal activities superior to simple silver nitrate.¹¹⁴ To the best of our knowledge yet, the only alcohol substituted NHC-platinum complex reported is a bis-carbenic platinum (II) complex prepared by the group of Strassner.²⁴⁵

In order to extend the library of known complexes and obtain alcohol functionalized NHC platinum complexes for anticancer tests, an alcohol NHC platinum complex **44** has been synthesized (**Figure 43**). Regardless the presence of the hydroxyl function, reaction yield is comparable to “innocent” alkane complexes. The stability of this complex is proved by successful Williamson etherification. The alcohol is deprotonated *in situ* by potassium *tert*-butoxide and let to react with benzyl bromide to yield 48% of ether complex **45**.

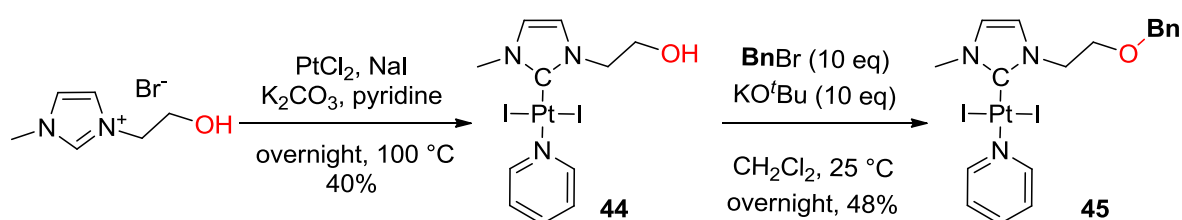


Figure 43: Synthesis of a hydroxyl functionalized NHC Pt complex **44 and post-functionalization by Williamson-type etherification**

Mono crystals suitable for X-ray diffraction analysis have been obtained (**Figure 44**), confirming the *trans* geometry of the complex **44**. In the solid state, no platinum-hydroxyl interactions were visible, validating its inertness toward the metal centre. The presence of hydroxyl groups usually lead to the formation of hydrogen bonds. Surprisingly, we did not observe any hydrogen bonds between the OH groups or OH and iodide ligands of complex **44**.

²³⁷ Ray, L.; Katiyar, C.; Raihan, M. J.; Nanavati, H.; Shaikh, M. M.; Ghosh, P. *Eur. J. Inorg. Chem.* **2006**, 3724; Ray, L.; Katiyar, V.; Barman, S.; Raihan, M. J.; Nanavati, H.; Shaikh, M. M.; Ghosh, P. *J. Organomet. Chem.* **2007**, 692, 4259; Dominique, F. J.-B.; Gornitzka, H.; Sournia-Saquet, A.; Hemmert, C. *Dalton Trans.* **2009**, 340; Jacques, B.; Hueber, D.; Hameury, S.; Braunstein, P.; Pale, P.; Blanc, A.; De Frémont, P. *Organometallics* **2014**, 33, 2326.

²³⁸ Hameury, S.; De Frémont, P.; Breuil, P.-A. R.; Olivier-Bourbigou, H.; Braunstein, P. *Dalton Trans.* **2014**, 43, 4700;

²³⁹ Arduengo, A. J., III; Dolphin, J. S.; Gurău, G.; Marshall, W. J.; Nelson, J. C.; Petrov, V. A.; Runyon, J. W. *Angew. Chem. Int. Ed.* **2013**, 52, 5110.

²⁴⁰ Arnold, P. L.; Scarisbrick, A. C.; Blake, A. J.; Wilson, C. *Chem. Commun.* **2001**, 2340; Arnold, P. L.; Rodden, M.; Davis, K. M.; Scarisbrick, A. C.; Blake, A. J.; Wilson, C. *Chem. Commun.* **2004**, 1612.

²⁴¹ Benítez, M.; Mas-Marzá, E.; Mata, J. E.; Peris, E. *Chem. Eur. J.* **2011**, 17, 10453.

²⁴² Bartoszewicz, A.; Marcos, R.; Sahoo, S.; Inge, A. K.; Zou, X.; Martín-Matute, B. *Chem. Eur. J.* **2012**, 18, 14510

²⁴³ Liddle, S. T.; Edworthy, I. S.; Arnold, P. L. *Chem. Soc. Rev.* **2007**, 36, 1732.

²⁴⁴ For ether functionalized ruthenium and rhodium complexes, see e.g.: Çetinkaya, B.; Özdemir, I.; Dixneuf, P. H. *J. Organomet. Chem.* **1997**, 534, 153; for iridium (II) complexes: Martín-Matute *et al.*²⁴²

²⁴⁵ Meyer, A.; Unger, Y.; Poethig, A.; Strassner, T. *Organometallics* **2011**, 30, 2980.

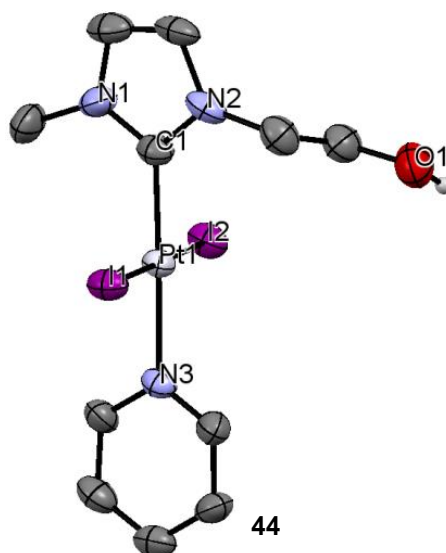


Figure 44: X-ray structure of an alcohol functionalized NHC platinum complex **44**. Selected bond lengths (Å) and angles (°): C-Pt: 1.986; Pt-N: 2.090; Pt-I: 2.603, 2.613; I-Pt-I: 179.01; C-Pt-N: 178.05; C-Pt-I: 88.11, 91.50; N-C-N: 106.20; N-C-Pt-I: 82.24, 96.85; (N-C)_{NHC}-(N-C)_{Pyr}: 6.10.

Morpholine-based *N*-substituents were also introduced (**46** and **48**, **Figure 45**). Interestingly, protonation of the morpholine containing Pt complex **46** by formic acid gave high solubility to **47** in polar solvents like ethanol and even in water.

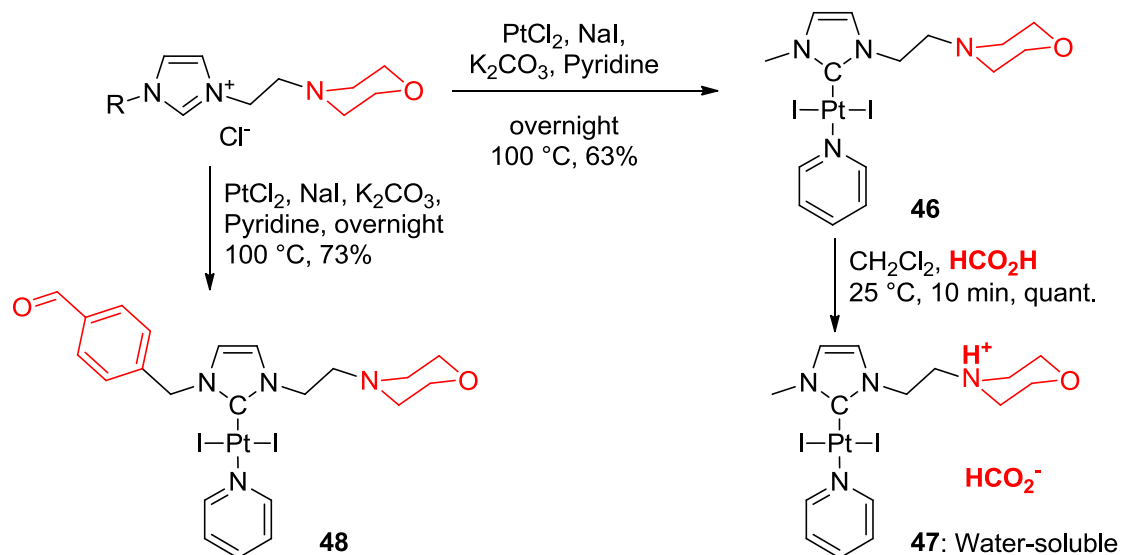


Figure 45: Water-soluble complexes: morpholine substituted NHC platinum complexes

Both complexes **46** and **48** crystallize as single crystals suitable for X-ray diffraction (**Figure 46**, **Table 2**). The molecular structures confirm the expected *trans* geometry between the NHC and pyridine and the chair conformation of the morpholine moiety.

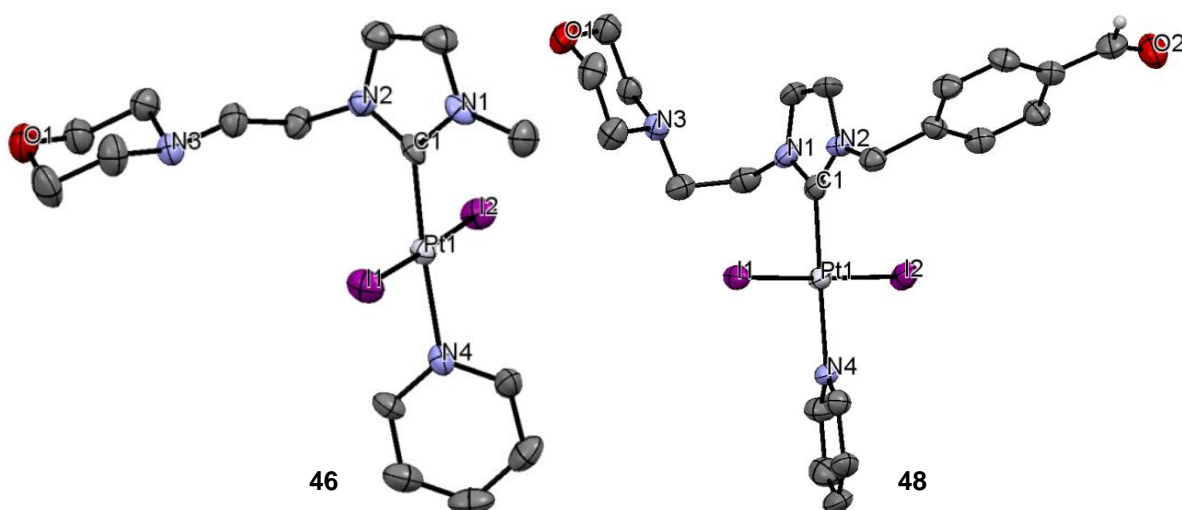


Figure 46: Molecular structures of the complexes 46 and 48

Complexes	C-Pt	Pt-N	Pt-I	I-Pt-I	N-C-N
46	1.972	2.100	2.587, 2.589	178.34	105.52
48	1.978	2.101	2.602, 2.604	178.42	105.75

Table 2: Selected bond lengths (Å) and angles (°) of morpholine substituted NHC complexes 46 and 48

The palladium-morpholine congener **49** was also synthesized (Figure 47). After its protonation by formic acid (**49.HCO₂H**), its solubility in ethanol or water is enhanced. This water-soluble palladium complex is a promising agent for potential catalytic reactions in water.

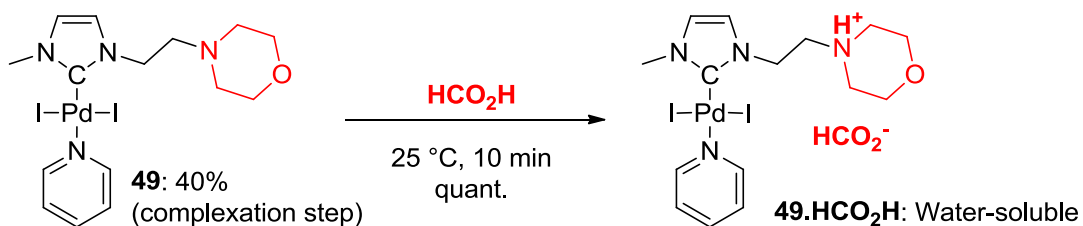


Figure 47: Water-soluble morpholine substituted NHC palladium complexes

The biological properties of these compounds will be described in chapter 5.1.2. *Cytotoxicity of prefunctionalized [(NHC)PtI₂(amine)] complexes.*

2.2.3 Pt-NHC complexes N-functionalized by nitriles, carboxylic acids and their derivatives

Nitriles, typically acetonitrile or benzonitrile, are neutral ligands commonly employed in coordination chemistry. Incorporated into NHC backbone, the nitrile group, a relatively inert chemical function, remains less common. In literature, ruthenium,²⁴⁶ palladium,²⁴⁷ silver and rhodium²⁴⁸ nitrile functionalized NHC complexes can be found. Veiros, Chetcuti and co-workers reported C-H activation of a nitrile ligand on a NHC-Ni (II) centre.²⁴⁹ The group of Morris investigated the reactivity of palladium (II) and platinum (II) complexes featuring a nitrile-functionalized NHC ligand.²⁵⁰ The nitrile group, depending on the solvent, could coordinate a metal centre to form dimeric species.

To study the influence of a nitrile group on biological activity, we synthesized an acetonitrile substituted NHC-platinum (II) pyridine complex **50** from 3-(cyanomethyl)-1-methyl-1H-imidazol-3-ium bromide (**Figure 48**). Starting from pyridine complex, the NHC-Pt (II) cyclohexylamine complex **51** could be obtained by ligand exchange at room temperature, while heating at 40 °C leads to the decomposition of the compound. Nitriles are precursors of oxazolines. Attempts to modify complex **50** into a bis-dentate NHC-oxazoline using standard conditions (nitrile, EtOH, NaH_(cat.)) resulted in undefined species.²⁵¹

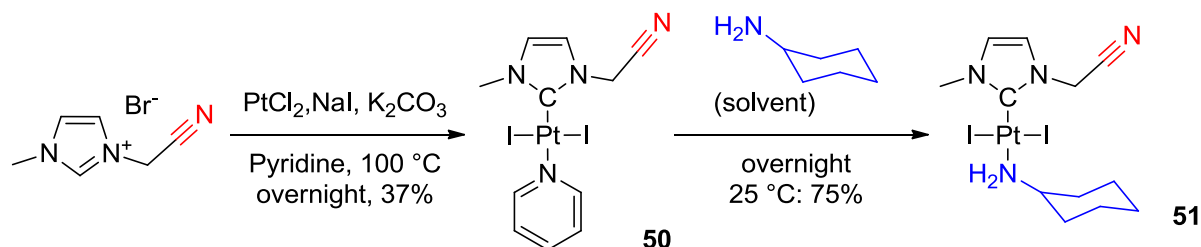


Figure 48: Synthesis of acetonitrile substituted NHC complexes 50 and 51

We were also interested by the carboxylic acid and its derivatives (esters, amides, acyl halides and anhydride acids). Presence of carboxylic acids on a molecule should enhance its water solubility, which is a key factor for biological applications.²⁵² Compatibility between acid derivatives and NHC complexes has been proven by several examples from the literature. Beside several known NHC-

²⁴⁶ Fürstner, A.; Krause, H.; Ackermann, L.; Lehmann, C. W. *Chem. Commun.* **2001**, 2240

²⁴⁷ Fei, Z.; Zhao, D.; Pieraccini, D.; Ang, W. H.; Geldbach, T. J.; Scopelliti, R.; Chiappe, C.; Dyson, P. J. *Organometallics* **2007**, 26, 1588; Huynh, H. V.; Wu, J. J. *Organomet. Chem.* **2009**, 694, 323.

²⁴⁸ O, W. W. N.; Lough, A. J.; Morris, R. H. *Organometallics* **2009**, 28, 853.

²⁴⁹ Oertel, A. M.; Ritleng, V.; Chetcuti, M. J.; Veiros, L. F. *J. Am. Chem. Soc.* **2010**, 132, 13588; Oertel, A. M.; Freudenreich, J.; Gein, J.; Ritleng, V.; Veiros, L. F.; Chetcuti, M. J.; Veiros, L. F. *Organometallics* **2011**, 30, 3400.

²⁵⁰ O, W. W. N.; Lough, A. J.; Morris, R. H. *Organometallics* **2010**, 29, 570.

²⁵¹ Herrmann, W. A.; Goossen, L. J.; Spiegler, M. *Organometallics* **1998**, 17, 2162.

²⁵² For a review of water-soluble NHC complexes, see: Schaper, L.-A.; Hock, S. J.; Herrmann, W. A.; Kühn, F. E. *Angew. Chem. Int. Ed.* **2013**, 52, 270.

amide or ester functionalized rhodium,²⁵³ iridium,²⁵⁴ silver,²⁵⁵ gold,²⁵⁶ palladium^{257,258} or nickel²⁵⁹ complexes, relatively few Pt (II) analogues were reported. For example, Unger and Strassner synthesized amide-functionalized bis-NHC Pt complexes.²⁶⁰ Beside carboxylic acids, water-solubility can be induced by sulfonate groups on NHC complexes.^{261,262} Nevertheless, under standard conditions, free sulfonates or carboxylic acids would lead to competition reaction with the platinum. For this reason, our attention was focused on esters acting as protecting groups during complexation. In a first step, we synthesized Pt-NHC complexes functionalized with esters. Then, hydrolysis of the ester function into a carboxylic acid was achieved in order to afford water-soluble compounds.

The expected Pt ester complexes **52** and **53** were obtained with similar yields compared to alkane complexes (**Figure 49**, a), proving the ester to be innocent toward complexation. The methylester complex could be further functionalized by ligand exchange with *tert*-butyl protected amino acid (**54**).

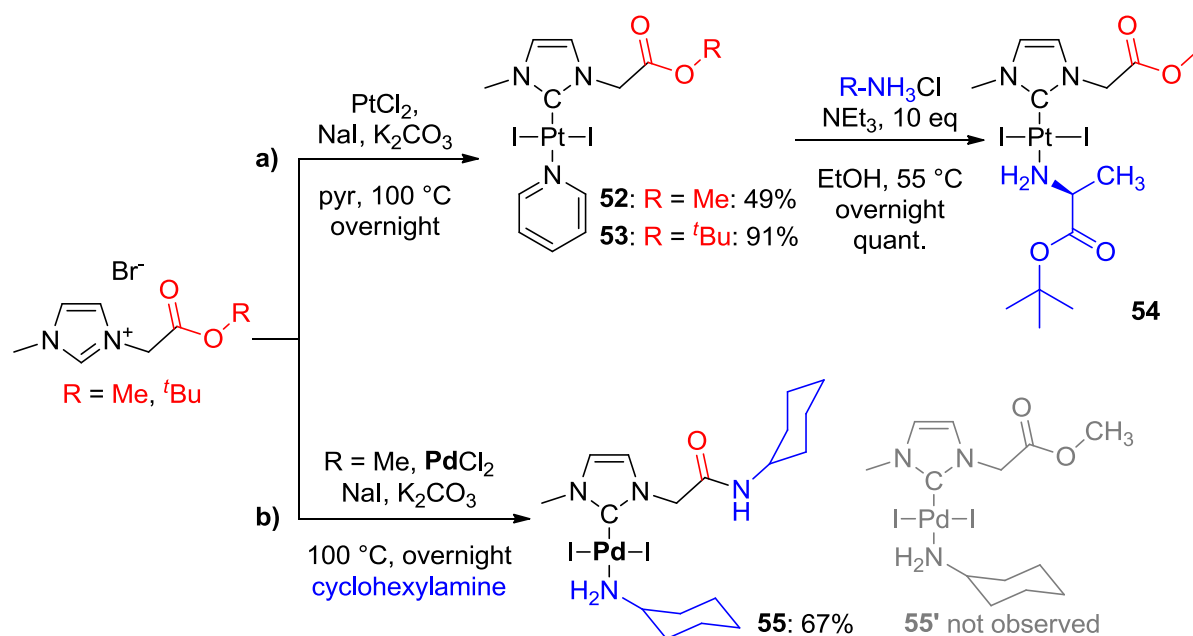


Figure 49: Synthesis of a) ester functionalized Pt complexes and b) amide functionalized Pd complex

²⁵³ Herrmann, W. A.; Gooßen, L. J.; Spiegler, M. *J. Organomet. Chem.* **1997**, 547, 357; For a review, see: John, A.; Ghosh, P. *Dalton Trans.* **2010**, 39, 7183.

²⁵⁴ Gülcemal, D.; Gökçe, A. G.; Gülcemal, S.; Çetinkaya, B. *RSC Adv.* **2014**, 4, 26222.

²⁵⁵ Samantaray, M. K.; Katiyar, V.; Roy, D.; Pang, K.; Nanavati, H.; Stephen, R.; Sunoj, R. B.; Ghosh, P. *Eur. J. Inorg. Chem.* **2006**, 2975; Samantaray, M. K.; Katiyar, V.; Pang, K.; Nanavati, H.; Ghosh, P. *J. Organomet. Chem.* **2007**, 692, 1672; Liao, C. Y.; Chan, K. T.; Chiu, P. L.; Chen, C. Y.; Lee, H. M. *Inorg. Chim. Acta* **2008**, 361, 2973.

²⁵⁶ Pellei, M.; Gandin, V.; Marinelli, M.; Marzano, C.; Yousufuddin, M.; Dias, H. V. R.; Santini, C. *Inorg. Chem.* **2012**, 51, 9873; Samantaray, M. K.; Pang, K.; Shaikh, M. M.; Ghosh, P. *Inorg. Chem.* **2008**, 47, 4153.

²⁵⁷ Kumar, S.; Shaikh, M. M.; Ghosh, P. *J. Organomet. Chem.* **2009**, 694, 4162; Kamisue, R.; Sakaguchi, S. *J. Organomet. Chem.* **2011**, 696, 1910.

²⁵⁸ McGuinness, D. S.; Cavell, K. J. *Organometallics* **2000**, 19, 741.

²⁵⁹ Samantaray, M. K.; Shaikh, M. M.; Ghosh, P. *Organometallics* **2009**, 28, 2267.

²⁶⁰ Unger, Y.; Strassner, T. *J. Organomet. Chem.* **2012**, 713, 203.

²⁶¹ Azua, A.; Sanz, S.; Peris, E. *Organometallics* **2010**, 29, 3661.

²⁶² Godoy, F.; Segarra, C.; Poyatos, M.; Peris, E. *Organometallics* **2011**, 30, 684.

To obtain the cyclohexylamine-palladium analogue, the methylester imidazolium salt was reacted with palladium chloride in cyclohexylamine as solvent (b). The expected ester complex was not observed. Instead, an amide complex **55** was formed. In cyclohexylamine, the ester is directly attacked by the stronger nucleophile. Saponification trials of both $[(\text{OMe-ester-NHC})\text{PtI}_2(\text{pyr})]$ **52** and $[(\text{Amide-NHC})\text{PdI}_2(\text{CHA})]$ **55** complexes under different conditions (MeOH/H₂O 2 days, 25 °C; H₂O/NaOH or: H₂O/HCl) afforded the starting material with decomposition products. These negative results led us to disrupt the exploration of further methylester complexes (e.g. a $[(\text{OMe-ester-NHC})\text{PtI}_2(\text{CHA})]$ complex) and other carboxylic acids protective groups²⁶³ were considered. While deprotection of most esters is carried out under basic conditions, *tert*-butyl esters react under strong acid conditions. By stirring the *tert*-butyl ester complex **53** in formic acid/dichloromethane, the acid complex **56** was quantitatively obtained after evaporation of the volatiles (**Figure 50**). The acid derivative is poorly water-soluble up to 1 mg/ml at 30 °C (and soluble in acetone but insoluble in CH₂Cl₂). Formic acid is a good candidate as deprotecting agent: low price, the contra-ion is less coordinating, excess acid could be removed by simple evaporation and the deprotection reaction is driven to completion by formation of *isobutylene* gas. In presence of triethylamine, the acid is quantitatively deprotonated to form a water-soluble triethylammonium carboxylate **57**. The stability of our carboxylic acid platinum complexes in both acid and basic conditions makes them suitable candidates for bioconjugation by solid-phase peptide synthesis.

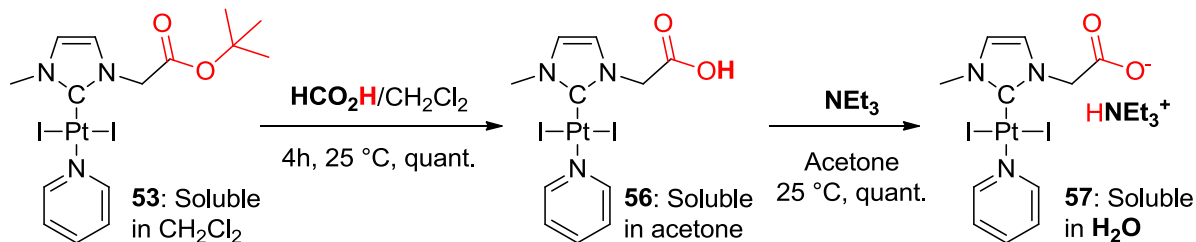


Figure 50: Deprotection of *tert*-butyl ester NHC complex by formic acid: water-soluble complexes

Introducing several acids should enhance the water-solubility of an NHC complex. For this reason, dicarboxylic acids **58-60** were synthesized (**Figure 51**, a). Compound **59** is not soluble in water (but in acetone or ethanol) despite the presence of two acid groups. The direct synthesis of *t*butyl ester complexes from azolium salt is limited to the use of pyridine as solvent, since only decomposition products were obtained in presence of cyclohexylamine. We were also interested in mixed carboxylic acid-benzaldehyde functionalized NHC-platinum-pyridine complexes **61-63**. The presence of the benzaldehyde group makes them possible precursors for further oxime ligation (b).²⁶⁴

²⁶³ Green, T. W.; Wuts, P. G. M. *Protective Groups in Organic Synthesis* **1999**, Wiley-Interscience, New York.

²⁶⁴ See chapter *Post-synthetic modification of NHC complexes by hydrazone and oxime*.

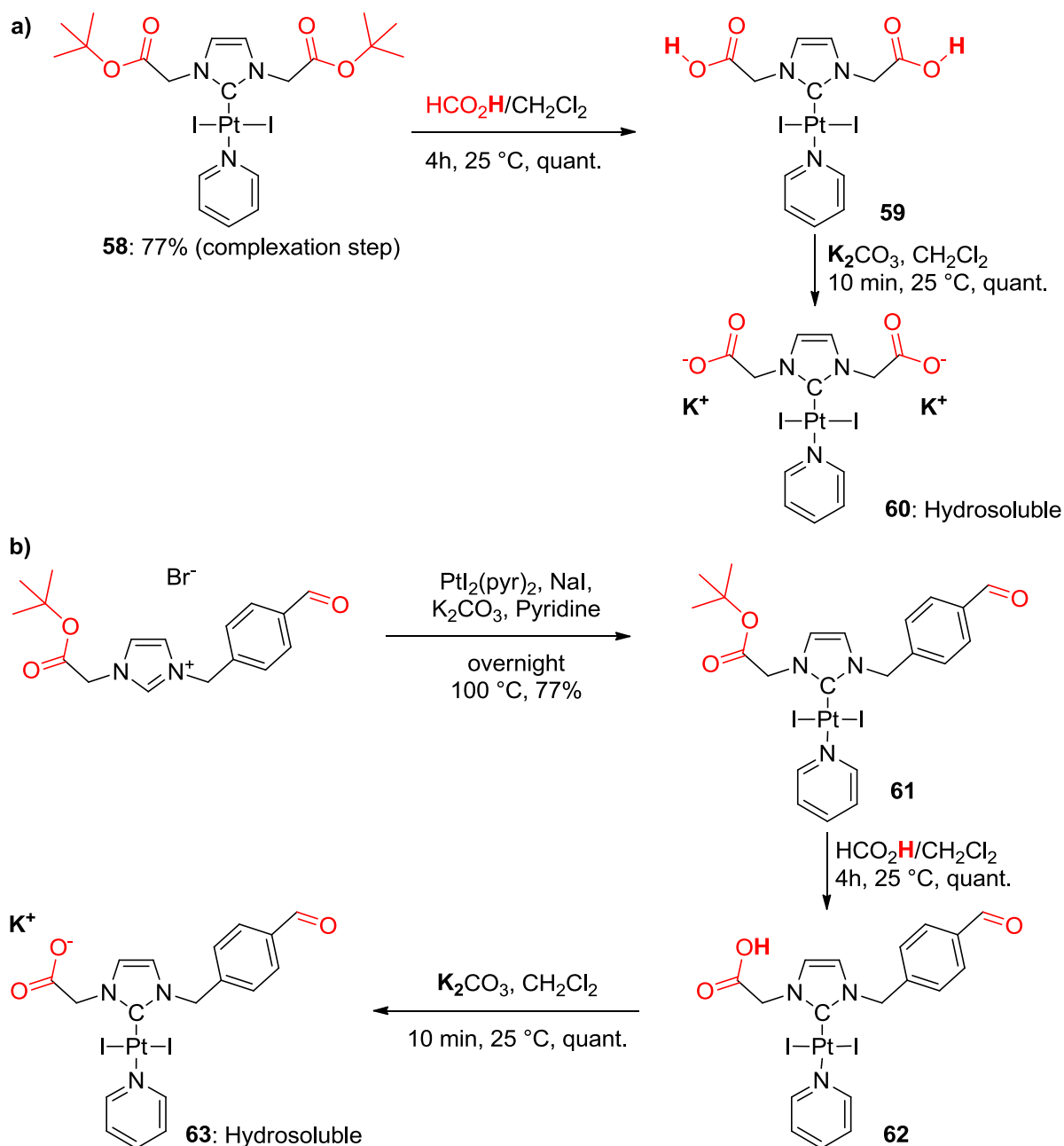


Figure 51: Synthesis of di-carboxylic acid and carboxylic acid-benzaldehyde complexes

Besides bringing in the *tert*-butyl esters to the NHC, we also introduced *tert*-butyl ester protected amino acids. A mixture of two equivalents of *L*-glutamic acid derivative (H-*L*-Glu(*t*Bu)-OtBu*HCl), PtCl₂ in presence of sodium iodide and potassium carbonate in pyridine afforded **64** in 43% yield (Figure 52). During the course of the reaction, the amino ester exchanged the pyridine ligand of [(NHC)PtI₂(pyridine)] formed *in situ*. Unfortunately, deprotection reaction conducted to an unidentifiable mixture.

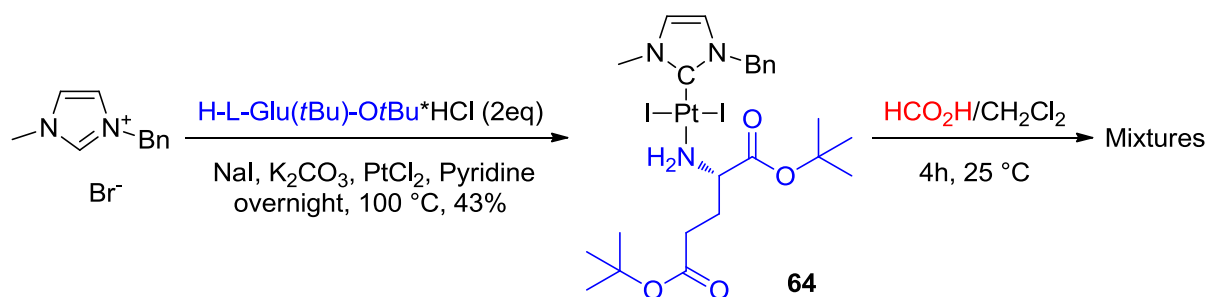


Figure 52: Synthesis of [(NHC)Pt₂(L-Glutamic acid di-*t*-butyl ester)] **64 by in situ ligand exchange**

Single crystals, obtained by diffusion of pentane in concentrated dichloromethane solutions of the acetonitrile complex **50** and the methyl ester complex **52**, were analysed by X-ray diffraction confirming the absence of coordination by the nitrile nitrogen respectively the ester group (**Figure 53**). The nitrile and ester groups are not changing significantly the Pt-ligand bond lengths (**Table 3**). Both complexes adopt the expected square planar geometry with *trans* configuration of the NHC toward the pyridine ligand. The biological properties of these compounds will be described in chapter 5.1.2. *Cytotoxicity of prefunctionalized [(NHC)PtI₂(amine)] complexes.*

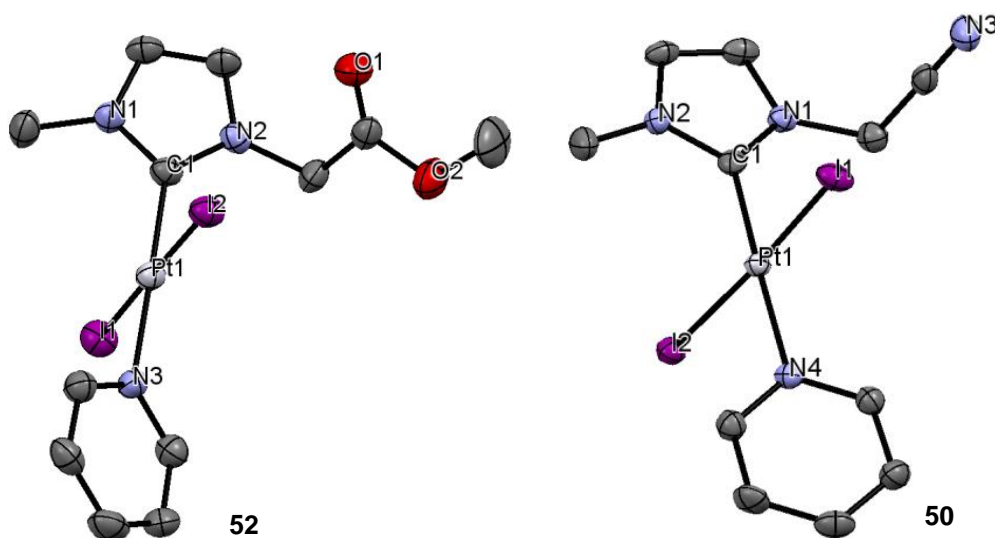


Figure 53: X-ray structure of methyl-ester functionalized platinum complex **52 and of acetonitrile substituted NHC Pt complex **50**.**

Complexes	C-Pt	Pt-N _{pyr}	Pt-I	N-C-Pt-I	C=O	C(O)-O	O-C=O	C≡N
50	1.959	2.084	2.604, 2.606	72.77, 103.26	/	/	/	1.141
52	1.977	2.093	2.601, 2.604	76.82, 104.84	1.190	1.340	125.25	/

Table 3: Selected bond lengths (Å) and angles (°) of complexes **50** and **52**

Palladium (carboxylic-NHC) complexes **65-68** were also synthesized (**Figure 54**). The cyclohexylamine complex **67** was obtained by ligand exchange. Noteworthy, in contrast to complex **55**, the expected ester was obtained in this case. This can be attributed to the less harsh conditions (25 °C). These compounds were water-soluble while deprotect. Water-soluble transition metal complexes are of great interest for applications as catalysts in water (by far the most inoffensive and cheapest solvent).²⁶⁵ Different strategies are reported to render NHC-complexes water-soluble: either using ionic (mostly cationic) ligands, or attach polar²²⁹ or charged functional groups: for example sulfonates,²⁶⁶ or protonated amines²⁶⁷. To test the catalytic activity of our complexes functionalized with free carboxylic acids, copper-free Sonogashira²⁶⁸ reaction in water²⁶⁹ was carried out. Using 1-iodo-4-nitrobenzene and ethynylbenzene with only 1% of palladium catalyst **66**, 1-nitro-4-(phenylethynyl)benzene was obtained (**Figure 55**). Organic products were extracted by ethyl acetate, evaporated and analysed by NMR and GC-MS. C-C coupling results can be found in **Table 4**.

²⁶⁵ For the concept of water soluble complexes, see: Herrmann, W. A.; Kohlpaintner, C. W. *Angew. Chem. Int. Ed. Engl.* **1993**, 32, 1524.

²⁶⁶ Azua, A.; Sa, S.; Peris, E. *Chem. Eur. J.* **2011**, 17, 3963; Czégényi, C. E.; Papp, G.; Kathó, Á.; Joó, F. *J. Mol. Catal. A: Chem.* **2011**, 340, 1; Türklen, H.; Çetinkaya, B.; *J. Mol. Catal. A: Chem.* **2011**, 348, 88; Silbestri, G. F.; Flores, J. C.; De Jesús, E. *Organometallics* **2012**, 31, 3355.

²⁶⁷ Özdemir, I.; Yiğit, B.; Çetinkaya, B.; Ülkü, D.; Tahir, M. N.; Arıcı, C. *J. Organomet. Chem.* **2001**, 633, 27.

²⁶⁸ For palladium catalysed coupling reactions, see: Valente, C.; Çalimsiz, S.; Hoi, K. H.; Mallik, D.; Sayah, M.; Organ, M. *G. Angew. Chem. Int. Ed.* **2012**, 51, 3314.

²⁶⁹ Samantaray, M. K.; Shaikh, M. M.; Ghosh, P. *J. Organomet. Chem.* **2009**, 694, 3477; Wang, X.; Zhang, J.; Wang, Y.; Liu, Y. *Cat. Comm.* **2013**, 40, 23; John, A.; Modak, S.; Madasu, M.; Katari, M.; Ghosh, P. *Polyhedron*, **2013**, 64, 20.

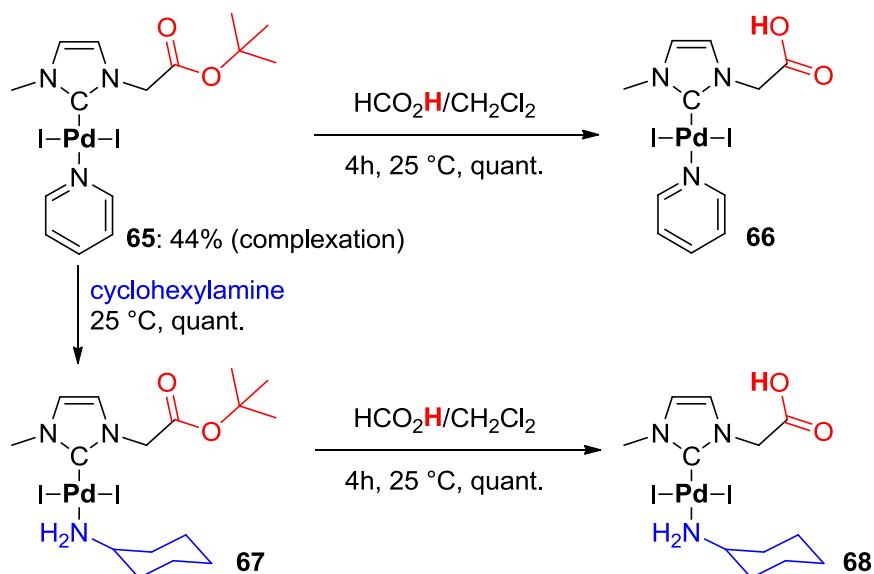


Figure 54: Synthesis of tert-butyl ester and carboxylic acid NHC palladium complexes

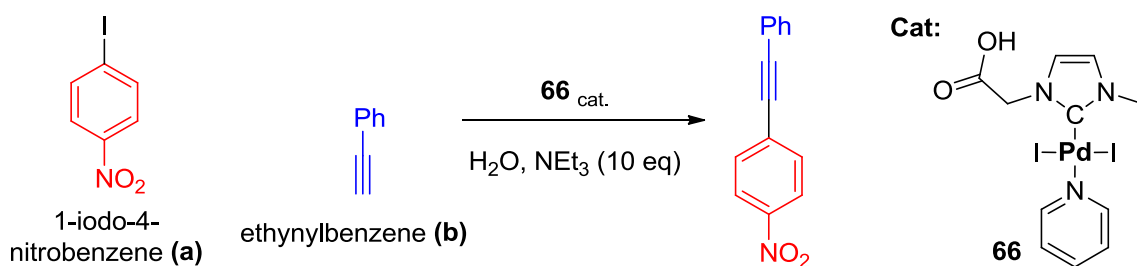


Figure 55: Copper-free Sonogashira catalyzed by a carboxylic acid NHC palladium complex

Entry	b/a	% of 66	T (°C)	Time	% of coupling product	Unreacted (a) recovered
1	1/1	1.5	40 °C, then 25 °C	1 day, then 3 days	71%*	26%
2	1/1	1	80 °C	overnight	11%	89%
3	2/1	1	60 °C	overnight	37%	61%
4	1/1	1	40 °C	2 days	90%	10%

Table 4: Conditions tested for Sonogashira reaction: conversion measured by GC-MS (* isolated product)

Entry 2 and 3 suggest that increase of temperature resulted in a decrease of yields, probably caused by catalyst decomposition (entry 2). Heating 2 days at 40 °C gave coupling product in 90% yield without other side products except starting material 1-nitro-4-(phenylethynyl)benzene (entry 4). The ease of synthesis in only two steps and their stability in water and air make our palladium NHC complexes

user-friendly. These preliminary non-optimized results are promising to extend further the scope of these soluble complexes in various C-C coupling reactions.

2.2.4 Pt-NHC complexes functionalized by aldehydes and acetals

Aldehyde function is of special interest since it allows a relatively easy derivatization through imine (hydrazone, oxime) formation, as depicted out in section 4.2. *Post-synthetic modification of NHC-Pt complexes.*

We first studied the direct attachment of formyl functionality to the alkene backbone of the NHC moiety. 1,3-dibenzyl-5-formyl-1H-imidazol-3-ium bromide was directly obtained from 4-imidazolecarboxaldehyde in base free-conditions (**Figure 56**).²⁷⁰ Complexation attempts afforded a 1/1 mixture of desired complex **69** and the decarbonylated product **70**. The polarity of both complexes is similar making impossible the separation by classical silica gel chromatography. The same reaction in cyclohexylamine gave decomposition products.

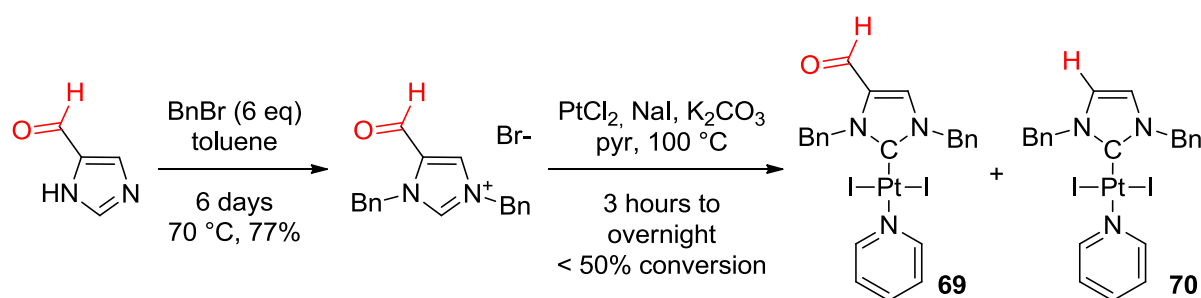
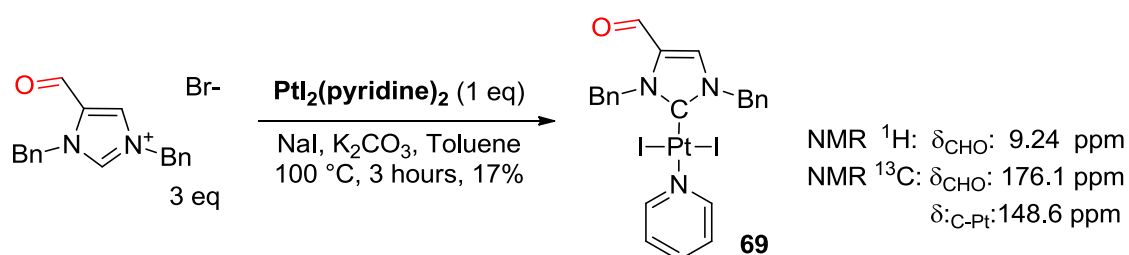


Figure 56: Unsuccessful (CHO)-NHC-Pt(II)-pyridine synthesis attempts

As the imidazolium salt was found to be instable under strong basic conditions,²⁷¹ the reaction conditions were optimized to reduce the presence of free carbene. Poorly soluble PtCl_2 was replaced by the more soluble $\text{PtI}_2(\text{pyr})_2$. Anhydrous toluene was chosen as solvent and the mixture of NaI, K_2CO_3 , $\text{PtI}_2(\text{pyr})_2$ with an excess of imidazolium salt were heated for only three hours at 100 °C. Under pyridine-free conditions, decarbonylation side reaction could be prevented and the carbonyl complex **69** obtained albeit in poor yield (17%) (**Figure 57**). The short reaction time helped to prevent side reactions; however, a majority of the imidazolium precursor did not react.

²⁷⁰ Crandall, I. E.; Szarek, W. A.; Vlahakis, J. Z. **2011**, WO2010025558, pages 80-81.

²⁷¹ Stability was tested in THF with different bases (NaOH/H₂O, pyridine or K_2CO_3) yielding decomposition products.

Figure 57: Synthesis of $[(\text{CHO-NHC})\text{Pt(II)}(\text{pyridine})]$ under mild conditions

NHC carbenes are well established as organic catalysts²⁷² for benzoin²⁷³ or Stetter²⁷⁴ reactions.²⁷⁵ The decarbonylation of our formyl imidazolium can be explained by a mechanism with autocatalytic action of our product. Probably, the reaction passes either through a Breslow-type intermediate²⁷⁶ thus giving directly decarbonylated compound by release of carbon monoxide, or conjugation of a NHC to a second molecule by 1,4 addition on the α,β -unsaturated carbonyl.²⁷⁷ By blocking position 5 on the backbone, decarbonylation reaction should be foreclosed if decarbonylation is passing by second mechanism. Two methyl-substituted formyl imidazolium salts were synthesized starting from 4-methyl-1H-imidazole-5-carbaldehyde (**Figure 58**). Both proligands gave the desired pyridine complexes **71-74** in good yields (72-89%) indicating that position 5 protection successfully inhibits decarbonylation.

X-ray diffraction studies on (1,3,5-trimethyl-2,3-dihydro-1H-imidazolylidene-4-carbaldehyde)PtI₂-pyridine **72** established the molecular structure of the compound (**Figure 59**). A notable difference of bond length was noticed compared to a “simple” imidazolylidene platinum (II) complex (e.g. **14**): C=C double bond of formyl complex **72** (1.368 Å) is elongated compared to **14** (1.326 Å) probably due to electronic conjugation with C=O.

²⁷² These catalysts are also present in living systems: thiamine diphosphate, a thiazolium derivative, is a coenzyme for different enzymes: Schenk, G.; Duggleby, R. G.; Nixon, P. F. *Int. J. Biochem. Cell Biol* **1998**, *30*, 1297; Zhao, H.; Foss, F. W.; Breslow, R. *J. Am. Chem. Soc.* **2008**, *130*, 12590.

²⁷³ Enders, D. Kalfass, U. *Angew. Chem. Int. Ed.* **2002**, *41*, 1743; Gao, G.; Yuan, Y.; Zhou, C.-H.; You, J.; Xie, R.-G. *J. Chem. Res.* **2002**, 262.

²⁷⁴ Rong, Z.-Q.; Li, Y.; Yang, G.-Q.; You, S.-L. *Synlett*, **2011**, 7, 1033.

²⁷⁵ Enders, D.; Balensiefer, T. *Acc. Chem. Res.* **2004**, *37*, 534; Bugaut, X.; Glorius, F. *Chem. Soc. Rev.* **2012**, *41*, 3511.

²⁷⁶ Wittig, G.; Davis P.; Koenig, G. *Chem. Ber.* **1951**, *84*, 627; Seebach, D. *Angew. Chem. Int. Ed.* **1979**, *18*, 239; Berkessel, A.; Elfert, S.; Yatham, V. R.; Neudörfl, J.-M.; Schlörer, N. E.; Teles, J. H. *Angew. Chem. Int. Ed.* **2012**, *51*, 12370.

²⁷⁷ Berkessel, A.; Elfert, S.; Etzenbach-Effers, K.; Teles, J. H. *Angew. Chem.* **2010**, *122*, 7275.

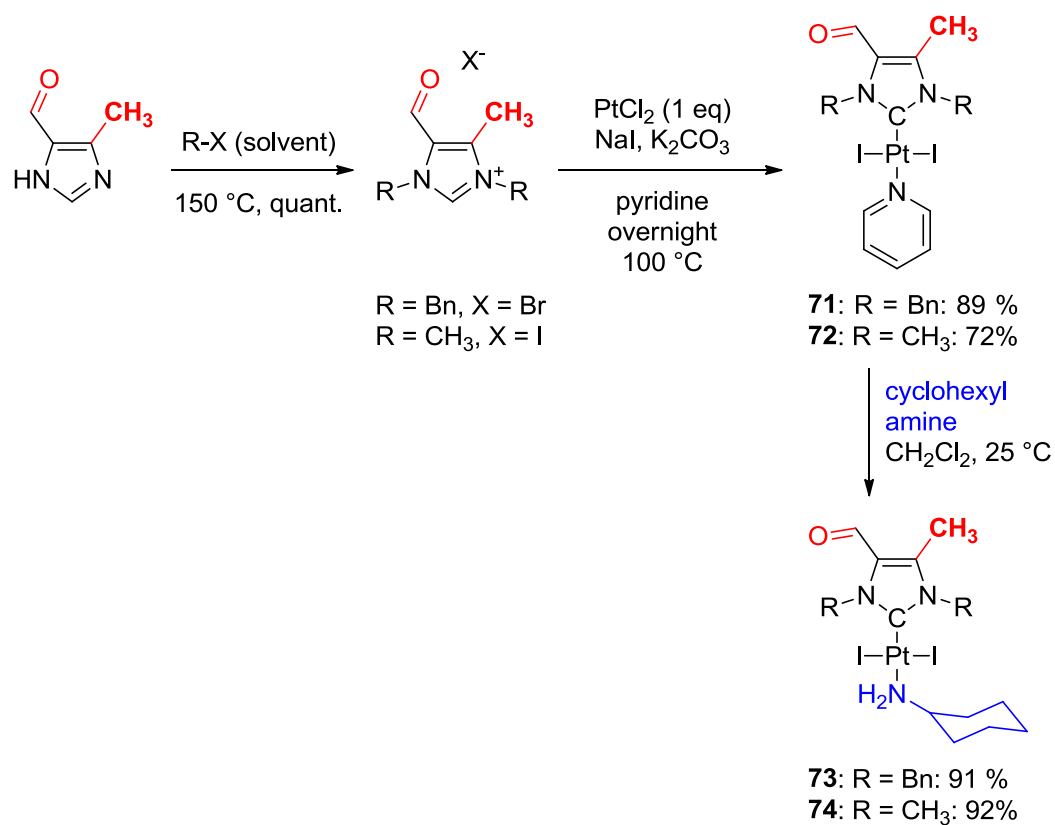


Figure 58: NHC-platinum complexes 71-74 derived from 4-methyl-1H-imidazole-5-carbaldehyde

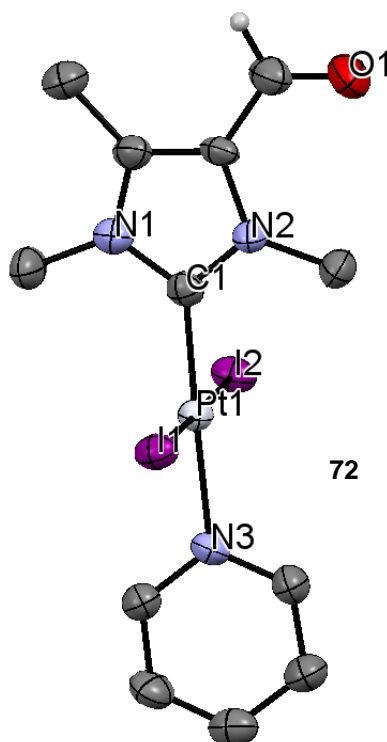


Figure 59: X-ray structure of 72. Selected bond lengths (Å) and angles (°): C-Pt: 1.963; N_{pyr}-Pt: 2.092; Pt-I: 2.596, 2.602; C=O: 1.209; N-C-N: 105.28; C-Pt-I: 89.04, 89.81; (N-C)_{NHC}-(N-C)_{Pyr}: 11.91

To access *N*-substituted aldehydes, we decided to introduce acetal-protected carbonyls as a valuable function for further functionalization. Various silver (I) and gold (I) mono acetal-NHC-complexes,²⁷⁸ silver (I), nickel (II) and palladium (II) diacetal complexes,²⁷⁹ acetal-benzimidazol-2-ylidene-Ag (I) complexes,²⁸⁰ or palladium (II) acetal complexes²⁸¹ are already known in literature. We obtained the acetal substituted NHC complex **75** with classical yield (56%) from 3-(2,2-diethoxyethyl)-1-methyl-1H-imidazol-3-ium bromide (**Figure 60**). Acetal function appeared to be inert under the employed reaction conditions.

²⁷⁸ Leitner, S.; List, M.; Monkowius, U. *Z. Naturforsch.* **2011**, 66b, 1255.

²⁷⁹ Yang, W.-H.; Lee, C.-S.; Pal, S.; Chen, Y.-N.; Hwang, W.-S.; Lin, I. J. B.; Wang, J.-C. *J. Organomet. Chem.* **2008**, 693, 3729.

²⁸⁰ Özdemir, İ.; Gürbüz, N.; Doğan, Ö.; Günel, S.; Özdemir, İ. *Appl. Organometal. Chem.* **2010**, 24, 758; Doğan, Ö.; Kaloğlu, N.; Demir, S.; Özdemir, İ.; Günel, S.; Özdemir, İ. *Monatsh. Chem.* **2013**, 144, 313.

²⁸¹ Özdemir, İ.; Gürbüz, N.; Kaloğlu, N.; Doğan, Ö.; Kaloğlu, M.; Bruneau, C.; Doucet, H. *Beilstein J. Org. Chem.* **2013**, 9, 303.

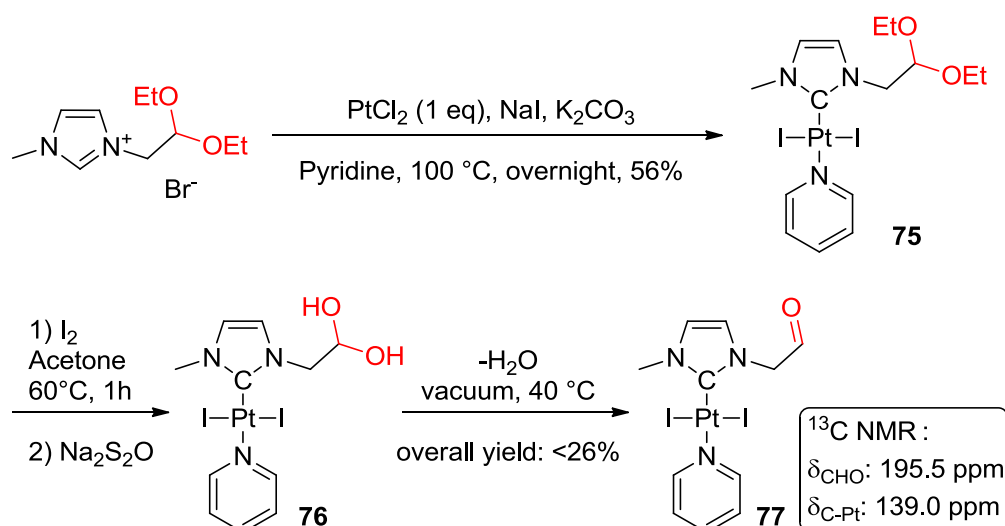


Figure 60: Synthesis and hydrolysis attempts of an acetal substituted NHC platinum complex

Various tests were conducted to hydrolyse the acetal moiety into aldehyde. Classical acid deprotection (HCl) at 60 °C gave the impure dihydroxy product **76**. By water elimination, aldehyde complex **77** could be obtained accompanied by by-products. To try a less harsh deprotection with iodine, acetal complex was heated at 60 °C in acetone;²⁸² excess of I_2 was removed by washing with $\text{Na}_2\text{S}_2\text{O}_3(\text{aq})$. Overnight drying under vacuum at 40 °C finally gave the desired aldehyde complex **77** (accompanied by small amount of **76**). This aldehyde complex seems to be of limited stability under anhydrous conditions, but immediately reacts in presence of traces of water to dihydroxy analogue. The hygroscopic nature of NHC-aldehyde complexes is in agreement with the work of Yang *et al.* showing an equilibrium between aldehyde and dihydroxy NHC palladium complexes.²⁷⁹ Youngs and co-workers also reported a stable silver NHC *gem*-diol.²⁸³ To obtain a more stable complex than the pyridine derivative, we synthesized the cyclohexylamine complex **78** in 49% yield (**Figure 61**). Deprotection attempts ($\text{HCl}/\text{H}_2\text{O}$ or wet SiO_2) also afford a mixture of dihydroxy complex, impurities and desired aldehyde.

Condensation reactions²⁸⁴ of the platinum aldehyde with cyclohexylamine, aniline, phenylhydrazine or methylhydrazine result in unidentifiable mixtures. Cyclohexylamine in large excess in presence of a drying agent (Na_2SO_4) did not lead to the desired condensation reaction. The pyridine was totally exchanged by the cyclohexylamine and the acetal group was partly deprotected. Thus, a mixture of both cyclohexyl-platinum-aldehyde and cyclohexyl-platinum-dihydroxy complexes was obtained.

²⁸² Sun, J.; Dong, Y.; Cao, L.; Wang, X.; Wang, S.; Hu, Y. *J. Org. Chem.* **2004**, 69, 8932.

²⁸³ Melaiye, A.; Sun, Z.; Hindi, K.; Milsted, A.; Ely, D.; Reneker, D. H.; Tessier, C. A.; Youngs, W. J. *J. Am. Chem. Soc.* **2005**, 127, 2285.

²⁸⁴ For detailed description of condensation and ligand exchange reactions, see chapter 4. *Introducing diversity in NHC-Platinum complexes: Post-synthetic derivatization*.

A single crystal suitable for X-ray diffraction of the acetal complex **78** was obtained (**Figure 61**). Again, the molecular structure confirms the square planar geometry of the platinum. No interactions between the metal and the oxygen atoms of the acetal were revealed in solid state.

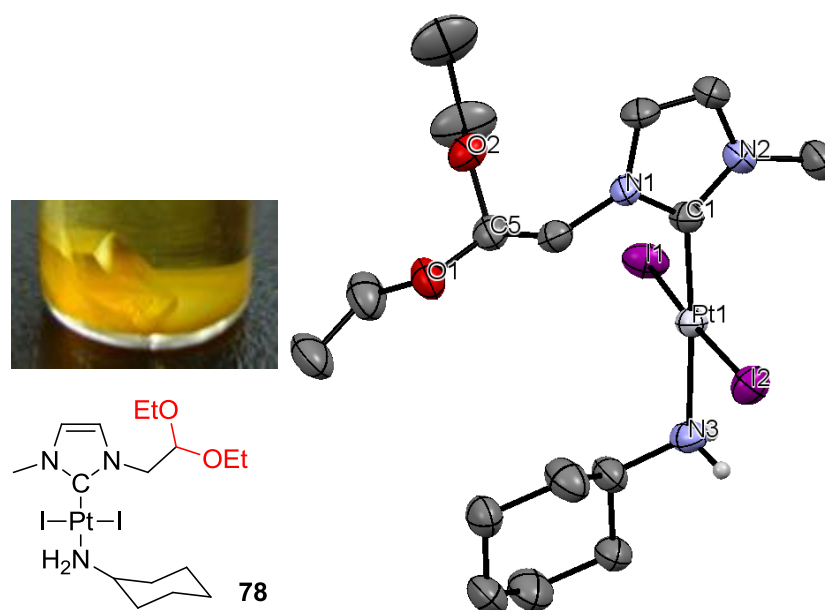


Figure 61: Single crystal X-ray structure of $[(\text{acetal-NHC})\text{PtI}_2(\text{cyclohexylamine})]$ **79**. Selected bond lengths (Å) and angles (°): C-Pt: 1.981; Pt-I: 2.595, 2.602; Pt-N: 2.128; C-Pt-N: 175.97; C-Pt-I: 90.03, 91.50; N-C-N: 105.46; N-C-Pt-I: 79.08, 95.97;

The difficulty of deprotecting the acetal and especially the tendency of the aldehyde located close to the imidazolidine to form a dihydroxy compound obliged us to develop another synthetic strategy.

As shown for $[(\text{CHO-NHC})\text{Pt}(\text{II})(\text{pyr})]$ complex **69**, a direct linkage between imidazolidine moiety and the formyl should be avoided. Therefore, both functionalities should be separated by a linker entity. First, 4-halogenobenzaldehydes were tried as starting product. 4-bromobenzaldehyde did not yield the desired products neither with methylimidazole at 130 °C nor imidazole in presence of supported copper catalyst $\text{Cu}(\text{II})\text{NaY}$ and potassium carbonate under microwave irradiation following a reported procedure (Ullman reaction) (**Figure 62, a and b**).²⁸⁵ Finally, desired 4-(1H-imidazol-1-yl)benzaldehyde was obtained by refluxing 4-fluorobenzaldehyde with imidazole, anhydrous K_2CO_3 and catalytic amount of Aliquat 336 (Starks' catalyst, a phase transfer agent) in DMF (**Figure 62, c**).²⁸⁶ The 4-(1H-imidazol-1-yl)benzaldehyde could be further alkylated with 2 different halogenoalkanes (MeI, BnBr) to give the corresponding azolium salts.

²⁸⁵ Fouchet, J.; Douce, L.; Heinrich, B.; Welter, R.; Louati, A. *Beilstein J. Org. Chem.* **2009**, *5*, 51.

²⁸⁶ Liang, Z.-Q.; Wang, C.-X.; Yang, J.-X.; Gao, H.-W.; Tian, Y.-P.; Tao, X.-T.; Jiang, M.-H. *New J. Chem.* **2007**, *31*, 906.

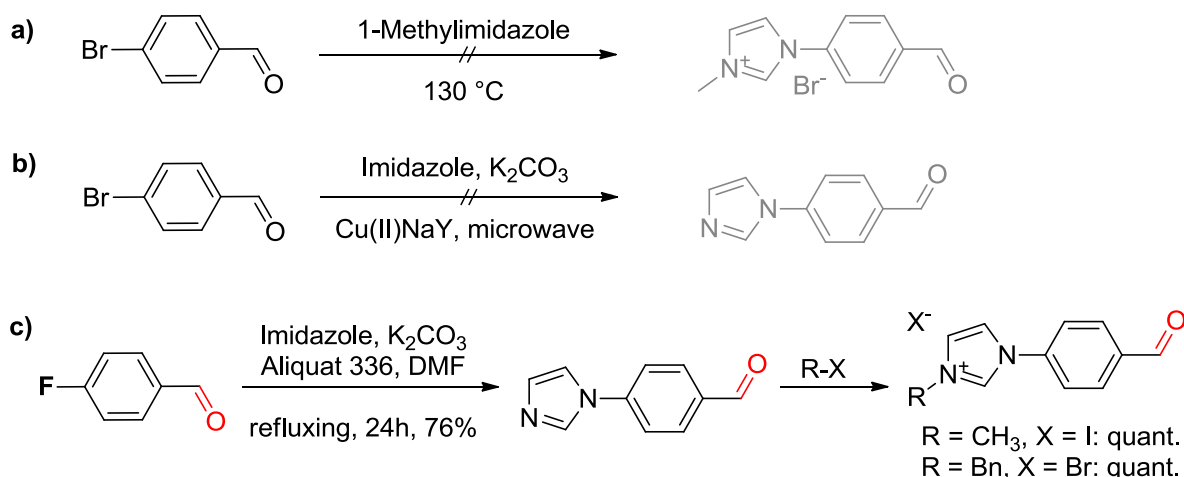


Figure 62: Trials to obtain imidazole-benzaldehyde derivatives by a) reaction with methylimidazole, b) Ullman coupling and c) from fluorobenzaldehyde

We have also synthesized imidazolium compounds featured with a CH_2 -benzaldehyde group. The starting material (4-(diethoxymethyl)phenyl)methanol was obtained following a reported procedure (**Figure 63**).²⁸⁷ Bromination with PBr_3 did not give the expected bromo acetal derivative, but deprotection of the acetal group (pathway a). This compound, after mesityl activation, reacted with methylimidazole in the presence of NaI to afford the desired azolium salt. To optimize the overall yield, bromination step was carried out with SOBr_2 , which also deprotect the acetal in only one-step (pathway b). 4-(bromomethyl)benzaldehyde is obtained quantitatively as a white powder and reacts quantitatively with 1-methylimidazole to afford the proligand 3-(4-(formylbenzyl)-1-methyl-1H-imidazol-3-ium bromide, a white powder. This three-step pathway **b**) works up to gram scale (2.5 g, 9 mol).

²⁸⁷ Sarri, P.; Venturi, F.; Cuda, F.; Roelens, S. *J. Org. Chem.* **2004**, 69, 3654.

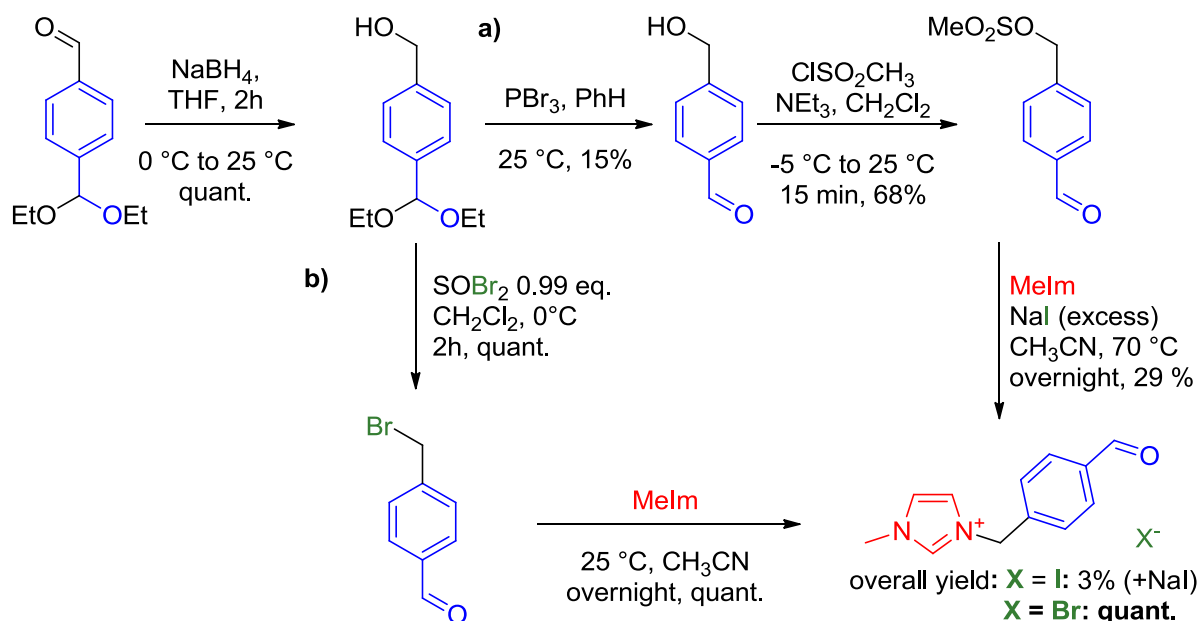


Figure 63: Synthesis of 3-(4-formylbenzyl)-1-methyl-1H-imidazol-3-ium halide (Melm = 1-methylimidazole)

A third imidazolium-benzaldehyde molecule was investigated. In this molecule, a $\text{CH}_2\text{CH}_2\text{O}$ -bridge connects the benzaldehyde to the imidazolium core (Figure 64). 4-(2-bromoethoxy)benzaldehyde, obtained according to reported procedure,²⁸⁸ reacts quantitatively with 1-methylimidazole to 3-(2-(4-formylphenoxy)ethyl)-1-methyl-1H-imidazol-3-ium bromide.

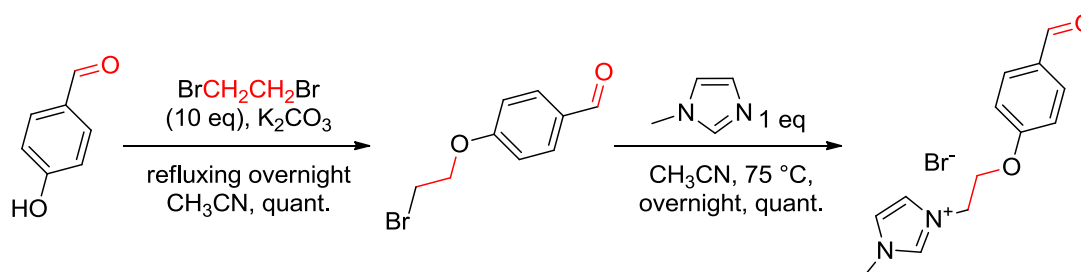


Figure 64: Two-step synthesis of 3-(2-(4-formylphenoxy)ethyl)-1-methyl-1H-imidazol-3-ium bromide

A first complexation test was done with 3-(4-formylbenzyl)-1-methyl-1H-imidazol-3-ium iodide, PtCl_2 , K_2CO_3 and NaI in pyridine at 100 °C giving complex **79** in only 12% yield (Figure 65, a). The same reaction with cyclohexylamine as solvent gave the expected complex **81** with better yield (33%) (b). Longer reaction times did not increase yields. Ligand exchange reaction of the labile pyridine by cyclohexylamine in excess conducted to the desired ligand exchange, but at the same time also to an

²⁸⁸ Gimenez-Lopez, M. del C.; Räisänen, M. T.; Chamberlain, T. W.; Weber, U.; Lebedeva, M.; Rance, G. A.; Briggs, G. A. D.; Pettifor, D.; Burlakov, V.; Buck, M.; Khlobystov, A. N. *Langmuir* **2011**, 27, 10977.

imine condensation of the cyclohexylamine **80** (c).²⁸⁹ Formation of same imine product **80** during direct synthesis of **81** (pathway b) was confirmed by analysis of crude reaction (pathway d). Imine product **80** could be isolated by chromatography column with triethylamine-deactivated silica gel ($\text{SiO}_2/\text{NEt}_3$, CH_2Cl_2), whereas the imine compound after second chromatography column with non triethylamine-deactivated silica gel (pathway e) gave the aldehyde complex **81** with 21% overall yield.

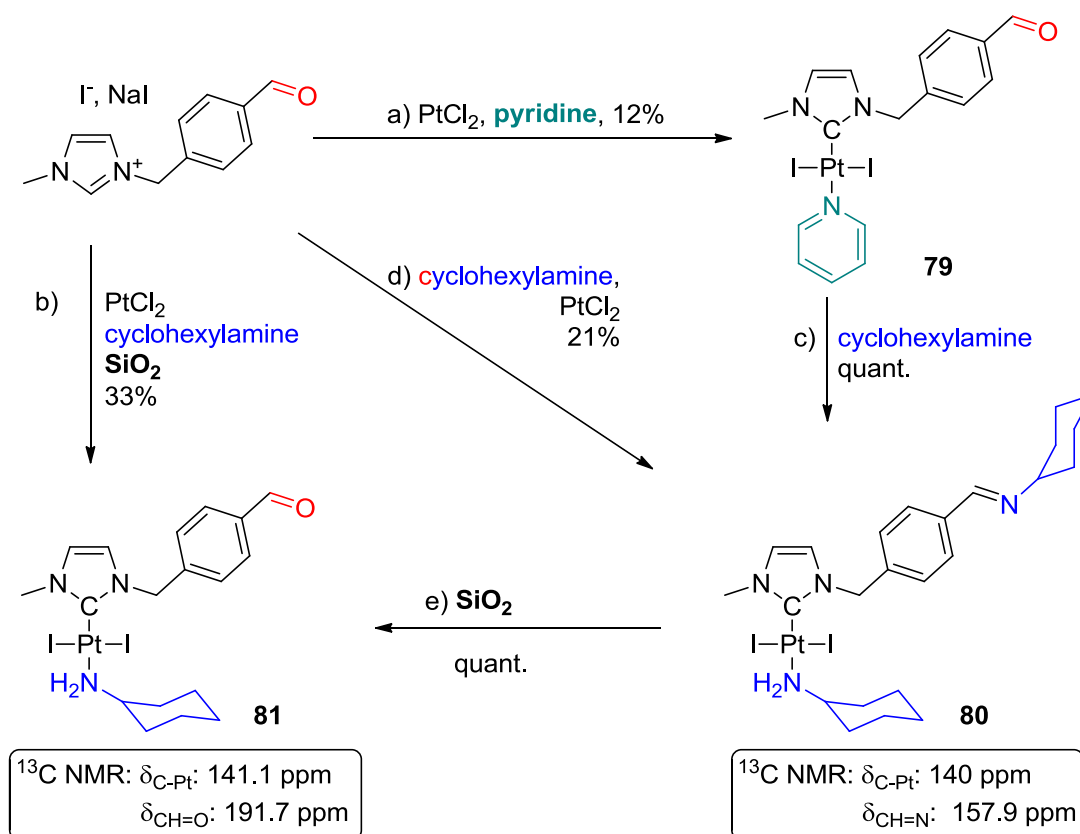


Figure 65: Synthesis of [(benzaldehyde-NHC)PtI₂(cyclohexylamine)] complex. Reactions conditions: a) PtCl_2 , NaI, K_2CO_3 , pyridine, overnight, 100 °C; b) and d) cyclohexylamine (solvent), NaI, K_2CO_3 , 100 °C, PtCl_2 c) cyclohexylamine (solvent), Na_2SO_4 , 25 °C, overnight e) SiO_2 , CH_2Cl_2 , 25 °C

²⁸⁹ Ligand exchange reactions and imine condensation are described in detail in chapter 4.1. *Ligand exchange* and 4.2.2. *Post-synthetic modification of NHC complexes by imine*.

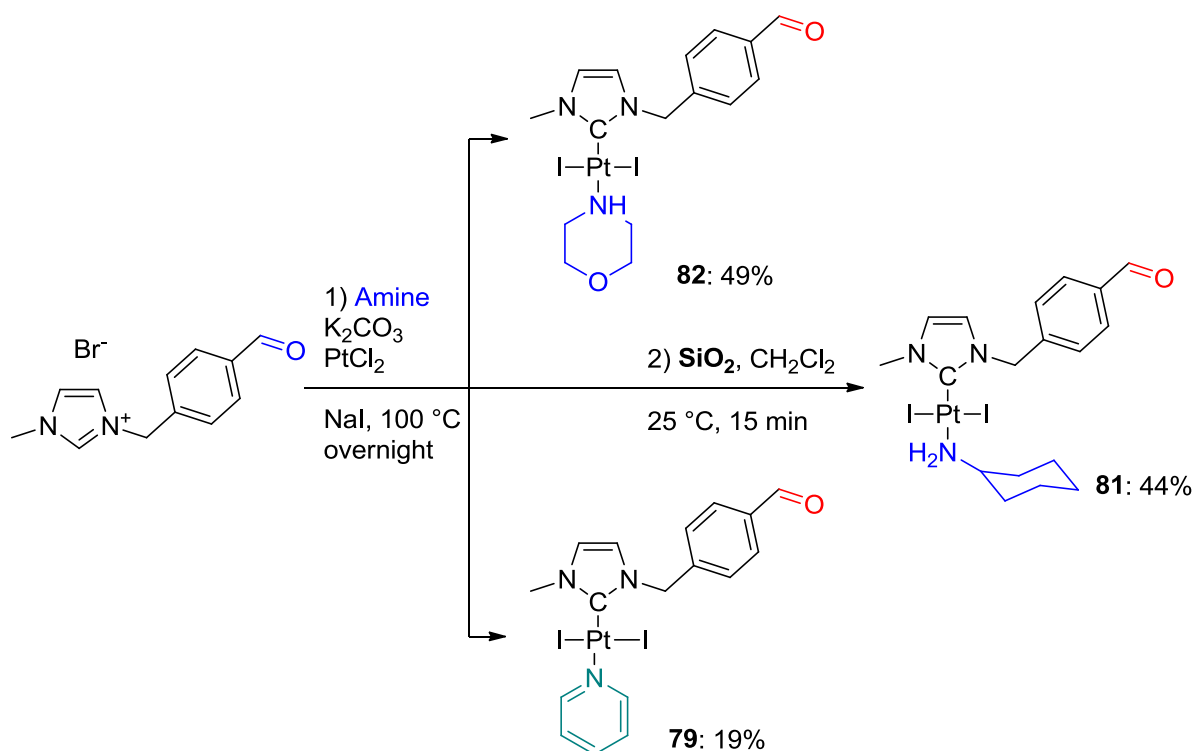


Figure 66: Synthesis of [(benzaldehyde-NHC)PtI₂(amine)] complexes **79**, **81** and **82** from 3-(4-formylbenzyl)-1-methyl-1H-imidazol-3-ium bromide

The complexation reaction of $PtCl_2$ with 3-(4-formylbenzyl)-1-methyl-1H-imidazol-3-ium iodide only gave the corresponding complex **79** in moderate yield (**Figure 65, a**). 3-(4-formylbenzyl)-1-methyl-1H-imidazol-3-ium bromide afforded [(benzaldehyde-NHC)PtI₂(cyclohexylamine)] complex **81** in good yield (44%), but only 19% of [(benzaldehyde-NHC)PtI₂(pyr)] complex **79** (**Figure 66**). The morpholine derivative **82** could be also obtained in a better yield (49%). Thus, we generally observed a significant lower yield for the reaction with pyridine (19%) when compared to amines, cyclohexylamine (44%) and morpholine (49%). *In situ*, these amines can form imine respectively iminium intermediates with the benzaldehyde group during the complexation reaction. To test the role as *in situ* formed protection groups, imidazolium imine was synthesized and allowed to react with platinum chloride in pyridine (**Figure 67**). The expected [(imine-NHC)PtI₂(pyridine)] complex was not obtained. Instead, only [(imine-NHC)PtI₂(cyclohexylamine)] complex **80** was isolated. This suggests the presence of an equilibrium between imine and aldehyde.

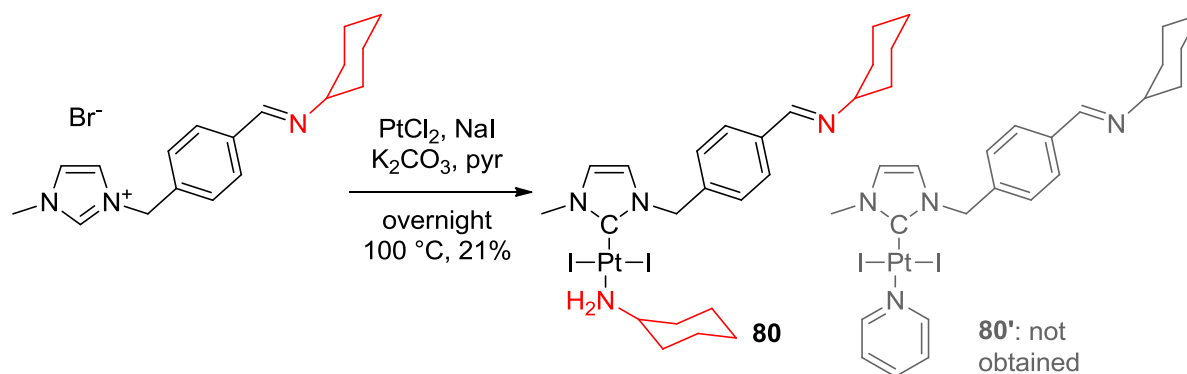


Figure 67: Reactivity of (E)-3-(4-((cyclohexylimino)methyl)benzyl)-1-methyl-1H-imidazol-3-ium bromide

The imine protection seems to be not inert. For this reason, an acetal-protected imidazolium proligand was investigated to avoid potential secondary reactions (**Figure 68**). Surprisingly, the acetal group was deprotected into aldehyde group during the case of the reaction. The [(benzaldehyde-NHC)PtI₂(pyr)] complex **79** is obtained in moderate yield (41%) comparable to other innocent imidazolium precursors. This result shows that in presence of carbene, the (benz)aldehyde is not an innocent function. Thus, it should be protected before the synthesis or *in situ* by imine formation to obtain higher yields. This is probably due to benzoin-type reactivity.

The reaction with more soluble platinum (II) precursors than PtCl₂ was investigated (reaction of the *in situ* formed carbene only with Pt) to favour complexation reaction rather than side reaction. Starting from PtCl₂(cod) (cod = 1,5-Cyclooctadiene), [(benzaldehyde-NHC)PtI₂(pyr)] **79** was obtained by good 80% yield. The enhanced solubility of this platinum source probably allows quickly trapping of the *in situ* formed carbene, thus preventing side reactions due to this aldehyde moiety.

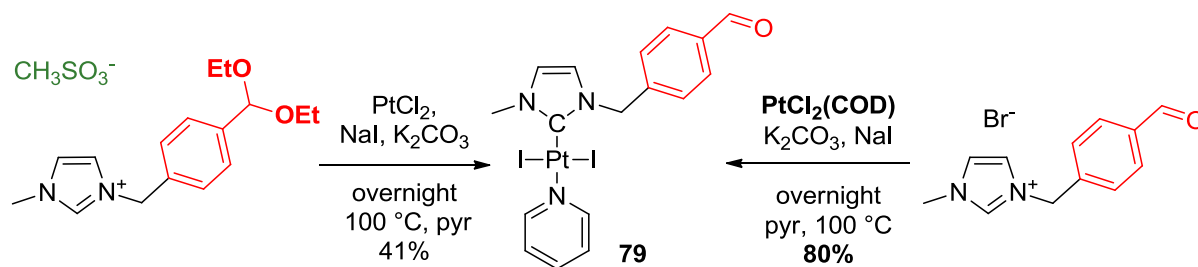


Figure 68: Optimized synthesis of [(benzaldehyde-NHC)PtI₂(pyr)] **79 from an acetal-protected imidazolium proligand, or from PtCl₂(cod)**

Finally, by using various imidazolium bromide salts and various neutral L ligands, a whole family of aldehyde complexes could be obtained (**Figure 69**). Five complexes **69**, **71-74** were obtained with formyl group directly on the NHC (a). Various *N*-substituted NHC-CH₂-benzaldehyde complexes **48**, **61**, **79**, **81-86** with three different L ligands (pyr, cyclohexylamine, morpholine) were obtained (b).

Four complexes **87-91** were bearing the benzaldehyde *via* a CH₂CH₂O linker (c). Benzimidazolylidene complex **92** could also be obtained (d) as well as NHC-benzaldehyde derivatives **93-94**.

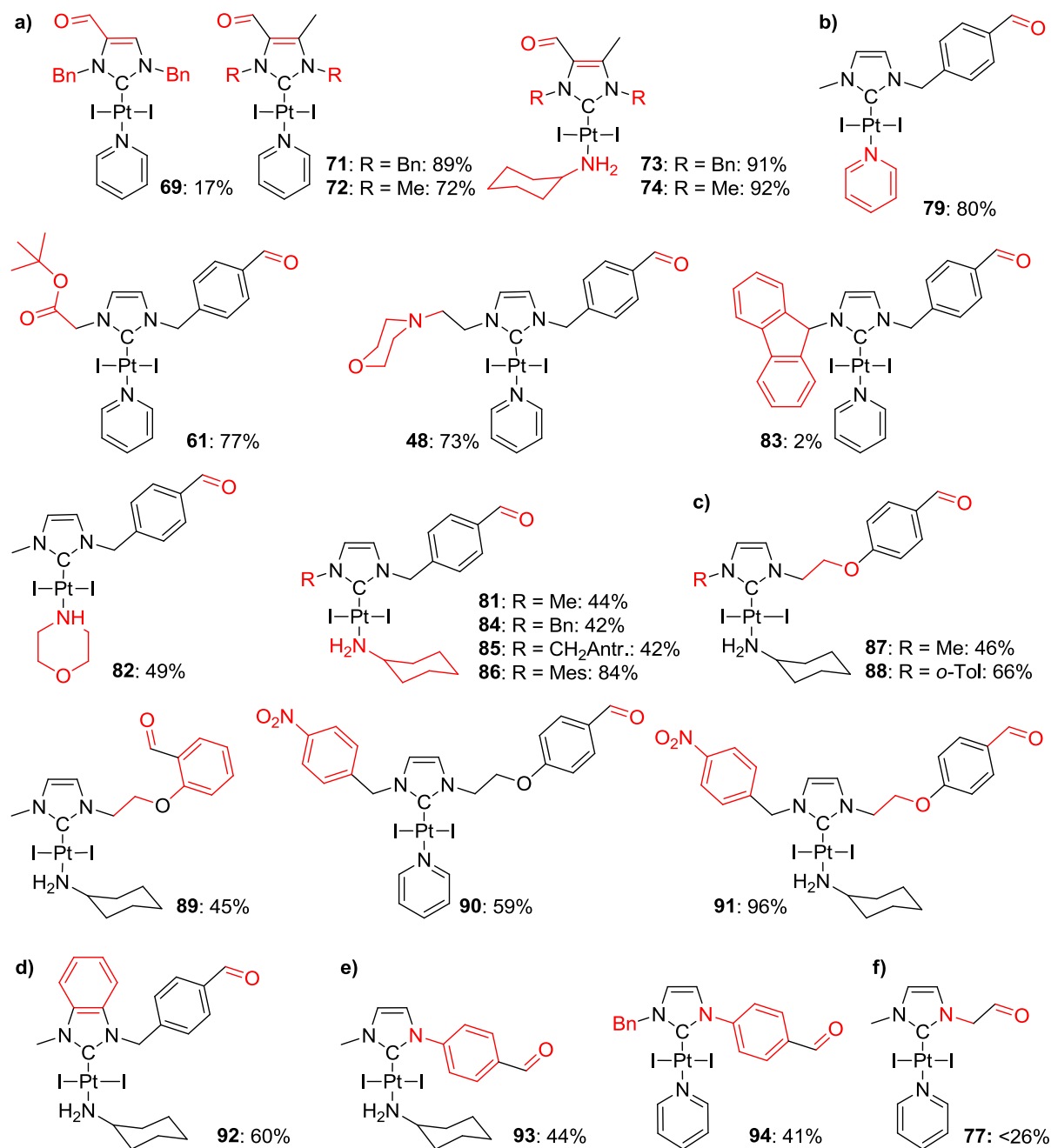


Figure 69: Diversity creation with benzaldehyde based NHC-Pt complexes (%: yield of complexation step)

Single crystals suitable for X-ray diffraction were obtained for two of these complexes (**79** and **94**) (**Figure 70**) confirming the classical arrangement around the metal. In the crystal packing, complex **79** shows an interaction between HC_{imidazolylidene} and the O_{carbonyl} of neighbouring molecule (Van der Waals radii C+O = 3.22Å > 3.123Å) conducting to a step-like arrangement.

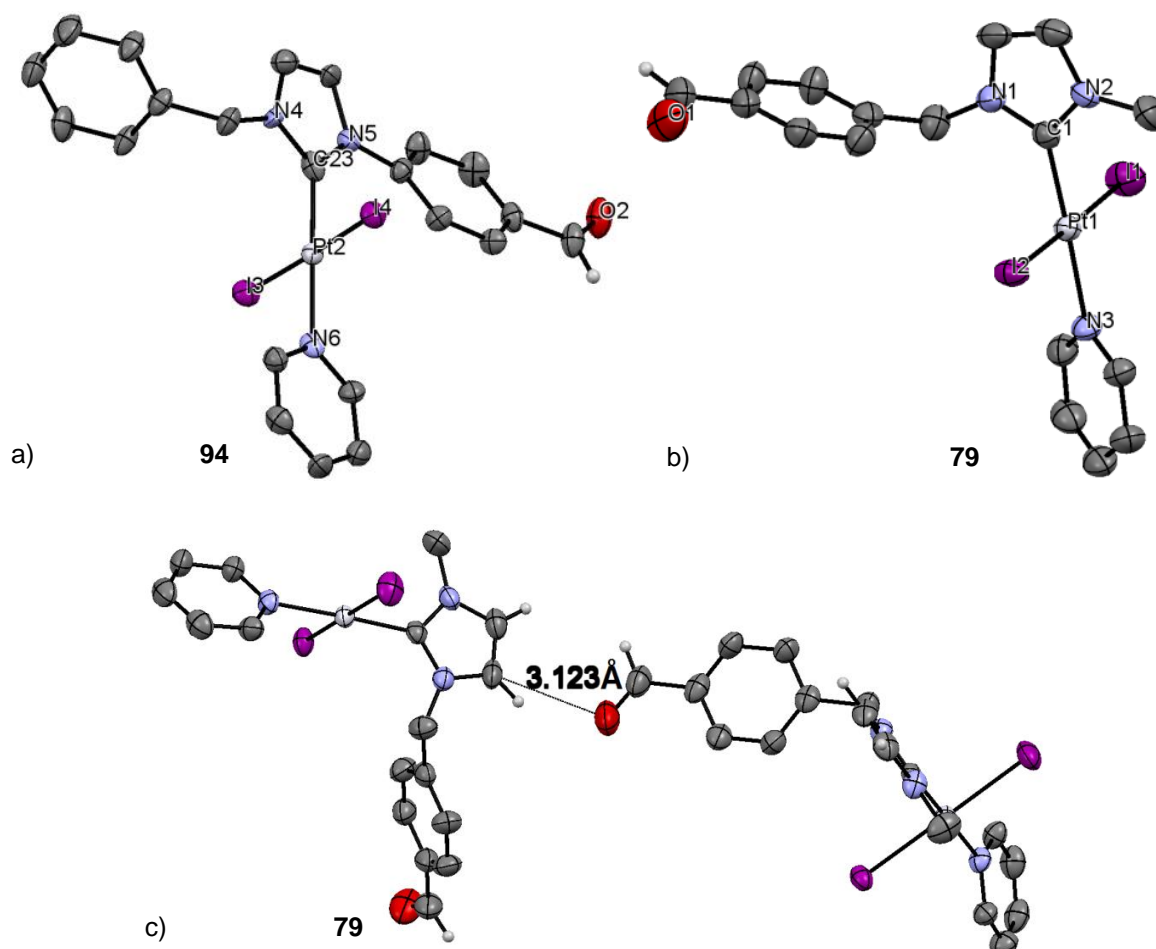


Figure 70: a, b) X-ray structures for two benzaldehyde-platinum-pyridine complexes 94 and 79, c) Interaction between HC_{imidazolylidene} and the O_{carbonyl} of complex 79

After successful complexation with platinum, coordination toward palladium was attempted to extend our strategy of benzaldehyde-featured precursors. The corresponding mono-NHC-benzaldehyde **93-95** and bis-NHC-benzaldehyde **98** palladium complexes were obtained with rather poor yields and showed a lower stability, especially in solution, compared to their platinum analogues (**Figure 71**).

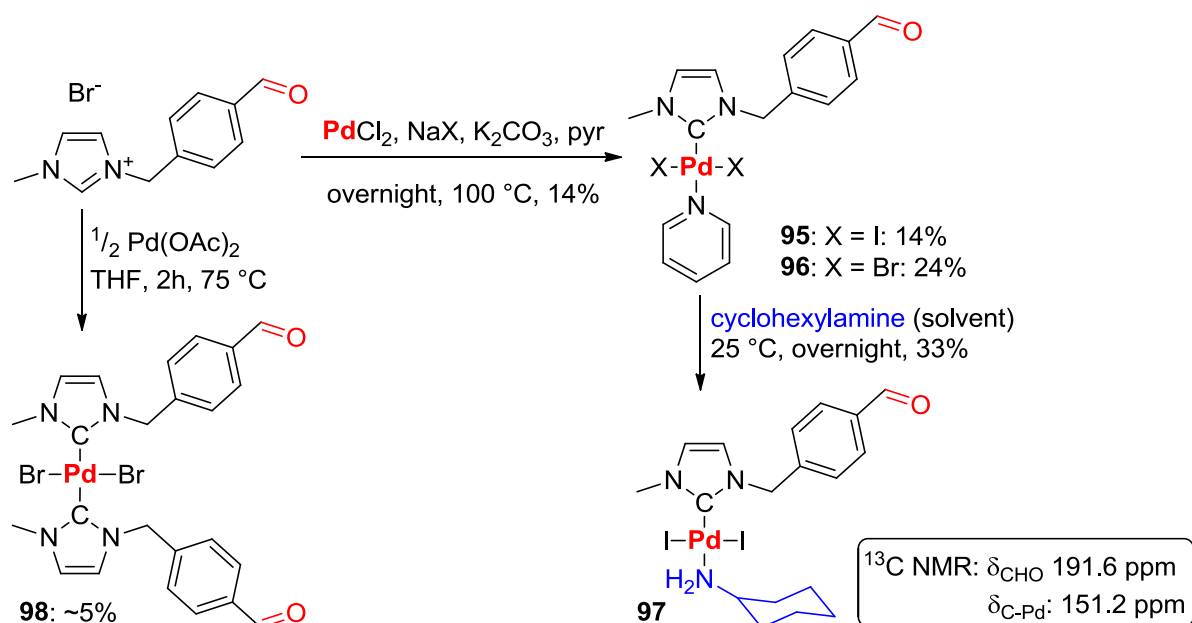


Figure 71: Synthesis of palladium-benzaldehyde complexes

[(Benzaldehyde-NHC) PdBr_2 (pyridine)] **96** gave crystals suitable for X-ray diffraction (**Figure 72**). The complex displays the expected square planar geometry. NHC and pyridine ligands adopt a *trans* location. This square planar complex also shows an interaction between $\text{HC}_{\text{imidazolylidene}}$ and $\text{O}_{\text{carbonyl}}$ of neighbouring molecules (Van der Waals radii $\text{C}+\text{O} = 3.22\text{\AA} > 3.071\text{\AA}$)

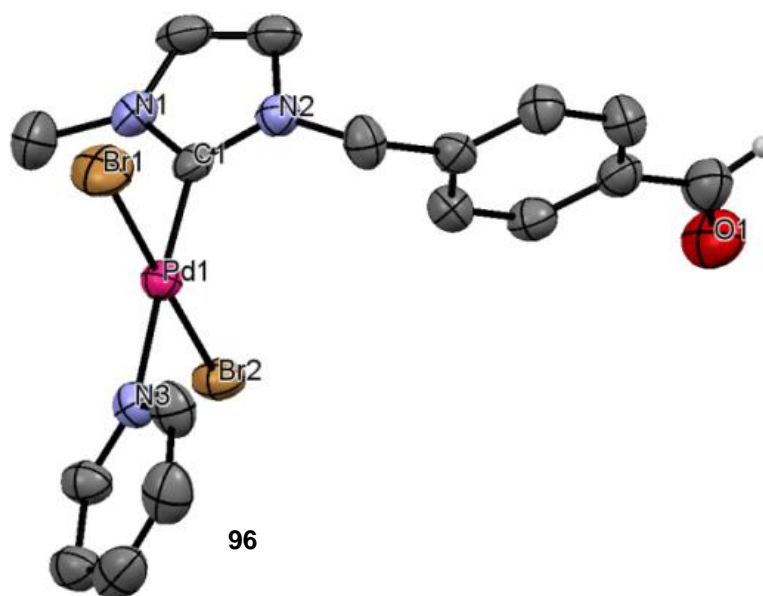


Figure 72: X-ray structure of [(Benzaldehyde-NHC) PdBr_2 (pyr)] complex **96**. Selected bond lengths (\AA) and angles ($^\circ$): C-Pd: 1.961; Pd-Br: 2.443, 2.423; Pd-N: 2.100; C-Pd-N: 177.04; N-C-Pd-I: 87.87, 90.00.

As conclusion, benzaldehyde featured imidazolium salts are proved to be suitable precursors to access various platinum complexes. These compounds give the opportunity of further derivatization by oxime conjugation. In contrast, lower stability of palladium analogues hampers their potential for post-functionalization.

2.2.5 Polynuclear platinum NHC complexes

Simultaneous presence of several metal centres within the same structure can play a collaborative effect or modulate the reactivity of the second metal ion. Beautiful examples are found in nature. For example, copper-zinc superoxide dismutase catalyses the dismutation into oxygen and hydrogen peroxide of toxic superoxide radical (O_2^-).²⁹⁰

The simplest way to obtain polynuclear platinum complexes derived from cisplatin constitutes the use of di or polyamine spacers²⁹¹ to connect platinum atoms.²⁹² Polynuclear compounds have demonstrated different²⁹³ and sometimes new binding modes to DNA and therefore new mechanism of cytotoxicity.²⁹⁴ This is especially promising to circumvent the cellular resistance mechanisms against cisplatin.²⁹⁵ In the case of triplatin tetranitrate^{23,296} (*BBR3464*) (discontinued in phase II trials), the cationic trinuclear complex binds to DNA through hydrogen bonding and electrostatic interactions along the phosphate backbone in a binding mode called by Farrell and co-workers as DNA “backbone tracking”.²⁹⁷ Marinetti and co-workers have reported diamine linked *trans*-platinum (II) NHC complexes provoking cell death by mechanisms different from those of cisplatin.¹²³ Instead of bridging amine, metal centres can be linked by Janus-type ditopic NHC ligands.²⁹⁸ Beside this special kind of ligand, two or more NHC ligands linked by alkane or phenyl bridges are synthetically readily

²⁹⁰ Tainer, J. A.; Getzoff, E. D.; Richardson, J. S.; Richardson, D. C. *Nature* **1983**, 306, 284.

²⁹¹ Dependence of DNA interaction to the nature of the linker between the two platinum atoms is demonstrated on two similar dinuclear platinum complexes by Guo *et al.*: Zhu, J.; Lin, M.; Fan, D.; Wu, Z.; Chen, Y.; Zhang, J.; Lu, Y.; Guo, Z. *Dalton Trans.* **2009**, 48, 10889.

²⁹² Selected studies of polynuclear platinum compounds: Hegmans, A.; Qu, Y.; Kelland, L. R.; Roberts, J. D.; Farrell, N. *Inorg. Chem.* **2001**, 40, 6108; Qu, Y.; Harris, A.; Hegmans, A.; Petz, A.; Kabolizadeh, P.; Penazova, H.; Farrell, N. *J. Inorg. Biochem.* **2004**, 98, 1591; Van der Schilden, K. *PhD Thesis* **2006**, University of Leiden; Marques, M. P. M. *ISRN Spectroscopy* **2013**, 2013, Article ID 287353. For a review, see: Farrell, N. *Cancer Drug Discovery and Development in Platinum-Based Drugs in Cancer Therapy* **2000**, 321, Humana Press; Wheate, N. J.; Collins, J. G. *Coord. Chem. Rev.* **2003**, 241, 133.

²⁹³ McGregor, T. D.; Bousfield, W.; Qu, Y.; Farrell, N. *J. Inorg. Biochem.* **2002**, 91, 212.

²⁹⁴ Roberts, J. D.; Peroutka, J.; Farrell, N. *J. Inorg. Biochem.* **1999**, 77, 51.

²⁹⁵ Cisplatin induces mainly apoptosis. To compare, Farrell, Böglér and co-workers studied mechanism of BBR3610, a multiplatinum compound that induced G2/M arrest in the absence of cell death: Billecke, C.; Finniss, S.; Tahash, L.; Miller, C.; Mikkelsen, T.; Farrell, N. P.; Böglér, O. *Neuro-oncol.* **2006**, 8, 215.

²⁹⁶ [*trans*-PtCl(NH₃)₂]₂-μ-*trans*-Pt(NH₃)₂{NH₂(CH₂)₆NH₂]₂]⁴⁺(NO₃)₄.

²⁹⁷ Harris, A.; Qu, Y.; Farrell, N. *Inorg. Chem.* **2005**, 44, 1196; Komeda, S.; Moulai, T.; Woods, K. K.; Chikuma, M.; Farrell, N. P.; Williams, L. D. *J. Am. Chem. Soc.* **2006**, 128, 16092.

²⁹⁸ For examples, see: Guerret, O.; Solé, S.; Gornitzka, H.; Teichert, M.; Trinquier, G.; Bertrand, G. *J. Am. Chem. Soc.* **1997**, 119, 6668; Boydston, A. J.; Rice, J. D.; Sanderson, M. D.; Dykhno, O. L.; Bielawski, C. W. *Organometallics* **2006**, 25, 6087; Khranov, D. M.; Boydston, A. J.; Bielawski, C. W. *Angew. Chem. Int. Ed.* **2006**, 45, 6186; Schmidtendorf, M.; Schulte to Brinke, C.; Hahn, F. E. *J. Organomet. Chem.* **2014**, 751, 620; Gonell, S.; Poyatos, M.; Peris, E. *Chem. Eur. J.* **2014**, 20, 9716.

accessible.²⁹⁹ The length of the linker appears to be a main factor between bridging two metals and chelating one single metal.³⁰⁰ Heterobi- and tri-metallic complexes obtained by a single-step site-selective metalation have been described by Hahn and co-workers.³⁰¹

Biological activity of poly metallic platinum complexes linked by multi NHC ligands has never been reported. To explore this field, several multi imidazolium precursors (**Figure 73**) were synthesized and complexation reactions were tested under standard conditions (**Figure 74**). Linkers between two imidazolium units (propane, dodecane, *m*-xylene, *p*-xylene, 9,10-dimethylantracene) and number of imidazolium units (2, 3, 4, 6) were varied.

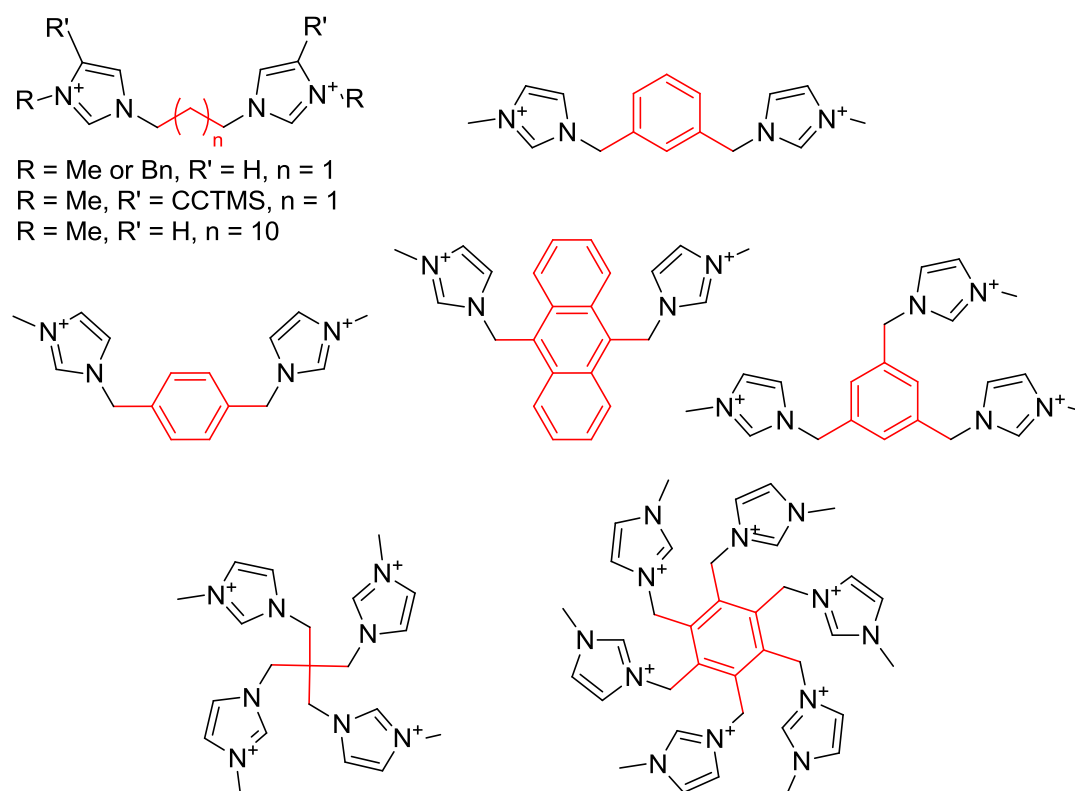


Figure 73: Bis, tri, tetra and hexa-imidazolium precursors (Contra-anions: Br⁻) obtained from R-imidazole and polybromoalkanes

With propane linker, no complexes were obtained even with the use of excess of platinum chloride or other more soluble platinum (II) sources (PtI₂Pyr₂, PtCl₂(cod)). *P*-xylene linked bis-imidazolium is not yielding any complex with pyridine. In cyclohexylamine, desired complex **101** is obtained in poor yield (19%) from this precursor. In contrast, 9,10-dimethylantracene is reacting in 42% yield to form

²⁹⁹ Hu, X. L.; Meyer, K. J. *Organomet. Chem.* **2005**, 690, 5474; Poyatos, M.; Mata, J. A.; Peris, E. *Chem. Rev.* **2009**, 109, 3677; Rit, A.; Pape, T.; Hepp, A.; Hahn, F. E. *Organometallics* **2011**, 30, 334; Rit, A.; Pape, T.; Hahn, F. E. *Organometallics* **2011**, 30, 6393; Maity, R.; Rit, A.; Schulte to Brinke, C.; Daniliuc, C. G.; Hahn, F. E. *Chem. Commun.* **2013**, 49, 1011.

³⁰⁰ Mata, J. A.; Chianese, A. R.; Miecznikowski, J. R.; Poyatos, M.; Peris, E.; Faller, J. W.; Crabtree, R. H. *Organometallics* **2004**, 23, 1253.

³⁰¹ Maity, R.; Koppetz, H.; Hepp, A.; Hahn, F. E. *J. Am. Chem. Soc.* **2013**, 135, 4966; Maity, R.; Schulte to Brinke, C.; Hahn, F. E. *Dalton Trans.* **2013**, 42, 12857.

a di-nuclear complex **100** nearly insoluble in common solvents (MeOH, CH₂Cl₂, acetone, C₆H₁₂, AcOEt or THF) and also *m*-xylene bis-imidazolium is reacting in 52% yield (**52**). Mesitylene tri-imidazolium ligand gave a trinuclear complex **102** in 22% yields. Tetra and hexa-imidazolium precursors did not give any complex. Nevertheless, inhibition of reaction for propane-linked imidazolium and poor reactivity of *p*-xylene both remain obscure. In **103** (63%), dodecane linker is believed to separate enough both imidazolylidene-platinum moieties to act as independent units. Successful ligand exchange reaction with an amino ester (complex **104**) indicated similar reactivity of this compound compared to classical mononuclear complexes.

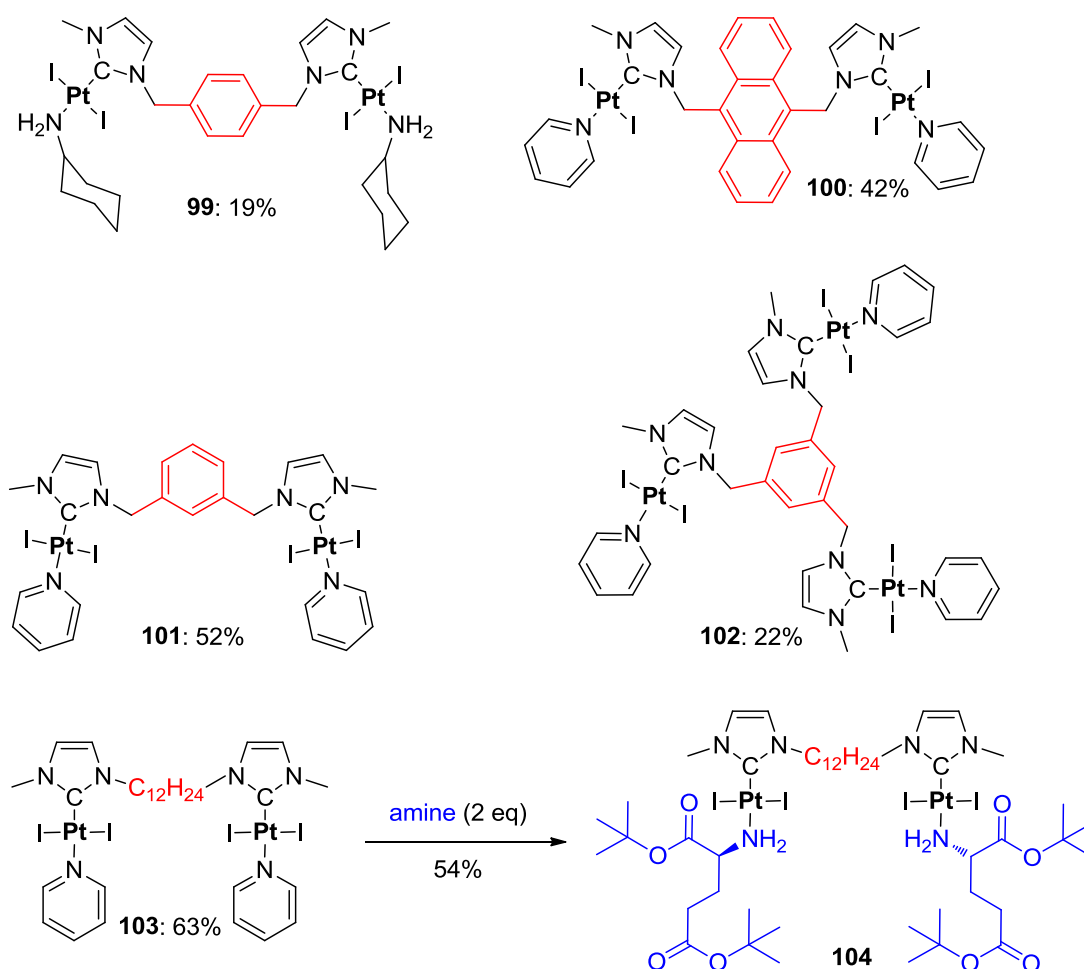


Figure 74: Poly-nuclear platinum complexes (%: yield of the complexation step)

Other possible strategy to access binuclear species consists in dimerization of mononuclear complex. Dimerization of an alkene complex using first Generation Grubbs Catalyst resulted in a mixture of E/Z compound **105** in ratio of 1.6/0.4 (Figure 75).

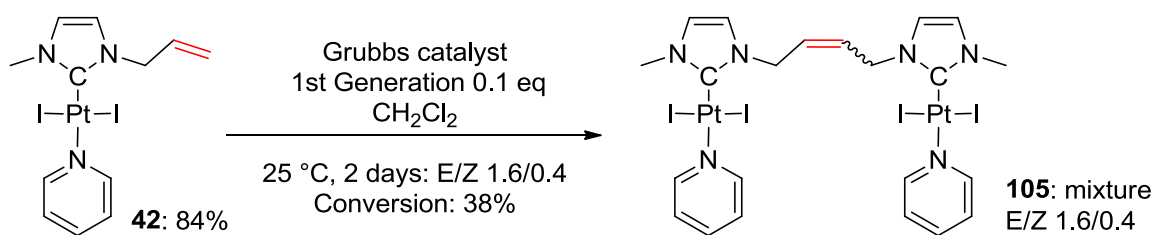


Figure 75: Dimerization of an alkene complex by olefin metathesis

These examples show that our general synthetic strategy is also adapted to afford several polymetallic species, whose biological properties will be reported in this work (chapter 5.1.2.5 *Polynuclear complexes*).

2.3 Variation of the alkene substituents of the NHC-backbone

In previous sections, mainly *N*-substituents of the imidazolidene were varied with several functionalities. In this section, we present several structural variations on the alkene moiety of the NHC-backbone in order to introduce other functionalities for potential biological applications. In the literature, various 5-membered imidazolidene ligands³⁰² featured with functional groups directly on alkene backbone of the NHC are reported. Various NHC-platinum (II)-amine complexes bearing imidazolidene, benzimidazolidene, 4,5-diphenyl-imidazolidene, triazolidene and tetramethylxantin-8-ylidene ligands were reported by the group of Marinetti.¹²² Thiazolidene based platinum complexes were communicated by Stone,³⁰³ Cavell,³⁰⁴ and Huynh.³⁰⁵ Alkyne substituted imidazolidene complexes have also been synthesized in our laboratory.^{126,127} The variation of alkene backbone substituents influences the electronic properties of the NHC more than its steric hindrance and so allows evaluation of the influence of these parameters on biological activity.

³⁰² NHC ligand bearing 1) an enol: Glorius *et al.*¹⁵³; Lavigne *et al.*¹⁵⁴; 2) an alkyne: Bellemin-Laponnaz *et al.*^{126,127}; 3) an amine: Lavigne *et al.*¹⁵⁵; Danopoulos, A. A.; Monakhov, K. Y.; Braunstein, P. *Chem. Eur. J.* **2013**, *19*, 450; Zhang, Y.; César, V.; Storch, G.; Lugan, N.; Lavigne, G. *Angew. Chem. Int. Ed.* **2014**, *53*, 6482; 4) a phosphine: Mendoza-Espinosa, D.; Donnadiou, B.; Bertrand, G. *Chem. Asian J.* **2011**, *6*, 1099; 5) a borate: Kolychev, E. L.; Kronig, S.; Brandhorst, K.; Freytag, M.; Jones, P. G.; Tamm, M. *J. Am. Chem. Soc.* **2013**, *135*, 12448; 6) chlorine atoms: Hoi, K. H.; Coggan, J. A.; Organ, M. G. *Chem. Eur. J.* **2013**, *19*, 843.

³⁰³ Fraser, P. J.; Roper, W. R.; Stone, F. G. A. *J. Chem. Soc., Dalton Trans.* **1974**, 102.

³⁰⁴ Graham, D. C.; Cavell, K. J.; Yates, B. F. *Dalton Trans.* **2007**, 4650; McGuinness, D. S.; Cavell, K. J.; Yates, B. F.; Skelton, B. W.; White, A. H. *J. Am. Chem. Soc.* **2001**, *123*, 8317.

³⁰⁵ Yen, S. K.; Young, D. J.; Huynh, H. V.; Koh, L. L.; Hor, T. S. A. *Chem. Commun.* **2009**, 6831.

Various imidazolium salts (triazolium, thiazolium, benzimidazolium,³⁰⁶ 4,5-diphenyl-imidazolium and 4,5-dichloro-imidazolium) have been synthesized following a one-step procedure by mono or dialkylation of commercially available products. Under standard conditions, these azolium salts lead to the corresponding 4,5-diphenyl-imidazolylidene **106**, benzimidazolylidene **107-110**, triazolylidene **111**, 4,5-dichloro-imidazolylidene³⁰⁷ **113-114** and thiazolylidene **115** complexes in comparable yield to imidazolylidene complexes (**Figure 76**). These examples prove that our synthetic strategy is not limited to imidazolylidene-based complexes.

X-ray diffraction structure of triazolylidene Pt complex **111** ascertained its *trans* configuration as well as the absence of abnormal NHC coordination, or coordination through the nitrogen atom of the NHC backbone (**Figure 77**). Platinum-C_{NHC} bond length is comparable to imidazolylidene-based complexes. Pt-pyridine and Pt-I bond lengths were slightly increased compared to imidazolylidene complexes (e.g. **Table 1**) indicating an increased donor potential of the triazolylidene structure.

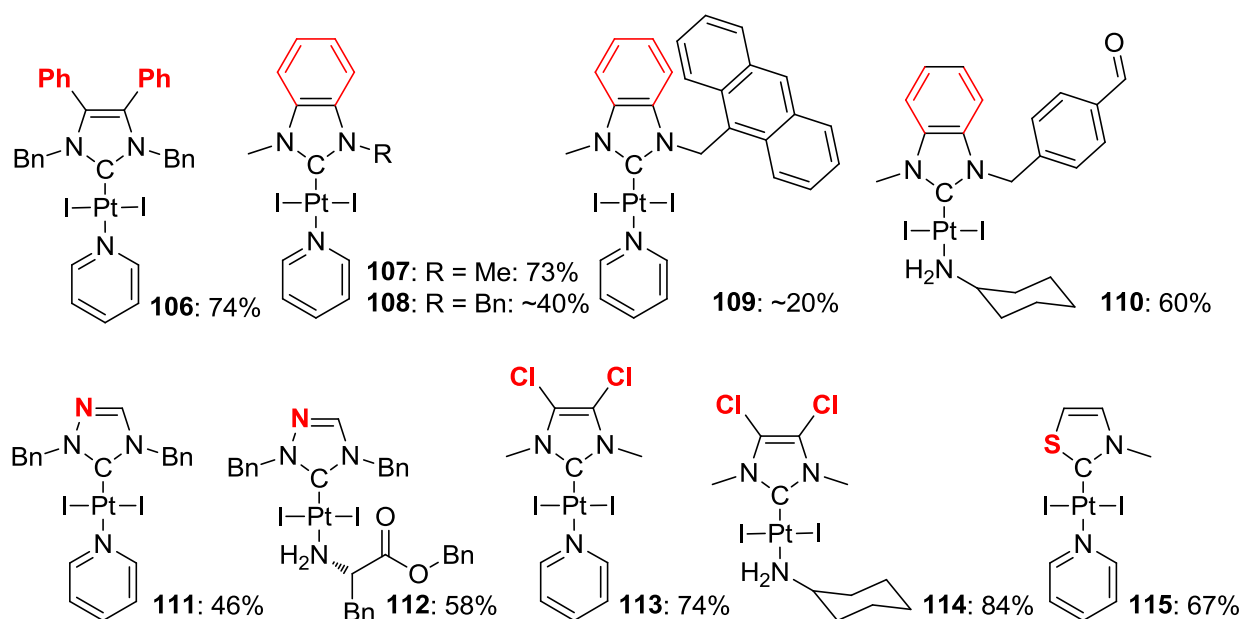


Figure 76: Backbone functionalized NHC platinum complexes studied in this work (yields refer to complexation step, respectively to ligand exchange (114, 116))

³⁰⁶ For a review of use of benzimidazolylidene ligands, see: Muskawar, P. N.; Karthikeyan, P.; Aswar, S. A.; Bhagat, P. R.; Kumar, S. S. *Arabian J. Chem.* **2012**, DOI: 10.1016/j.arabjc.2012.04.040.

³⁰⁷ Fernandez *et al.* reported a rare platinum (0) 4,5-dichloro-imidazolylidene complex as catalysts for diboration: Lillo, V.; Mata, J. A.; Segarra, A. M.; Peris, E.; Fernandez, E. *Chem. Commun.* **2007**, 2184; Lillo, V.; Mata, J.; Ramirez, J.; Peris, E.; Fernandez, E. *Organometallics* **2006**, 25, 5829.

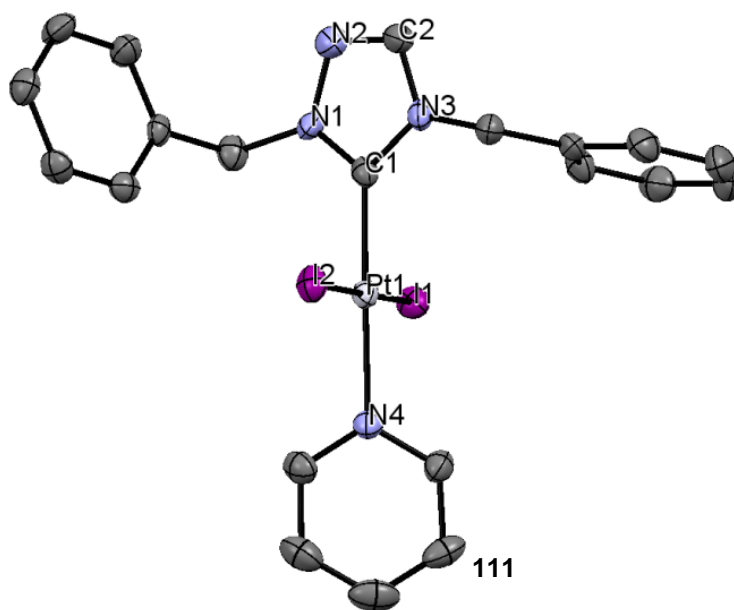


Figure 77: X-ray structure of triazolylidene platinum complex 111 Selected bond lengths (Å) and angles (°): C-Pt: 1.967; Pt-I: 2.603, 2.610; Pt-N_{pyr}: 2.102; C=N: 1.296; C-Pt-N: 178.94; C-Pt-I: 88.72, 90.60; N-C-N: 103.16; N-C-Pt-I: 69.91, 102.42; (N-C_{NHC})-(N-C_{pyr}): 43.07.

Alkyne substitution of the alkene backbone of imidazolylidene allows electronic conjugation from the carbene to the triple bond. In our laboratory, alkyne complexes have been studied for derivatization by RuAAC.^{126,127} Sonogashira coupling³⁰⁸ between this alkyne complex and 1-iodo-4-nitrobenzene under ligand-, copper-, and amine-free conditions³⁰⁹ gave the expected coupling product **116** with 37% yield (**Figure 78**). Noteworthy, the same reaction with the palladium analogue (pyr)PdI₂(NHC-alkyne) resulted in unidentifiable products.

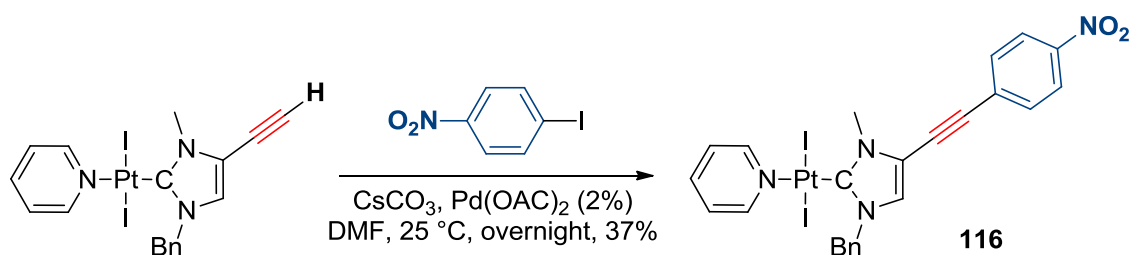


Figure 78: NHC-alkyne complex functionalized by Sonogashira coupling

N-substituents do not influence significantly the electronic properties of the carbene as showed by ¹³C-NMR shifts of the carbonyl carbon for [(NHC)PtI₂(L)] complexes (**Figure 79**). (For example, benzyl instead of methyl group as *N*-substituent increases chemical shift value less than 3 ppm.) L ligands neither significantly influence the chemical shift of the carbene (a difference in the range of 3 to 4 ppm

³⁰⁸ Chinchilla, R.; Nájera, C. *Chem. Rev.* **2007**, 107, 874.

³⁰⁹ Urgaonkar, S.; Verkade, J. G. *J. Org. Chem.* **2004**, 69, 5752.

of the chemical shift between cyclohexylamine and pyridine complexes was noticed). In contrast, alkene substituents have huge influence: variation of five-membered NHC backbone results in chemical shift variation from 135 to 167 ppm. The NHC ligands can be classified by increased frequency: imidazolylidene, 4,5-diphenyl-imidazolylidene, 4,5-dichloro-imidazolylidene and alkyne-imidazolylidene, triazolylidene, formyl-imidazolylidene, benzimidazolylidene, and finally thiazolylidene. This means that an increase of chemical shift is observed by incorporation of heteroatoms (N, S) inside the five membered ring as wells as by attaching functional groups on the alkene (alkynes, chlorine atoms, benzene rings, or formyl groups).

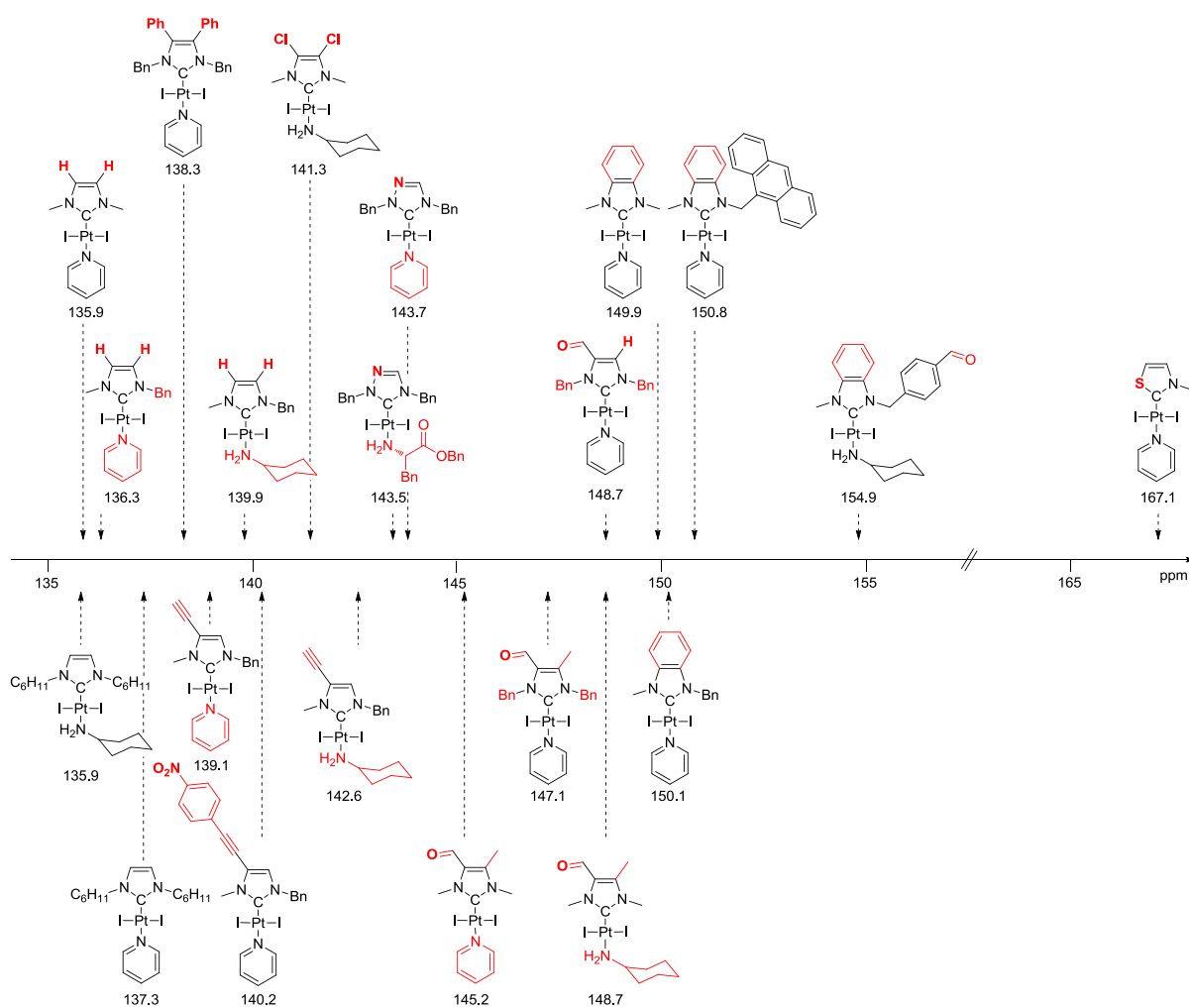
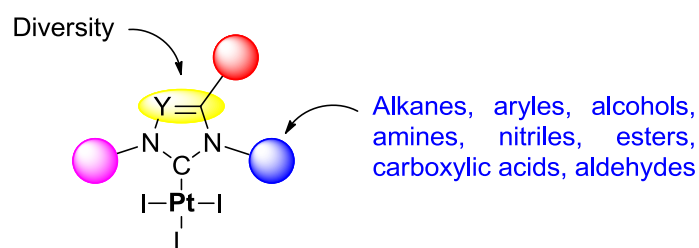


Figure 79: ^{13}C -NMR shifts of $\text{C}_{\text{Carbene}}\text{-Pt}$ for various $[(\text{NHC})\text{Pt}_2(\text{L})]$ complexes (CDCl_3 , 398K)

The difference of electronic properties of the carbene is an interesting factor to tune the biological properties of NHC complexes. The activity of several of these complexes will be evaluated *in vitro* (chapter 7.3.1.6. *Synthesis of complexes with variations of the alkene substituents of the NHC-backbone*).

2.4 Conclusion: diversity introduction by prefunctionalized azolium precursors

In this chapter, we have demonstrated the versatile character of diversity introduction in an ylide-platinum core using prefunctionalized azolium salts. Our classical platinum complexation reaction proves to be inert to various chemical functions (alkane, aryl, hydroxyl, amine, nitrile, acetal and ester groups).



Carboxylic acids-Pt complexes could be obtained by post-deprotection of *tert*-butyl ester complexes. After further deprotonation, these compounds were found to be water-soluble.

Aldehyde featured platinum complexes are interesting precursors for further derivatization by oxime conjugation. The aldehyde function seems to be a non-inert group upon complexation. Nevertheless, we obtained several aldehyde-featured complexes by *in situ* protection by imine formation or changing the Pt source ($\text{PtCl}_2(\text{cod})$).

The synthesis of several polynuclear platinum complexes has been achieved in order to increase the local platinum concentration. We were also interested in alkene substituents modification on the NHC backbone. Then, imidazolylidene, 4,5-diphenyl-imidazolylidene, 4,5-dichloro-imidazolylidene, alkyne-imidazolylidene, triazolylidene, benzimidazolylidene and thiazolylidene based complexes were synthesized in order to modulate the electronic properties of the NHC.

Finally, biological properties of these complexes have been evaluated *in vitro* and the results will be discussed in chapter 5.1.2 Cytotoxicity of prefunctionalized $[(\text{NHC})\text{PtI}_2(\text{amine})]$ complexes.

3 Synthesis of Pt complexes containing tridentate ligands

In 2010, the group of Che demonstrated that cyclometalated platinum NHC complexes are interesting structures for the development of new anticancer drugs (**Figure 80**).^{310,129} These [(C[^]N[^]N)Pt^{II}(NHC)]PF₆ complexes display high cytotoxicity as well as strong luminescent properties allowing mechanistic studies by fluorescence microscopy.^{311,312} Biological investigations showed that these complexes accumulate in cytoplasm. Bidentate NHC complexes featuring various (C[^]N) ligands also show high luminescence properties and can induce cancer cell apoptosis by endoplasmic reticulum and mitochondrial stress.³¹³ Similar complexes were also studied by Uesugi *et al.*³¹⁴ (N[^]N[^]N)Pt^{II}(pyridine) derivatives were reported by the group of De Cola.³¹⁵ These neutral complexes show enhanced emission properties together with high stability making them suitable for bioimaging.³¹⁶ Fluorescence confocal microscopy investigations revealed inhibition by biomolecules conducting to expulsion of the Pt centre from the cells. Altogether, these potential biological applications combined with enhanced stability of polydentate ligands let us to investigate the scope of tridentate ligands based platinum complexes.

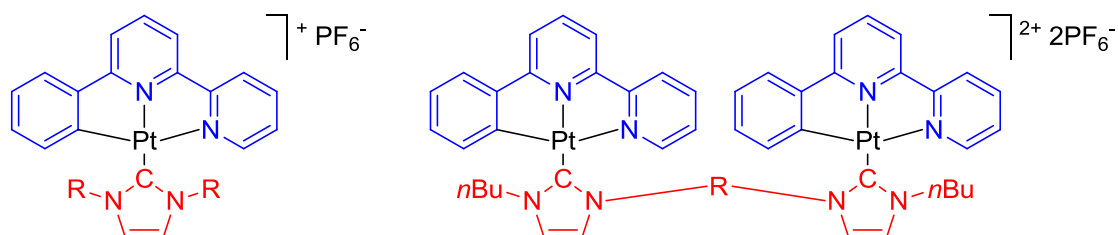


Figure 80: Cyclometalated (C[^]N[^]N) NHC Pt (II) complexes displaying high cytotoxicity adjunct to strong luminescence (Che and collaborators)¹²⁹

³¹⁰ For a review about cyclometalated transition metals, see: Albrecht, M. *Chem. Rev.* **2010**, *110*, 576.

³¹¹ Thorp-Greenwood, F. L. *Organometallics* **2012**, *31*, 5686.

³¹² Platinum (II) complexes conjugated with (C[^]N[^]N) ligands are reported to be luminescent also in absence of NHC ligand, see for example: Xiao, X.-S.; Kwong, W.-L.; Guan, X.; Yang, C.; Lu, W.; Che, C.-M. *Chem. Eur. J.* **2013**, *19*, 9457; Other conjugated polydentate ligands Pt complexes are well known for their luminescence properties. Among innumerable examples, see e.g.: Baldo, M. A.; O'Brien, D. F.; You, Y.; Shoustikov, A.; Silbley, S.; Thompson, M. E.; Forrest, S. R. *Nature* **1998**, *395*, 151; Kui, S. C. F.; Chow, P. K.; Tong, G. S. M.; Lai, S.-L.; Cheng, G.; Kwok, C.-C.; Low, K.-H.; Ko, M. Y.; Che, C.-M. *Chem. Commun.* **2013**, *49*, 1497; Hang, X.-C.; Fleetham, T.; Turner, E.; Brooks, J.; Li, J. *Angew. Chem., Int. Ed.* **2013**, *52*, 6753; These strong luminescence properties made platinum complexes interesting for Organic Light-Emitting Devices (OLEDs): Yang, X.; Yao, C.; Zhou, G. *Platinum Metals Rev.* **2013**, *57*, 2; Mauro, M.; Aliprandi, A.; Septiadi, D.; Kehr, N. S.; De Cola, L. *Chem. Soc. Rev.* **2014**, *43*, 4144.

³¹³ Zou, T.; Lok, C.-N.; Fung, Y.M.E.; Che, C.-M. *Chem. Commun.* **2013**, *49*, 5423.

³¹⁴ Uesugi, H.; Tsukuda, T.; Takao, K.; Tsubomura, T. *Dalton Trans.* **2013**, *42*, 7396.

³¹⁵ Septiadi, D.; Aliprandi, A.; Mauro, M.; De Cola, L. *RSC Adv.* **2014**, *4*, 25709.

³¹⁶ For a review of complexes in cell imaging, see: Coogan, M. P.; Fernandez-Moreira, V. *Chem. Commun.* **2014**, *50*, 384.

3.1 Tridentate (O⁺C⁺O) ligand based complexes

In our group, a (O⁺C⁺O)³¹⁷ ligand incorporating an imidazolidinylidene moiety was synthesized and successfully coordinated toward various transition metals including vanadium, manganese or group 4 metals.³¹⁸ The corresponding titanium and zirconium complexes were successfully used as catalysts in ring opening polymerization of *rac*-Lactide.³¹⁹ Redox and luminescent properties of group 4 (Ti, Zr, Hf) bis-(O⁺C⁺O) complexes have also been reported.³²⁰ In line with these results and to further extend the scope of this work, antitumor properties of (O⁺C⁺O) Pt-type complexes were tested. This ligand should generate a different electronic and steric environment around the platinum core compared to previously described complexes based on monodentate NHC ligands. Moreover, access to luminescent probe for mechanistic studies should be possible for this new class of compounds.³²¹

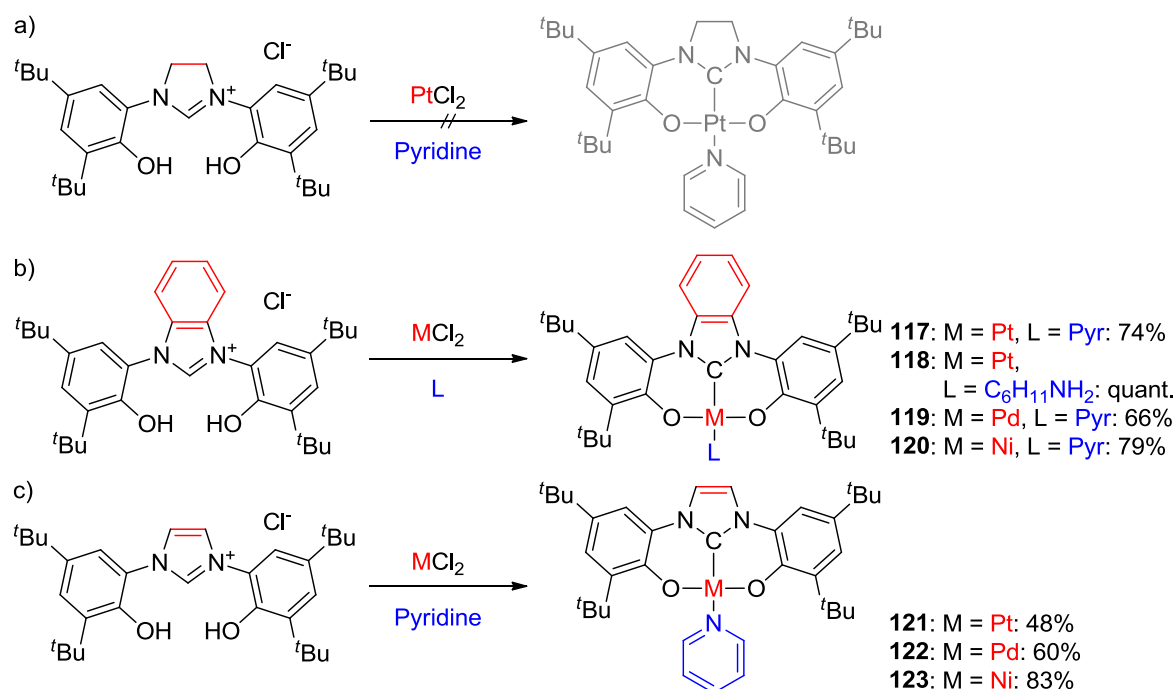


Figure 81: Tridentate (O⁺C⁺O) ligand-based complexes of group 10 metals.³²² Reactions conditions: MCl₂ (1eq.), L (solvent), K₂CO₃ (30 eq.), 100 °C, overnight

³¹⁷ For a O⁺C⁺O tridentate NHC containing ligands, see: Weinberg, D. R.; Hazari, N.; Labinger, J. A.; Bercaw, J. E. *Organometallics* **2010**, 29, 89; for a C⁺O didentate NHC containing ligand, see: Boydston, A. J.; Rice, J. D.; Sanderson, M. D.; Dykhno, O. L.; Bielawski, C. W. *Organometallics* **2006**, 25, 6087; a dodecamethylene bridged bis-(C⁺O) tetradentate NHC containing ligand: Komiya, N.; Yoshida, A.; Naota, T. *Inorg. Chem. Commun.* **2013**, 27, 122; and for thiol analogues S⁺C⁺S: Sellmann, D.; Prechtel, W.; Knoch, F.; Moll, M. *Inorg. Chem.* **1993**, 32, 538.

³¹⁸ Dagorne, S.; Bellemin-Lapponnaz, S.; Romain, C. *Organometallics* **2012**, 32, 2736; Bellemin-Lapponnaz, S.; Welter, R.; Brelot, L.; Dagorne, S. *J. Organomet. Chem.* **2009**, 694, 604.

³¹⁹ Romain, C.; Brelot, L.; Bellemin-Lapponnaz, S.; Dagorne, S. *Organometallics* **2010**, 29, 1191; Romain, C.; Heinrich, B.; Bellemin-Lapponnaz, S.; Dagorne, S. *Chem. Commun.* **2012**, 48, 2213.

³²⁰ Romain, C.; Choua, S.; Collin, J.-P.; Heinrich, M.; Bailly, C.; Karmazin-Brelot, L.; Bellemin-Lapponnaz, S.; Dagorne, S. *Inorg. Chem.* **2014**, 53, 7371.

³²¹ Ma, D.-L.; He, H.-Z.; Leung, K.-H.; Chan, D. S.-H.; Leung, C.-H. *Angew. Chem. Int. Ed.* **2013**, 52, 7666.

³²² Complexes 121-125 were synthesized in collaboration with Dr. E. Borré.

We first studied the imidazolidinylidene based ($O^{\wedge}C^{\wedge}O$) ligand (**Figure 81, a**). Platinum complexation with this tridentate ligand was tested under standard conditions.³²³ Unfortunately, no product was obtained. The unsaturated benzimidazolyliidene analogue appeared to be a more adequate precursor for platinum (**117, 118**) as well as palladium (**119**) and nickel (**120**) complexes (b).³²⁴ Successful metal complexation reaction was verified by 1H and ^{13}C -NMR ($\delta_{C_{carbene-M}}$: Ni: 162.4, Pd: 165.3 and Pt: 153.6 ppm).³²⁵ Besides, the nickel complex **120** was found to be diamagnetic, in line with a square-planar environment around the metal.

Unfortunately, attempts in growing monocrystals from the complexes only afforded crystals of insufficient quality for total resolving of the structure. Nevertheless, a preliminary X-ray structure of the platinum complex **117** could be obtained (R-factor = 10.62). Despite the insufficient quality for refinement, atom connectivity could be established confirming the proposed structure (**Figure 82**). This molecular structure indicates absence of planarity of the ($O^{\wedge}C^{\wedge}O$) ligand diminishing probability of electronic delocalisation.

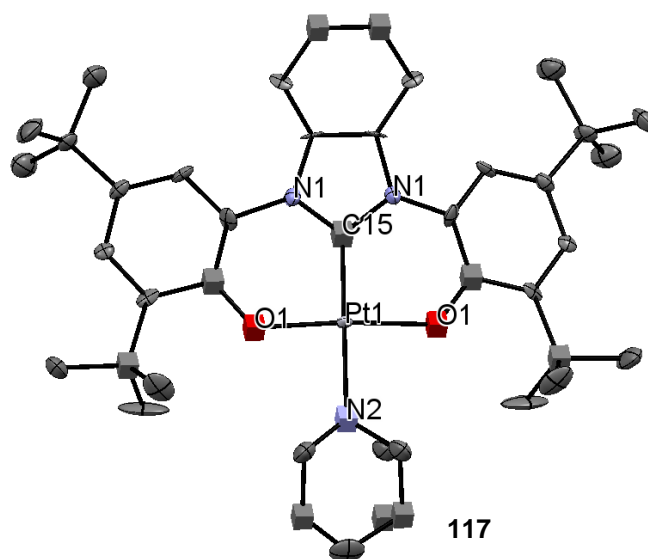


Figure 82: Preliminary molecular structure of $[(O^{\wedge}C^{\wedge}O)Pt(pyridine)]$ **117 obtained by X-ray diffraction**

Most of the complexes presented in previous chapter were imidazolyliidene based. For comparison, an imidazolyliidene containing tridentate ligand was prepared and successfully reacted with Pt, Pd and Ni (complexes **121-123**) (**Figure 81, c**). Differences in reactivity between both imidazolyliidene and benzimidazolyliidene based complexes was noticed. Whereas pyridine did not exchange easily with benzimidazolyliidene complexes, the corresponding imidazolyliidene complexes were more reactive.

³²³ For a review on NHC-based bi- and tridentate ligands, see: Mata, J. A.; Poyatos M.; Peris, E. *Coord. Chem. Rev.* **2007**, 251, 841; Pugh, D.; Danopoulos, A. A. *Chem. Rev.* **2007**, 251, 610.

³²⁴ Borr , E.; Dahm, G.; Aliprandi, A.; Mauro, M.; Dagorne, S.; Bellemin-Laponnaz, S. *Organometallics* **2014**, 33, 4374.

³²⁵ Similar chemical shift values were found for monodentate benzimidazolyliidene platinum complex, see: *Figure 79*.

For example, addition of triphenylphosphine to the imidazolylidene platinum compound **121** afforded the corresponding phosphine adduct **124** in 80% yield, whereas no product could be obtained from benzimidazolylidene complex **117** (**Figure 83**). However, using neat conditions, the pyridine could be quantitatively exchanged by cyclohexylamine to afford **118**. Unsuccessful trial of selective decoordination of the phenoxy groups (addition of TFA and NaI) showed their importance for these groups for the stability of the complexes (chelate effect).

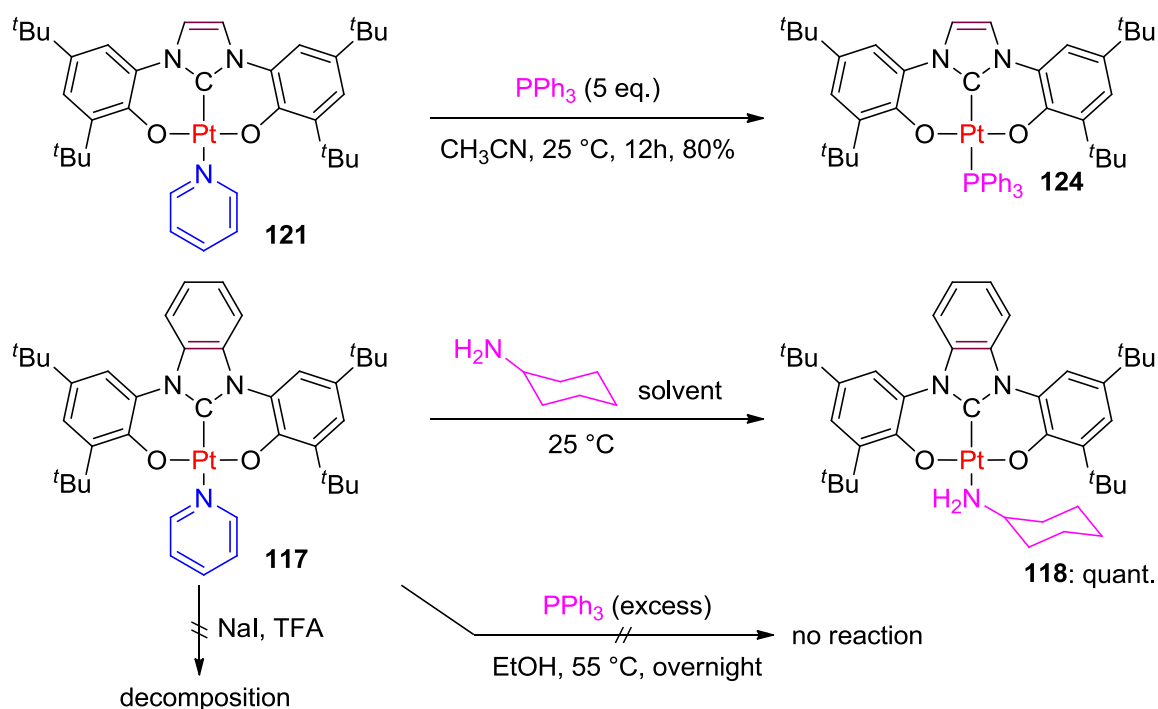


Figure 83: Reactivity of the (O[^]C[^]O) complexes towards neutral ligands or acids³²²

UV-visible absorbance, density functional theory (DFT) and time-dependent DFT (TD-DFT) calculations were carried out under both vacuum and solvent on this system.³²⁶ Noteworthy, at 77 K, the Pt complexes **117**, **118** and **121** in frozen glassy matrix present a weak photoluminescence in green region of the visible spectrum with μ s excited-state lifetimes. Absence of emission in solution at room temperature is attributed to the absence of planarity of the (O[^]C[^]O) ligands as well as to the free rotation of the pyridine respectively the cyclohexylamine ligand.

A second class of more flexible (O[^]C[^]O) ligands was also envisaged. Thanks to ketone-enol equilibrium, a di- acetophenone substituted imidazolium gave the desired complex **125** under standard conditions (**Figure 84**). Interestingly, the methyl analogue was not afforded following the same pathway. The low solubility of this compound did not facilitate crystals growing and only an X-ray

³²⁶ Collaboration with Dr. Matteo Mauro from Institut de Science et d'Ingénierie Supramoléculaires (ISIS) of Strasbourg.

diffraction structure of moderate quality (R-factor = 6.22) could be obtained. The molecular structure reveals absence of planarity of this ligand too and its tridentate coordination mode.

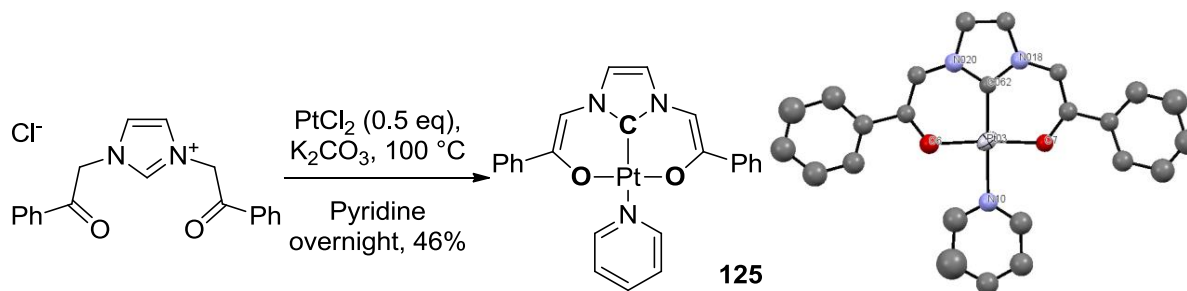


Figure 84: [(O⁺C⁺O)Pt(pyridine)] complex 125 obtained from di-acetophenone imidazolium and its preliminary X-ray structure

3.2 Tridentate (O⁺N⁺O) ligand based complexes

In light of the moderate luminescent properties of (O⁺C⁺O) based complexes, we decided to study other tridentate ligands. These ligands should be easily available and tuneable to generate a greater diversity of compounds and modulate their properties. A triazole based (O⁺N⁺O) (NHC-free) ligand attracted our attention (**Figure 85**). This iron-chelating drug, known under trade name Deferasirox (*Exjade*), is commercialized by Novartis for oral treatment of chronic iron overload.³²⁷ Vanadium complexes based on this tridentate structure exhibit anti-diabetic properties.³²⁸ Interestingly, derivatives of this tridentate ligand are easily accessible from a two-step procedure reported by the group of Hegetschweiler.³²⁹ Variation of the R group attached to the 1,2,4-triazole may modulate electronic properties of the ligand and obviously of the afforded complexes. Our aim was the synthesis of various complexes bearing this tridentate ligand. Additionally, luminescence and biological activities of the new complexes will be evaluated.

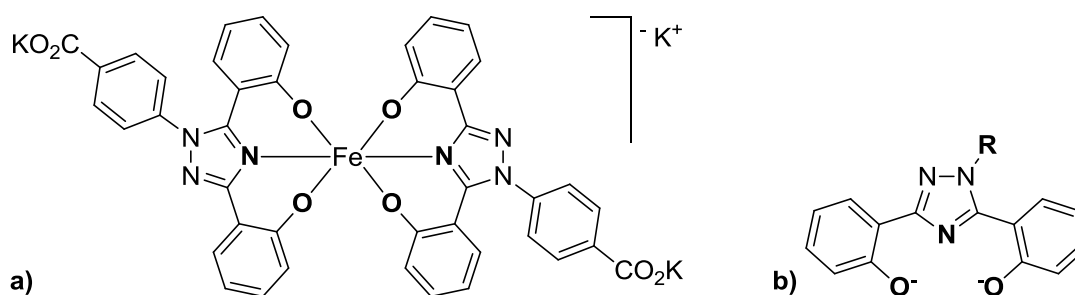


Figure 85: a) 2 Deferasirox ligands chelating iron (III) and b) derived (O⁺N⁺O) ligand studied

³²⁷ Choudhry, V. P.; Naithani, R. *Ind. J. Pediatr.* **2007**, 74, 759.

³²⁸ Yoshikawa, Y.; Sakurai, H.; Crans, D. C.; Micera, G.; Garribba, E. *Dalton Trans.* **2014**, 43, 6965.

³²⁹ Steinhäuser, S.; Heinz, U.; Bartholomä, M.; Weyhermüller, T.; Nick, H.; Hegetschweiler, K. *Eur. J. Inorg. Chem.* **2004**, 2004, 4177.

3.2.1.1 Synthesis of $[(O^{\wedge}N^{\wedge}O)M(L)]$ complexes

Using classical complexation conditions, a whole series of complexes was obtained from Deferasirox derivatives³³⁰ as yellow powders with good to excellent yields. Diversity was introduced by varying the R group of the ligand and the metal (Pt or Pd) (**Figure 86**). Successful synthesis was confirmed by ^1H -NMR (disappearance of phenolic protons, L ligand coordination) and ^{13}C -NMR. The influence of three parameters on luminescence was evaluated: i) the influence of the metal (Pd or Pt), ii) the R group and iii) the neutral ligand L.

Unfortunately, none of the palladium complexes **126-129** showed luminescence under UV irradiation at 365 nm in the solid state (**Table 5**).

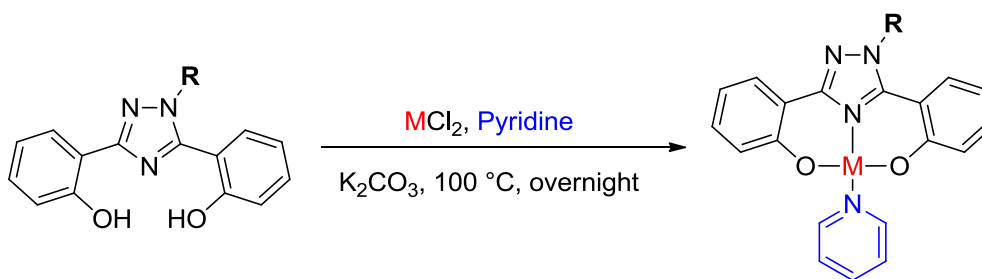


Figure 86: Synthesis of $[(O^{\wedge}N^{\wedge}O)M(\text{pyr})]$ complexes ($M = \text{Pt or Pd}$)

Entry	Complex	($M = \text{Pd}$), R =	Yield (%) ^[1]	Luminescence
1	126	Me	63	
2	127		86	
3	128		Quant.	
4	129		50	

Table 5: $[(O^{\wedge}N^{\wedge}O)\text{Pd}(\text{pyridine})]$ complexes: no luminescence was observed under UV irradiation (365 nm). ^[1] Yield of complexation.

³³⁰ Synthesis in collaboration with Changkan Fu: Fu, C. *Master Thesis* 2014, University of Strasbourg.

In contrast, several synthesized Pt complexes **130-139** showed promising luminescence properties. As shown in **Table 6**, in the solid state under UV irradiation at 365 nm, the Pt complexes, with the exception of methyl-substituted complex **130**, emit yellow light. Among these complexes, compound **136** with 1,3-bis(CF₃)benzene group seems to present the strongest emission (entry 7). Noteworthy, a red shift is also observed in these complexes when the substituent group R contains electron-withdrawing groups.



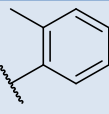

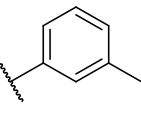
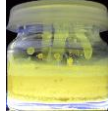
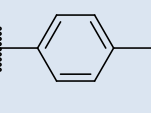

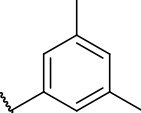

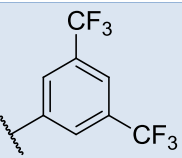

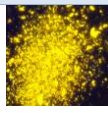
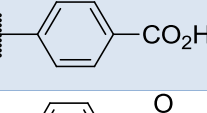
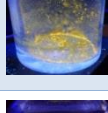
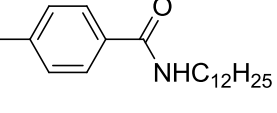

Entry	Complex	(M = Pt), R =	Yield (%) ^[1]	Luminescence
1 *	130	- CH ₃	89	
2	131	- Phenyl	86	
3	132		68	
4	133		Quant.	
5	134		Quant.	
6	135		Quant.	
7	136		Quant.	
8	137	-C ₆ F ₅	81	
9	138		81	
10	139		78	

Table 6: [(O^{^-}N^{^+}O)Pt(pyridine)] complexes: influence of R group variation on luminescence under UV irradiation (365 nm). ^[1]Yield of complexation.

To compare the influence of the monodentate L ligand, various neutral ligands other than pyridine were studied. For example, using the same procedure, cyclohexylamine could be introduced quantitatively to a platinum complex **140** (**Figure 87**). Unfortunately, this complex did not display any luminescence in the solid state.

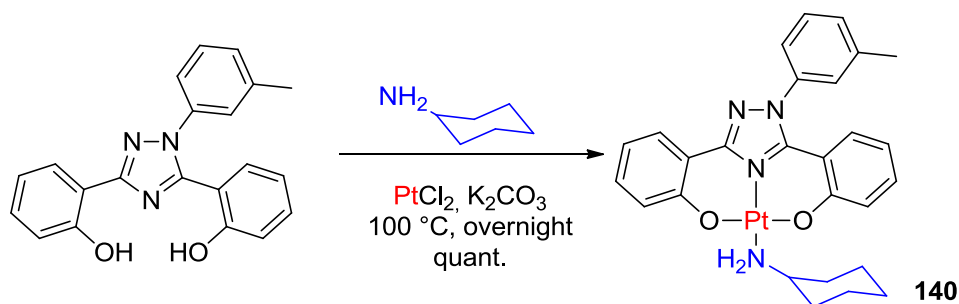


Figure 87: [(O[−]N[−]O)Pt(cyclohexylamine)] complex synthesis

As complexes featured with 1,3-bis(CF₃)benzene R group seem to demonstrate the strongest emission, we selected this fragment and further scanned the neutral ligand L (**Figure 88**). We selected several pyridine derivatives with electron donating or withdrawing groups, strong donor ligands (PPh₃, AsPh₃, NHC), and nitrogen-based ligands (acetonitrile and NH₃).

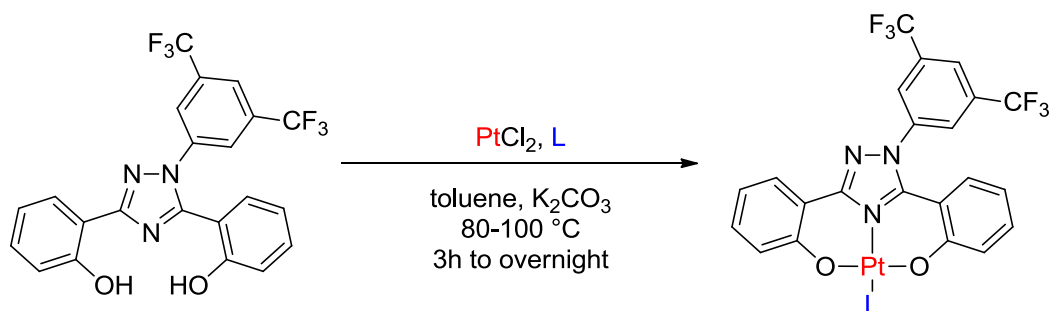


Figure 88: Synthesis of [(O[−]N[−]O)Pt(L)] complexes: variation of the monodentate L ligand

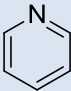

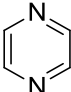

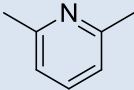

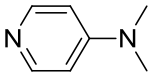

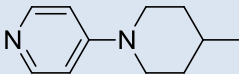
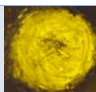
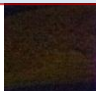

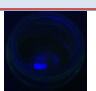
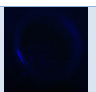
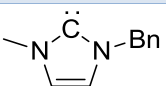
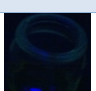
Entry	Complex	(M = Pt), L	Yield (%) ^[1]	Luminescence
1	136		Quant.	
2	141		52	
3	142		50	
4	143		88	
5	144		94	
6	145	NH ₃	92	
7	146	CH ₃ CN	<5	
8	147	PPh ₃ ^[2]	74	
9	148	AsPh ₃ ^[2]	34	
10	149		59	

Table 7: [(O[^]N[^]O)Pt(L)] complexes: influence of L ligand variation on luminescence under UV irradiation (365 nm). ^[1] Yield of complexation. R = 1,3-bis(CF₃)benzene except ^[2] R = Ph.

All pyridine derivatives **136**, **141-144** showed a yellow-orange emission similar to pyridine derivative **136** (Table 7, entry 1-5). This offers the possibility to modulate the wavelength of the emission in relation with the nature of pyridine derivative. Other neutral ligands (**145-149**) inhibit this phenomenon (entry 6-10). Even for nitrogen-based ligands NH₃ or CH₃CN (**145**, **146**), no emission was visible. As a conclusion, the combination of 1,3-bis(CF₃)benzene substituted (O[^]N[^]O) with pyridine derivatives seems the best choice for further studies.

The scope of the (O[^]N[^]O) ligands was expanded by introducing NHCs as L ligands. The NHC could be introduced by ligand replacement reaction (Figure 89, a.). During this reaction, the tridentate ligand exchanged both pyridine and chloride ligands on a preformed NHC complex to afford complex **149**. Complexes **150** and **151** were synthesized *in pot* from (O[^]N[^]O)H₂ and imidazolium precursors and PtCl₂ in pyridine (b).

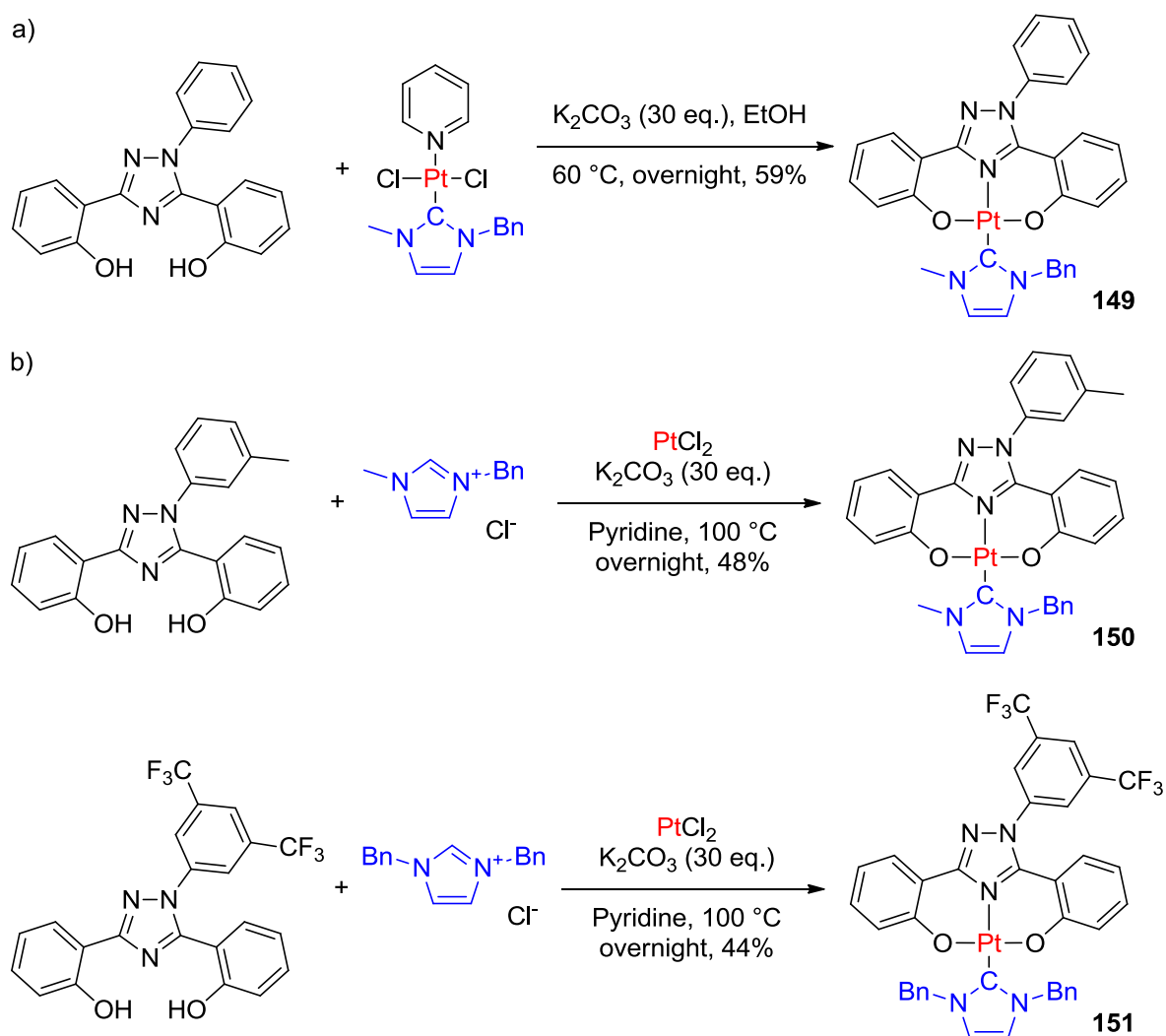
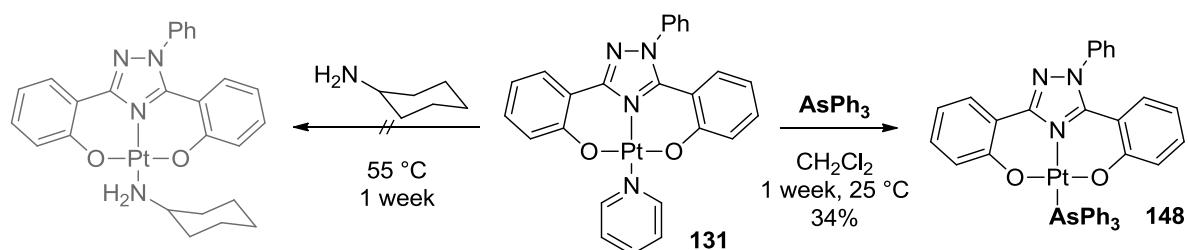


Figure 89: Easy O[^]N[^]O complexation with a preformed [(NHC)PtCl₂(pyridine)] complex

In this context, it is noteworthy to mention the difference of reactivity of (O[^]N[^]O)Pt(pyridine) and previous described [(NHC)PtI₂(pyridine)] complexes (e.g. complex **14**). In the case of (O[^]N[^]O)Pt(pyridine) complex, the pyridine ligand could not be exchanged by amines. The (O[^]N[^]O) ligand does not weaken the pyridine ligand located *trans* to the nitrogen atom. Exchange trial with triphenylarsine in ethanol at 55 °C led to decomposition. Fortunately, at room temperature, the desired compound **148** was obtained after one-week reaction (**Figure 90**).

Figure 90: Ligand exchange reactivity of $[(O^N^O)Pt(pyridine)]$

4,4'-bipyridine introduction resulted in a mixture of mono- and di-platinum complexes that were easily separated by chromatography (**Figure 91**). In presence of one equivalent of bipyridine, the mono Pt complex **152** was obtained in good yield (70%), but also small amount (20%) of binuclear compound **153** was isolated. Complex **152** is strongly emitting under 365 nm irradiation in the solid state. The emission disappears after addition of iodomethane (**154**) or trifluoroacetic acid (**155**) (**Figure 92**). These preliminary qualitative results promise interesting applications of this complex, e.g. for the design of pH switchable OLED's.

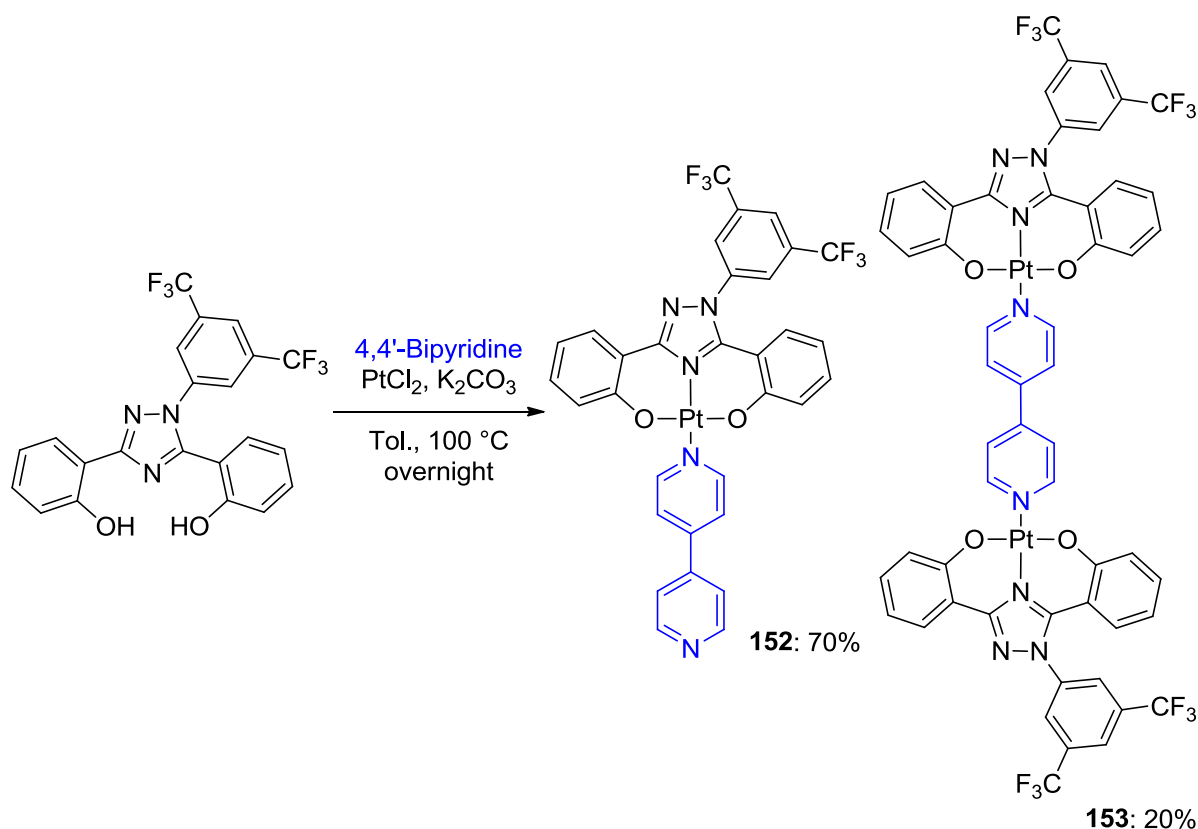


Figure 91: Synthesis of mono and binuclear 4,4'-bipyridine complexes

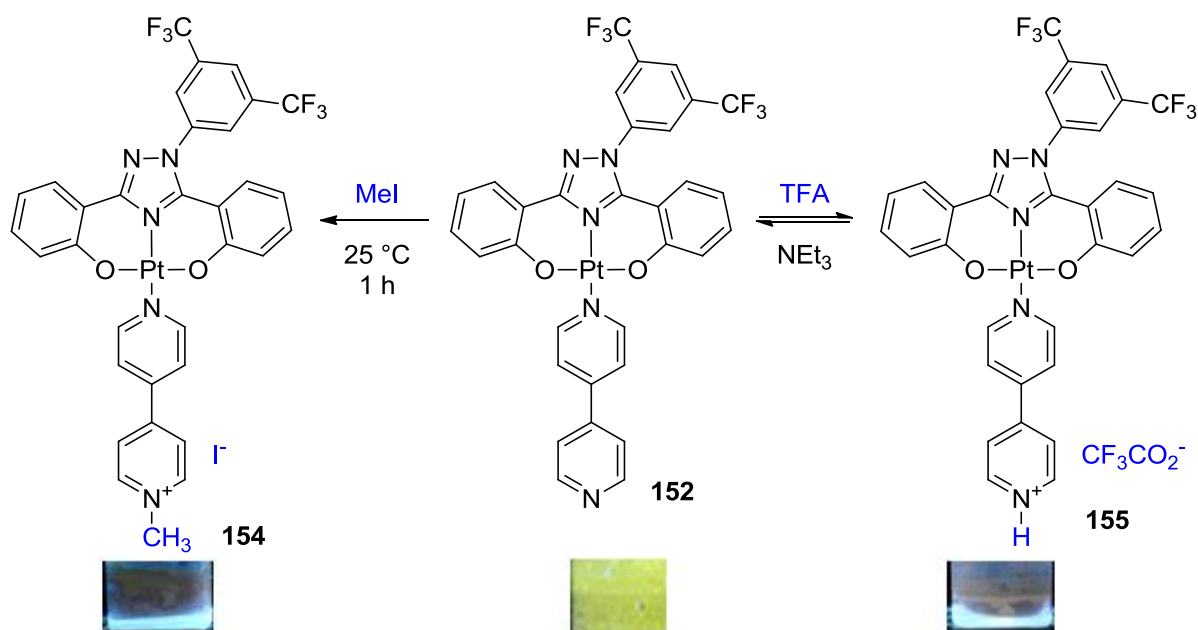


Figure 92: Switch of luminescence of [(O[^]N[^]O)Pt(4,4'-bipyridine)] complex

3.2.1.2 Study of molecular structures of the (O[^]N[^]O)M(L) complexes

Single crystals of several complexes suitable for X-ray diffraction studies were obtained. These molecular structures allow better understanding of their properties (**Figure 93**, **Figure 94** and **Figure 95**). Most pertinent structural informations are depicted in **Table 8**. The three (O[^]N[^]O)M(L) complexes **126**, **131** and **150** adopt square planar geometry around the metal centre. Going from **126** to **131**, the bond lengths between the metal and the (O[^]N[^]O) ligand are elongated, in accord with larger atomic radius of platinum relative to palladium (entry 1-3). Indeed, the smaller palladium atom forces the tridentate ligand to a strong distortion (entry 11). [(O[^]N[^]O)Pt(L)] complexes **131** and **150** illustrate the influence of the NHC on the neighbouring (O[^]N[^]O) ligand. The strong electro donation of the NHC elongates the (O[^]N[^]O)-M bonds (entry 1-3) resulting in a distortion of the (O[^]N[^]O) ligand of **150** (entry 11). Between these three compounds, only one (**131**) with nearly planar (O[^]N[^]O) ligand allows electronic delocalisation, explaining the luminescent emission observed only for these Pt pyridine derivatives.

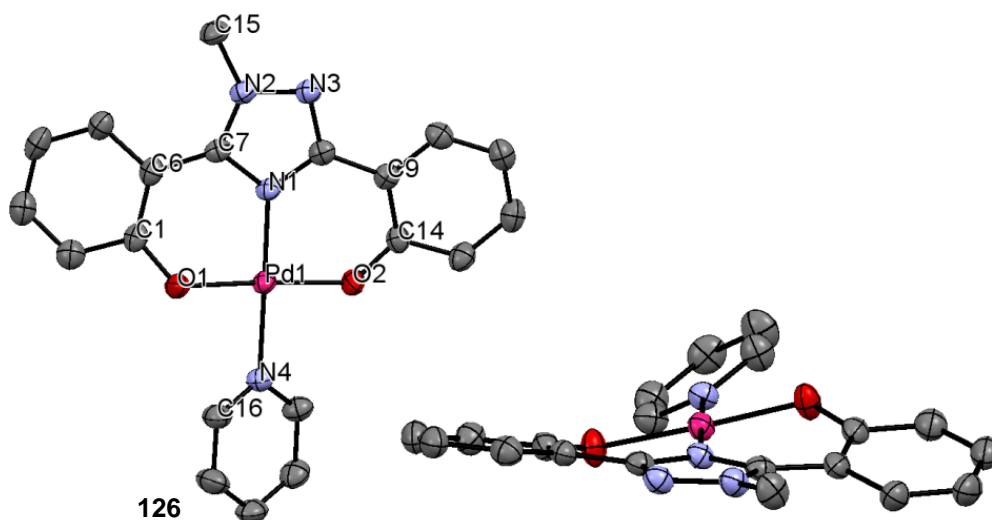


Figure 93: X-ray diffraction structure of palladium complex 126

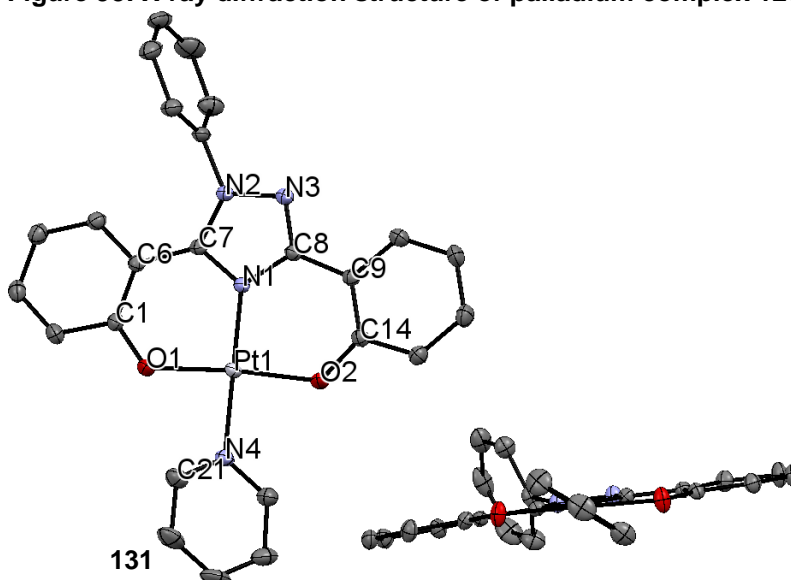


Figure 94: X-ray diffraction structure of platinum complex 131

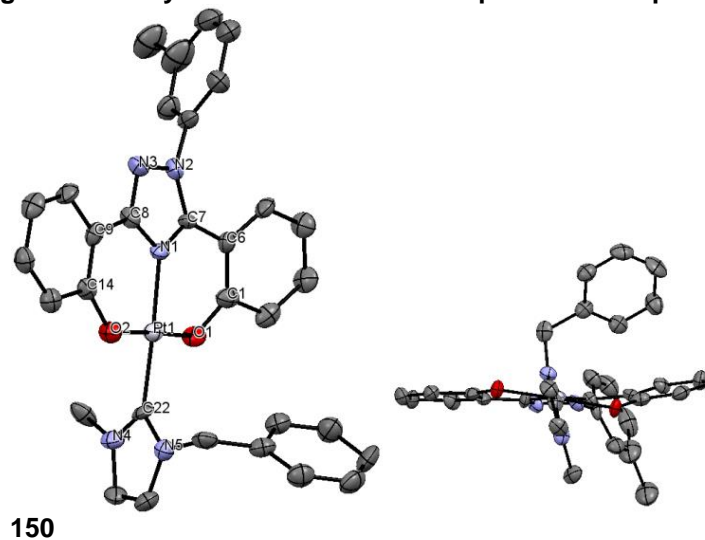
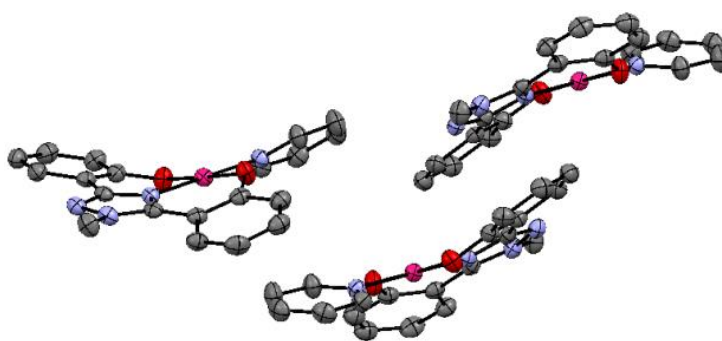


Figure 95: X-ray diffraction structure of platinum complex 150

Entry	Bond lengths and angles	(O [^] N [^] O)Pd(pyr) 126	(O [^] N [^] O)Pt(pyr) 131	(O [^] N [^] O)Pt(NHC) 150
1	M-O ¹	1.976	1.984	1.992
2	M-O ²	1.986	1.996	2.008
3	M-N ¹	1.949	1.961	2.012
4	M-N ⁴	2.060	2.024	/
5	M-C _{Carbene}	/	/	1.987
6	N ¹ -M-O ¹	90.80	92.00	88.03
7	N _{Pyr} -M-O ²	89.06	86.57	/
8	C _{Carbene} -M-O ²	/	/	88.03
9	O ² -M-N ⁴ -C _{Pyr}	20.81	35.36	/
10	O ² -M-C _{Carbene} -N ⁵	/	/	69.24
11	C ¹ -C ⁶ -C ⁹ -C ¹⁴	20.62	3.25	13.44

Table 8: Bond lengths (Å) and angles (°) of three [(O[^]N[^]O)M(L)] complexes

Solid-state staking of both complexes [(O[^]N[^]O)Pd(pyridine)] **126** and [(O[^]N[^]O)Pt(pyridine)] **131** shows a π stacking between the aromatic planes of (O[^]N[^]O) ligands conducting to antiparallel layers (**Figure 96**, **Figure 97**). However, π stacking interactions between pyridine groups are present in palladium complex **126**. In solid state, the [(O[^]N[^]O)Pt(NHC)] **150** complex forms dimeric anti-parallel structures by π -interaction between the triazole moieties (**Figure 98**).

Figure 96: Packing of [(O[^]N[^]O)Pd(pyridine)] complex 126: absence of π interactions

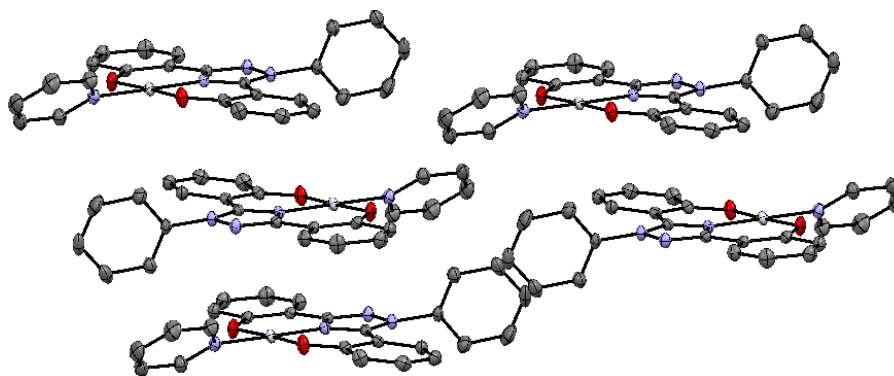


Figure 97: Packing of [(O^NO)Pt(pyridine)] complex 131: long-range π stacking between O^NO moieties

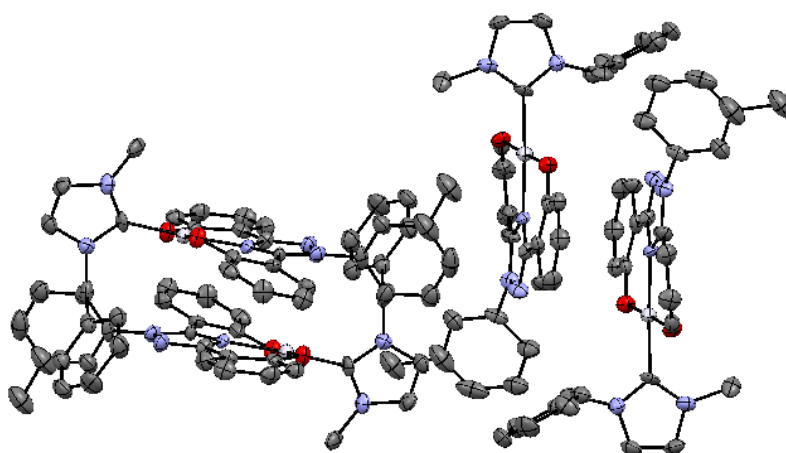


Figure 98: Packing of [(O^NO)Pt(NHC)] complex 150: dimer formation by π stacking

3.2.1.3 Photophysical characterization of the [(O^NO)Pt(pyridine)] complexes

Preliminary photophysical studies of four [(O^NO)Pt(NHC)] type complexes (R = Ph, 3,5-bis(CF₃)phenyl, 3,5-dimethylphenyl, and *p*-tolyl) were performed in 2-MethylTHF solution (5×10^{-5} M, 25 °C).³²⁶ Upon excitation at 350 nm, all the complexes showed a broad emission with moderate intensity in the green-to-orange range of the visible spectrum. The emission wavelength of the 3,5-bis(CF₃)phenyl complex **136** redshifts by ca. 40 nm compared to three other complexes having very close emission spectrum (**Figure 99**).

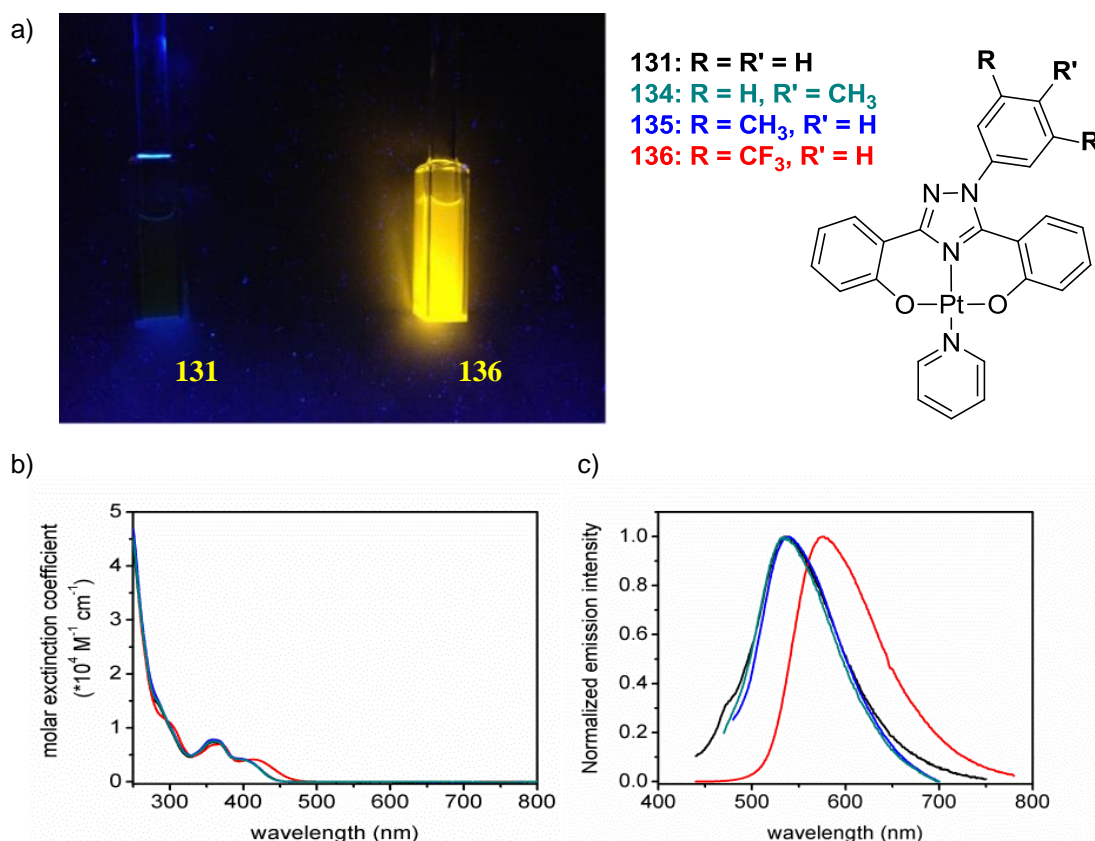


Figure 99: a) Emission of phenyl 131 (left) and 3,5-bis(CF₃)phenyl 136 (right) complex in 2-MeTHF, b) absorption and c) emission spectra of four (O[^]N[^]O) platinum complexes

The fluorinated complex **136** absorption differs by a significant redshift from the three other complexes (**Table 9**). In air-equilibrated or degassed solution, the three non-fluorinated complexes display short radiative de-excitation kinetics. The CF₃ complex **136** shows a longer excited state lifetime (148 ns) in normal solution and two magnitudes longer in degassed solution (1380 ns). This finding clearly indicates the triplet-manifold nature of the emitting excited state for such complexes. Moderate photoluminescence quantum yield of fluorinated derivative **136** was found (7%).

Complex: R =	$\lambda_{\text{abs max}} (\epsilon) [\text{nm}, (\times 10^4 \text{ M}^{-1} \text{ cm}^{-1})]$	$\lambda_{\text{em}} [\text{nm}]$	$T[\text{ns}]$	$\lambda_{\text{em}} [\text{nm}]$	$T[\text{ns}]$
131 Ph	286 (1.43), 360 (0.75), 403 (0.4)	537	18.3	537	22.7
134 <i>p</i> -tolyl	286 (1.43), 360 (0.75), 403 (0.4)	535	12.5	535	13.3
135 3,5-di(CH ₃)Ph	286 (1.46), 360 (0.78), 403 (0.4)	540	13.3	540	15.3
136 3,5-bis(CF ₃)Ph	302 (1.06), 368 (0.70), 419 (0.41)	577	148	577	1380

Table 9: [(O[^]N[^]O)Pt(NHC)] complexes: absorbance and emission maxima (λ) and excited state lifetime (T) in air-equilibrated and degassed 2-MeTHF

3.2.1.4 $[(O^{\wedge}N^{\wedge}O)Pt(\text{pyridine})]$ complexes: Molecular Orbital Calculations

DFT calculations were performed on each complex for better understanding of their electronic properties.³²⁶ As shown on **Figure 100**, the HOMO (Highest Occupied Molecular Orbital) is always located on the $(O^{\wedge}N^{\wedge}O)$ -Pt moiety. However, we notice a remarkable difference between the LUMO (Lowest Unoccupied Molecular Orbital) of the three non-fluorinated complexes **131**, **135**, **134** (LUMO on the pyridine) and the CF_3 complex **136**: electron-withdrawing effect of CF_3 displaces the LUMO towards the triazole and the 5-phenyl rings. These results imply the correlation between electron-withdrawing R groups and increase in emission intensity for such complexes and emission wavelength shifts. It remains to be investigated whether other electron-withdrawing groups, such as pentafluorophenyl or nitrobenzene, can further enhance the emission.

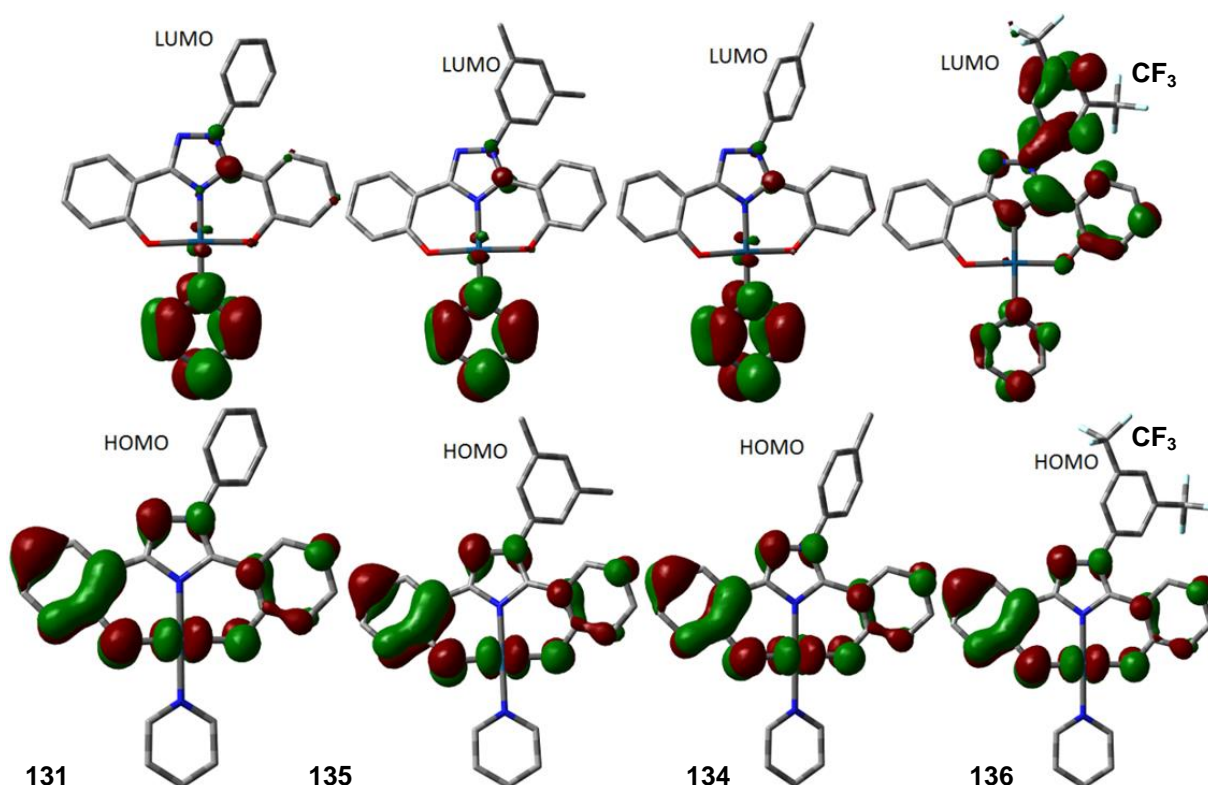
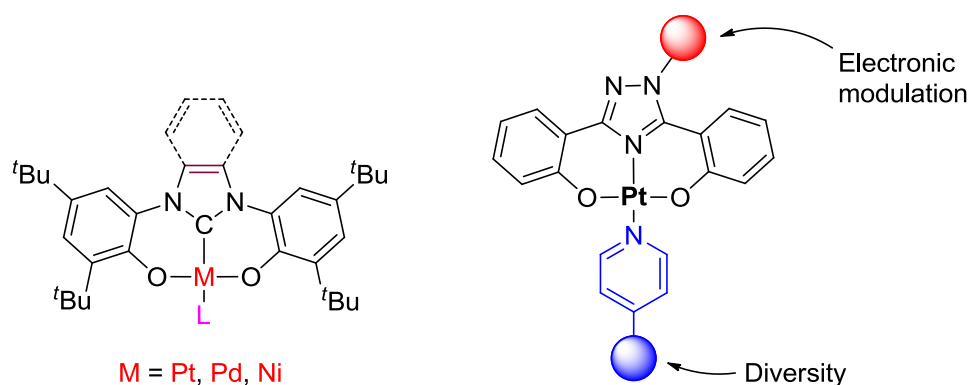


Figure 100: Locations of LUMOs and HOMOs on the $(O^{\wedge}N^{\wedge}O)$ platinum complexes: influence of the CF_3 group on the LUMO

3.3 Conclusion on Pt complexes containing tridentate ligands

In this chapter, we described successful synthesis and characterization of two families of complexes containing tridentate ($O^{\wedge}C^{\wedge}O$) or ($O^{\wedge}N^{\wedge}O$) ligands.



The preliminary photophysical studies are currently ongoing. ($O^{\wedge}C^{\wedge}O$) based complexes depict relatively poor luminescence strength. In contrast, the ($O^{\wedge}N^{\wedge}O$) based Pt complexes exhibit strong luminescence in solid state. Variation of the R group and monodentate L ligand shows promising luminescent properties for R = 3,5-bis(CF_3)phenyl and L = pyridine system. The planarity of the ($O^{\wedge}N^{\wedge}O$) ligand and subsequently electronic delocalisation may explain the luminescence observed for ($O^{\wedge}N^{\wedge}O$)Pt pyridine derivatives. DFT calculations show the influence of electron-withdrawing groups (CF_3) on the LUMO localisation of the complexes. Cytotoxic properties of these compounds will be further discussed in this thesis.

4 Introducing diversity in NHC-Platinum complexes: Post-synthetic derivatization

Post-synthetic functionalization allows introduction of further diversity to relatively simple precursors. In this chapter, we functionalized previously described simple NHC platinum complexes following three strategies:

- Ligand exchange reactions
- Imine formation on a NHC complex bearing an aldehyde function
- Halogen exchange reactions

Ligand exchange of a labile pyridine with various neutral ligands allows introduction of various amines as well as more exotic pnictogen based ligands (phosphines, arsines, stibines). The use of polyamines will further permit to obtain polynuclear and cationic species. This derivatization strategy can be combined with imine/oxime formation on a benzaldehyde Pt complex. Especially oxime formation gave various stable complexes. Halogen exchange of bromide ligands by iodide allowed a fast and quantitative introduction of radioactive iodine isotopes to NHC platinum complexes.

4.1 Ligand exchange reaction on a pyridine platinum NHC complex

The pyridine-platinum bond located in *trans* configuration to the NHC,³³¹ is weakened by its strong donor property. This effect was earlier observed by Grubbs and co-workers for [(pyr)Ru(NHC)] complexes.³³² Thanks to its lability, pyridine complexes, especially 3-chloropyridine, allowed the preparation and stabilization of NHC-palladium complexes (concept of PEPPSI: pyridine-enhanced precatalyst preparation, stabilization, and initiation) for various palladium-catalysed cross coupling reactions.^{333,268}

Ligand exchange has always been a strategy of choice for post-synthetic modification of metal complexes. However, ligands possessing several donor atoms rarely allow a direct ligand substitution. Inspired by the straightforward NHC palladium synthesis described by Organ and co-workers,³³³ a direct synthesis of *trans* [(pyridine)Pt(NHC)X₂] complexes was developed in our laboratory.^{124,125} This

³³¹ For a description of *trans*-effect in platinum complexes, see: Orgel, L. E. *J. Inorg. Nucl. Chem.* **1956**, 2, 137.

³³² Trnka, T. M.; Morgan, J. P.; Sanford, M. S.; Wilhelm, T. E.; Scholl, M.; Choi, T.-L.; Ding, S.; Day M. W. Grubbs, R. H. *J. Am. Chem. Soc.*, **2003**, 125, 2546; Sanford, M. S.; Love, J. A. Grubbs, R. H. *Organometallics* **2001**, 20, 5314; Emrick, T. S. *US 7,960,555*, **2011**.

³³³ O'Brien, C. J.; Kantchev, E. A. B.; Valente, C.; Hadei, N.; Chass, G. A.; Lough, A.; Hopkinson, A. C.; Organ, M. G. *Chem. Eur. J.* **2006**, 12, 4743.

way, numerous post-synthetic modifications are easily accessible through simple ligand exchange of pyridine (**Figure 101**).

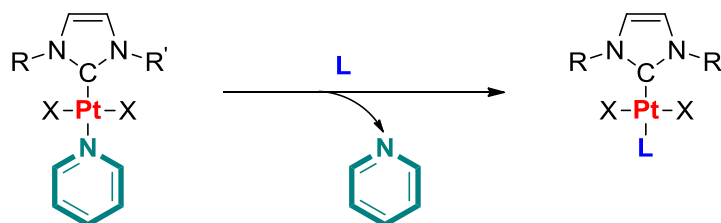


Figure 101: Post-synthetic modification by ligand substitution on a platinum-NHC complex

This methodology allowed easy derivatization of nitrogen-based ligands such as amines, hydrazines, amino acids, di and tri-peptides or ureic acid derivatives (**Figure 102**).^{124,125,128} Of interest, no competition for coordination toward the metal centre were observed for other functional groups such as alcohols, esters, amides, guanidinium or carbamates, present on the amino backbone. Nevertheless, incorporation of carboxylic acid groups on the molecule conducts to non-identified products resulting from a contest between forehead groups. This problem could be circumvented by protecting the carboxylic acid prior the coordination on the platinum centre. However, it is noteworthy that after formation of the amino ester platinum complex, deprotection to regenerate the acid was not possible.

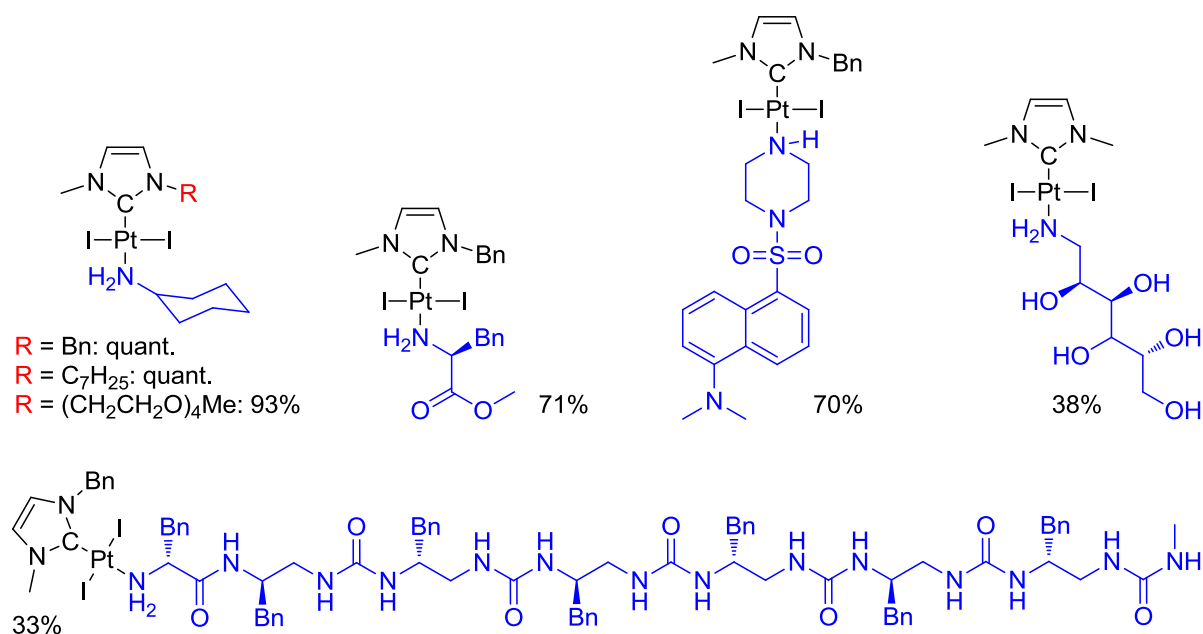


Figure 102: Examples of N-ligand functionalized platinum complexes (% refers to isolated product obtained from pyridine precursor)

Introduction of dansyl groups³³⁴ endow the complexes with a fluorescent moiety interesting for monitoring *in vitro* fluorescence. Enhanced water-solubility of glucamine, ethanol or polyethylene glycol (PEG) complexes allows potential biomedical applications. While simple amines (cyclohexylamine) or hydrazines were introduced nearly quantitatively, polar groups and dipeptides impeded purification by silica gel chromatography and decreased reaction yield.

4.1.1 Introducing nitrogen based ligands by ligand exchange

In order to increase the diversity of such potential bioactive molecules, other nitrogen containing ligands were prepared. We thus considered various biological interesting amines, (metronidazole and phosphonate derivatives) and hydroxylamines to study the influence of adjacent oxygen atom as well as polyethylenimine (PEI) for enhanced water solubility.

4.1.1.1 One-step introduction of volatile amines

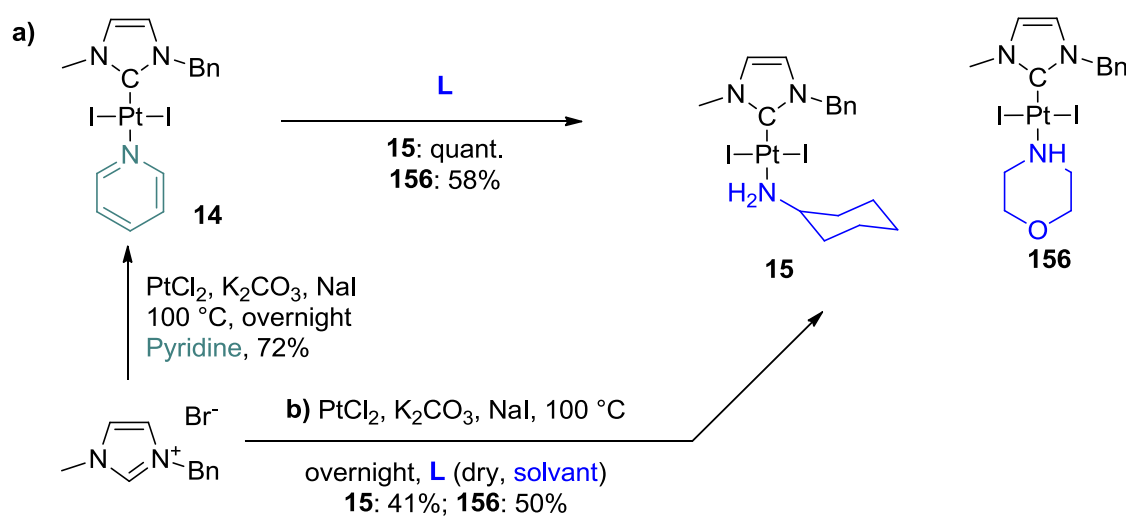


Figure 103: Ligand exchange **a)** and **b)** direct synthesis of [(NHC)PtI₂(amine)] complexes

Simple and volatile amines (cyclohexylamine, morpholine, etc.) could be introduced to pyridine-platinum-NHC complexes by ligand exchange as previously reported through pathway **a)** (**Figure 103**). Alternatively, these ligands could also easily be introduced by replacement of the pyridine by the

³³⁴ Bartzatt, R. J. *Pharmacol. Toxicol. Methods*. **2001**, *45*, 247.

corresponding amine to obtain the desired complexes **15** and **156** more quickly and in comparable yields (pathway b).

4.1.1.2 Introduction of alkylating and targeting ligands to platinum NHC complexes

The first di-alkylating antineoplastic agent discovered was mechlorethamine (*Mustargen*).³³⁵ It was used to treat Hodgkin diseases or leukaemia, giving rise to a whole family of nitrogen mustard-based³³⁶ drugs. These molecules (*Cyclophosphamide*, *Chlorambucil*, *Bendamustine*, *Trofosfamide*, *Prednimustine*, *Uramustine*, *Melphalan*, or *Estramustine*) form cross-linkage of two 7-*N*-guanines of different DNA-strands.³³⁷ To enhance the cytotoxic properties of our platinum complex, we investigated the introduction of bis(2-chloroethyl)amine *trans* to the NHC (**Figure 104**).³³⁸ The mild conditions (3 days, 25 °C) yielded the desired complex **157** in 85% yields preventing hydrolysis of chlorine groups.

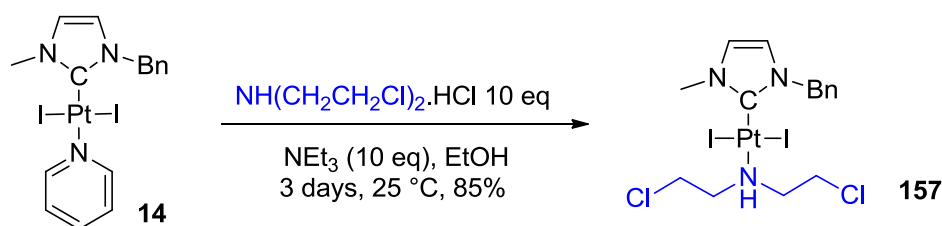


Figure 104: Synthesis of nitrogen mustard platinum derivative 157

In order to combine another biological activity with the platinum core, metronidazole was also considered. Indeed this class of compounds is well known to have some antibiotic properties³³⁹ especially against anaerobic bacteria infections.³⁴⁰

³³⁵ Ariel, I.; M.; Kanter, L. *Am. J. Surg.* **1949**, 77, 509; Joensuu, H. *Lancet Oncol.* **2008**, 9, 304.

³³⁶ Marrs, T. C.; Maynad, R. L.; Sidell, F. R. *Chemical Warfare Agents: Toxicology and Treatment* **2007**, John Wiley & Sons

³³⁷ Mattes, W. B.; Hartley, J. A.; Kohn, K. W. *Nucleic Acids Res.* **1986**, 14, 2971.

³³⁸ In mustard-Co(III) complexes, the cobalt(III) is used as carrier of the prodrug. Reducing into Co(II) in hypoxic cancer cells is supposed to release the mustard agent: Ware, D. C.; Wilson, W. R.; Denny, W. A.; Richard, J. C. E. F. *Chem. Soc., Chem. Commun.* **1991**, 1171; Ware, D. C.; Palmer, B. D.; Wilson, W. R.; Denny, W. A. *J. Med. Chem.* **1993**, 36, 1839.

³³⁹ *18th List of Essential Medicines* **2013**, World Health Organization.

³⁴⁰ Lindmark, D. G.; Müller, M. *Antimicrob. Agents Chemother.* **1976**, 10, 476; Brogden, R. N.; Heel, R. C.; Speight, T. M.; Avery, G. S. *Drugs* **1978**, 16, 387.

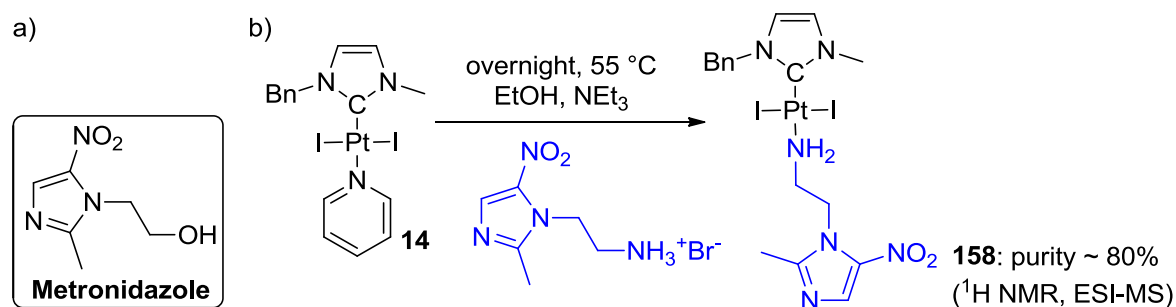


Figure 105: a) Metronidazole and b) introduction trial to Pt-NHC complexes of an amino derivative of it

The amino-metronidazole was obtained from commercially available metronidazole.³⁴¹ Then ligand exchange was performed using our standard conditions (**Figure 105**). Once more, the presence of the expected complex **158** was observed by mass spectrometry and ¹H-NMR thanks to disappearance of the coordinated pyridine signal. Slow decomposition occurred upon chromatography purification (SiO₂) and so product was always obtained in only 80% purity.

4.1.1.3 Amino-phosphonate linkers for nano-particle functionalization

Phosphonate (R-PO(OR')₂ with R = alkyl and R' = H or alkyl) is an organophosphorous (P^V) class derived from phosphorous acid (H-PO(OH)₂). These molecules are an important class of valuable synthetic intermediate to access phosphorous containing compounds³⁴² such as chiral phosphines and oligonucleotides.³⁴³ Aminophosphonic acids derivatives are well known for their interesting biological properties.³⁴⁴ Since the beginning of 21st century, phosphonates have been studied as linkage groups on amorphous iron oxide nanoparticles³⁴⁵, iron oxide colloids³⁴⁶ or on magnetite nanoparticles.³⁴⁷ Its high binding efficiency by electrostatic interactions to nanoparticles opens a large field for (biological)

³⁴¹ Bertinaria, M.; Galli, U.; Sorba, G.; Fruttero, R.; Gasco, A.; Brenciaglia, M. I.; Scaltrito, M. M.; Dubini, F. *Drug Dev. Res.* **2003**, *60*, 225.

³⁴² Kraszewski, A.; Stawinski, J. *Pure Appl. Chem.* **2007**, *79*, 2217.

³⁴³ Pertusati, F.; Serpi, M.; McGuigan, C. *Antiviral Chem. Chemother.* **2012**, *22*, 181.

³⁴⁴ Naydenova, E. D.; Todorov, P. T.; Troev, K. D. *Amino Acids* **2010**, *38*, 23; Fleisch, H. *Breast Cancer Res* **2002**, *4*, 30; Green, J. R. *Oncologist*. **2004**, *9*, 3.

³⁴⁵ Yee, C.; Kataby, G.; Ulman, A.; Prozorov, T.; White, H.; King, A.; Rafailovich, M.; Sokolov, J.; Gedanken A. *Langmuir* **1999**, *15*, 7111.

³⁴⁶ Portet, D.; Denizot, B.; Rump, E.; Lejeune, J.-J.; Jallet, P. *J. Colloid Interface Sci.* **2001**, *238*, 37.

³⁴⁷ Sahoo, Y.; Pizem, H.; Fried, T.; Golodnitsky, D.; Burstein, L.; Sukenik, C. N.; Markovich, G. *Langmuir* **2001**, *17*, 7907.

applications.³⁴⁸ Nanoparticles, coated with PEG (polyethylene glycol) chains, are water-soluble and can be functionalized with a wide range of functionalities.³⁴⁹

Several groups have associated phosphonate groups with metals (**Figure 106**),³⁵⁰ the phosphonate moiety acting as a ligand onto the platinum³⁵¹ or it is incorporated into the ligand.³⁵²

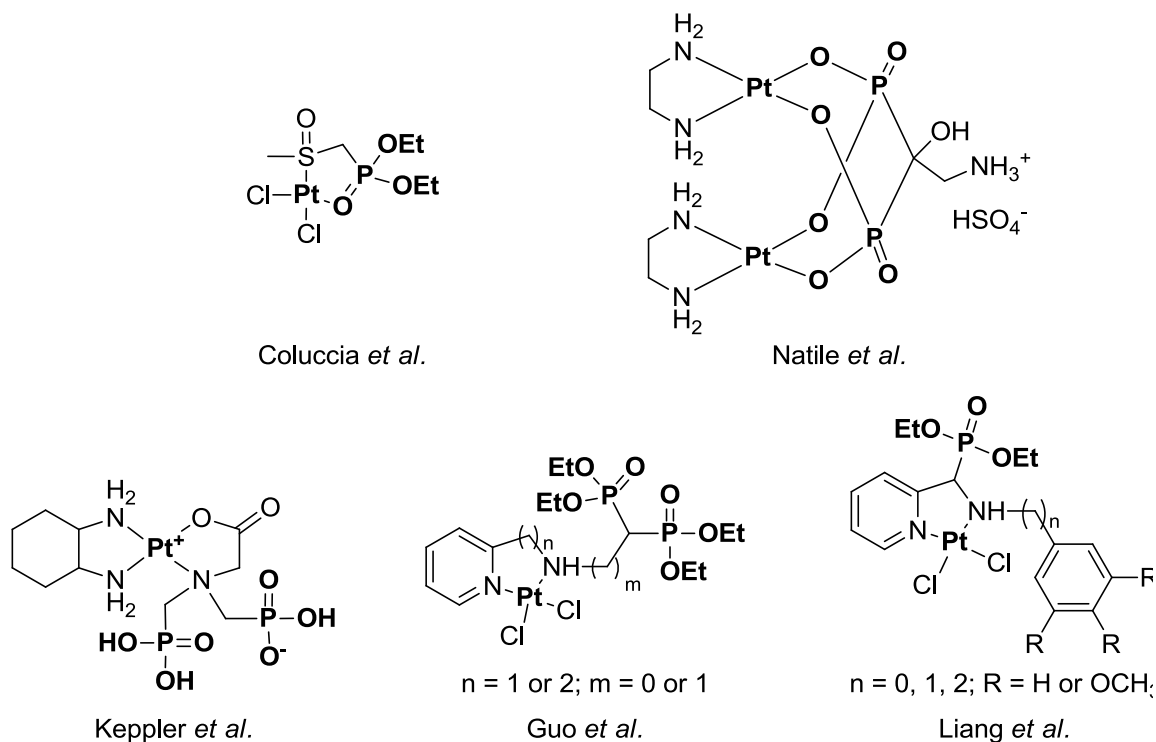


Figure 106: Platinum-phosphonate conjugates tested for anticancer applications^{351,352}

Considering high antiproliferative properties of our Pt NHC complexes, it was then decided to synthesize a class of non-coordinating phosphonate complexes. The phosphonate would potentially modulate the toxicity of the platinum core, but also give access to conjugate the complex to iron nanoparticles. For this purpose, phosphonate group was either attached to the NHC backbone, or attached on the amine ligand. The phosphonate imidazolium derivative was synthesized in two steps in

³⁴⁸ White, M. A.; Johnson, J. A.; Koberstein, J. T.; Turro, N. J. *J. Am. Chem. Soc.* **2006**, *128*, 1135; Thanh, N. T. K.; Green, L. A. W. *Nano Today* **2010**, *5*, 213; Sapsford, K. E.; Algar, W. R.; Berti, L.; Gemmill, K. B.; Casey, B. J.; Oh, E.; Stewart, M. H.; Medintz, I. L. *Chem. Rev.* **2013**, *113*, 1904.

³⁴⁹ Susumu, K.; Uyeda, H. T.; Medintz, I. L.; Pons, T.; Delehanty, J. B.; Mattoussi, H. *J. Am. Chem. Soc.* **2007**, *129*, 13987; Juteaek, N.; Nayoun, W.; Jiwon, B.; Ho, J.; Joonhyuck, P.; Sungwook, J.; Sanghwa, J.; Youngrong, P.; Sungjee, K. *Adv. Drug. Deliv. Rev.* **2013**, *65*, 622.

³⁵⁰ Galezowska, J.; Gumienna-Kontecka, E. *Coord. Chem. Rev.* **2012**, *256*, 105.

³⁵¹ Sasanelli, R.; Boccarelli, A.; Giordano, D.; Laforgia, M.; Arnesano, F.; Natile, G.; Cardellicchio, C.; Capozzi, M. A. M.; Coluccia, M. *J. Med. Chem.* **2007**, *50*, 3434; Piccinonna, S.; Margiotta, N.; Pacifico, C.; Lopalco, C.; Denora, N.; Fedi, S.; Corsini, M.; Natile, G. *Dalton Trans.* **2012**, *41*, 9689.

³⁵² Galanski, M.; Slaby, S.; Jakupec, M. A.; Kepler, B. K. *J. Med. Chem.* **2003**, *46*, 4946; Xue, Z.; Lin, M.; Zhu, J.; Zhang, J.; Li, Y.; Guo, Z. *Chem. Commun.* **2010**, *46*, 1212; Huang, K.-B.; Chen, Z.-F.; Liu, Y.-C.; Li, Z.-Q.; Wei, J.-H.; Wang, M.; Zhang, G.-H.; Liang, H. *Eur. J. Med. Chem.* **2013**, *63*, 76; Huang, K.-B.; Chen, Z.-F.; Liu, Y.-C.; Li, Z.-Q.; Wei, J.-H.; Wang, M.; Xie, X.-L.; Liang, H. *Eur. J. Med. Chem.* **2013**, *64*, 554.

moderate yield from diethyl 4-hydroxybenzylphosphonate.³⁵³ The phosphonic acid derivative (R-P(O)(OH)₂) was discarded for a straight synthesis to prevent competitive coordination through the metal centre. We choose a diethyl phosphonate ester instead of phosphonic acid derivative to prevent competing coordination of the phosphonate group. Using standard conditions, the corresponding Pt-pyridine complex **159** was obtained in good yield (**Figure 107**). High polarity of the resulting complex did not allow easy purification on silica gel chromatography (ethyl acetate, $R_f = 0.2$). In contrast, standard complex synthesis conditions with cyclohexylamine as solvent only afforded decomposition products. Ligand exchange involving cyclohexylamine in large excess afforded the desired complex **160** in poor yield (15%). It appeared that the complex decomposes in cyclohexylamine media. [(NHC)Pt(cyclohexylamine)] complex **160** is even more polar, as acetone was needed to elute the compound over SiO₂ chromatography column. Besides, it is only soluble in polar solvents such as acetone, MeOH, EtOH, etc.

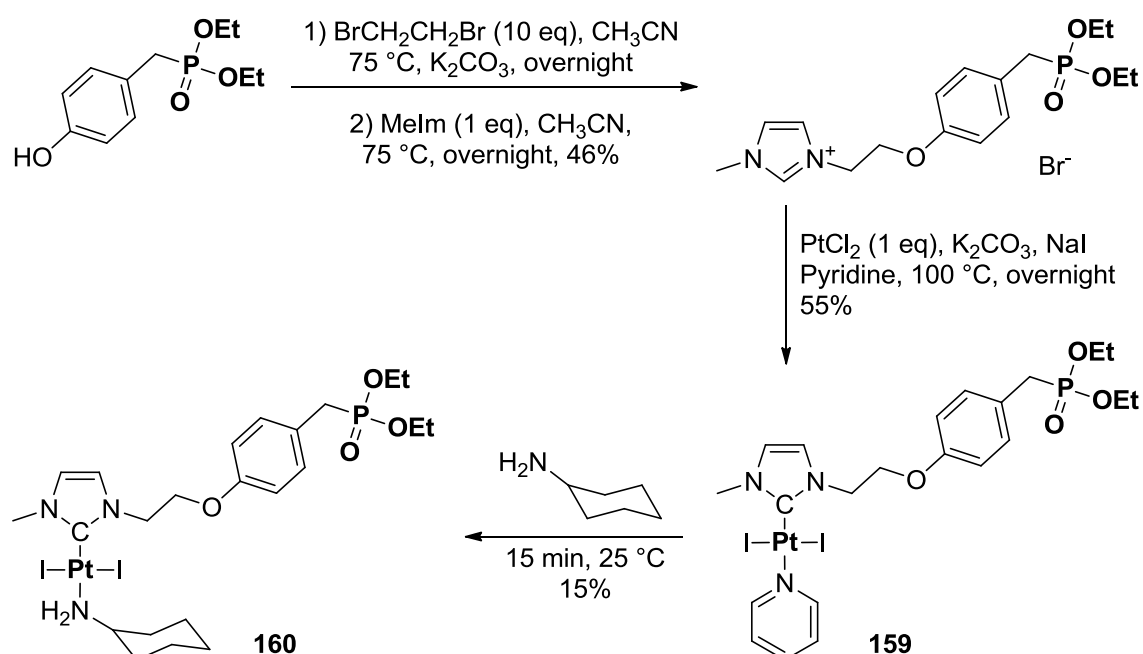
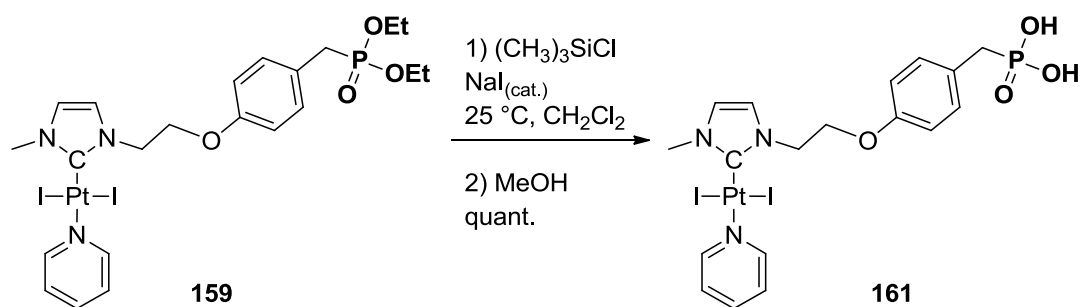


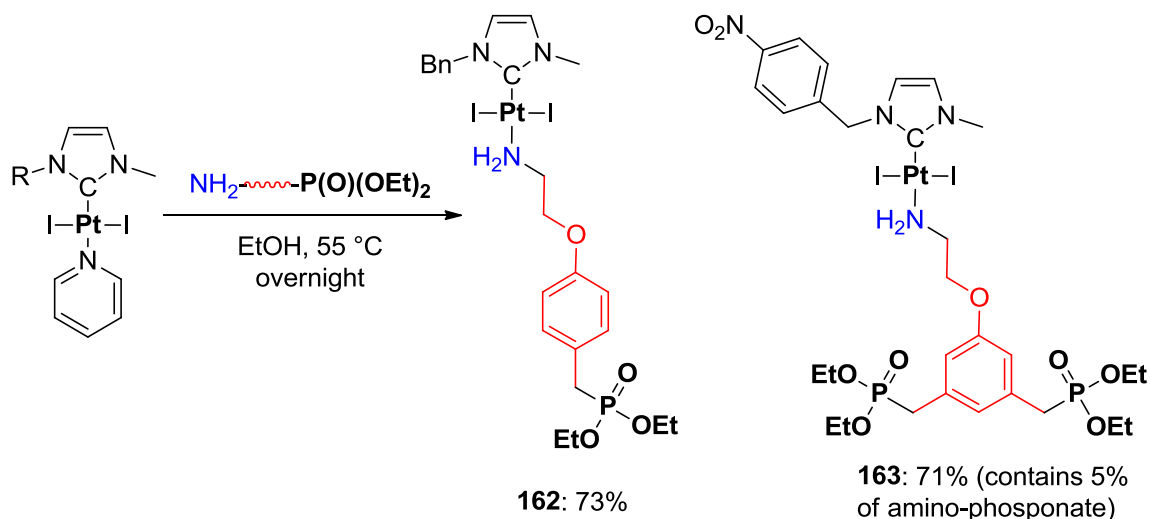
Figure 107: Synthesis of Phosphonate-NHC-platinum conjugates 159 and 160

Several hydrolytic conditions were tested to generate the free phosphonic acid. No reaction is observed in presence of HCO₂H or TMS-Cl, and TFA leads to mixtures. Finally, combination of TMS-Cl and catalytic amount of sodium iodide afforded a phosphonate trimethylsilyl conjugate. The desired compound **161** is obtained pure in quantitative yield after methanol addition, filtration and evaporation of volatiles. The obtained phosphonic acid is soluble in polar solvents (methanol) and indeed in water.

³⁵³ Diethyl 4-hydroxybenzylphosphonate precursor was prepared in the DMO-IPCMS group by Catalina Bordeianu under Dr. D. Felder-Flesch.

**Table 10: Mild hydrolysis of phosphonic ester**

This experiment demonstrates the possibility to easily access phosphonic acid featured complexes. To introduce potentially cleavable linker between the nanoparticle and the Pt, we decided to introduce an amino-phosphonate linker by ligand exchange. The two amino-linker-phosphonate derivatives (diethyl 4-(2-aminoethoxy)benzylphosphonate and tetraethyl ((5-(2-aminoethoxy)-1,3-phenylene)bis(methylene))bis(phosphonate)) were synthesized according a procedure developed in the DMO laboratory by Catalina Bordeianu under supervision of Dr. D. Felder-Flesch. Starting from the standard pyridine complex, these linkers afforded the desired complexes **162** and **163** in good yields after silica gel purification (**Figure 108**).

**Figure 108: Introduction of phosphonate linkers by ligand exchange (%: yield of ligand exchange step)**

These phosphonic linker-containing molecules are very promising water-soluble anticancer drugs but also building block for nanoparticles (NP). Actually, the group of Dr. Felder-Flesch (DMO, IPCMS) developed an elegant synthesis of water-soluble dendronized iron nanoparticles studied as contrast agents in nuclear magnetic resonance imagery (MRI).³⁵⁴ Water-solubility of these NP results from covering of these particles with PEG groups attached by phosphonate linkers. Knowing that combining metal complexes and NPs provides new interesting material for anticancer therapy,³⁵⁵ combination of our platinum complexes with phosphonate-iron NPs was started (**Figure 109**).³⁵⁶ This promising theranostic³⁵⁷ agent is currently under investigation in collaboration with the group of Dr. Felder-Flesch.³⁵⁸

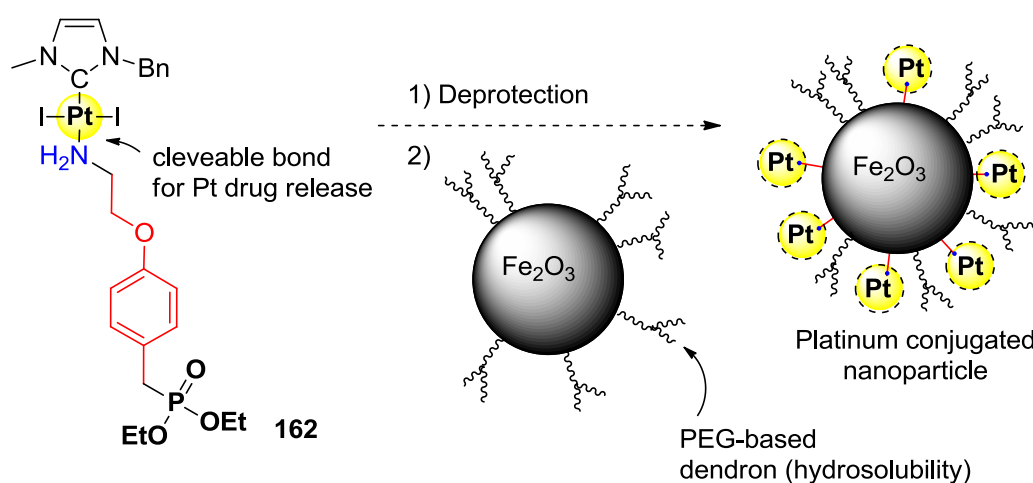


Figure 109: Proposed functionalization of nanoparticles with NHC-platinum complexes

³⁵⁴ Basly, B.; Felder-Flesch, D.; Perriat, P.; Billotey, C.; Taleb, J.; Pourroy, G.; Begin-Colin, S. *Chem. Commun.* **2010**, 46, 985; Basly, B.; Popa, G.; Fleutot, S.; Pichon, B. P.; Garofalo, A.; Ghobril, C.; Billotey, C.; Berniard, A.; Bonazza, P.; Martinez, H.; Felder-Flesch, D.; Begin-Colin, S. *Dalton Trans.* **2013**, 42, 2146.

³⁵⁵ Maldonado, C. R.; Salassa, L.; Gomez-Blanco, N.; Mareque-Rivas, J. C. *Coord. Chem. Rev.* **2013**, 257, 2668.

³⁵⁶ Several works on platinum incorporating nanoparticles appeared in last 5 years: Gadolinium-DTPA/DACH-Platinum-loaded micelles: Kaida, S.; Cabral, H.; Kumagai, M.; Kishimura, A.; Terada, Y.; Sekino, M.; Aoki, I.; Nishiyama, N.; Tani, T.; Kataoka, K. *Cancer Res.* **2010**, 70, 7031; Gold Nanoparticles: Brown, S. D.; Nativo, P.; Smith, J. A.; Stirling, D.; Edwards, P. R.; Venugopal, B.; Flint, D. J.; Plumb, J. A.; Graham, D.; Wheate, J. N. *J. Am. Chem. Soc.* **2010**, 132, 4678; Min, Y.; Mao, C.-Q.; Chen, S.; Ma, G.; Wang, J.; Liu, Y. *Angew. Chem. Int. Ed.* **2012**, 51, 6742; or Hydrogel nanoparticles: Shirakura, T.; Kelson, T. J.; Ray, A.; Malyarenko, A. E. Kopelman, R. *ACS Macro Lett.* **2014**, 3, 602.

³⁵⁷ Wang, D.; Lin, B.; Ai, H. *Pharm. Res.* **2014**, 31, 1390; Arrowsmith, R. L.; Pascu, S. I.; Smugowski, H. *Organomet. Chem.* **2012**, 38, 1.

³⁵⁸ Bouché, M. *Master Thesis* **2014**, University of Strasbourg.

4.1.1.4 Introduction of hydroxylamines to NHC-Pt complexes

As already mentioned, chemical diversity can be accessed by using various nitrogen sources. To complete this work, other nitrogen-based ligands have been investigated such as hydroxylamine (aminoxy) ligands of general formula $\text{NH}_2\text{-O-R}$.³⁵⁹ Similar to amino esters, hydroxylamines were generated *in situ* by deprotonation of the corresponding ammonium salt in presence of triethylamine (**Figure 110**).¹²⁴ The reaction with pyridine complex **14** was found to be effective with yields ranging from 39 to 76% (complexes **164-166**).

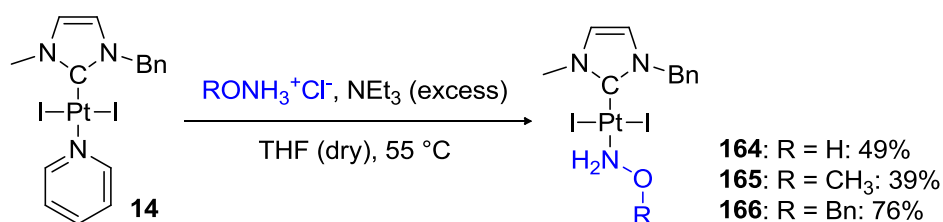


Figure 110: Ligand exchange reaction applied to hydroxylamines (%: yield of exchange step)

Reaction conditions were optimized by varying solvents or reaction time. Neither methanol nor toluene was found as effective as THF for this transformation. Moreover, increase of reaction time (4 days) was found detrimental for the stability of the product. Sodium hydroxide employed as a base instead than triethylamine extinguished the reaction by decomposition of the starting material.

The presence of the neighbouring oxygen atom should increase the nucleophilicity of the nitrogen of hydroxylamines compared to amines (α -effect).³⁶⁰ A bis-functionalized amino-hydroxylamine derivative should prefer the coordination of the hydroxylamine rather than amine allowing selective coordination of hetero-functionalized compounds. This would be especially interesting to introduce selectively e.g. a hydroxylamine-functionalized peptide by the hydroxylamine function. To test this hypothesis, competition experiment between benzylamine and benzyhydroxylamine gave after three days (equilibrium) a mixture of **167** / **166** = 3/1 proving the preferential complexation of amines over hydroxylamines (**Figure 111**). The presence of equilibrium renders impossible potential introduction of hydroxylamine-amine derivatives selectively by one single function.

³⁵⁹ Hydroxylamines are well known as antimalarial agents for parasite inhibition: Berger, B. J. *Antimicrob. Agents Chemother.* **2000**, 44, 2540.

³⁶⁰ Ren, Y.; Yamataka, H. *J. Org. Chem.* **2007**, 72, 5660.

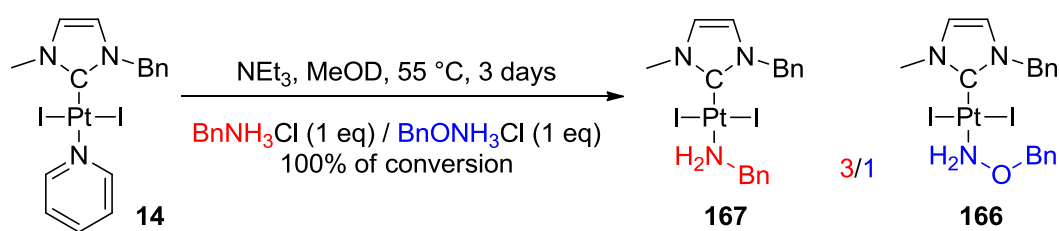


Figure 111: Competition experiment between benzylamine and benzylhydroxylamine

Single crystals of two $[(\text{NHC})\text{PtI}_2(\text{hydroxylamine})]$ complexes **164** and **166** suitable for X-ray diffraction analysis were obtained by slow diffusion of pentane in a solution of dichloromethane. Both complexes adopt the typical square planar conformation akin to the previous complexes (**Figure 112**). Selected bond lengths of hydroxylamine and amino complexes are summarized in **Table 11** to demonstrate the influence of the neighbouring oxygen atom of the hydroxylamine. $\text{C}_{\text{carbene}}$ -platinum bond of benzylhydroxylamine complex **166** is elongated compared with cyclohexylamine analogue **15**. Platinum-nitrogen bonds of both hydroxylamine complexes **164** and **166** are slightly shortened compared to cyclohexylamine. The packing of $[(\text{NHC})\text{PtI}_2(\text{NH}_2\text{OH})]$ **166** is first directed by hydrogen bonds between OH moiety and iodine ligands (3.450(6) Å) and secondarily by O- $\text{HC}_{\text{imidazolyldiene}}$ interactions (3.133(7) Å < sum of Van der Waals radii (3.22 Å) of O (1.52 Å) and C (1.70 Å)).

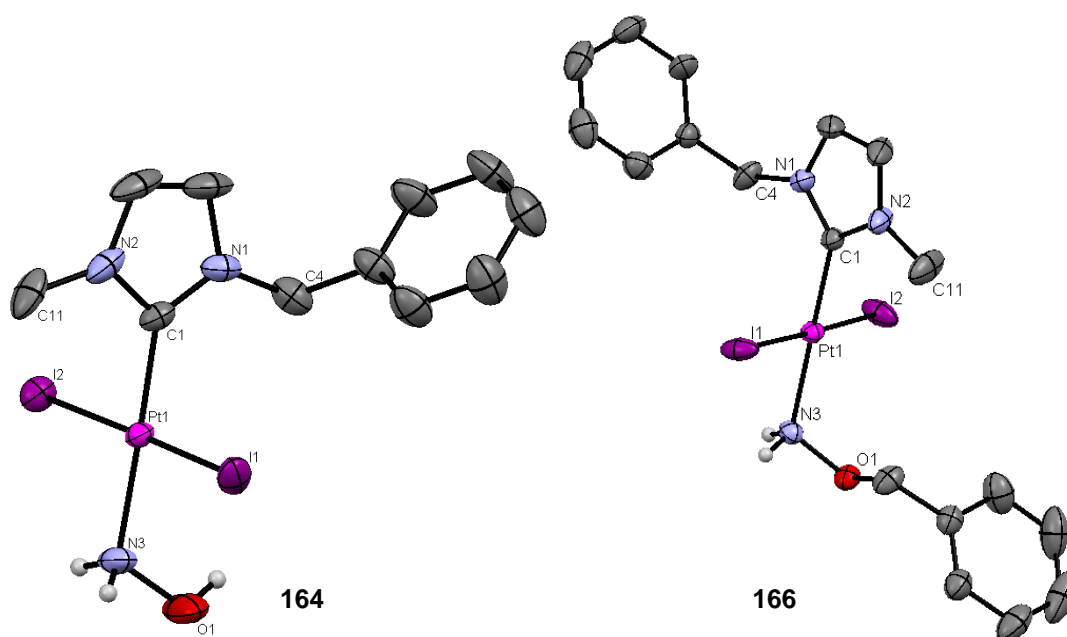


Figure 112: X-ray diffraction structures of $[(\text{NHC})\text{PtI}_2(\text{NH}_2\text{OH})]$ **164 and $[(\text{NHC})\text{PtI}_2(\text{benzylhydroxylamine})]$ **166****

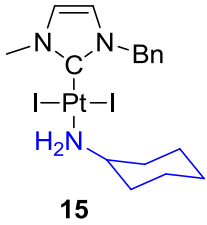
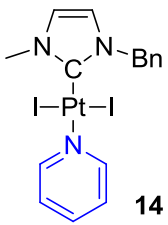
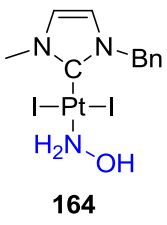
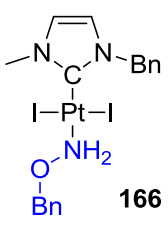
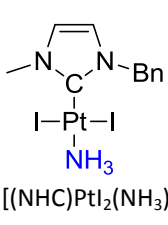
Bond lengths (Å)	 15	 14	 164	 166	 [(NHC)PtI ₂ (NH ₃)]
C-Pt	1.964(5)	1.974(7)	1.961(4)	1.971(4)	1.971(6)
Pt-N	2.121(5)	2.094(6)	2.098(4)	2.103(4)	1.971(6)
Pt-I	2.6011(5) 2.5891(5)	2.5934(5) 2.6025(5)	2.5929(4) 2.5935(4)	2.5853(4) 2.5940(4)	2.6081(3) 2.5929(3)

Table 11: Comparison of bond lengths of hydroxylamine and amino complexes¹²⁴

4.1.2 Reactivity of platinum NHC complexes towards polyamines

We fix our attention on introduction of polyamines to our platinum complexes in order to reassemble several platinum moieties in one single molecule and increase the platinum loading (increase of local Pt concentration). Small polyamines (ethylenediamine, diethylenetriamine) coordinate in κ^2 respectively κ^3 (chelate effect) to form cationic species. Larger polyamines bind several platinum atoms thus increasing the platinum percentage per molecule. We first discuss the reactivity of di and tri-coordinating amines and further extend the scope to polyethylenimine (PEI).

4.1.2.1 Reactivity of (NHC)Pt(II)(pyridine) complexes with di and tri-amines

Ligand exchange reactions with various amines were conducted in our laboratory to introduce diversity into NHC-Pt complexes. To extend this post-synthetic functionalization to other complexes, we also tried substitution reaction with a dibromo complex. During these experiments, we observed different reactivity of bromide compared to the iodide complexes. For example, [(NHC)PtI₂(pyridine)] **14** complex reacts in presence of a model primary amine, e.g. cyclohexylamine, by exchange of the labile pyridine ligand to quantitatively yield the [(NHC)PtI₂(cyclohexylamine)] **15** complex (**Figure 113**).¹²⁵ To note, diamino-platinum complexes never were observed stating with the bis-iodide-platinum complexes. Even when using harsher conditions such as 100 °C with amine as solvent, no exchange with iodide was noticed. [(NHC)PtBr₂(pyridine)] **168** in presence of cyclohexylamine in

CH_2Cl_2 is giving the expected mono-substituted complex *trans*-[(NHC)PtBr₂(cyclohexylamine)] **169**. However, changing the conditions, the bromo platinum derivative generated cationic species thanks to the weaker bromo platinum bond strength. For example, using cyclohexylamine as solvent at 25 °C for 1 hour afforded after purification a white cationic species [(NHC)PtBr(cyclohexylamine)₂]⁺Br⁻ **170** in good yield (68%). The coordination of two amines to platinum centre was evidenced by mass spectrometry and NMR analysis.

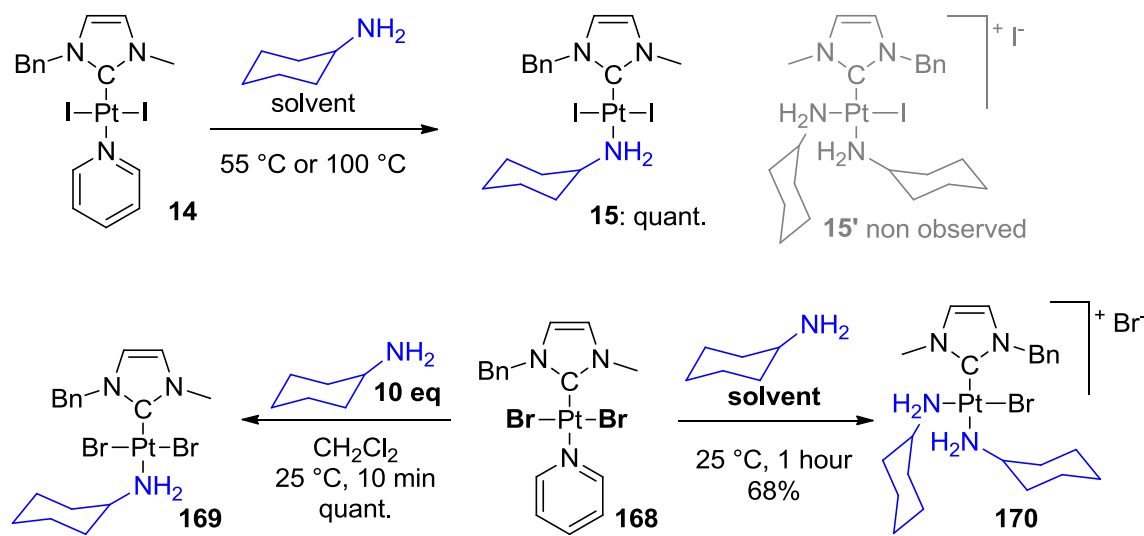


Figure 113: Ligand exchange on [(NHC)PtX₂(pyr)] with cyclohexylamine: Influence of halogen ligands

In contrast to monodentate amines, bidentate ligands such as ethylenediamine only form the corresponding cationic complex **171** thanks to the chelating effect (**Figure 114**).¹²⁴ A tridentate ligand conducts to full displacement of every other ligands than the NHC by the diethylenetriamine to form the di-cationic complex **172** as proved by single crystal X-ray diffraction. It is noteworthy that in solution, a dynamic equilibrium is observed between bis and tri coordinated ligand (verified by mass spectrometry). As expected, all those cationic complexes were found to be water-soluble. In view of the reactivity of ethylenediamine and diethylenetriamine, it seems obvious to extend to longer amino chains based on the same repeating NHCH_2CH_2 unit to arise polycationic and polymetallic species.

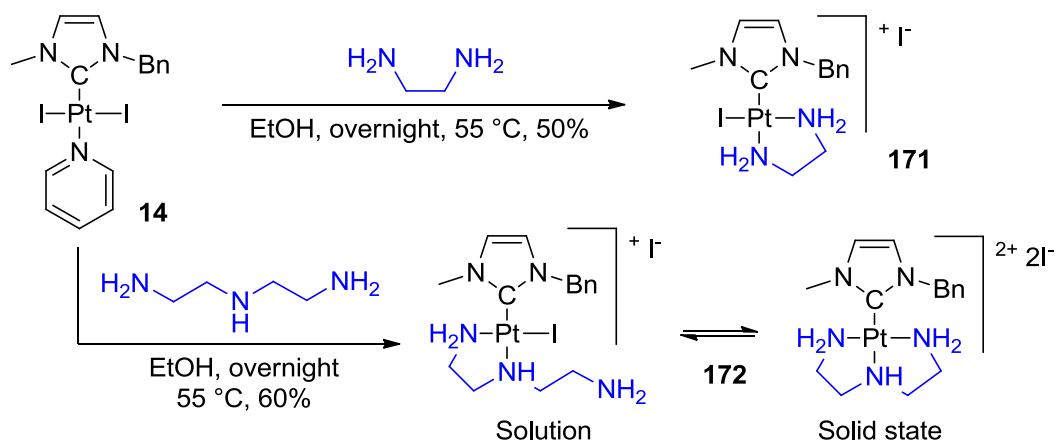


Figure 114: Ligand exchange on [(NHC)Pt₂(pyridine)] **14** with di and tri-amines: cationic complexes¹²⁴

4.1.2.2 Biological applications of polyethylenimine (PEI)

Polyethylenimine (PEI)³⁶¹ is an organic polymer formally formed by polymerization of aziridine (C₂H₅N) (**Figure 115**). Commercially available Linear PEI (LPEI) is produced by acidic hydrolysis³⁶² of methyl-initiated poly(2-ethyl-2-oxazoline) (PEtOx) obtained by cationic ring-opening polymerization of 2-oxazolines³⁶³ with well-defined molecular mass distribution.³⁶⁴ Branched PEI (BPEI) is obtained by acid-catalysed polymerization of aziridine.³⁶⁵

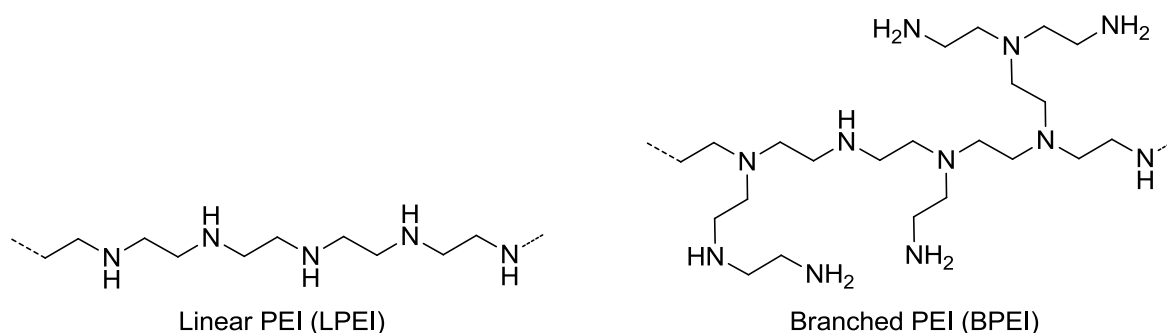


Figure 115: Structures of linear and branched PEI

³⁶¹ Demeneix, B.; Behr, J. P. *Adv. Genet.* **2005**, 53, 217.

³⁶² Kem, K. M. *J. Polym. Sci. Polym. Chem. Ed.* **1979**, 17, 1977.

³⁶³ Bodner, T.; Ellmaier, L.; Schenk, V.; Albering, J.; Wiesbrock, F. *Polym. Int.* **2011**, 60, 1173.

³⁶⁴ Adib, A.; Stock, F.; Erbacher, P. *US20100197888 A1* **2010**.

³⁶⁵ Dick, C. R.; Ham, G. E. *J. Macromol. Sci. Part A - Chem.* **1970**, 4, 1301; V. Harpe, A.; Peterson, H.; Li, Y.; Kissel, T. *J. Control. Release* **2000**, 69, 309.

PEI is employed for numerous applications including: detergents, adhesives, water treatment agents and cosmetics.³⁶⁶ PEI derivatives are as well involved in CO₂ capture,³⁶⁷ and found biological application as attachment promoter³⁶⁸ and transfection agent.³⁶⁹ Therefore, it is not surprising that PEI have been investigated by chemical companies and sold mainly by BASF under the brand name of *Polymin SK* as dewatering aid for effluent sludge during the manufacture of paper and board.³⁷⁰ Vancha *et al.* explored PEI as attachment factor on the plastic surface of culture dishes for weakly anchoring cell lines and primary cells.³⁶⁸ DNA plasmid PEI conjugates was investigated as promising immunogenes.³⁷¹

Gene delivery promises a great potential for live science fundamental research as for disease treatment by correcting genetic defects.³⁷² In 1995, the group of Behr discovered the transfection properties of PEI for gene transfer³⁷³ into cells thanks to its protonation reservoir ability.^{369,374,369} It is commonly admitted that molecules ranging between 5 and 25 kDalton are the most convenient for gene transfer. Among various PEI tested, relatively low molecular weight linear polymer seemed to combine low cytotoxicity³⁷⁵ with high gene delivery potential,³⁷⁶ whereas higher molecular weight increases significantly the cytotoxicity.³⁷⁷

Under physiological conditions, amino nitrogen atoms of the PEI are protonated (proton sponge) resulting in highly water-soluble polycation. Its condensation and complexation behaviour to DNA is dependent on the molecular weight, the number and the charge density of the PEI and finally the ratio of polymer to DNA. The condensation DNA-PEI processes is mostly relied to electrostatic interactions.³⁷⁸ Internalization of the cationic particles is assumed to be undertaken by adsorptive endocytosis or secondarily by clathrin-coated pit mechanism. Release in intracellular environment by endosomal escape is believed to be caused by the proton-sponge effect. Endosomal membrane ATPase enzymes actively transport protons into the endosome thus lowering pH inside the vesicle. PEI acting

³⁶⁶ Sigma-Aldrich Product Information, **2014**.

³⁶⁷ Goeppert, A.; Czaun, M.; May, R. B.; Prakash, G. K. S.; Olah, G. A.; Narayanan, S. R. *J. Am. Chem. Soc.* **2011**, *13*, 20164

³⁶⁸ Vancha, A. R.; Govindaraju, S.; Parsa, K. V.L.; Jasti, M.; González-García, M.; Ballester, R. P. *BMC Biotechnology* **2004**, *4*, 23.

³⁶⁹ Boussif, O.; Lezoualc'h, F.; Zanta, M. A.; Mergny, M. D.; Scherman, D.; Demeneix, B.; Behr, J. P. *Proc. Natl. Acad. Sci. U S A.* **1995**, *92*, 7297.

³⁷⁰ BASF Product Information, **2014**.

³⁷¹ Grant, E. V.; Thomas, M.; Fortune, J.; Klibanov, A. M.; Letvin, N. L. *Eur. J. Immunol.* **2012**, *42*, 2937.

³⁷² Neu, M.; Fischer, D.; Kissel, T. *J. Gene Med.* **2005**, *7*, 992.

³⁷³ Godbey, W. T.; Wu, K. K.; Mikos, A. M. *J. Control. Release* **1999**, *60*, 149; Lungwitz, U.; Breunig, M.; Blunk, T.; Göpferich, A. *Eur. J. Pharm. Biopharm.* **2005**, *60*, 247; Nguyen, D. N.; Green, J. J.; Chan, J. M.; Langer, R.; Anderson, D. G. *Adv. Mater.* **2008**, *20*, 1; Amiji, M. M.; Ogris, M. *Polymeric Gene Delivery: Principles and Applications*, Part II. A. Chapter 7, CRC Press **2010**.

³⁷⁴ Suh, J.; Paik, H. J.; Hwang, B. K. *Bioorg. Chem.* **1994**, *22*, 318.

³⁷⁵ Bonnet, M.-E.; Erbacher, P.; Bolcato-Bellemin, A.-L. *Pharm. Res.* **2008**, *25*, 2972.

³⁷⁶ Fischer, D.; Bieber, T.; Li, Y.; Elsassner, H. P.; Kissel, T. *Pharm. Res.* **1999**, *16*, 1273; Breunig, M.; Lungwitz, R.; Liebl, C.; Fontanari, J.; Kurtz, A. *J. Gene Med.* **2005**, *7*, 1287.

³⁷⁷ Fischer, D.; Li, Y.; Ahlemeyer, B.; Krieglstein, J.; Kissel, T. *Biomaterials*, **2003**, *24*, 1121.

³⁷⁸ Bloomfield, V. A. *Curr. Opin. Struct. Biol.* **1996**, *6*, 334; Bronich T.; Kabanov, A. V.; Marky, L. A. *J. Phys. Chem. B* **2001**, *105*, 6042.

as a proton-sponge conducts to increased ATPase enzymes activity. The escorting counter-ions of internalized protons provoke osmotic swelling and final rupture of the endosomal membrane.³⁷⁹

Especially branched PEI offer a high potential of functionalization because of its high number of final amino groups. BPEI and LPEI were functionalized with a tremendous variety of compounds.³⁸⁰ A non-exhaustive list contains functionalization of PEI with: dopamine for electrochemical quantification of NADH,³⁸¹ mesoporous silica nanoparticles,³⁸² carbon nanotubes for delivery of siRNA,³⁸³ graphene oxide composites used as ammonia sensors,³⁸⁴ gold nanoparticles,³⁸⁵ galactose,³⁸⁶ retinoic acid,³⁸⁷ dextran,³⁸⁸ chitosan as a gene carrier,³⁸⁹ or hydrophobic poly(γ -benzyl l-glutamate) segments (PBLG) for DNA complexation.³⁹⁰

A second-generation polymer incorporating PEG (polyethylene glycol) units have been widely investigated to form new PEI-copolymers.³⁹¹ This strategy is often used to bring more variety on the polymer backbone. Therefore, PEI-PEG copolymers were reported to complex Exon-Skipping Oligonucleotides,³⁹² functionalized with uronic acids as novel synthetic gene carriers,³⁹³ or forming a block copolymer with poly(γ -benzyl l-glutamate) self-assembled in to micelles.³⁹⁴

4.1.2.3 Combining NHC-Pt complexes with polyethylenimine: Towards new antitumor drugs

Considering high PEI affinity for DNA and high cytotoxicity of our NHC-platinum complexes, combination has been attempted to give rise to a new innovative and versatile family of polymer-drug

³⁷⁹ Morille, M.; Passirani, C.; Vonarbourg, A.; Clavreul, A.; Benoit, J.-P. *Biomaterials* **2008**, 29, 3477.

³⁸⁰ For a review of gene-transfer vector design, see: Kissel *et al.*³⁷²

³⁸¹ Rubianes, M. D.; Strumia, M. C. *Electroanalysis* **2010**, 22, 1200.

³⁸² Ufer, B.; Rosenholm, J. M.; Duchanoy, A.; Bergman, L.; Lindén, M. *Studies in Surface Science and Catalysis* **2008**, 174, 353.

³⁸³ Huang, Y.-P.; Lin, I.-J.; Chen, C.-C.; Hsu, Y.-C.; Chang, C.-C.; Lee, M.-J.; *Nanoscale Research Letters* **2013**, 8, 267.

³⁸⁴ Song, M.; Xu, J. *Electroanalysis* **2013**, 25, 523.

³⁸⁵ Tencomnao, T.; Apijaraskul, A.; Rakkhithawatthana, V.; Chaleawlerumpon, S.; Pimpa, N.; Sajomsang, W.; Saengkrit, N. *Carbohydr. Polym.* **2011**, 84, 216; Sharma, A.; Tandon, A.; Tovey, J.C.; Gupta, R.; Robertson, J. D.; Fortune, J.A.; Klibanov, A.M.; Cowden, J.W.; Rieger, F.G.; Mohan, R.R. *Nanomedicine* **2011**, 7, 505; Fortune, J.A.; Novobrantseva, T.I.; Klibanov, A.M. *J. Drug Del.* **2011**, 2011, 204058.

³⁸⁶ Kunath, K.; von Harpe, A.; Fischer, D.; Kissel, T. *J. Control. Release* **2003**, 88, 159.

³⁸⁷ Thünemann, A. F.; Beyermann, J. *Macromolecules* **2000**, 33, 6878.

³⁸⁸ Tseng, W.-C.; Jong, C.-M. *Biomacromolecules* **2003**, 1277.

³⁸⁹ Jiang, H.-L.; Kim, Y.-K.; Arote, R.; Nah, J.-W.; Cho, M.-H.; Choi, Y.-J.; Akaike, T.; Cho, C.-S. *J. Control. Release* **2007**, 117, 273.

³⁹⁰ Tian, J.; Xiong, W.; Wei, J.; Wang, Y.; Chen, X.; Jing, X.; Zhu, Q. *Biomaterials* **2007**, 28, 2899.

³⁹¹ Petersen, H.; Fechner, P. M.; Fischer, D.; Kissel, T. *Macromolecules* **2002**, 35, 6867.

³⁹² Sirsi, S. R.; Schray, R. C.; Guan, X.; Lykens, N. M.; Williams, J. H.; Erney, M. L.; Lutz, G. J. *Human Gene Therapy* **2008**, 19, 795.

³⁹³ Weiss, S. I.; Sieverling, N.; Niclase, M.; Maucksch, C.; Thünemann, A. F.; Möhwald, H.; Reinhardt, D.; Rosenecker, J.; Rudolph, C. *Biomaterials* **2006**, 27, 2302.

³⁹⁴ Tian, H. Y.; Deng, C.; Lin, H.; Sun, J.; Deng, M.; Chen, X.; Jing, X. *Biomaterials* **2005**, 26, 4209.

conjugates.³⁹⁵ Here water-soluble PEI would not only serve as carrier for the poor water-soluble platinum to reach its destination, but also protects the metal from side reactions with undesired molecules.³⁹⁶ Other motivation for PEI-platinum derivatives originates from several promising examples of platinopolymers, nanoscale coordination polymers and polymer-platinum conjugates from literature.³⁹⁷ Such platinum polymeric systems not only depict anticancer³⁹⁸ but also antiviral properties.³⁹⁹

After cell entering by endocytosis, low pH⁴⁰⁰ media in endosomes should provoke active platinum species release (**Figure 116**).⁴⁰¹ Poly-metallic amino⁴⁰² compound pledges to a higher local concentration of cytotoxic platinum in cancer cell. Platinum-PEI molecules fulfil the five conditions of polymer-drug conjugates of Ringsdorf's model⁴⁰³ defined for designing pharmaceutical active polymers: polymeric backbone (PEI), drug (the platinum-NHC complex), cleavable spacer (nitrogen_{PEI}-platinum coordination bond), targeting group (not introduced yet, we only took advantage of EPR effect) and solubilising agent (intrinsic water solubility of the PEI).

³⁹⁵ For selected reviews of the opportunities of polymer-drug conjugates, see: Duncan, R.; Vicent, M. J.; Greco, F.; Nicholson, R. I. *Endocrine-Related Cancer* **2005**, 12, 189; Duncan, R. *Nature Reviews Drug Discovery* **2003**, 2, 347; Callari, M.; Aldrich-Wright, J. R.; de Souza, P. L.; Stenzel, M. H. *Prog. Polym. Sci.* **2014**, 39, 1614; Duncan, R. *J. Control. Release* **2014**, 190, 371.

³⁹⁶ For drug delivery, see: Karsa, D. R.; Stephenson, R. A. *Chemical Aspects of Drug Delivery Systems* **1996**, Book News, Inc., Portland, Or.

³⁹⁷ Filipová-Vopršalová, M.; Drobník, J.; Šrámek, B.; Květina, K. *J. Control. Release* **1991**, 17, 89; Siegmann-Louda, D. W.; Carraher, C. E. Jr. *Polymeric platinum containing drugs in the treatment of cancer in Macromolecules Containing Metal and Metal-like Elements, Volume 3: Biomedical Applications*, **2004**, 119, Wiley, New York; Sood, P.; Thurmond, K. B. II.; Jacob, J. E.; Waller, L. K.; Silva, G. O.; Stewart, D. R.; Nowotnik, D. P. *Bioconjugate Chem.* **2006**, 17, 1270; Komane, L. L.; Neuse, E. W. *Metal-based Drugs* **2007**, 2008, 1; Mukaya, E. H.; Neuse, E. W.; van Rensburg, C. E. J. *J. Inorg. Organomet. Polym.* **2008**, 18, 111; N'Da, D. D.; Neuse, E. W. *J. Inorg. Organomet. Polym.* **2010**, 20, 468; Rieter, W. J.; Pott, K. M. Taylor, K. M. L.; Lin, W. *J. Am. Chem. Soc.* **2008**, 130, 11584; Haxton, K. J.; Burt, H. M. *J. Pharm. Sci.* **2009**, 98, 2299; Wild, A.; Babiuch, K.; König, M.; Winter, A.; Hager, M. D.; Gottschaldt, M.; Prokop, A.; Schubert, U. S. *Chem. Commun.* **2012**, 48, 6357; Oberoi, H. S.; Nukolova, N. V.; Kabanov, A. V.; Bronich, T. K. *Adv. Drug Deliv. Rev.* **2013**, 65, 1667.

³⁹⁸ Carraher, C. E.; Scott, W. J.; Lopez, I.; Cerutis, D. R.; Manek, T. *Polymeric Derivatives Based on cis-Diamminedichloroplatinum (II) as Antineoplastic Agents in Biological Activities of Polymers* **1982**, 221; Carraher, C. E.; Ademu-John, C.; Fortman, J. J.; Giron, D. J.; Linville, R. *Polymeric Materials Science and Engineering, Proceedings of the ACS Division of Polymeric Materials Science and Engineering* **1983**, 49, 210.

³⁹⁹ Jun, Y.; J.; Kim, J. I.; Jun, M. J.; Sohn, Y. S. *J. Inorg. Biochem.* **2005**, 99, 1593; Campone, M.; Rademaker-Lakhai, J. M.; Bennouna, J.; Howell, S. B.; Nowotnik, D. P.; Beijnen, J. H.; Schellens, J. H. M. *Cancer Chemotherapy and Pharmacology* **2007**, 60, 523; Roner, M.R.; Carraher Jr. C.E.; Dhanji, S.; Barot, G. *J. Polymer Mat.* **2007**, 24, 371; Roner, M.R.; Carraher Jr. C.E. *Cisplatin Derivatives as Antiviral Agents in Inorganic and Organometallic Macromolecules: Design and Applications*. **2008**, 193, Springer; Haxton, K. J.; Burt, H. M. *J. Pharm. Sci.* **2009**, 98, 2299; Roner, M.R.; Carraher Jr. C.E.; Shahi, K.; Barot, G. *Materials* **2011**, 4, 991.

⁴⁰⁰ Cancer cells present decreased pH. This property is exploited by ProLindac (AP5346), a platinum hydroxypropylmethacrylamide (HPMA) conjugate studied in phase II, to hydrolyse a pH-sensitive linker between the polymer and the metal in cancer cells: Nowotnik, D. P.; Cvitkovic, E. *Adv. Drug. Deliv. Rev.* **2009**, 61, 1214.

⁴⁰¹ pH-depending release of active species, see e.g.: Ulbrich, K.; Šubr, V. *Adv. Drug Del. Rev.* **2004**, 56, 1023; Zheng, H.; Xing, L.; Cao, Y.; Che, S. *Coord. Chem. Rev.* **2013**, 257, 2013.

⁴⁰² Magalhães Silva, T.; Andersson, S.; Kumar Sukumaran, S.; Marques, M. P.; Persson, L.; Oredsson, S. *PLoS ONE* **2013**, 8, 55651.

⁴⁰³ Ringsdorf, H. *J. Polym. Sci. Symp.* **1975**, 51, 135; Hoste, K.; De Winne, K.; Schacht, E. *Int. J. Pharm.* **2004**, 277, 119; Rohini, N. A.; Anupam, J.; Alok, M. *J. Antivir Antiretrovir* **2013**, 15.

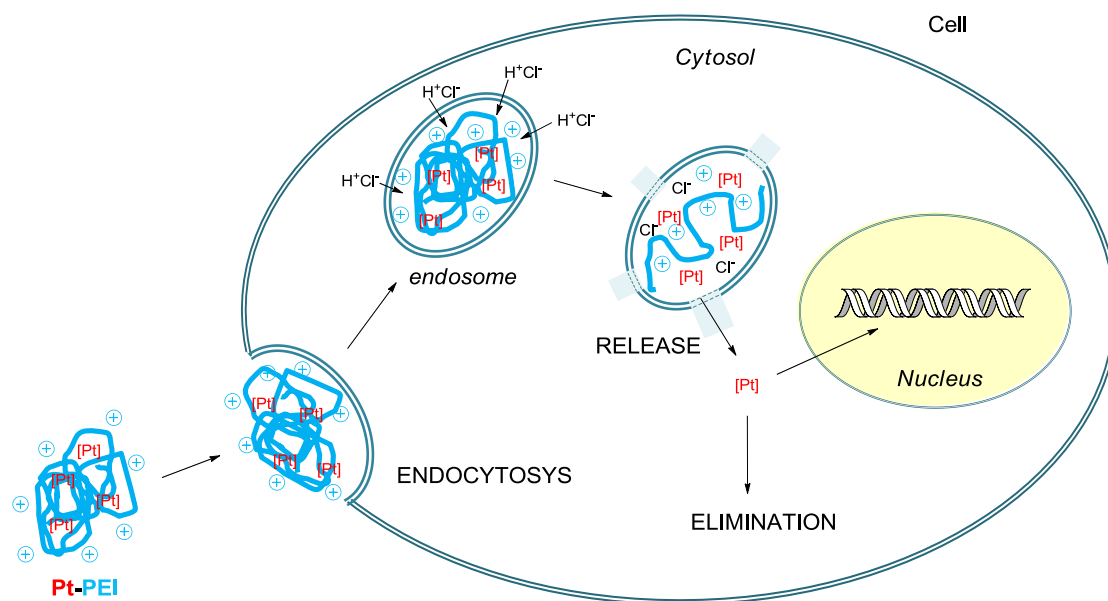


Figure 116: Envisaged PEI-platinum cellular uptake and activity⁴⁰⁴

Additionally, large macromolecules (such as PEI above 22 kDalton) could benefit of the EPR effect for solid tumours.⁴⁰⁵ This effect was first described in 1976 by Matsumura and Maeda.⁴⁰⁶ In solid cancers, tumour vasculature necessary for tumour supply with nutriment grows in an unbridled way resulting in abnormalities like hyper-vasculature and extensive production of vascular permeability factors stimulating extravasation within tumour tissues.⁴⁰⁷ This enhanced permeability allows diffusion of macromolecules into the tumour interstitial space. Poor lymphatic drainage allows macromolecules to stay and maintain constant serum concentration. Macromolecules exceed also the limit of renal excretion threshold and thus plasma half-lifetime is increased.⁴⁰⁸ Finally, this effect results in higher concentration of macromolecules in the solid tumour compared to healthy tissue.

⁴⁰⁴ Picture modified from: Chardon, E. *PhD Defence* **2011**.

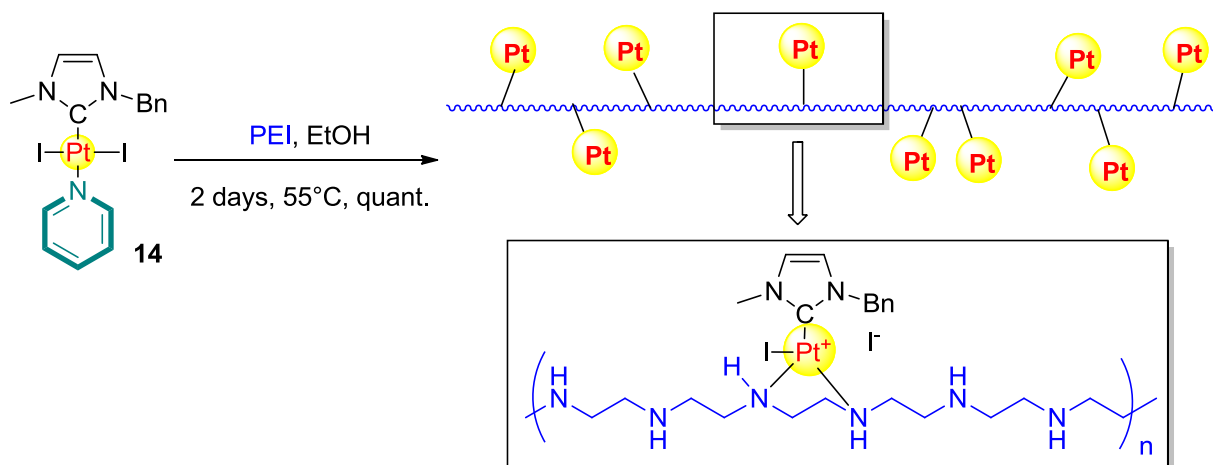
⁴⁰⁵ Iyer, A. K.; Khaled, G.; Fang, J.; Maeda, H. *Drug Discovery Today*, **2006**, *11*, 812; Maeda, H.; Bharate, G. Y.; Daruwalla, J. *Eur. J. Pharma. Biopharma* **2009**, *71*, 409; Greish, K. *Methods Mol. Biol.* **2010**, *624*, 25; Fang, J.; Nakamura, H.; Maeda, J. *Adv. Drug Del. Rev.* **2011**, *63*, 136; Maeda, H. *J. Control. Release* **2012**, *164*, 138; Prabhakar, U.; Maeda, H.; Jain, R. K.; Sevik-Muraca, E. M.; Zamboni, W.; Farokhzad, O. C.; Barry, S. T.; Gabizon, A.; Grodzinski, P.; Blakey, D. C. *Cancer Res.* **2013**, *73*, 2412.

⁴⁰⁶ Matsumura, Y.; Maeda, H. *Cancer Res.* **1986**, *46*, 6387.

⁴⁰⁷ Wu, J.; Akaike, T.; Maeda, H. *Cancer Res.* **1998**, *58*, 159.

⁴⁰⁸ Noguchi, Y.; Wu, J.; Duncan, R.; Strohalm, J.; Ulbrich, K.; Akaike, T.; Maeda, H. *Jpn. J. Cancer Res.* **1998**, *89*, 307.

4.1.2.4 Synthesis of (NHC)Pt(II)-PEI compounds

Figure 117: Synthesis of (NHC)Pt(II)-PEI compounds by ligand exchange⁴⁰⁹

[(PEI)Pt(NHC)] complexes were generated in quantitative yield starting from appropriate PEI and [(NHC)Pt(II)(pyridine)] complex (**Figure 117**).¹²⁸ The exchange reaction in ethanol needs heating over 2 days to be complete (followed by TLC). Neighbouring positive charges probably decrease nucleophilicity of the nitrogens thus slowing down exchange kinetics. By NMR, the disappearance of the signals of coordinated pyridine at 9 ppm indicates the formation of new compounds.

Reaction done in a mixture of refluxing $\text{CH}_2\text{Cl}_2/\text{water}$ or in methanol/water at 55 °C over 2 days resulted in recovered impure starting material respectively a mixture of PEI and pyridine complexes. However, in presence of water, the PEI is protonated preventing the reaction.

Several parameters such as the nature of PEI (linear or branched), its molecular weight, the ratio between platinum centre and nitrogen atoms and NHC backbone (R^1 , R^2) can be easily tuned.

For clarity reasons, polyethylenimine derivatives will be annotated PEI (M, n, b/l) where M represents the molecular weight of the initial PEI (kDalton), n the ratio between nitrogens of the PEI and platinum, and b/l for branched or linear PEI. The various combinations using platinum complexes derived from the 3-benzyl-1-methyl-imidazolyldene were represented in **Table 12**.

⁴⁰⁹ On this representation, we represent the PEI conjugate as a ligand bi-coordinating the Pt atom. Regarding the results of diethylenetriamine, it should be kept in mind that in solution, equilibrium between several coordination modes (mono, bi and tri coordination) exists (broad NMR signals).

M (kDalton)	1.8 (b)	2.5	2.5	2.5	21.5	21.5	25	25	25	250	250	250
n (N/Pt)	15	10	20	30	20	30	10	20	30	15	20	35

Table 12: NHC Pt PEI conjugates synthesized: Variation of the molecular weight of the linear PEI (M) and the ratio $n=N_{PEI}/Pt$ for different [(NHC)PtI₂-PEI(M,n,(b))] compounds (NHC = 3-benzyl-1-methyl-imidazolydene)

It is noteworthy that attempts to increase the amount of Pt ($n = 2.5$ or 5) per PEI (2.5 , 1) always generated a mixture of starting Pt complex and PEI-Pt polymer with N/Pt ratio always higher than seven. This limiting ratio could easily be explained by electrostatic repulsion and the folding of the polymer that could hide some coordinating nitrogen atoms.

Then using these conditions, a library of PEI complexes were prepared with various NHC precursors as presented in **Figure 118**. Again, these metallopolymers were obtained quantitatively after washing with diethylether.

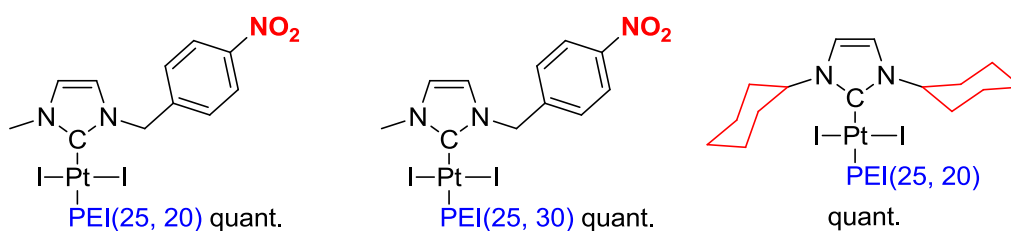


Figure 118: Variation of the nature of the NHC ligand of various linear PEI [(NHC)PtI₂-PEI(M,n)] or diethylenetriamine compounds (yields refer to the exchange reaction)

Antitumor properties of these compounds have been explored *in vitro* and *in vivo* analysis and were described in this thesis (chapters 5.1.7. *In vitro* studies of polyethylenimine platinum complexes and 5.2. *Preliminary in vivo* studies of PEI platinum NHC conjugates).

4.1.3 Introduction of pnictogen based ligands: Phosphines, arsines and stibines

After having widely explored the chemistry of nitrogen-based ligands, enlarged variation on the nature of the neutral L type ligand had been investigated. Thus modulation of both electronic and steric properties should be accessed and so influence its biological properties (solubility, cell entrance, hydrolysis rate, DNA platination). As phosphinated ligands are of great interest for biological purpose, synthesis of combined NHC-phosphine derivatives have been undertaken. To extend even further the scope⁴¹⁰ of complexes available through this procedure, the following arsine and antimony pnictogens⁴¹¹ have been explored.

4.1.3.1 Literature overview of selected [(NHC)Pt(II)(phosphine)] and [(NHC)Pt(II)(phosphine)₂] compounds

Synthesis of [(NHC)Pt(II)(phosphine)] or [(NHC)Pt(II)(phosphine)₂] complexes had already been reported in the literature even though the examples remain rare. Most of them are multi-step reactions or sensible to air or moisture. Surprisingly, easily available L-type ligand AsPh₃ is (except one rare exception⁴¹²) not used for modulation of a NHC-Palladium-L catalytic system. [(NHC)Pd(AsPh₃)] examples^{413,414} are few explored and only one family of [(NHC)Pd(SbPh₃)] complexes⁴¹⁴ is reported. In palladium phosphine chemistry, Guo and Huynh reported ligand exchange of labile acetonitrile by monodentate and chelating phosphines on a dicarbene-bridged dipalladium (II) complex.⁴¹⁵ Lee and co-workers successfully replaced pyridine ligand of an abnormal [(NHC)PdCl₂(pyr)] complex by PPh₃ and obtained the corresponding *cis* palladium derivative.⁴¹⁶ For catalytic purposes, platinum complexes are less considered compared to the well-developed palladium chemistry. Nevertheless, platinum-NHC-complexes have been used for example for reductive cyclization of diynes and enynes⁴¹⁷, for catalytic diboration of unsaturated molecules or tandem hydroboration-cross coupling reactions³⁰⁷.

⁴¹⁰ Nearly every chemical element is of clinical use. For an overview, see: Barry, N. P. E.; Sadler, P. J. *Chem. Commun.* **2013**, 49, 5106.

⁴¹¹ A pnictogen, name suggested by Anton Eduard van Arkel in the 1950thes and derived from Greek root *pnikta*, “suffocating product” (Girolami, G. S. *J. Chem. Educ.* **2009**, 86, 1200), is an element of group 15 of periodic table (Connelly, N. G.; Damhus, T.; Hartshorn, R. M.; Hutton, A. T. *Nomenclature of Inorganic Chemistry: IUPAC Recommendations 2005*).

⁴¹² DelPozo, J.; Casares, J. A.; Espinet, P. *Chem. Commun.* **2013**, 49, 7246.

⁴¹³ Ng K. H.; Li Y.; Tan W. X.; Chiang M.; Pullarkat S. A. *Chirality*. **2013**, 25, 149.

⁴¹⁴ Yang, J.; Li, P.; Zhang, Y.; Wang, L. *Dalton Trans.* **2014**, 43, 14114.

⁴¹⁵ Guo, S.; Huynh, H. V. *Organometallics* **2014**, 33, 2004.

⁴¹⁶ Chen, S.-J.; Lin, Y.-D.; Chiang, Y.-H.; Lee, H. M. *Eur. J. Inorg. Chem.* **2014**, 2014, 1492.

⁴¹⁷ Jung, I. G.; Seo, J.; Lee, S. I.; Choi, S. Y.; Chung, Y. K. *Organometallics* **2006**, 25, 4240.

Interestingly, in 1971, Muir and co-workers synthesized the first *trans*-[(NHC)PtCl₂(P(Et)₃)] complex by reacting an olefin with Pt(PEt₃)₂Cl₂.⁴¹⁸ One year later, they also reported the thermal isomerization of the *trans* complex to the thermodynamically more stable⁴¹⁹ *cis* compound (**Figure 119**).⁴²⁰ Muir noticed colour change between both complexes (*cis* white, *trans* yellow), greater coupling constants $J(^{195}\text{Pt}-^{31}\text{P})$ in NMR for *cis*-complex (*cis* 3.3-4.1 kHz, *trans* 2.4-2.5 kHz)⁴²¹ or lower Pt-P and Pt-C_{carbene} bonds length for *cis* compound.

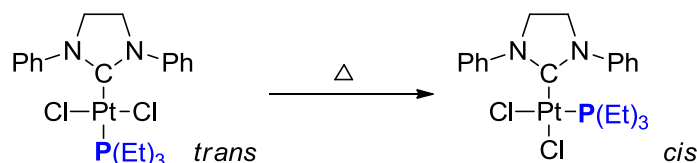


Figure 119: Thermal *trans* to *cis* isomerization of a NHC-Pt-phosphine complex⁴²⁰

Han *et al.* synthesized a *trans*-Pt-phosphine complex starting from the imidazolium salt and PtBr₂ in DMSO with sodium acetate as base.⁴²² Then, ligand exchange from DMSO only afforded the kinetic *trans* complex, which in refluxing dichloromethane isomerized to the thermodynamic *cis* product (**Figure 120**).

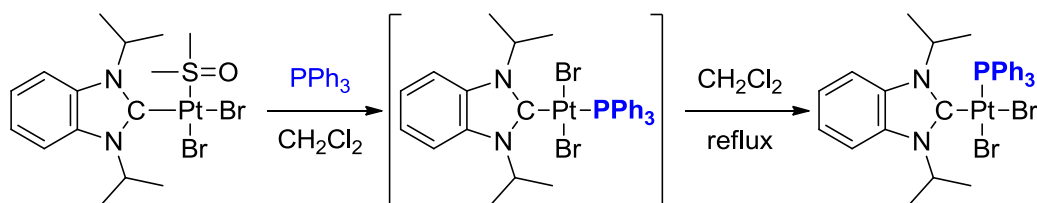


Figure 120: *Trans* to *cis* isomerization of a [(NHC)PtBr₂(PPh₃)] complex⁴²²

The group of Marinetti described a 3 steps synthesis involving the formation of a Pt (0)-NHC complex using *Karstedt catalyst* as platinum precursor,⁴²³ followed by its oxidation into platinum (II) by halide and finally substitution of labile divinyltetramethyldisiloxane with phosphines⁴²⁴ or phosphoramidites

⁴¹⁸ Cardin, D. J.; Çetinkaya, B.; Lappert, M. F.; Manojlovic-Muir, L_J.; Muir, K. W. *J. Chem. Soc. D*, **1971**, 400.

⁴¹⁹ Vicente and co-workers reported the difficulty of coordinating a phosphine *trans* to carbon donors such as aryl or aroyl in palladium complexes and called this phenomena *transphobia* (Vicente, J.; Arcas, A.; Bautista, D.; Jones, P. G. *Organometallics* **1997**, 16, 2127; Vicente, J.; Abad, J. A.; Frankland, A. D.; Ramírez de Arellano, M. C. *Chem.-Eur. J.* **1999**, 5, 3066).

⁴²⁰ Cardin, D. J.; Çetinkaya, B.; Çetinkaya, Engin.; Lappert, M. F.; Manojlovic-Muir, L_J.; Muir, K. W. *J. Organomet. Chem.* **1972**, 44, 59.

⁴²¹ Cardin, D. J.; Çetinkaya, B.; Lappert, M. F. *J. Organomet. Chem.* **1974**, 72, 139.

⁴²² Han, Y.; Huynh, H. V.; Tan, G. K. *Organometallics* **2007**, 26, 4612.

⁴²³ Markó, I. E.; Stérin, S.; Buisine, O.; Berthon, G.; Michaud, G.; Tinant B.; Declercq, J.-P. *Adv. Synth. Catal.* **2004**, 346, 1429; Buisine, O.; Berthon-Gelloz, G.; Brière, J.-F.; Stérin, S.; Mignani, G.; Branlard, P.; Tinant, B.; Declercq, J.-P.; Markó, I. E. *Chem. Commun.* **2005**, 3856; Berthon-Gelloz, G.; Buisine, O.; Brière, J.-F.; Michaud, G.; Stérin, S.; Mignani, G.; Tinant, B.; Declercq, J.-P.; Chapon D.; Markó, I. E. *J. Organomet. Chem.* **2005**, 690, 6156.

⁴²⁴ Brissy, D.; Skander, M.; Retaillieu, P.; Frison, G.; Marinetti, A. *Organometallics* **2009**, 28, 140.

(**Figure 121**).⁴²⁵ These phosphorous containing platinum complexes were active in transformations such as enantioselective cycloisomerizations. Notably, depending of its nature, the phosphoramidite ligand adopts either a *cis* or a *trans* geometry regarding the NHC.

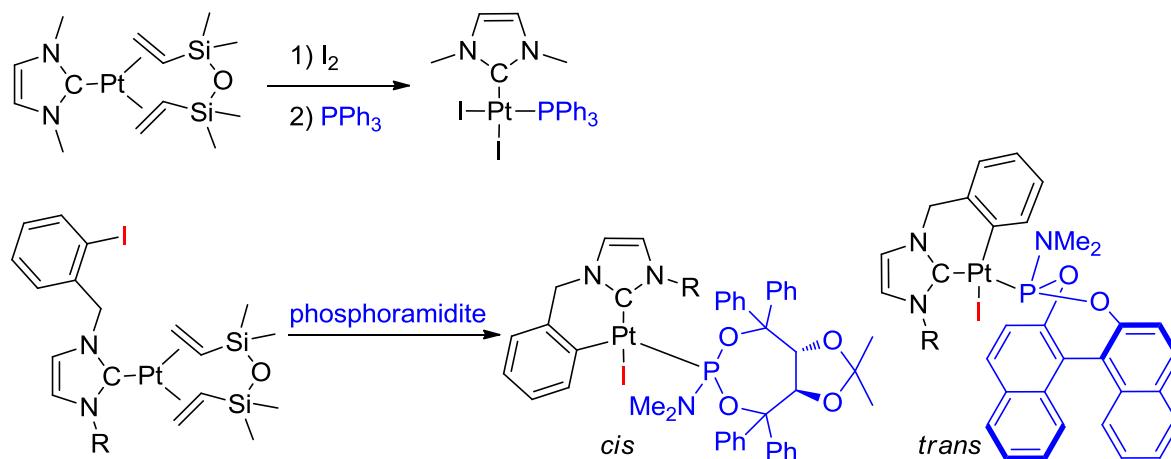


Figure 121: Phosphine and phosphoramidite complexes reported by Marinetti *et al.*^{424,425}

Mirkin and co-workers studied the binding mode of a P,S-bidentate ligand over a Pt(NHC) complex. The coordination in either mono or bidentate mode generated neutral and cationic complexes respectively (**Figure 122**).⁴²⁶

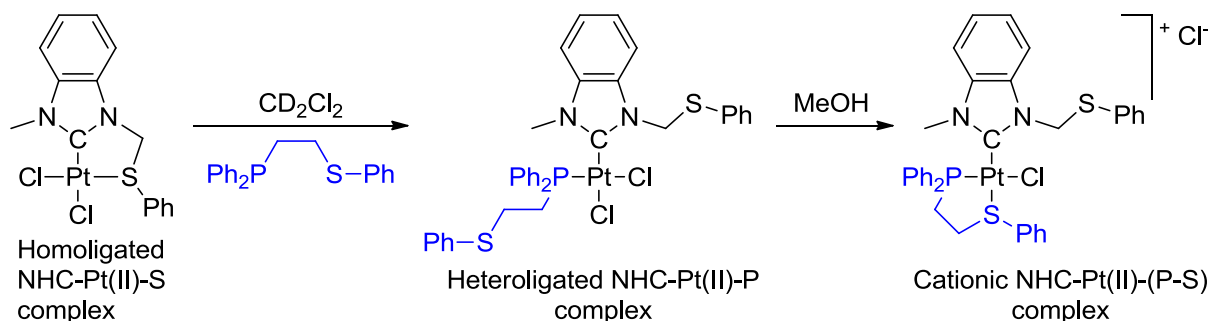


Figure 122: Reactivity of a bidentate phosphine-thioether ligand coordinating NHC complex⁴²⁶

Cationic complexes can even be obtained without chelating ligands. For example, the group of Yates formed a platinum-diphosphine complex by oxidative addition of 2-iodo-imidazolium to Pt(PPh₃)₄ or

⁴²⁵ Zhang, Y.; Jullien, H.; Brissy, D.; Retailleau, P.; Voituriez, A.; Marinetti, A. *ChemCatChem* **2013**, 5, 2051; Jullien, H.; Brissy, D.; Retailleau, P.; Marinetti, A. *Eur. J. Inorg. Chem.* **2011**, 2011, 5083; Jullien, H.; Brissy, D.; Sylvain, R.; Retailleau, P.; Naubron, J.-V.; Gladiali, S.; Marinetti, A. *Adv. Synth. Catal.* **2011**, 353, 1109; Brissy, D.; Skander, M.; Jullien, H.; Retailleau, P.; Marinetti, A. *Org. Lett.* **2009**, 11, 2137.

⁴²⁶ Rosen, M. S.; Stern, C. L.; Mirkin, C. A. *Chem. Sci.* **2013**, 4, 4193.

imidazolium to $\text{Pt}(\text{PPh}_3)_2$ (**Figure 123**).^{304,427} Depending of imidazolium and platinum precursor, the phosphines adopt a *cis* or *trans* position respecting each other.

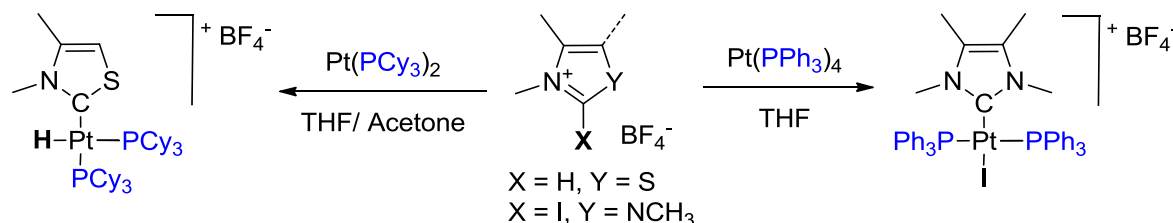


Figure 123: Cationic NHC diphosphine complexes formed by oxidative addition to a Pt (0) precursor

Also by ligand displacement of DMSO, Rourke and collaborators synthesized $[(\text{NHC})\text{Pt}(\text{II})(\text{PPh}_3)]$ from the corresponding $[(\text{NHC})\text{Pt}(\text{II})(\text{DMSO})]$ complex itself obtained by transmetalation (**Figure 124**).⁴²⁸ Addition of PPh_3 to this complex gave the cationic $[(\text{NHC})\text{Pt}(\text{II})(\text{PPh}_3)_2]$ complex.

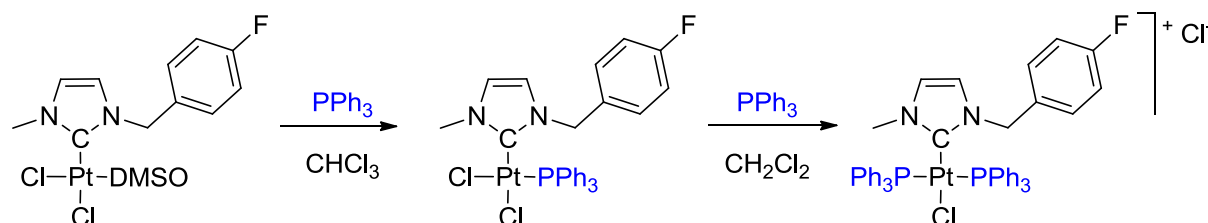


Figure 124: Rourke's two-step synthesis of $(\text{NHC})\text{Pt}(\text{II})(\text{PPh}_3)$ and $(\text{NHC})\text{Pt}(\text{II})(\text{PPh}_3)_2$ complexes⁴²⁸

Oxidative addition of purine based ligands as caffeine or 9-Methyladenine and azoles to $\text{Pt}(\text{PPh}_3)_4$ gave neutral *cis*- $[(\text{NR},\text{N-NHC})\text{PtCl}(\text{PPh}_3)_2]$ complexes which itself react with acid to cationic $[(\text{NR},\text{NH-NHC})\text{PtCl}(\text{PPh}_3)_2]^+\text{BF}_4^-$ complexes.⁴²⁹

Chelate effect can equally be exploited when using di- or triphosphine ligands. Several examples using diphosphines as 1,2-bis(diphenylphosphino)ethane (dppe) or bis(dimethylphosphino)ethane (dmpe) are reported (**Figure 125**).^{430,431}

⁴²⁷ McGuinness, D. S.; Cavell, K. J.; Yates, B. F. *Chem. Commun.* **2001**, 355.

⁴²⁸ Newman, C. P.; Deeth, R. J.; Clarkson, G. J.; Rourke, J. P. *Organometallics* **2007**, 26, 6225.

⁴²⁹ Kösterke, T.; Pape, T.; Hahn, F. E. *J. Am. Chem. Soc.* **2011**, 133, 2112; Kösterke, T.; Kösters, J.; Würthwein, E.-U.; Mück-Lichtenfeld, C.; Schulte to Brinke, C.; Lahoz, F.; Hahn, F. E. *Chem.-Eur. J.* **2012**, 18, 14594; Brackemeyer, D.; Hervé, A.; Schulte to Brinke, C.; Jahnke, M. C.; Hahn, F. E. *J. Am. Chem. Soc.* **2014**, 136, 7841.

⁴³⁰ Schmidtendorf, M.; Pape, T.; Hahn, F. E. *Dalton Trans.* **2013**, 42, 16128.

⁴³¹ Brissy, D.; Skander, D.; Retailleau, P.; Marinetti, A. *Organometallics* **2007**, 26, 5782.

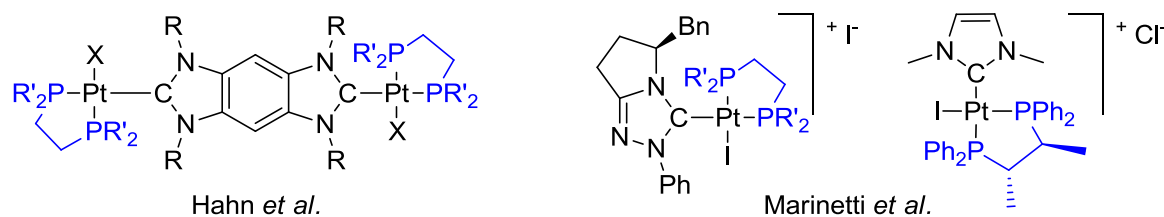


Figure 125: Examples of chelating diphosphines^{430,431}

Recently hybrid ligand containing both NHC and phosphine motif have raised a lot of attention.⁴³² This is mainly due to easy access to a large library of compounds in order to increase notably binding efficiency at the metal centre. Those phosphorous compounds can be classified in four main families: NHC-phosphonium salt, *N*-phosphorylated imidazolium salt, 4-phosphino or 4,5-diphosphino substituted imidazolium salts and phosphino substituents bound on various positions on the imidazolium salt.⁴³³

Chelating tridentate diphosphine-NHC complexes reported by Fryzuk and co-workers are obtained by oxidative addition of the pro-ligand precursor to Pt (0) (**Figure 126**).⁴³⁴ A similar complex is reported by Pan *et al.*⁴³⁵ Hahn *et al.* synthesized unsaturated analogues and NHC-monophosphines by classic trans-metalation procedure from the corresponding silver complexes.⁴³⁶ Chelating tridentate diphosphine-NHC complexes were used for template-controlled synthesis by the same group to achieve bis-cationic bis-phosphine bis-NHC macrocycle platinum complex.⁴³⁷

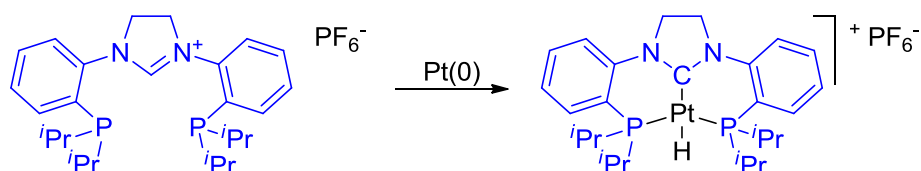


Figure 126: Chelating tridentate Diphosphine-NHC complexes of Fryzuk⁴³⁴

To the best of our knowledge, biological properties of [(NHC)Pt(II)(phosphine)] derivatives are not explored yet despite the fact that [PtP₂Cl₂] type compounds present moderate anticancer activity.⁴³⁸

⁴³² For a review, see: Gaillard, S.; Renaud, J.-L. *Dalton Trans.* **2013**, 42, 7255.

⁴³³ Gaillard, S.; Renaud, J.-L. *Dalton Trans.* **2013**, 42, 7255.

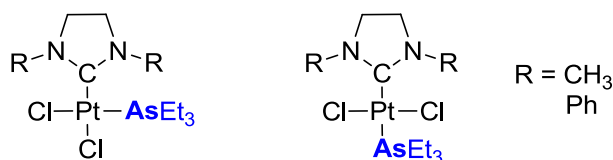
⁴³⁴ Steinke, T.; Shaw, B. K.; Jong, H.; Patrick, B. O.; Fryzuk, M. D. *Organometallics* **2009**, 28, 2830.

⁴³⁵ Pan, B.; Pierre, S.; Bezpalko, M. W.; Napoline, J. W.; Foxman, B. M.; Thomas, C. M. *Organometallics* **2013**, 32, 704.

⁴³⁶ Hahn, F. E.; Jahnke, M. C.; Pape, T. *Organometallics* **2006**, 25, 5927.

⁴³⁷ Flores-Figueroa, A.; Pape, T.; Feldmann, K.-O.; Hahn, F. E. *Chem. Commun.* **2010**, 46, 324.

⁴³⁸ Mügge, C.; Rothenburger, C.; Beyer, A.; Gorls, H.; Gabbiani, C.; Casini, A.; Michelucci, E.; Landini, I.; Nobili, S.; Mini, E.; Messori, L.; Weigand, W. *Dalton Trans.* **2011**, 40, 2006.

Figure 127: *Cis* and *trans* NHC-Platinum-arsine⁴³⁹

Extension of this synthetic pass way to the softer arsenic (As) and antimony (Sb), other members of the pnictogen family, remains rare. Only one example of (NHC)Pt(AsR₃) complex was depicted in the late 70^s in the literature. At that time, Lappert studied in detail far infrared and NMR properties of various *cis* and *trans*-[(NHC)Pt(phosphine)] and [(NHC)Pt(arsine)] complexes (Figure 127).⁴³⁹ Despite arsine⁴⁴⁰ or antimony⁴⁴¹ ligands⁴⁴² are well known and these elements established as drug for several pathologies, no NHC-Pt derivatives were reported.

4.1.3.2 Use of arsenic or antimony compounds for medical applications

Nowadays, chemotherapy by metallodrugs is generally associated with platinum complexes. We should keep in mind that chemotherapy started with other metal elements. World's first modern chemotherapeutic drug *Salvarsan* (initially called *compound 606*) (Figure 128), was found by systematic screening⁴⁴³ of hundreds of arsenical chemicals. It was introduced in 1910 by Sahachiro Hata and Paul Ehrlich as antisyphilitic drug.⁴⁴⁴ In 1912, *Salvarsan* was superseded by the more water-soluble neoarsphenamine (*Neosalvarsan*), also developed by Ehrlich. In 1924, Raiziss, Stokes and Chambers introduced a combined arsenic bismuth compound, *Bismarsen*, which has the advantage of being less toxic and easier to administrate. Arsenic based drugs⁴⁴⁵ are currently employed: melarsoprol (*Arsobal*) for 2nd stage African trypanosomiasis (sleeping sickness),³³⁹ or under investigation: *GSAO* (4-(N-(S-glutathionylacetyl)amino)-phenylarsenoxide), a trivalent arsenical peptide⁴⁴⁶ or *ZIO-101* (S-

⁴³⁹ Cardin, D. J.; Çetinkaya, B.; Lappert, M. F. *J. Organomet. Chem.* **1974**, *4*, 139; Cardin, D. J.; Çetinkaya, B.; Çetinkaya, E.; Lappert, M. F.; Randall, E. W.; Rosenberg, E. *Dalton Trans.* **1973**, 1982.

⁴⁴⁰ See e.g.: Burt, J.; Levason, W.; Reid, G. *Coord. Chem. Rev.* **2014**, *260*, 65; Jeram, S.; Henderson, W.; Nicholson, B. K.; Hor, A. T. S. *J. Organomet. Chem.* **2006**, *691*, 2827; Chooi, S. Y. M.; Leung, P.-H.; Sim, K. Y. *Tetrahedron: Asymmetry* **1994**, *5*, 49; Hill, W. E.; Minahan, D. M. A. *Inorganica Chimica Acta*, **1979**, *36*, L394; L.; Levason, W.; Reid, G. *Reference Module in Chemistry, Molecular Sciences and Chemical Engineering* **2013**, 475.

⁴⁴¹ See e.g.: Champness, N. R.; Levason, W. *Coord. Chem. Rev.* **1994**, *133*, 115; Levason, W.; Reid, G. *Coord. Chem. Rev.* **2006**, *250*, 2565; Brynda, M. *Coord. Chem. Rev.* **2005**, *249*, 2013.

⁴⁴² In contrast to platinum, *trans* [(NHC)PdCl₂(L)] with L = AsPh₃ or SbPh₃ are reported: Yang *et al.*⁴¹⁴

⁴⁴³ Ehrlich introduced the concept of drug development by systematic screening of chemicals (often derived from dye industry), to target specifically the bacterium (magic bullet concept): “wir müssen zielen lernen, chemisch zielen lernen”; for a review, see: Strebhardt, K.; Ullrich, A. *Nature Reviews Cancer* **2008**, *8*, 473.

⁴⁴⁴ Gibaud, S.; Jaouen, G. *Topics in Organometallic Chemistry* **2010**, *32*, 1.

⁴⁴⁵ Zhu, J.; Chen, Z.; Lallemand-Breitenbach, V.; de Thé, H. *Nature Reviews Cancer* **2002**, *2*, 705.

⁴⁴⁶ Don, A. S.; Kisker, O.; Dilda, P.; Donoghue, N.; Zhao, X.; Decollogne, S.; Creighton, B.; Flynn, E.; Folkman, J.; Hogg, P. *Cancer Cell.* **2003**, *3*, 497.

dimethylarsino-glutathione, or *Darinaparsin*),⁴⁴⁷ both for the treatment of solid tumours. *Nitarson* (*Histostat*) prevents blackhead disease in veterinary (Figure 129).

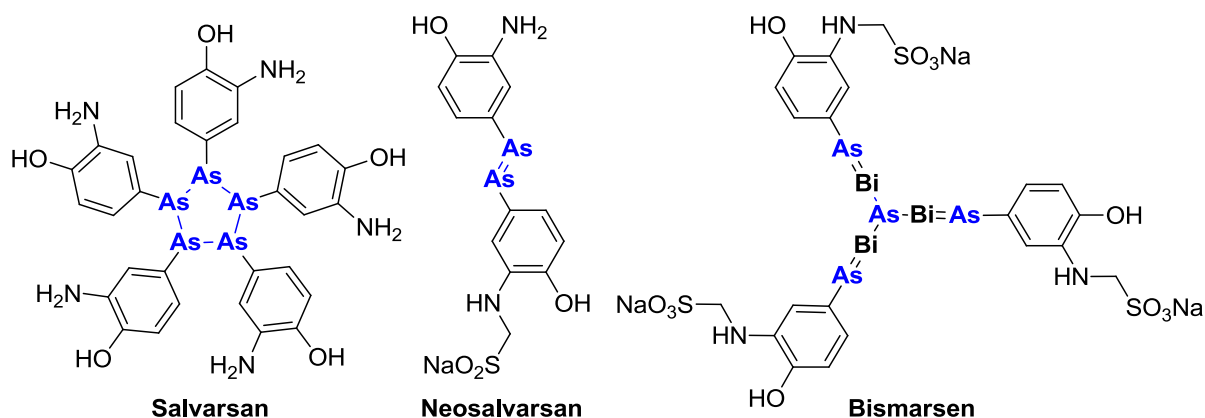


Figure 128: Salvarsan,⁴⁴⁸ Neosalvarsan and Bismarsen: the world's first modern chemotherapeutic drugs

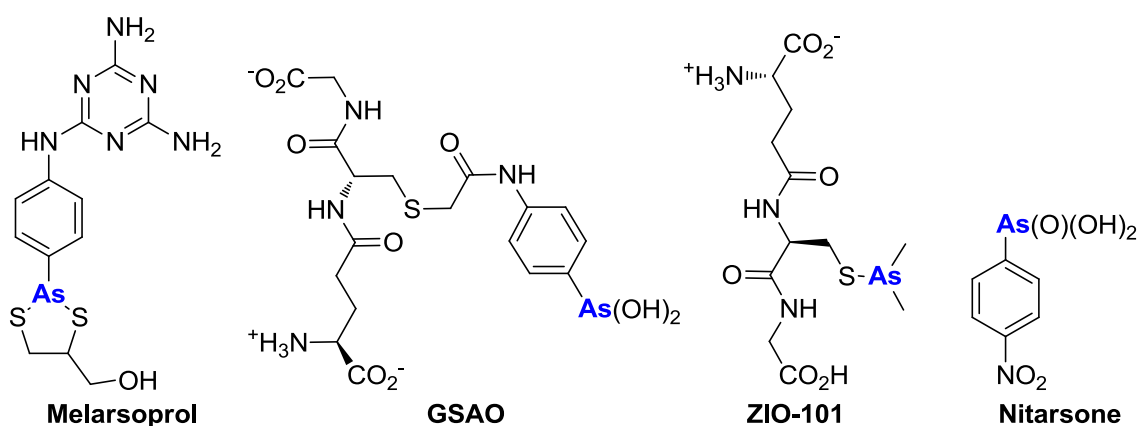


Figure 129: Arsenic-based drugs: Melarsoprol, GSAO, ZIO-101 and Nitarson

Despite the high toxicity of arsenic compounds,⁴⁴⁹ the potential of arsenic trioxide (As₂O₃) was tested by Chinese physicians on patients suffering from leukaemia.⁴⁵⁰ These encouraging results led to further investigations in western countries⁴⁵¹ showing that arsenic trioxide is the single most effective

⁴⁴⁷ Camacho, L. H.; Hong, D. S.; Gutierrez, C.; Vertovsek, S.; Tannir, N.; Parker, C. A.; Purdom, M. A.; Lewis, J.; Gale R. P.; Kurzrock R. *J. Clin. Oncol.* **2006**, *24*, 13041; Marcoux, S. *Master Thesis*, **2007**, McGill University.

⁴⁴⁸ Salvarsan is probably a mixture of trimeric and pentameric cyclopolyarsines: Lloyd, N. C.; Morgan, H. W.; Nicholson, B. K.; Ronimus, R. S. *Angew. Chem. Int. Ed.* **2005**, *44*, 941.

⁴⁴⁹ Thomas, D. J.; Styblo, M.; Lin, S. *Toxicology and Applied Pharmacology* **2001**, *176*, 127; Hughes, M. F. *Toxicology Letters* **2002**, *133*, 1; Choong, T. S. Y.; Chuah, T. G.; Robiah, Y.; Koay, F. L. G.; Azni, I. *Desalination* **2007**, *217*, 139; Nordberg, G. F.; Fowler, B. A.; Nordberg, M.; Friberg, L. *Handbook on the Toxicology of Metals* **2007**, Elsevier, Burlington

⁴⁵⁰ Degos, L. *British Journal of Haematology* **2003**, *122*, 539.

⁴⁵¹ Evens, A. M.; Tallman, M. S.; Gartenhaus, R. B. *Leuk. Res.* **2004**, *28*, 891; Soignet, S. L.; Frankel, S. R.; Douer, D.; Tallman, M. S.; Kantarjian, H.; Calleja, E.; Stone, R. M.; Kalaycio, M.; Scheinberg, D. a.; Steinherz, P.; Sievers, E. L.;

agent for treating Acute Promyelocytic Leukaemia (APL).⁴⁵² Derivatives of As (III)⁴⁵³ are under investigation as well as As (V) compounds.⁴⁵⁴

Interestingly, in 2013, the group of O'Halloran established the synergistic anticancer properties of a combined platinum arsenic compound (*arsenoplatin*) (**Figure 130**) with better cytotoxic activity than either cisplatin or As₂O₃ in colon and glioblastoma.⁴⁵⁵

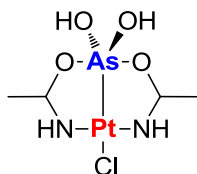


Figure 130: Assemble As and Pt: O'Halloran's highly cytotoxic arsenoplatin complex⁴⁵⁵

Antimony was utilized since prehistoric time for medical applications⁴⁵⁶ despite its high toxicity⁴⁵⁷. Especially the use as emetic agent⁴⁵⁸ of antimony potassium tartrate, known as *tartarus stibiatus emeticus* (K₂Sb₂C₈H₄O₁₂·3H₂O) is notorious since Roman times. Pentavalent antimonial in form of sodium stibogluconate (*Pentostam*)⁴⁵⁹ or meglumine antimoniate (*Glucantime*)⁴⁶⁰ is used as an antiprotozoal agent against leishmaniasis (**Figure 131**).³³⁹ Research to find new promising derivatives⁴⁶¹ as antimicrobials⁴⁶² or in oncology⁴⁶³ are undergoing, but less is known about the

Coutr , S.; Dahlberg, S.; Ellison, R.; Warrell, R. P. J. *J. Clin. Onco.* **2001**, *19*, 3852; R llig, C.; Illmer, T. *Cancer Treatment Reviews* **2009**, *35*, 425; Bailey, K. A.; Hester, S. D.; Knapp, G. W.; Owen, R. D.; Thai, S.-F. *Mol. Carcinog.* **2010**, *49*, 981; Emadi, A.; Gore, S. D. *Blood Reviews*, **2010**, *24*, 191; Sun, R. C.; Board, P. G.; Blackburn, A. C. *Molecular Cancer* **2011**, *10*, 142.

⁴⁵² Ghavamzadeh, A.; Alimoghaddam, K.; Rostami, S.; Ghaffari, S. H.; Jahani, M.; Irvani, M.; Mousavi, S. A.; Bahar, B.; Jalili, M. *J. Clin. Oncol.* **2011**, *29*, 2753.

⁴⁵³ Liu, Y.; Duan, D.; Yao, J.; Zhang, B.; Peng, S.; Ma, H.; Song, Y.; Fang, J. *J. Med. Chem.* **2014**, *57*, 5203.

⁴⁵⁴ Fr zard, F.; Demicheli, C.; Kato, K.C.; Reis, P. G.; Lizarazo-Jaimes, E. H. *Reviews Inorg. Chem.* **2013**, *33*, 1.

⁴⁵⁵ Miodragovi ,  . U.; Quentzel, J. A.; Kurutz, J. W.; Stern, C. L.; Ahn, R. W.; Kandela, I.; Mazar, A.; O'Halloran, T. V. *Angew. Chem. Int. Ed.* **2013**, *52*, 10749; Swindell, E. P.; Hankins, P. L.; Chen, H.; Miodragovi ,  . U.; O'Halloran, T. V. *Inorg. Chem.* **2013**, *52*, 12292.

⁴⁵⁶ Fr zard, F.; Demicheli, C.; Ribeiro, P. R. *Molecules* **2009**, *14*, 2317.

⁴⁵⁷ Nordberg, G. F.; Fowler, B. A.; Nordberg, M.; Friberg, L. *Handbook on the Toxicology of Metals*, **2007**, Elsevier, Burlington.

⁴⁵⁸ Weiss, S.; Hatcher, R. A. *J. Exp. Med.* **1923**, *37*, 97.

⁴⁵⁹ Roychoudhury, J.; Ali, N. *Ind. J. Biochem. Biophys.* **2008**, *45*, 16.

⁴⁶⁰ Soto, J.; Fuya, P.; Herrera, R.; Berman, J. *Clin. Infect. Dis.* **2008**, *26*, 56.

⁴⁶¹ Ferreira, W. A.; Islam, A.; Andrade, A. P. S.; Fernandes, F. R.; Fr zard, F.; Demicheli, C. *Molecules* **2014**, *19*, 5478

⁴⁶² Islam, A.; Da Silva, J. G.; Berbet, F. M.; Da Silva, S. M.; Rodrigues, B. L.; Beraldo, H.; Melo, M. N.; Fr zard, F.; Demicheli, C. *Molecules* **2014**, *19*, 6009; Lizarazo-Jaimes, E.H.; Reis, P.G.; Bezerra, F.M.; Rodrigues, B.L.; Monte-Neto, R.L.; Melo, M.N.; Fr zard, F.; Demicheli, C. *J. Inorg. Biochem.* **2014**, *132*, 30; Ali, M. I.; Rauf, M. K.; Badshah, A.; Kumar, I.; Forsyth, C. M.; Junk, P. C.; Kedzierski, L.; Andrews, P. C. *Dalton Trans.* **2013**, *42*, 16733; Khan, N. U. H.; Sultana, K.; Nadeem, H. *Middle-East J. Sci. Research* **2013**, *16*, 1109; Lizarazo-Jaimes, E. H.; Monte-Neto, R. L.; Reis, P. G.; Fernandes, N. G.; Speziali, N. L.; Melo, M. N.; Fr zard, F.; Demicheli, C. *Molecules* **2012**, *17*, 12622.

⁴⁶³ Sharma, P.; Perez, D.; Cabrera, A.; Rosas, N.; Arias, J. L. *Acta Pharmacol. Sin.* **2008**, *29*, 881.

mechanism of (geno)toxicity of antimonials.⁴⁶⁴ The presumed mechanism of the pentavalent antimony Sb (V) seems to be its intracellular reduction into active Sb (III) form.⁴⁶⁵

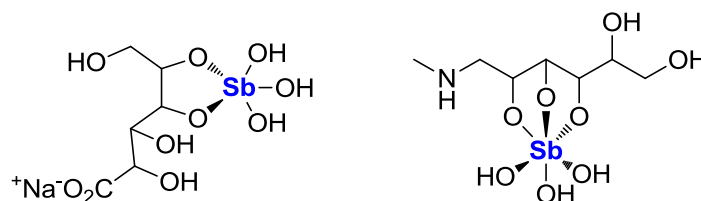


Figure 131: Antimony based drugs: Sodium stibogluconate and meglumine antimoniate

4.1.3.3 Introduction of phosphines, arsines and stibines to NHC-Pt complexes

In this context, we were expecting that combination of our NHC-Pt complexes with softer As or Sb ligands would provide a synergic effect on biological activity. These pnictogen ligands *cis* to the NHC might modulate activity and have an impact on the organism when released. Thus, a range of [(NHC)Pt(L)] (L = phosphine⁴⁶⁶, arsine or stibine⁴⁶⁷) complexes were synthesized using our well-established procedure by ligand exchange.^{125,126} For the whole discussion, the NHC will be set as a reference and a complex *trans* would mean that the L ligand would be in *trans* to the NHC, and *cis* complex, *cis* to the NHC (**Figure 132**). This agreement, due to the presence of NHC in both reactive and final product, would allow easy comparison between different complexes.

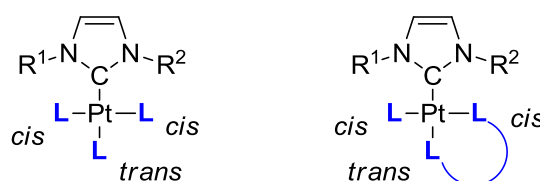


Figure 132: Adopted convention of cis/trans ligands

⁴⁶⁴ Gebel, T. *Chemico-Biological Interactions* **1997**, 107, 131; De Boeck, M.; Kirsch-Volders, M.; Lison, D. *Mutation Research* **2003**, 533, 135.

⁴⁶⁵ Sereno, D.; Holzmüller, P.; Mangot, I.; Cuny, G.; Ouassiss, A.; Lemesre, J.L. *Antimicrob. Agents Chemother.* **2001**, 45, 2064.

⁴⁶⁶ Pyridine substitution by triphenylphosphine on a NHC-Pd(II)-pyridine complex was investigated by Ghosh *et al.*: Kumar, A.; Katari, M.; Ghosh, P. *Polyhedron* **2013**, 52, 524.

⁴⁶⁷ Stibines (or Stibanes following IUPAC nomenclature) are the organo derivatives of antimony.

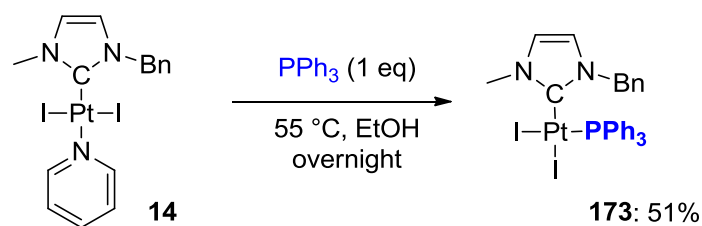


Figure 133: Synthesis of a [(NHC)Pt(PPh₃)] complex by ligand exchange

The pyridine precursor **14** and one equivalent of PPh₃, the simplest phosphine ligand, were stirred overnight in ethanol at 55 °C to afford after purification by silica gel chromatography the desired complex **173** in moderate yield (51%) (**Figure 133**). The expected ³¹P {¹H} NMR spectrum with ¹⁹⁵Pt satellites showed a centred signal and a doublet due to the *J*_{P-Pt}. The direct assignment *cis* or *trans* configuration is based on the *J* values between Pt and phosphorous (**Table 13**). The *J*_{P-Pt} = 3684 Hz measured correspond to typical value for *cis* complexes (*J*_{P-Pt} ~3500 Hz), whereas *trans* complexes usually have *J*_{P-Pt} = ~2500 Hz.⁴⁶⁸ The *cis* geometry proposed in **Figure 133** is probably imposed by NHC strong σ donor ability that would prevent *trans* coordination of other σ donating ligand. The ¹H-NMR spectrum shows two diastereotopic protons of the N-CH₂ group of the NHC (doublets at 4.32 and 5.84 ppm; *J* = 14 Hz). The presence of the bulky PPh₃⁸⁵ prevents the free rotation of the CH₂-Ph group and so benzylic protons do not have the same chemical environment.

Phosphine can also be generated by deprotonation *in situ* of tributylphosphonium to afford complex **174** (**Figure 134**).⁴⁶⁹

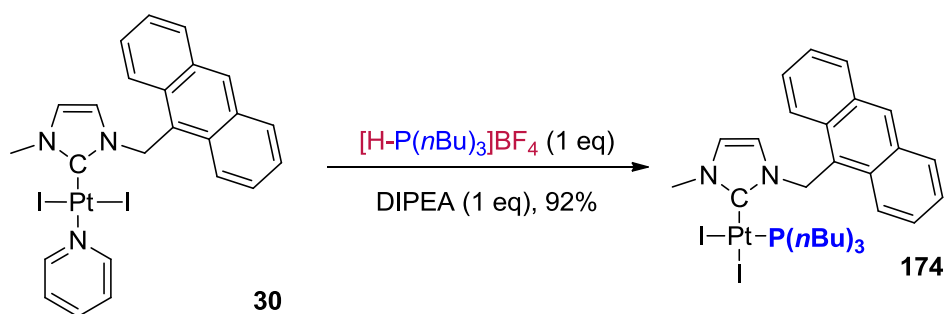


Figure 134: Synthesis of platinum complex 174 bearing tributylphosphine

Previously cited literature examples of di-phosphine NHC complexes revealed several cationic species. Charged complexes are *a priori* more water-soluble and so more adapted for biological

⁴⁶⁸ Dixon, K. R.; Fakley, M.; Pidcock, A. *Can. J. Chem.* **1976**, *54*, 2733; Favez, R.; Roulet, R.; Pinkerton, A. A.; Schwabenbach, D. *Inorg. Chem.* **1980**, *19*, 1356.

⁴⁶⁹ Synthesized in collaboration with Mathilde Bouché.³⁵⁸

applications. Cationic complex **175** was obtained by reaction of an excess of phosphine (**Figure 135**). Again, a cautious analysis of ^1H (diastereotopic $\text{CH}_2\text{-Ph}$ protons), ^{31}P and ^{13}C -NMR indicate a complex where the two phosphines are *cis* to the NHC (**Table 13**).

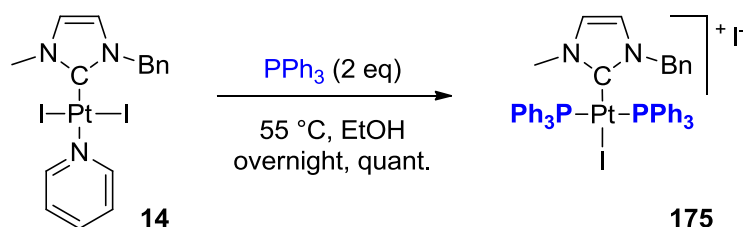


Figure 135: Synthesis of a cationic $[(\text{NHC})\text{PtI}(\text{PPh}_3)_2]^+$ complex by ligand exchange

Using a bidentate phosphine ligand leads directly to the formation of the cationic compound rather than the κ^1 -complex (**Figure 136**). 1,2-Bis(diphenylphosphino)ethane (dppe) can be introduced to either phenyl and nitrobenzyl⁴⁷⁰ substituted NHC-Pt complexes **176** and **177** respectively.

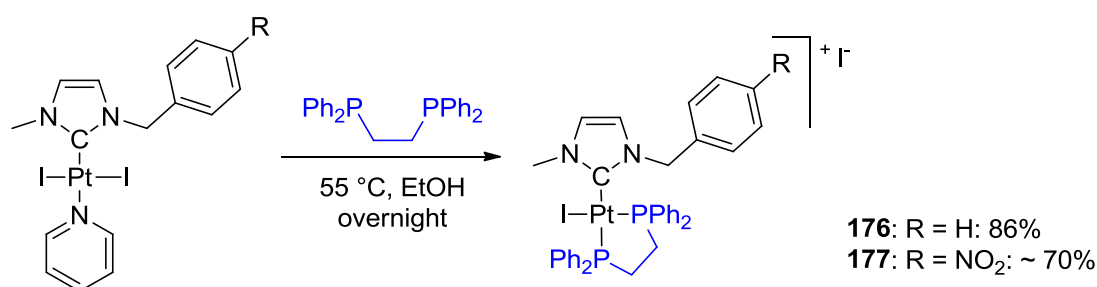


Figure 136: Synthesis of a cationic $[(\text{NHC})\text{PtI}(\text{dppe})]^+$ complex by ligand exchange

The same comments for ^1H -NMR and ^{13}C -NMR as before can be done. The two phosphorous atoms are not equivalent as they are either in a *cis* respectively *trans* configuration to the NHC, conducting to two different sets of signals in ^{31}P -NMR ($J_{\text{P-Pt}} = 2221$ Hz for *trans* P, and 3306 Hz for *cis* P) (**Table 13**) and (**Figure 137**).

⁴⁷⁰ The nitro derivative 177 was synthesized in collaboration with Mathilde Bouché.³⁵⁸

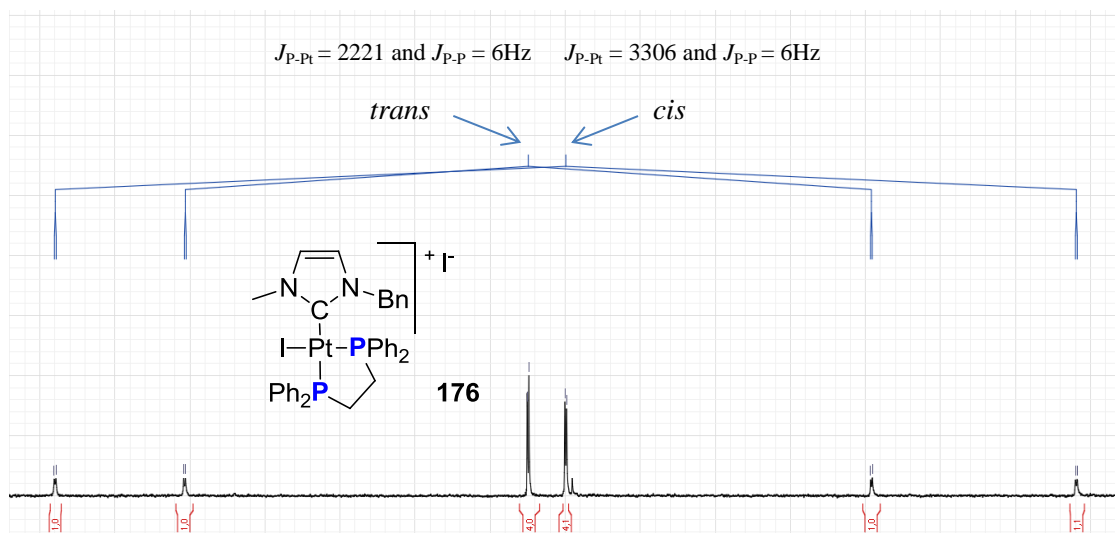


Figure 137: NMR ^{31}P spectrum of $[(\text{NHC})\text{PtI}(\text{dppe})]\text{I}$ complex **176**: evidence of cis and trans P

Attempts to introduce 1,1'-Bis(diphenylphosphino)ferrocene (dppf) failed. At 25 °C no reaction occurs, and at 60 °C decomposition of platinum complex was observed, potentially caused by redox side reactions. For the bulkier BINAP (2,2'-Bis(diphenylphosphino)-1,1'-binaphthyl) as well, no coordination was noticed.

After successful introduction of phosphine ligands, other simple pnictogen derivatives such as triphenylarsine (AsPh_3) and triphenylstibine (SbPh_3)^{471,472} were tested affording complexes **178-182**.

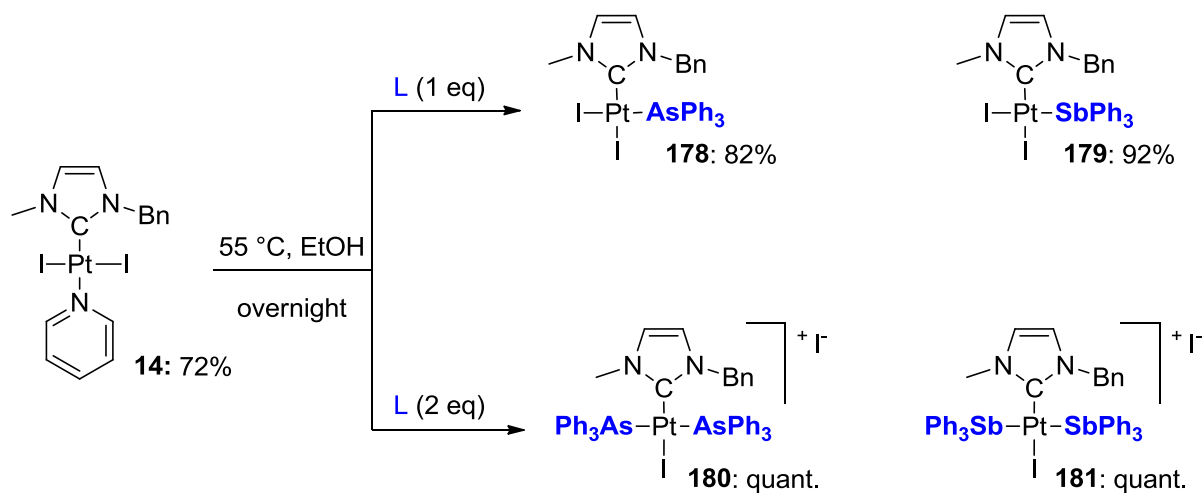


Figure 138: Ligand substitution reactions with triphenylarsine and triphenylstibine

⁴⁷¹ Triphenylantimony (III) or triphenylstibine (IUPAC).

⁴⁷² In this context, it is worth mentioning that antimony (III) was complexed by cyclic alkyl(amino)carbenes (CAACs) to form a CAAC-SbCl₃ complex: Kretschmer, R.; Ruiz, D. A.; Moore, C. E.; Rheingold, A. L.; Bertrand, G. *Angew. Chem. Int. Ed.* **2014**, 53, 8176.

Comparable reactivity as PPh_3 was observed for either AsPh_3 or SbPh_3 , which generated *cis* complexes **178** and **179** respectively in good yield (**Figure 138**). Using an excess of ligand led to the formation of bis *cis*-cationic complexes **180** and **181** in high yield. First difference observed to *trans* complexes, all *cis* complexes are white or white-yellow colour.⁴⁷³

^1H and ^{13}C -NMR analysis (**Table 13**) showed some interesting trends in chemical shift. In all complexes containing pnictogen ligand except the dppe complex **176** (166 ppm), the carbon of carbene is downfield at around 150 ppm which can be considered as fingerprint for *cis* imidazolylidene complexes, compared to pyridine complex **14** at 136 ppm (entry 1). In ^1H -NMR, N-CH_3 and N-CH_2 protons are deshielded changing from pyridine to phosphine. The chemical shift is softly increasing from phosphine to stibine (entry 2 and 3). As observed for **173**, coordination of AsPh_3 and SbPh_3 usually disymmetrize the benzylic protons as two doublets in ^1H -NMR (entry 3 and 4) (except **175**). As typical example, the spectrum of $[(\text{NHC})\text{Pt}(\text{II})(\text{SbPh}_3)]$ **179** is presented in **Figure 139**. A variable temperature NMR was conducted for Sb complex **179**, no coalescence of the two doublet signals was observed up to 323K in CDCl_3 . Increased heating at 363K in DMSO-d_6 leads to slow decomposition of the complex.

Entry	NMR δ (ppm), J (Hz)	14 (Pyr)	173 (PPh_3)	178 (AsPh_3)	179 (SbPh_3)
1	^{13}C : $\delta_{\text{C-Pt}}$	136.3	154.0	151.5	150.1
2	^1H : $\delta_{\text{N-CH}_3}$	3.97	3.53	3.56	3.58
3	^1H : $\delta_{\text{N-CH}_2}$	5.72	4.32, 5.84	4.57, 5.77	5.11, 5.50
4	^1H : $J_{(\text{N-CH}_2)}$	/	14.0	14.1	14.2
5	^{31}P : δ_{P}	/	8.46	/	/
6	^{31}P : $J_{(\text{Pt-P})}$	/	3648	/	/

Entry	NMR δ (ppm), J (Hz)	175 (Bis- PPh_3)	180 (Bis- AsPh_3)	181 (Bis- SbPh_3)	176 (Dppe*)
1	^{13}C : $\delta_{\text{C-Pt}}$	150.7	n.d.	150.7	165.5
	^{13}C : $J_{(\text{Pt-C})}$ and (P-C)	/	/	/	138.3, 7.8
2	^1H : $\delta_{\text{N-CH}_3}$	3.31	3.49	3.58	3.37
3	^1H : $\delta_{\text{N-CH}_2}$	4.71	4.50, 5.70	5.12, 5.50	4.18, 5.24
4	^1H : $J_{(\text{N-CH}_2)}$	/	14.0	14.2	14.6
5	^{31}P : δ_{P}	13.01	/	/	41.0, 40.0
6	^{31}P : $J_{(\text{Pt-P})}$	2448	/	/	2221, 3306
7	^{31}P : $J_{(\text{P-P})}$	/	/	/	6

Table 13: Characteristic NMR data for Pnictogen Imidazol-2-ylidene complexes (25 °C, Solvent: CDCl_3 , *MeOD)

⁴⁷³ Muir *et al.* reported the typical white colour for *cis* complexes of phosphines and arsines.⁴²⁰

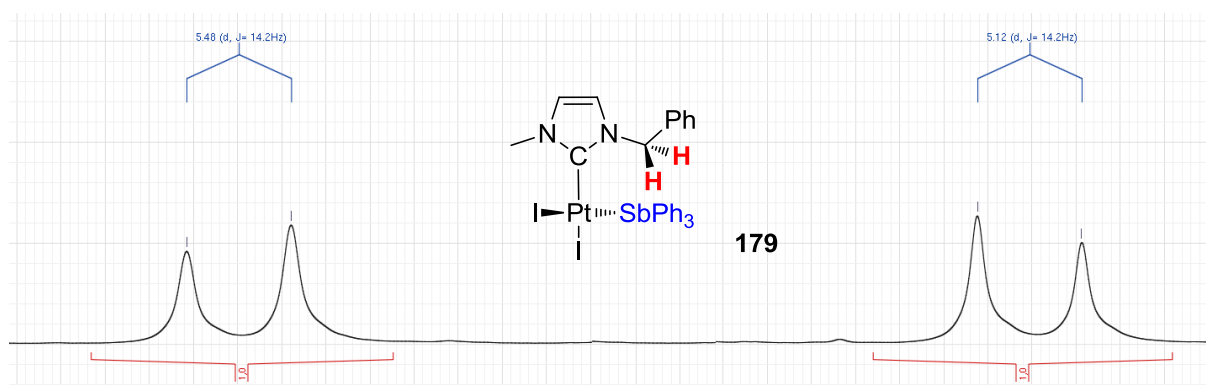


Figure 139: ^1H -NMR spectrum of NHC-Pt(II)-SbPh₃ **179**: disymmetrisation of the two hydrogens of the N-CH₂ (Nota: CH₂Cl₂ pic at 5.3 ppm omitted for clarity)

Suitable crystals were obtained by vapour diffusion of pentane in saturated CDCl₃ respective CH₂Cl₂ solutions of [(NHC)Pt(II)(AsPh₃)] **178** and of [(NHC)Pt(II)(SbPh₃)] **179** complexes and characterized by X-ray diffraction (**Figure 140**).

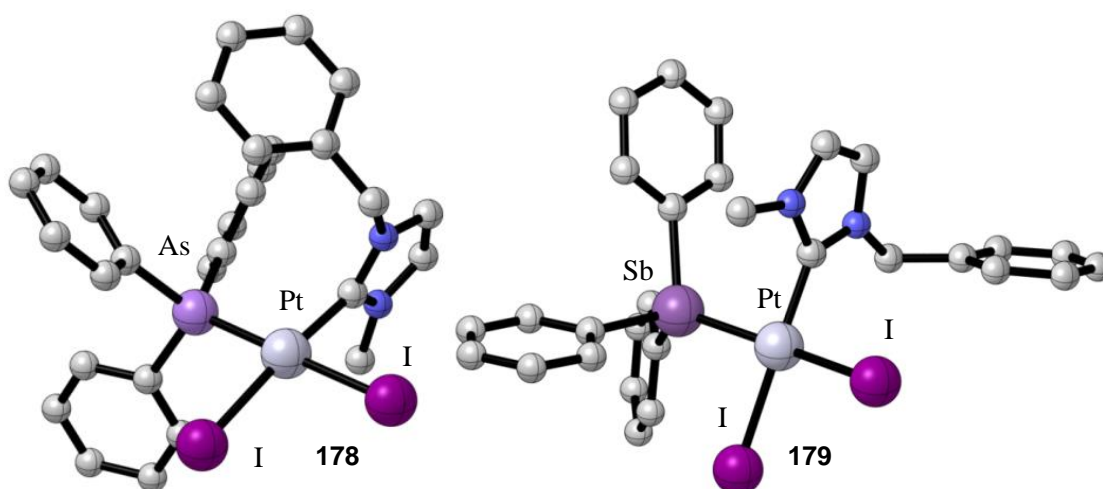


Figure 140: X-ray diffraction structure of (NHC)Pt(II)(AsPh₃) **178** and of (NHC)Pt(II)(SbPh₃) **179**

Complex **178** crystallized in P_1 space group with one molecule of chloroform and complex **179** in Pbc space group.

Entry	(NHC)Pt(II)(L) complexes	14 (Pyridine)	178 (AsPh ₃)	179 (SbPh ₃)
1	Space group	<i>P</i> 2 ₁ /c	<i>P</i> ₁	<i>P</i> b c a
2	C _{carbene} -Pt (Å)	1.973	1.993	1.983
3	Pt-L (Å)	2.094	2.634	2.507
4	Pt-I _{cis} (Å)	2.601, 2.594	2.629	2.649
5	Pt-I _{trans} (Å)	/	2.655	2.638
6	C _{carbene} -Pt-L (°)	177.51	93.20	91.10
7	N _{CH3} -C _{carbene} -Pt-I _{cis} (°)	76.49, 104.56	101.63	91.20
8	C _{carbene} -Pt-I _{trans} (°)	/	174.84	176.77
9	C _{carbene} -Pt-I _{cis} (°)	89.41, 90.61	86.19	89.16
10	C _{carbene} -I _{cis} (Å)	3.243, 3.282	3.192	3.285

Table 14: Selected bond lengths (Å) and angles (°) of [(NHC)Pt(II)I₂(ligand)] complexes

Selected bond lengths and angles of the solid state structures of three NHC-Pt(II)-L complexes (pyridine **14**, arsine **178** and stibine **179**) are assembled in **Table 14**. Three arsine complexes found in literature^{474,475} are mentioned in **Table 15** for comparison purpose.

Entry	Arsine complexes	<i>Trans</i> -[(pyr)PtI ₂ (AsPh ₃)] ⁴⁷⁴	[(PtI ₃ AsPh ₃) ⁻ (N _n But) ₃ ⁺] ⁴⁷⁴	<i>Trans</i> -[PtCl ₂ (AsPh ₃) ₂] ⁴⁷⁵
1	Space group	<i>P</i> 2 ₁ /n	<i>P</i> 2 ₁ /n	<i>P</i> 2 ₁ /n
2	N _{pyridine} -Pt	2.109	/	/
3	Pt-As	2.357	2.375	2.410
4	Pt-I _{trans} to As	/	2.658	/
5	Pt-X _{cis} to As	2.606, 2.585	2.611 2.618	2.300

Table 15: Data from selected platinum arsine complexes from literature (Bond lengths Å)

Solid-state molecular structure of both arsine **178** and stibine **179** complexes confirmed the square planar coordination at the platinum centre, with *cis* geometry of arsine or stibine relative to the NHC (*entry 6 and 8*). Compared to pyridine complex **14** (1.973 Å), C_{carbene}-Pt is elongated for stibine **179** (0.010 Å) and arsine **178** (0.020 Å) complexes (*entry 2*). It probably results of stronger electron donating ability of these ligands compared to pyridine. Platinum-arsine (2.634 Å) and platinum stibine (2.507 Å) bond lengths are in the same magnitude as platinum-iodine bond (average *cis*: 2.639 Å; average *trans*: 2.645 Å), but longer (0.55 Å average) than platinum-pyridine bond (*entry 3*). The presence of arsine and stibine on the metal centre locate the two iodine *trans* to stronger σ donating ligand (both NHC and As or Sb) and so elongated the Pt-I bond length (+0.045 Å) compared to Pt-I

⁴⁷⁴ Kuznik, N.; Wendt, O. F. *J. Chem. Soc. Dalton Trans.* **2002**, 3074.⁴⁷⁵ Johansson, M. H.; Otto, S.; Roodt A.; Oskarsson, Å, *Acta Cryst.* **2000**, B56, 226.

bond observed for pyridine complex (*entry 4 and 5*). The presence of the NHC on the metal centre result in an elongation of the Pt-As (2.634 Å) bond compared to other NHC-free platinum arsine complexes (average 2.38 Å) (**Table 15**, entry 3). The C_{carbene}-Pt-I_{cis} angle expected as 90° for square planar geometry, perfectly adopts this value for pyridine and stibine complex, but is deviated for arsine complex to 86° (entry 9). Interatomic distances for C_{carbene}-I_{cis} (*entry 10*) for all complexes are within the sum of van der Waals radii (~3.68 Å) for carbon (~1.70 Å) and iodine (~1.98 Å). Especially for the arsine complex, these three values indicate interactions between lone pairs of electrons of I *cis* to the NHC ligand and formally vacant antibonding NHC *p* orbital, feature already observed for platinum-NHC¹²⁴ or early transition metal-NHC complexes.⁴⁷⁶ For (NHC)Pt(II)-stibine **179**, an edge to face (T-shape) π - π interaction⁴⁷⁷ is established between phenyl ring and imidazole ring of a second molecule (Ph_{centroid}-C distance: 3.384 Å) (**Figure 141**).

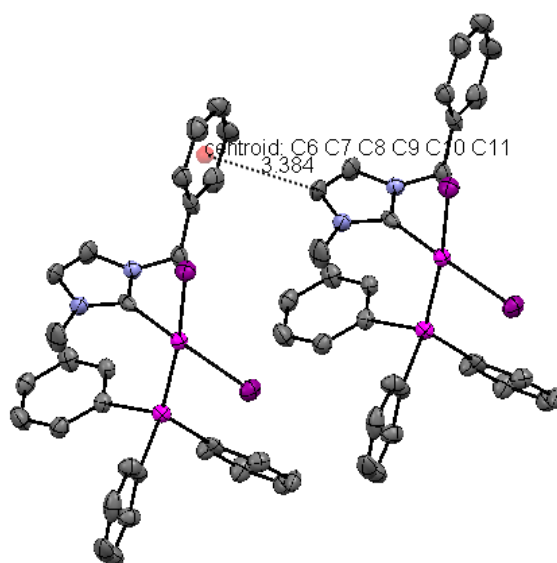


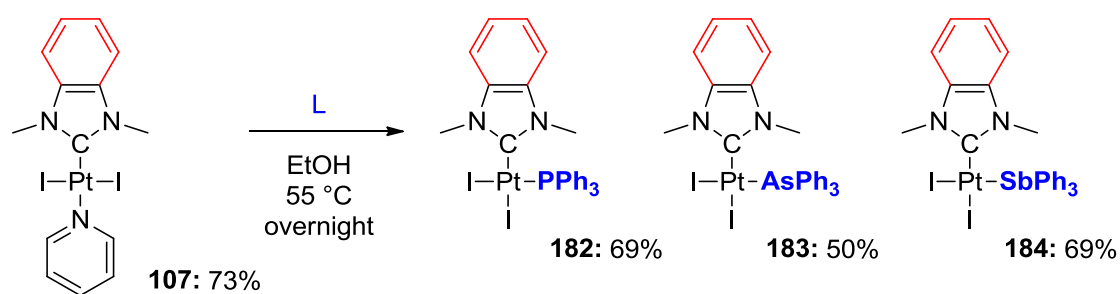
Figure 141: Solid-state π - π interaction established between a phenyl ring and imidazole ring two stibine complexes **179**

The nature of the NHC backbone was then changed. With a benzimidazol-2-ylidene symmetrical core, mono substituted *cis* pnictogen platinum complexes **182-184** (white powders) were synthesized in moderate yield (**Figure 142**). Surprisingly, even an excess of L ligand did not generated the expected cationic complexes as only neutral mono-substituted complexes were obtained. The low donating ability of benzimidazol-2-ylidene carbenes⁴⁷⁸ (in regard to imidazol-2-ylidene carbenes) probably is not strong enough to weaken the Pt-I bond to allow its displacement and stabilize the cationic species.

⁴⁷⁶ Bellemin-Laponnaz, S.; Welter, R.; Brelot, L.; Dagorne, S. *J. Organomet. Chem.* **2009**, 694, 604.

⁴⁷⁷ Martinez, C. R.; Iverson, B. L. *Chem. Sci.* **2012**, 3, 2191; Xu, X.; Pooi, B.; Hirao, H.; Hong, S. H. *Angew. Chem. Int. Ed.* **2014**, 53, 1283.

⁴⁷⁸ Huynh, H. V.; Han, Y.; Jothibas, R.; Yang, J. A. *Organometallics* **2009**, 28, 5395.

Figure 142: Synthesis of benzimidazol-2-ylidene-Pt-pnictogen complexes **182**, **183** and **184**

Entry	NMR δ (ppm), J (Hz)	107 (Pyridine)	182 (PPh ₃)	183 (AsPh ₃)	184 (SbPh ₃)
1	¹³ C: $\delta_{\text{C-Pt}}$	149.9	166.3	163.9	163.2
2	³¹ P: δ_{P}	/	8.3	/	/
3	$J(\text{P-Pt})$	/	d, 3665	/	/
4	¹ H: $\delta_{\text{N-CH}_3}$	4.17	3.75	3.78	3.82

Table 16: NMR data for benzimidazol-2-ylidene complexes **182-184** (25 °C, solvent CDCl₃)

In order to access higher diversity, imidazolylidene backbone was modified. Influence of the *N*-substituents of the NHC (C₅H₉, benzaldehyde for possible further functionalization, CH₃, Anthracene) was investigated by introduction of one equivalent of arsine (**Figure 143**). No obvious reactivity modification was observed and each corresponding complexes **185**, **186**, **187**, **189**, **191** were obtained in moderate to good yield. In addition, two cationic imidazolylidene arsine complexes **186** and **188** could be isolated.

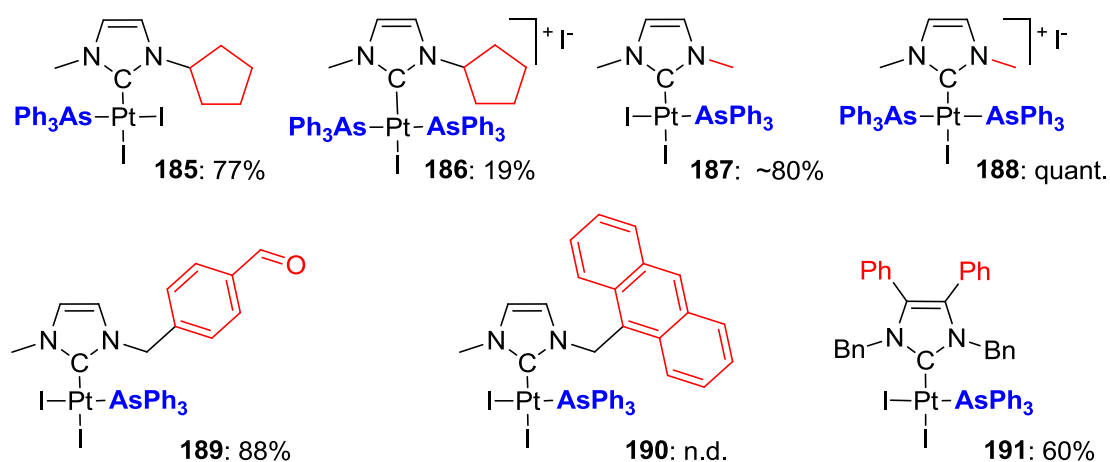
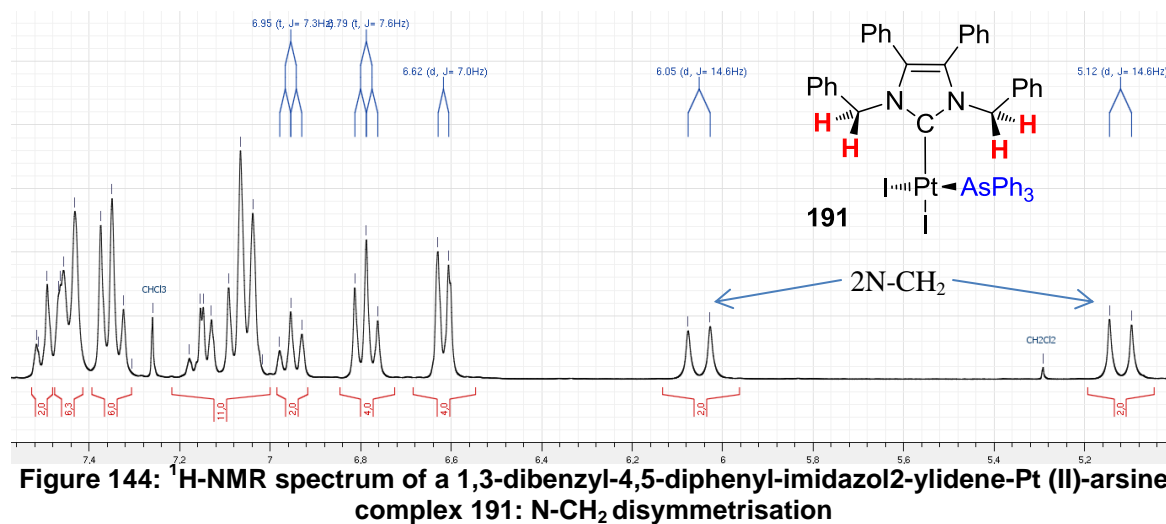
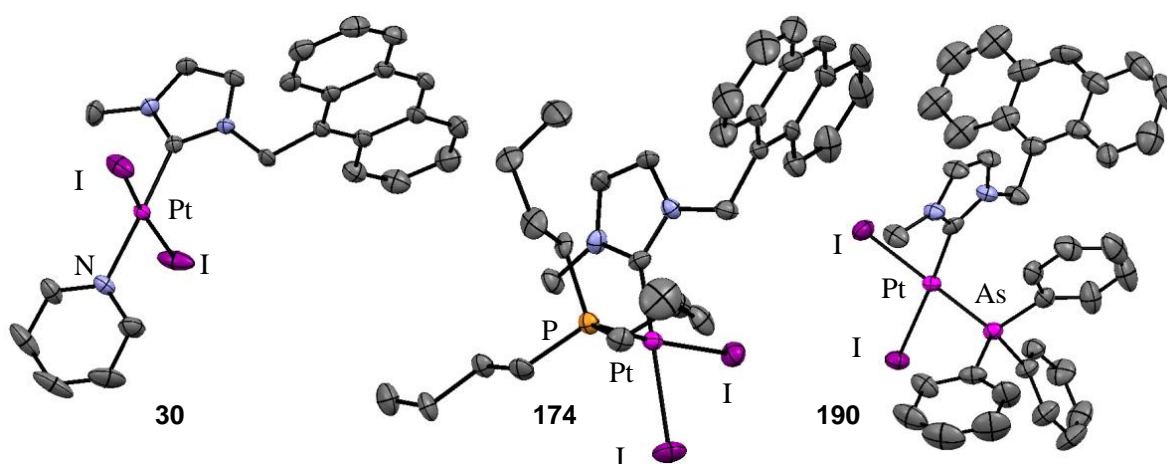


Figure 143: Triphenylarsine complexes with various NHC derivatives (%: yield of exchange step)

Once again, ^1H -NMR spectrum of symmetric 1,3-dibenzyl-4,5-diphenyl-imidazol-2-ylidene-Pt (II)-arsine complex **191** shows disymmetrisation of hydrogens of both CH_2 of the benzyl groups ($J=14.6\text{Hz}$) (**Figure 144**).



Vapor diffusion afforded crystals suitable for X-ray diffraction studies of three different (Anthracene-NHC)Pt(II)-ligand complexes **30**, **174** and **190** confirming the square planar geometry around platinum and the expected *cis* configuration of the ligands (**Figure 145**).



Entry	[(Anthracene-NHC)PtI ₂ (L)] complexes	30 (pyr)	174 (P(<i>n</i> Bu) ₃)	190 (AsPh ₃)
1	Space group	P 2 ₁ /c	P 2 ₁ /c	P 2 ₁ /c
2	C _{carbene} -Pt (Å)	1.961	1.965	1.992
3	Pt-L (Å)	2.088	2.253	2.355
4	Pt-I _{cis} (Å)	2.601, 2.573	2.668	2.626
5	Pt-I _{trans} (Å)	/	2.659	2.649
6	C _{carbene} -Pt-L (°)	174.90	92.25	92.33
7	N _{CH3} -C _{carbene} -Pt-I _{cis} (°)	87.88, 99.72	96.45	83.30
8	C _{carbene} -Pt-I _{trans} (°)	/	176.78	175.49
9	C _{carbene} -Pt-I _{cis} (°)	92.02, 87.72	85.27	87.50
10	C _{carbene} -I _{cis} (Å)	3.173, 3.312	3.180	3.226

Table 17: Selected bond lengths (Å) and angles (°) of (Anthracene-NHC)PtI₂(L) complexes

Table 17 indicates C_{NHC}-Pt bond length elongation for triphenylarsine complex **190** compared to pyridine **30** or tributylphosphine **174** (*entry 2*). Tributylphosphine-platinum bond is comprised between short platinum-pyridine and longer platinum-arsine bond (*entry 3*). Similar to previous described NHC-Pt(II)-L complexes, I_{cis} as well as AsPh₃ and SbPh₃ ligands point perpendicularly toward the NHC ligand plane (*entry 7*). C_{carbene}-Pt-I_{cis} angle is deviated from ideal 90° in case of all three complexes (*entry 9*). Interatomic distances for C_{carbene}-I_{cis} (*entry 10*) for all complexes are within the sum of van der Waals radii for carbon and iodine (~1.98 Å). For every complex, these three values indicate interactions between lone pairs of electrons of iodine I_{cis} *cis* to the NHC ligand and formally vacant antibonding *p* orbital of the NHC carbon atom.

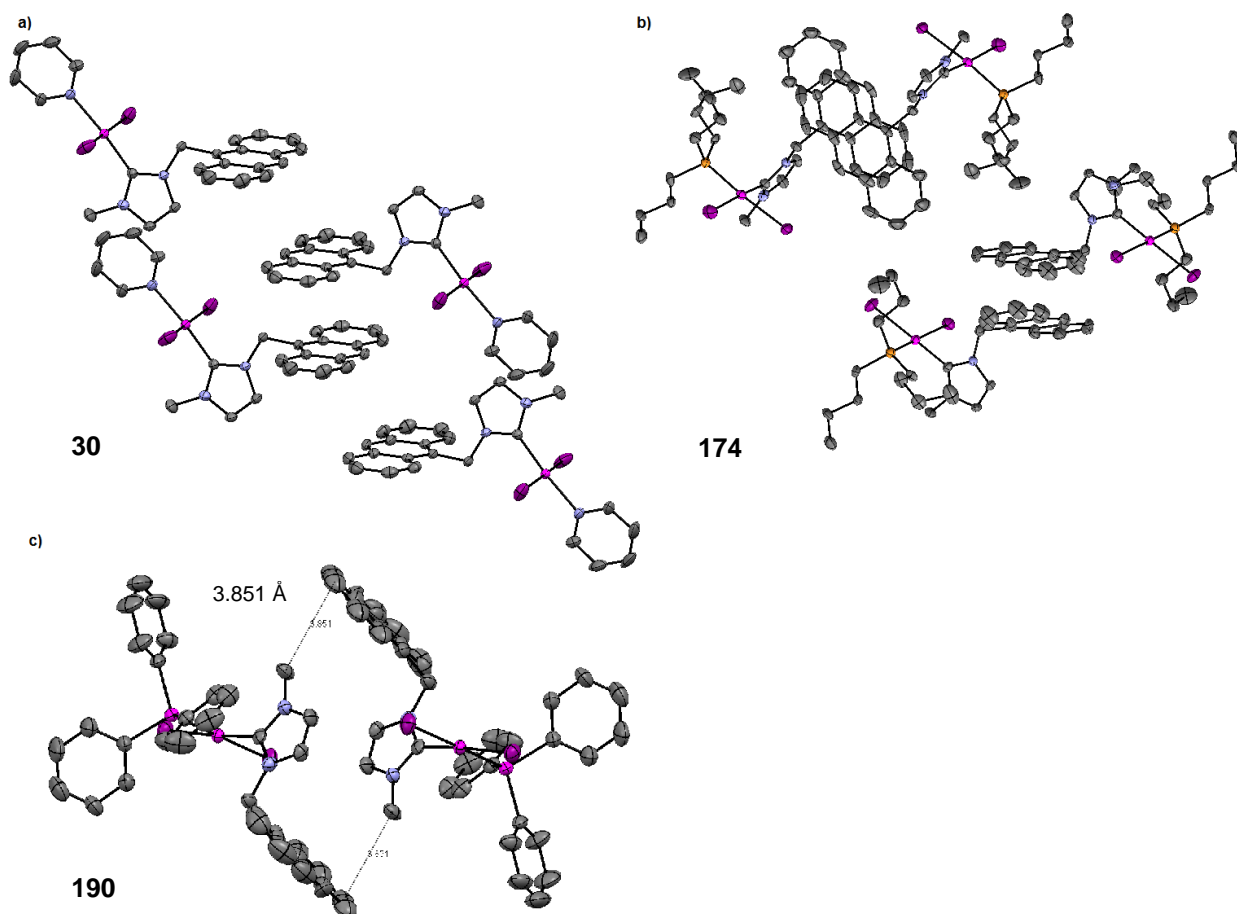


Figure 146: Solid state of (Anthracene-NHC)-Pt complexes with a) pyridine (**30**) b) tributylphosphine (**174**) and c) arsinic acid (**190**) ligands

Figure 146 summarizes complex organisation in solid state: pyridine complex **30** is forming ‘‘polymeric’’ structures by π - π interactions between anthracene moieties (a). Tributylphosphine complex **174** is organized in dimers linked also by parallel-displaced π - π interactions (b). Surprisingly, no π - π interactions between anthracene groups are present in the triphenylarsine compound **190**, which is forming dimeric structures by $\text{CH}_{\text{N-CH}_3}\cdots\pi_{\text{anthracene}}$ interactions (3.851 Å) (c)

During purification of complex **191**, a minor by-product **192** was also isolated (9%). The yellow colour as well the singlet signal of the N-CH₂ group in ¹H-NMR suggests the formation of the corresponding *trans* complex. X-rays revealed the formation of a *trans* NHC-platinum (II) complex linked to triphenylarsine oxide OAsPh₃. In crystal cell, also one molecule of OAsPh₃ co-crystallized with the complex (**Figure 147**).

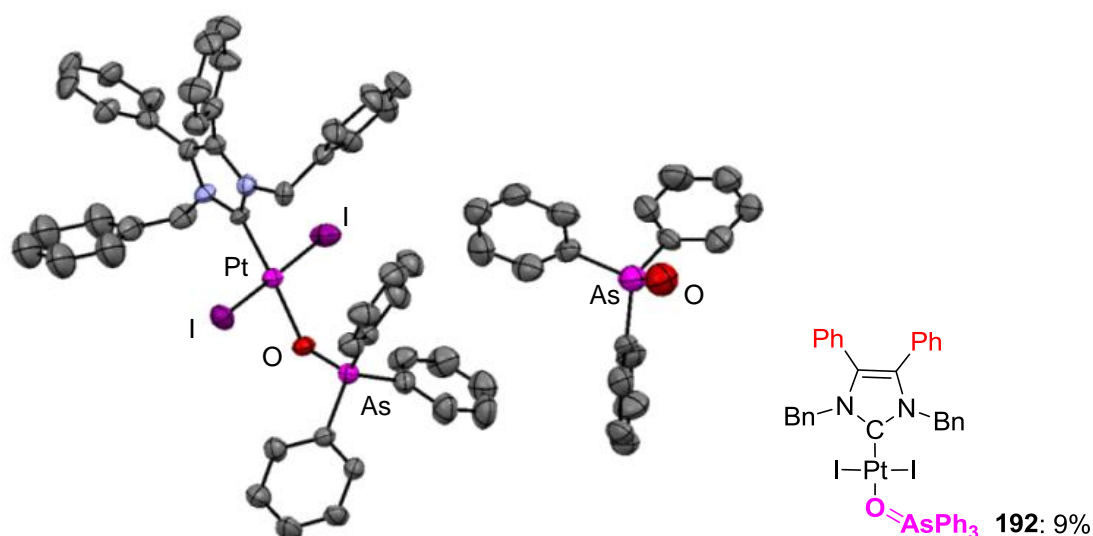


Figure 147: X-rays structure of an unexpected triphenylarsine oxide complex **192** (%: yield of exchange step)

Platinum-carbene distance is characteristic for *trans*-NHC complexes (1.941 Å), the geometry is square planar with both iodine ligands nearly perpendicular to NHC plane (**Table 18**). Arsenic-oxygen bonding length in OAsPh₃ (free OAsPh₃ < OAsPh₃·H₂O (1.644 Å)⁴⁷⁹ < Pt-OAsPh₃) is compatible with double bond character for no-coordinated ligand and single bond like character for platinum-coordinated ligand. The solid packing is determined by oxygen-C_{Phenyl} interactions (Sum of van der Waals Radii: (O: 1.52 Å + C: 1.70 Å = 3.22 Å) of neighbour coordinated OAsPh₃ moieties (interatomic distance: 3.173 Å) as well by Oxygen-C_{Phenyl} interactions between neighbour coordinated OAsPh₃ moieties (interatomic distance: 3.124-3.128 Å) (**Figure 148**).

C-Pt	Pt-O	As-O	As-O (free OAsPh ₃)	Pt-I	C-Pt-O	Pt-O-As	C-Pt-I
1.941	2.084	1.678	1.630	2.591, 2.597	176.19	123.99	89.91, 88.48

Table 18: Selected angles (°) and bond lengths (Å) for triphenylarsine oxide platinum complex **192**

⁴⁷⁹ Ferguson, G.; Macaulay, E. W. *J. Chem. Soc. A* **1969**, 1.

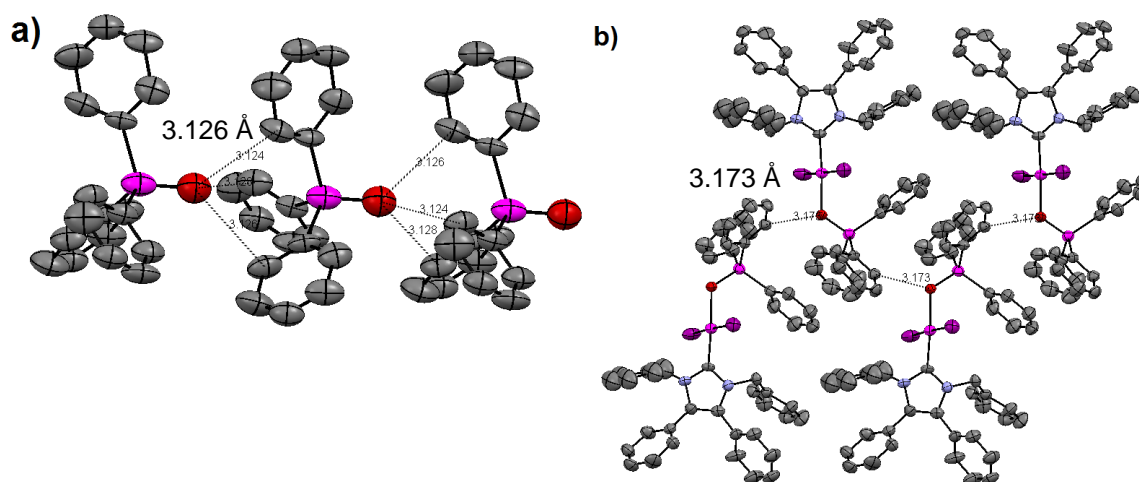


Figure 148: Oxygen-C_{Phenyl} interactions of non-coordinated a) and coordinated b) OAsPh₃ moieties

The major non-oxidized complex **191** is stable in CDCl₃ solution or in solid state under air over days. On TLC before chromatography, this side product **192** was not present and appeared only until the product **191** migrated on chromatography. Probably, released under air, the complex **191** oxidized on silica gel chromatography from arsine (III) to arsine (V). The oxidized ligand having less donor strength than triphenylarsine, it rearranged to the *trans* configuration.

On a binuclear complex **103**, one pyridine can be selectively substituted affording a mixt pyridine-arsine complex **193** to combine the different properties of both Pt-pyridine and Pt-As moieties in one single molecule (**Figure 149**).

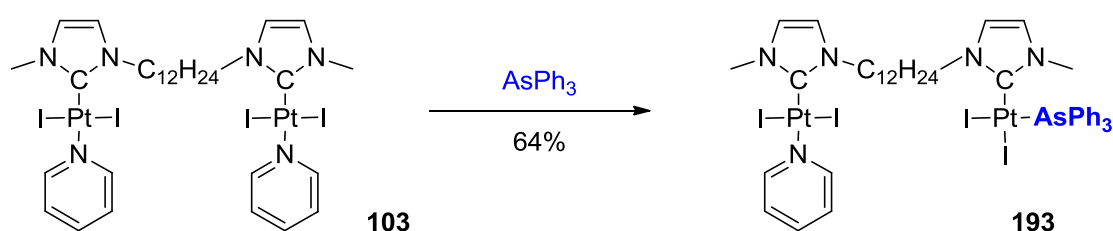


Figure 149: Binuclear NHC complex 198 with pyridine and arsine ligands

NMR spectra of this compound depict properties of both ligands (**Figure 150**).

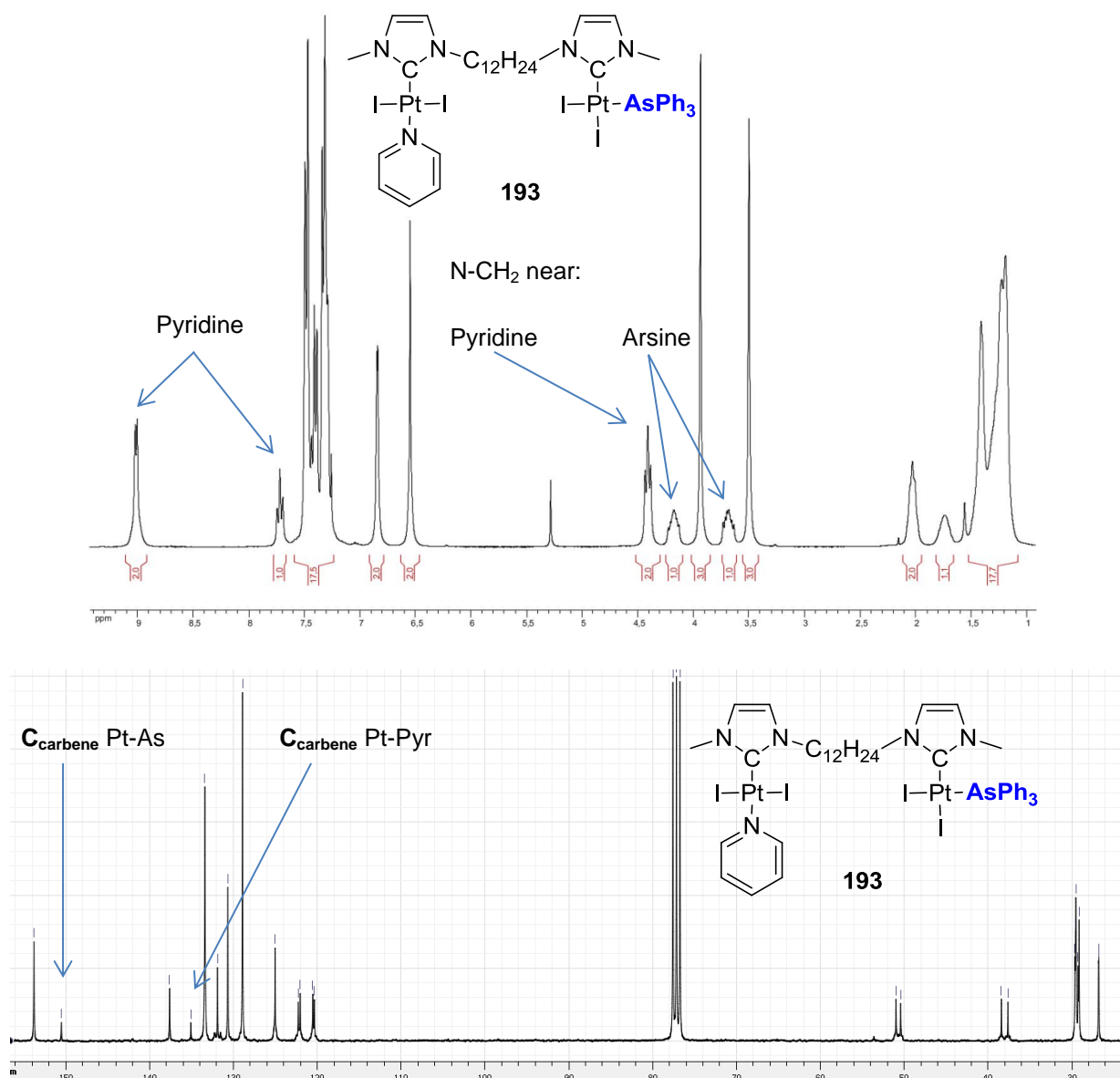


Figure 150: 1H and ^{13}C -NMR spectra of a binuclear NHC complex 193 with pyridine and arsine ligands

These examples show the versatility of our ligand exchange strategy, which allowed the introduction of various neutral ligands. Depending of the reactions conditions, cationic species could be obtained. We will describe the interesting *in vitro* results of several of these pnictogen ligand based compounds in chapter 5.1.6 *Cytotoxicity of platinum complexes*.

4.2 Post-synthetic modification of NHC-Pt complexes featuring benzaldehyde

One of the most famous reaction of aldehyde⁴⁸⁰ is the formation of imine derivatives, also known as Schiff bases (**Figure 151**).⁴⁸¹ Schiff bases obtained from aromatic aldehydes are well known in catalysis as they generate the family of Salen ligands. Thanks to their flexibility, a large library of chemical analogues can be prepared.⁴⁸² The condensation reaction is (Lewis) acid catalysed⁴⁸³ and water is generated as side product.

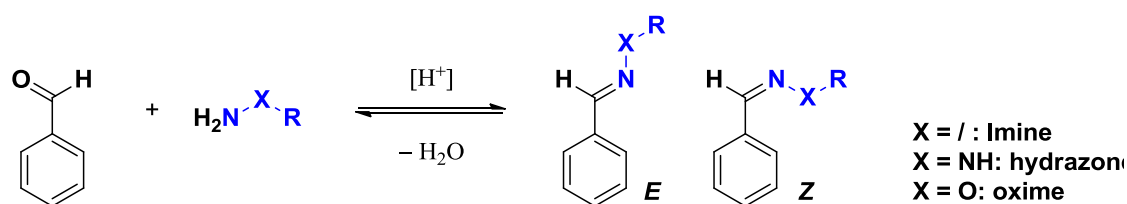


Figure 151: Condensation between amino derivatives and benzaldehyde

Stability of final product towards hydrolysis depends on the nature of the X atom neighbouring the amine (α -effect) (imine \ll hydrazone $<$ oxime).⁴⁸⁴ Two explanations are generally evoked for the greater stability of hydrazones and oximes: i) stabilization by delocalisation of electron doublet of the neighbouring heteroatom to the $\text{C}=\text{X}$ carbon thus decreasing its electrophilicity⁴⁸⁰ (**Figure 152**), and ii) decrease of the repulsion between lone pairs of nitrogen and X atoms in the resulting product.⁴⁸⁵

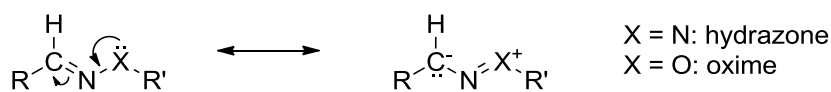


Figure 152: Mesomeric forms of hydrazones and oximes: stabilization towards hydrolysis

⁴⁸⁰ Carey, F. A. Sunberg, R. J. Addition, Condensation and Substitution Reactions of Carbonyl Compounds in *Advanced Organic Chemistry* **2007**, Springer Science+Business Media, LLC.

⁴⁸¹ W. P. Jencks, *Prog. Phys. Org. Chem.* **1964**, 2, 63; Hall N. E.; Smith, B. I. *J. Phys. Chem. A* **1998**, 102, 4930.

⁴⁸² Rajavel, R.; Vadivu, M. S.; Anitha, C. *Eur. J. Chem.* **2008**, 5, 620.

⁴⁸³ An acceleration of oxime and hydrazone formation can be obtained by nucleophilic catalytic aniline acting as transamination agent: Dirksen, A.; Hackeng, T. M.; Dawson, P. E. *Angew. Chem. Int. Ed.* **2006**, 45, 7581; Dirksen, A.; Dirksen, S.; Hackeng, T. M.; Dawson, P. E. *J. Am. Chem. Soc.* **2006**, 128, 15602.

⁴⁸⁴ Sander, E. G.; Jencks, W. P. *J. Am. Chem. Soc.* **1968**, 90, 6154; Cordes E. H.; Jencks, W. P. *J. Am. Chem. Soc.* **1963**, 85, 2843; Hine J.; Yeh, C. Y. *J. Am. Chem. Soc.* **1967**, 89, 2669; Hine, J.; Yeh, C. Y.; Schmalstieg, F. C. *J. Org. Chem.* **1970**, 35, 340; Hine, J.; Craig, J. C. Jr.; Underwood, J. G. II.; Via, F. A. *J. Am. Chem. Soc.* **1970**, 92, 5194; Kalia, J.; Raines, R. T. *Angew. Chem.* **2008**, 120, 7633.

⁴⁸⁵ Wiberg, K. B.; Glaser, R. *J. Am. Chem. Soc.* **1992**, 114, 841.

4.2.1 Functionalization of NHC complexes featuring benzaldehyde by oxime formation

Such condensation reaction fulfils (in principle) all criteria of Sharpless click chemistry reactions:¹³⁵ it is compatible with most (bio) functionalities⁴⁸⁶ and suitable as fast and easy applicable reaction for connection of two entities to create a library of compounds.⁴⁸⁷ A representative example is the work of the group of Dumy on attachment of carbohydrates and/or peptides to cyclopeptide scaffolds to afford artificial vectors for drug delivery, imaging probes, synthetic vaccines, or functional arrays (**Figure 153**).⁴⁸⁸

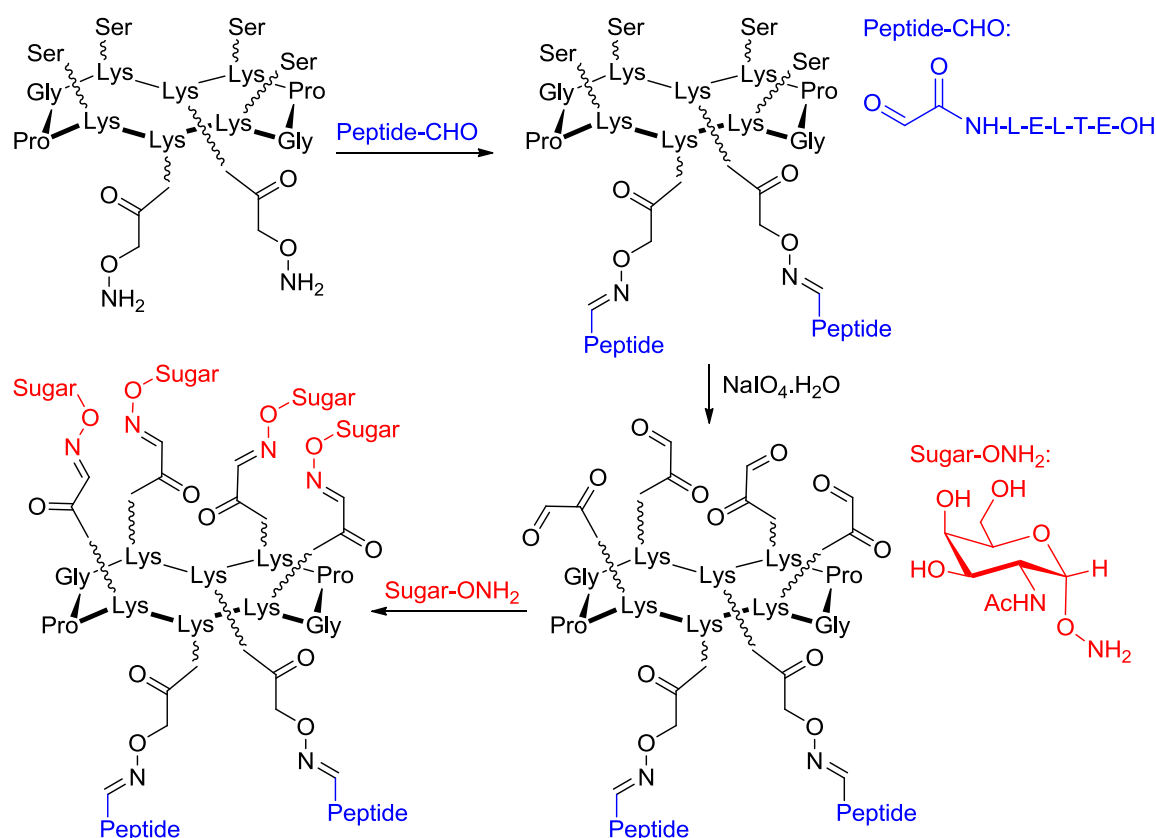


Figure 153: Representative oxime conjugation: functionalization of cyclopeptides with sugars and peptides by oxime ligation⁴⁸⁸

⁴⁸⁶ Rose, K. *J. Am. Chem. Soc.* **1994**, *116*, 30; Lemieux, G. A.; Bertozzi, C.R. *Trends Biotechnol.* **1998**, *16*, 506; Boturyn, D.; Constant, J.-F.; Defrancq, E.; Lhomme, J.; Barbin, A.; Wild, C. P. *Chem. Res. Toxicol.* **1999**, *12*, 476; Houdiera, S.; Legrand, M.; Boturyn, D.; Crozeb, S.; Defrancq, E.; Lhomme, J. *Analytica Chimica Acta* **1999**, *382*, 253; Falsey, J. R.; Renil, M.; Park, S.; Li, S.; Lam, K. S. *Bioconjugate Chem.* **2001**, *12*, 346; Hang, H.; Bertozzi, C. R. *Acc. Chem. Res.* **2001**, *34*, 727; Lelièvre, D.; Bure, C.; Laot, F.; Delmas, A. *Tetrahedron Lett.* **2001**, *42*, 235; Renaudet, O.; Reymond, J.-L. *Org. Lett.* **2003**, *5*, 4693; Chen, X.; Lee, G. S.; Zettl, A.; Bertozzi, C. R. *Chem. Int. Ed.* **2004**, *43*, 6111; Cremer, G.-A.; Bureaud, N.; Piller, V.; Kunz, H.; Piller, F.; Delmas, A. F. *ChemMedChem* **2006**, *1*, 965; Zhou, X.; Zhou, J. *Biosens. Bioelectron.* **2006**, *21*, 1451; Hecker, J. G.; Berger, G. O.; Scarfo, K. A.; Zou, S.; Nantz, M. H. *ChemMedChem* **2008**, *3*, 1356; Renaudet, O. *Mini-Rev. Org. Chem.* **2008**, *5*, 274; Dirksen, A.; Dawson, P. E. *Bioconjugate Chem.* **2008**, *19*, 2543; Meyer, A.; Spinelli, N.; Dumy, P.; Vasseur, J.-J.; Morvan, F.; Defrancq, E. *J. Org. Chem.* **2010**, *75*, 3927; Biswas, S.; Knipp, R. J.; Gordon, L. E.; Nandula, S. R.; Gorr, S.-U.; Clark, G. J.; Nantz, M. H. *ChemMedChem* **2011**, *6*, 2063.

⁴⁸⁷ For a review, see: Prescher, J. A.; Bertozzi, C. R. *Nature Chemical Biology* **2005**, *1*, 13.

⁴⁸⁸ Ulrich, S.; Boturyn, D.; Marra, A.; Renaudet, O.; Dumy, P. *Chem. Eur. J.* **2014**, *20*, 34; Daskhan, G. C.; Garcia, J.; Fiore, M.; Dumy, P.; Sulc, M.; Křen, V.; Renaudet, O. *Carbohydr. Res.* **2014**, *393*, 9.

Reversibility of imine bond enables a target-driven one-pot screening approach for probing secondary interactions to identify multi-point binding ligands of biomolecules (dynamic combinatorial chemistry)⁴⁸⁹ and developing of constitutional dynamic libraries.⁴⁹⁰

In organometallic chemistry, condensation reaction was first introduced on ruthenium (II) complexes. Ruthenium arene complexes have been studied for their antimetastatic properties.⁴⁹¹ In 2007, Ang, Dyson and co-workers designed a ruthenium (II) arene PTA (PTA = 1,3,5-triaza-7-phosphatricyclo-[3.3.1.1]decane) complex (RAPTA) bearing benzaldehyde. By hydrazone formation, this complex was successfully conjugated to human serum albumin, a protein that may accumulate in tumours (**Figure 154**).⁴⁹²

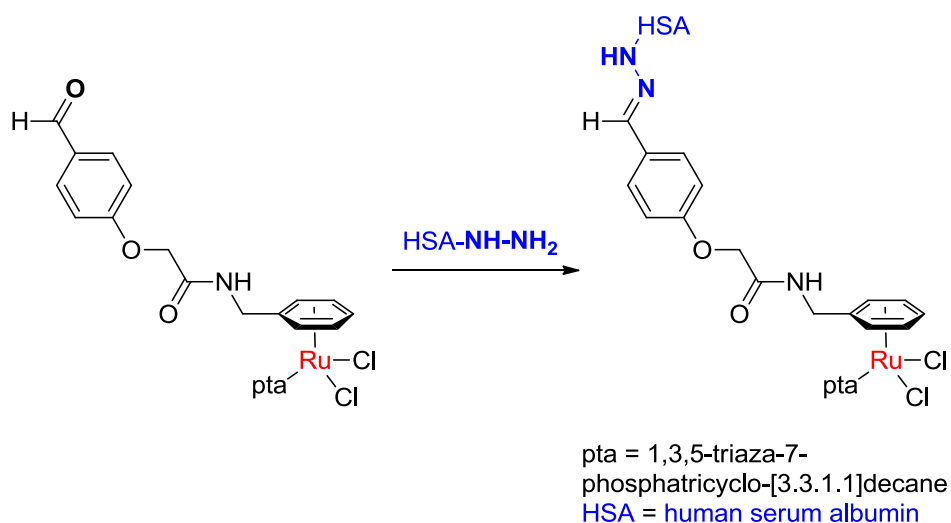


Figure 154: Ruthenium-HAS conjugate obtained by hydrazone formation⁴⁹²

Because the presence of the hydrophobic benzaldehyde may modify the biological properties of the complex, Ang and co-workers synthesized a ruthenium species with an acetal chain linked onto the arene. The acetal was deprotected under acid conditions into free aldehyde, which was then successfully condensed with benzylhydroxylamine (**Figure 155**).⁴⁹³

⁴⁸⁹ Ulrich, S.; Duly, P. *Chem. Commun.* **2014**, 50, 5810.

⁴⁹⁰ Vantomme, G.; Jiang, S.; Lehn, J.-M. *J. Am. Chem. Soc.* **2014**, 136, 9509.

⁴⁹¹ Dyson, P. J.; Sava, G. *Dalton Trans.* **2006**, 1929; Casini, A.; Mastrobuoni, G.; Ang, W.; Gabbiani, C.; Pieraccini, G.; Moneti, G.; Dyson, P. J.; Messori, L. *ChemMedChem*, **2007**, 2, 631; Bergamo, A.; Masi, A.; Dyson, P. J.; Sava, G. *Int. J. Oncol.* **2008**, 33, 1281; Süß-Fink, G. *Dalton Trans.* **2010**, 39, 1673; Antonarakis, E.S.; Emadi, A. *Cancer Chemother. Pharmacol.* **2010**, 66, 1.

⁴⁹² Ang, W. H.; Daldini, E.; Juillerat-Jeanneret, L.; Dyson, P. J. *Inorg. Chem.* **2007**, 46, 9048.

⁴⁹³ Tan, Y. Q.; Dyson, P. J.; Ang, W. H. *Organometallics* **2011**, 30, 5965.

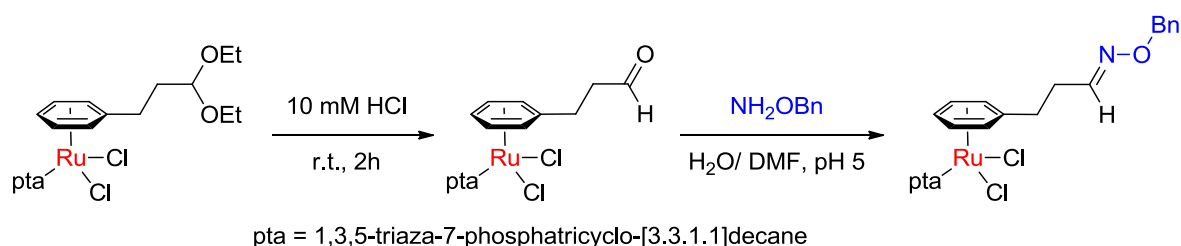


Figure 155: Condensation of a Ruthenium-aldehyde complex and benzylhydroxylamine⁴⁹³

More recently, a whole library of Ru-arene Schiff-base (RAS) complexes were synthesized in one-pot combinatorial three-component assembly reaction and screened for anticancer activity by same group.⁴⁹⁴ The methodology was expanded to Pt (IV) complexes armed with 4-formylbenzoate groups. Various substrates (hydrazides, hydroxylamines, oligopeptide derivatives) are introduced by imine ligation and stability of formed complexes was demonstrated (**Figure 156**).⁴⁹⁵ Five different peptides targeting FPR1/2 formyl peptide receptors, which are highly expressed in immune cells, could be chemo-selectively conjugated.⁴⁹⁶ As cisplatin derivatives prove some immune-stimulating activity, the authors claim to combine chemotherapy with immunotherapy to achieve a therapeutic synergy.

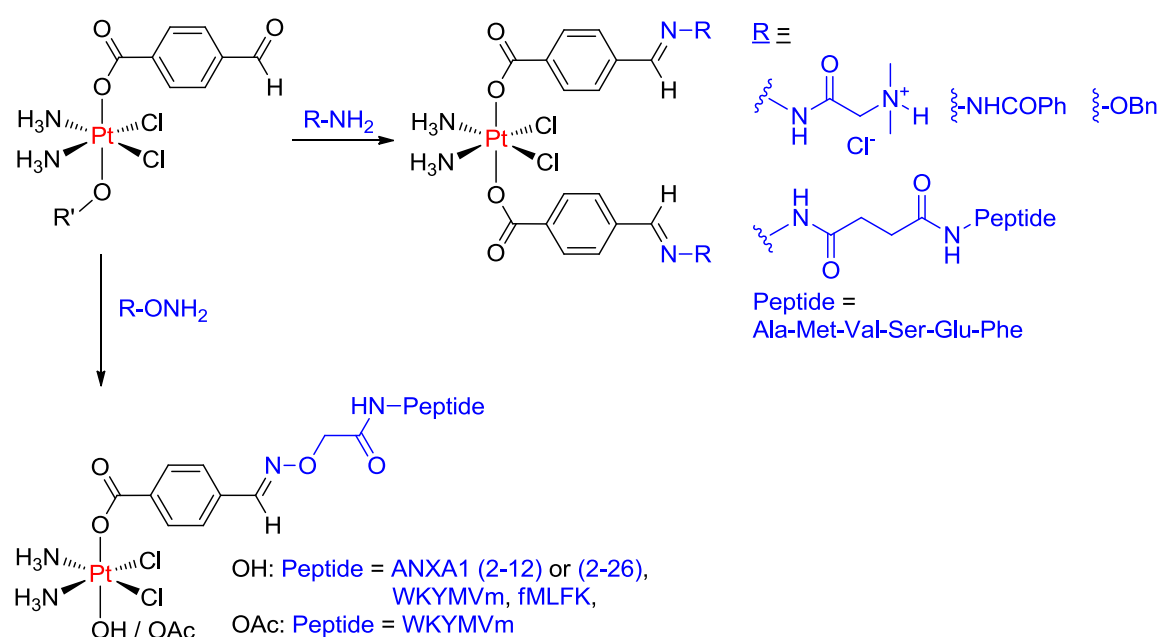


Figure 156: Conjugation of platinum (IV) complexes with various hydrazides or hydroxylamines⁴⁹⁵

⁴⁹⁴ Chow, M. J.; Licon, C.; Wong, D. Y. Q.; Pastorin, G.; Gaidon, C.; Ang, W. H. *J. Med. Chem.* **2014**, DOI: 10.1021/jm500455p.

⁴⁹⁵ Wong, D. Y. Q.; Lau, J. Y.; Ang, W. H. *Dalton Trans.* **2012**, 41, 6104.

⁴⁹⁶ Wong, D. Y. Q.; Yeo, C. H. F.; Ang, W. H. *Angew. Chem. Int. Ed.* **2014**, 53, 6752.

Considering the promising reactivity of Schiff bases, we decided to explore herein the scope and limitations of conjugation reaction between stable NHC-platinum complexes bearing a benzaldehyde moiety with various amines, hydrazines and hydroxylamines. Among various aldehyde bearing complexes synthesized (chapter 2.2.4 *Pt-NHC complexes functionalized by aldehydes and acetals*), two NHC-structures with different L ligands were selected for the ease of preparation (**Figure 157**).

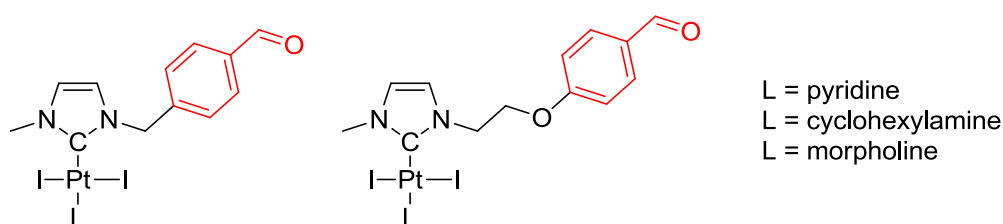


Figure 157: Benzaldehyde complexes chosen for conjugation with nitrogen derivatives

4.2.2 Post-synthetic modification of NHC complexes by imine formation

The desired imine containing NHC-Pt complexes were synthesized by simple condensation reaction in presence of the appropriate amine. Cyclohexylamine was first used in this study. Benzaldehyde platinum complex **81** in presence of a large excess of cyclohexylamine and Na₂SO₄ afforded quantitatively the desired imine complex **80** (**Figure 158**). Dry Na₂SO₄ was added in excess to trap the formed water and displace the equilibrium towards imine formation. The remaining cyclohexylamine was then evaporated *in vacuo* and the compound purified by silica gel chromatography (CH₂Cl₂, NEt₃).⁴⁹⁷ Interestingly, the imine compound could easily be hydrolysed in presence of wet SiO₂ / CH₂Cl₂ giving the starting aldehyde complex **81**. This result shows the relative instability of the imine bond towards hydrolysis susceptible to release the Pt-aldehyde derivative **81** in aqueous (cellular) medium.

⁴⁹⁷ Deactivation of the silica gel with NEt₃ was necessary to prevent decomposition of the imine.

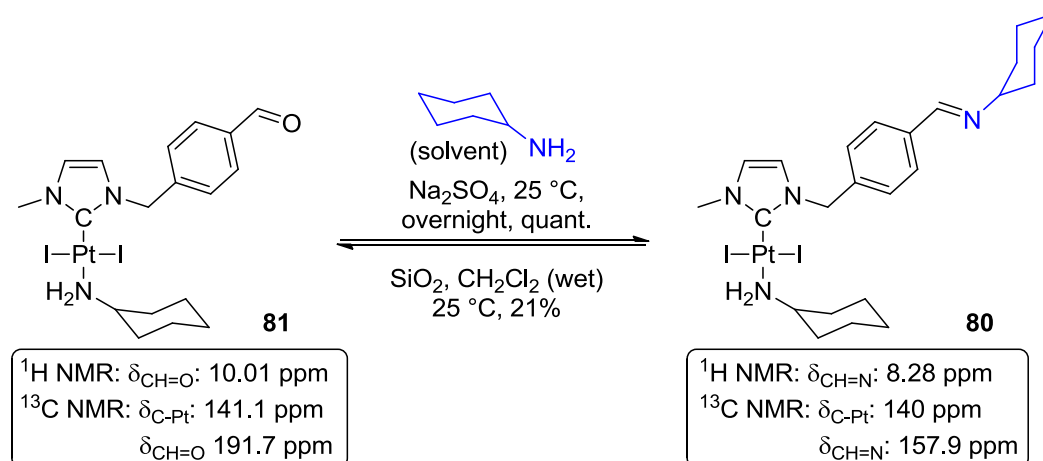


Figure 158: Condensation reaction between benzaldehyde complex and cyclohexylamine

The imine formation was easily followed by ^1H -NMR thanks to typical signals at 10.0 ppm and 8.3 ppm for CH=O and CH=N respectively. For all herein presented complexes, only one signal is obtained in ^1H and ^{13}C -NMR spectroscopy for the imine group CH=N indicating the presence of only stereoisomer *E*.⁴⁹⁸

The kinetics of reaction was followed by NMR. **Figure 159** displays the imine formation as a function of time.

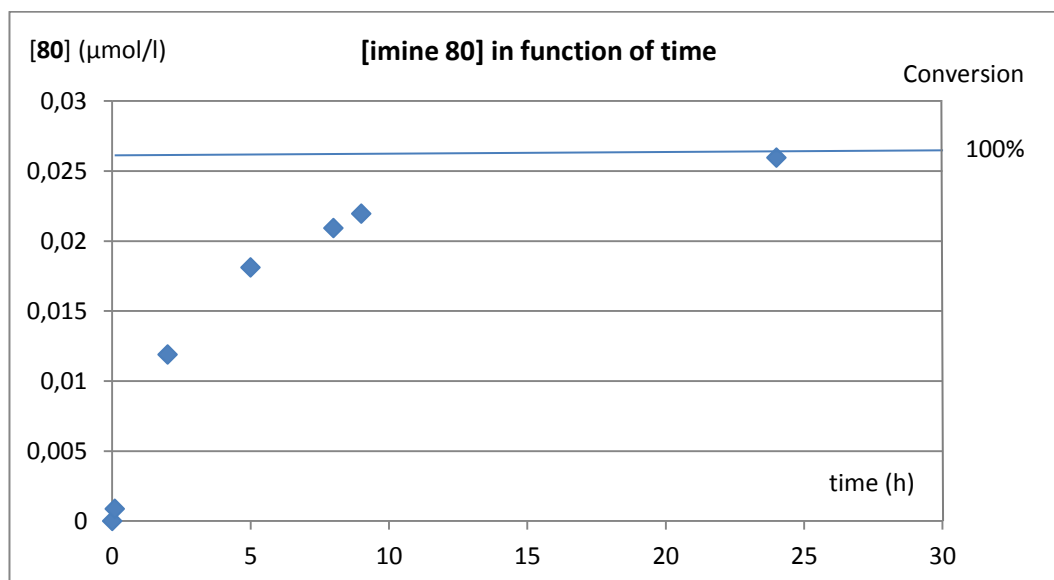


Figure 159: Imine 80 concentration (μM) as function of time (h) (conditions: initial [81] = [cyclohexylamine] = 26.8 μM, Solvent CD_2Cl_2 (0.5 mL), molecular sieve, 25 °C)

⁴⁹⁸ Chemical shifts of CH=N group of our imine complex **80** in ^1H and ^{13}C -NMR (8.28 ppm respectively 157.9 ppm) both correspond to values found in literature for similar (*E*)-imine molecules (8.34 ppm respectively 159.2 ppm). See e.g.: Pelletier, G.; Bechara, W. S.; Charette, A. B. *J. Am. Chem. Soc.* **2010**, 132, 12817. This also correlates with the greater stability of the *E* configuration: Bjørge, J.; Boyd, D. R.; Watson, C. G.; Jennings, W. B.; Jerina, D. M. *J. Chem. Soc., Perkin Trans. 2* **1974**, 1081.

After one day, imine / aldehyde ratio reached 34/1. After 3 days, a final equilibrium was obtained with imine / aldehyde ratio = 266/1 ($^1\text{H-NMR}$) showing that imine formation is favoured under water-free conditions. **Figure 160** displays the inverse of the concentration of imine as a function of time, demonstrating that the overall order of the reaction is 2.

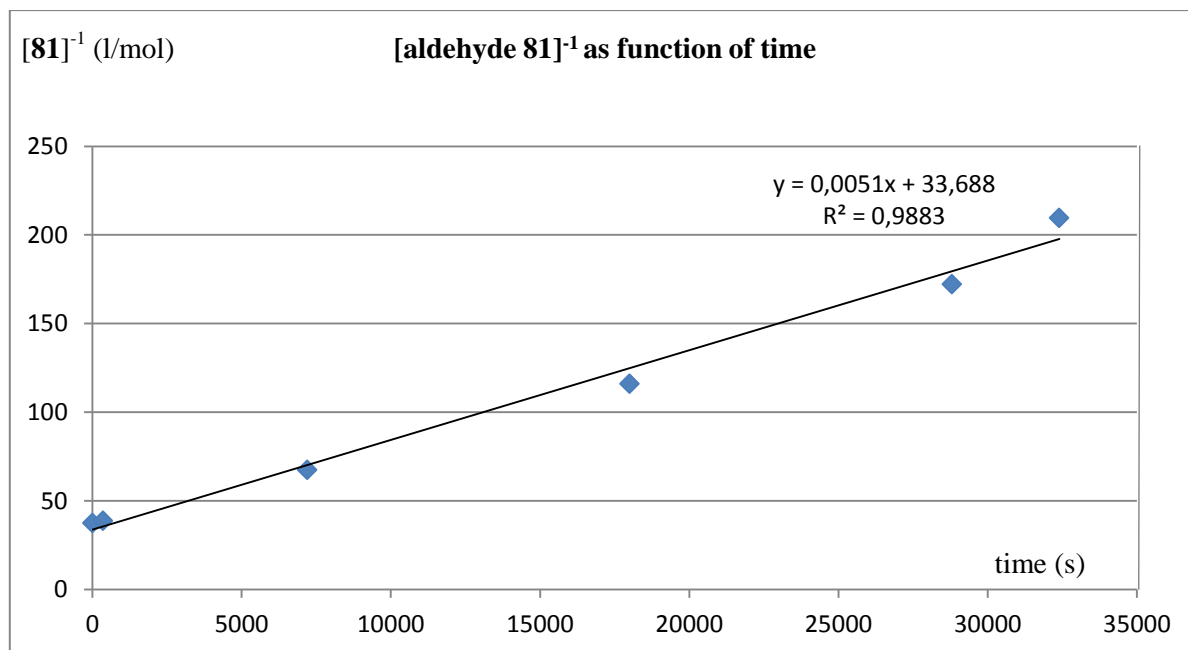


Figure 160: $[\text{81}]^{-1}$ (l/mol) as function of time (s) (conditions: initial $[\text{81}] = [\text{cyclohexylamine}] = 26.8 \mu\text{M}$, Solvent CD_2Cl_2 (0.5 mL), molecular sieve, 25°C)

Following the same procedure, cyclohexylamine condensation with the O-benzaldehyde complex **89** is yielding quantitatively the imine complex **194** (**Figure 161**).

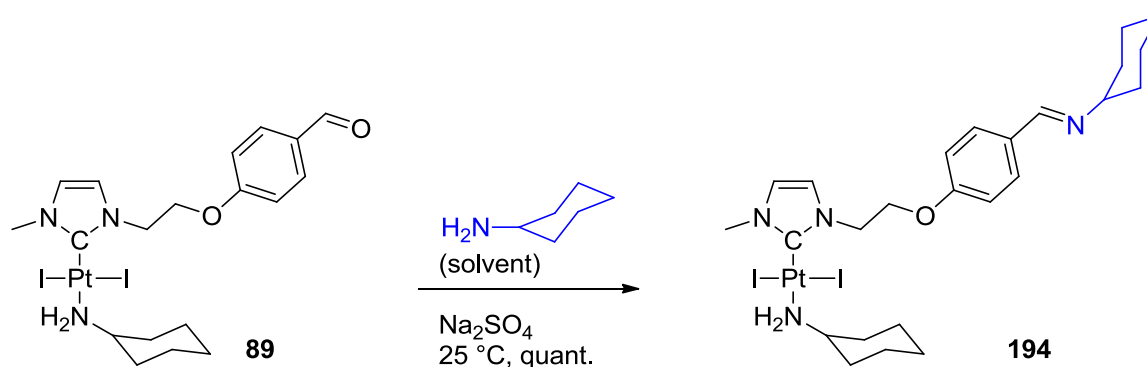


Figure 161: Condensation reaction with an O-benzaldehyde complex and cyclohexylamine.

Pyridine NHC complexes are prompted to exchange reactions with amines. Thus, in the presence of Pt complex **79**, the cyclohexylamine (solvent) react both on Pt centre and with the aldehyde moiety. The corresponding complex **80** was obtained in quantitative yield (**Figure 162**).

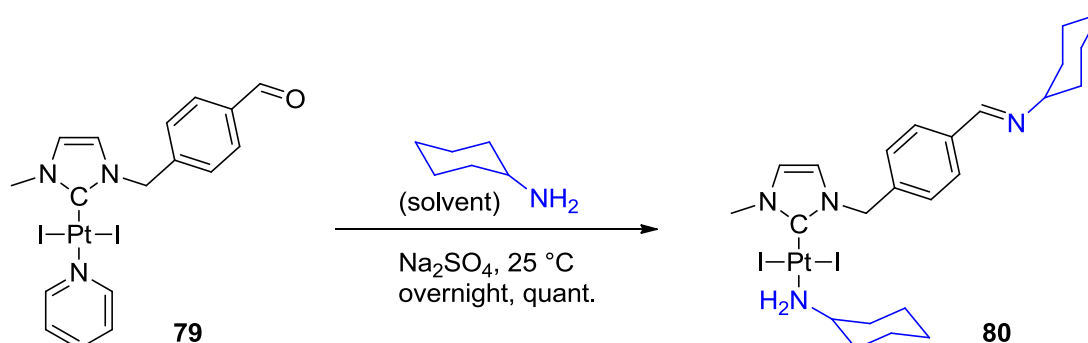


Figure 162: Bis-functionalization of [(pyridine)PtI₂(NHC-benzaldehyde)] **79 by *in situ* ligand exchange and condensation**

The cyclohexylamine complexes allow further derivatization by addition of a different amine to form the corresponding imine. Indeed, with an excess of aniline the corresponding imines **195** and **196** were formed (CH₂Cl₂, Na₂SO₄) (**Figure 163**). Anthracen-2-imine derivative **196** was obtained in only 25% yield due to its moderate on silica.

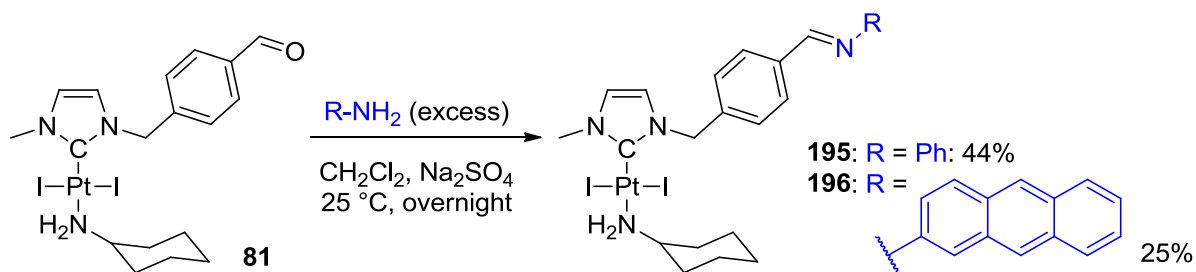


Figure 163: Functionalization of Pt complexes

To obtain potentially water-soluble compounds, ligation with glucosamine, glucamine or ethanolamine (**Figure 164**) was tried resulting in imine/aldehyde mixture or decomposition. Presumed, neighbouring hydroxyl group was catalysing hydrolysis of the compound. 2-(aminooxy)acetic acid was reacting with benzaldehyde complex **81** yielding only small amount of this highly polar compound, demonstrating the need to protect polar functions (carboxylic acids, alcohols, ...).

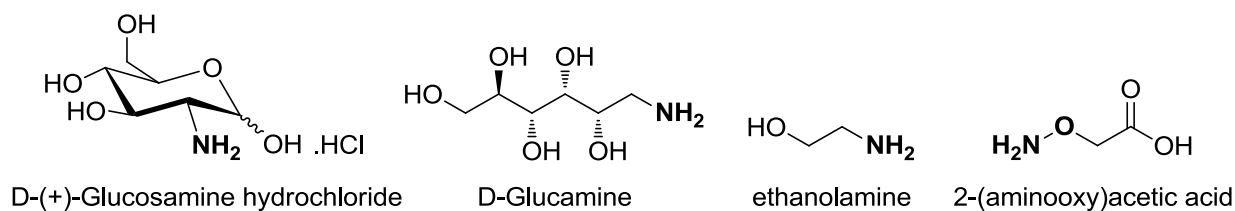


Figure 164: Water-soluble (hydroxyl)amines unsuccessfully tested for imine condensation

O-protected **amino acids** were also introduced as ammonium salts deprotonated *in situ* by triethylamine (**Figure 165**). The corresponding complex **197** could be isolated in 70%.

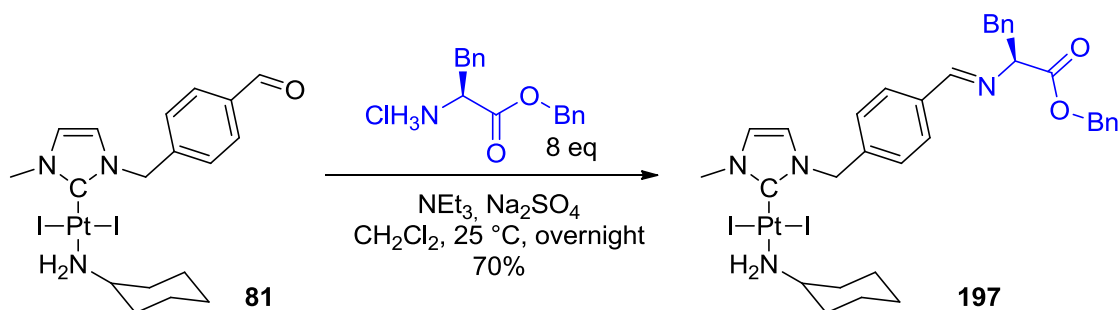


Figure 165: Amino acid conjugation to platinum complexes

Starting from [(morpholine)PtI₂(NHC-benzaldehyde)] complex **82**, one equivalent of amino ester was added giving imine complex **198**. Noteworthy, the amino must be *O*-protected. In excess, an amino ester (a less steric hindered primary amine) displaced the morpholine ligand (a secondary amine), yielding a homo-bis-functionalized complex **199** (**Figure 166**).

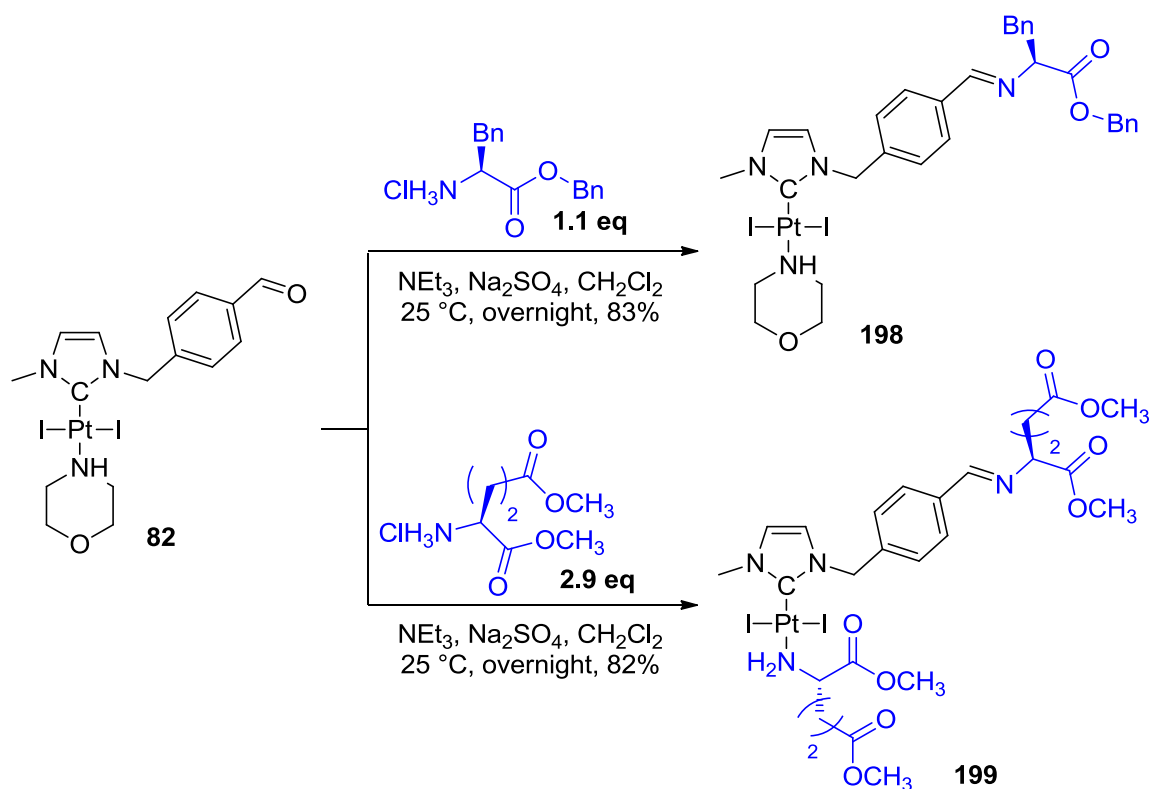


Figure 166: Functionalization of $[(\text{morpholine})\text{PtI}_2(\text{NHC-benzaldehyde})]$ complex with amino esters

In the presence of a larger excess of non *N*-protected lysine, four different inseparable products **200** were obtained: the lysine reacted with amine N^2 or N^6 to form the imine and coordinate to the Pt. On the other hand, half equivalent of lysine gave a di-metallic⁴⁹⁹ species **201** (Figure 167).

⁴⁹⁹ For polynuclear species, see also section 2.2.5. *Polynuclear platinum NHC complexes*.

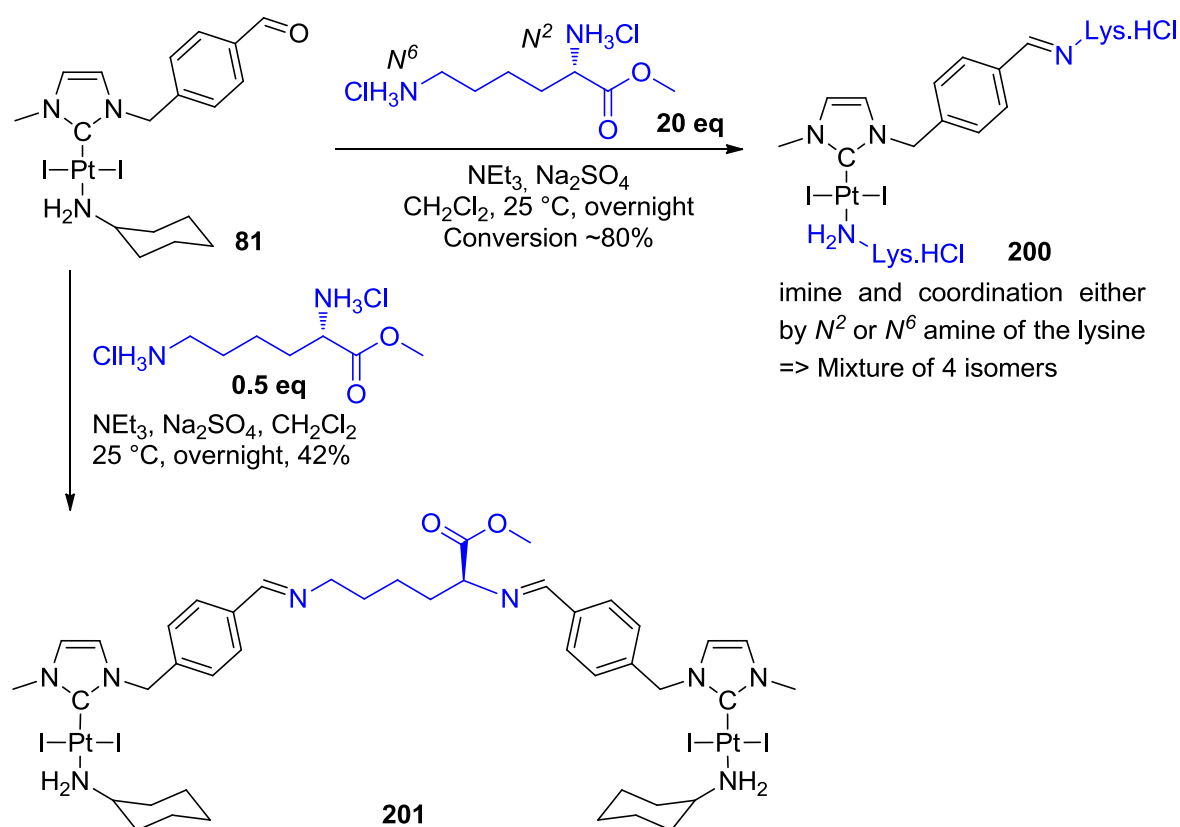


Figure 167: Reactivity of lysine with platinum complexes

By our methodology, we successfully introduced *O*-protected amino acids to the platinum benzaldehyde complex. This proof of concept allows envisaging introduction of biological moieties that are of interest for applications. Hydrazones and oximes, which are known to be more stable than imines, have also been investigated.

4.2.3 Post-synthetic modification of NHC complexes by hydrazone and oxime formation

In previous section, we successfully reacted various amines to NHC complexes featuring benzaldehyde. The poor water stability of these compounds let us to investigate hydrazone and oxime formation. These functions are less sensible to water. Only under strong acidic conditions, e.g. in lysosomes, these functions are prompt to hydrolyse. These would guaranty a higher stability of the Pt hydrazone conjugates as well as possible more efficient release of the active Pt core in the cell.

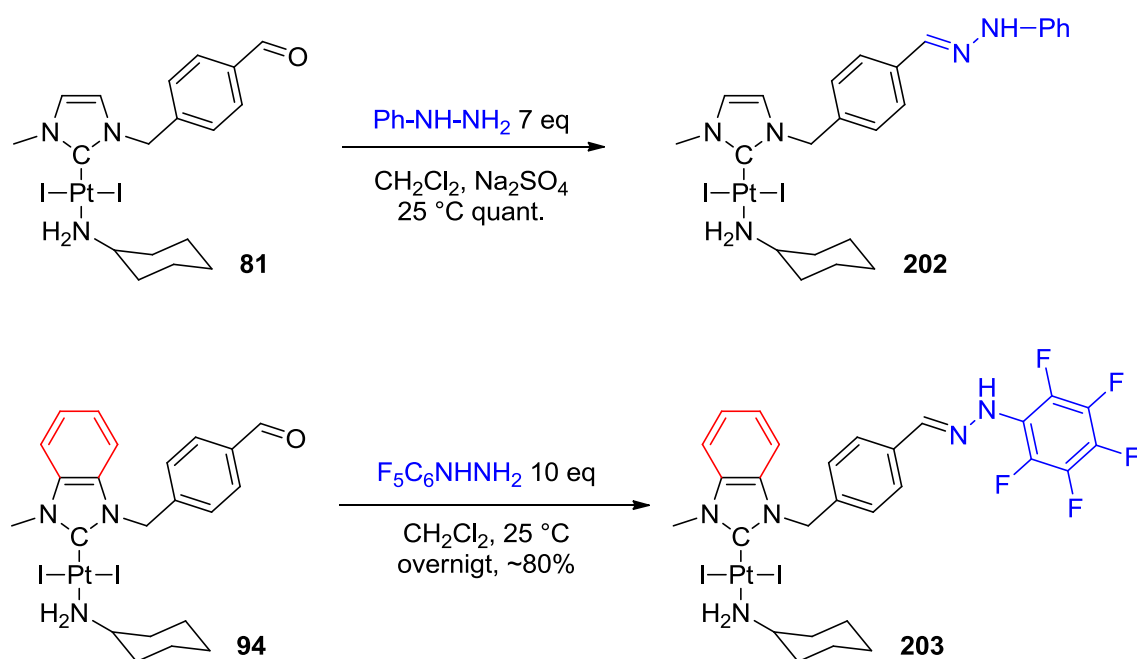


Figure 168: Hydrazone formation with benzaldehyde complexes

Phenylhydrazone complex **202** was obtained quantitatively after reaction in CH_2Cl_2 overnight (Figure 168). The reaction was found to be reversible: after one night in wet CDCl_3 , a mixture ($\mathbf{81}/\mathbf{202} = 1/3$) is observed. Variation of nature of the NHC (benzimidazolylidene) and hydrazine (perfluorophenylhydrazine) did not change the reactivity (complex **203**).

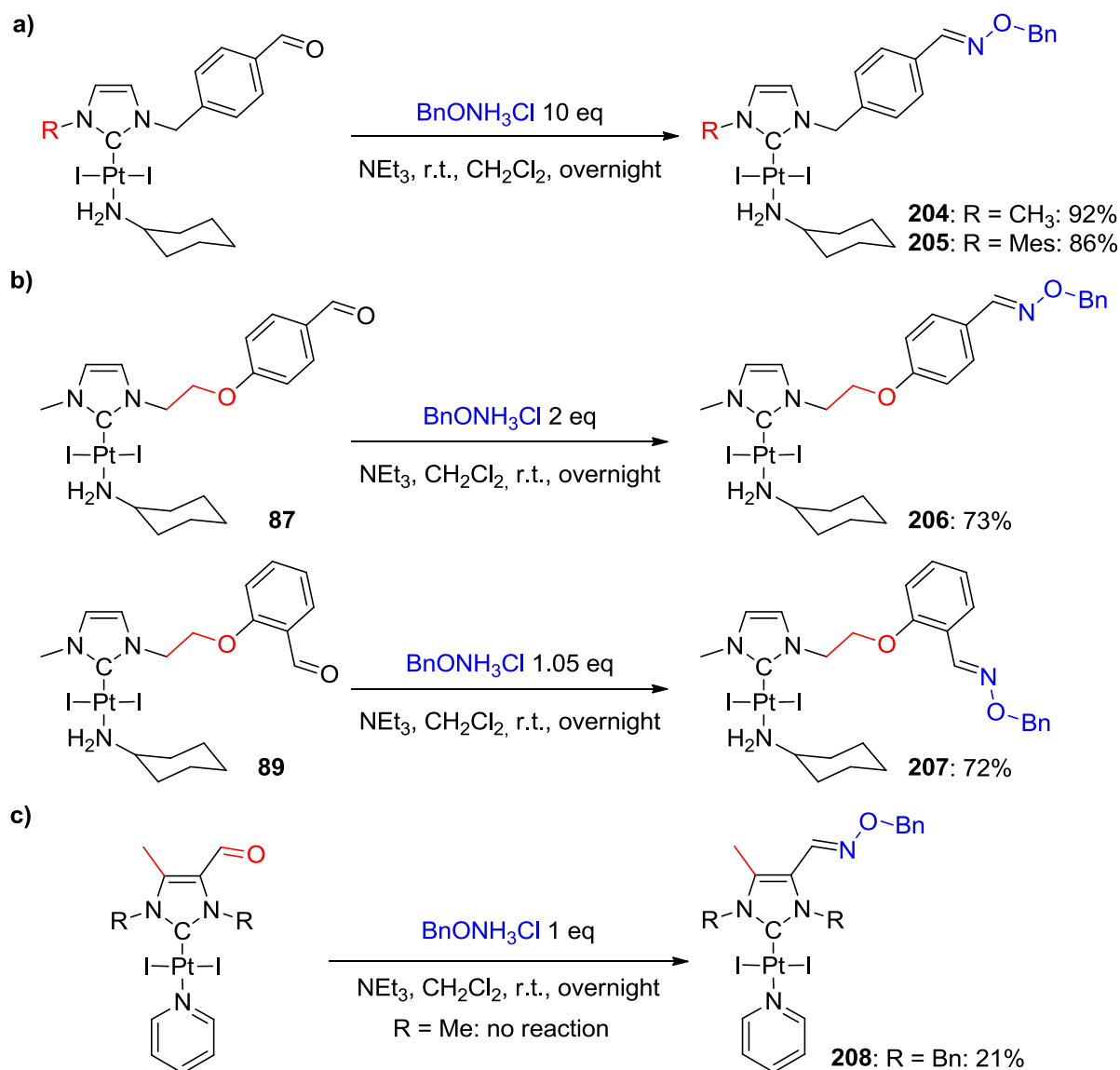


Figure 169: NHC-Pt complexes post-synthetic functionalization: oxime formation with benzylhydroxylamine (%: yield of condensation step)

As expected, *E*-oxime⁵⁰⁰ complexes **204** and **205** were formed from [(cyclohexylamine)PtI₂(NHC-benzaldehyde)] complexes **81** and **86** (**Figure 169 a**). They were found to be stable on silica gel or in wet solvents (no hydrolysis after one night in wet CD₃COCD₃). These compounds were easier to purify than their imine analogues and so were generally obtained in better yield. Even in a *water*/dimethylformamide mixture, the reaction gave the oxime **204** in 71% yields. Changing the aldehyde did not change the reactivity (complexes **206** and **207**) (**Figure 169 b**). Moreover, when the aldehyde is present on the NHC backbone (c), the condensation was found to be less efficient (21% yield for

⁵⁰⁰ In ¹H and ¹³C-NMR, only one signal for CH=NO was observed at 8.0 and 148 ppm respectively, respectively, indicating the presence of only one diastereomer. *E*-oxime protons are deshielded relative to *Z*-oxime analogues, for comparison see: Ewan, H. S.; Muli, C. S.; Touba, S.; Bellinghiere, A. T.; Veitschegger, A. M.; Smith, T. B.; Pistel II, W. L.; Jewell, W. T.; Rowe, R. K.; Hagen, J. P.; Palandoken, H. *Tetrahedron Lett.* **2014**, 55, 4962 and herein cited references.

208) (**Figure 169 c**). O-(anthracen-9-ylmethyl)hydroxylamine reacted nearly quantitatively with aldehyde complex **81** giving a fluorescent complex **209** suitable for luminescent studies (**Figure 170**).

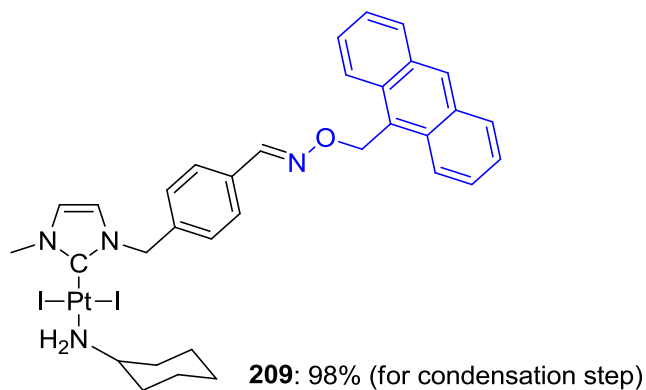


Figure 170: Anthracene functionalized platinum complex 209

Monocrystals suitable for X-ray diffraction were obtained for oxime-functionalized complexes **204** and **209** by slow vapour diffusion of pentane into a dichloromethane solution. X-ray diffraction structure of both oxime complexes confirmed the *E* configuration of the oxime double bond (**Figure 171** and **Figure 172**).

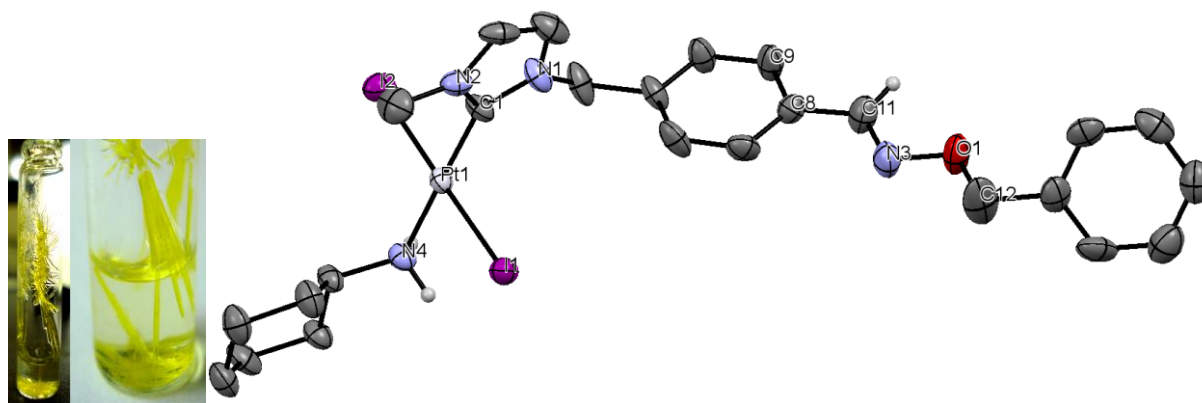
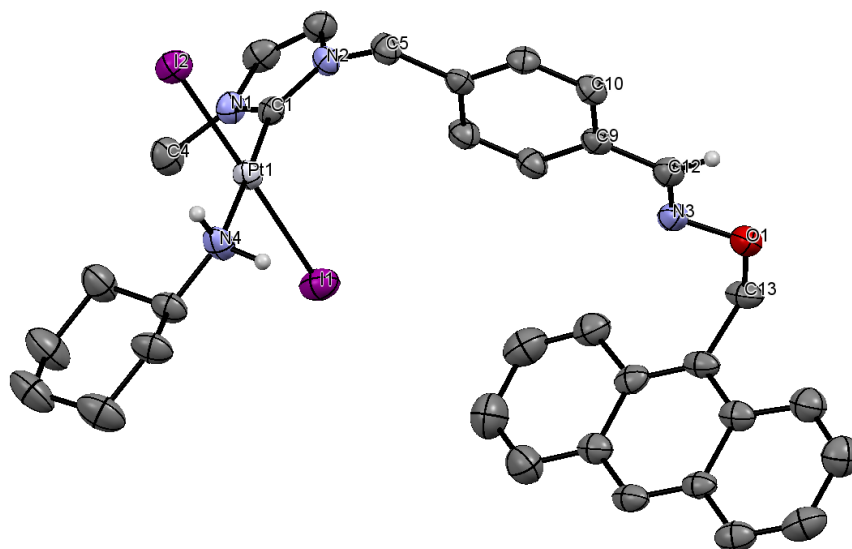


Figure 171: X-ray structure of benzyloxime complex 204

Figure 172: X-ray structure of anthracene-oxime complex **209**

The 3-D packing of benzyloxime complex **204** displays a hydrogen bond between O_{oxime} and NH_2 groups of two complexes ($O-N$: 3.230 Å). In contrast, neither hydrogen bonds nor π - π interactions between anthracene-moieties are visible for anthracene-oxime compound **209**.

Bond lengths and angles of these two oxime NHC complexes have been collected in **Table 19** together with a cyclohexylamine- PtI_2 -NHC complex and a pyridine-aldehyde (**15** and **79**). Platinum-carbene bonds are identical for both oxime complexes (*column 1*). Iodine-platinum bonds are similar for all complexes except benzyloxime complex **204** (*column 3*). $C_{\text{carbene}}\text{-Pt-I}$ angles are comparable for anthracene derivative and cyclohexylamine- PtI_2 -NHC complex (*column 4*).

Bond lengths, angles	Pt-C	Pt-N	Pt-I	C-Pt-I	N-O	C=N	C=N-O
Complex	1	2	3	4	5	6	7
204	1.971	2.111	2.801; 2.590	87.45; 90.43	1.385	1.283	110.37
209	1.970	2.127	2.608; 2.602	90.24; 90.51	1.398	1.289	110.70
15	1.964	2.121	2.601; 2.589	89.94; 90.86	/	/	/
79	1.981	2.091	2.603; 2.592	88.57; 88.99	/	/	/

Table 19: Selected bond lengths (Å) and angles (°) of oxime complexes **204** and **209**, and non-functionalized complexes **15** and **79**

By using hydroxylamine in large excess, also the amine ligand of **81** could be exchanged affording complex **210** in moderate yields (**Figure 173**).

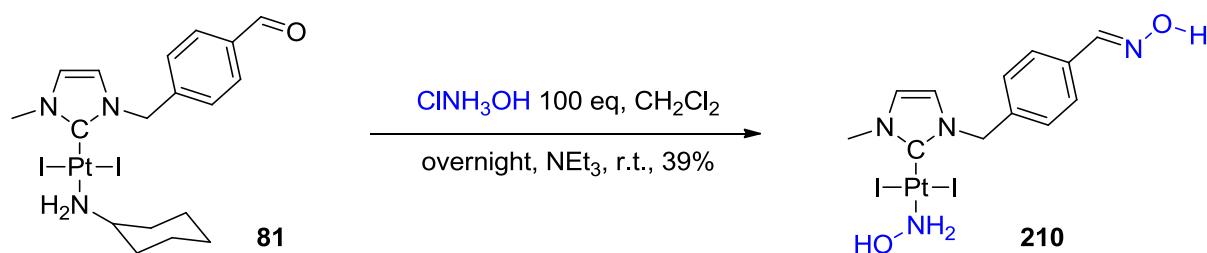


Figure 173: Bis-functionalization of 81 using an excess of hydroxylamine

These examples show the versatility and relatively ease of derivatization of NHC complexes by oxime formation. Bis-functionalization could be achieved by introduction of various moieties (used generally in large excess) by both condensation and ligand exchange. Bis-functionalization with two different groups remains of interest to increase the diversity of compounds for further cytotoxic studies. Therefore, we combined ligand exchange reaction with oxime condensation. Two strategies were investigated: condensation reaction followed by ligand exchange or the inverse process (**Figure 174**).

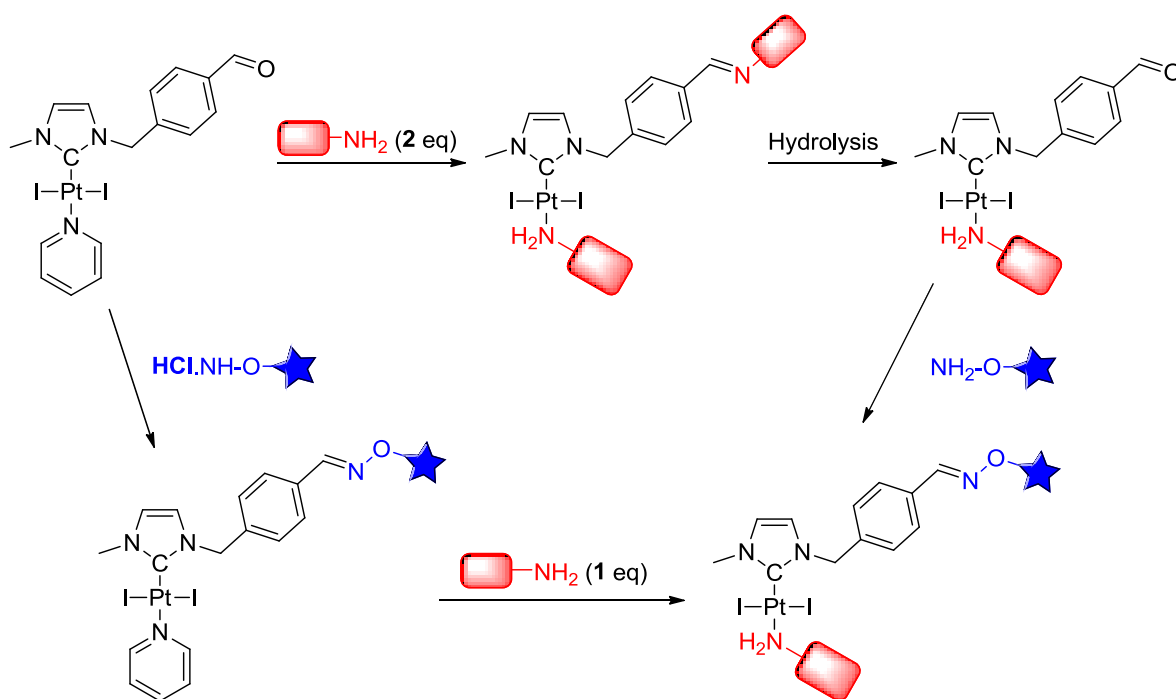


Figure 174: Strategies of bis-heterofunctionalization of NHC-Pt complexes studied in this work

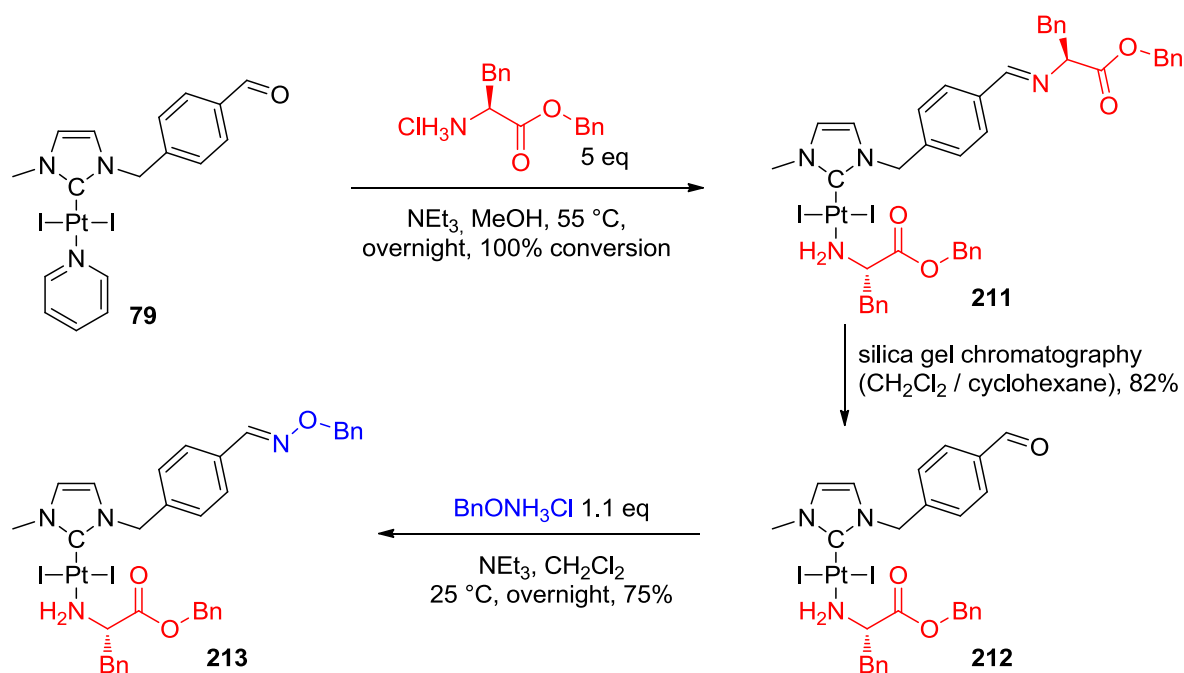


Figure 175: Bis-functionalization of a pyridine benzaldehyde complex with two different groups

Reaction of complex **79** with 5 equivalents of phenylalanine ester gave the functionalized complex **211** in 100% conversion. The reversibility of imine formation allowed the hydrolysis of the imine on silica gel to obtain a mono-functionalized complex **212** in 82% yields. Then, this compound could be selectively modified by condensation with one equivalent of benzylhydroxylamine to afford the hetero-bis-functionalized complex **213** (**Figure 175**). The drawback of the strategy remains the need of two equivalents of amine (one equivalent sacrificed) in the first step to avoid mixtures.

We tried to invert the reaction steps by starting with oxime condensation. Pyridine exchange was not occurring under acidic conditions (**Figure 176 a**). On a $[(\text{pyridine})\text{PtI}_2(\text{NHC-benzaldehyde})]$ complex **81**, hydroxylammonium chloride reacted with the benzaldehyde, the pyridine ligand remained untouched through this pathway (complexes **214** and **215**). Then, in a second step, the pyridine could be selectively exchanged by an amino acid (complex **216**) (**Figure 176 b**). Compared to the first strategy (62%), the overall yield was lower (22%).

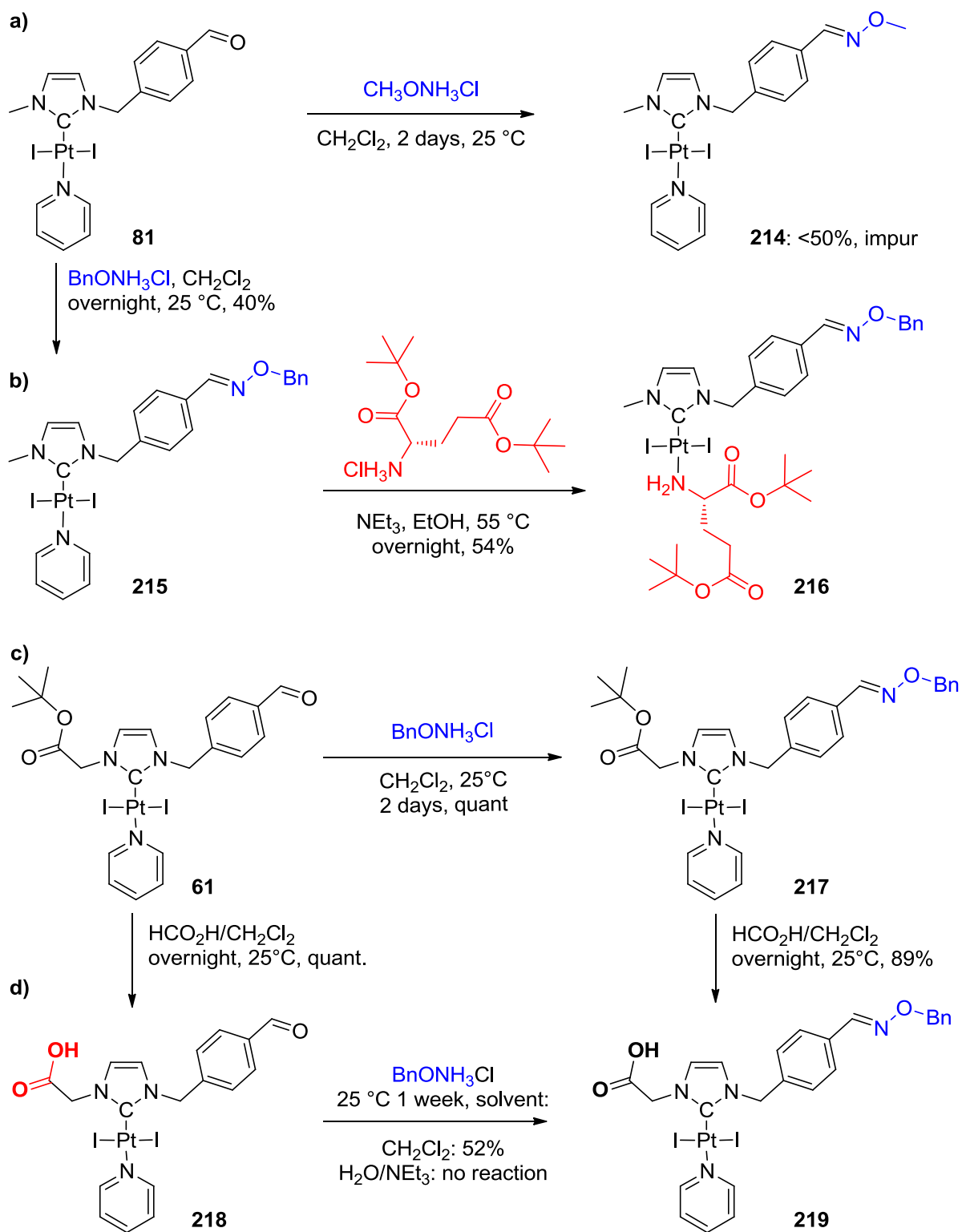


Figure 176: Selectively oxime formation on a pyridine complex followed by post-synthetic modification

Interestingly, *tert*-butylester group of an oxime containing complex **217** could be selectively deprotected⁵⁰¹ giving water-soluble carboxylic acid complex **219** (Figure 176 c). Alternatively, this carboxylic acid-oxime complex **219** could also be obtained from the carboxylic acid-aldehyde complex **218** through oxime formation in dichloromethane (d).

We explored a simplified procedure and investigated ligand exchange as well as oxime condensation in one single step. As observed in chapter 4.1.1.4. *Introduction of hydroxylamines*, ligand exchange reaction occurred preferentially with amines. Competition experiment between benzylamine (ligand exchange) and hydroxylamine (condensation) resulted in the formation of a major product in 50% yield (Figure 177).

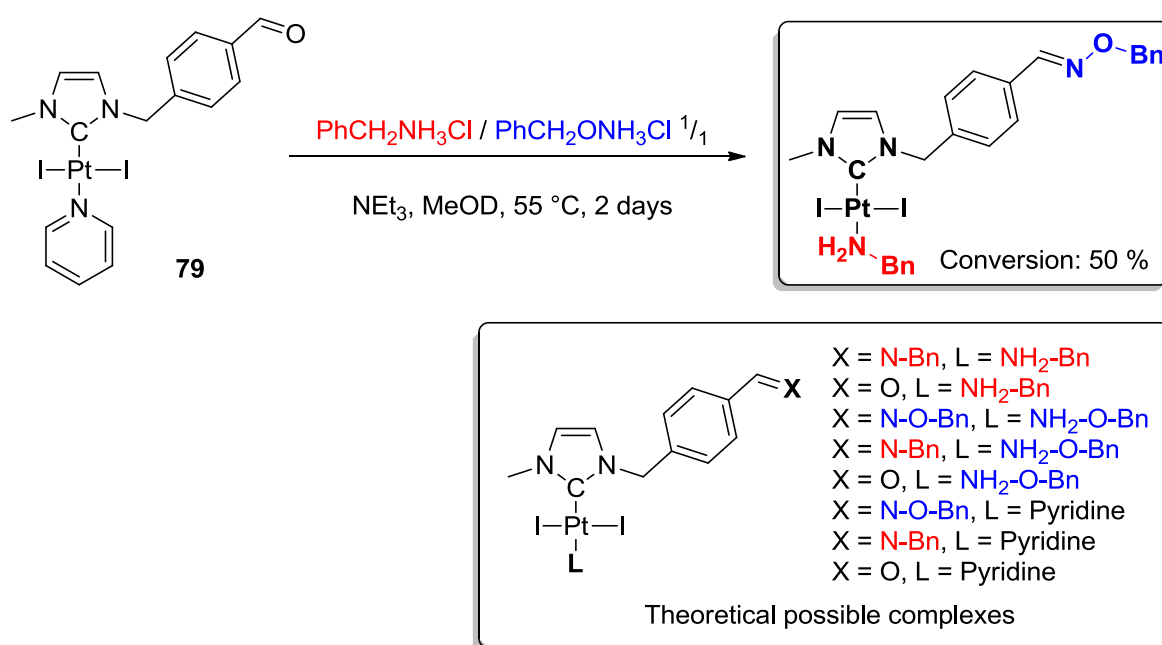


Figure 177: Competition experiment between amine and oxime on a [(pyridine)PtI₂(NHC-benzaldehyde)] complex: relative selectivity of oxime formation and ligand exchange

Post-synthetic modification of benzaldehyde complexes is not limited to platinum complexes. We also successfully functionalized two palladium complexes with benzylhydroxylamine (Figure 178). Surprisingly, complexes **220** and **223** were stable in solution, whereas the quite similar complexes **221** and **224** presented only limited stability in solution.

⁵⁰¹ For deprotection of *tert*-butyl esters into carboxylic acids, see section 2.2.3. *Pt-NHC complexes N-functionalized by nitriles, carboxylic acids and their derivatives.*

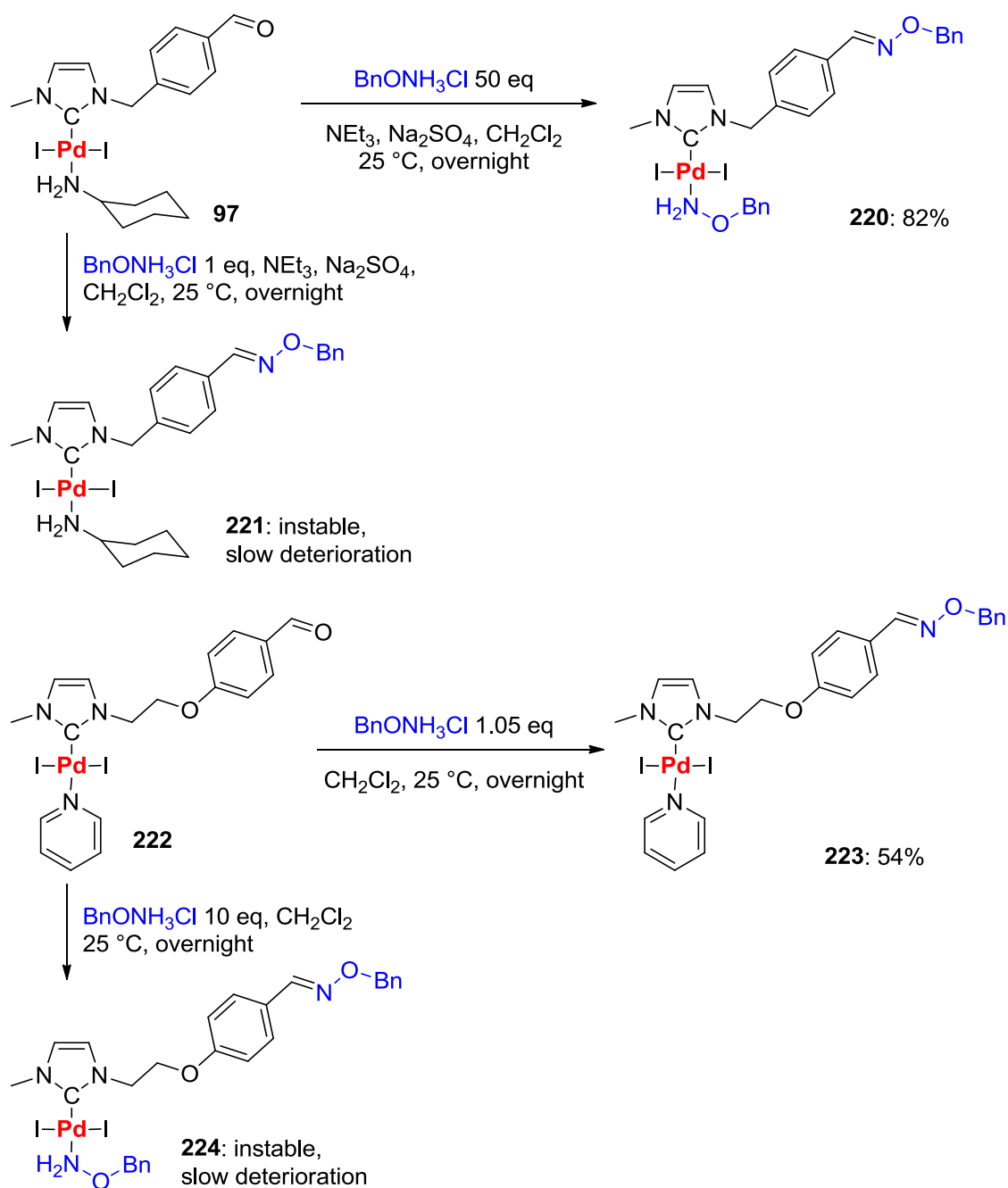


Figure 178: Functionalization of benzaldehyde palladium complexes (%: yield of condensation step)

The solid-state structure of bis-functionalized palladium complex **220** displays the expected *E* configuration for the oxime (**Figure 179, a**) and the presence of intermolecular hydrogen bonds between the NH₂ of coordinated hydroxylamine and O and I respectively (b).

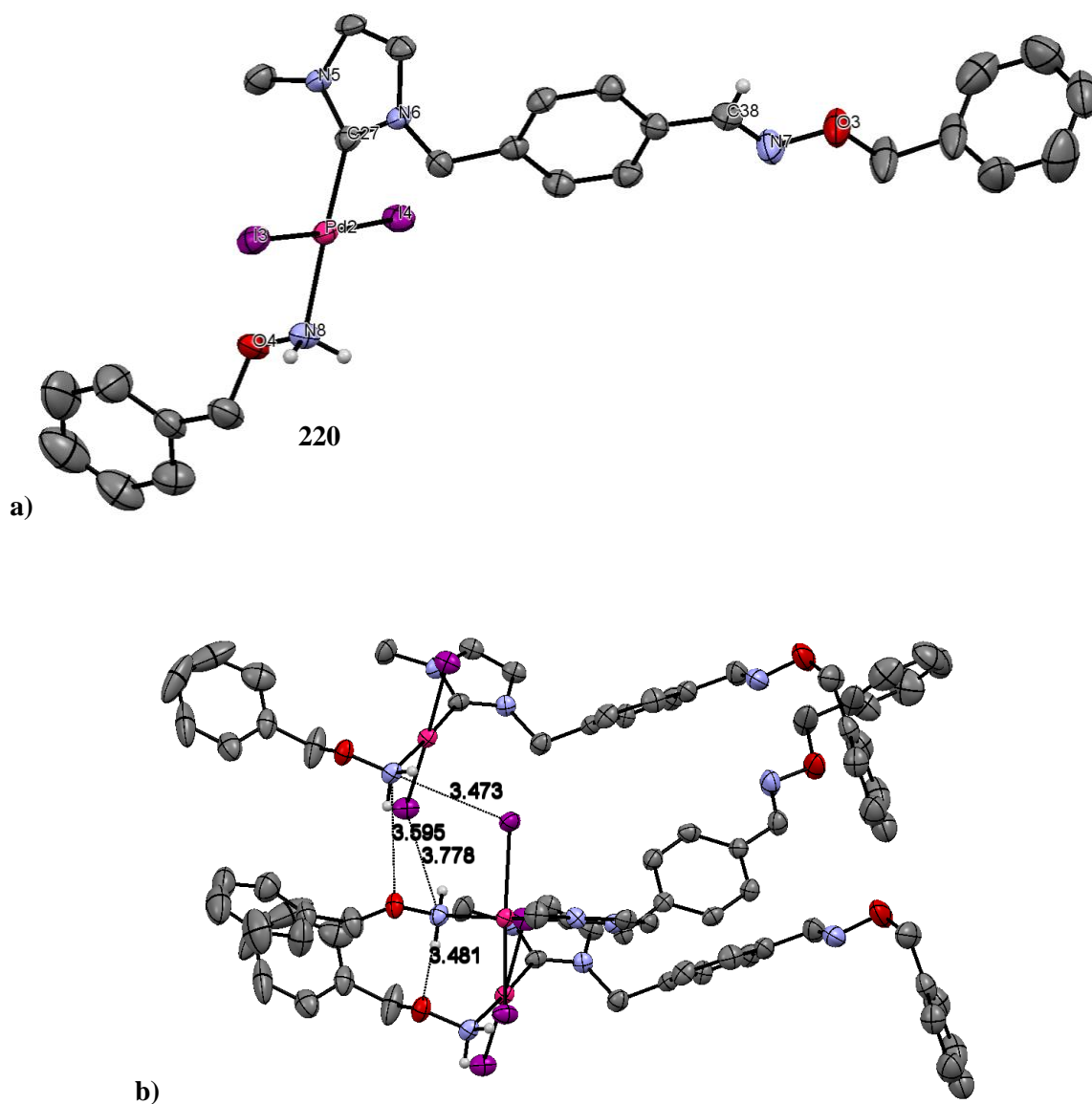


Figure 179: a) X-ray structure of palladium oxime complex 220 and b) intermolecular H-bonds

As a conclusion, diversity introduction by oxime formation was successfully established with various platinum benzaldehyde complexes. Extension to palladium analogues remains a challenge due to limited stability of these complexes.

4.2.4 Post-synthetic modification of NHC complexes by imine reduction

Imines derivatives, in contrast to oximes, are highly sensible to hydrolysis. To gain more stability after post-synthetic modification by imine formation, we tried to reduce the imine bond to a stable amine bond.⁵⁰² Among various reduction agents ($\text{H}_2/\text{C}/\text{Pd}$, NH_4CHO_2 ,⁵⁰³ LiAlH_4 , NaBH_4 , NaBH_3CN) tested on cyclohexylimine complex **80**, only sodium triacetoxyborohydride ($\text{NaBH}(\text{CH}_3\text{CO}_2)_3$)⁵⁰⁴ in CH_2Cl_2 gave the desired amine **225** with moderate yield (**Figure 180**).

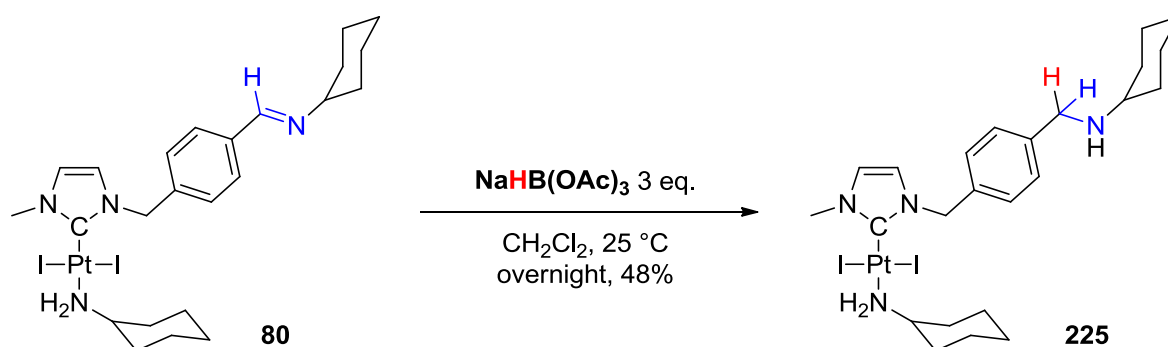


Figure 180: Imine reduction with sodium triacetoxyborohydride

The reaction was also suitable with polyethylene glycol-imine and with amino acids affording the corresponding amines **226**, **229** and **230** (**Figure 181**). In addition, $[(\text{cyclohexylamine})\text{PtI}_2(\text{NHC-benzaldehyde})]$ could be reduced to the corresponding alcohol **227**. We noticed two limitations for this reaction: direct amination of the carbonyl ($\text{R-CH=O} + \text{amine} + \text{hydride} \rightarrow \text{amine}$) resulted in decomposition, thus the imine complex needed to be isolated prior to reduction. Secondly, in contrast to imines, oximes could not be reduced by this reducing agent.

⁵⁰² Lo and co-workers conjugate aldehyde groups of $[\text{Ir}(\text{pba})_2(\text{N}^{\wedge}\text{N})](\text{PF}_6)$ ($\text{pba} = 4\text{-(2-pyridyl)benzaldehyde}$) with 2 molecules of *N*-biotinyl-1,6-diaminohexane. In pot, these imines are reduced by NaBH_4 ; Zhang, K. Y.; Lo, K. K.-W. *Inorg. Chem.* **2009**, 48, 6011.

⁵⁰³ O'Connor, D.; Lauria, A.; Bondi, S. P.; Saba, S. *Tetrahedron Lett.* **2011**, 52, 129.

⁵⁰⁴ Abdel-Magid, A. F.; Carson, K. G.; Harris, B. D.; Maryanoff, C. A.; Shah, R. D. *J. Org. Chem.* **1996**, 61, 3849.

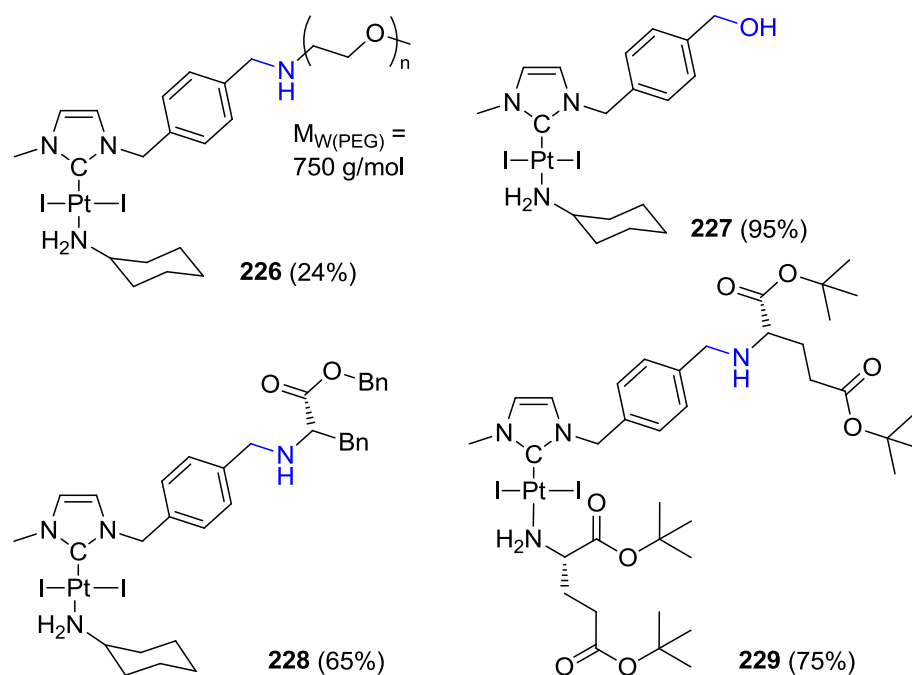


Figure 181: Post-synthetic modified Pt complexes obtained by imine reduction (%: yield of reduction step)

4.2.5 Conjugation of Pt-NHC complexes with a PSMA targeting urea

In developed countries, prostate cancer is the most detected and third fatal cancer for males.⁵⁰⁵ Survival rate is nearly quantitatively when detected early, but decreases dramatically after starting of metastasis. Prostate-specific membrane antigen (PSMA), a transmembrane glycoprotein, has two unique enzymatic functions, folate hydrolase and NAALADase. PSMA is highly and specific expressed by prostate cancer and by neovasculature of most of the solid tumours making it a target for imaging⁵⁰⁶ and therapy.⁵⁰⁷ Beside antibodies,⁵⁰⁸ simpler urea derivatives⁵⁰⁹ proved to be excellent targeting agents for PSMA suitable to radiolabeling.⁵¹⁰ Combined iodine ^{123}I urea derivatives reached clinical phase I (**Figure 182**).⁵¹¹

⁵⁰⁵ Jemal, A.; Bray, F.; Center, M. M.; Ferlay, J.; Ward, E.; Forman, D. *CA-Cancer J. Clin.* **2011**, *61*, 69.

⁵⁰⁶ Chen, Y.; Pullambhatla, M.; Banerjee, S.; Byun, Y.; Stathis, M.; Rojas, C.; Slusher, B. S.; Mease, R. C.; Pomper, M. G. *Bioconjugate Chem.* **2012**, *23*, 2377.

Chen, Y.; Dhara, S.; Banerjee, S. R.; Byun, Y.; Pullambhatla, M.; Mease, R. C.; Pomper, M. G. *Biochem. Biophys. Res. Commun.* **2009**, *390*, 624.

⁵⁰⁷ Schülke, N.; Varlamova, O. A.; Donovan, G. P.; Ma, D.; Gardner, J. P.; Morrissey, D. M.; Arrigale, R. R.; Zhan, C.; Chodera, A. J.; Surowitz, K. G.; Maddon, P. J.; Heston, W. D.; Olson, W. C. *PNAS* **2003**, *100*, 12590; Nakajima, T.; Mitsunaga, M.; Bander, N. H.; Heston, W. D.; Choyke, P. L.; Kobayashi, H. *Bioconjugate Chem.* **2011**, *22*, 1700.

⁵⁰⁸ Kinoshita, Y.; Kuratsukuri, K.; Newman, N.; Rovito, P. M.; Kaumaya, P. T. P.; Wang, C. Y.; Haas, G. P. *Prostate Cancer Prostatic Dis.* **2005**, *8*, 359; Bühler, P.; Wolf, P.; Elsässer-Beile, U. *Immunotherapy* **2009**, *1*, 471.

⁵⁰⁹ Kozikowski, A. P.; Nan, F.; Conti, P.; Zhang, J.; Ramadan, E.; Bzdega, T.; Wroblewska, B.; Neale, J. H.; Pshenichkin, S.; Wroblewski, J. T. *J. Med. Chem.* **2001**, *44*, 298.

⁵¹⁰ Pomper, M. G.; Musachio, J. L.; Zhang, J.; Scheffel, U.; Zhou, Y.; Hilton, J.; Maini, A.; Dannals, R. F.; Wong, D. F.; Kozikowski, A. P. *Mol. Imaging* **2002**, *1*, 96; Chen, Y.; Foss, C. A.; Byun, Y.; Nimmagadda, S.; Pullambhatla, M.; Fox, J. J.; Castanares, M.; Lupold, S. E.; Babich, J. W.; Mease, R. C.; Pomper, M. G. *J. Med. Chem.* **2008**, *51*, 7933; Hillier, S. M.;

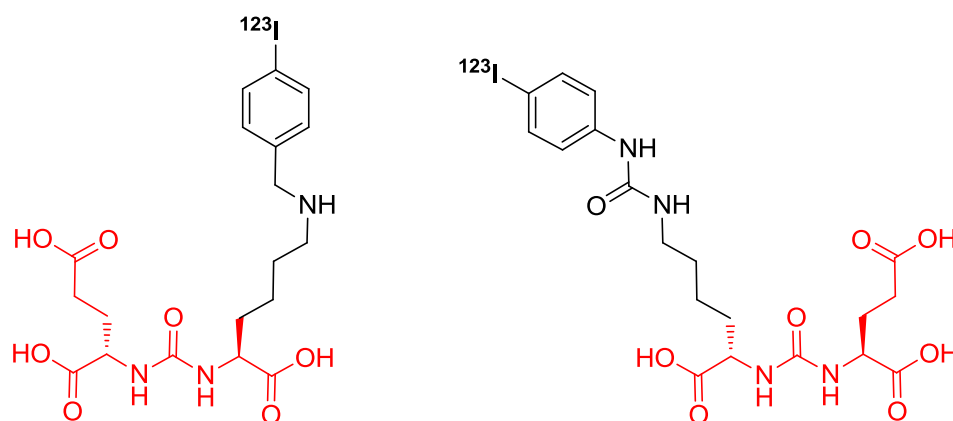


Figure 182: PSMA targeting radio-iodated urea derivatives tested in phase I

We thus decided to combine the urea ligand with a Pt NHC complex through oxime formation. A hydroxylamine derivative of this small molecule was synthesized and conjugated to benzaldehyde-platinum complex (**Figure 183**).⁵¹² The desired complex **230** was obtained (¹H NMR, mass spectrometry) together with unreacted aldehyde complex and urea starting material. The mixture could not be completely purified by silica gel chromatography caused by the high polarity of the compound (90% of purity of best). To remove unreacted products and obtain the necessary purity for medical applications, HPLC purification should be a solution (currently underway).

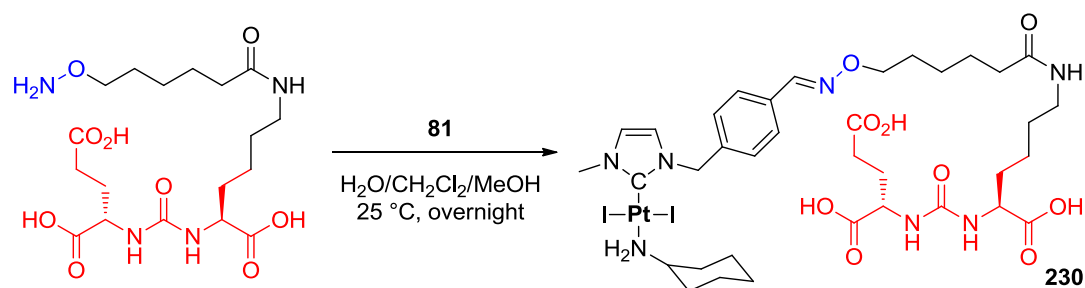


Figure 183: Conjugation of a platinum complex with a PSMA targeting urea

Maresca, K.P.; Lu, G.; Merkin, R. D.; Marquis, J. C.; Zimmerman, C. N.; Eckelman, W. C.; Joyal, J. L.; Babich, J. W. *J. Nucl. Med.* **2013**, *54*, 1369.

⁵¹¹ Barrett, J. A.; Coleman, R. E.; Goldsmith, S. J.; Vallabhajosula, S.; Petry, N. A.; Cho, S.; Armor, T.; Stubbs, J. B.; Maresca, K. P.; Stabin, M. G.; Joyal, J. L.; Eckelman, W. C.; Babich, J. W. *J. Nucl. Med.* **2013**, *54*, 380.

⁵¹² Synthesis by Dr Etienne Borré.

4.2.6 Introduction of fullerenes (C₆₀) to NHC-Pt complexes

Fullerenes are a class of spherical molecules entirely composed of sp²-hybridized carbon. This carbon allotrope was discovered in 1985 by Smalley and co-workers during investigations of the mechanisms by which long-chain carbon molecules are formed in interstellar space.⁵¹³ The structure of fullerene, composed by 2(10+M) carbon atoms, is a trivalent convex polyhedron with 12 pentagonal and M hexagonal faces (Euler-Poincaré characteristic). First discovered and most studied fullerene is icosahedral C₆₀, also called Buckminsterfullerene.⁵¹⁴ The *I_h* symmetry implies equivalence of all 60 atoms.⁵¹⁵ Fullerenes and its derivatives exhibit great potentialities in medicinal field.⁵¹⁶ Beside more curious studies,⁵¹⁷ radioprotective,⁵¹⁸ antibacterial,⁵¹⁹ antiviral,⁵²⁰ and antitumor⁵²¹ properties and photodynamic therapy (PDT)⁵²² applications are reported. Several reactions are known to functionalize fullerenes: cycloadditions,⁵²³ hydroxylation,⁵²⁴ metal complexation,⁵²⁵ Bingel reaction⁵²⁶ or Prato reaction.⁵²⁷ To combine the effects of C₆₀ and our NHC-platinum complexes, an ethyl malonate substituted NHC-platinum complex **231** was prepared. Unfortunately, harsh Bingel conditions⁵²⁸ resulted in decomposition products. Presumably the enolate group formed *in situ* reacted with a platinum centre, or the presence of iodine led to instable platinum IV species (**Figure 184**).

⁵¹³ Kroto, H.W.; Heath, J.R.; O'Brien, S.C.; Curl, R.F.; Smalley R.E. *Nature* **1985**, *318*, 162.

⁵¹⁴ Billups, W. E.; Ciufolini, M. A. *Buckminsterfullerenes* **1993**, John Wiley & Sons.

⁵¹⁵ Haymet, A. D. J. *J. Am. Chem. Soc.* **1986**, *108*, 319; Johnson, R. D.; Meijer, G.; Bethune, D. S. *J. Am. Chem. Soc.* **1990**, *112*, 8983.

⁵¹⁶ Bosi, S.; Da Ros, T.; Spalluto, G.; Prato, M. *Eur. J. Med. Chem.* **2003**, *38*, 913; Ma, H. L.; Liang, X. *J. Sci. China Chem.* **2010**, *53*, 2233; Xu, Y.; Zhu, J.; Xiang, K.; Li, Y.; Sun, R.; Ma, J.; Sun, H.; Liu, Y. *Biomaterials*. **2011**, *32*, 9940; Baati, T.; Bourasset, F.; Gharbi, N.; Njim, L.; Abderrabba, M.; Kerkeni, A.; Szwarc, H.; Moussa, F. *Biomaterials* **2012**, *33*, 6292.

⁵¹⁷ Zhou, Z.; Lenk, R.; Dellinger, A.; MacFarland, D.; Kumar, K.; Wilson, S. R.; Kepley, C. L. *Nanomed. Nanotechnol. Biol. Med.* **2009**, *5*, 202.

⁵¹⁸ Cai, X.; Hao, J.; Zhang, X.; Yu, B.; Ren, J.; Luo, C.; Li, Q.; Huang, Q.; Shi, X.; Li, W.; Liu, J. *Toxicol. Appl. Pharm.* **2010**, *243*, 27.

⁵¹⁹ Spesia, M. B.; Milanesio, M. E.; Durantini, E. N. *Eur. J. Med. Chem.* **2008**, *43*, 853.

⁵²⁰ Bosi, S.; Da Ros, T.; Spalluto, G.; Balzarini, J.; Prato, M. *Bioorg. Med. Chem. Lett.* **2003**, *13*, 4437.

⁵²¹ Zhu, J.; Ji, Z.; Wang, J.; Sun, R.; Zhang, X.; Gao, Y.; Sun, H.; Liu, Y.; Wang, Z.; Li, A.; Ma, J.; Wang, T.; Jia, G.; Gu, Y. *Small* **2008**, *4*, 1168; Meng, H.; Xing, G.; Sun, B.; Zhao, F.; Lei, H.; Li, W.; Song, Y.; Chen, Z.; Yuan, H.; Wang, X.; Long, J.; Chen, C.; Liang, X.; Zhang, N.; Chai, Z.; Zhao, Y. *ACS Nano*, **2010**, *4*, 2773.

⁵²² Mroz, P.; Pawlak, A.; Satti, M.; Lee, H.; Wharton, T.; Gali, H.; Sarna, T.; Hamblin, M. R. *Free Radic. Biol. Med.* **2007**, *43*, 711; Hu, Z.; Zhang, C.; Huang, Y.; Sun, S.; Guan, W.; Yao, Y. *Chem. Biol. Interact.* **2012**, *195*, 86.

⁵²³ Briggs, J.B.; Miller, G.P. *C. R. Chimie* **2006**, *9*, 916.

⁵²⁴ Li, J.; Takeuchi, A.; Ozawa, M.; Li, X.; Saigo, K.; Kitazawa, K. *J. Chem. Soc., Chem. Commun.* **1993**, 1784.

⁵²⁵ Fagan, P.J.; Calabrese, J.C.; Malone, B. *Science* **1991**, *252*, 1160; Fagan, P. J.; Calabrese, J. C.; Malone, B. *J. Am. Chem. Soc.* **1991**, *113*, 9408; Denisovich, L. I.; Peregodova, S. M.; Novikov, Y. N. *Russ. J. Electrochem.* **2010**, *46*, 1.

⁵²⁶ Bingel, C. *Chem. Ber.* **1993**, *126*, 1957.

⁵²⁷ Maggini, M.; Scorrano, G.; Prato, M. *J. Am. Chem. Soc.* **1993**, *115*, 9798; Piotrowski, P.; Pawłowska, J.; Pawłowski, J.; Więckowska, A.; Bilewicz, R.; Kaim, A. *J. Mater. Chem. A*, **2014**, *2*, 2353.

⁵²⁸ Nierengarten, J.-F.; Herrmann, A.; Tykwinski, R. R.; Riittmann, M.; Diederich, F.; Boudon, C.; Gisselbrecht, J.-P.; Gross, M. *Helv. Chim. Acta* **1997**, *80*, 293; Nakamura, Y.; Suzuki, M.; Imai, Y.; Nishimura, J. *Org. Lett.* **2004**, *6*, 2797.

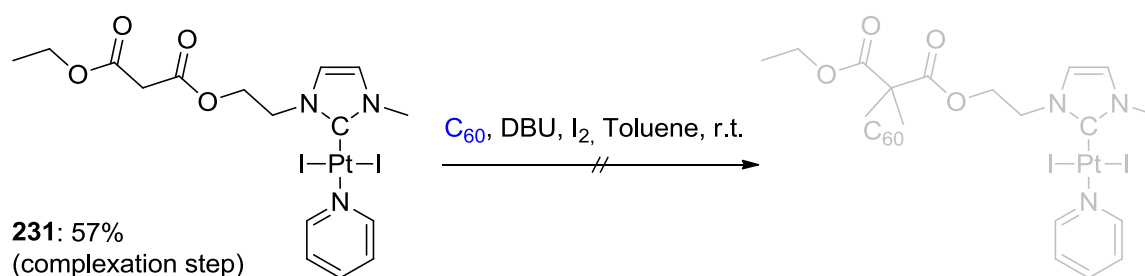


Figure 184: Unsuccessful trial of NHC-platinum complex functionalization with C_{60} moiety by Bingel reaction

After failure of Bingel reaction, we successfully tested the Prato reaction. Starting from benzaldehyde-NHC-Pt complex **81** and C_{60} , desired product **232** was afforded in 37% yield (**Figure 185**). This complex is a promising product for further electrochemical studies.

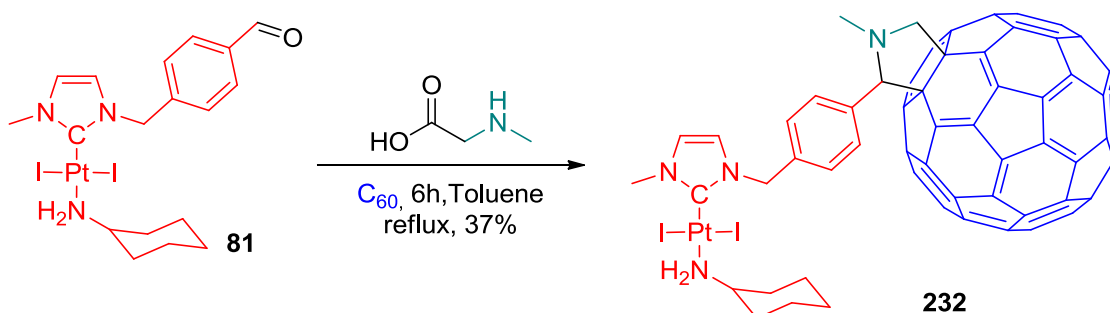


Figure 185: C_{60} functionalization of a NHC-Pt complex by Prato reaction

4.3 Halide exchange reactions

4.3.1 Introducing radioactivity to organometallic complexes

In nuclear medicine, compounds doped by radioactive isotopes are widely used.⁵²⁹ The marking of molecules by radioactive elements allows *in vivo* studies to determine their biodistribution and their elimination pathways.³⁵⁷

Our platinum complexes bear two iodide ligands. In the case of iodine, only one stable isotope of iodine is known: ^{127}I ; all other 36 isotopes are radioactive. Among these isotopes, ^{123}I , ^{125}I and ^{131}I are commonly employed for diagnostic or therapeutic purposes.⁵³⁰

Iodine ^{123}I is prepared from ^{123}Te by proton bombardment in a cyclotron. This nuclide has a half decay of 13 hours and it is emitting gamma ray of 159 keV.⁵³¹ This half decay is long enough to make ^{123}I suitable for medicinal applications and incorporation in organic or organometallic molecules. An iodobenzene derivative can be radiolabeled by isotope exchange of stable ^{127}I to ^{123}I .⁵³² The thyroid scanning by ^{123}I derivatives was investigated.⁵³³ Ioflupane (^{123}I) has become a valuable agent in medical imaging for differentiating of Parkinsonian disease,⁵³⁴ Ioazenil to detect benzodiazepine receptors in the human brain⁵³⁵ or iofetamine (^{123}I) for Alzheimer detection (**Figure 186**).⁵³⁶

Iodine ^{125}I , a 27 keV gamma emitter having a half-life of 60 days, is used for brachytherapy, a radiotherapy where radioactive source is placed in or near target tissues.⁵³⁷ Iodine ^{131}I , produced from tellurium in cyclotrons, has a half-life of 8 days.⁵³⁸ Emission of beta (608 keV) and gamma radiation (364 keV) is responsible for the highly mutagens capacity of this isotope when incorporated in living organisms. Especially iodophilicity of thyroid gland increases the risk for thyroid cancer after exposure to radioactive ^{131}I .⁵³⁹ On other hand, the specific accumulation of iodine in thyroid allows to threat hyperthyroidism. In case of thyroid cancers,⁵⁴⁰ iodine 131 is also employed as a theranostic

⁵²⁹ Ceresa, C.; Bravin, A.; Cavaletti, G.; Pellei, M.; Santini, C. *Curr Med Chem.* **2014**, *21*, 2237.

⁵³⁰ Silberstein, E. B. *Semin. Nucl. Med.* **2012**, *42*, 164.

⁵³¹ Hupf, H. B.; Eldridge, J. S.; Beaver, J. E. *Int. J. Appl. Radiat. I.* **1968**, *19*, 345.

⁵³² Emran, A. M. **1992**, *New Trends in Radiopharmaceutical Synthesis, Quality Assurance, and Regulatory Control*, Springer.

⁵³³ Park, H-M. *J. Nucl. Med.* **2002**, *43*, 77.

⁵³⁴ Wanner *et al*, *J. Nucl. Med.* **2012**, *53*, 154.

⁵³⁵ Höll, K.; Deisenhammer, E.; Dauth, J.; Carmann H.; Schubiger, P. A. *Int. J. Rad. Appl. Instrum. B* **1989**, *16*, 759.

⁵³⁶ Druckenbrod, R. W.; Williams, C. C.; Gelfand, M. J. *DICP: the Annals of Pharmacotherapy* **1989**, *23*, 19.

⁵³⁷ Kanikowski, M.; Skowronek, J.; Kubaszewska, M.; Chichel, A.; Milecki, P. *Rep. Pract. Oncol. Radiother.* **2008**, *13*, 150.

⁵³⁸ El-Absy, M. A.; El-Garhy, M. A.; El-Amir, M. A.; Fasih, T. W.; El-Shahat, M. F. *Sep. Purif. Technol.* **2010**, *71*, 1.

⁵³⁹ Holm, L.-E. *Acta Oncol.* **2006**, *45*, 1037.

⁵⁴⁰ Rasmuson, T. *Acta Oncol.* **2006**, *45*, 1011.

agent.⁵⁴¹ Meta-iodobenzylguanidine (MIBG) is used in the diagnosis (^{123}I) and therapy (^{131}I) of endocrine tumours.⁵⁴²

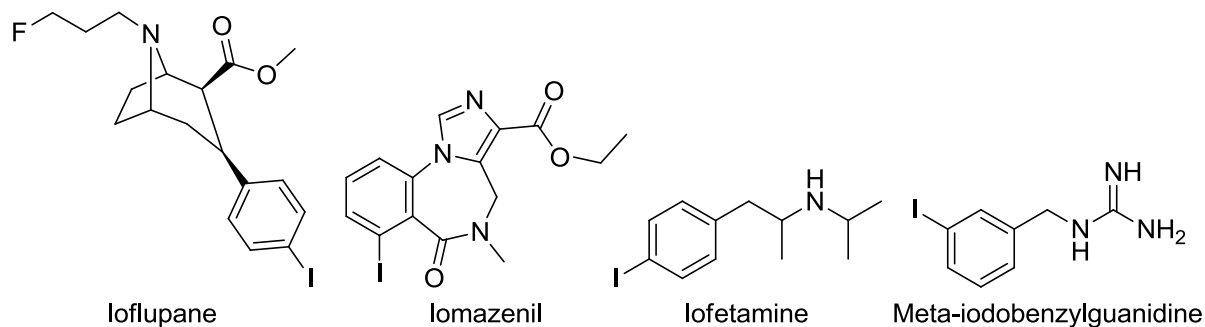


Figure 186: Examples of radioactive iodine labelled drugs

For better understanding of the biological acting of our complexes, a labelling by iodine ^{123}I would be a tool to elucidate mechanistic pathways. Introduction of iodine ^{131}I will allow combining the cytotoxic properties of the platinum with the toxicity induced by radioactivity. We can assume that DNA repair mechanisms will be inhibited by radioactivity, which may inhibit this resistance mechanism.

In literature, we only found few examples of complexes labelled by radionuclides⁵⁴³ and beside them, only two examples of radiolabelled NHC-metal complexes. In 2013, Braband and co-workers published mono and bi-dentate $^{99\text{m}}\text{Tc}$ -NHC complexes (**Figure 187**).⁵⁴⁴ One year later, the group of Herrmann synthesized a ^{188}Re labelled carbene complex.⁵⁴⁵ In both cases, it is the metal itself, which is radioactive and not his NHC or oxygen ligands.

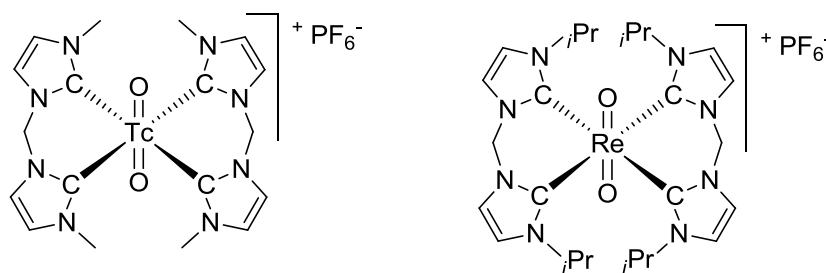


Figure 187: Radiolabelled NHC-technetium 99 and rhenium 188 complexes^{544,545}

⁵⁴¹ For a discussion of the concept of Theranosis, see: DeNardo, G. L.; DeNardo, S. J. *Semin. Nucl. Med.* **2012**, 42, 147.

⁵⁴² Sisson, J. C.; Yanik, G. A. *Semin. Nucl. Med.* **2012**, 42, 171.

⁵⁴³ Adriaenssens, L.; Liu, Q.; Chaux-Picquet, F.; Tazan, S.; Picquet, M.; Denat, F.; Le Gendre, P.; Marques, F.; Fernandes, C.; Mendes, F.; Gano, L.; Campello, M. P. C.; Bodio, E. *ChemMedChem* **2014**, 9, 1567.

⁵⁴⁴ Benz, M.; Spingler, B.; Alberto, R.; Braband, H. *J. Am. Chem. Soc.* **2013**, 135, 17566.

⁵⁴⁵ Wagner, T.; Zeglis, B. M.; Groveman, S.; Hille, C.; Pöthig, A.; Francesconi, L. C.; Herrmann, W. A.; Kühn, F. E.; Reiner, T. *J. Label Compd. Radiopharm.* **2014**, 57, 441.

In parallel to our work, Gestin and his group developed the introduction of radioactive iodine ^{125}I or astatine ^{211}At ligands to a NHC-rhodium complex by ligand exchange (**Figure 188**).⁵⁴⁶

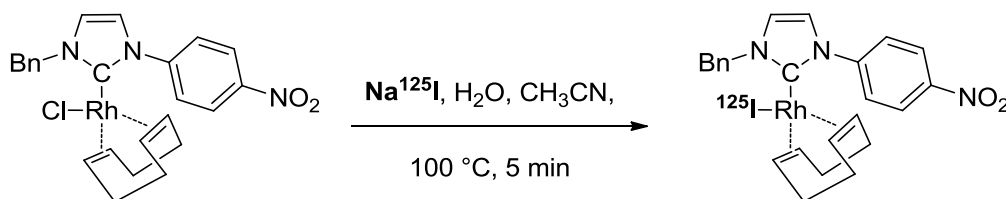


Figure 188: Synthesis of radio-iodinated NHC-Rhodium complex by Gestin.⁵⁴⁶

4.3.2 Introduction of iodine to NHC-Pt complexes by ligand exchange

Our general synthesis starting from imidazolium salt and platinum (II) does not allow the synthesis of radioactive compounds. This synthesis needs iodide in excess and a long reaction time. Purification by silica gel chromatography would create a large amount of radioactive waste. For these reasons, a short time and quantitative reaction needing no purification step must be developed ideally

In coordination chemistry, neutral ligands (L) or anionic ligands (X) are acting as Lewis bases (electron pair donors) and the metal as a Lewis acid (electron pair acceptor). In 1963, Ralph G. Pearson introduced the concept of Hard and Soft Acids and Bases (HSAB) for classification of acids and bases to predict metathesis equilibrium.⁵⁴⁷ Hard acids prefer bonding to hard bases (charged or highly polarized species). The interaction is ionic type. Soft acids prefer bonding to soft bases (non-charged species or the electrical charge is diffused on a big volume). The interaction is covalent type.

The application of the HSAB theory on the halide group displays the following order: $\text{I}^- > \text{Br}^- > \text{Cl}^- > \text{F}^-$. As platinum (II) is a soft acid, it will coordinate the halide following the same order: $\text{I}^- > \text{Br}^- > \text{Cl}^- > \text{F}^-$. Playing with the different affinity of the halides, it should be easy to introduce the iodide ligands by exchange with chloride or bromide platinum complexes.

⁵⁴⁶ Rajerison, H.; Guérard, F.; Mougin-Degraef, M.; Bourgeois, M.; Da Silva, I.; Chérel, M.; Barbet, J.; Faivre-Chauvet, A.; Gestin, J-F. *Nucl. Med. Biol.* **2014**, *41*, e23.

⁵⁴⁷ Pearson, R. G. *J. Am. Chem. Soc.* **1963**, *85*, 3533; Pearson, R. G. *Chemical Hardness*, **2005**, Wiley-VCH.

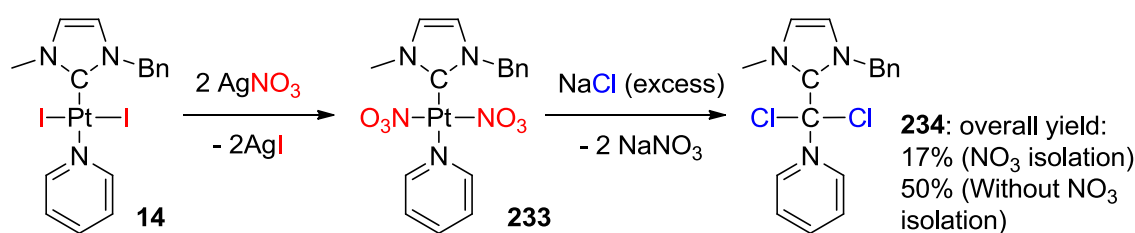


Figure 189: Synthesis of $[(\text{NHC})\text{PtCl}_2(\text{pyridine})]$ from $[(\text{NHC})\text{Pt}(\text{NO}_3)_2(\text{pyridine})]$

First ligand exchange reaction was starting from the bis-nitro complex **233**.¹²² Following a synthetic pathway described by Marinetti, we obtained this complex from $[(\text{NHC})\text{PtI}_2(\text{pyr})]$ complex **14** by reaction with silver nitrate (**Figure 189**). This ligand exchange is forced by the precipitation of insoluble silver iodide. The obtained bis-nitro complex **233** was instable and decomposed slowly under air. Compared to halides, NO_3 is a less coordinating ligand allowing an easy exchange. After adding an excess of sodium chloride, the corresponding $[(\text{NHC})\text{PtCl}_2(\text{pyr})]$ complex **234** was obtained in a global yield of 17%. The poor yield of the reaction can be explained by the limited stability of the isolated bis-nitro complex **233**. To increase the yield, the isolation of bis-nitro complex should be avoided. Adding sodium chloride to *in situ* formed complex **233** in acetonitrile, we obtained **234** in 50% yields.

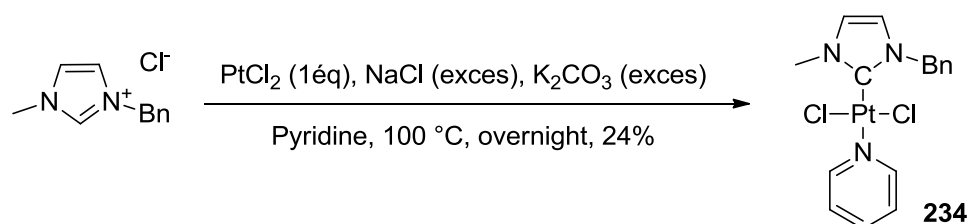


Figure 190: Synthesis of $[(\text{NHC})\text{PtCl}_2(\text{pyridine})]$ from the imidazolium chloride

The bis-chloro complex **234** could also be obtained from the corresponding imidazolium chloride using the previous described synthesis of NHC-complexes in 24% yield (**Figure 190**). Purification by chromatography on silica gel was found to be difficult since impurities $(\text{PtCl}_2(\text{pyr})_2)$ have a similar polarity. Attempts to increase the yield by longer reaction time (2 days) or imidazolium chloride in excess conducted to decomposition and even lower yield (12%). To improve the purification, a less polar complex $[(\text{Ph-NHC})\text{PtCl}_2(\text{pyridine})]$ **235** was synthesized with a more acceptable yield (36%) (**Figure 191**). Nevertheless, the desired $[(\text{NHC})\text{PtCl}_2(\text{pyridine})]$ type complex cannot be easily obtained by this strategy. Therefore, we decided to continue with bis-bromo complexes, which are stable and easy to purify.

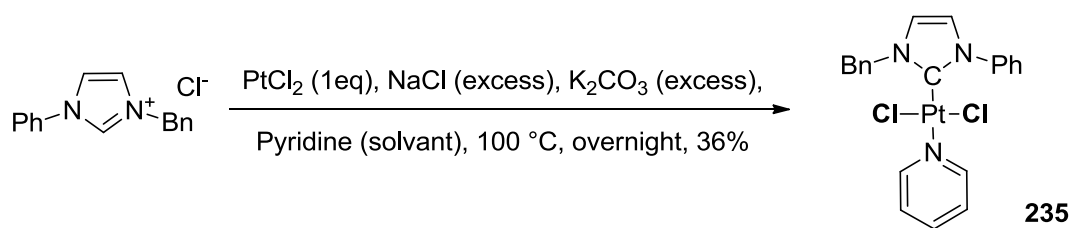


Figure 191: Synthesis of [(Ph-NHC)PtCl₂(pyridine)] 235 from the imidazolium chloride

[(NHC)PtBr₂(pyr)] complex **168** was easily obtained in comparable yield than bis-iodine NHC complexes (52%) (**Figure 192**). The purification by chromatography was simple and the complex stable both under air and in solution.

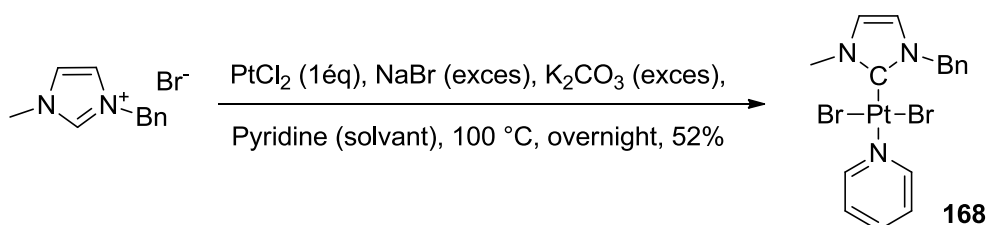


Figure 192: Synthesis of [(NHC)PtBr₂(pyr)] complex 168 from the imidazolium chloride

By ligand exchange, [(NHC)PtBr₂(cyclohexylamine)] complex **169** was obtained quantitatively (**Figure 193**). Only slight excess of cyclohexylamine should be introduced to avoid formation of cationic species.⁵⁴⁸

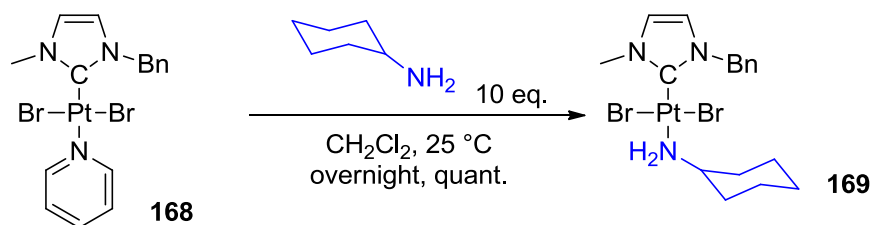


Figure 193: Synthesis of [(NHC)PtBr₂(cyclohexylamine)] complex 169 by ligand exchange

⁵⁴⁸ Detailed in section 4.1.2.1. Reactivity of (NHC)Pt(II)(pyridine) complexes with di and tri-amines.

Entry	Complex	14 (I)	168 (Br)	234 (Cl)
1	Solid (Colour)	Yellow	Yellow	Yellow
2	Polarity on TLC (R_f in CH_2Cl_2)	0.70	0.45	0.35
3	^{13}C -NMR (CDCl_3): $\delta_{\text{C-Pt}}$ (ppm)	136.3	138.2	139.8
4	^{13}C -NMR (CDCl_3): $\delta_{\text{C}_{\text{Capyr}}}$ (ppm)	153.7	152.3	151.3
5	^1H -NMR (CDCl_3): $\delta_{\text{N-CH}_3}$ (ppm)	3.97	4.11	4.14
6	^1H -NMR (CDCl_3): $\delta_{\text{N-CH}_2}$ (ppm)	5.72	5.83	5.78
7	Yield (%)	72	52	36

Table 20: Comparison between the different $[(\text{NHC})\text{PtX}_2(\text{pyr})]$ complexes **14**, **168** and **234**

By ^1H and ^{13}C -NMR, the three different $[(\text{NHC})\text{PtX}_2(\text{pyr})]$ complexes **14**, **168** and **234** could be unambiguously differentiated due to their typical chemical shift values (Table 20, entry 3-6). The decreasing polarity from the chloro **234** to the iodine complex **14** is reflecting the decreasing hardness of the X ligands (entry 2). It also allows easy distinguishing of the complexes by thin layer chromatography.

In order to introduce (potentially) radioactive iodide ligands to our complexes, the halogen reaction was studied with chloro and bromo complexes **234** and **168**. The goal was to find the best conditions in order to form easily and quantitatively the iodine Pt complex (Figure 194).

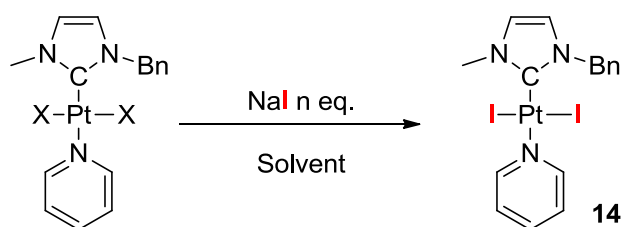


Figure 194: Introduction of iodine by X ligand exchange

Entry	Nal (eq.)	Solvent	Temperature and reaction Time	Result
1	4	CD ₃ CN	30 min 25 °C,	14/234 : 50% / 50%
2	4	CH ₃ CN	40 min 50 °C,	14/234 : 67% / 33%
			overnight reflux	14 (impure)
			overnight, reflux	72% of 14 (after chromatography)
3	4	CH ₃ CN	2h, reflux,	14/234 : 33% / 67%
4	2.2	Acetone*	2h, reflux,	14/234 : 70% / 30%
5	2.2	MeOH/Acetone 1/1	2h, reflux	85% of 14 , 15% impurity
6	10	Acetone, 1 drop of MeOH	2h, reflux	100% of 14
7	10	H ₂ O / MeOH	overnight, 55 °C	234 + decomposition products

Table 21: Tested conditions for converting chloride 234 into iodide 14 complex (* low solubility in acetone)

Table 21 suggests that entry 5 presents the best conversion with only 2.2 equivalents in a short time, however only 85% of Pt iodine complex **14** was observed. Finally, the best condition was obtained with acetone and a minimum of MeOH giving the product **14** in 100% after 2 hours (entry 6).

These experiences showed the possibility to exchange chloro ligands quantitatively by iodine ligands. Driven by the difficult synthesis of the chloro complex **234**, we decided to continue the same reactions with the more easily available bromo complex **168** (**Table 22**).

Entry	Nal (eq.)	Reaction Time	Result
1	10	120 min	Iodide complex 14 only (after chromatography)
2	10	60 min	Iodide complex 14 only (after chromatography)
3	2.2	0 min	Bromide complex 168 *
		10 min	168/14 = 3/2 *
		30 min	168/14 = 3/17 *
		60 min	168/14 = 1/21 *
		90 min	After chromatography: 100 % of pure 14
4	2.2	60 min	100% of 14 after evaporation + filtration

Table 22: Tested conditions for converting bromide 168 into iodide 14 complex (Temperature: reflux, solvent: acetone, * determined by NMR spectroscopy)

Following the ligand exchange by NMR, the reaction was completed after 90 minutes by using only 2.2 equivalents of sodium iodide (entry 3). To enhance the rate of the reaction, sodium iodide was in a second step crushed before use and the reaction was done under air and moisture (entry 4). Under

these conditions, the reaction was quantitative after only one hour and using only 2.2 equivalents of sodium iodide. Since no side products were observed, the purification requires only evaporation of acetone, filtration in dichloromethane on a bed of cotton and final drying. The whole procedure was done in only 70 minutes. Within the same time and under same conditions, exchange could also be performed using sodium iodide (2.2 eq.) in water solution.

This reaction is also independent of the nature of the fourth L-type ligand: [(NHC)PtBr₂(cyclohexylamine)] **169** was converted using the same conditions to the corresponding [(NHC)PtI₂(cyclohexylamine)] complex **15**. To combine the reaction with the possibility of further complex functionalization by oxime formation, a [(benzaldehyde-NHC)PtBr₂(cyclohexylamine)] **236** was synthesized by ligand exchange from [(benzaldehyde-NHC)PtBr₂(pyridine)] **237**. The iodides were then introduced using the same procedure, giving the compound **81** in quantitative yield (**Figure 195**).

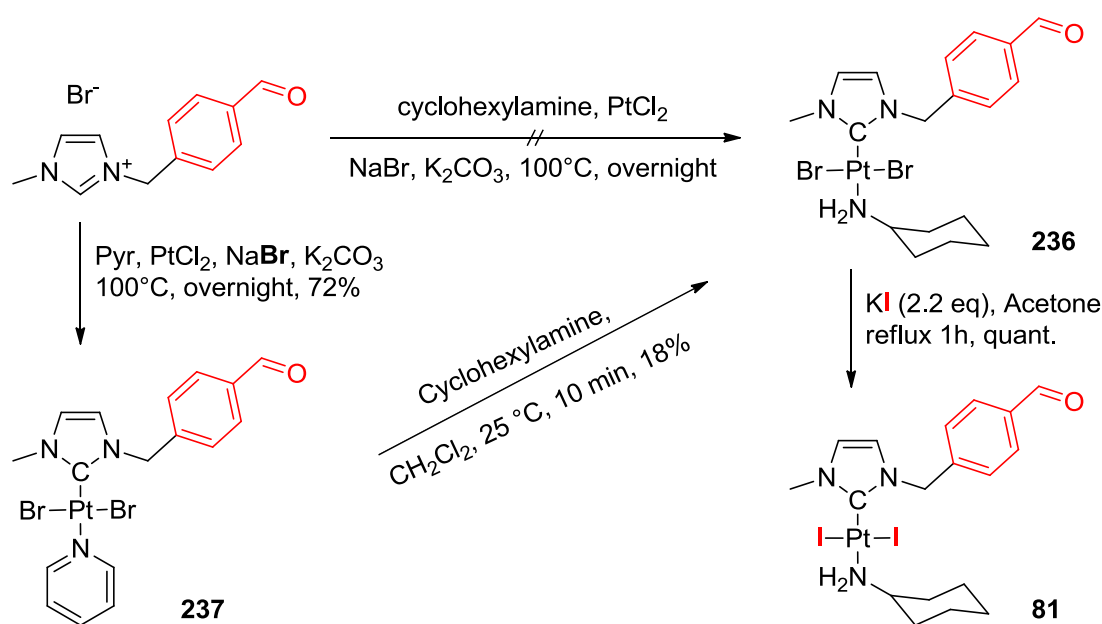


Figure 195: Synthesis of [(benzaldehyde-NHC)PtBr₂(cyclohexylamine)]: a reactive for iodide introduction

As a conclusion, iodide ligands could be quantitatively introduced from the bromine complexes in a straightforward manner with easy purification. The methodology is suitable to be applied in nuclear medicine under clinical conditions.

4.3.3 Introduction of ^{123}I

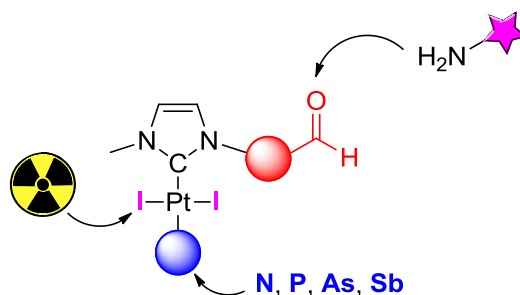
Altogether, these results allow applying the reaction with success to ^{123}I .

The introduction of ^{123}I on platinum NHC complexes was successfully done by C. Darcissac and A. Clotagatide from Radiopharmacie CHU de Saint Etienne. The reaction could be validated by HPLC experiments. The group of Pr. C. Billotey in Saint Etienne currently investigates these ^{123}I Pt NHC complexes *in vivo* on mice model.

These results allow continuing to *in vivo* tests to elucidate the mechanism and biodistribution of our NHC-Pt complexes.

4.4 Conclusion: diversity introduction by post-synthetic modifications

Post-synthetic functionalization allowed introducing diversity to preformed NHC complexes.



By ligand exchange reaction, we could functionalize NHC Pt complexes with various neutral ligands: amines, polyethylenimine (PEI) or pnictogen based ligands (phosphines, arsines, stibines)

Condensation reaction between benzaldehyde featured NHC complexes and amines, hydrazines or hydroxylamines led to a whole family of compounds, especially fluorescent anthracene moiety as well as a PSMA targeting urea could be introduced. The ease of synthesis and stability of oxime complexes should be mentioned.

A fast and user-friendly introduction of iodide ligands to NHC Pt complexes was developed and successfully applied to radioactive iodine isotopes.

The biological properties of these compounds will be described in *chapter 5. Biological studies*.

5 Biological studies of NHC-Pt complexes

5.1 In vitro studies of platinum NHC complexes

Various cancerous and non-cancerous cell lines models⁵⁴⁹ had been used for preliminary cytotoxicity studies. The cytotoxicity of the compounds was quantified using a MTS assay that measure cell metabolism. The results are expressed either in **cell viability inhibition percentage** at a given concentration of the studied compound (generally 10^{-5} or 10^{-6} M) or in half-maximal inhibitory concentration (**IC₅₀**) in μM . Cisplatin was used as a reference. **Table 23** and **24** describe a list of cells that have been used in this work.

Cell line	Description
HeLa	cervix carcinoma
KB	cervix carcinoma (derivative of HeLa)
U87	glioblastoma
BJAB	Burkitt lymphoma
SK-OV3	ovary adenocarcinoma *
OVCAR-8	ovarian carcinoma
HL60	acute myeloid leukaemia
MCF7	breast adenocarcinoma expressing the oestrogen receptor
HCT116	colorectal adenocarcinoma
PC3	prostate carcinoma

Table 23: Human cancerous cell lines (* cisplatin resistant cells) used in this work

Cell line	Origin	Description
MRC5	Human	foetus lung fibroblast
Vero	African green monkey	kidney
EPC	Fathead minnow	skin epithelial progenitor cells

Table 24: Non-cancer cell lines used in this work

⁵⁴⁹ The accuracy and clinical value of cell line models are discussed: Gillet, J.-P.; Varma, S.; Gottesman, M. M. *J. Natl. Cancer Inst.* **2013**, *105*, 452; Masters, J. R. W. *Nat. Rev. Mol. Cell Biol.* **2000**, *1*, 233.

5.1.1 State of the art: anticancer properties of platinum NHC complexes

First cell viability inhibition studies of NHC platinum complexes were performed by the group of Marinetti.^{122,123} Their IC₅₀ values were inferior or comparable to cisplatin and oxaliplatin making them promising agents. Besides toxicity comparison of [(NHC)PtX₂(amine)] complexes with X = I, Br or NO₂, iodide ligands gave the best results. Thus [(NHC)PtX₂(amine)] complexes proved to be active against cisplatin resistant cells suggesting a mechanistic pathway different from cisplatin.

In our preliminary studies, toxicities of various [(NHC)PtI₂(amine)] complexes against HeLa, U87 or BJAB cell lines were shown to be higher than cisplatin.^{124,125,128} Platinum-NHC complexes appeared to be more cytotoxic than palladium-NHC and no activity was noticed for imidazolium precursors. Moreover, no loss of activity was observed even after days in DMSO solution proving their high stability. Selectivity studies did not depict any differentiation between cancerous and non-cancerous cell lines, except for oestrogen-functionalized complex toward ovarian and colon cancer cells. Usually, variation of the amine ligand did not affect cytotoxicity excepted for urea and polyethylene glycol derivatives. Cationic complexes bearing polyamines showed interesting behaviour: ethylenediamine and diethylenetriamine derivatives were completely inactive while polyethylenimine conjugates showed high cell viability inhibition capacity. Noteworthy, the polyethylenimine complexes presented selectivity towards cancerous cell lines compared to healthy cells (*in vitro*).

Thus high cytotoxicity values were reported for relatively simple [(NHC)PtI₂(amine)] complexes. Obviously, cationic polyethylenimine platinum derivatives are highly promising candidates for antitumor applications. In the following section, we will focus on biological properties of novel NHC complexes with backbone modifications.

5.1.2 Cytotoxicity of prefunctionalized [(NHC)PtI₂(amine)] complexes

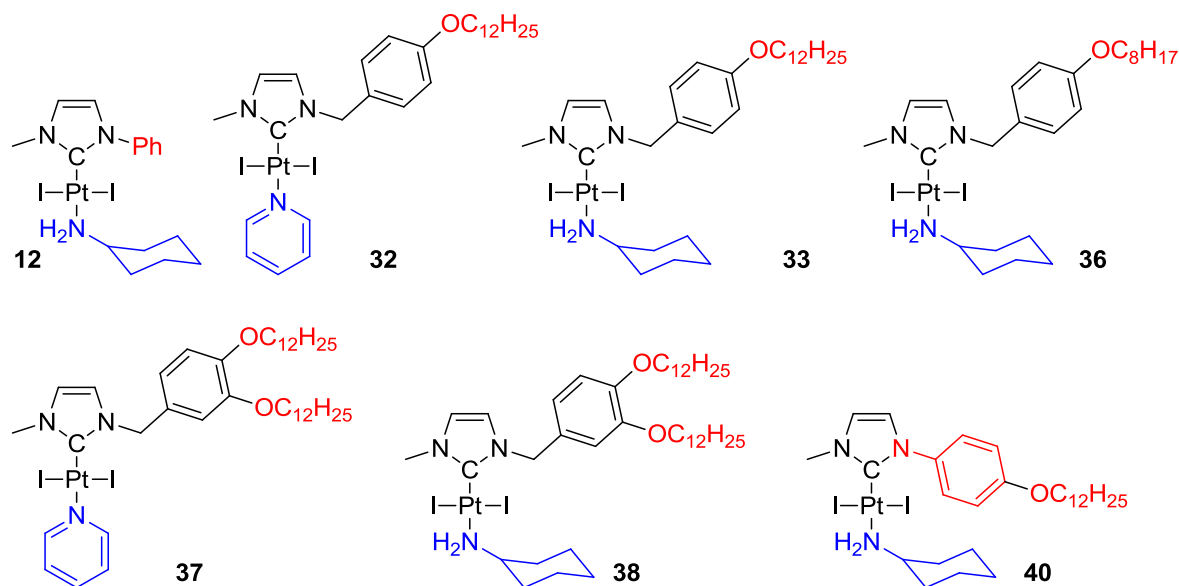
In this part, we will discuss the *in vitro* cytotoxicity of the compounds as a function of three main parameters, namely *N*-substituents on the NHC, L ligands, and NHC backbone. *N*-substituents functionalities studied here are:

- Alkyl / polyethylene glycol chains and aryl groups
- Complexes with various functional groups (alcohol, nitrile, malonate)
- Phosphonate derivatives (potential nanoparticle functionalization)
- Water-soluble complexes (carboxylic acid and morpholine functions)
- Polynuclear complexes
- Benzaldehyde featured complexes as precursors for further derivatization

In vitro measurements were carried out in the Laboratory of Conception and Application of Bioactive Molecules from the Faculty of Pharmacy of Strasbourg and by the Ciblotheque Laboratory of Institute of Chemistry of Naturel Substances (ICSN) from Gif-Sur-Yvette. Usually, measurements were undertaken in triplicate (cell viability inhibition percentage) respectively in duplicate (IC₅₀). Samples were prepared by compounds dissolution in DMSO at stock concentration of 10 mM, except for cisplatin which was dissolved in water.

5.1.2.1 Influence on cytotoxicity of alkyl chains and aryls as *N*-substituents of NHC complexes

The influence of alkyl chains was studied using several chain lengths (C₁₂ or C₈) and one or two chains per complex (**Table 25** and **Table 26**). Cell viability inhibition percentages measured at 10⁻⁵ (**Table 25**) and 10⁻⁶ M (**Table 26**) for these complexes highlighted several trends. Cyclohexylamine complexes (**33**, **38**) proved to be more toxic than pyridine analogues (**32**, **37**). Introduction of two alkyl chains (**37**, **38**) resulted in inactive complexes. The complex containing a C₁₂ chain (**33**) presented higher cytotoxicity than its C₈ analogue (**36**). Introduction of the phenyl-OC₁₂H₂₅ group directly on the NHC (without a CH₂ bridge) (**40**) gave increased activity. The simple phenyl complex **12** depicted the best activity and finally led us to conclude that introduction of alkyl chains did not allowed access to the expected cytotoxicity enhancement.

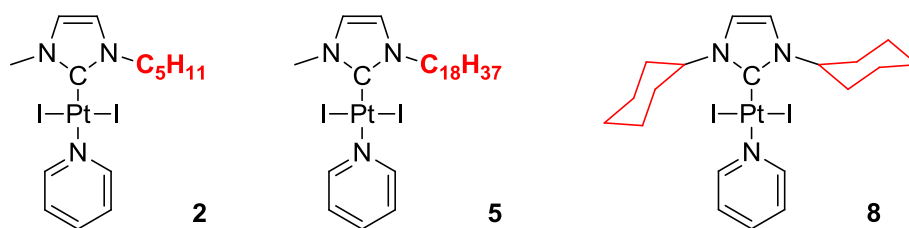


Complex	Cisplatin	12	32	33	36	37	38	40
KB	4	100	60	92	100	8	-18	92
MCF7	-4	98	21	86	89	-13	-6	96
HCT116	3	95	43	90	95	8	-3	98
PC3	-6	93	15	24	81	1	-22	85
SK-OV3	4	95	29	68	87	5	8	94
OVCAR-8	-2	99	22	95	78	-4	0	96
HL60	-11	97	0	75	68	13	11	90
MRC5	-20	99	0	91	96	-1	-9	99
Vero	-4	100	0	20	13	-1	-10	86
EPC	-1	96	38	62	96	4	19	98

Table 25: Cell viability inhibition percentage ($\pm 5\%$) at 10^{-5} M: influence of alkyl chains

Complex	Cisplatin	12	32	33	36	37	38	40
KB	24	16	1	2	38	8	22	22
HCT116	0	31	11	11	3	8	9	20
MCF7	-1	17	5	17	6	-13	5	21
PC3	9	8	0	0	-3	1	-12	1
SK-OV3	2	5	12	16	11	5	9	14
OVCAR-8	3	11	0	0	0	-4	9	5
HL60	-8	0	0	0	1	13	2	17
MRC5	-9	0	0	0	-15	-1	-4	-25
Vero	-6	38	0	0	0	-1	-1	7
EPC	-0	2	5	0	8	4	13	32

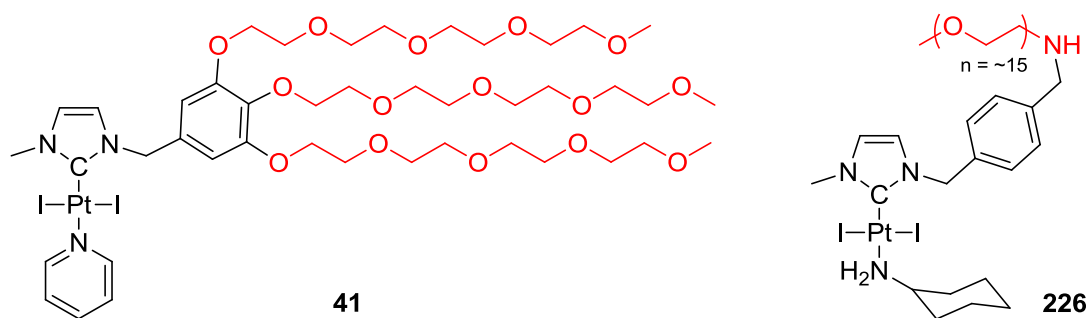
Table 26: Cell viability inhibition percentage ($\pm 5\%$) at 10^{-6} M: influence of alkyl chains



Complex	MCF7	HCT116	PC3	OV3	MRC5	EPC
cisplatin	19.8±0.6	6.4±0.2	10±1	18±2	12.5±0.1	76±10
2	0.23±0.01	0.04±0.01	0.09±0.01	0.07±0.01	0.07±0.01	0.21±0.02
5	82±1	46±5	44±5	53±2	91±7	>100
8	0.22±0.01	0.45±0.04	0.35±0	0.29±0.01	0.295±0.005	0.54±0.01

Table 27: IC₅₀ values (μM) of alkane chain complexes: low cytotoxicity

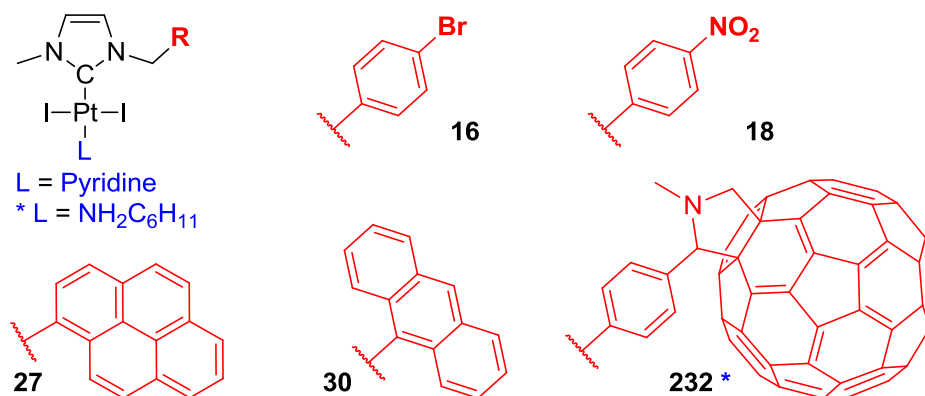
Biological activities of three complexes **5**, **2** and **8** bearing alkane chains were compared in **Table 27**. While the short chain C₅ complex **2** ($0.04 < \text{IC}_{50} < 0.23 \mu\text{M}$) and the cyclohexyl complex **8** ($0.22 < \text{IC}_{50} < 0.54 \mu\text{M}$) presented excellent activities, longer chain C₁₈ analogue **5** ($44 < \text{IC}_{50}$) was less active than cisplatin. These results also suggested that shorter alkyl chains might be better choice as *N*-substituents of [(NHC)PtI₂(L)] complexes.



Complex	MCF7	HCT116	PC3	OV3	MRC5	EPC
cisplatin	19.8±0.6	6.4±0.2	10±1	18±2	12.5±0.1	76±10
41	64.9±0.7	42±2	74±8	67±2	56±2	32±6
226	13±2	4.0±0.8	15±1	12.1±0.4	4.4±0.7	24.7±0.6

Table 28: IC₅₀ values (μM) for PEG featured NHC complexes: low toxicity of PEG Pt complexes

Table 28 indicates IC₅₀ values of two water-soluble complexes containing PEG chains. Both polar complexes **226** and **41** depicted relatively poor cytotoxic properties, consistent with poor cell viability inhibitions further observed with other polar or charged compounds (**Table 34** and **Table 35**). Surprisingly, both lipophilic and hydrophilic longer chains (alkanes or PEG) led to decreased activity of the corresponding Pt complexes.

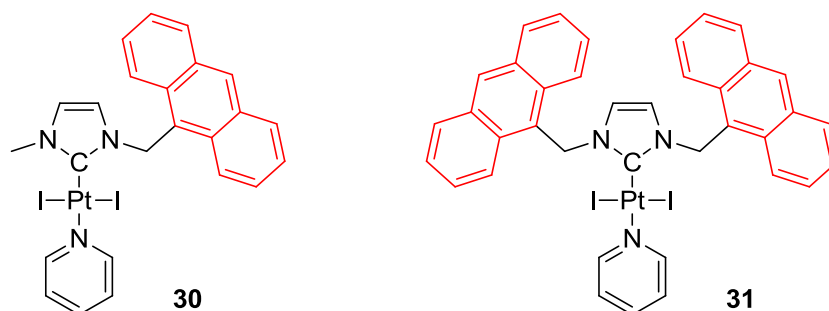


Complex	MCF7	HCT116	PC3	OV3	MRC5	EPC
cisplatin	19.8±0.6	6.4±0.2	10±1	18±2	12.5±0.1	76±10
16	0.36±0.01	0.30±0.02	n.d.	n.d.	n.d.	0.81±0.02
18	0.035±0.005	<0.005	0.9±0.2	0.075±0.005	<0.005	0.075±0.005
27	0.145±0.005	0.010±0.005	0.16±0.02	0.165±0.005	0.03±0	0.11±0.01
30	0.085±0.005	0.01±0.01	0.035±0.005	0.02±0.01	0.02±0.01	0.085±0.005
232	NI	NI	n.d.	n.d.	n.d.	NI

Table 29: IC₅₀ values (μM) for aromatic groups featured complexes (NI: no inhibition at 33.3μM): high activity of aryl complexes

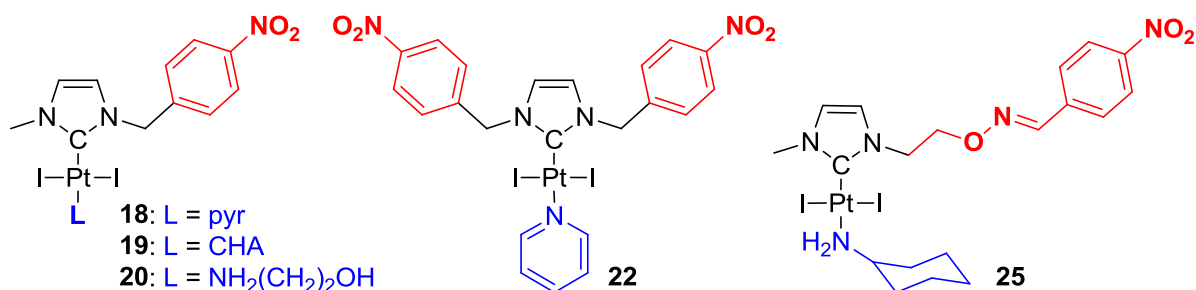
Further investigations led us to consider the influence of various aryl groups as *N*-substituents. NHC platinum complexes **16**, **18**, **27**, **30** (except C₆₀ conjugate **235**) had inhibition concentrations at or below micromolar range (**Table 29**). Among these complexes, anthracene **30** and nitrobenzyl **18** derivatives presented excellent cytotoxicity. Thus to enhance their biological activity, various complexes bearing anthracene or nitrobenzyl group were tested (**Table 30** and **Table 31**). Surprisingly, the bis-anthracene derivative **31** was inactive, probably due to its low solubility. Most of nitrobenzyl complexes (**18**, **19**, **22**, **20** and **25**) gave acceptable inhibition abilities; nevertheless the most simple pyridine derivative **18** remained the most active. The cyclohexylamine complex **19** gave even lower results than its pyridine analogue. Besides polar ethanolamine derivative **20** appeared to be the less active compound of this series. Finally, we highlighted two complexes (nitrobenzyl **18** and

anthracene **30** derivatives) that are active at the nanomolar range. Obviously, these compounds are promising candidates for further investigations e.g. for nanoparticle or polymer conjugation or liposomal formulations.



Complex	MCF7	HCT116	PC3	OV3	MRC5	EPC
cisplatin	19.8±0.6	6.4±0.2	10±1	18±2	12.5±0.1	76±10
30	0.085±0.005	0.01±0.01	0.035±0.005	0.02±0.01	0.02±0.01	0.085±0.005
31	89±7	40±6	76±1	84.0±0.1	47±11	>100

Table 30: IC₅₀ values (μM) for two anthracene featured complexes: low activity of bis-anthracene complex 31



Complex	MCF7	HCT116	EPC
cisplatin	19.8±0.6	6.4±0.2	76±10
18	0.035±0.005	<0.005	0.075±0.005
19	1.1±0.6	1.1±0.1	1.7±0.3
20	4.5±0.2	2.75±0.05	8.5±0.1
22	0.36±0.05	0.25±0.01	0.54±0.08
25	1.25±0.05	1.45±0.05	1.2±0.6

Table 31: IC₅₀ values (μM) for different nitrobenzyl featured NHC complexes: influence of *N*-substituents and L ligands

5.1.2.2 Biological incidence of introduction of miscellaneous functional groups

Table 32 shows cell viability inhibition percentages at 10^{-5} and 10^{-6} M of NHC complexes **51** and **75**. Simple variation of a cyano group (**51**) by an acetal (**75**) dramatically increases the cytotoxicity: at 10^{-6} M, the cyano complex **51** is inactive while the acetal derivative **75** inhibited over 80% of the tested cells. Thus IC_{50} values were lower to 10^{-6} M for the acetal derivative **75** and lower to 10^{-5} for cyano complex **51**. IC_{50} value of the ethanol derivative **44** was also in the 10^{-5} M range (**Table 33**). Malonate **4** featured complex was highly active with IC_{50} values ranging from 0.2 to 1.2 μ M. In contrast, a low activity is depicted by the more polar alcohol functionalized complex **44**. These examples indicated similar activities for malonate **231** and acetal **75** derivatives while decreased toxicity was observed for cyano **51** and alcohol **44** complexes.

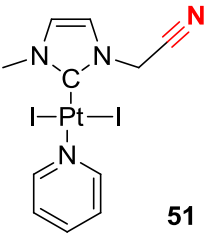
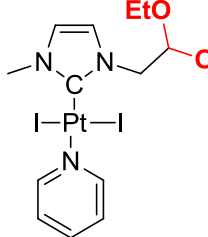
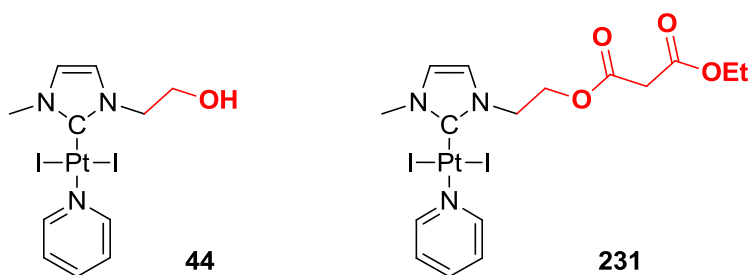
Complex				
	51		75	
[c] (M)	10^{-5}	10^{-6}	10^{-5}	10^{-6}
KB	99	23	100	91
MCF7	97	22	99	86
HCT116	90	27	95	84
PC3	85	0	90	52
SK-OV3	93	28	96	82
OVCAR-8	91	0	99	95
HL60	87	14	97	86
MRC5	100	0	100	100
Vero	100	11	100	99
EPC	100	0	100	79

Table 32: Cell viability inhibition percentage ($\pm 5\%$) at 10^{-5} / 10^{-6} M of two NHC complexes with nitrile and acetal groups

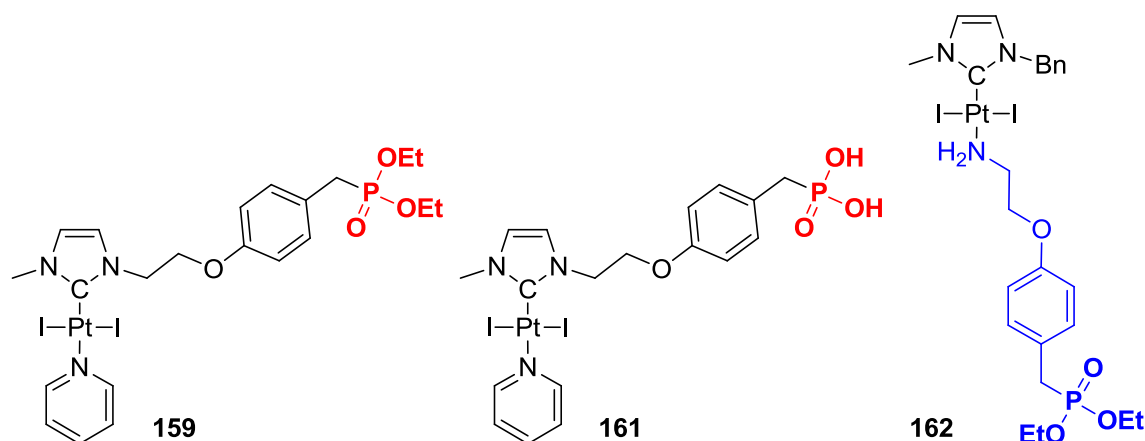


Complex	MCF7	HCT116	PC3	OV3	MRC5	EPC
cisplatin	19.8±0.6	6.4±0.2	10±1	18±2	12.5±0.1	76±10
44	5±1	11±2	9.0±0.3	7.6±0.6	6.4±0.04	11.2±0.1
231	0.325±0.005	0.46±0.09	n.d.	n.d.	n.d.	1.2±0.1

Table 33: Pt complexes functionalized with hydroxyl and malonate functional groups: IC₅₀ (μM)

5.1.2.3 NHC complexes featured with phosphonate groups

Phosphonate groups are interesting functions to allow strong grafting of our complexes to nanoparticles. Ethylester protected phosphonate derivatives **159** and **162** (Table 34) had high cytotoxic values. However, deprotection of the phosphonate ester rendered **161** inoffensive. This result was consistent with activity loss observed for other charged platinum NHC complexes. As polar groups decreased the activity of our complexes, it is necessary to keep away the cytotoxic NHC-Pt core from the polar phosphonate group in order to make candidates for further nanoparticle functionalization. So, introduction of a cleavable linker Pt-linker bond, e.g. a phosphonate-amine linker (**162**) was investigated. This would allow release of the active (phosphonate group-free) NHC-Pt complex after cell entering of the combined Pt-nanoparticle. This promising project of grafting platinum NHC complexes via cleavable amino-phosphonate linkers on iron nanoparticles will constitute a part of the PhD thesis of M. Bouché.

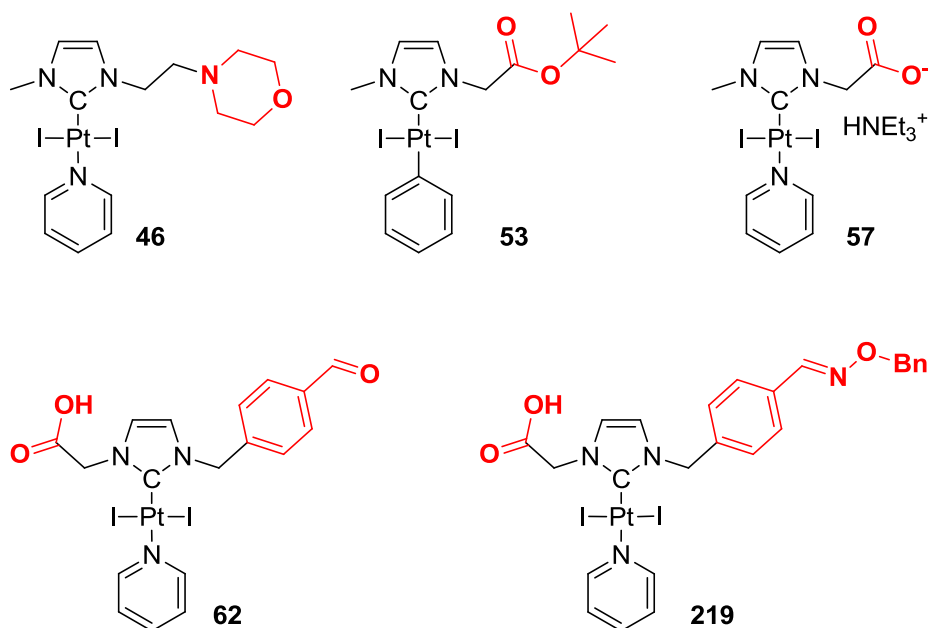


Complex	HCT116	MCF7	EPC
Cisplatin	6.4±0.2	19.8±0.6	76±10
159	0.925±0.005	0.8±0.1	1.2±0.1
161	NI	NI	NI
162	0.73±0.02	0.735±0.005	0.8±0.1

Table 34: IC₅₀ values (μM) of phosphonate derivatives (NI: no inhibition at 33.3μM): no inhibition for deprotected phosphonate complex 161

5.1.2.4 High water solubility: biological incidences

Low water-solubility remains the major drawback of cisplatin. Thus, water-soluble NHC platinum complexes bearing acid or morpholine groups had been explored. Cytotoxicity comparison of various acid functionalized complexes with unprotected ester **53** revealed the limitations of this strategy (Table 35). Indeed, while the small and lipophilic ester complex **53** showed comparable activity to other [(NHC)PtI₂(pyr)] complexes, the acid and carboxylate analogues **57**, **62** and **219** all presented IC₅₀ values above 20 μM. These poor results could be explained by the difficulty of anionic complexes to pass through cell membrane, as well as by the electronic repulsion between negatively charged DNA and these complexes. In contrast, the morpholine derivative **46** presented comparable to better cytotoxicity than cisplatin. Therefore, a more efficient strategy was necessary to access water-soluble complexes. Introduction of water-soluble groups not directly on the complex was considered. Instead, water solubility should be accessible from conjugation of vectoring moieties (nanoparticles, PEI) to lead lipophilic complex.

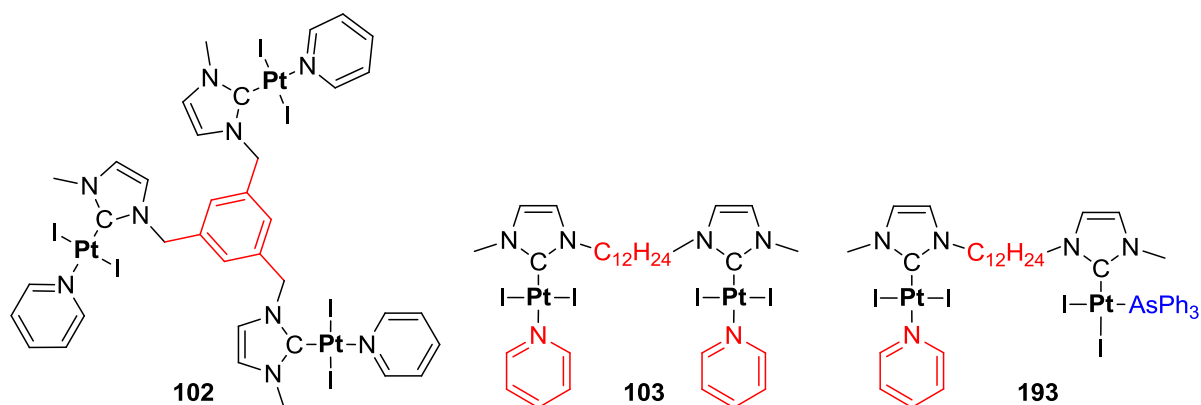


Complex	MCF7	HCT116	PC3	OV3	MRC5	EPC
cisplatin	19.8±0.6	6.4±0.2	10±1	18±2	12.5±0.1	76±10
53	0.22±0.01	0.01±0.1	1.52±0.02	0.12±0.01	0.04±0.01	0.10±0.02
57	>100	57±6	>100	>100	88±10	>100
62	62±3	19.9±0.2	38.2±0.5	83±4	51±11	72±28
219	36.3±0.7	29.1±0.5	76±15	92±5	71±5	39±2
46	13.3±0.4	1.5±0.1	17±6	9±2	2.1±0.3	10±1

Table 35: IC₅₀ values (μM) of water-soluble complexes: absence of activity of charged complexes

5.1.2.5 Polynuclear complexes

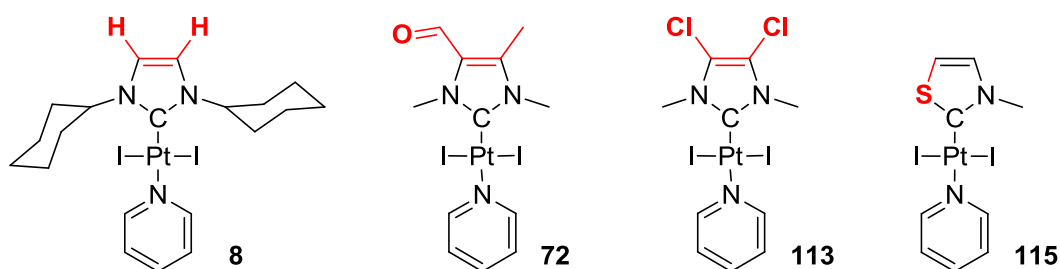
Polynuclear complexes were tested to access poly-coordination of DNA and to increase local platinum concentration. Unfortunately, IC₅₀ values of polynuclear complexes **102**, **103** and **193** (Table 36) were not as good as expected. A trimetallic complex **102** as well as di-pyridine complex **103** showed low toxicity. Even its mixt pyridine-arsine analogue **193** was not toxic at all. Surprisingly, compared to mononuclear species, these compounds appeared to be less active.



Complex	HCT116	MCF7	EPC
Cisplatin	6.4±0.2	19.8±0.6	76±10
102	4.5±0.2	8±2	5±2
103	1.1±0.1	2.4±0.3	5.5±0.7
193	13±1	NI	NI

Table 36: IC₅₀ values (μM) of polynuclear compounds (NI: no inhibition at 33.3μM)

5.1.2.6 NHC backbone: alkene modifications

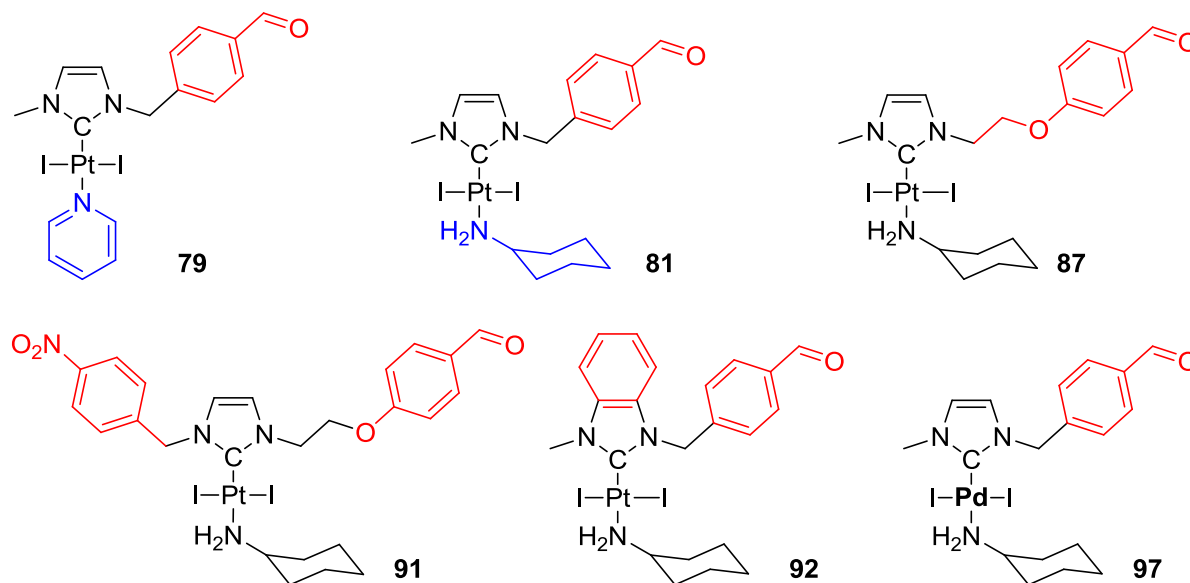


Complex	HCT116	MCF7	MRC5	EPC
Cisplatin	6.4±0.2	19.8±0.6	12.5±0.1	76±10
8	0.45±0.03	0.22±0.01	n.d.	0.54±0.01
72	2.1±0.1	1.6±0.2	n.d.	4.6±0.2
113	0.7±0.1	0.7±0.1	n.d.	1.3±0.1
115	6,3±0.6	7,5±0.2	4,7±0.5	4,4±0.7

Table 37: IC₅₀ values (μM) of backbone modified NHC

NHC-alkene backbone modifications did not show clear trend (Table 37). Introduction of an acetal (72) or two chlorine atoms (113) is expected to make the NHC less donating and so change its reactivity (and pyridine exchange). Nevertheless, the chlorine derivative 113 depicted slightly decreased activity compared to the highly donating 1,3-dicyclohexyl-imidazolylidene complex 8. The aldehyde derivative 72 was even less active. The thiazolylidene based complex 115 also presented low activities. Imidazolylidene based NHC remains the best structure to access highly active compounds.

5.1.2.7 Biological properties of NHC platinum complexes featuring benzaldehyde



complex	MCF7	HCT116	PC3	OV3	MRC5	EPC
cisplatin	19.8±0.6	6.4±0.2	10±1	18±2	12.5±0.1	76±10
79	0.49±0.07	4±3	0.93±0.03	1.5±0.4	0.60±0.02	1.8±0.2
81	0.78±0.05	0.17±0.07	0.79±0.06	0.55±0.09	0.30±0.07	1.08±0.03
87	0.74±0.06	0.14±0.01	4±3	0.86±0.03	0.48±0.08	1.0±0.2
91	1.75±0.05	2.1±0.2	n.d.	n.d.	n.d.	3.05±0.05
92	0.85±0.01	0.50±0.02	1.09±0.02	1.0±0.1	0.445±0.005	2.7±0.2
97	24.7±0.01	3.9±0.6	7.9±0.2	9.9±0.4	8.9±0.3	52±17

Table 38: IC₅₀ values (μM) of benzaldehyde complexes: active precursors for further derivatization

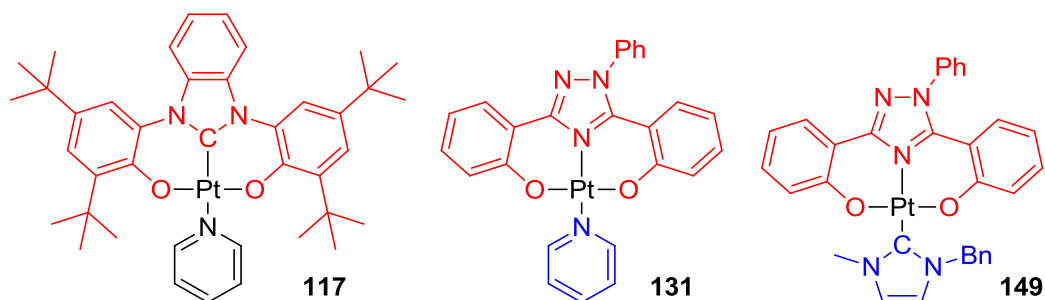
Cytotoxicity of various benzaldehyde derivatives has been tested toward several cancerous cell lines (Table 38). As expected, cyclohexylamine complex **81** was more active than its pyridine analogue **79**; but palladium complex **97** was less active than the platinum one **81**. Variation of the NHC backbone (imidazolylidene **81** / benzimidazolylidene **92**) did not influence the activity. IC₅₀ values of the complexes were influenced by the linker between the N_{NHC} and the benzaldehyde: Complex **81** gave better results than complex **87**. Introduction of functionalities to the second N_{NHC} (nitrobenzyl complex **91**) resulted in an increase of the IC₅₀ values. Finally our Pt benzaldehyde complexes all present good activities and consequently are valuable starting material for further derivatization by oxime coupling.

5.1.3 Preliminary conclusion on *in vitro* results of functionalized NHC complexes

Some main tendencies could be drawn considering each result previously obtained:

- Long alkane chains (C₁₂-C₁₈) led to decreased activity.
- Generally, cyclohexylamine complexes were more active than their pyridine analogues.
- Polar functions (alcohols, nitriles, PEG) conducted to less active compounds and charged species (phosphonates, acids) were inactive.
- The best NHC backbone remains the imidazolylidene based structure.
- Polynuclear complexes were less active than their mononuclear analogues.
- Complexes featured with benzaldehyde were promising candidates for further derivatization by oxime ligation.
- The best IC₅₀ values were obtained for two simple [(NHC)PtI₂(pyr)] complexes **18** and **30** with nitrobenzene and anthracene moieties as *N*-substituents.

5.1.4 Platinum complexes bearing tridentate ligands



Complex	MCF7	HCT116	PC3	OV3	MRC5	EPC
cisplatin	19.8±0.6	6.4±0.2	10±1	18±2	12.5±0.1	76±10
117	>100	70±4	>100	69±31	52±17	>100
131	20±8	4.4±0.3	52±7	21±1	29±3	5.88±0.01
149	85±13	2.9±0.4	53±6	24±3	58±2	>100

Table 39: IC₅₀ values of tridentate complexes: failure of these structures

Luminescence properties of platinum complexes made them interesting potential biological probes. Inhibition concentration of three tridentate complexes [(O[^]C[^]O)Pt(pyr)] **117**, [(O[^]N[^]O)Pt(pyr)] **137** and [(O[^]N[^]O)Pt(NHC)] **149** were measured (**Table 39**).

[(O[^]C[^]O)Pt(pyridine)] complex **117** was inactive against all cell lines. Complex **117** might be to hindered (*t*Bu groups) to interact with biological moieties.

In contrast, [(O[^]N[^]O)Pt(pyridine)] **131** was moderately active against only HCT116 and EPC cells. In this complex, the pyridine-platinum bond was stronger than for classical NHC-Pt-pyr complexes impeding an easy substitution of the pyridine by nucleophiles. [(O[^]N[^]O)Pt(NHC)] **149** presented moderate activity against only one cell line (HCT116). This complex has no labile ligand under mild conditions that could be substituted by DNA or other biomolecule.

5.1.5 Biological properties of post-synthetic modified complexes by ligand exchange and imine condensation

Post-synthetic modification by ligand exchange allowed easy access to various compounds. IC₅₀ (μM) of a mustard platinum derivative **157** is presented in **Table 40**. This compound has good cytotoxic properties in the micromolar range comparable to previously described non-functionalized complexes, thus showing that the mustard fragment did not improve efficiency.

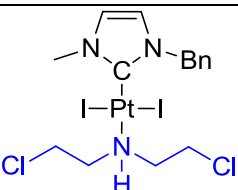
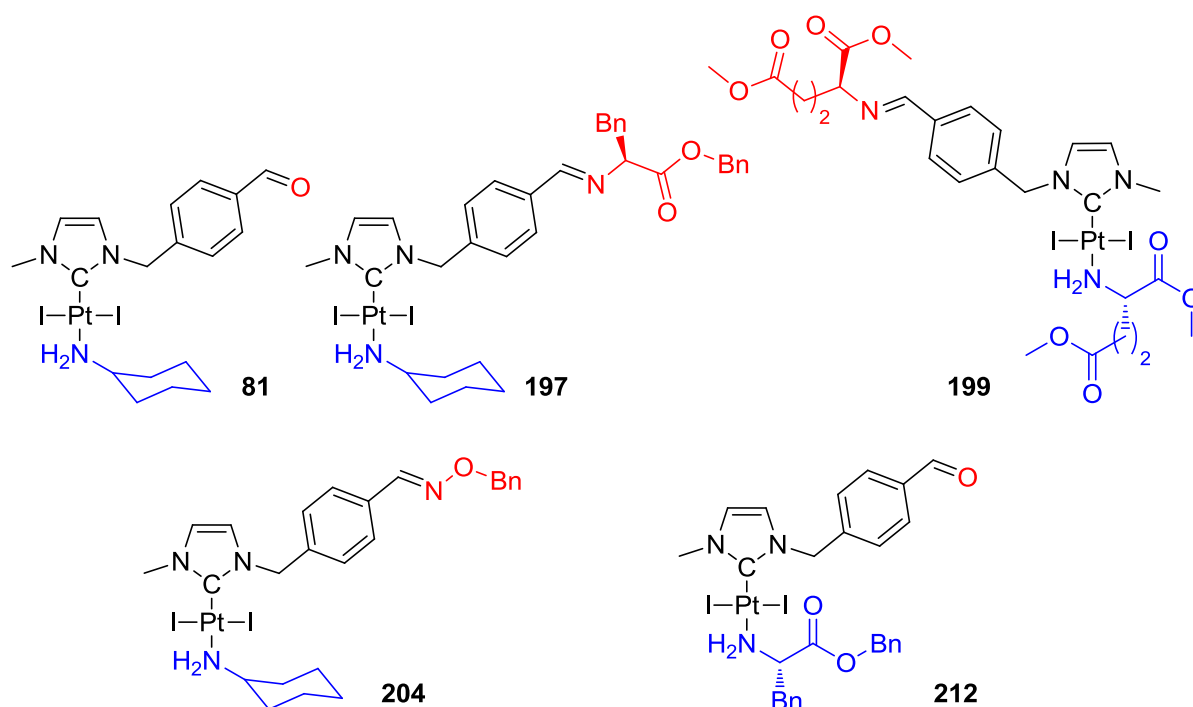
Complex	HCT116	MCF7	MRC5	PC3
 157	1.21±0.08	1.68±0.05	2.63±0.06	0.68±0.04

Table 40: IC₅₀ (μM) of a mustard platinum derivative 157

Post-synthetic modification of aldehyde complexes by imine or oxime conjugation allowed us to generate a huge library of various complexes. The biological activity of non-functionalized compounds was used as a reference to quantify the impact of introduction of several functionalities (amino acids, urea derivatives).

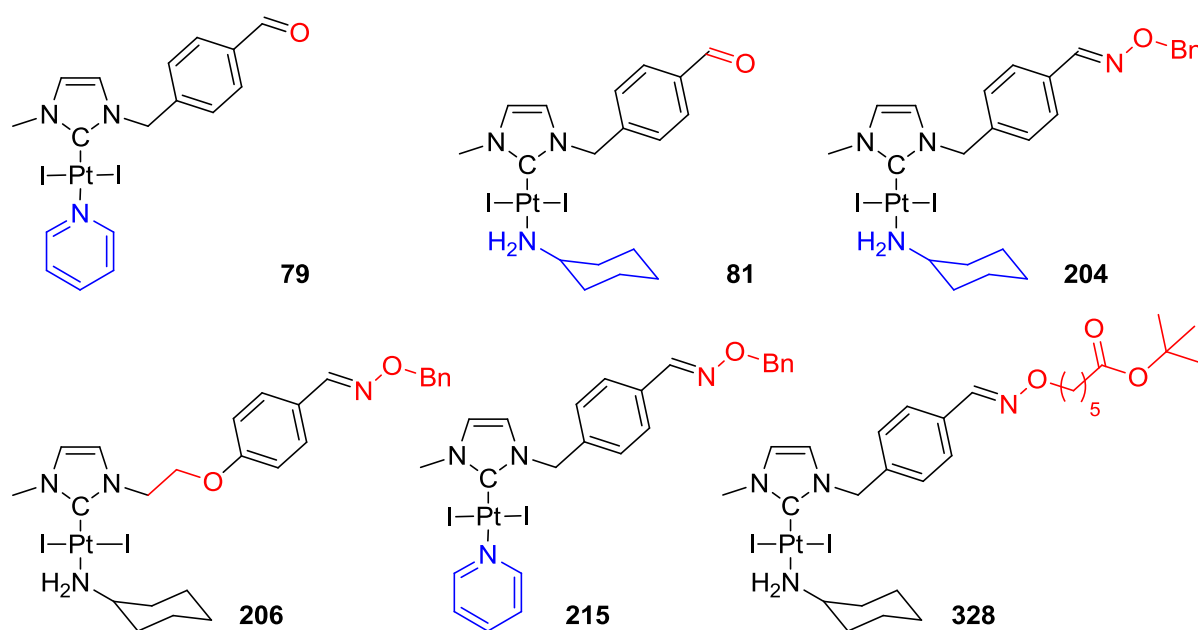
Table 41 summarizes inhibition percentages of complexes **197**, **199**, **204** and **212** functionalized by imine formation as well as by ligand exchange. Compared to the non-functionalized benzaldehyde complex **81**, it is of great importance to note that oxime or imine formation did not affect inhibition potential. We suppose that imine hydrolysis released the simple benzaldehyde complex **81** in biological media leading to similar toxicity. Nevertheless the stability of oximes does not allow this hypothesis and their similar toxicity should rather be explained by the innocent character of oximes that do not modify solubility or steric properties of the corresponding complexes (**204**). Ligand exchange with an amino acid (**212**) did not allow increased toxicity. Surprisingly, double functionalization (imine and ligand exchange) with *O*-CH₃ protected glutamic methylester made compound **199** inactive even at 10⁻⁵ M.



Complex	81		197		199		204		212	
[c] (M)	10 ⁻⁵	10 ⁻⁶	10 ⁻⁵	10 ⁻⁶	10 ⁻⁵	10 ⁻⁶	10 ⁻⁵	10 ⁻⁶	10 ⁻⁵	10 ⁻⁶
KB	100	39	100	51	7	0	100	58	100	52
MCF7	99	22	99	22	14	0	100	29	99	37
HCT116	97	49	97	70	1	0	97	79	97	73
PC3	93	17	91	18	11	3	94	26	93	22
SK-OV3	97	23	98	29	12	0	98	31	95	32
OVCAR-8	99	32	98	62	15	4	100	63	99	69
HL60	94	30	95	55	12	0	98	51	95	61
MRC5	99	8	98	48	2	0	99	60	98	74
Vero	100	42	100	68	17	15	100	53	100	59
EPC	98	16	79	0	0	26	100	27	95	40

Table 41: Cell viability inhibition percentage (±5%) of complexes functionalized by imine formation / ligand exchange

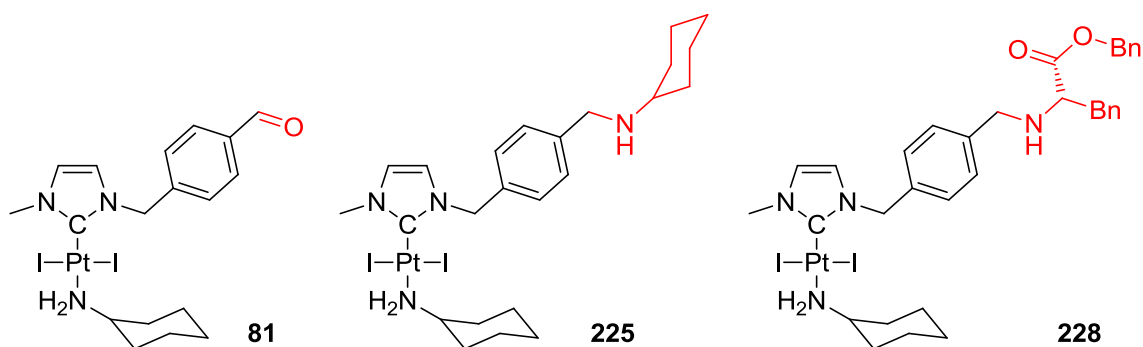
IC₅₀ values were measured for several oxime-functionalized complexes **204**, **206**, **215**, and **328** (Table 42) to ascertain inertness of oxime towards activity. As the complexes all showed similar activities, oxime ligation may be a tool for functionality introduction (targeting agents, fluorescent groups, etc.) without modifying the cytotoxicity due to the NHC-Pt(II) moiety.



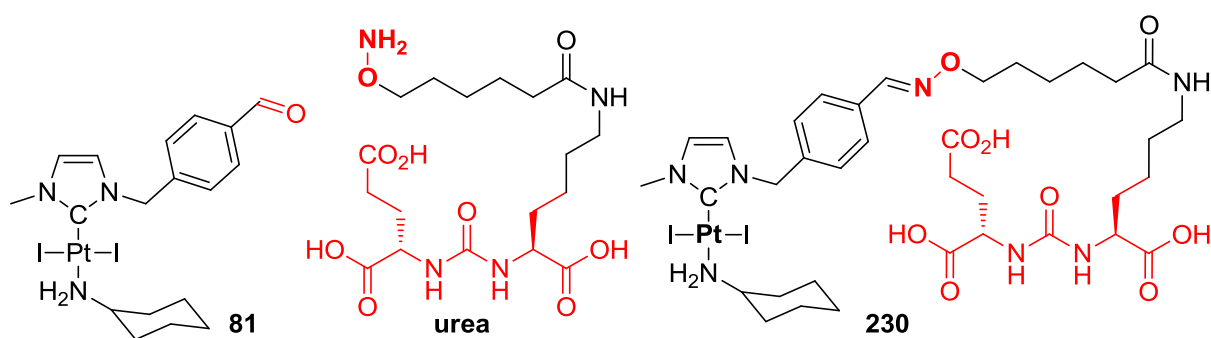
Complex	MCF7	HCT116	PC3	OV3	MRC5	EPC
cisplatin	19.8±0.6	6.4±0.2	10±1	18±2	12.5±0.1	76±10
79	0.49±0.07	4.6±3.3	0.93±0.03	1.5±0.4	0.60±0.02	1.8±0.2
81	0.8±0.2	0.26±0.02	0.50±0.03	0.28±0.02	0.40±0.01	0.94±0.03
204	0.35±0.03	0.13±0.02	0.28±0.02	0.19±0.01	0.14±0.01	0.33±0.07
206	0.885±0.005	0.09±0.02	2.6±0.6	1.31±0.03	0.7±0.2	1.14±0.06
215	2.4±0.3	1.1±0.1	n.d.	n.d.	n.d.	5.5±0.7
328	1.11±0.03	0.445±0.005	1.1±0.1	0.67±0.02	0.66±0.05	1.0±0.3

Table 42: IC₅₀ (μM) of oxime functionalized platinum complexes: maintain of activity after derivatization

IC₅₀ values of reduced imines **225** and **228** (Table 43) were similar to benzaldehyde precursor **81**. This variation of *N*-substituents seemed to be far enough from the platinum core and thus did not affect its activity. This strategy allows generation of amino acid featured complexes without alteration of platinum activity.



Complex	MCF7	HCT116	PC3	OV3	MRC5	EPC
cisplatin	19.8±0.6	6.4±0.2	10±1	18±2	12.5±0.1	76±10
81	0.8±0.1	0.255±0.005	0.50±0.03	0.28±0.02	0.40±0.01	0.94±0.003
225	0.855±0.005	0.09±0.01	0.375±0.005	0.26±0.03	0.16±0.02	0.41±0.01
228	0.515±0.005	0.175±0.005	0.50±0.02	0.345±0.005	0.285±0.005	1.5±0.2

Table 43: IC₅₀ values (μM) for reduced imines: maintain of activity after derivatization

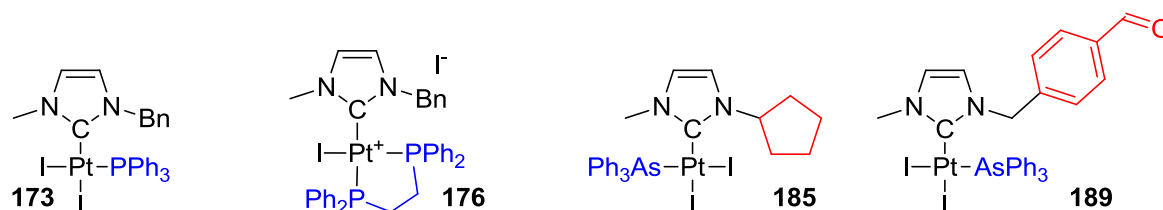
Complex	MCF7	HCT116	PC3	OV3	MRC5	EPC
cisplatin	19.8±0.6	6.4±0.2	10±1	18±2	12.5±0.1	76±10
81	0.8±0.1	0.255±0.005	0.50±0.03	0.28±0.02	0.40±0.01	0.94±0.3
urea	>100	>100	>100	>100	>100	>100
230	87±7	26±4	58±20	70±28	88±9	94±6

Table 44: IC₅₀ values (μM) of a Pt urea derivative: Moderate activity

Finally, **Table 44** displays the activity of non-functionalized benzaldehyde complex **81**, of a PSMA targeting urea-hydroxylamine derivative and of the final conjugate **233**. While the urea alone was inactive, the conjugation with platinum **230** resulted in a molecule with moderate activity. Compared to non-functionalized complex **81**, IC_{50} values were two orders of magnitude higher for the conjugate **230** clearly indicating that conjugation of the urea leads to diminished cytotoxicity. To access targeting, further investigations should be undertaken with PSMA expressing cell lines (PC3 cells (prostate carcinoma) are PSMA negative).

5.1.6 Cytotoxicity of platinum complexes containing pnictogen ligands

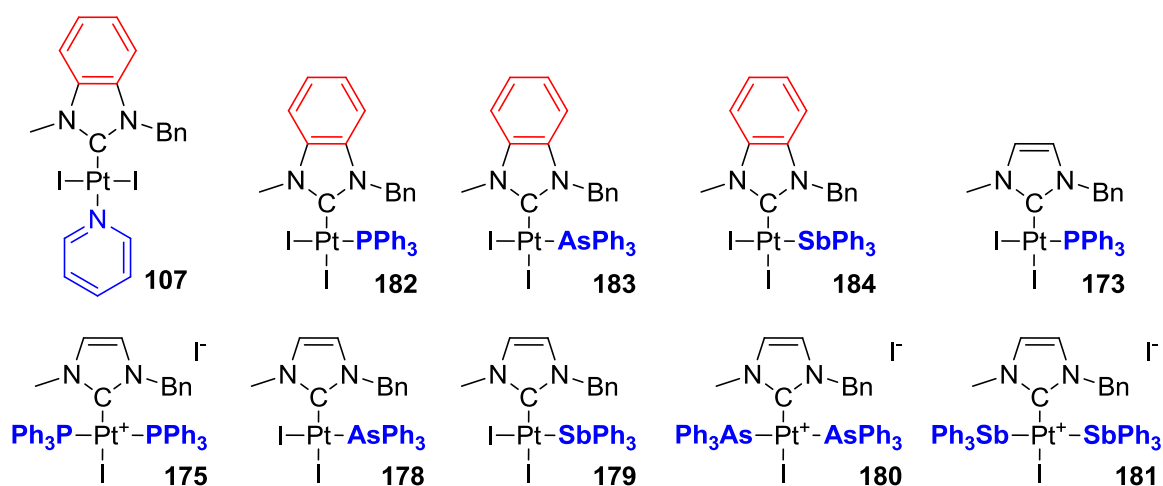
The influence of neutral ligands on NHC complexes biological activities was investigated by introduction of various pnictogen ligands (**Table 45**). While $[(C_5H_9-NHC)PtI_2(AsPh_3)]$ complex **185** was extremely active, its benzaldehyde analogue **189** was less active. Even its pyridine **79** or cyclohexylamine analogues **81** were more active than **189**. $[(NHC)PtI_2(PPh_3)]$ complex **173** had very interesting activities against all cell lines except MCF7 and EPC. Cationic $[(NHC)PtI(dppe)]^+ I^-$ complex **176** presented good activities, especially in comparison to the previously mentioned morpholine featured complex. These properties made the cationic diphosphine complex a promising example for development of a new class of platinum complexes combining NHC with phosphine ligands.



Complex	MCF7	HCT116	PC3	OV3	MRC5	EPC
cisplatin	19.8±0.6	6.4±0.2	10±1	18±2	12.5±0.1	76±10
173	8.4±0.9	1.9±0.9	4.9±0.8	0.9±0.3	3.3±0.9	12.1±0.4
176	1.5±0.3	0.50±0.04	n.d.	n.d.	n.d.	2.2±0.2
185	0.8±0.1	0.065±0.005	0.28±0.01	0.11±0.01	0.12±0.02	0.98±0.05
189	18.0±0.5	1.8±0.3	6.3±0.6	2.30±0.02	2.69±0.08	34.8±0.6

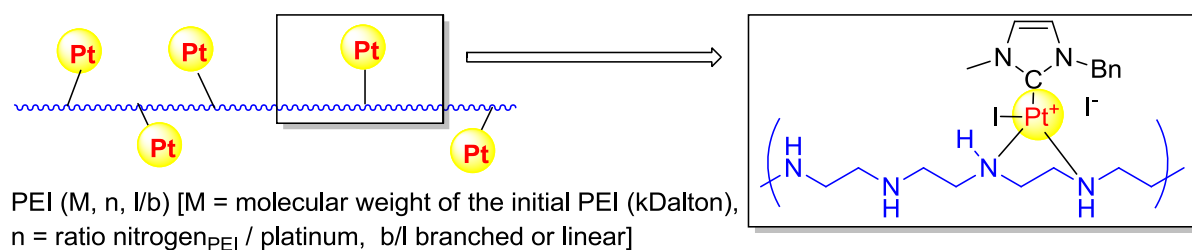
Table 45: IC_{50} (μM) of pnictogen Pt NHC complexes: complexes outstripping cisplatin

To better understand the influence of pnictogen elements and compare neutral / cationic complexes, we summarized the IC₅₀ (μM) values of two series of Pt complexes containing pnictogen ligand in **Table 46**. Three benzimidazolylidene complexes **182-184** were compared with their pyridine precursor **102** which remained the most active. The phosphine complex **182**, arsine complex **183** and stibine complex **184** present moderate activity. Between the three neutral imidazolylidene **173**, **178** and **179** complexes, only the phosphine complex **173** presented moderate activities. Between the three cationic imidazolylidene **175**, **180** and **181** complexes, the stibine complex **181** was only moderately active. Luckily, both arsine **180** and phosphine **175** complexes presented high cytotoxicity. Noteworthy, the cationic complexes (**175**, **180**, and **181**) always were more active than their neutral analogues. To conclude, these cationic complexes showed the best activities of the series.



Complex	HCT116	MCF7	MRC5	PC3
Cisplatin	ND	ND	ND	ND
107	0.96±0.56	1.32±0.17	5.52±0.78	2.82±0.92
182	ND	ND	8.77±1.94	3.14±1.21
183	2.32±0.38	2.05±0.52	2.48±0.24	3.49±0.58
184	4.05 ±0.69	9.93±0.26	ND	ND
173	3.48±0.15	5.69±0.51	5.73±0.68	4.42±0.56
175	1.76±0.07	1.87±0.57	1.47±0.66	1.83±0.77
178	7.40±0.74	ND	11.60±2.31	5.72±0.29
180	0.75±0.38	1.58±0.08	1.59±0.79	2.60±0.59
179	7.54±2.60	ND	8.51±1.52	5.05±1.62
181	3.92±0.66	5.02±0.5	3.99±0.11	4.69±0.88

Table 46: IC₅₀ (μM) of pnictogen ligand functionalized Pt NHC complexes. (ND: no activity below 10 μM)

5.1.7 *In vitro* studies of polyethylenimine platinum complexes**Figure 196: Schematic representation of PEI (M, n, b/l) platinum complexes used in this work**

Polyethylenimine (PEI) conjugates are interesting vectors to allow solubilisation of our complexes in biological media. In preliminary studies, the cytotoxicity of PEI (3.17, 20, b) and PEI (52.6, 10, l) were been studied and showed very promising results.¹²⁸ Inhibition concentration investigations⁵⁵⁰ showed high inhibition (64-99%) of the linear compound at 10^{-5} M, whereas only modest results were obtained for branched PEI-Pt (<43%). Cationic [(NHC)Pt(diethylenetriamine)]²⁺ 2I⁻ **173** remained completely inactive, confirming previous observations of poor toxicity for most charged complexes. These results led us to further investigate linear PEI-Pt complexes.

PEI	(1.8,15, b)		(2.5,10)		(2.500,20)		(2.5,30)		(25,20)		(250.000,20)	
[c] (M)	10^{-5}	10^{-6}	10^{-5}	10^{-6}	10^{-5}	10^{-6}	10^{-5}	10^{-6}	10^{-5}	10^{-6}	10^{-5}	10^{-6}
KB	5	0	14	13	28	6	57	0	92	5	9	0
MCF7	0	0	87	2	91	0	99	0	99	0	0	0
HCT116	0	0	69	18	91	0	95	5	95	8	14	0
PC3	13	2	82	3	82	10	95	7	91	0	22	0
SK-OV3	0	0	96	5	98	9	99	46	100	0	70	0
OVCAR-8	10	14	69	3	99	27	100	34	100	5	52	5
HL60	0	0	96	1	95	1	96	38	96	0	57	0
MRC5	0	0	13	0	91	5	100	1	100	4	45	0
Vero	0	0	21	24	78	19	98	9	98	0	2	0
EPC	25	16	68	15	96	25	98	39	97	16	44	7

Table 47: Cell viability inhibition percentage ($\pm 5\%$) at 10^{-5} and 10^{-6} M of PEI (M, n, l) complexes dissolved in EtOH⁵⁵⁰ For comparison purposes, all concentrations referre to platinum concentration.

Table 47 summarizes inhibition percentage at 10^{-5} and 10^{-6} M of PEI complexes with various chain lengths and N_{PEI}/Pt ratio (M, n, l). Comparison of PEI (M, 20, l) with various molecular weights (2.5, 25 and 250 kD) (and N/Pt constant) revealed poor inhibition for M = 2.5 and absence of activity for M = 250 kD whereas the best activities were measured for 2.5 and 25 kD. The disappointing result for 250kD can be explained by its low solubility in both ethanol and water. Good results for 2.5 and 25 kD may be correlated to the well-known transfection ability inherent in PEI 22 kD. Switching the ratio of N/Pt from 10 to 30 for PEI (2.5, n, l) (in this case M = constant) gave moderate results for n = 10 and high antiproliferative properties for n = 20 and especially for n = 30. We can suppose that compound n = 30 was the most similar of all PEI-Pt to free PEI and so the PEI transfection properties were less affected. In PEI (2.5, 10, l), high Pt concentration may completely modify their physico-chemical properties (H^+ sponge properties, solubility, cell penetration and DNA complexation ability). As a conclusion, linear PEI-Pt with platinum loading of from n = 20 to 30 were best candidates for anticancer applications.

To confirm this result, IC_{50} values were measured on BJAB cells (**Table 48**) and PEI (250, 20, l) showed excellent activity but its poor solubility make it hard to reproduce. In this case, we did not observed the same trend as for PEI complexes n = 20 and 30 which had better activities than complex n = 10. PEI-Pt n = 30 presented similar activity than PEI-Pt n = 10.

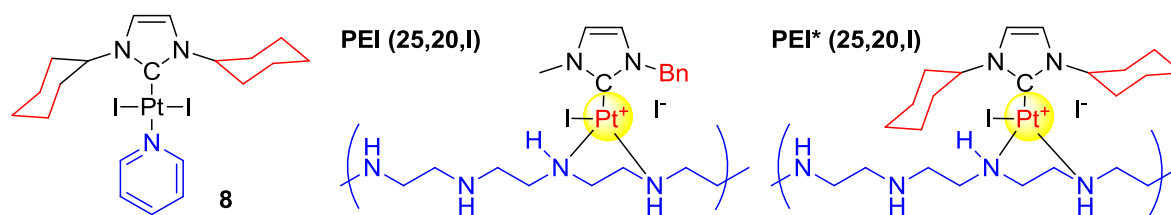
PEI (M, n, l)	(1.8,15)	(2.5,10)	(2.5,20)	(2.5,30)	(25,20)	(250, 20)
IC_{50} (μM)	11.386	17.837	8.574	19.119	13.646	0.950

Table 48: IC_{50} (μM) of PEI (M, n, l) platinum complexes dissolved in DMSO against BJAB cells

PEI (25,n,l)	MCF7	HCT116	PC3	OV3	MRC5	EPC
(25,10)	28 \pm 1	21.65 \pm 0.05	32.4 \pm 0.7	24 \pm 4	28 \pm 4	33.1 \pm 0.3
(25,20)	0.60 \pm 0.01	0.755 \pm 0.005	0.90 \pm 0.02	0.58 \pm 0.01	1.1 \pm 0.2	1.8 \pm 0.5
(25,30)	0.9 \pm 0.2	1.205 \pm 0.005	0.94 \pm 0.06	0.3 \pm 0.2	1.0 \pm 0.2	1.94 \pm 0.02

Table 49: IC_{50} (μM) of PEI (25, n, l) platinum complexes dissolved in EtOH against 6 cell lines

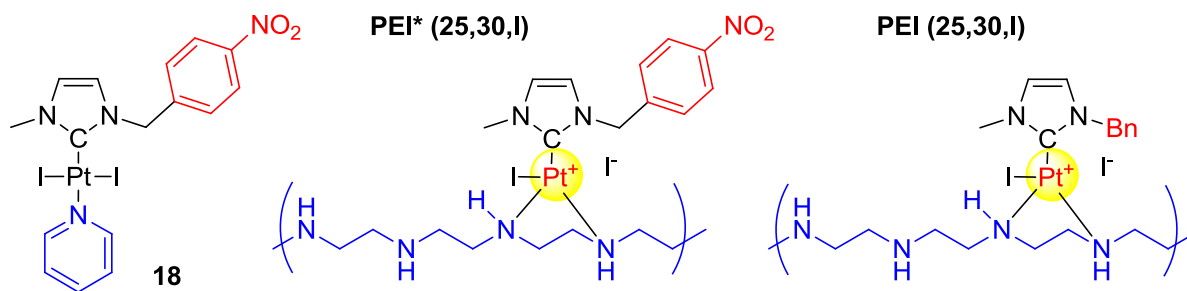
To obtain more informations about biological properties of these compounds, IC_{50} (μM) of PEI (25, n, l) of various ratio N/Pt were measured (**Table 49**). Cytotoxicity appeared to be cell line independent except for EPC (lower toxicity). We clearly see that n = 10 presented low activity (IC_{50} 20-33 μM), whereas activities of PEI (25, 20, l) and PEI (25, 30, l) were both in the micromolar range (0.5-2.3 μM). as a conclusion, we can state that PEI Pt complexes (M, n, l) with M = 2.5 and 25 and n = 20 and 30 were the best candidates for further exploration of antiproliferative properties.



Complex	Solvent	MCF7	HCT116	PC3	OV3	MRC5	EPC
cisplatin	H ₂ O	19.8±0.6	6.4±0.2	10±1	18±2	12.5±0.1	76±10
8	DMSO	0.22±0.02	2±2	0.35±0.01	0.29±0.01	0.295±0.005	0.54±0.01
PEI (25,20,I)	EtOH	0.60±0.01	0.755±0.005	0.90±0.02	0.58±0	1.1±0.2	1.8±0.5
PEI* (25,20,I)	EtOH	6.0±0.4	3.4±0.3	6.0±0.1	3.4±0.2	6.5±0.2	19±5

Table 50: IC₅₀ (μM) of a PEI* (25,20,I) complexes with a di-cyclohexyl *N*-substituted NHC

The last modification to investigate was the influence of the NHC structure on PEI-Pt complexes inhibition. A PEI adducts containing a NHC with two cyclohexyl groups as *N*-substituents PEI* (25,20,I) was compared with our usual (Me, Bn)NHC PEI (25,20,I) (Table 50). Both PEI compounds had IC₅₀ lower than the benchmark cisplatin. Nevertheless, our usual (Me, Bn)NHC PEI (25,20,I) was one magnitude more active than its cyclohexyl analogue. Additionally, the cyclohexyl-NHC PEI conjugate also was less active than its neutral [(NHC)PtI₂(pyr)] precursor 8.



Complex	HCT116	MCF7	EPC
Cisplatin	6.4±0.2	19.8±0.6	76±10
PEI* (25,30,I)	1.55±0.05	1.65±0.05	1.85±0.05
PEI (25,30,I)	1.205±0.005	0.9±0.2	1.94±0.02
18	<0.005	0.035±0.005	0.075±0.005

Table 51: IC₅₀ (μM) of a PEI* (25,30,I) Pt with a *N*-nitrotoluene substituted NHC structure

As nitrotoluene *N*-substituted complex **18** presented excellent cytotoxic activity, we also tested its PEI conjugate PEI* (25,30,1) (**Table 51**). Surprisingly, this conjugate was less active than its neutral precursor as well as our usual NHC PEI (25,30,1) with a benzyl as *N* substituent,

As a conclusion, the *N*-benzyl substituted NHC platinum moiety seemed to be the best candidate for further investigations. PEI (25,30,1) compound, which overall showed the best *in vitro* activities, was chosen for *in vivo* tests.

5.1.8 Conclusions on *in vitro* biological activities of NHC Pt complexes

From these *in vitro* results, general trend could be envisioned. Thus three functionalities types should be avoided to keep high cytotoxicity of [(NHC)PtI₂(L)] type complexes: polar functionalities, charged functional groups and long alkane or PEG chains. Polynuclear complexes or tridentate ligands based structures were poorly active.

Overall, three structures presented excellent results: simple [(NHC)PtI₂(pyr)] complexes **18** and **30** with nitrotoluene and anthracene as *N*-substituents, cationic [(NHC)PtI(dppe)]⁺I⁻ complex **176** and neutral NHC-arsine derivate **185**.

Functionalization of benzaldehyde-based complexes maintained similar activity in the case of innocent oximes. A urea derivative presented poor toxicity, nevertheless its potential as targeting agent should be further investigated. Pt-PEI (25,30,1) complex gave easy access to water-solubility and enhanced activity allowing it to further investigate its *in vivo* properties.

5.2 Preliminary *in vivo* studies of PEI platinum NHC conjugates

In vivo studies were undertaken in collaboration with Pr. Sylvie Fournel and Neila Chekkat (University of Strasbourg, Faculty of Pharmacy, Laboratory of conception and application of bioactive molecules - UMR 7199 CNRS - Illkirch). Herein the first preliminary results recently obtained on mice will be discussed. To immunodeficient 5-week-old mice were intraperitoneal injected 5.10^6 HCT116 cells (human adenocarcinoma). After 5 days, the cancer xenograft was palpable and the animals were randomly sorted into four treatment groups presenting a mean tumour volume of 25 mm³. Three groups were used as control groups and treated in intraperitoneal injection route over 48h during 15 days by:

- NaCl (0.9%): to evaluate the consequences of vehicle injection on mice
- EtOH (10%) and NaCl (0.9%): to evaluate toxicity due to ethanol itself
- Oxaliplatin (10 mg/kg, i.e. 25 μ mol of Pt/kg), EtOH (10%), NaCl (0.9%) (Sigma Aldrich, # O9512),: oxaliplatin was the benchmark drug

Fourth group was treated with our PEI (25,30,I) compound (10 mg/kg, i.e. 5 μ mol of Pt/kg) dissolved in a serum solution (EtOH (10%) / NaCl (0.9%)). Noteworthy, at 10 mg/kg, oxaliplatin contained five times higher Pt (II) molar concentration than the PEI (25,30,I) complex at 10 mg/kg.

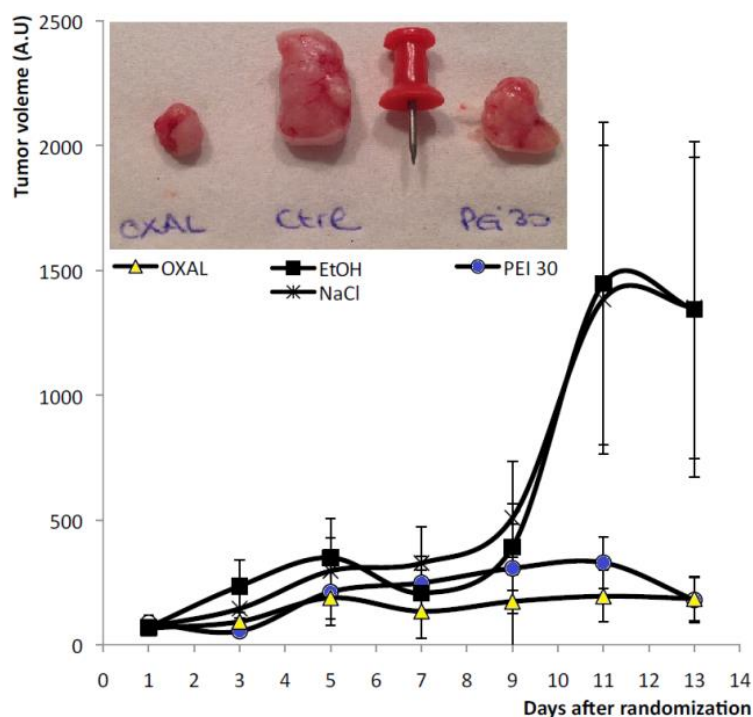


Figure 197: Xenograft volume growth on mice treated by PEI (25,30,I) Pt (5 μ mol of Pt/kg) and control groups: at 10 mg/kg, similar inhibition of our compounds and well-established oxaliplatin (25 μ mol of Pt/kg) was observed

This treatment was repeated every two days and tumour volume was determined by calibre measurement and normalized toward the tumour volume observed at the beginning of the treatment. Tumour volume, reported in **Figure 197**, showed the expected uncontrolled growth for the two control groups. After 5 days, tumour size of PEI treated mice outmatched the size of oxaliplatin reference group. This experiment was stopped after 13 days for ethical reasons (tumour size of control groups exceeds ethically acceptable size). At this day, mean tumour volume was identical for PEI treated mice and oxaliplatin group.

Only in the case of oxaliplatin treated mice, severe side effect was observed (**Figure 198**). These animals were subject to hematomas caused by platinum drug, a side effect also observed in human oxaliplatin treatment.⁵⁵¹ Fortunately, this side effect was not observed for our PEI-Pt derivative.



Figure 198: Tumour (arrow marked) of control group (left); oxaliplatin treated mouse (right): hematomas caused by oxaliplatin not observed for PEI conjugates

⁵⁵¹ Koutras, A. K.; Makatsoris, T.; Paliogianni, F.; Kopsida, G.; Onyenadum, A.; Gogos, C. A.; Mouzaki, A.; Kalofonos, H. P. *Oncology* **2004**, 67, 179.

Treatment efficiency of our platinum complex was also demonstrated by its mice survival curve (**Figure 199**). Until 13 days, all PEI (25,30,l) treated animals were still alive, while one of oxaliplatin control group was already dead. The 13th days, three PEI-Pt and three other oxaliplatin treated animals were sacrificed, finally 16th day the rest of the mice. Similar phenomena for non-platinum control groups: after 13 days, 4 animals and on 16th day the last one, were sacrificed. Noteworthy, survival probability of PEI (25,30,l) seems to surpass oxaliplatin.

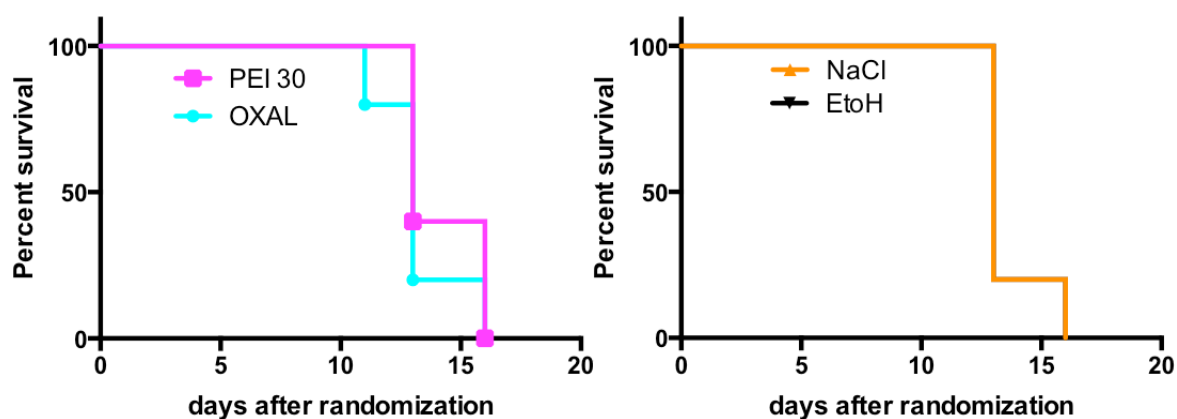


Figure 199: Mice survival curve of PEI (25,30,l) treated mice and control groups

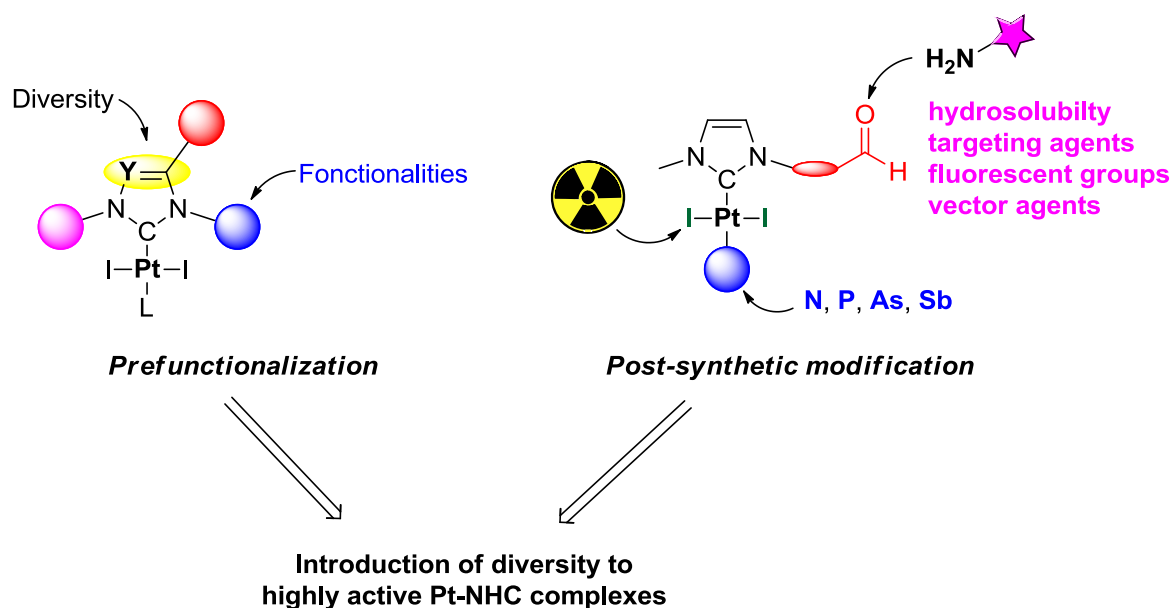
Finally, these *in vivo* results proved our platinum NHC PEI conjugate to have higher antitumor activity than the well-established oxaliplatin even when administrated at 5 times lower dose. Additionally, mice treated with our complex did not show any apparent side effects. Further investigations should elucidate several points:

- Long-time survival probability
- Dose-dependency of the PEI-Pt
- Bio-distribution of the PEI-Pt complex
- Combination treatment with established non-platinum anticancer drugs
- Mechanistic and toxicity studies *in vitro* and *in silico*

The ease of access and the modularity of these water-soluble compounds will allow fine-tuning of their properties to access new drugs.

6 General conclusion

Metal *N*-Heterocyclic Carbene (NHC) complexes are organometallic compounds which have already proved their potential for cancer therapy. In particular, *in vitro* studies confirmed the evidence of various NHC-containing platinum compounds, which have a significantly higher cytotoxicity than cisplatin. However, the (pre)clinical development of these new drugs induces several challenges that are inherent of *in vivo* validation. Parameters such as solubility or stability in aqueous solution become crucial at this point. *In vivo*, the molecule should also be inert towards biological environment before reaching the targeted cells thus avoiding interference and deactivation. They should exhibit high selectivity toward cancer cells and rapid clearance from non-targeted cells. Active targeting with a suitable ligand displaying high affinity for specific receptors is thus needed. All these requirements should be pre-evaluated and modulated by means of simple synthetic and highly tuneable pathways. At this stage, the development of modular approaches allowing quick access to functionalized and conjugated NHC metal complexes is of capital use for selecting the best candidates for further clinical development.



In this work, we synthesized a large library of new platinum complexes stabilized by *N*-Heterocyclic Carbenes with general formula [(NHC)PtX₂(L)], where X represent a halogen ligand and L a neutral ligand. We focused our attention on introduction of molecular diversity on these complexes. The first step was the coordination of NHC precursors containing various substituents to platinum. As a second strategy, post-synthetic functionalization of platinum complexes has been fully investigated by:

- imines, hydrazones or oxime formation

- ligand exchange reaction with various amines (including polyamines) and pnictogen-based ligands (phosphines, arsines, stibines)
- halogen exchange for iodide isotopes introduction

Moreover, these post-synthetic modifications could be combined thus giving an access to increased diversity.

Using the first approach (i.e. pre-functionalization), we synthesized a whole library of Pt-NHC compounds bearing various chemical functions such as hydroxyl, amines, nitriles, esters, acids or phosphonates. The second approach was found to be more promising as it allows generation of large number of molecules. For example, Prostate-Specific Membrane Antigen (PSMA) targeting urea hydroxylamine derivative could be introduced by oxime conjugation onto the NHC-platinum. These complexes could also be stabilized by PEI polymers giving highly water-soluble products.

Cytotoxic properties of these new compounds were evaluated *in vitro* on several cancerous and non-cancerous cell lines revealing various trends. Lipophilic molecules generally showed IC₅₀ values in micromolar or nanomolar concentration at best. A decrease of activity was noticed with polar or charged complexes with the exception of cationic phosphine complex and PEI conjugates.

Finally, antitumor properties of a PEI-Pt conjugate were tested *in vivo* on mice model. This compound showed similar tumour inhibition as oxaliplatin. Besides, no “visual” side effects were detected in contrast to oxaliplatin (hematomas). These preliminary results make these compounds promising anticancer agents for further investigations.

Some of the complexes reported here also showed interesting luminescent properties. Tridentate-based (O⁺C⁺O) and (O⁺N⁺O) ligands were synthesized and coordinated toward metals of the group 10 (Ni, Pd, Pt). (O⁺C⁺O) type complexes presented a weak luminescence in solution only at low temperature (77K) whereas (O⁺N⁺O) complexes showed strong luminescence properties in the solid state.

These outstanding results opened up new perspectives in the field of platinum-based drugs. Modular bis-functionalization may be applied to introduce further of functionalities to the complexes. Especially, conjugation with targeting agents or fluorescent groups can be envisioned to increase selectivity toward cancerous cells. Double functionalization should allow potential *in vivo* investigations by fluorescence and FRET technics. Cleavability of hydrazone or oxime linkers in acid conditions may be of huge interest for efficient intracellular drug release. We also should consider the possibility of grafting our complexes *via* phosphonate-amine or phosphonate-oxime linkers to nanoparticles or incorporation of the complexes into liposomes to obtain both selectivity and water solubility. Iodine isotope incorporation may allow *in vivo* bio distribution investigations of the complexes and enhance its cytotoxicity thanks to additional radioactivity.

7 Experimental part

7.1 General considerations

All manipulations were carried out using standard Schlenk techniques unless stated otherwise. Reagents were purchased from commercial chemical suppliers (mainly Acros, Aldrich, Alfa Aesar, TCI Europe and Strem) and used without further purification. Solvents were dried according to standard procedures. Solvents employed during complexation reactions (pyridine, cyclohexylamine, morpholine) were distilled over calcium hydride and carefully stored under argon. Metal complexes were synthesized using distilled solvents. ^1H , ^{13}C { ^1H } nuclear magnetic resonance (NMR) spectra were recorded on a Bruker Avance 300 spectrometer. ^{13}C assignments were confirmed when necessary with the use of DEPT-135 experiments. ^1H and ^{13}C -NMR spectra were referenced using the residual solvent peak (CDCl_3 : $\delta_{\text{H}} = 7.26$ ppm; $\delta_{\text{C}} = 77.16$ ppm; DMSO : $\delta_{\text{H}} = 2.50$ ppm; $\delta_{\text{C}} = 39.52$ ppm; CD_3OD : $\delta_{\text{H}} = 3.31$ ppm; $\delta_{\text{C}} = 49.00$ ppm; D_2O : $\delta_{\text{H}} = 4.79$ ppm; CD_2Cl_2 : $\delta_{\text{H}} = 5.32$ ppm; $\delta_{\text{C}} = 53.84$ ppm; Acetone: $\delta_{\text{H}} = 2.05$ ppm; $\delta_{\text{C}} = 29.84$ and 206.26 ppm) at 295K. Chemical shifts δ are given in ppm whereas coupling constants J are stated in Hertz (Hz). The following abbreviations are used to classify the multiplicity of the observed signals: s = singlet, d = doublet, t = triplet, q = quartet, quint = quintuplet, dd = doublet from doublet, dt = doublet from triplet, m = complex multiplet or broad signal, pyr = pyridine proton, CHA = cyclohexylamine proton, (CH=) = NHC alkene proton. Positive mode electrospray ionization mass spectra (ESI-MS) were recorded on microTOF, Bruker Daltonics by *Hélène Nierengarten* and *Mélanie Lebreton* at Institut de Chimie Mass Spectrometry Facility of the University of Strasbourg. UV-visible absorption spectra were recorded on a HITACHI U-3000 spectrophotometer, and fluorescence spectra on a Photon Technology International MD-5020. Measurements were carried out in aerated CH_2Cl_2 or CH_3CN solutions. X-Ray diffraction studies were carried out by *Dr. Lydia Brelot* at Institut de Chimie X-ray Facility of the University of Strasbourg. Crystal data were collected at 173 K using a $\text{MoK}\alpha$ graphite monochromated ($\lambda = 0.71073$ Å) radiation on a Nonius KappaCCD diffractometer. The structures were solved using direct methods with SHELXS97⁵⁵² and refined against F2 using the SHELXL97 software.⁵⁵³ Non-hydrogen atoms were refined anisotropically. Hydrogen atoms were generated according to stereochemistry and refined using a riding model in SHELXL97. Iodine isotope introduction experiments were undertaken by *Dr. Anthony Clotagatide* and *C. Darcissac* from Radiopharmacie CHU of Saint Etienne.

⁵⁵² L. Palatinus, G. Chapuis, *J. Appl. Cryst.* **2007**, 40, 786.

⁵⁵³ (a) G.-M. Sheldrick, *SHELXL97, Program for the refinement of Crystal Structures*, University of Göttingen: Göttingen, Germany, **1997**; (b) G.-M. Sheldrick, *Acta Cryst.* **2008**, A64, 112.

7.2 Synthesis of azolium salts

Unless mentioned, azolium salts are obtained using standard synthesis procedures in 250 mg to 1g scale. Monoalkylated imidazole precursors are obtained from imidazole and **halogenoalkanes** using standard procedures.⁵⁵⁴ Symmetrical imidazolium salts are obtained by a) Arduengo's classic multicomponent cyclization (1,3-dicyclohexyl-1H-imidazol-3-ium bromide)^{221,63}, b) reaction between (trimethylsilyl)imidazole and two equivalents of **halogenoalkane** in CH_2Cl_2 ²²² or c) refluxing of azole derivatives with excess of volatile **halogenoalkane** in toluene²²⁴. Unsymmetrical azolium salts are obtained by d) alkylation of azole derivatives with one equivalent of **halogenoalkanes** in CH_3CN overnight at 75 °C, or e) refluxing of azole derivative in volatile **halogenoalkanes** (MeI, BnBr, ...). Polyimidazolium salts are obtained by f) refluxing an excess of methylimidazole and **polybromoalkane** in CH_3CN at 75 °C overnight or g) alkylation by **halogenoalkane** of an polyimidazole derivative. In all cases, after evaporation of the volatiles, the crude product is first recrystallized in boiling pentane or diethylether, then dissolved in CH_2Cl_2 or methanol and precipitated by cold diethyl ether or pentane. The obtained product is used for complexation without further purification. **3-(anthracen-9-ylmethyl)-1-methyl-1H-imidazol-3-ium chloride**, **3-benzyl-1-methyl-1H-imidazol-3-ium bromide** and **3-benzyl-1-methyl-1H-imidazol-3-ium chloride** were obtained according to literature procedures.^{124, 555}

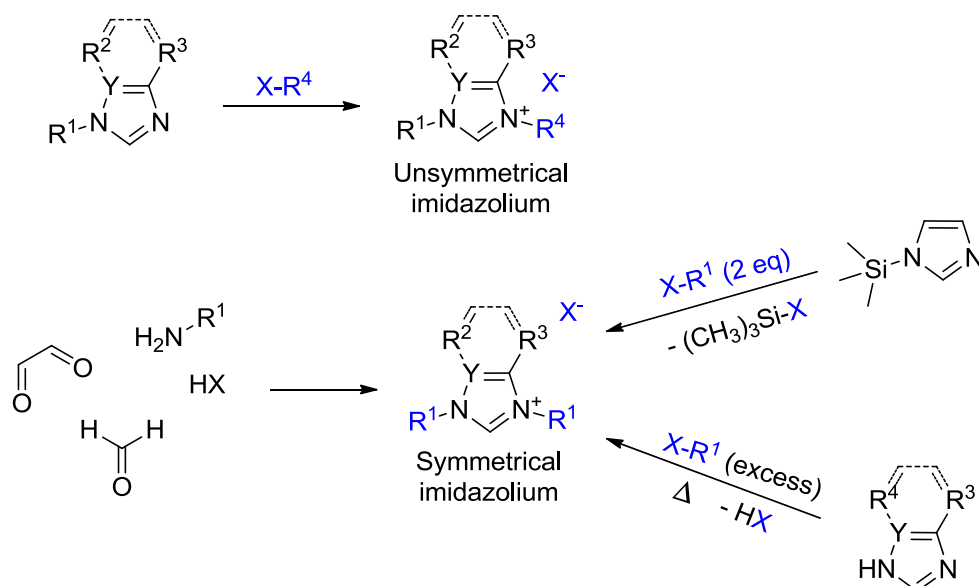
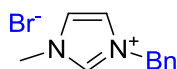


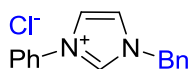
Figure 200: Imidazolium synthesis

⁵⁵⁴ Jiang, N.; Zhai, X.; Zhao, Y.; Liu, Y.; Qi, B.; Tao, H.; Gong, P. *Eur. J. Med. Chem.* **2012**, *54*, 534.

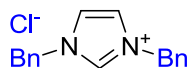
⁵⁵⁵ Fei, Z.; Zhu, D. R.; Yang, X.; Meng, L.; Lu, Q.; Ang, W. H.; Scopelliti, R.; Hartinger, C. G.; Dyson, P. J. *Chem. Eur. J.* **2010**, *16*, 6473.



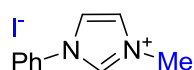
3-benzyl-1-methyl-1H-imidazol-3-ium bromide: Synthesis *e*: 92%, ^1H -NMR (CDCl_3 , 300 MHz, 20 $^\circ\text{C}$): δ 4.08 (s, 3H, N- CH_3), 5.58 (s, 2H, N- CH_2), 7.17 (s, 1H, CH), 7.23 (s, 1H, CH), 7.38-7.50 (m, 5H, CH_{ar}), 10.79 (s, 1H, NCHN). ^{13}C -NMR (CDCl_3 , 75 MHz, 20 $^\circ\text{C}$): δ 36.6 (N- CH_3), 52.8 (N- CH_2), 122.1 (CH), 123.8 (CH), 128.8 (CH_{arom}), 129.1 (CH_{ar}), 129.2 (CH_{ar}), 133.2 ($\text{C}_{\text{IV ar}}$), 136.6 (NCHN).



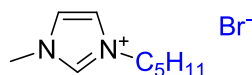
1-benzyl-3-phenyl-1H-imidazol-3-ium chloride: Synthesis *e*: quant. ^1H -NMR (CDCl_3 , 300 MHz, 20 $^\circ\text{C}$): δ 5.55 (s, 2H, N- CH_2), 6.98-7.21 (m, 6H, 6H_{ar}), 7.40-7.53 (m, 4H, 4H_{ar}), 7.00 (t, $J = 1.8\text{Hz}$, 1H, CH=), 7.82 (t, $J = 1.8\text{Hz}$, 1H, CH=), 77.15 (t, $J = 1.8\text{Hz}$, 1H, NCHN). ^{13}C -NMR (CDCl_3 , 75 MHz, 20 $^\circ\text{C}$): δ 52.9 (N- CH_2), 120.9 (CH=), 121.2 (CH_{ar}), 123.1 (CH=), 129.0 129.1 129.7 130.2 (CH_{ar}), 133.4 (C_{ar}), 134.2 (C_{ar}), 135.3 (NCHN).



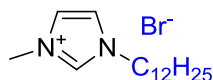
1,3-dibenzyl-1H-imidazol-3-ium chloride: Synthesis *c*: quant. ^1H -NMR (CDCl_3 , 300 MHz, 20 $^\circ\text{C}$): δ 5.55 (s, 4H, 2N- CH_2), 7.27-7.52 (m, 12H, 10H_{ar} and CH=CH), 10.92 (s, 1H, NCHN).



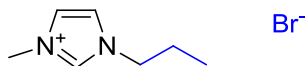
3-methyl-1-phenyl-1H-imidazol-3-ium iodide: Synthesis *e*: quant. ^1H -NMR (CDCl_3 , 300 MHz, 20 $^\circ\text{C}$): δ 4.13 (s, 3H, N- CH_3), 7.423 (m, 3H, 3H_{ar}), 7.67 (m, 2H, 2H_{ar}), 7.75 (t, $J = 1.8\text{Hz}$, 1H, CH=), 7.78 (t, $J = 1.8\text{Hz}$, 1H, CH=), 10.09 (s, 1H, NCHN). ^{13}C -NMR (CDCl_3 , 75 MHz, 20 $^\circ\text{C}$): δ 37.5 (N- CH_3), 121.1 (CH=), 122.0 (CH_{ar}), 125.0 (CH=), 130.3 (CH_{ar}), 130.5 (CH_{ar}), 134.3 (C_{ar}), 135.4 (NCHN).



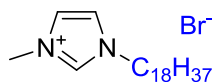
1-methyl-3-pentyl-1H-imidazol-3-ium bromide: Synthesis *d*: 92%, ^1H -NMR (CDCl_3 , 300 MHz, 20 °C): 0.48 (t, J = 6.9Hz, 3H, CH_3), 0.94 (m, 4H, 2CH_2), 1.54 (quint, J = 7.4Hz, 2H, CH_2), 3.75 (s, 3H, N- CH_3), 3.96 (t, J = 7.4Hz, 2H, N- CH_2), 7.30 (t, J = 1.8Hz, 1H, CH=), 7.43 (t, J = 1.8Hz, 1H, CH=), 9.86 (s, 1H, NCHN). δ ^{13}C -NMR (CDCl_3 , 75 MHz, 20 °C): δ 1.3.5 (CH_3), 21.7 27.8 29.6 (CH_2), 26.3 (N- CH_3), 49.6 (N- CH_2), 122.1 (CH=), 123.6 (CH=), 136.5 (NCHN).



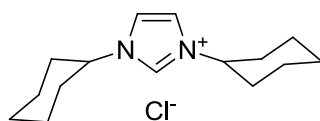
1-dodecyl-3-methyl-1H-imidazol-3-ium bromide: Synthesis *d*: 96%, ^1H -NMR (DMSO, 300 MHz, 20 °C): δ 0.83 (t, J = 6.6Hz, 3H, CH_3), 1.22 (m, 18H, 9CH_2), 1.76 (m, 2H, CH_2), 3.87 (s, 3H, N- CH_3), 4.17 (t, J = 7.1Hz, 2H, N- CH_2), 7.77 (t, J = 1.8Hz, 1H, CH=), 7.84 (t, J = 1.8Hz, 1H, CH=), 9.30 (s, 1H, NCHN). ^{13}C -NMR (CDCl_3 , 75 MHz, 20 °C): δ 13.9 (CH_3), 22.1 25.5 28.4 28.7 28.8 29.0 29.4 31.3 (CH_2), 35.7 (N- CH_3), 48.7 (N- CH_2), 122.2 (CH=), 123.5 (CH=), 136.5 (NCHN).



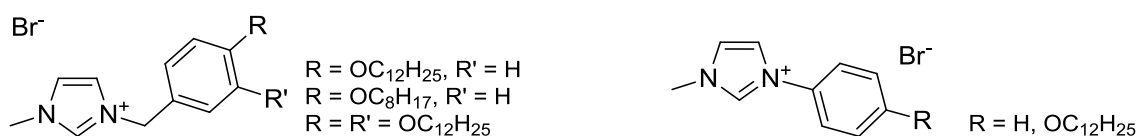
3-methyl-1-propyl-1H-imidazol-3-ium bromide: Synthesis *e*: quant. ^1H -NMR (DMSO, 300 MHz, 20 °C): δ 0.83 (t, J = 7.3Hz, 3H, CH_3), 1.79 (t, J = 7.2Hz, 2H, CH_2), 3.88 (s, 3H, N- CH_3), 4.16 (t, J = 7.1Hz, 2H, N- CH_2), 7.79 (s, 1H, CH=), 7.87 (s, 1H, CH=), 9.36 (s, 1H, NCHN). ^{13}C -NMR (CDCl_3 , 75 MHz, 20 °C): δ 13.9 (CH_3), 22.1 25.5 28.4 28.7 28.8 29.0 29.4 31.3 (CH_2), 35.7 (N- CH_3), 48.7 (N- CH_2), 122.2 (CH=), 123.5 (CH=), 136.5 (NCHN).



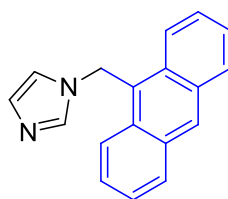
3-methyl-1-octadecyl-1H-imidazol-3-ium bromide: Synthesis *d*: 44%, ^1H -NMR (CDCl_3 , 300 MHz, 20 °C): δ 0.85 (t, J = 6.6Hz, 3H, CH_3), 1.22 (m, 30H, 15CH_2), 2.11 (m, 2H, CH_2), 4.11 (s, 3H, N- CH_3), 4.29 (t, J = 7.5Hz, 2H, N- CH_2), 7.36 (t, J = 1.8Hz, 1H, CH=), 7.52 (t, J = 1.8Hz, 1H, CH=), 10.44 (s, 1H, NCHN). ^{13}C -NMR (CDCl_3 , 75 MHz, 20 °C): δ 14.1 (CH_3), 22.6 26.2 29.0 29.3 29.5 29.7 30.3 31.9 (CH_2), 36.7 (N- CH_3), 50.2 (N- CH_2), 121.7 (CH=), 123.5 (CH=), 137.6 (NCHN).



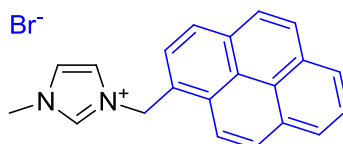
1,3-dicyclohexyl-1H-imidazol-3-ium chloride: Synthesis *a*:^{63,221} <50%, ¹H-NMR (MeOD, 300 MHz): δ 1.10-2.21 (m, 20H, Cy), 4.36 (m, 2H, 2N-CH), 7.79 (d, J = 1.5Hz, 2H, CH=CH), 9.24 (s, 1H, NCHN). ¹³C-NMR (CD₃OD, 75 MHz, 20 °C): δ 26.0 (CH₂ Cy), 32.0 (CH₂ Cy), 34.4 (CH₂ Cy), 61.3 (N-CH), 122.1 (CH=CH), 134.8 (NCHN).



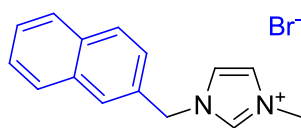
Alkane chain featured imidazolium bromide salts were obtained according to literature.²²⁷



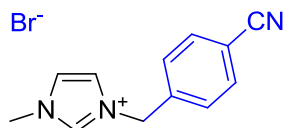
1-(anthracen-9-ylmethyl)-1H-imidazole: Synthesis adopting a literature process:⁵⁵⁴ ¹H-NMR (CDCl₃, 300 MHz, 20 °C): δ 5.88 (s, 2H, N-CH₂), 6.79 (s, 1H, CH=), 6.95 (s, 1H, CH=), 7.39-7.53 (m, 5H, 5H_{ar}), 7.96 (d, J = 8.2Hz, 2H, 2H_{ar}), 8.07 (d, J = 8.2Hz, 2H, 2H_{ar}), 8.43 (s, 1H, NCHN). ¹³C-NMR (CDCl₃, 75 MHz, 20 °C): δ 43.2 (N-CH₂), 119.3 (CH=), 121.7 122.9 125.4 127.5 128.8 129.5 130.8 131.4 135.1 (C_{ar}) and CH=), 136.7 (NCHN).



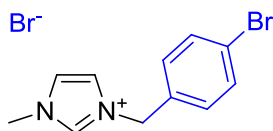
1-methyl-3-(pyren-1-ylmethyl)-1H-imidazol-3-ium bromide: Synthesis *d*: quant. ¹H-NMR (DMSO, 300 MHz, 20 °C): δ 3.83 (s, 3H, N-CH₃), 6.24 (s, 2H, N-CH₂), 7.76 (t, J = 1.7Hz, 1H, CH=), 7.90 (t, J = 1.7Hz, 1H, CH=), 8.09-8.59 (m, 9H, 9H_{ar}), 9.23 (s, 1H, NCHN). ¹³C-NMR (DMSO₃, 75 MHz, 20 °C): δ 37.8 (N-CH₃), 51.8 (N-CH₂), 124.3 124.5 125.6 125.8 126.0 127.1 127.7 127.9 128.6 129.2 129.3 129.9 130.1 130.5 130.7 132.0 132.6 133.4 (16C_{ar}+CH=CH), 138.6 (NCHN).



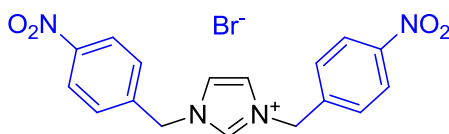
3-methyl-1-(naphthalen-2-ylmethyl)-1H-imidazol-3-ium bromide: Synthesis *d*: quant, ^1H -NMR (CD_2Cl_2 , 300 MHz, 20 °C): δ 3.81 (s, 3H, N-CH₃), 5.86 81 (s, 3H, N-CH₂), 7.25-7.81 (m, 8H, 6H_{ar} + CH=CH), 7.99 (s, 1H, 1H_{ar}), 10.11 (s, 1H, NCHN). ^{13}C -NMR (CD_2Cl_2 , 75 MHz, 20 °C): δ 36.9 (CH₃), 49.5 (N-CH₂), 122.7 124.1 (CH=CH), 136.2 126.4 127.1 127.3 128.1 128.4 128.8 129.4 131.9 133.4 133.5 (C_{ar}), 137.3 (NCHN).



3-(4-cyanobenzyl)-1-methyl-1H-imidazol-3-ium bromide: Synthesis *d*: ^1H -NMR (MeOD, 300 MHz, 20 °C): δ 3.95 (s, 3H, N-CH₃), 5.57 (s, 2H, N-CH₂), 7.56-7.79 (m, 6H, 4CH_{ar} and CH=CH), 9.14 (s, 1H, NCHN).

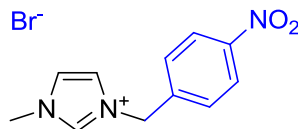


3-(4-bromobenzyl)-1-methyl-1H-imidazol-3-ium bromide: Synthesis *d*: quant. ^1H -NMR (DMSO, 300 MHz, 20 °C): δ 3.87 (s, 3H, N-CH₃), 5.49 (s, 2H, N-CH₂), 7.45 (d, J= 8.3Hz, 2H, 2CH_{ar}), 7.61 (d, J= 8.3Hz, 2H, 2CH_{ar}), 7.78 (t, J= 1.7Hz, 1H, CH=), 7.88(t, J= 1.7Hz, 1H, CH=), 9.40 (s, 1H, NCHN). ^{13}C -NMR (DMSO, 75 MHz, 20 °C): δ 35.9 (N-CH₃), 50.9 (N-CH₂), 122.0 (C_{ar}-Br), 122.2 123.9 (CH=CH), 130.7 131.8 (CH_{ar}), 134.3 (C_{ar}), 136.7 (NCHN).

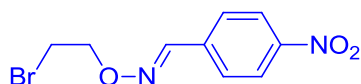


1,3-bis(4-nitrobenzyl)-1H-imidazol-3-ium bromide: Synthesis *b*: quant. ^1H -NMR (DMSO, 300 MHz, 20 °C): δ 5.71 (s, 4H, 2N-CH₂), 7.74 (d, J= 8.5Hz, 4H, 4H_{ar}), 7.99 (s, 2H, CH=CH), 8.27 (d, J=

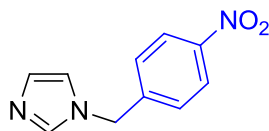
8.5Hz, 4H, 4H_{ar}), 9.66 (s, 1H, NCHN). ¹³C-NMR (DMSO, 75 MHz, 20 °C): δ 51.1 (N-CH₂), 123.2 (CH=CH), 124.0 (CH_{ar}), 129.7 (CH_{ar}), 137.2 (NCHN), 141.9 (C_{ar}), 147.5 (C_{ar}-NO₂).



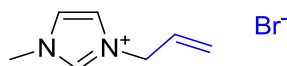
1-methyl-3-(4-nitrobenzyl)-1H-imidazol-3-ium bromide: Synthesis *d*: quant. ¹H-NMR (DMSO, 300 MHz, 20 °C): δ 3.88 (s, 3H, N-CH₃), 5.65 (s, 2H, N-CH₂), 7.69 (d, J= 8.6Hz, 2H, 2CH_{ar}), 7.79 (t, J= 1.7Hz, 1H, CH=), 7.86 (t, J= 1.7Hz, 1H, CH=), 8.28 (d, J= 8.6Hz, 2H, 2CH_{ar}), 9.34 (s, 1H, NCHN). ¹³C-NMR (DMSO, 75 MHz, 20 °C): δ 36.0 (N-CH₃), 50.8 (N-CH₂), 122.5 (CH=), 124.0 (CH_{ar}), 124.2 (CH=), 129.5 (CH_{ar}), 137.1 (NCHN), 142.2 (C_{ar}), 147.5 (C_{ar}-NO₂).



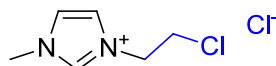
(E)-4-nitrobenzaldehyde O-(2-bromoethyl) oxime: A solution of (E)-4-nitrobenzaldehyde oxime (1 eq.), K₂CO₃ (10 eq.) and dibromoethane (10 eq.) in acetonitrile was refluxed overnight in acetonitrile. After evaporation of the volatiles, ethyl acetate was added and the organic layer was washed with water. quant. ¹H-NMR (CDCl₃, 300 MHz, 20 °C): δ 3.59 (t, J= 6.2Hz, 2H, CH₂), 4.44 (t, J= 6.2Hz, 2H, CH₂), 7.69 (d, J= 8.7Hz, 2H, 2H_{ar}), 8.13 (s, 1H, CH=N), 8.15 (d, J= 8.7Hz, 2H, 2H_{ar}). ¹³C-NMR (CDCl₃, 75 MHz, 20 °C): δ 29.6 (CH₂-Br), 74.0 (CH₂-O), 123.9 (CH_{ar}), 127.6 (CH_{ar}), 137.8 (C_{ar}), 147.4 (C_{ar}-NO₂), 148.3 (CH=N).



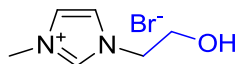
1-(4-nitrobenzyl)-1H-imidazole: Synthesis *d*: quant. ¹H-NMR (CDCl₃, 300 MHz, 20 °C): δ 5.15 (s, 2H, N-CH₂), 6.82 (d, J= 1.0Hz, 1H, CH=), 6.93 (d, J= 1.0Hz, 1H, CH=), 7.14 (d, J= 8.7Hz, 2H, 2H_{ar}), 7.46 (s, 1H, NCHN), 7.96 (d, J= 8.7Hz, 2H, 2H_{ar}). ¹³C-NMR (CDCl₃, 75 MHz, 20 °C): δ 49.4 (N-CH₂), 119.1 (CH=), 123.7 (CH_{ar}), 127.5 (CH_{ar}), 129.6 (CH=), 137.2 (NCHN), 143.5 (C_{ar}), 147.2 (C_{ar}-NO₂).



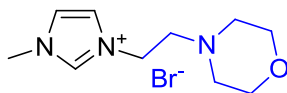
3-allyl-1-methyl-1H-imidazol-3-ium bromide: Synthesis *e*: quant. ^1H -NMR (CDCl_3 , 300 MHz, 20 $^\circ\text{C}$): δ 3.85 (s, 3H, N- CH_3), 4.76 (d, J = 6.2Hz, 2H, N- CH_2), 5.13-5.25 (m, 2H, 2 H_{alkene}), 5.69-5.83 (m, 1H, 1 H_{alkene}) 7.35 (t, J = 1.8Hz, 1H, CH=), 7.53 (t, J = 1.8Hz, 1H, CH=), 9.86 (s, 1H, NCHN).



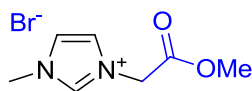
3-(2-chloroethyl)-1-methyl-1H-imidazol-3-ium chloride: Synthesis *e*: quant. ^1H -NMR (CDCl_3 , 300 MHz, 20 $^\circ\text{C}$): δ 4.08 (m, 5H, N- CH_3 and CH_2Cl), 4.88 (m, 2H, N- CH_2), 7.36 (s, 1H, CH=), 7.66 (s, 1H, CH=), 10.77 (s, 1H, NCHN). ^{13}C -NMR (CDCl_3 , 75 MHz, 20 $^\circ\text{C}$): δ 36.9 (N- CH_3), 53.5 ($\text{CH}_2\text{-Cl}$), 51.7 (N- CH_2), 122.7 123.4 (CH=CH), 138.9 (NCHN).



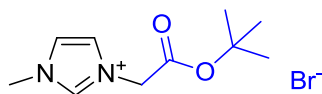
1-(2-hydroxyethyl)-3-methyl-1H-imidazol-3-ium bromide: Synthesis *e*: quant., ^1H -NMR (MeOD, 300 MHz, 20 $^\circ\text{C}$): δ 3.96 (t, J = 4.9Hz, 2H, CH_2), 4.05 (s, 3H, N- CH_3), 4.42 (t, J = 4.9Hz, 2H, CH_2), 4.84 (s, 1H, OH), 7.69 (t, J = 1.8Hz, 1H, CH=), 7.75 (t, J = 1.8Hz, 1H, CH=), 9.08 (s, 1H, NCHN). ^{13}C -NMR (CDCl_3 , 75 MHz, 20 $^\circ\text{C}$): δ 36.8 (N- CH_3), 53.4 (N- CH_2), 61.2 ($\text{CH}_2\text{-OH}$), 124.2 (CH), 124.9 (CH), 138.4 (NCHN).



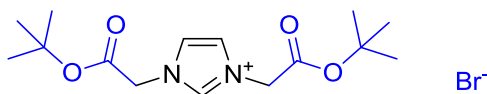
1-methyl-3-(2-morpholinoethyl)-1H-imidazol-3-ium bromide: Synthesis *d*: 33% ^1H -NMR (CDCl_3 , 300 MHz, 20 $^\circ\text{C}$): δ (t, J = 4.6Hz, 4H, 2 CH_2), 2.78 (t, J = 5.5Hz, 2H, 2 CH_2), 3.65 (t, J = 4.6Hz, 4H, 2 CH_2), 4.07 (s, 3H, N- CH_3), 4.48 (t, J = 5.5Hz, 2H, N- CH_2), 7.42 (t, J = 1.8Hz, 1H, CH=), 7.58 (t, J = 1.8Hz, 1H, CH=), 10.53 (s, 1H, NCHN). ^{13}C -NMR (CDCl_3 , 75 MHz, 20 $^\circ\text{C}$): δ 36.7 (CH_3), 46.5 (N- CH_2), 53.5 (CH_2), 57.8 (2N- CH_2), 66.9 (2O- CH_2), 122.8 (CH=CH), 138.5 (NCHN).



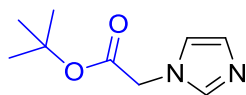
3-(2-methoxy-2-oxoethyl)-1-methyl-1H-imidazol-3-ium bromide: Synthesis *e*: quant. ^1H -NMR (CDCl_3 , 300 MHz, 20 °C): δ 3.79 (s, 3H, O-CH₃), 4.07 (s, 3H, N-CH₃), 5.57 (s, 2H, N-CH₂), 7.54 (t, J = 1.7Hz, 1H, CH=), 7.76 (t, J = 1.7Hz, 1H, CH=), 10.15 (s, 1H, NCHN). ^{13}C -NMR (CDCl_3 , 75 MHz, 20 °C): δ 37.0 (N-CH₃), 50.2 (N-CH₂), 53.5 (O-CH₃), 123.4 (CH=), 124.2 (CH=), 137.7 (NCHN), 166.8 (CH=O).



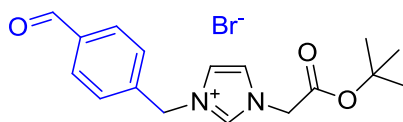
3-(2-(tert-butoxy)-2-oxoethyl)-1-methyl-1H-imidazol-3-ium bromide: Synthesis *e*: quant. ^{13}C -NMR (CDCl_3 , 75 MHz, 20 °C): δ 28.0 (CH₃), 36.8 (N-CH₃), 50.8 (N-CH₂), 84.8 (O-C), 123.0 123.8 (CH=CH), 138.3 (NCHN), 164.9 (C=O).



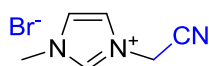
1,3-bis(2-(tert-butoxy)-2-oxoethyl)-1H-imidazol-3-ium bromide: Synthesis *b*: Quant. ^1H -NMR (CDCl_3 , 300 MHz, 20 °C): δ 1.25 (s, 18H, 6CH₃), 5.08 (s, 4H, 2N-CH₂), 7.58 (s, 2H, CH=CH), 9.84 (s, 1H, NCHN). ^{13}C -NMR (CDCl_3 , 75 MHz, 20 °C): δ 27.9 (CH₃), 50.7 (2N-CH₂), 84.3 (C_t-Bu), 123.3 (CH=CH), 138.5 (NCHN), 164.6 (C=O).



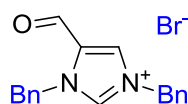
tert-butyl 2-(1H-imidazol-1-yl)acetate: Synthesis *b*: quant. ^1H -NMR (CDCl_3 , 300 MHz, 20 °C): δ 1.47 (s, 9H, 3CH₃), 4.62 (s, 2H, N-CH₂), 6.95 (s, 1H, CH=), 7.03 (s, 1H, CH=), 7.48 (s, 1H, NCHN). ^{13}C -NMR (CDCl_3 , 75 MHz, 20 °C): δ 27.7 (CH₃), 48.5 (N-CH₂), 82.7 (C_t-Bu), 119.9 129.0 (CH=CH), 137.7 (NCHN), 166.4 (C=O).



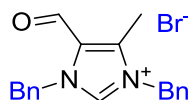
1-(2-(tert-butoxy)-2-oxoethyl)-3-(4-formylbenzyl)-1H-imidazol-3-ium bromide Synthesis *d*: 82%
 ^1H -NMR (DMSO, 300 MHz, 20 °C): δ 1.44 (s, 9H, 3CH₃), 5.18 (s, 2H, N-CH₂), 5.66 (s, 2H, N-CH₂), 7.61 (d, *J* = 8.1Hz, 2H, 2H_{ar}), 7.81 (s, 1H, CH=), 7.90 (s, 1H, CH=), 7.97 (d, *J* = 8.1Hz, 2H, 2H_{ar}), 9.36 (s, 1H, NCHN), 10.04 (s, 1H, CH=O). ^{13}C -NMR (DMSO₃, 75 MHz, 20 °C): δ 27.6 (3CH₃), 50.2 51.5 (2N-CH₂), 83.0 (C-O), 122.3 124.3 (CH=CH), 128.8 (CH_{ar}), 130.1 (CH_{ar}), 136.2 (C_{ar}), 137.7 (NCHN), 141.1 (C_{ar}), 165.6 (O-C=O), 192.7 (CH=O).



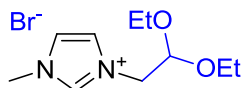
3-(cyanomethyl)-1-methyl-1H-imidazol-3-ium bromide: Synthesis *e*: quant. ^1H -NMR (MeOD, 300 MHz, 20 °C): δ 4.01 (s, 3H, N-CH₃), 5.57 (s, 2H, N-CH₂), 7.73 (s, 1H, CH=), 7.783 (s, 1H, CH=), 9.21 (s, 1H, NCHN). ^{13}C -NMR (CD₃OD, 75 MHz, 20 °C): δ 35.7 (N-CH₃), 36.6 (N-CH₂), 113.0 (CN), 122.5 (CH=), 124.5 (CH=), 137.7 (NCHN).



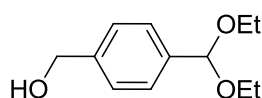
1,3-dibenzyl-5-formyl-1H-imidazol-3-ium bromide: Synthesis *c*: 77%. ^1H -NMR (CDCl₃, 300 MHz, 20 °C): δ 5.75 (s, 2H, N-CH₂), 5.82 (s, 2H, N-CH₂), 7.30-7.60 (m, 10H, 10CH_{ar}), 8.00 (s, 1H, CH=), 9.78 (s, 1H, NCHN), 11.24 (s, 1H, CH=O). ^{13}C -NMR (CDCl₃, 75 MHz, 20 °C): δ 52.8 (N-CH₂), 54.2 (N-CH₂), 128.9 129.4 129.5 129.6 129.7 129.9 130.0 131.8 132.1 132.7 (8C_{ar}, CH= and NCHN), 141.2 (C=), 178.0 (CHO).



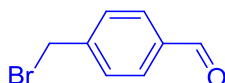
1,3-dibenzyl-5-formyl-4-methyl-1H-imidazol-3-ium bromide: Synthesis *c*: quant. ^1H -NMR (DMSO, 300 MHz, 20 °C): δ 2.56 (s, 3H, CH₃), 5.55 (s, 2H, N-CH₂), 5.72 (s, 2H, N-CH₂), 7.35-7.49 (m, 10H, 10H_{ar}), 9.68 (s, 1H), 9.93 (s, 1H). ^{13}C -NMR (DMSO, 75 MHz, 20 °C): δ 8.7 (CH₃), 49.9 (N-CH₂), 51.3 (N-CH₂), 125.8 127.8 128.1 128.6 128.8 128.8 129.1 133.3 134.3 139.8 142.2 (8C_{ar}, C=C and NCHN), 180.8 (CH=O).



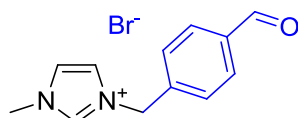
3-(2,2-diethoxyethyl)-1-methyl-1H-imidazol-3-ium bromide: Synthesis *e*: quant. $^1\text{H-NMR}$ (CDCl_3 , 300 MHz, 20 °C): δ 1.20 (t, $J = 7.1\text{Hz}$, 6H, 2 CH_3), 3.70 (m, 4H, 2 OCH_2), 3.76 (s, 3H, NCH_3), 4.48 (d, $J = 5.5\text{Hz}$, 2 H, NCH_2), 4.80 (t, $J = 5.5\text{Hz}$, 1H, CH), 7.40 (d, $J = 2.0\text{Hz}$, 1H, $\text{C}=\text{CH}$), 7.41 (d, $J = 2.0\text{Hz}$, 1H, $\text{C}=\text{CH}$), 10.33 (s, 1H, NCHN). $^{13}\text{C-NMR}$ (CDCl_3 , 75 MHz, 20 °C): δ 15.1 (2 CH_3), 36.7 (NCH_3), 51.9 (NCH_2), 64.2 (2 OCH_2), 99.4 (CH), 123.0 ($\text{C}=\text{C}$), 123.6 ($\text{C}=\text{C}$), 137.9 (NCHN).



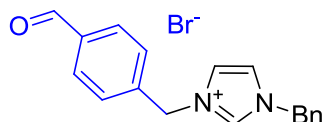
(4-(diethoxymethyl)phenyl)methanol: Synthesis according to literature²⁸⁷: quant. $^1\text{H-NMR}$ (CDCl_3 , 300 MHz, 20 °C): δ 1.23 (t, $J = 6.9\text{Hz}$, 6H, 2 CH_3), 3.57 (sept, $J = 6.9\text{Hz}$, 4H, 2O- CH_2), 4.65 (s, 2H, CH_2), 5.49 (s, 1H, CH), 7.33 (d, $J = 8.1\text{Hz}$, 2H, CH_{ar}), 7.45 (d, $J = 8.1\text{Hz}$, 2H, CH_{ar}). $^{13}\text{C-NMR}$ (CDCl_3 , 75 MHz, 20 °C): δ 15.1 (CH_3), 61.0 (O- CH_2), 101.3 (CH), 126.7 126.8 (CH_{ar}), 139.4 141.0 (C_{ar}).



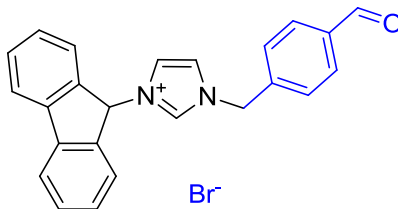
4-(bromomethyl)benzaldehyde: To a solution of (4-(diethoxymethyl)phenyl)methanol (2.1g, 10mmol) in CH_2Cl_2 (5mL) was added SOBr_2 (770 mL, 10mmol) at 0 °C. The reaction was stirred at room temperature for 2 hours, then quenched with water (5mL). The solution was washed with saturated NaHCO_3 (5ml) and water (5mL). The CH_2Cl_2 was removed under reduced pressure affording 4-(bromomethyl)benzaldehyde as a white powder (100%, 2.0g) $^1\text{H-NMR}$ (CDCl_3 , 300 MHz, 20 °C): δ 4.46 (s, 2H, $\text{CH}_2\text{-Br}$), 7.49 (d, $J = 8.1\text{Hz}$, 2H, CH_{ar}), 7.79 (d, $J = 8.1\text{Hz}$, 2H, CH_{ar}), 9.95 (s, 1H, $\text{CH}=\text{O}$). $^{13}\text{C-NMR}$ (CDCl_3 , 75 MHz, 20 °C): δ 32.2 ($\text{CH}_2\text{-Br}$), 129.7 (CH_{ar}), 130.1 (CH_{ar}), 136.1 (C_{ar}), 144.2 (C_{ar}), 191.5 ($\text{CH}=\text{O}$).



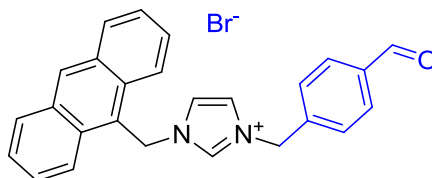
3-(4-formylbenzyl)-1-methyl-1H-imidazol-3-ium bromide: Synthesis *d*: quant. $^1\text{H-NMR}$ (CDCl_3 , 300 MHz, 20 °C): δ 4.09 (s, 3H, N- CH_3), 5.80 (s, 2H, N- CH_2), 7.26 (CH= hide by solvent), 7.30 (s, 1H, CH=), 7.72 (d, $J = 8.1\text{Hz}$, 2H, CH_{ar}), 7.92 (d, $J = 8.1\text{Hz}$, 2H, CH_{ar}), 10.03 (s, 1H, CH=O), 10.87 (s, 1H, NCHN). $^{13}\text{C-NMR}$ (DMSO, 75 MHz, 20 °C): δ 35.9 (N- CH_3), 51.2 (N- CH_2), 122.4 (CH=), 124.0 (CH=), 128.8 (CH_{ar}), 129.9 (CH_{ar}), 136.1 (C_{ar}), 137.0 (NCHN), 141.2 (C_{ar}), 192.7 (CH=O). MS (positive ESI): [M-Br]: calculated for $\text{C}_{12}\text{H}_{13}\text{N}_2\text{O}_1$: 201.10, found 201.10.



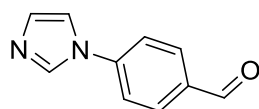
1-benzyl-3-(4-formylbenzyl)-1H-imidazol-3-ium bromide: Synthesis *d*: quant. $^1\text{H-NMR}$ (CDCl_3 , 300 MHz, 20 °C): δ 5.53 (s, 2H, N- CH_2), 5.76 (s, 2H, N- CH_2), 7.21-7.85 (m, 11H, 9H_{Ph} + HC=CH), 9.91 (s, 1H, CH=O), 10.58 (NCHN). $^{13}\text{C-NMR}$ (CDCl_3 , 75 MHz, 20 °C): δ 52.4 (N- CH_2), 53.2 (N- CH_2), 122.3 (CH=), 122.8 (CH=), 128.8 129.3 129.4 129.6 130.0 (CH_{ar}), 132.8 (C_{ar}), 136.6 (NCHN), 139.6 (C_{ar}), 191.6 (CH=O).



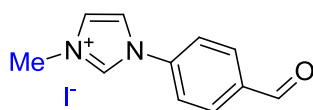
3-(9H-fluoren-9-yl)-1-(4-formylbenzyl)-1H-imidazol-3-ium bromide: Synthesis *d*: n.d. $^1\text{H-NMR}$ (MeOD, 300 MHz, 20 °C): δ 5.64 (s, 2H, N- CH_2), 6.76 (s, 1H, CH-N), 7.39-8.10 (m, 14H, HC=CH and 12H_{ar}), 9.48 (s, 1H, NCHN), 10.10 (s, 1H, CH=O).



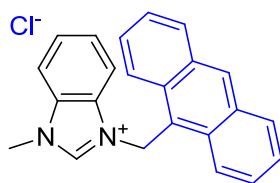
1-(anthracen-9-ylmethyl)-3-(4-formylbenzyl)-1H-imidazol-3-ium bromide: Synthesis *d*: quant. $^1\text{H-NMR}$ (CDCl_3 , 300 MHz, 20 °C): δ 5.74 (s, 2H, N- CH_2), 6.61 (s, 2H, N- CH_2), 6.66 (s, 1H, CH=), 6.96 (s, 1H, CH=), 7.50-8.38 (m, 10H, 10H_{ar}), 8.61 (s, 1H, H_{antr}), 9.95 (s, 1H, CH=O), 11.37 (s, 1H, NCHN).



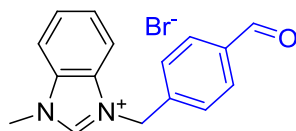
4-(1H-imidazol-1-yl)benzaldehyde: Synthesis according to literature.²⁸⁶ $^1\text{H-NMR}$ (CDCl_3 , 300 MHz, 20 °C): δ 7.22 (s, 1H, H_{im}), 7.36 (s, 1H, H_{im}), 7.56 (d, $J = 8.4\text{Hz}$, 2H, 2H_{ar}), 7.91-8.10 (m, 3H, 2H_{ar} and H_{im}), 10.01 (s, 1H, CH=O).



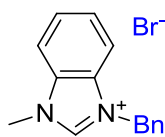
1-(4-formylphenyl)-3-methyl-1H-imidazol-3-ium iodide: Synthesis *e*: quant. $^1\text{H-NMR}$ (CDCl_3 , 300 MHz, 20 °C): δ 4.27 (s, 3H, N-CH_3), 7.54 (d, $J = 1.8\text{Hz}$, 1H, H_{im}), 7.71 (d, $J = 1.8\text{Hz}$, 1H, H_{im}), 8.02 (d, $J = 8.5\text{Hz}$, 2H, 2H_{ar}), 8.11 (d, $J = 8.5\text{Hz}$, 2H, 2H_{ar}), 10.09 (s, 1H, CH=O), 10.75 (s, 1H, NCHN).



3-(anthracen-9-ylmethyl)-1-methyl-1H-benzo[d]imidazol-3-ium chloride: Synthesis *d*: <5%, $^1\text{H-NMR}$ (DMSO , 300 MHz, 20 °C): 3.88 (s, 3H, N-CH_3), 6.71 (s, 2H, N-CH_2), 7.58-7.67 (m, 4H, 4H_{ar}), 7.80 (quint, $J = 8.0\text{Hz}$, 2H, 2H_{ar}), 8.03 (d, $J = 7.8\text{Hz}$, 1H, 1H_{ar}), 8.26 (m, 2H, 2H_{ar}), 8.37 (t, $J = 7.7\text{Hz}$, 3H, 3H_{ar}), 8.91 (d, $J = 7.2\text{Hz}$, 2H, 2H_{ar}).



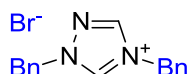
3-(4-formylbenzyl)-1-methyl-1H-benzo[d]imidazol-3-ium bromide: Synthesis *d*: quant. $^1\text{H-NMR}$ (CDCl_3 , 300 MHz, 20 °C): δ 4.39 (s, 3H, N-CH_3), 6.07 (s, 2H, N-CH_2), 7.44-7.94 (m, 8H, 8H_{ar}), 9.96 (s, 1H, CH=O), 11.70 (s, 1H, NCHN). $^{13}\text{C-NMR}$ (CDCl_3 , 75 MHz, 20 °C): δ 34.19 (N-CH_3), 50.9 (N-CH_2), 112.9 113.5 127.4 129.0 130.5 (CH_{ar}), 130.9 132.1 136.7 139.1 143.6 (C_{ar} and NCHN), 191.3 (CH=O).



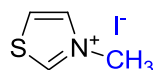
3-benzyl-1-methyl-1H-benzo[d]imidazol-3-ium bromide: Synthesis *e*: quant. $^1\text{H-NMR}$ (CDCl_3 , 300 MHz, 20 °C): δ 4.28 (s, 3H, N-CH₃), 5.86 (s, 2H, N-CH₂), 7.27-7.74 (m, 9H, 9H_{ar}), 11.57 (s, 1H, NCHN). $^{13}\text{C-NMR}$ (CDCl_3 , 75 MHz, 20 °C): δ 33.9 (N-CH₃), 51.4 (N-CH₂), 112.8 113.6 127.2 128.3 129.2 129.3 143.3 (C_{ar} and NCHN).



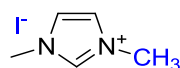
1,3-dimethyl-1H-benzo[d]imidazol-3-ium iodide: Synthesis *e*: quant. $^1\text{H-NMR}$ (CDCl_3 , 300 MHz, 20 °C): δ 4.28 (s, 6H, 2N-CH₃), 7.71 (m, 4H, 4H_{ar}), 11.04 (s, 1H, NCHN). $^1\text{H-NMR}$ (DMSO, 300 MHz, 20 °C): δ 4.08 (s, 6H, 2N-CH₃), 7.71 (m, 2H, 2H_{ar}), 8.02 (m, 2H, 2H_{ar}), 9.65 (s, 1H, NCHN). $^{13}\text{C-NMR}$ (CDCl_3 , 75 MHz, 20 °C): δ 33.2 (N-CH₃), 113.4 (CH_{ar}), 126.4 (CH_{ar}), 131.6 (C_{ar}), 143.1 (NCHN).



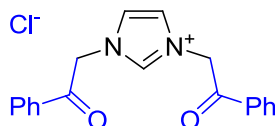
1,4-dibenzyl-1H-1,2,4-triazol-4-ium bromide: Synthesis *c*: quant. $^1\text{H-NMR}$ (CDCl_3 , 300 MHz, 20 °C): δ 5.63 (s, 2H, N-CH₂), 5.76 (s, 2H, N-CH₂), 7.28-7.38 (m, 6H, 6H_{ar}), 7.46-7.54 (m, 2H, 2H_{ar}), 7.56-7.62 (m, 2H, 2H_{ar}), 8.93 (s, 1H, CH=N), 11.78 (s, 1H, NCHN). $^{13}\text{C-NMR}$ (CDCl_3 , 75 MHz, 20 °C): δ 52.0 (N-CH₂), 56.3 (N-CH₂), 129.2 129.4 129.5 129.6 129.9 (CH_{ar}), 131.7 (C_{ar}), 131.9 (C_{ar}), 142.6 (NCHN), 143.7 (NCHN).



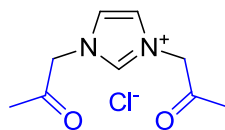
3-methylthiazol-3-ium iodide: Synthesis *e*: quant., $^1\text{H-NMR}$ (DMSO, 300 MHz, 20 °C): δ 4.21 (s, 3H, N-CH₃), 8.32 (m, 1H, CH=), 8.47 (m, 1H, CH=), 10.11 (s, 1H, SCHN).



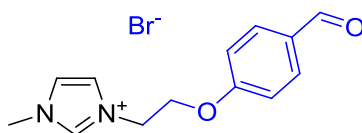
1,3-dimethyl-1H-imidazol-3-ium iodide: Synthesis *e*: quant. ^1H -NMR (DMSO, 300 MHz, 20 °C): δ 3.83 (s, 6H, 2N-CH₃), 7.69 (d, J = 1.6Hz, 2H, CH=CH), 9.08 (s, 1H, NCHN). ^{13}C -NMR (DMSO, 75 MHz, 20 °C): δ 35.8 (N-CH₃), 123.3 (CH=CH), 136.9 (NCHN).



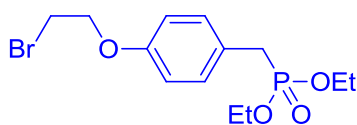
1,3-bis(2-oxo-2-phenylethyl)-1H-imidazol-3-ium chloride: Synthesis *b*: n.d. ^1H -NMR (CDCl₃, 300 MHz, 20 °C): δ 6.10 (s, 4H, 2N-CH₂), 7.58-7.77 and 8.09-8.13 (m, 12H, 10H_{ar} and CH=CH), 9.07 (s, 1H, NCHN). ^{13}C -NMR (CDCl₃, 75 MHz, 20 °C): δ 53.1 (N-CH₂), 122.1 (CH=CH), 128.8 (CH_{ar}), 129.2 (CH_{ar}), 133.1 (C_{ar}), 137.0 (NCHN), C=O (not observed).



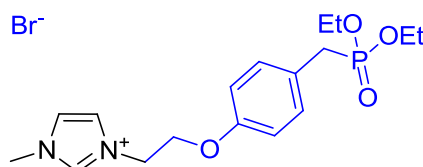
1,3-bis(2-oxopropyl)-1H-imidazol-3-ium chloride: Synthesis *b*: n.d. ^1H -NMR (DMSO, 300 MHz, 20 °C): δ 3.79 (s, 6H, 2CH₃), 5.72 (s, 4H, 2N-CH₂), 7.92 (s, 2H, CH=CH), 9.28 (s, 1H, NCHN). ^{13}C -NMR (DMSO, 75 MHz, 20 °C): δ 26.9 (CH₃), 57.6 (N-CH₂), 123.2 (CH=CH), 137.9 (NCHN), 199.9 (C=O).



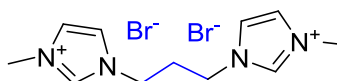
3-(2-(4-formylphenoxy)ethyl)-1-methyl-1H-imidazol-3-ium bromide: Synthesis *d*: quant. % ^1H -NMR (DMSO, 300 MHz, 20 °C): δ 3.89 (s, 3H, N-CH₃), 4.49 (t, J = 4.9Hz, 2H, CH₂), 4.64 (t, J = 4.9Hz, 2H, CH₂), 7.15 (s, 1H, CH=), 7.18 (s, 1H, CH=), 7.66-7.94 (m, 4H, 4H_{ar}), 9.26 (s, 1H, NCHN), 9.89 (s, 1H, CH=O). ^{13}C -NMR (DMSO, 75 MHz, 20 °C): δ 35.8 (N-CH₃), 48.3 (N-CH₂), 66.2 (O-CH₂), 115.1 (CH_{ar}), 122.8 123.6 (CH=CH), 130.2 (C_{ar}), 131.8 (CH_{ar}), 137.1 (NCHN), 162.5 (O-C_{ar}), 191.4 (CH=O).



diethyl 4-(2-bromoethoxy)benzylphosphonate: A solution of diethyl 4-hydroxybenzylphosphonate (1 eq), K_2CO_3 (10 eq) and dibromoethane (10 eq) in acetonitrile was refluxed overnight in acetonitrile. After evaporation of the volatiles, ethyl acetate was added and the product was washed with water. 52%. 1H -NMR ($CDCl_3$, 300 MHz, 20 °C): δ 1.13 (t, J = 7.1Hz, 6H, $2CH_3$), 2.98 (d, J_{PH} =21.1Hz, 2H, P- CH_2), 3.50 (t, J = 6.2Hz, 2H, Br- CH_2), 3.90 (t, J = 7.1Hz, 4H, 2O- CH_2), 4.14 (t, J = 6.2Hz, 2H, O- CH_2), 6.74 (d, J = 8.7Hz, 2H, $2H_{ar}$), 7.11 (d, J = 8.7Hz, 2H, $2H_{ar}$). ^{31}P -NMR ($CDCl_3$, 121 MHz, 20 °C): δ 26.5 (s, P). ^{13}C -NMR ($CDCl_3$, 75 MHz, 20 °C): δ 16.2 ($2CH_3$), 29.0 (Br- CH_2), 32.5 (P- CH_2), 61.8 (2O- CH_2), 67.7 (O- CH_2), 114.6 (CH_{ar}), 124.1 (C_{ar}), 130.6 (CH_{ar}), 156.9 (C_{ar}).



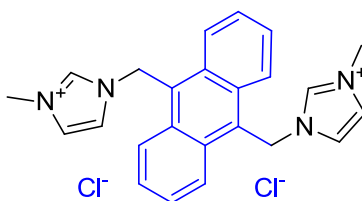
3-(2-(4-(((diethoxyphosphoryl)methyl)phenoxy)ethyl)-1-methyl-1H-imidazol-3-ium) bromide: Synthesis *d*: 88%. 1H -NMR ($CDCl_3$, 300 MHz, 20 °C): δ 1.07 (t, J = 7.1Hz, 6H, $2CH_3$), 2.88 (d, J_{PH} =21.1Hz, 2H, P- CH_2), 3.82 (t, J = 7.5Hz, 4H, 2O- CH_2), 3.88 (s, 3H, N- CH_3), 4.18 (s, 2H, CH_2), 4.66 (s, 2H, CH_2), 6.66 (d, J = 8.4Hz, 2H, $2H_{ar}$), 6.99 (d, J = 8.4Hz, 2H, $2H_{ar}$), 7.50 (s, 1H, CH=), 7.65 (s, 1H, CH=), 9.93 (s, 1H, NCHN). ^{31}P -NMR ($CDCl_3$, 121 MHz, 20 °C): δ 26.3 (s, P). ^{13}C -NMR ($CDCl_3$, 75 MHz, 20 °C): δ 16.0 16.1 ($2CH_3$), 31.3 33.1 (P- CH_2), 36.3 (N- CH_3), 49.0 (N- CH_2), 61.7 61.8 (2O- CH_2), 65.9 (O- CH_2), 114.3 (CH_{ar}), 122.9 (CH=), 123.2 (CH=), 124.3 124.9 (C_{ar}), 130.5 130.6 (CH_{ar}), 137.0 (NCHN), 156.2 156.2 (C_{ar}).



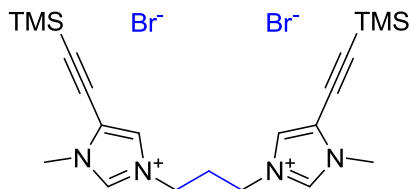
1,1'-(propane-1,3-diyl)bis(3-methyl-1H-imidazol-3-ium) bromide Synthesis *f*: quant. 1H -NMR (MeOD, 300 MHz, 20 °C): δ 2.58 (q, J = 7.4Hz, 2H, CH_2), 3.98 (s, 6H, 2 N- CH_3), 4.42 (t, J = 7.4Hz, 4H, 2 N- CH_2), 7.63 (d, J = 1.7Hz, 2H, $2CH=$), 7.77 (d, J = 1.7Hz, 2H, $2CH=$), 9.13 (s, 1H, NCHN). ^{13}C -NMR (MeOD, 75 MHz, 20 °C): δ 31.6 (CH_2), 36.9 (N- CH_3), 47.7 (N- CH_2), 123.9 (CH=), 125.4 (CH=), 138.4 (NCHN).



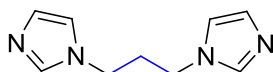
1,1'-(1,4-phenylenebis(methylene))bis(3-methyl-1H-imidazol-3-ium) bromide: Synthesis *f*: quant. $^1\text{H-NMR}$ (MeOD, 300 MHz, 20 °C): δ 3.95 (s, 6H, 2 N-CH₃), 5.48 (s, 4H, 2 N-CH₂), 7.54 (s, 4H, 4H_{ar}), 7.61 (s, 2H, 2CH=), 7.64 (s, 2H, 2CH=), 9.09 (s, 2H, 2 NCHN). $^{13}\text{C-NMR}$ (MeOD, 75 MHz, 20 °C): δ 34.84 (N-CH₃), 51.6 (N-CH₂), 121.8 (CH=), 123.5 (CH=), 128.8 (CH_{ar}), 135.6 (C_{ar}), 136.3 (NCHN). $^1\text{H-NMR}$ (DMSO, 300 MHz, 20 °C): δ 3.87 (s, 6H, 2 N-CH₃), 5.50 (s, 4H, 2 N-CH₂), 7.52 (s, 4H, 4H_{ar}), 7.77 (s, 2H, 2CH=), 7.88 (s, 2H, 2CH=), 9.44 (s, 2H, 2 NCHN). $^{13}\text{C-NMR}$ (DMSO, 75 MHz, 20 °C): δ 35.9 (N-CH₃), 51.2 (N-CH₂), 122.3 (CH=), 123.9 (CH=), 128.9 (CH_{ar}), 135.4 (C_{ar}), 136.6 (NCHN).



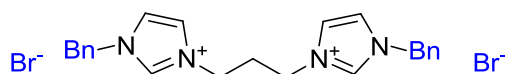
1,1'-(anthracene-9,10-diylbis(methylene))bis(3-methyl-1H-imidazol-3-ium) chloride: Synthesis *f*: n.d. $^1\text{H-NMR}$ (CDCl₃, 300 MHz, 20 °C): δ 3.70 (s, 6H, 2 N-CH₃), 6.58 (s, 4H, 2 N-CH₂), 7.03 (s, 2H, 2CH=), 7.25 (m, 4H, 4H_{ar}), 7.81 (m, 4H, 4H_{ar}), 8.90 (s, 2H, 2CH=), 9.22 (s, 2H, 2 NCHN). $^{13}\text{C-NMR}$ (CDCl₃, 75 MHz, 20 °C): δ 36.0 (2 N-CH₃), 50.8 (2 N-CH₂), 122.1 (2 CH=), 123.2 (4 CH_{ar}), 124.2 (4 C_{ar}), 124.3 (2 CH=), 127.5 (4 CH_{ar}), 130.0 (4 C_{ar}), 137.2 (2 NCHN).



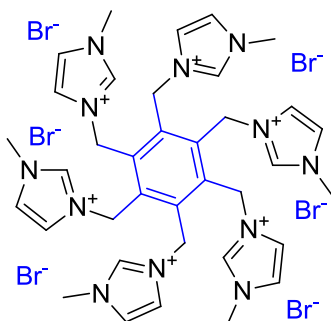
3,3'-(propane-1,3-diyl)bis(1-methyl-5-((trimethylsilyl)ethynyl)-1H-imidazol-3-ium) bromide: Synthesis *g*: 59%. $^1\text{H-NMR}$ (CDCl₃, 300 MHz, 20 °C): δ 0.28 (s, 18H, Si(CH₃)₃), 2.87 (q, *J* = 7.1 Hz, 2H, CH₂), 3.93 (s, 6H, N-CH₃), 4.77 (t, *J* = 7.1 Hz, 4H, N-CH₂), 8.23 (s, 2H, CH=), 10.28 (s, 2H, NCHN). $^{13}\text{C-NMR}$ (CDCl₃, 75 MHz, 20 °C): δ -0.7 (Si(CH₃)₃), 30.9 (CH₂), 34.7 (N-CH₃), 47.0 (N-CH₂), 86.5 (C_{alkyne}-Si), 108.8 (C_{alkyne}), 118.7 (CH=), 126.0 (C=), 137.1 (NCHN).



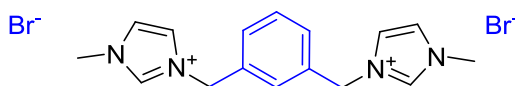
1,3-di(1H-imidazol-1-yl)propane: Synthesis adopting a literature procedure:⁵⁵⁴ 42% ¹H-NMR (CDCl₃, 300 MHz, 20 °C): δ 1.98 (q, J= 6.9Hz, 2H, CH₂), 3.63 (t, J= 6.9Hz, 4H, 2N-CH₂), 6.64 (d, J= 1.0Hz, 2H, CH=), 6.76 (d, J= 1.0Hz, 2H, CH=), 7.14 (s, 2H, 2NCHN). ¹³C-NMR (CDCl₃, 75 MHz, 20 °C): δ 31.6 (CH₂), 43.2 (2N-CH₂), 118.6 (CH=), 129.4 (CH=), 136.8 (NCHN).



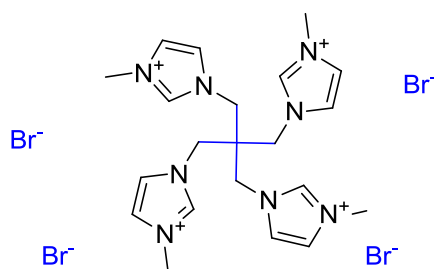
3,3'-(propane-1,3-diyl)bis(1-benzyl-1H-imidazol-3-ium) bromide: Synthesis g: quant. ¹H-NMR (MeOD, 300 MHz, 20 °C): δ 2.63 (quint, J= 7.3Hz, 2H, CH₂), 4.48 (t, J= 7.3Hz, 4H, 2N-CH₂), 5.54 (s, 4H, 2N-CH₂-Ph), 7.33-7.60 (10H, m, 10H_{ar}), 7.67 (d, J= 1.8Hz, 2H, 2CH=), 7.85 (d, J= 1.8Hz, 2H, 2CH=), 9.45 (s, 2H, 2NCHN). ¹³C-NMR (MeOD, 75 MHz, 20 °C): δ 31.5 (CH₂), 47.9 (N-CH₂), 54.2 (N-CH₂-Ph), 123.9 (CH=), 124.1 (CH=), 130.1 130.4 130.5 (CH_{ar}), 135.2 (C_{ar}), 137.6 (NCHN).



3,3',3'',3''',3'''',3'''''-(benzene-1,2,3,4,5,6-hexaylhexakis(methylene))hexakis(1-methyl-1H-imidazol-3-ium) bromide: Synthesis f: quant. ¹H-NMR (DMSO, 300 MHz, 20 °C): δ 3.83 (s, 3H, N-CH₃), 5.80 (s, 2H, N-CH₂), 7.67 (s, 1H, CH=), 7.81 (s, 1H, CH=), 9.32 (s, 1H, NCHN). ¹³C-NMR (DMSO, 75 MHz, 20 °C): δ 35.7 (N-CH₃), 47.4 (N-CH₂), 122.6 (CH=), 122.9 (CH=), 136.7 (CH_{ar}), 138.4 (NCHN).



3,3'-(1,3-phenylenebis(methylene))bis(1-methyl-1H-imidazol-3-ium) bromide: Synthesis *cf.* n.d. ^1H -NMR (DMSO, 300 MHz, 20 °C): δ 3.90 (s, 6H, 2N-CH₃), 5.53 (s, 4H, 2N-CH₂), 7.46 (m, 3H, 3CH_{ar}), 7.69 (s, 1H, 1CH_{ar}), 7.81 (t, J = 1.7Hz, 2H, 2CH=), 7.94 (t, J = 1.7Hz, 2H, 2CH=), 9.54 (s, 2H, 2NCHN). ^{13}C -NMR (CDCl₃, 75 MHz, 20 °C): δ 36.0 (N-CH₃), 51.2 (N-CH₂), 122.2 (CH=), 123.9 (CH=), 128.4 128.6 129.5 (CH_{ar}), 135.6 (C_{ar}), 136.7 (NCHN).



1,1'-(2,2-bis((3-methyl-1H-imidazol-3-ium-1-yl)methyl)propane-1,3-diyl)bis(3-methyl-1H-imidazol-3-ium) bromide: Synthesis *cf.* quant. ^1H -NMR (DMSO, 300 MHz, 20 °C): δ 3.87 (s, 3H, N-CH₃), 4.46 (s, 2H, 2N-CH₂), 7.68 (s, 1H, 1CH=), 7.77 (s, 1H, 1CH=), 9.07 (s, 1H, 1NCHN).

7.3 Synthesis of platinum NHC complexes

7.3.1 Synthesis of prefunctionalized [(NHC)PtI₂(L)] complexes

Unless mentioned, the following general procedures were used (20-100 mg, 30-150 μ mol scale):

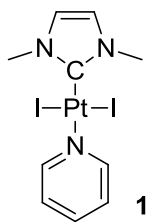
Procedure a: Synthesis of [(NHC)PtI₂(L)] from azolium precursor: (L = pyridine, cyclohexylamine or morpholine): Imidazolium halide (1.1 eq. 50-250 mg, 0.2-1 μ mol), PtCl₂ (1 eq), NaI (10 eq.) and K₂CO₃ (10 eq) were suspended under argon in anhydrous solvent (pyridine, cyclohexylamine, morpholine 10 mL). The mixture was sonicated during 10 minutes, heated overnight at 100 °C, then concentrated under reduced pressure, dissolved in CH₂Cl₂ and filtered through a celite plug. The residue was purified by a silica gel chromatography (gradient CH₂Cl₂/pentane 1/1, CH₂Cl₂, CH₂Cl₂/MeOH 20/1) affording the complex as a yellow oil or powder.

[(NHC)PdX₂(L)] were obtained employing the same procedure starting with PdCl₂.

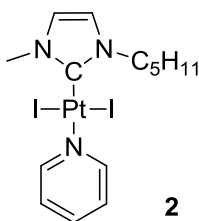
Procedure b: Synthesis of [(NHC)PtI₂(L)] by ligand exchange: (L = amine, amino acid, pnictogen ligand phosphine, arsine or stibine): the complex is obtained using reported procedures.^{124,125} To a solution of platinum pyridine in EtOH, the amine (1.1 eq) respectively the ammonium salt (1.1 eq) with triethylamine (10 eq) were added. The solution was stirred at 55 °C with TLC monitoring. The volatiles were removed and the crude product purified over silica gel chromatography (gradient CH₂Cl₂/pentane 1/1, CH₂Cl₂, CH₂Cl₂/MeOH 20/1) affording the complex as a yellow oil or powder.

Complexes **14**, **15** and **30** were reported by our group.^{124,125}

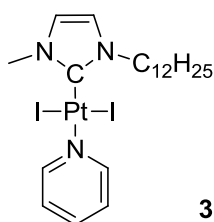
7.3.1.1 *Synthesis of Pt-NHC complexes bearing innocent N-substituents: alkanes, aromatic rings, alkenes and fluoroalkanes*



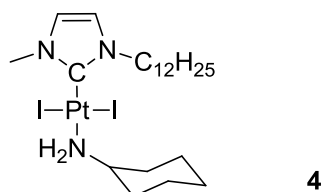
Procedure *a*: 93%. ^1H -NMR (CDCl_3 , 300 MHz, 20 °C): δ 3.93 (d, $J=0.7\text{Hz}$, 6H, 2N- CH_3), 6.82 (d, $J=0.7\text{Hz}$, 2H, $\text{CH}=\text{CH}$), 7.31 (t, $J= 6.8\text{Hz}$, 2H, 2H_{pyr}), 7.71 (td, $J= 7.6$ and 0.7Hz , 1H, 1H_{pyr}), 9.02 (m, 2H, 2H_{pyr}). ^{13}C -NMR (CDCl_3 , 75 MHz, 20 °C): δ 38.2 (N- CH_3), 121.9 ($\text{CH}=\text{CH}$), 125.0 (C_{pyr}), 135.9 (C-Pt), 137.5 (C_{pyr}), 153.7 (C_{pyr}).



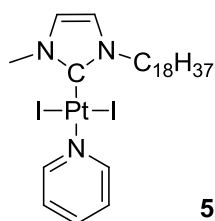
Procedure *a*: 51%. ^1H -NMR (CDCl_3 , 300 MHz, 20 °C): δ 0.95 (t, $J= 6.7\text{Hz}$, 3H, CH_3), 1.41 (m, 4H, 2CH_2), 2.03 (q, $J= 7.6\text{Hz}$, 2H, CH_2), 3.94 (s, 3H, N- CH_3), 4.41 (t, $J= 7.6\text{Hz}$, 2H, N- CH_2), 6.83 (s, 2H, $\text{CH}=\text{CH}$), 7.31 (t, $J= 6.7\text{Hz}$, 2H, 2H_{pyr}), 7.71 (tt, $J= 7.8\text{Hz}$ and 1.6Hz , 1H, H_{pyr}), 9.02 (m, 2H, 2H_{pyr}). ^{13}C -NMR (CDCl_3 , 75 MHz, 20 °C): δ 14.1 (CH_3), 22.3 (CH_2), 28.9 (CH_2), 29.3 (CH_2), 38.4 (N- CH_3), 50.9 (N- CH_2), 120.4 ($\text{CH}=\text{}$), 121.9 ($\text{CH}=\text{}$), 125.0 (C_{pyr}), 135.1 (C-Pt), 137.5 (C_{pyr}), 153.7 (C_{pyr}). MS (positive ESI) $[\text{M-I}]$: calculated for $\text{C}_{14}\text{H}_{21}\text{I}_1\text{N}_3\text{Pt}_1$: 553.04, found 553.04, $[\text{M-I}+\text{CH}_3\text{CN}]$: calculated for $\text{C}_{14}\text{H}_{21}\text{I}_1\text{N}_3\text{Pt}_1\text{CH}_3\text{CN}$: 594.07, found 594.07.



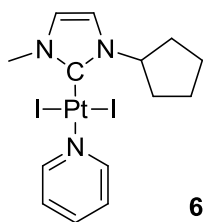
Procedure *a*: 85%. ^1H -NMR (CDCl_3 , 300 MHz, 20 °C): δ 0.87 (t, $J= 6.6\text{Hz}$, 3H, CH_3), 1.17-1.49 (m, 18H, 9CH_2), 2.02 (m, 2H, CH_2), 3.94 (s, 3H, N- CH_3), 4.41 (t, $J= 7.7\text{Hz}$, 2H, N- CH_2), 6.83 (s, 2H, $\text{CH}=\text{CH}$), 7.31 (t, $J= 6.9\text{Hz}$, 2H, 2H_{pyr}), 7.71 (tt, $J= 7.6$ and 1.6Hz , 1H, 1H_{pyr}), 9.02 (m, 2H, 2H_{pyr}). ^{13}C -NMR (CDCl_3 , 75 MHz, 20 °C): δ 14.2 (CH_3 alkane), 22.8 26.8 29.3 29.4 29.6 29.7 32.0 (CH_2 alkane), 38.4 (N- CH_3), 51.0 (N- CH_2), 121.4 ($\text{CH}=\text{}$), 122.0 ($\text{CH}=\text{}$), 125.0 (C_{pyr}), 135.2 (C-Pt), 137.5 (C_{pyr}), 153.8 (C_{pyr}).



Procedure b: 35%. $^1\text{H-NMR}$ (CDCl_3 , 300 MHz, 20 °C): δ 0.88 (t, J = 6.6Hz, 3H, CH_3), 1.12-2.47 (m, 30H, $10\text{H}_{\text{CHA}}+10\text{CH}_2$), 2.90 (m, 2H, Pt- NH_2), 3.25 (s, 1H, CH_{CHA}), 3.85 (s, 3H, N- CH_3), 4.30 (t, J = 7.6Hz, 2H, N- CH_2), 6.79 (s, 2H, $\text{CH}=\text{CH}$).

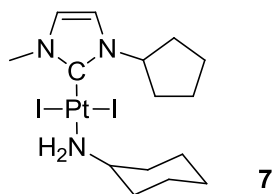


Procedure a: 35%. $^1\text{H-NMR}$ (CDCl_3 , 300 MHz, 20 °C): δ 0.87 (t, J = 6.7Hz, 3H, CH_3), 1.25 (m, 30H, 15CH_2), 2.03 (m, 2H, CH_2), 3.95 (s, 3H, N- CH_3), 4.42 t, J = 7.7Hz, 2H, N- CH_2), 6.83 (s, 2H, $\text{CH}=\text{CH}$), 7.31 (m, 2H, 2H_{pyr}), 7.71 (tt, J = 7.7 and 1.6Hz, 1H, 1H_{pyr}), 9.04 (m, 2H, 2H_{pyr}). $^{13}\text{C-NMR}$ (CDCl_3 , 75 MHz, 20 °C): δ 14.1 (CH_3 alkane), 22.7 26.7 29.2 29.3 29.5 29.6 29.7 31.9 (CH_2 alkane), 38.3 (N- CH_3), 50.9 (N- CH_2), 120.8 ($\text{CH}=\text{}$), 121.8 ($\text{CH}=\text{}$), 124.9 (C_{pyr}), 135.1 (C-Pt), 137.3 (C_{pyr}), 153.7 (C_{pyr}).

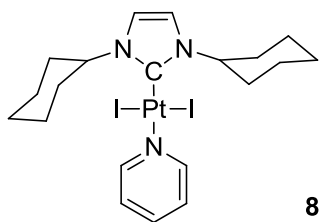


Procedure a: 67%. $^1\text{H-NMR}$ (CDCl_3 , 300 MHz, 20 °C): δ 1.53-1.91 (m, 6H, 6H_{cyp}), 2.41 (m, 2H, 2H_{cyp}), 3.92 (s, 3H, N- CH_3), 5.77 (q, J = 7.9Hz, 1H, N-CH), 6.85 (m, 2H, $\text{CH}=\text{CH}$), 7.30 (m, 2H, 2H_{pyr}), 7.71 (tt, J = 7.7Hz and 1.6Hz, 1H, H_{pyr}), 9.04 (m, 2H, 2H_{pyr}). $^{13}\text{C-NMR}$ (CDCl_3 , 75 MHz, 20 °C): δ 24.3 (CH_2), 33.1 (CH_2), 38.2 (CH_3), 61.3 (CH), 116.8 ($\text{CH}=\text{}$), 122.5 ($\text{CH}=\text{}$), 124.9 (CH_{pyr}), 134.8 (C-Pt), 137.4 (CH_{pyr}), 153.8 (CH_{pyr}). MS (positive ESI) [$\text{M}+\text{e}^-$]: calculated for $\text{C}_{14}\text{H}_{19}\text{I}_2\text{N}_3\text{Pt}$: 677.93,

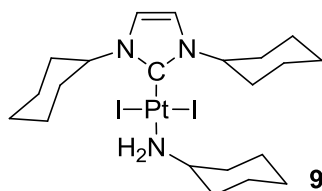
found 677.92, [M-2I-H]: calculated for $C_{14}H_{18}N_3Pt$: 423.11, found 423.11, [M-I]: calculated for $C_{14}H_{19}IN_3Pt$: 551.03, found 551.02



Procedure *b*: 42%. 1H -NMR ($CDCl_3$, 300 MHz, 20 °C): δ 1.02-1.87 (m, 14H, 7CH₂), 2.22 (m, 4H, 2CH₂), 2.89 (m, 2H, NH₂-Pt), 3.23 (m, 1H, CH), 3.82 (s, 3H, N-CH₃), 5.62 (q, J= 8.0Hz, 1H, N-CH), 6.81 (s, 2H, CH=CH). ^{13}C -NMR ($CDCl_3$, 75 MHz, 20 °C): δ 24.1 24.8 25.3 32.9 35.9 (5CH₂), 37.9 (N-CH₃), 54.7 (NH₂-CH), 61.1 (N-CH), 116.6 122.3 (CH=CH), 138.4 (C-Pt). MS (positive ESI) [M-I]: calculated for $C_{15}H_{27}IN_3Pt$: 571.09, found 571.09, [M-I+CH₃CN]: calculated for $C_{15}H_{27}IN_3PtCH_3CN$: 612.12, found 612.11, [M-2I-H]: calculated for $C_{15}H_{26}N_3Pt$: 443.18, found 443.18.

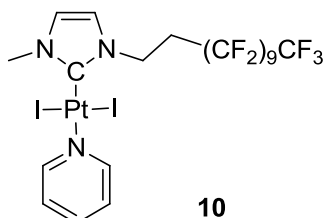


Procedure *a*: 43%. 1H -NMR ($CDCl_3$, 300 MHz, 20 °C): δ 1.02-2.00 (m, 16H, H_{Cy}), 2.36 (m, 4H, H_{Cy}), 5.31 (m, 2H, CH_{Cy}), 6.87 (s, 2H, CH=CH), 7.33 (m, 2H, CH_{pyr}), 7.71 (tt, J= 7.6 and 1.6Hz, 1H, CH_{pyr}), 9.09 (m, 2H, CH_{pyr}). ^{13}C -NMR ($CDCl_3$, 75 MHz, 20 °C): δ 25.4 (C_{Cy}), 25.6 (C_{Cy}), 33.0 (C_{Cy}), 59.5 (N-CH_{Cy}), 117 (CH=CH), 124.8 (C_{pyr}), 132.1 (C-Pt), 137.3 (C_{pyr}), 154.1 (C_{pyr}). MS (TOF MS ES+) [M-I+CH₃CN]: calculated for $C_{22}H_{32}IN_4Pt$: 674.13, found 674.15

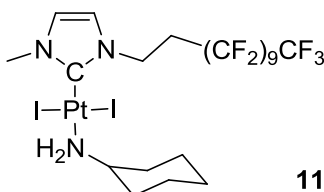


Procedure *b*: Quant. 1H -NMR ($CDCl_3$, 300 MHz, 20 °C): δ 1.05-1.97 (m, 24H, 24H_{CHA}), 2.31 (m, 6H, 6H_{CHA}), 2.92 (m, 2H, NH₂-Pt), 3.27 (m, 1H, CH), 5.19 (m, 2H, 2N-CH), 6.82 (s, 2H, CH=CH). ^{13}C -

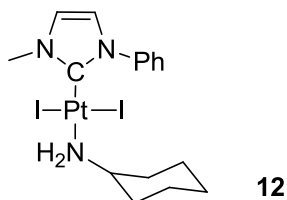
NMR (CDCl₃, 75 MHz, 20 °C): δ 24.8 25.4 25.6 26.9 32.9 35.9 (CH_{CHA}), 54.9 (NH₂-CH_{CHA}), 59.2 (2N-CH_{CHA}), 117.1 (CH=CH), 135.9 (C-Pt).



Procedure *a*: 73%. ¹H-NMR (CDCl₃, 300 MHz, 20 °C): δ 3.06 (m, 2H, CH₂), 3.95 (s, 3H, N-CH₃), 4.79 (t, J = 7.7Hz, 2H, N-CH₂), 6.89 (m, 2H, CH=CH), 7.32 (t, J = 6.9Hz, 2H, 2H_{Pyr}), 7.72 (t, J = 7.7Hz, 1H, 1H_{Pyr}), 8.97 (m, 2H, 2H_{Pyr}). ¹⁹F-NMR (CDCl₃, 300 MHz, 20 °C): δ -126.3 (m, 2F), -123.3 (s, 2F), -122.9 (s, 2F), -121.9 (m, 10F), -113.5 (quint, J = 16.2Hz, 2F), -81.0 (t, J = 10.0Hz, 3F). ¹³C-NMR (CDCl₃, 75 MHz, 20 °C): δ 31.5 (t, J = 21.3Hz, CH₂), 38.5 (s, N-CH₃), 43.0 (s, N-CH₂), 104.1-115.8 (m, CF), 117.7 (t, J = 32.4Hz, CF), 119.0 (t, J = 33.0Hz, CF), 120.9 (s, CH=), 122.6 (s, CH=), 125.1 (s, C_{Pyr}), 137.7 (s, C_{Pyr}), 153.7 (s, C_{Pyr}).

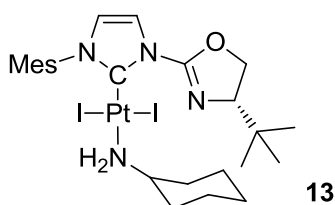


Procedure *b*: Quant., ¹H-NMR (CDCl₃, 300 MHz, 20 °C): δ 1.11-1.43 (m, 5H, 5H_{CHA}), 1.63 (m, 1H, 1H_{CHA}), 1.77 (m, 2H, 2H_{CHA}), 2.27 (m, 2H, 2H_{CHA}), 2.94 (m, 4H, NH₂+CH₂), 3.24 (m, 1H, CH_{CHA}), 3.86 (s, 3H, N-CH₃), 4.69 (t, J = 7.7, 2H, N-CH₂), 6.85 (s, 2H, CH=CH). ¹⁹F-NMR (CDCl₃, 300 MHz, 20 °C): δ -126.3 (s, 2F), -123.4 (s, 2F), -122.7 (s, 2F), -121.7 (m, 10F), -113.8 (s, 2F), -80.6 (t, J = 9.9Hz, 3F).

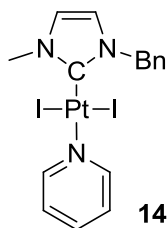


Procedure *a*: A mixture of 1-methyl-3-phenyl-1H-imidazol-3-ium iodide (20 mg, 0.070 mmol), sodium iodide (104.8 mg, 0.699 mmol), platinum dichloride (9.3 mg, 0.035 mmol) and potassium

carbonate (97 mg, 0.702 mmol) was suspended in cyclohexylamine (3 mL). The mixture was sonicated then stirred at 100°C overnight. The resulting suspension was concentrated under reduced pressure, then dissolved in dichloromethane, filtered through a celite plug and concentrated under reduced pressure. The residue was purified by silica gel chromatography (dichloromethane/cyclohexane 1:1) affording the complex as a yellow-brown oil (13.9 mg, 56%). ¹H-NMR (CDCl₃, 300MHz, 20 °C): δ 0.98-1.17 (m, 5H, 5H_{CHa}), 1.59-1.89 (m, 3H, 3H_{CHa}), 2.10 (m, 2H, 2H_{CHa}), 2.79 (m, 2H, Pt-NH₂), 3.06 (m, 1H, CH_{CHa}), 3.97 (s, 3H, N-CH₃), 6.97 (d, J= 2.1Hz, 1H, CH), 7.06 (d, J= 2.1Hz, 1H, CH), 7.30-7.53 (m, 3H, 3H_{ar}), 7.84 (d, J= 7.5, 2H, 2H_{ar}). ¹³C-NMR CDCl₃ (CDCl₃, 75 MHz, 20 °C): δ 24.7 (C_{CHa}), 25.2 (C_{CHa}), 35.6 (C_{CHa}), 38.4 (N-CH₃), 54.9 (CH_{CHa}), 121.9 (CH=), 122.2 (CH=), 126.9 (CH_{ar}), 128.3 (CH_{ar}), 128.6 (CH_{ar}), 139.8 (C_{ar}), 140.2 (C-Pt). MS (positive ESI) [M-I+CH₃CN]: calculated for C₁₆H₂₃I₁N₃Pt₁CH₃CN 620.08 found 620.08, [M-I]: calculated for C₁₆H₂₃I₁N₃Pt₁ 579.06 found 579.06.

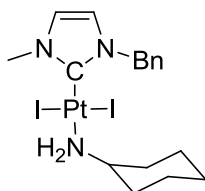


Procedure *a*: <5%, ¹H-NMR (CDCl₃, 300 MHz, 20 °C): δ 0.94 (s, 9H, C(CH₃)₃), 0.95-1.25 (m, 5H, 5H_{CHa}), 1.59-1.97 (m, 5H, 5H_{CHa}), 2.31 (s, 6H, 2CH₃ Mes), 2.33 (s, 3H, CH₃ Mes), 2.77 (m, 2H, Pt-NH₂), 2.94 (m, 2H, 1H_{CH2}+CH_{CHa}), 4.00 (dd, J= 14.0 and 4.3Hz, 1H, 1H_{CH2}), 4.26 (m, 1H, 1H_{CH2}), 6.74 (d, J= 1.9Hz, 1H, CH=), 6.93 (s, 2H, 2H_{ar}), 7.13 (d, J= 1.9Hz, 1H, CH=).

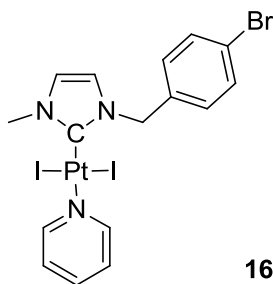


Procedure *a*: 72%: ¹H-NMR (CDCl₃, 300 MHz, 20 °C): δ 3.97 (s, 3H, N-CH₃), 5.72 (s, 2H, N-CH₂), 6.60 (s, 1H, CH=), 6.82 (s, 1H, CH=), 7.27-7.44 (m, 5H, 5H_{ar}), 7.52 (m, 2H, H_{Pyr}), 7.74 (m, 1H, H_{Pyr}), 9.09 (m, 2H, H_{Pyr}). ¹³C-NMR CDCl₃ (CDCl₃, 75 MHz, 20 °C): δ 38.3 (N-CH₃), 54.4 (N-CH₂), 119.8 (CH=), 122.2 (CH=), 124.8 (CH_{Pyr}), 128.3 (CH_{ar}), 128.8 (CH_{ar}), 129.1 (s, CH_{arom}), 135.4 (C_{Pyr}), 136.3 (C-Pt), 137.5 (s, C_{Pyr}), 153.7 (C_{Pyr}); MS (positive ESI) [M-I]: calculated for C₁₆H₁₇IN₃Pt: 573.011,

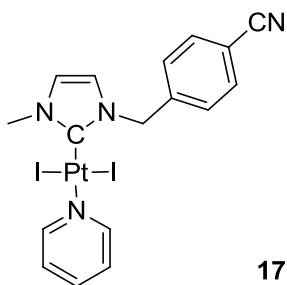
found 572.969. Microanalysis: Calculated for $C_{16}H_{17}I_2N_3Pt$: C, 27.44; H, 2.45; N, 6.00. Found: C, 26.97; H, 2.47; N, 5.82.

**15**

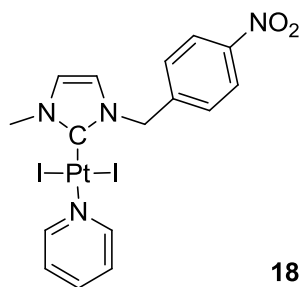
Cyclohexylamine (0.05 mL, 0.437 mmol) was added to a solution of **14** (10 mg, 0.014 mmol) in dichloromethane (1 mL). The reaction was stirred for 1 h at room temperature and filtered through silica gel plug with dichloromethane to afford the complex **15** as a yellow solid (11 mg, quantitative). 1H -NMR ($CDCl_3$, 300 MHz, 20°C): δ 0.96-1.32 (m, 5H, 5CH), 1.39-1.77 (m, 5H, 5CH), 2.71-3.00 (m, 2H, NH_2), 3.08-3.29 (m, 1H, CH_{CH_A}), 3.81 (s, 3H, N- CH_3), 5.51 (s, 2H, N- CH_2), 6.47 (d, $J = 1.8$ Hz, 1H, CH), 6.69 (d, $J = 1.9$ Hz, 1H, CH), 7.29-7.50 (m, 5H, Ar-H). ^{13}C -NMR ($CDCl_3$, 75 MHz, 20°C): δ 24.9 (CH_2), 25.3 (CH_2), 35.9 (CH_2), 38.1 (N- CH_3), 54.4 (N- CH_2), 54.9 (CH), 119.9 (CH), 122.2 (CH), 128.3 ($CH_{aromatic}$), 128.8 ($CH_{aromatic}$), 129.1 ($CH_{aromatic}$), 135.5 ($C_{aromatic}$), 139.9 (C-Pt). HRMS (positive ESI) [M-I]: Calculated for $C_{17}H_{25}IN_3Pt$ 593.074, found 593.071. Microanalysis: Calculated for $C_{17}H_{25}I_2N_3Pt$: C, 28.35; H, 3.50; N, 5.83. Found: C, 27.98; H, 3.42; N, 5.56.

**16**

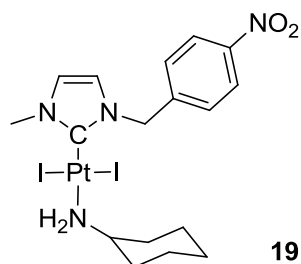
Procedure *a*: 89%. 1H -NMR ($CDCl_3$, 300 MHz, 20 °C): δ 3.98 (s, 3H, N- CH_3), 5.68 (s, 2H, N- CH_2), 6.59 (d, $J = 1.7$ Hz, 1H, CH=), 6.84 (d, $J = 1.7$ Hz, 1H, CH=), 7.31(t, $J = 6.7$ Hz, 2H, $2H_{Pyr}$), 7.38 (d, $J = 8.3$ Hz, 2H, $2H_{ar}$), 7.50 (d, $J = 8.3$ Hz, 2H, $2H_{ar}$), 7.71 (t, $J = 7.6$ Hz, 2H, $2H_{Pyr}$), 9.02 (m, 2H, $2H_{pyr}$). ^{13}C -NMR ($CDCl_3$, 75 MHz, 20 °C): δ 38.5 (N- CH_3), 53.9 (N- CH_2), 119.9 (CH=), 122.5 (C_{ar-Br}), 122.6 (CH=), 125.1 (C_{Pyr}), 130.8 (CH_{ar}), 132.1 (CH_{ar}), 134.5 (C_{ar}), 137.0 (C-Pt), 137.6 (C_{Pyr}), 153.8 (C_{Pyr}). MS (positive ESI) [M+Na]: calculated for $C_{16}H_{16}I_2N_3Pt_1Br_1Na$: 801.8121, found 801.8301, [M-I]: calculated for $C_{16}H_{16}I_1N_3Pt_1Br_1$: 651.9179, found 651.9341.



Procedure *a*: 34%. $^1\text{H-NMR}$ (CDCl_3 , 300 MHz, 20 °C): δ 4.01 (s, 3H, N- CH_3), 5.81 (s, 2H, N- CH_2), 6.65 (d, J = 2.0Hz, 1H, CH=), 6.90 (d, J = 2.0Hz, 1H, CH=), 7.32 (m, 2H, 2H_{pyr}), 7.58-7.76 (m, 5H, 4H_{ar} and 1H_{pyr}), 9.00 (m, 2H, 2H_{pyr}). $^{13}\text{C-NMR}$ (CDCl_3 , 75 MHz, 20 °C): δ 38.6 (N- CH_3), 54.1 (N- CH_2), 112.4 ($\text{C}_{\text{ar-CN}}$), 118.6 (CN), 120.1 (CH=), 123.1 (CH=), 125.1 (C_{pyr}), 129.6 (CH_{ar}), 132.7 (CH_{ar}), 137.7 (C_{pyr}), 138.2 (C-Pt), 140.9 (C_{ar}), 153.8 (C_{pyr}).

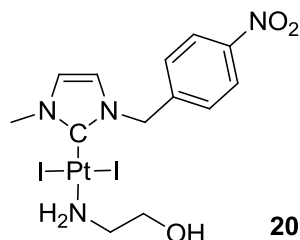


Procedure *a*: 86%. $^1\text{H-NMR}$ (CDCl_3 , 300 MHz, 20 °C): δ 4.01 (s, 3H, N- CH_3), 5.85 (s, 2H, N- CH_2), 6.68 (d, J = 2.1Hz, 1H, CH=), 6.92 (d, J = 2.1Hz, 1H, CH=), 7.32 (t, J = 7.0Hz, 2H, 2H_{pyr}), 7.65 (d, J = 8.7Hz, 2H, 2H_{ar}), 7.72 (tt, J = 7.8 and 1.6Hz, 1H, H_{pyr}), 8.22 (d, J = 8.7Hz, 2H, 2H_{ar}), 8.99 (m, 2H, 2H_{pyr}). $^{13}\text{C-NMR}$ (CDCl_3 , 75 MHz, 20 °C): δ 38.6 (N- CH_3), 53.7 (N- CH_2), 120.2 (CH=), 123.2 (CH=), 124.1 (CH_{ar}), 125.1 (C_{pyr}), 129.6 (CH_{ar}), 137.7 (C_{pyr}), 138.2 (C-Pt), 142.8 (C_{ar}), 147.9 (C_{ar}), 153.7 (C_{pyr}).

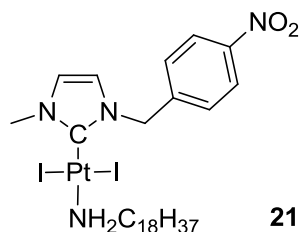


Procedure *b* : Quant. $^1\text{H-NMR}$ (CDCl_3 , 300 MHz, 20 °C): δ 1.09-1.37 (m, 5H, 5H_{CHA}), 1.54-1.81 (m, 3H, 3H_{CHA}), 2.24 (m, 2H, 2H_{CHA}), 2.92 (m, 2H, Pt- NH_2), 3.21 (m, 1H, CH_{CHA}), 3.91 (s, 3H, N- CH_3),

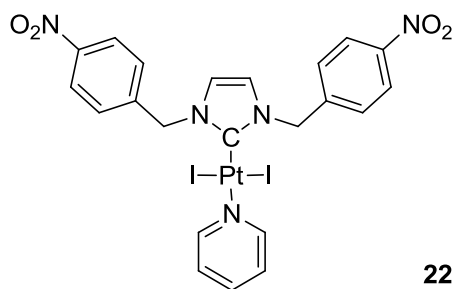
5.73 (s, 2H, N-CH₂), 6.65 (d, J= 2.1Hz, 1H, CH=), 6.88 (d, J= 2.1Hz, 1H, CH=), 7.59 (d, J= 8.7Hz, 2H, 2H_{ar}), 8.21 (d, J= 8.7Hz, 2H, 2H_{ar}). ¹³C-NMR (CDCl₃, 75 MHz, 20 °C): δ 24.9 (C_{CHA}), 25.4 (C_{CHA}), 36.0 (C_{CHA}), 38.4 (N-CH₃), 53.6 (N-CH₂), 55.0 (CH_{CHA}), 120.1 123.1 (CH=CH), 124.1 (CH_{ar}), 129.5 (CH_{ar}), 141.7 (C-Pt), 142.9 (C_{ar}), 147.9 (C_{ar}). MS (positive ESI) [M-I]: calculated for C₁₇H₂₄I₁N₄Pt₁O₂ 638.0588, found 638.0609, [M₂+Na]: calculated for C₃₄H₄₈I₄N₈Pt₂O₄Na 1552.9159, found 1552.9125.



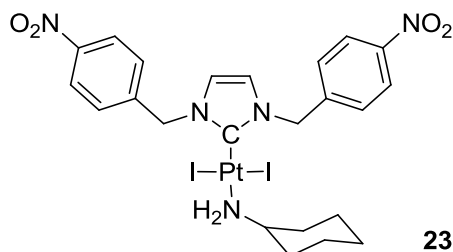
Procedure *b*: ~20%. ¹H-NMR (CDCl₃, 300 MHz, 20 °C): δ 3.16-3.25 (m, 4H, Pt-NH₂+CH₂), 3.91 (m, 5H, N-CH₃ and CH₂), 5.74 (s, 2H, N-CH₂), 6.66 (s, 1H, CH=), 6.89 (s, 1H, CH=), 7.58 (d, J= 8.5Hz, 2H, 2H_{ar}), 8.23 (d, J= 8.5Hz, 2H, 2H_{ar}). ¹³C-NMR (CDCl₃, 75 MHz, 20 °C): δ 38.5 (N-CH₃), 47.4 (CH₂), 53.6 (N-CH₂), 61.0 (CH₂-OH), 120.2 (CH=), 123.2 (CH=), 124.2 (CH_{ar}), 129.5 (CH_{ar}), 141.0 (C-Pt), 142.7 (C_{ar}), 148.0 (C_{ar}-NO₂).



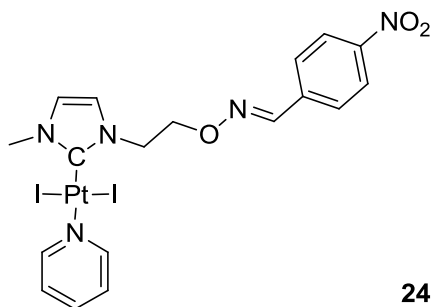
Procedure *b*: 85%. ¹H-NMR (CDCl₃, 300 MHz, 20 °C): δ 0.88 (t, J= 6.7Hz, 3H, CH₃), 1.17-1.41 (m, 30H, 15CH₂), 1.56 (m, 2H, CH₂), 2.94 (m, 4H, CH₂+NH₂), 3.91 (s, 3H, N-CH₃), 5.74 (s, 2H, N-CH₂), 6.64 (d, J= 2.1Hz, 1H, CH=), 6.87 (d, J= 2.1Hz, 1H, CH=), 7.59 (d, J= 8.7Hz, 2H, 2H_{ar}), 8.22 (d, J= 8.7Hz, 2H, 2H_{ar}). ¹³C-NMR (CDCl₃, 75 MHz, 20 °C): δ 14.3 (CH₃ alkane), 22.9 26.6 29.3 29.5 29.6 29.7 29.8 32.1 32.3 (CH₂ alkane), 38.5 (N-CH₃), 45.7 (CH₂ alkane), 53.7 (N-CH₂), 120.1 (CH=), 123.1 (CH=), 124.1 (CH_{ar}), 129.5 (CH_{ar}), 141.5 (C-Pt), 142.9 (C_{ar}), 148.0 (C_{ar}-NO₂).



Procedure *a*: 49%. $^1\text{H-NMR}$ (CDCl_3 , 300 MHz, 20 °C): δ 5.91 (s, 4H, 4N- CH_2), 6.77 (s, 2H, $\text{CH}=\text{CH}$), 7.32 (t, $J = 6.7\text{Hz}$, 2H, 2H_{pyr}), 7.63-7.78 (m, 5H, 4H_{ar} and 1H_{pyr}), 8.25 (d, $J = 8.7\text{Hz}$, 4H, 4H_{ar}), 8.95 (m, 2H, 2H_{pyr}). $^{13}\text{C-NMR}$ (CDCl_3 , 75 MHz, 20 °C): δ

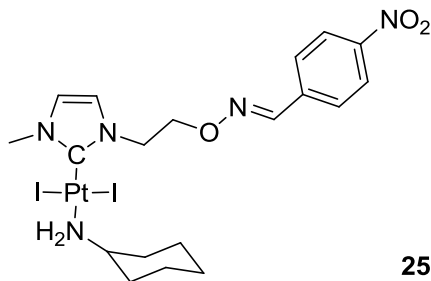


Procedure *b*: Quant. $^1\text{H-NMR}$ (CDCl_3 , 300 MHz, 20 °C): δ 1.08-1.35 (m, 5H, 5H_{CHA}), 1.59-1.79 (m, 3H, 3H_{CHA}), 2.90 (m, 2H, 2H_{CHA}), 2.95 (m, 2H, Pt-NH_2), 3.20 (m, 1H, CH_{CHA}), 5.79 (s, 4H, 2N-CH_2), 6.73 (s, 2H, $\text{CH}=\text{CH}$), 7.63 (d, $J = 8.3\text{Hz}$, 4H, 4H_{ar}), 8.24 (d, $J = 8.3\text{Hz}$, 4H, 4H_{ar}). $^{13}\text{C-NMR}$ (CDCl_3 , 75 MHz, 20 °C): δ 24.89 (C_{CHA}), 25.3 (C_{CHA}), 36.0 (C_{CHA}), 54.0 (N-CH_2), 55.2 (CH_{CHA}), 121.4 ($\text{CH}=\text{CH}$), 124.2 (CH_{ar}), 129.6 (CH_{ar}), 142.4 (C_{ar}), 143.8 (C-Pt), 148.1 ($\text{C}_{\text{ar-NO}_2}$).

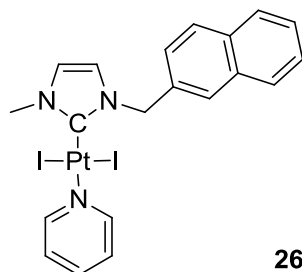


Procedure *a*: 44%. $^1\text{H-NMR}$ (CDCl_3 , 300 MHz, 20 °C): δ 3.96 (s, 3H, N-CH_3), 4.83 (m, 4H, $\text{N-CH}_2\text{-CH}_2\text{-O}$), 6.84 (d, $J = 2.0\text{Hz}$, 1H, CH), 6.91 (d, $J = 2.0\text{Hz}$, 1H, CH), 7.31 (ddd, $J = 7.6$, 5.0 and 1.5Hz, 2H, 2H_{pyr}), 7.73 (tt, $J = 7.7$ and 1.6Hz, 1H, 1H_{pyr}), 7.77 (d, $J = 8.7\text{Hz}$, 2H, 2H_{ar}), 8.22 (m, 3H, 2H_{ar} and $\text{CH}=\text{N}$), 9.02 (m, 2H, 2H_{pyr}). $^{13}\text{C-NMR}$ (CDCl_3 , 75 MHz, 20 °C): δ 38.5 (N-CH_3), 49.9 (N-CH_2), 73.0

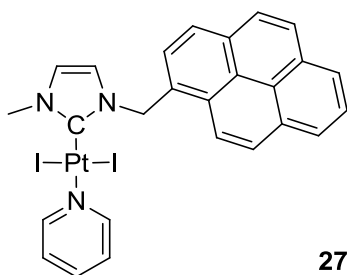
(O-CH₂), 121.7 122.1 (CH=CH), 124.1 (CH_{ar}), 125.1 (C_{Pyr}), 127.9 (CH_{ar}), 136.4 (C-Pt), 137.6 (C_{Pyr}), 138.1 (C_{ar}), 147.7 (CH=N), 148.6 (C_{ar}-NO₂), 153.8 (C_{Pyr}).



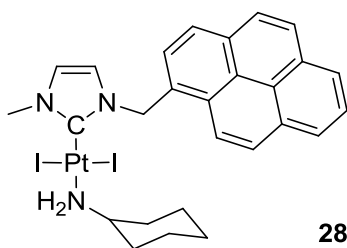
Procedure *b*: quant. ¹H-NMR (CDCl₃, 300 MHz, 20 °C): δ 1.06-1.39 (m, 5H, 5H_{CHA}), 1.57-1.81 (m, 3H, 3H_{CHA}), 2.27 (m, 2H, 2H_{CHA}), 2.92 (m, 2H, Pt-NH₂), 3.25 (m, 1H, CH_{CHA}), 3.87 (s, 3H, N-CH₃), 4.75 (s, 4H, N-CH₂-CH₂-O), 6.80 (d, J= 2.0Hz, 1H, CH), 6.87 (d, J= 2.0Hz, 1H, CH), 7.76 (d, J= 8.8Hz, 2H, 2H_{ar}), 8.18 (s, 1H, CH=N), 8.24 (d, J= 8.8Hz, 2H, 2H_{ar}). ¹³C-NMR (CDCl₃, 75 MHz, 20 °C): δ 24.8 (C_{CHA}), 25.2 (C_{CHA}), 35.9 (C_{CHA}), 38.1 (N-CH₃), 49.6 (N-CH₂), 54.8 (CH_{CHA}), 72.9 (O-CH₂), 121.5 121.8 (CH=CH), 124.0 (CH_{ar}), 127.7 (CH_{ar}), 137.9 (C_{ar}), 139.8 (C-Pt), 147.4 (CH=N), 148.5 (C_{ar}-NO₂).



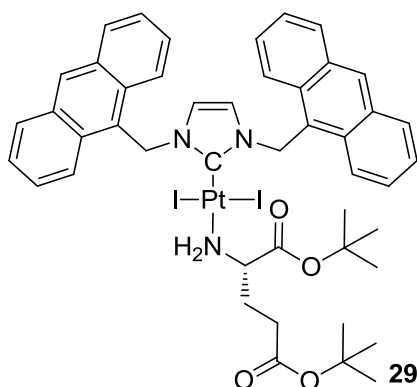
Procedure *a*: 78%. ¹H-NMR (CDCl₃, 300 MHz, 20 °C): δ 3.99 (s, 3H, N-CH₃), 5.88 (s, 2H, N-CH₂), 6.56 (d, J= 2.1Hz, 1H, CH=), 6.80 (d, J= 2.1Hz, 1H, CH=), 7.26 (ddd, J= 7.6, 5.2 and 1.4Hz, 2H, 2H_{Pyr}), 7.46-7.55 (m, 2H, 2H_{ar}), 7.61-7.71 (m, 2H, 2H_{ar}), 7.80-7.91 (m, 2H, 2H_{ar}), 7.96 (s, 1H, 1 H_{ar}), 9.04 (m, 2H, 2H_{Pyr}). ¹³C-NMR (CDCl₃, 75 MHz, 20 °C): δ 38.3 (N-CH₃), 54.6 (N-CH₂), 119.9 122.4 (CH=CH), 124.9 (C_{Pyr}), 126.3 126.4 126.6 127.7 127.9 128.1 128.7 (CH_{ar}), 132.8 133.0 133.1 (C_{ar}), 136.3 (C-Pt), 137.4 (C_{Pyr}), 153.5 (C_{Pyr}). MS (positive ESI) [M-I-Pyr]: calculated for C₁₅H₁₄I₁N₃Pt: 543.9845, found 543.9864, [M-I]: calculated for C₂₀H₁₉I₁N₃Pt: 623.0268, found 623.0224, [M-I-HI]: calculated for C₂₀H₁₉N₃Pt: 495.1145, found 495.1567.



Procedure *a*: 60%. $^1\text{H-NMR}$ (CDCl_3 , 300 MHz, 20 °C): δ 4.04 (s, 3H, N- CH_3), 6.26 (d, J = 2.0Hz, 1H, CH=), 6.36 (s, 2H, N- CH_2), 6.69 (d, J = 2.0Hz, 1H, CH=), 7.35 (ddd, J = 7.6, 5.2 and 1.3Hz, 2H, 2H_{Pyr}), 7.74 (tt, J = 7.6 and 1.5Hz, 1H, 1H_{Pyr}), 7.99-8.26 (m, 8H, 8H_{ar}), 8.55 (d, J = 9.2Hz, 1H, 1H_{ar}), 9.12 (m, 2H, 2H_{Pyr}). $^{13}\text{C-NMR}$ (CDCl_3 , 75 MHz, 20 °C): δ 38.6 (N- CH_3), 53.6 (N- CH_2), 120.1 121.9 (CH=CH), 124.0 124.7 125.0 125.1 125.7 125.8 126.4 127.5 127.7 128.2 128.9 129.1 130.0 131.0 131.3 132.1 (C_{ar} + C_{Pyr}), 136.1 (C-Pt), 137.6 (C_{Pyr}), 153.9 (C_{Pyr}).

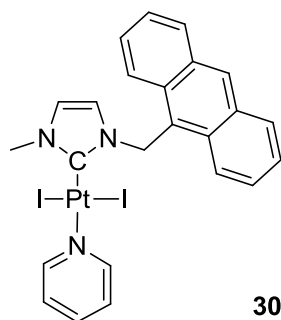


Procedure *b*: 98%. $^1\text{H-NMR}$ (CDCl_3 , 300 MHz, 20 °C): δ 1.05-1.74 (m, 8H, 8H_{CHA}), 2.34 (m, 2H, 2H_{CHA}), 3.02 (m, 2H, Pt- NH_2), 3.34 (m, 1H, CH_{CHA}), 3.94 (s, 3H, N- CH_3), 6.23 (s, 3H, N- CH_2 and CH=), 6.65 (d, J = 2.0Hz, 1H, CH=), 8.00-8.24 (m, 8H, 8H_{ar}), 8.48 (d, J = 9.3Hz, 1H, 1H_{ar}).

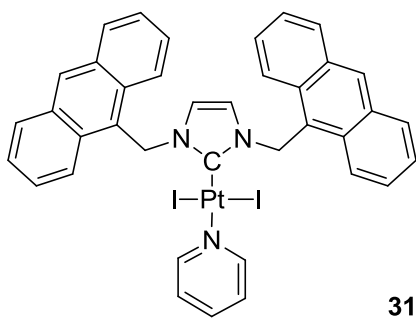


Procedure *b*: ~80%. $^1\text{H-NMR}$ (CDCl_3 , 300 MHz, 20 °C): δ 1.19 (s, 9H, O- t -Bu), 1.52 (s, 9H, O- t -Bu), 2.32-2.96 (m, 4H, 4H_{Glu}), 3.72 (m, 2H, NH_2 -Pt), 4.42 (m, 1H, CH_{Glu}), 5.74 (s, 2H, CH=CH), 6.54 (s, 4H, 2N- CH_2), 7.44-7.63 (m, 8H, 8H_{antr}), 8.02 (d, 4H, 4H_{antr}), 8.47 (m, 6H, 6H_{antr}). $^{13}\text{C-NMR}$ (CDCl_3 ,

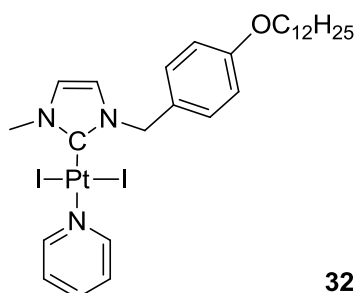
75 MHz, 20 °C): δ 26.9 (CH_2_{Glu}), 27.9 ($\text{CH}_3_{t\text{Bu}}$), 28.1 ($\text{CH}_3_{t\text{Bu}}$), 31.6 (CH_2_{Glu}), 48.0 (N- CH_2), 58.1 (CH_{Glu}), 80.6 (O- $\text{C}_{t\text{Bu}}$), 83.2 (O- $\text{C}_{t\text{Bu}}$), 119.1 ($\text{CH}=\text{CH}$), 124.5 124.6 125.4 127.4 129.0 129.4 131.3 131.4 (C_{antr}), 136.6 (C-Pt), 171.5 (C=O), 172.3 (C=O). MS (positive ESI) [M-I]: calculated for $\text{C}_{46}\text{H}_{49}\text{I}_1\text{N}_3\text{O}_4\text{Pt}_1$ 1029.24, found 1029.24, [M+Na]: calculated for $\text{C}_{46}\text{H}_{49}\text{I}_2\text{N}_3\text{O}_4\text{Pt}_1\text{Na}$ 1179.14 found 1179.13.



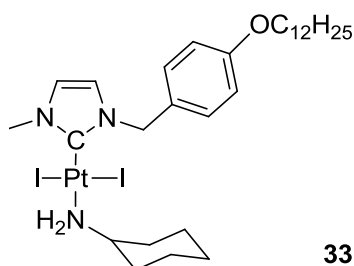
Procedure *a*: 63%. ^1H -NMR (CDCl_3 , 300 MHz, 20 °C): δ 4.04 (s, 3H, CH_3), 5.98 (d, J = 2.1 Hz, 1H, $\text{CH}=\text{}$), 6.58 (s, 2H, NCH_2), 6.60 (d, J = 1.8 Hz, 1H, $\text{CH}=\text{}$), 7.39 (m, 2H, 2CH_{Pyr}), 7.55 (m, 4H, $4\text{H}_{\text{anthracenyl}}$), 7.77 (m, 1H, CH_{Pyr}), 8.09 (d, J = 7.8 Hz, 2H, $2\text{H}_{\text{anthracenyl}}$), 8.46 (d, J = 5.7 Hz, 2H, $2\text{H}_{\text{anthracenyl}}$), 8.59 (s, 1H, $\text{H}_{\text{anthracenyl}}$), 9.18 ppm (m, 2H, 2H_{Pyr}); HRMS (positive ESI) [M-I]: calculated for $\text{C}_{24}\text{H}_{21}\text{IN}_3\text{Pt}$ 673.043, found 673.045; UV/Vis (CH_2Cl_2) λ_{max} (nm) (e, $\text{M}^{-1}\text{cm}^{-1}$): 276 (9480), 334 (3490), 351 (5930), 368 (8890), 389 (8230). luminescent properties: λ_{exc} =368 nm; λ_{em} =400-470 nm.



Procedure *a*: ~40%. ^1H -NMR (CDCl_3 , 300 MHz, 20 °C): δ 5.76 (s, 2H, $\text{CH}=\text{CH}$), 6.68 (s, 4H, 2N-CH_2), 7.36-7.65 (m, 10H, $8\text{H}_{\text{antr}}+2\text{H}_{\text{pyr}}$), 7.79 (m, 1H, 1H_{pyr}), 8.03 (m, 4H, 4H_{antr}), 8.52 (m, 6H, 6H_{antr}), 9.30 (m, 2H, 2H_{pyr}). ^{13}C -NMR (CDCl_3 , 75 MHz, 20 °C): δ 48.2 (N- CH_2), 119.1 ($\text{CH}=\text{CH}$), 124.5 124.6 124.8 125.1 125.4 127.4 129.0 129.3 131.4 ($8\text{C}_{\text{antr}}+\text{C}_{\text{Pyr}}$), 135.1 (C-Pt), 137.5 (C_{Pyr}), 153.9 (C_{Pyr}). MS (positive ESI) [M-I]: calculated for $\text{C}_{38}\text{H}_{29}\text{IN}_3\text{Pt}$: 849.11, found 849.10.

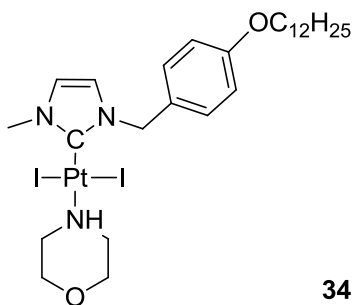


3-(4-(dodecyloxy)benzyl)-1-methyl-1H-imidazol-3-ium bromide (20 mg, 0.046 mmol), PtCl_2 (13.4 mg, 0.050 mmol), NaI (69 mg, 0.460 mmol) and K_2CO_3 (63 mg, 0.457 mmol) were suspended in pyridine (3 mL). The mixture was refluxed overnight at 100 °C, then concentrated under reduced pressure, dissolved in CH_2Cl_2 and filtered through a celite plug. The residue was purified by a silica gel chromatography ($\text{CH}_2\text{Cl}_2/\text{cyclohexane}$) affording the complex as a yellow oil (21.3 mg, 53%). ^1H -NMR (CDCl_3 , 300MHz, 20 °C): δ 0.88 (t, J = 6.9Hz, 3H, CH_3), 1.09-1.44 (m, 18H, CH_2), 1.78 (m, 2H, CH_2), 3.94 (t, J = 6.6Hz, 2H, O- CH_2), 3.98 (s, 3H, N- CH_3), 5.64 (s, 2H, N- CH_2), 6.57 (d, J = 1.8Hz, 1H, CH=), 6.79 (d J = 1.8Hz, 1H, CH=), 6.90 (m, 2H, 2H_{ar}), 7.31(m, 2H, CH_{pyr}), 7.47 (m, 2H, 2H_{ar}), 7.73(m, 1H, CH_{pyr}), 9.06 (m, 2H, CH_{pyr}). ^{13}C -NMR (CDCl_3 , 75 MHz, 20 °C): δ 14.1 (CH_3), 22.7 (CH_2CH_3), 26.1 (CH_2), 29.3 (CH_2), 29.4 (CH_2), 29.6 (CH_2), 29.7 (CH_2), 31.9 (CH_2), 38.3 (N- CH_3), 54.1 (N- CH_2), 68.1 (O- CH_2), 114.8 (CH_{ar}), 119.8 (C=C), 122.2 (C=C), 124.9 (CH_{pyr}), 127.2 (C_{ar}), 130.6 (CH_{ar}), 135.9 (C-Pt), 137.4 (CH_{pyr}), 153 (CH_{pyr}), 159.3 (C_{ar} -O). MS (positive ESI) $[\text{M}-\text{I}]$: calculated for $\text{C}_{28}\text{H}_{41}\text{I}_1\text{N}_3\text{O}_1\text{Pt}_1$ 757.19, found 577.18, $[\text{M}-\text{I}+\text{CH}_3\text{CN}]$ calculated for $\text{C}_{28}\text{H}_{41}\text{I}_1\text{N}_3\text{O}_1\text{Pt}_1\text{CH}_3\text{CN}$ 798.22, found 798.20.

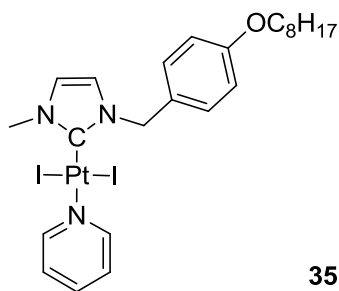


3-(4-(dodecyloxy)benzyl)-1-methyl-1H-imidazol-3-ium bromide (20 mg, 0.046 mmol), PtCl_2 (13.4 mg, 0.050 mmol), NaI (69 mg, 0.460 mmol) and K_2CO_3 (63 mg, 0.457 mmol) were suspended in cyclohexylamine (3 mL). The mixture was refluxed overnight at 100 °C, then concentrated under reduced pressure, dissolved in CH_2Cl_2 and filtered through a celite plug. The residue was purified by a silica gel chromatography ($\text{CH}_2\text{Cl}_2/\text{cyclohexane}$) affording the complex as a yellow oil (21.8 mg, 53%). ^1H -NMR (CDCl_3 , 300MHz, 20 °C): δ 0.87 (t, J = 6.9Hz, 3H, CH_3), 0.96-1.78 (m, 26H, CH_2 and 4. CH_{CHA}), 1.78 (m, 2H, CH_2), 2.28 (d, J = 11.7Hz, 2H, CH_2) 2.85 (m, 2H, NH_2), 3.27 (m, 1H, CH_{CHA}), 3.86 (s, 3H, N- CH_3), 3.93 (t, J = 6.6Hz, 2H, O- CH_2), 5.50 (s, 2H, N- CH_2), 6.52 (d, J = 1.8Hz, 1H,

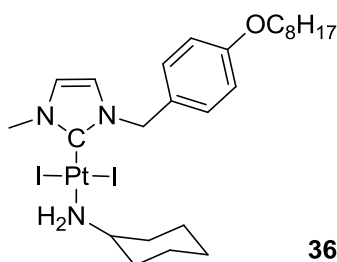
CH=), 6.75 (d, J = 1.8Hz, 1H, CH=), 6.87 (d J = 8.7Hz, 2H, $2H_{ar}$), 7.37 (d, J = 8.7 2H, $2H_{ar}$). ^{13}C -NMR ($CDCl_3$, 75 MHz, 20 °C): δ 14.2 (CH_3), 22.7 (CH_2CH_3), 24.7 (CH_2), 24.9 (CH_2), 25.3 (CH_2), 26.1 (CH_2), 29.3 (CH_2), 29.5 (CH_2), 29.6 (CH_2), 29.8 (CH_2), 31.9 (CH_2), 35.8 (CH_2), 35.9 (CH_2), 36.0 (CH_{CHA}), 38.1 (N- CH_3), 53.8 (CH_2), 54.8 (N- CH_2), 68.1 (O- CH_2), 114.7 (CH_{ar}), 119.7 (C=C), 122.1 (C=C), 127.0 (C_{ar}) 130.5 (CH_{ar}), 139.3 (C-Pt), 159.2 (C_{ar} -O). 1H -NMR (DMSO, 300MHz, 20 °C): δ 0.83 (t, J = 6.5Hz, 3H, CH_3), 0.92-1.78 (m, 26H, CH_2 , NH_2 and 4. CH_{CHA}), 1.65 (m, 2H, CH_2), 2.16 (m, 2H, CH_2), 3.05 (m, 1H, CH_{CHA}), 3.74 (s, 3H, N- CH_3), 3.91 (t, J = 6.5Hz, 2H, O- CH_2), 5.44 (s, 2H, N- CH_2), 6.86 (d J = 8.4Hz, 2H, $2H_{ar}$), 6.91 (d, J = 1.8Hz, 1H, CH=), 7.22 (d, J = 1.8Hz, 1H, CH=), 7.42 (d, J = 8.4 2H, $2H_{ar}$). ^{13}C -NMR (DMSO, 75 MHz, 20 °C): δ 14.2 (CH_3), 22.6 (CH_2CH_3), 24.9 (CH_2), 25.6 (CH_2), 26.0 (CH_2), 29.2 (CH_2), 29.3 (CH_2), 29.5 (CH_2), 31.8 (CH_2), 35.0 (CH_{CHA}), 37.7 (N- CH_3), 52.8 (CH_2), 54.6 (N- CH_2), 67.9 (O- CH_2), 114.8 (CH_{ar}), 120.6 (C=C), 123.5 (C=C), 128.5 (C_{ar}) 130.6 (CH_{ar}), 140.0 (C-Pt), 158.9 (C_{ar} -O). MS (positive ESI) $[M-I]$: calculated for $C_{29}H_{49}I_1N_3O_1Pt_1$ 777.26, found 777.26.



3-(4-(dodecyloxy)benzyl)-1-methyl-1H-imidazol-3-ium bromide (20 mg, 0.046 mmol), $PtCl_2$ (13.4 mg, 0.050 mmol), NaI (69 mg, 0.460 mmol) and K_2CO_3 (63 mg, 0.457 mmol) were suspended in morpholine (3 mL). The mixture was refluxed overnight at 100 °C, then concentrated under reduced pressure, dissolved in CH_2Cl_2 and filtered through a celite plug. The residue was purified by a silica gel chromatography (CH_2Cl_2 /cyclohexane) affording the complex as a yellow oil (22.4 mg, 44%). 1H -NMR ($CDCl_3$, 300MHz, 20 °C): δ 0.88 (t, J = 6.9.Hz, 3H, CH_3), 1.15-1.49 (m, 20H, CH_2), 1.77 (m, 2H, CH_2), 2.290 (m, 2H, $2H_{Mo}$), 3.34 (m, 1H, NH), 3.56 (m, 4H, CH_{Mo}). 3.85 (s, 3H, N- CH_3), 3.94 (t, J = 6.6Hz, 2H, O- CH_2), 5.47 (s, 2H, N- CH_2), 6.53 (d, J = 1.8Hz, 1H, CH=), 6.75 (d, J = 1.8Hz, 1H, CH=), 6.87 (d J = 8.7Hz, 2H, $2H_{ar}$), 7.35 (d, J = 8.7 2H, $2H_{ar}$). MS (positive ESI) $[M-I]$: calculated for $C_{27}H_{45}I_1N_3O_2Pt_1$ 765.22, found 765.21.

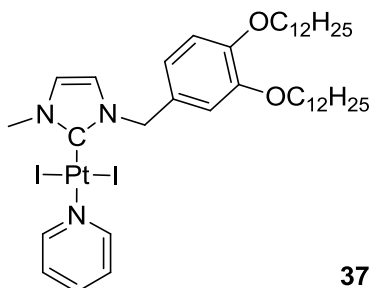


A mixture of 1-methyl-3-(4'-octyloxy)phenyl-1*H*-imidazol-3-ium bromide (62 mg, 0.162 mmol), sodium iodide (240 mg, 1.6 mmol), platinum dichloride (43 mg, 0.162 mmol) and potassium carbonate (221 mg, 2.232 mmol) was suspended in pyridine (2 mL). The mixture was stirred overnight at 100°C. The resulting suspension was concentrated *in vacuo*, then dissolved in dichloromethane, filtered through a celite plug and concentrated in vacuo. The residue was purified by a silica gel chromatography (dichloromethane/cyclohexane 3:2) affording the complex as a yellow-orange powder (83 mg, 62%). ¹H-NMR (CDCl₃, 300 MHz, 20°C): δ 0.89 (t, J= 8.3 Hz, 3H, CH₃), 1.37 (m, 10H, alkyl chain), 1.75 (m, 2H, alkyl chain), 3.95 (t, J= 6.0 Hz, 2H, OCH₂), 3.98 (s, 3H, N-CH₃), 5.64 (s, 2H, CH₂ benzyl), 6.57 (d, J= 2.1 Hz, 1H, CH_{imidazole}), 6.80 (d, J= 2.1 Hz, 1H, CH_{imidazole}), 6.90 (dd, J= 8.7, J= 2.1, 2H, CH_{phenyl}), 7.32 (m, 2H, CH_{py}), 7.43 (dd, J= 8.7, J= 1.8, 2H, CH_{phenyl}), 7.72 (t, J= 7.8 Hz, 1H, CH_{py}), 9.05 (d, J = 6.3 Hz, 2H, CH_{py}). ¹³C-NMR (CDCl₃, 125 MHz, 20°C): δ 14.1 (Me), 22.7, 26.1, 29.3 (m, alkyl chain), 31.8, 38.3, 54.1, 68.1 (N-Me), 114.8 (C_{imidazole}), 119.8 (CH_{aromatic}), 122.2 (CH_{aromatic}), 124.9 (CH_{imidazole}), 127.2 (CH_{pyridine}), 130.6 (C-Pt), 137.5 (CH_{pyridine}), 153.7 (CH_{pyridine}), 159.2 (OC_{aromatic}). Mass Spectrometry (positive ESI) [M-I]: Calculated for C₂₂H₃₃IN₃O Pt 701.24, found 701.13

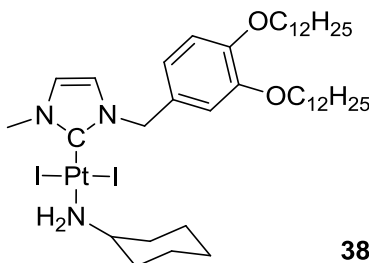


Complex (40 mg, 0.048 mmol) was dissolved in 1 mL of cyclohexylamine and stirred at 25 °C. After 10 min the solvent was removed in vacuo, affording the complex as a yellow powder (27 mg, 67%). ¹H-NMR (CDCl₃, 300 MHz, 20°C): δ 0.88 (m, 3H, CH₃), 1.00-1.90 (m, 18H, alkyl chain and cyclohexylamine), 2.32 (m, 2H, cyclohexylamine), 2.94 (m, 2H, cyclohexylamine), 3.26 (m, 1H, cyclohexylamine), 3.88 (s, 3H, N-CH₃), 3.95 (t, J= 6.6 Hz, OCH₂), 5.52 (s, 2H, benzyl), 6.54 (d, J= 2.1 Hz, 1H, CH_{imidazole}), 6.75 (d, J= 2.1 Hz, 1H, CH_{imidazole}), 6.88 (d, J= 8.4 Hz, 2H, CH_{phenyl}), 7.38 (d, J = 8.7 Hz, 2H, CH_{phenyl}). ¹³C-NMR (CDCl₃, 125 MHz, 20°C): δ 14.1 (Me), 22.7, 24.8, 25.3, 26.1, (m,

cyclohexylamine), 29.3 (m, alkyl chain), 29.7, 30.9, 31.8, 35.9, 38.1, 53.8, 54.8, 68.1 (N-Me), 114.8 ($\text{CH}_{\text{aromatic}}$), 119.7 ($\text{C}_{\text{imidazole}}$), 122.3 ($\text{C}_{\text{imidazole}}$), 127.2 ($\text{CH}_{\text{aromatic}}$), 130.5 ($\text{CH}_{\text{aromatic}}$), 139.3 (C-Pt), 159.2 (NH_2CH).

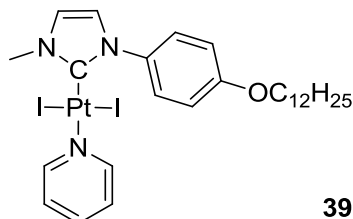


A mixture of 1-methyl-3-(3',4'-didodecyloxy)phenyl-1*H*-imidazol-3-ium bromide (101 mg, 0.162 mmol), sodium iodide (240 mg, 1.6 mmol), platinum dichloride (43 mg, 0.162 mmol) and potassium carbonate (221 mg, 2.232 mmol) was suspended in pyridine (2 mL). The mixture was stirred overnight at 100°C. The resulting suspension was concentrated in vacuo, then dissolved in dichloromethane, filtered through a celite plug and concentrated in vacuo. The residue was purified by a silica gel chromatography (dichloromethane/cyclohexane 3:2) affording the complex as a yellow-orange powder (96 mg, 62%). ^1H -NMR (CDCl_3 , 300 MHz, 20°C): δ 0.88 (m, 6H, 2CH_3), 1.27 (m, 40H, alkyl chain), 1.79 (m, 4H, alkyl chain), 3.99 (m, 7H, N-Me and 2OCH_2), 5.63 (s, 2H, CH_2 benzyl), 6.60 (d, $J = 2.1$ Hz, 1H, $\text{CH}_{\text{imidazole}}$), 6.80 (d, $J = 2.1$ Hz, 1H, $\text{CH}_{\text{imidazole}}$), 6.83-7.15 (m, 3H, $\text{CH}_{\text{phenyl}}$), 7.32 (m, 2H, CH_{py}), 7.72 (t, $J = 7.8$ Hz, 1H, CH_{py}), 9.06 (d, $J = 4.8$ Hz, 2H, CH_{py}). ^{13}C -NMR (CDCl_3 , 125 MHz, 20°C): δ 14.2 (Me), 22.7, 26.1, 29.3 (m, alkyl chain), 31.9, 38.3, 54.4, 69.4 (N-Me), 113.5 ($\text{C}_{\text{imidazole}}$), 114.5 ($\text{CH}_{\text{aromatic}}$), 119.8 ($\text{CH}_{\text{aromatic}}$), 121.4 ($\text{CH}_{\text{imidazole}}$), 122.3 ($\text{CH}_{\text{aromatic}}$), 124.9 ($\text{CH}_{\text{pyridine}}$), 128.1 (C-Pt), 137.4 ($\text{CH}_{\text{pyridine}}$), 149.1 (OCH_2), 149.7, (OCH_2), 153.7 ($\text{CH}_{\text{pyridine}}$). Mass Spectrometry (positive ESI) $[\text{M}+\text{Na}]$: Calculated for $\text{C}_{40}\text{H}_{65}\text{I}_2\text{N}_3\text{O}_2\text{Pt}+\text{Na}$ 1091.28, found 1091.28

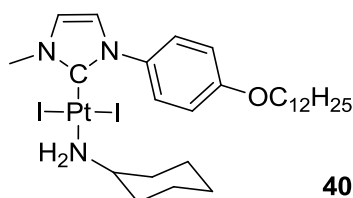


Complex (51 mg, 0.048 mmol) was dissolved in 1 mL of cyclohexylamine and stirred at 25 °C. After 10 min the solvent was removed in vacuo, affording the complex as a yellow powder (30 mg, 58%). ^1H -NMR (CDCl_3 , 300 MHz, 20°C): δ 0.88 (m, 3H, CH_3), 1.00-1.90 (m, 52H, alkyl chain and

cyclohexylamine), 2.29 (m, 2H, cyclohexylamine), 2.94 (m, 2H, cyclohexylamine), 3.26 (m, 1H, cyclohexylamine), 3.86 (s, 3H, N-CH₃), 3.98 (m, 2OCH₂), 5.50 (s, 2H, benzyl), 6.57 (d, J = 2.1 Hz, 1H, CH_{imidazole}), 6.76 (d, J = 2.1 Hz, 1H, CH_{imidazole}), 6.81-7.09 (m, 3H, CH_{phenyl}). ¹³C-NMR (CDCl₃, 125 MHz, 20°C): δ 14.3 (2Me), 22.9, 25.0, 25.5, 26.3 (m, cyclohexylamine), 29.7 (m, alkyl chain), 32.1, 36.2, 38.3, 54.4, 55.0, 69.6 (N-Me), 113.7 (CH_{aromatic}), 114.7 (C_{imidazole}), 119.9 (CH_{aromatic}), 121.6 (CH_{aromatic}), 122.3 (C_{imidazole}), 128.3 (CH_{aromatic}), 149.3 (C-Pt), 149.9 (NH₂CH).

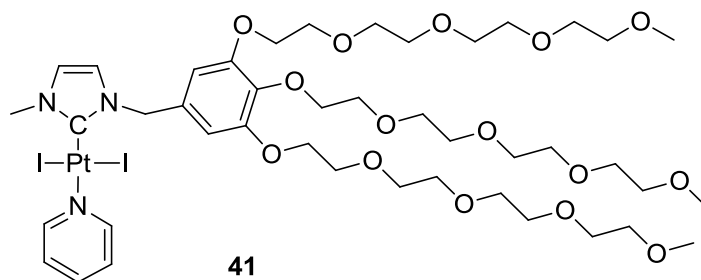


A mixture of 1-methyl-3-(4'-dodecyloxy)phenyl-1*H*-imidazol-3-ium iodide (76 mg, 0.162 mmol), sodium iodide (240 mg, 1.6 mmol), platinum dichloride (43 mg, 0.162 mmol) and potassium carbonate (221 mg, 2.232 mmol) was suspended in pyridine (2 mL). The mixture was stirred overnight at 100°C. The resulting suspension was concentrated in vacuo, then dissolved in dichloromethane, filtered through a celite plug and concentrated in vacuo. The residue was purified by a silica gel chromatography (dichloromethane/cyclohexane 3:2) affording the complex **9** as a yellow-orange powder (78 mg, 55%). ¹H-NMR (CDCl₃, 300 MHz, 20°C): δ 0.91 (t, J = 6.9 Hz, 3H, CH₃), 1.30 (m, 18H, alkyl chain), 1.85 (m, 2H, alkyl chain), 4.03 (t, J = 6.6 Hz, OCH₂), 4.07 (s, 3H, N-CH₃), 7.01 (m, 4H, CH_{imidazole} and CH_{phenyl}), 7.27 (m, 2H, CH_{py}), 7.67 (m, 1H, CH_{py}), 7.83 (d, J = 8.7 Hz, 2H, CH_{phenyl}), 8.88 (d, J = 8.0 Hz, 2H, CH_{py}). ¹³C-NMR (CDCl₃, 125 MHz, 20°C): δ 14.2 (Me), 22.7, 26.1, 29.5 (m, alkyl chain), 31.9, 38.6, 68.3 (N-Me), 114.26 (C_{imidazole}), 122.1 (CH_{aromatic}), 122.30 (CH_{aromatic}), 124.7 (CH_{imidazole}), 125.2 (CH_{pyridine}), 128.0 (CH_{aromatic}), 132.8 (C-Pt), 137.3 (CH_{pyridine}), 153.5 (CH_{pyridine}), 155.6 (C_{aromatic}), 158.9 (OC_{aromatic}). Mass Spectrometry (positive ESI) [M+Na]: Calculated for C₂₇H₃₉I₂N₃OPt+Na 893.07, found 893.07.

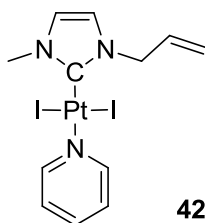


Complex **9** (42 mg, 0.048 mmol) was dissolved in 1 mL of cyclohexylamine and stirred at 25 °C. After 10 min the solvent was removed in vacuo, affording the complex **12** as a yellow powder (30 mg,

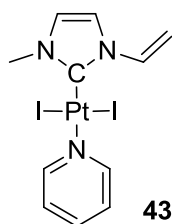
70%). $^1\text{H-NMR}$ (CDCl_3 , 300 MHz, 20°C): δ 0.88 (m, 3H, CH_3), 1.28 (m, 20H, alkyl chain), 1.00-1.83 (m, 8H, alkyl chain and cyclohexylamine), 2.08 (m, 2H, cyclohexylamine), 2.77 (m, 2H, NH_2), 3.08 (m, 1H, cyclohexylamine), 3.95 (s, 3H, N- CH_3), 3.97 (t, $J = 6.6$ Hz, OCH_2), 6.94 (d, $J = 2.1$ Hz, 1H, $\text{CH}_{\text{imidazole}}$), 6.95 (d, $J = 9.0$ Hz, 2H, $\text{CH}_{\text{phenyl}}$), 7.00 (d, $J = 2.1$ Hz, 1H, $\text{CH}_{\text{imidazole}}$), 7.70 (d, $J = 9.0$ Hz, 2H, $\text{CH}_{\text{phenyl}}$). $^{13}\text{C-NMR}$ (CDCl_3 , 125 MHz, 20°C): δ 14.1 (Me), 22.7, 24.8-26.1 (m, cyclohexylamine), 29.5 (m, alkyl chain), 30.9, 31.9, 35.7, 36.8, 38.3, 54.9, 68.3 (N-Me), 114.26 ($\text{CH}_{\text{aromatic}}$), 121.7 ($\text{C}_{\text{imidazole}}$), 122.2 ($\text{C}_{\text{imidazole}}$), 128.7 ($\text{CH}_{\text{aromatic}}$), 132.6 (C-Pt), 158.9 (NH_2CH). Mass Spectrometry (positive ESI) $[\text{M}+\text{CH}_2\text{-CH}_3]$: Calculated for $\text{C}_{27}\text{H}_{39}\text{I}_2\text{N}_3\text{OPt-CH}_2\text{CH}_3$ 890.15, found 863.07.



Procedure *a*: 21%. $^1\text{H-NMR}$ (CDCl_3 , 300 MHz, 20°C): δ 3.25 (s, 9H, 3O- CH_3), 3.42-3.91 (m, 42H, CH_2 PEG), 3.95 (s, 3H, N- CH_3), 4.22 (m, 6H, 3O- CH_2), 5.62 (s, 2H, N- CH_2), 6.86-6.95 (m, 4H, $\text{CH}=\text{CH}+2\text{H}_{\text{ar}}$), 7.32 (t, $J = 6.7$ Hz, 2H, 2H_{pyr}), 7.72 (t, $J = 7.6$ Hz, 1H, 1H_{pyr}), 8.97 (m, 2H, 2H_{pyr}). $^{13}\text{C-NMR}$ (CDCl_3 , 75 MHz, 20°C): δ 38.3 (N- CH_3), 54.0 (N- CH_2), 59.1 (O- CH_3), 68.2 68.9 69.2 69.3 69.4 69.7 69.8 71.4 (CH_2 PEG), 107.8 (CH_{ar}), 120.7 ($\text{CH}=\text{}$), 123.1 ($\text{CH}=\text{}$), 125.0 (C_{pyr}), 133.1 (C_{ar}), 135.0 ($\text{CH}_{\text{ar-O}}$), 135.9 (C-Pt), 137.6 (C_{pyr}), 151.7 ($2\text{CH}_{\text{ar-O}}$), 153.6 (C_{pyr}). MS (positive ESI) $[\text{M}+\text{Na}]$: calculated for $\text{C}_{45}\text{H}_{71}\text{I}_2\text{N}_3\text{O}_{15}\text{Pt}_1\text{Na}$: 1341.25 found 1341.26.



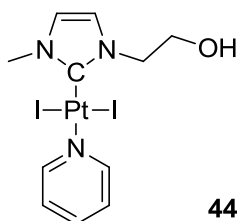
Procedure *a*: 84%. $^1\text{H-NMR}$ (CDCl_3 , 300 MHz, 20°C): δ 3.93 (s, 3H, N- CH_3), 5.11 (d, $J = 6.2$ Hz, 2H, N- CH_2), 5.54 (m, 2H, $2\text{H}_{\text{alkene}}$), 6.06-6.26 (m, 1H, $1\text{H}_{\text{alkene}}$), 6.83 (m, 2H, $\text{CH}=\text{CH}$), 7.30 (t, $J = 6.9$ Hz, 2H, 2H_{pyr}), 7.70 (t, $J = 7.6$ Hz, 1H, 1H_{pyr}), 9.01 (m, 2H, 2H_{pyr}). $^{13}\text{C-NMR}$ (CDCl_3 , 75 MHz, 20°C): δ 38.3 (N- CH_3), 53.4 (N- CH_2), 119.7 (C_{alkene}), 120.0 ($\text{CH}=\text{}$), 122.3 ($\text{CH}=\text{}$), 125.0 (C_{pyr}), 132.5 (C_{alkene}), 136.0 2 (C-Pt), 137.5 (C_{pyr}), 153.7 (C_{pyr}). MS (positive ESI) $[\text{M-I}]$: calculated for $\text{C}_{12}\text{H}_{15}\text{I}_1\text{N}_3\text{Pt}_1$: 522.9954, found 522.9924.



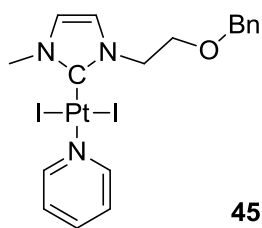
Procedure *a*: 21%. $^1\text{H-NMR}$ (CDCl_3 , 300 MHz, 20 °C): δ 4.00 (s, 3H, N- CH_3), 5.07 (dd, J = 9.0 and 2.0Hz, 1H, $1\text{H}_{\text{alkene}}$), 5.28 (dd, J = 16.0 and 2.0Hz, 1H, $1\text{H}_{\text{alkene}}$), 6.90 (d, J = 2.1Hz, 1H, CH=), 7.18 (d, J = 2.1Hz, 1H, CH=), 7.33 (t, J = 7.0Hz, 2H, 2H_{pyr}), 7.73 (tt, J = 7.6 and 1.6Hz, 1H, 1H_{pyr}), 8.09 (dd, J = 16.0 and 9.0Hz, 1H, $1\text{H}_{\text{alkene}}$), 9.04 (m, 2H, 2H_{pyr}).¹

7.3.1.2 Synthesis of Pt-NHC complexes N-functionalized by hydroxyl groups or amines

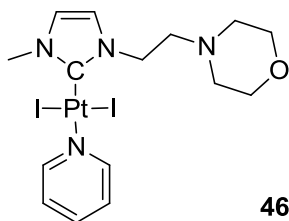
General procedure for protonated amine complexes (**47**, **49.HCO₂H**): A solution of the amine precursor (**46** and **49** respectively) in $\text{CH}_2\text{Cl}_2/\text{HCO}_2\text{H}$ 1/1 was stirred for 20 min at room temperature. The protonated complexes were obtained quantitatively after evaporation of the volatiles and drying under reduced pressure.



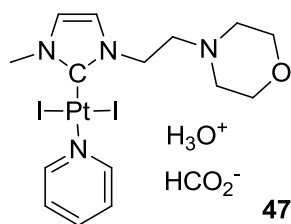
Procedure *a*: 40%. $^1\text{H-NMR}$ (CDCl_3 , 300 MHz, 20 °C): δ 2.19 (m, 1H, OH), 3.96 (s, 3H, N- CH_3), 4.32 (t, J = 5.3Hz, 2H, CH_2), 4.55 (t, J = 5.3Hz, 2H, CH_2), 6.86 (d, J = 2.1Hz, 1H, CH=), 6.97 (d, J = 2.1Hz, 1H, CH=), 7.33 (m, 2H, 2H_{pyr}), 7.72 (tt, J = 7.7Hz and 1.4Hz, 1H, 1H_{pyr}), 9.01 (m, 2H, 2H_{pyr}). $^{13}\text{C-NMR}$ (CDCl_3 , 75 MHz, 20 °C): δ 38.4 (N- CH_3), 52.9 (N- CH_2), 60.7 ($\text{CH}_2\text{-OH}$), 121.8 (CH=), 122.4 (CH=), 125.0 (C_{pyr}), 135.2 (C-Pt), 137.5 (C_{pyr}), 153.7 (C_{pyr}). MS (positive ESI) [M-I]: calculated for $\text{C}_{11}\text{H}_{15}\text{I}_1\text{N}_3\text{O}_1\text{Pt}_1$: 526.99, found 526.99, [M+Na]: calculated for $\text{C}_{11}\text{H}_{15}\text{I}_2\text{N}_3\text{O}_1\text{Pt}_1\text{Na}$: 676.88, found 676.89, [M-I+ CH_3CN]: calculated for $\text{C}_{13}\text{H}_{18}\text{I}_1\text{N}_4\text{O}_1\text{Pt}_1$: 568.02, found 568.02, [M-2I-H]: calculated for $\text{C}_{11}\text{H}_{14}\text{N}_3\text{O}_1\text{Pt}_1$: 399.08, found 399.08.



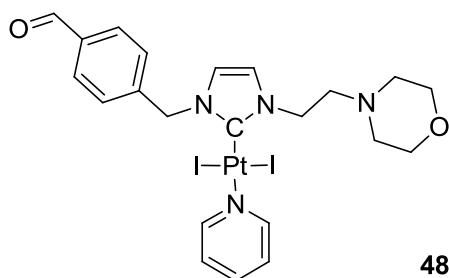
To a solution of **44** (1 eq) in CH_2Cl_2 , $\text{KO}t\text{Bu}$ (10 eq) and benzylbromide (10 eq) were added. The solution was stirred overnight at room temperature. After evaporation of the volatiles, the crude product was purified by silica gel chromatography ($\text{CH}_2\text{Cl}_2/\text{cyclohexane}$ 1/1): 48% ^1H -NMR (CDCl_3 , 300 MHz, 20 °C): δ 3.97 (s, 3H, N- CH_3), 4.08 (t, J = 5.3Hz, 2H, CH_2), 4.57 (s, 2H, O- CH_2), 4.67 (t, J = 5.3Hz, 2H, CH_2), 6.82 (d, J = 2.1Hz, 1H, $\text{CH}=\text{}$), 7.07 (d, J = 2.1Hz, 1H, $\text{CH}=\text{}$), 7.27-7.45 (m, 7H, 5H_{ar} and 2H_{pyr}), 7.73 (m, 1H, 1H_{pyr}), 9.03 (m, 2H, 2H_{pyr}). MS (positive ESI) $[\text{M}-\text{I}]$: calculated for $\text{C}_{18}\text{H}_{21}\text{I}_1\text{N}_3\text{O}_1\text{Pt}_1$: 617.04, found 617.04, $[\text{M}+\text{Na}]$: calculated for $\text{C}_{18}\text{H}_{21}\text{I}_2\text{N}_3\text{O}_1\text{Pt}_1\text{Na}$: 766.93, found 766.93, $[\text{M}-\text{I}+\text{CH}_3\text{CN}]$: calculated for $\text{C}_{18}\text{H}_{21}\text{I}_1\text{N}_3\text{O}_1\text{Pt}_1\text{CH}_3\text{CN}$: 658.06, found 658.06.



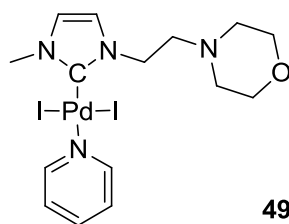
Procedure *a*: 63%. ^1H -NMR (CDCl_3 , 300 MHz, 20 °C): δ 2.56 (t, J = 4.6Hz, 4H, $2\text{N}-\text{CH}_2$), 2.96 (t, J = 6.3Hz, 2H, $\text{N}-\text{CH}_2$ Morpholine), 3.69 (t, J = 4.6Hz, 4H, $2\text{O}-\text{CH}_2$), 3.92 (s, 3H, N- CH_3), 4.54 (t, J = 6.3Hz, 2H, $\text{N}-\text{CH}_2$), 6.80 (d, J = 2.1Hz, 1H, $\text{CH}=\text{}$), 7.01 (d, J = 2.1Hz, 1H, $\text{CH}=\text{}$), 7.30 (ddd, J = 7.6, 5.1 and 1.5Hz, 2H, 2H_{pyr}), 7.70 (tt, J = 7.7 and 1.5Hz, 1H, 1H_{pyr}), 8.99 (m, 2H, 2H_{pyr}). ^{13}C -NMR (CDCl_3 , 75 MHz, 20 °C): δ 38.3 (N- CH_3), 47.5 (N- CH_2 Morpholine), 53.6 (N- CH_2), 57.3 ($2\text{N}-\text{CH}_2$), 67.1 ($2\text{O}-\text{CH}_2$), 121.5 121.7 ($\text{CH}=\text{CH}$), 125.0 (C_{pyr}), 135.4 (C-Pt), 137.5 (C_{pyr}), 153.7 (C_{pyr}). MS (positive ESI) $[\text{M}+\text{H}]$: calculated for $\text{C}_{15}\text{H}_{22}\text{I}_2\text{N}_4\text{Pt}_1\text{O}_1\text{H}_1$: 723.9605, found 723.9589, $[\text{M}-\text{I}]$: calculated for $\text{C}_{15}\text{H}_{22}\text{I}_1\text{N}_4\text{Pt}_1\text{O}_1$: 596.0482, found 596.0465.



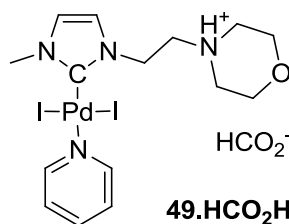
Quant. $^1\text{H-NMR}$ (CDCl_3 , 300 MHz, 20 °C): δ 2.97 (t, J = 4.8Hz, 4H, 2N-CH₂), 3.49 (t, J = 6.9Hz, 2H, N-CH₂ Morpholine), 3.85 (t, J = 4.8Hz, 4H, 2O-CH₂), 3.96 (s, 3H, N-CH₃), 4.76 (t, J = 6.9Hz, 2H, N-CH₂), 6.66 (large, 3H, H₃O⁺), 6.86 (d, J = 2.1Hz, 1H, CH=), 7.13 (d, J = 2.1Hz, 1H, CH=), 7.34 (t, J = 6.3Hz, 2H, 2H_{Pyr}), 7.75 (tt, J = 7.7 and 1.5Hz, 1H, 1H_{Pyr}), 9.02 (m, 2H, 2H_{Pyr}). $^{13}\text{C-NMR}$ (CDCl_3 , 75 MHz, 20 °C): δ 38.6 (N-CH₃), 46.4 (N-CH₂ Morpholine), 53.1 (N-CH₂), 56.2 (2N-CH₂), 65.6 (2O-CH₂), 121.9 122.3 (CH=CH), 125.2 (C_{Pyr}), 137.7 (C_{Pyr}), 153.9 (C_{Pyr}), 165.2 (HCO₂H).



Procedure *a*: 73%. $^1\text{H-NMR}$ (CDCl_3 , 300 MHz, 20 °C): δ 2.57 (t, J = 4.3Hz, 4H, 2N-CH₂), 2.99 (t, J = 6.3Hz, 2H, N-CH₂ Morpholine), 3.67 (t, J = 4.3Hz, 4H, 2O-CH₂), 4.59 (t, J = 6.3Hz, 2H, N-CH₂), 5.78 (s, 2H, N-CH₂), 6.63 (d, J = 1.9Hz, 1H, CH=), 7.08 (d, J = 1.9Hz, 1H, CH=), 7.28 (t, J = 6.8Hz, 2H, 2H_{Pyr}), 7.62 (d, J = 8.1Hz, 2H, 2H_{ar}), 7.68 (t, J = 7.7Hz, 1H, 1H_{Pyr}), 7.85 (d, J = 8.1Hz, 2H, 2H_{ar}), 8.95 (m, 2H, 2H_{Pyr}), 9.98 (s, 1H, CH=O). $^{13}\text{C-NMR}$ (CDCl_3 , 75 MHz, 20 °C): δ 47.7 (N-CH₂ Morpholine), 53.6 (N-CH₂), 54.2 (N-CH₂), 57.2 (2N-CH₂), 67.0 (2O-CH₂), 119.9 122.4 (CH=CH), 125.0 (C_{Pyr}), 129.4 (CH_{ar}), 130.1 (CH_{ar}), 136.1 (C_{ar}), 136.9 (C-Pt), 137.6 (C_{Pyr}), 142.1 (C_{ar}), 153.6 (C_{Pyr}), 191.7 (CH=O). MS (positive ESI) [M+H]: calculated for C₂₂H₂₆I₂N₄PtO₂H₁: 827.9867, found 827.9879, [M-I]: calculated for C₂₂H₂₆I₁N₄PtO₂: 700.0745, found 700.0761, [M-I+CH₃CN]: calculated for C₂₂H₂₆I₁N₄PtO₂CH₃CN: 741.1010, found 741.1036.

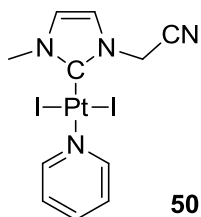


Procedure *a*: 40%. $^1\text{H-NMR}$ (CDCl_3 , 300 MHz, 20 °C): δ 2.55 (t, J = 4.6Hz, 4H, 2N-CH₂), 2.96 (t, J = 6.2Hz, 2H, N-CH₂ Morpholine), 3.67 (t, J = 4.6Hz, 4H, 2O-CH₂), 3.92 (s, 3H, N-CH₃), 4.47 (t, J = 6.2Hz, 2H, N-CH₂), 6.89 (d, J = 2.0Hz, 1H, CH=), 7.12 (d, J = 2.0Hz, 1H, CH=), 7.28 (ddd, J = 7.7, 5.1 and 1.3Hz, 2H, 2H_{Pyr}), 7.70 (tt, J = 7.7 and 1.6Hz, 1H, 1H_{Pyr}), 8.98 (m, 2H, 2H_{Pyr}). $^{13}\text{C-NMR}$ (CDCl_3 , 75 MHz, 20 °C): δ 39.1 (N-CH₃), 48.1 (N-CH₂ Morpholine), 53.5 (N-CH₂), 57.0 (2N-CH₂), 67.0 (2O-CH₂), 122.7 122.9 (CH=CH), 124.4 (C_{Pyr}), 137.7 (C_{Pyr}), 145.0 (C-Pd), 153.7 (C_{Pyr}). MS (positive ESI) [M+H]: calculated for C₁₅H₂₂I₂N₄PdO₁H: 634.8997, found 634.8863.



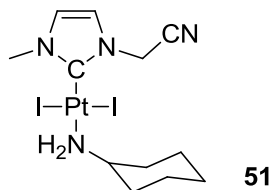
Quant. $^1\text{H-NMR}$ (CDCl_3 , 300 MHz, 20 °C): δ 2.86 (t, J = 4.4Hz, 4H, 2N-CH₂), 3.35 (t, J = 6.7Hz, 2H, N-CH₂ Morpholine), 3.80 (t, J = 4.7Hz, 4H, 2O-CH₂), 3.95 (s, 3H, N-CH₃), 4.66 (t, J = 6.7Hz, 2H, N-CH₂), 6.93 (d, J = 2.0Hz, 1H, CH=), 7.20 (d, J = 2.0Hz, 1H, CH=), 7.73 (t, J = 6.7Hz, 2H, 2H_{Pyr}), 7.73 (t, J = 7.5Hz, 1H, 1H_{Pyr}), 8.28 (s, 1H, HCO₂⁻), 9.00 (m, 2H, 2H_{Pyr}), 11.80 (s, 1H, NH⁺). $^{13}\text{C-NMR}$ (CDCl_3 , 75 MHz, 20 °C): δ 39.2 (N-CH₃), 48.2 (N-CH₂ Morpholine), 53.6 (N-CH₂), 57.1 (2N-CH₂), 67.0 (2O-CH₂), 122.8 123.9=0 (CH=CH), 124.5 (C_{Pyr}), 137.7 (C_{Pyr}), 145.2 (C-Pd), 153.8 (C_{Pyr}).

7.3.1.3 Synthesis of Pt-NHC complexes N-functionalized by nitriles, carboxylic acids and their derivatives

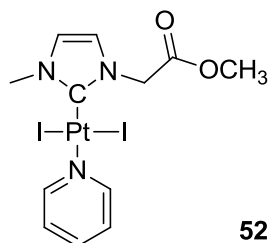


Procedure *a*: 37%. $^1\text{H-NMR}$ (CDCl_3 , 300 MHz, 20 °C): δ 3.98 (s, 3H, N-CH₃), 5.54 (s, 2H, N-CH₂), 6.97 (d, J = 2.1Hz, 1H, CH=), 7.13 (d, J = 2.1Hz, 1H, CH=), 7.36 (m, 2H, CH_{Pyr}), 7.75 (t, J = 9.6Hz,

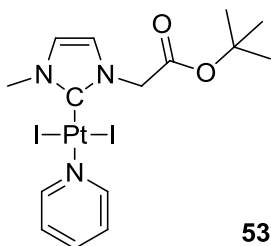
1H, CH_{pyr}), 9.01 (m, 2H, CH_{pyr}). ¹H-NMR (Acetone, 300 MHz, 20 °C): δ 3.97 (s, 3H, N-CH₃), 5.73 (s, 2H, N-CH₂), 7.36 (d, J = 1.5Hz, 1H, CH=), 7.40-7.57 (m, 3H, CH= and 2CH_{pyr}), 7.95 (m, 1H, CH_{pyr}), 9.01 (m, 2H, CH_{pyr}). ¹³C-NMR (Acetone, 75 MHz, 20 °C): δ 37.7 (N-CH₃), 38.0 (N-CH₂), 114.5 (CN), 120.8 (CH=), 123.8 (CH=), 125.2 (CH_{pyr}), 138.2 (CH_{pyr}), 139.6 (C-Pt), 153.5 (CH_{pyr}). MS (positive ESI) [M-I]: calculated for C₁₁H₁₂I₁N₄Pt₁ 521.975, found 521.975, [M-I+CH₃CN]: calculated for C₁₁H₁₂I₁N₄Pt₁ CH₃CN 563.002, found 563.003.



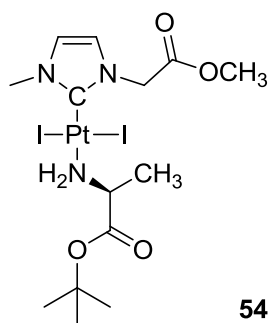
Procedure *b* was modified: reaction temperature 25 °C, cyclohexylamine was used as solvent: 37%. ¹H-NMR (CDCl₃, 300 MHz, 20 °C): δ 1.05-1.45 (m, 5H, CHA), 1.55-1.87 (m, 3H, CHA), 2.25 (m, 2H, CH₂), 2.99 (m, 2H, NH₂), 3.25 (m, 1H, CH_{CHA}), 3.89 (s, 3H, N-CH₃), 5.42 (s, 2H, N-CH₂), 6.93 (d, J= 2.2Hz, 1H, CH=), 7.09 (d, J= 2.2Hz, 1H, CH=).



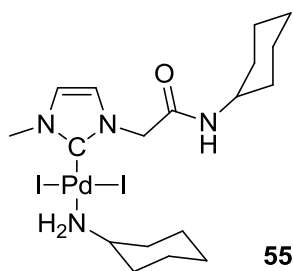
Procedure *a*: 49%. ¹H-NMR (CDCl₃, 300 MHz, 20 °C): δ 3.80 (s, 3H, O-CH₃), 3.95 (s, 3H, N-CH₃), 5.30 (s, 2H, N-CH₂), 6.90 (d, J= 2.1Hz, 1H, CH=), 6.99 (d, J= 2.1Hz, 1H, CH=), 7.31 (t, J= 6.8Hz, 2H, 2H_{pyr}), 7.71 (tt, J= 7.6 and 1.2Hz, 1H, 1H_{pyr}), 8.98 (m, 2H, 2H_{pyr}).



Procedure *a*: 91%. $^1\text{H-NMR}$ (CDCl_3 , 300 MHz, 20 °C): δ 1.51 (s, 9H, $\text{C}(\text{CH}_3)_3$), 3.95 (s, 3H, N- CH_3), 5.22 (s, 2H, N- CH_2), 6.88 (d, J = 2.1Hz, 1H, CH=), 7.00 (d, J = 2.1Hz, 1H, CH=), 7.32 (t, J = 6.7Hz, 2H, 2H_{Pyr}), 7.72 (tt, J = 6.7 and 1.2Hz, 1H, 1H_{Pyr}), 9.02 (m, 2H, 2H_{Pyr}). $^{13}\text{C-NMR}$ (CDCl_3 , 75 MHz, 20 °C): δ 28.2 (CH_3), 38.3 (N- CH_3), 52.1 (N- CH_2), 83.0 (O-C), 121.8 122.2 (CH=CH), 125.0 (C_{Pyr}), 137.5 (C_{Pyr}), 137.6 (C-Pt), 153.7 (C_{Pyr}), 166.2 (C=O). MS (positive ESI) $[\text{M}+\text{Na}]$: calculated for $\text{C}_{15}\text{H}_{21}\text{I}_2\text{N}_3\text{Pt}_1\text{O}_2\text{Na}$ 746.9264, found 746.9299, $[\text{M}_2+\text{Na}]$: calculated for $\text{C}_{30}\text{H}_{42}\text{I}_4\text{N}_6\text{Pt}_2\text{O}_4\text{Na}$ 1470.8627, found 1470.8629, $[\text{M-I}]$: calculated for $\text{C}_{15}\text{H}_{21}\text{I}_1\text{N}_3\text{Pt}_1\text{O}_2$ 597.0322, found 597.0371



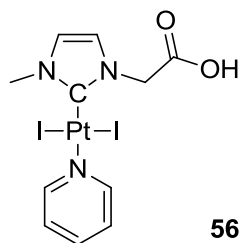
Procedure *b*: quant. $^1\text{H-NMR}$ (CDCl_3 , 300 MHz, 20 °C): δ 1.47 (s, 9H, 3CH_3), 1.64 (d, J = 7.2Hz, 3H, CH_3_{Ala}), 3.40 (m, 2H, $\text{NH}_2\text{-Pt}$), 3.80 (s, 3H, O- CH_3), 3.87 (s, 3H, N- CH_3), 4.08 (m, 1H, CH_{Ala}), 5.19 (s, 2H, N- CH_2), 6.87 (d, J = 2.1Hz, 1H, CH=), 6.97 (d, J = 2.1Hz, 1H, CH=). $^{13}\text{C-NMR}$ (CDCl_3 , 75 MHz, 20 °C): δ 19.3 (CH_3_{Ala}), 20.1 (O-C(CH_3) $_3$), 38.3 (N- CH_3), 51.6 (N- CH_2), 52.9 54.5 (CH and O- CH_3), 82.8 (O-C(CH_3) $_3$), 121.9 122.4 (CH=CH), 140.5 (C-Pt), 167.6 (C=O), 173.5 (C=O). MS (positive ESI) $[\text{M}+\text{Na}]$: calculated for $\text{C}_{14}\text{H}_{25}\text{I}_2\text{N}_3\text{O}_4\text{Pt}_1\text{Na}$: 770.95, found 770.95.



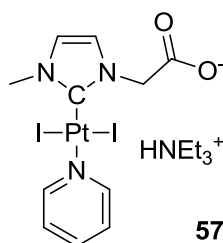
Procedure *a* was modified: the starting azolium precursor employed was 1-(2-methoxy-2-oxoethyl)-3-methyl-1H-imidazol-3-ium bromide. 67%. $^1\text{H-NMR}$ (CDCl_3 , 300 MHz, 20 °C): δ 1.00-1.43 (m, 10H, 10H_{CHA}), 1.49-1.84 (m, 8H, 8H_{CHA}), 2.17 (m, 2H, 2H_{CHA}), 2.30 (d, J = 7.1Hz, 2H, NH_2), 3.08 (m, 1H, CH_{CHA}), 3.72 (m, 1H, CH_{CHA}), 3.85 (s, 3H, N- CH_3), 4.96 (s, 2H, N- CH_2), 6.24 (d, J = 8.0Hz, 1H, NH), 6.96 (d, J = 2.1Hz, 1H, CH=), 7.00 (d, J = 2.1Hz, 1H, CH=). $^{13}\text{C-NMR}$ (CDCl_3 , 75 MHz, 20 °C): δ 24.9 25.0 25.2 25.4 32.6 36.3 (C_{CHA}), 36.0 (N- CH_3), 49.2 (NH- CH_{CHA}), 53.9 (C_{CHA}), 55.0 (N- CH_2), 122.0

(CH=), 124.5 (CH=), 151.6 (C-Pd), 165.4 (C=O). MS (positive ESI) [M-I]: calculated for $C_{18}H_{32}I_1N_4O_1Pd$: 553.07, found 553.09.

General procedure for *tert*-butyl ester deprotection: A solution of ester complexes (**53**, **58**, **61**, **65** and **67** respectively) in $CH_2Cl_2/HCOOH$ (1/1) was stirred at room temperature and TLC monitored until total disappearance of starting material. The volatiles are removed under reduced pressure. CH_2Cl_2 was added and the mixture evaporated. After drying under reduced pressure overnight, the acid complexes (**56**, **62**, **66**, **60** respectively) were obtained. The carboxylates were obtained by stirring a solution of the corresponding carboxylic acid in CH_2Cl_2 and NEt_3 (10 eq) at 25 °C during 10 min and evaporation of volatiles under reduced pressure. CH_2Cl_2 was added and the mixture evaporated. After drying under reduced pressure overnight, the carboxylate complexes **57** and **60** respectively were obtained.

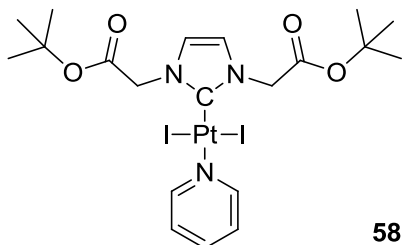


Quant. 1H -NMR (Acetone, 300 MHz, 20 °C): δ 3.95 (s, 3H, N-CH₃), 5.41 (s, 2H, N-CH₂), 7.22 (d, J= 2.1Hz, 1H, CH=), 7.29 (d, J= 2.1Hz, 1H, CH=), 7.51 (ddd, J= 7.6, 5.1 and 1.5Hz, 2H, 2H_{pyr}), 7.51 (tt, J= 7.7 and 1.5Hz, 1H, 1H_{pyr}), 9.00 (m, 2H, 2H_{pyr}). ^{13}C -NMR (Acetone, 75 MHz, 20 °C): δ 38.3 (N-CH₃), 51.6 (N-CH₂), 123.2 (CH=CH), 126.0 (C_{pyr}), 138.2 (C-Pt), 138.9 (C_{pyr}), 154.4 (C_{pyr}), 168.6 (C=O). MS (positive ESI) [M+Na]: calculated for $C_{11}H_{13}I_2N_3O_2Pt_1Na$: 690.86, found 690.87, [M-I]: calculated for $C_{11}H_{13}I_1N_3O_2Pt_1$: 540.97, found 540.97.

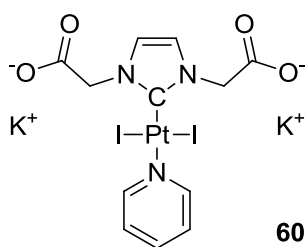


Quant. 1H -NMR (Acetone, 300 MHz, 20 °C): δ 1.11 (t, J= 7.2, 9H, 3CH₃), 2.92 (q, J= 7.2, 6H, 3CH₂), 3.92 (s, 3H, N-CH₃), 5.111 (s, 2H, N-CH₂), 7.11 (s, 1H, CH=), 7.35 (s, 1H, CH=), 7.49 (t, J= 6.8Hz, 2H, 2H_{pyr}), 7.91 (tt, J= 7.6 and 1.4Hz, 1H, 1H_{pyr}), 9.02 (m, 2H, 2H_{pyr}). ^{13}C -NMR (Acetone, 75 MHz, 20 °C): δ 9.9 (3CH₃), 38.2 (N-CH₃), 46.2 (3CH₂), 69.2 (N-CH₂), 122.2 123.5 (CH=CH), 125.9 (C_{pyr}),

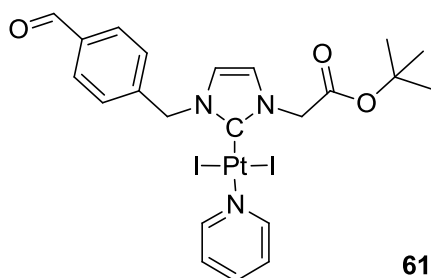
138.7 (C_{Pyr}), 154.5 (C_{Pyr}), 210.0 ($C=O$). MS (positive ESI) $[M-I]$: calculated for $C_{17}H_{28}I_1N_4O_2Pt_1$: 642.09, found 642.08, $[M-I-NEt_3]$: calculated for $C_{11}H_{13}I_1N_3O_2Pt_1$: 540.97, found 540.97.



Procedure *a*: 77%. 1H -NMR ($CDCl_3$, 300 MHz, 20 °C): δ 1.51 (s, 18H, $2C(CH_3)_3$), 5.24 (s, 4H, $2N-CH_2$), 7.05 (s, 2H, $CH=CH$), 7.32 (t, $J = 6.9\text{Hz}$, 2H, $2H_{\text{Pyr}}$), 7.72 (t, $J = 7.6\text{Hz}$, 1H, $1H_{\text{Pyr}}$), 9.02 (m, 2H, $2H_{\text{Pyr}}$). ^{13}C -NMR ($CDCl_3$, 75 MHz, 20 °C): δ 28.3 (CH_3), 52.3 ($N-CH_2$), 83.2 ($O-C$), 122.1 ($CH=CH$), 125.0 (C_{Pyr}), 137.6 (C_{Pyr}), 139.4 ($C-Pt$), 153.9 (C_{Pyr}), 166.1 ($C=O$).

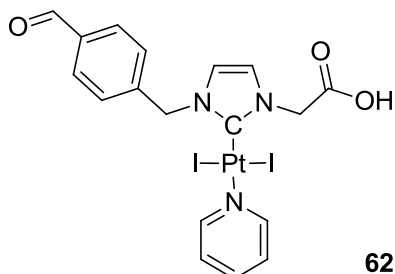


Quant. 1H -NMR (D_2O , 300 MHz, 20 °C): δ 4.98 (s, 4H, $2N-CH_2$), 7.04 (s, 2H, $CH=CH$), 7.35 (t, $J = 6.7\text{Hz}$, 2H, $2H_{\text{Pyr}}$), 7.74 (t, $J = 7.7\text{Hz}$, 1H, $1H_{\text{Pyr}}$), 8.76 (m, 2H, $2H_{\text{Pyr}}$).

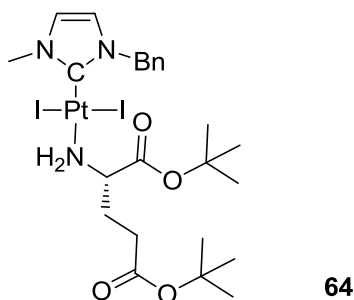


Procedure *a* was modified: $PtI_2(pyr)_2$ was used as platinum precursor: 77%. 1H -NMR ($CDCl_3$, 300 MHz, 20 °C): δ 1.52 (s, 9H, $C(CH_3)_3$), 5.72 (s, 2H, $N-CH_2$), 5.82 (s, 2H, $N-CH_2$), 6.69 (d, $J = 2.1\text{Hz}$, 1H, $CH=$), 7.05 (d, $J = 2.1\text{Hz}$, 1H, $CH=$), 7.30 (ddd, $J = 5.1, 7.6$ and 1.5Hz , 2H, $2H_{\text{pyr}}$), 7.64 (d, $J = 8.1\text{Hz}$, 2H, $2H_{\text{ar}}$), 7.71 (tt, $J = 7.6$ and 1.5Hz , 1H, $1H_{\text{pyr}}$), 7.88 (d, $J = 8.1\text{Hz}$, 2H, $2H_{\text{ar}}$), 8.98 (m, 2H, $2H_{\text{pyr}}$), 10.00 (s, 1H, $CH=O$). ^{13}C -NMR ($CDCl_3$, 75 MHz, 20 °C): δ 28.3 (CH_3), 52.3 ($N-CH_2$), 54.3

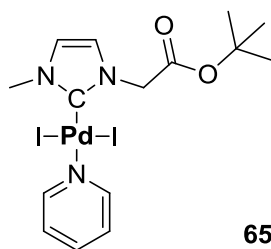
(N-CH₂), 83.2 (O-C), 120.4 122.9 (CH=CH), 125.0 (C_{Pyr}), 129.4 (CH_{ar}), 130.2 (CH_{ar}), 136.3 (C_{ar}), 137.7 (C_{Pyr}), 139.2 (C-Pt), 142.0 (C_{ar}), 153.7 (C_{Pyr}), 166.1 (C=O), 191.8 (CH=O). MS (positive ESI) [M-I]: calculated for C₂₂H₂₅I₁N₃Pt₁O₃: 701.06, found 701.06.



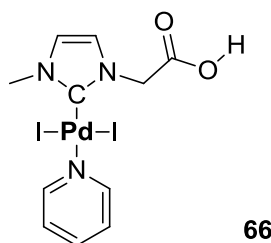
Quant. ¹H-NMR (Acetone, 300 MHz, 20 °C): δ 5.48 (s, 2H, N-CH₂), 5.89 (s, 2H, N-CH₂), 7.14 (d, J= 2.1Hz, 1H, CH=), 7.38 (d, J= 2.1Hz, 1H, CH=), 7.51 (t, J= 7.1, 2H, 2H_{pyr}), 7.78-7.99 (m, 5H, 4H_{ar}+1H_{pyr}), 8.99 (m, 2H, 2H_{pyr}), 10.07 (s, 1H, CH=O). ¹³C-NMR (CDCl₃, 75 MHz, 20 °C): δ 52.0 (N-CH₂), 54.6 (N-CH₂), 121.8 124.3 (CH=CH), 126.0 (C_{Pyr}), 130.4 (2CH_{ar}), 137.3 (C_{ar}), 139.0 (C_{Pyr}), 139.7 (C-Pt), 143.7 (C_{ar}), 154.4 (C_{Pyr}), 168.6 (C=O), 192.6 (CH=O).



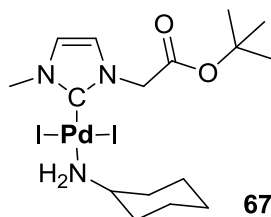
Procedure *a* was modified: To the initial solution in pyridine, 2 eq. of the aminium ester ((S)-1,5-di-tert-butoxy-1,5-dioxopentane-2-aminium chloride) was added: 43%. ¹H-NMR (CDCl₃, 300 MHz, 20 °C): δ 1.41 (s, 9H, O-*t*Bu), 1.48 (s, 9H, O-*t*Bu), 2.15-2.51 (m, 3H, 3H_{Glu}), 2.71-2.82 (m, 1H, CH_{Glu}), 3.41 (m, 2H, NH₂-Pt), 3.08 (s, 3H, N-CH₃), 4.17 (m, 1H, CH_{Glu}), 5.57 (s, 2H, N-CH₂), 6.55 (d, J= 2.1Hz, 1H, CH=), 6.78 (d, J= 2.1Hz, 1H, CH=), 7.26-7.44 (m, 5H, 5H_{ar}). ¹³C-NMR (CDCl₃, 75 MHz, 20 °C): δ 26.9 (CH₂ Glu), 27.6 (CH₂ Glu), 28.0 (CH₃ O-*t*Bu), 28.1 (CH₃ O-*t*Bu), 38.1 (N-CH₃), 54.3 (N-CH₂), 57.8 (CH Glu), 80.5 (O-C *t*Bu), 83.0 (O-C *t*Bu), 119.9 (CH=), 122.3 (CH=), 128.3 128.8 129.1 (CH_{ar}), 135.3 (C_{ar}), 137.9 (C-Pt), 171.5 (C=O), 172.1 (C=O). MS (positive ESI) [M+Na]: calculated for C₂₄H₃₇I₂N₃O₄PtNa: 903.04, found 903.05, [M-I]: calculated for C₂₄H₃₇I₁N₃O₄Pt: 753.15, found 753.15.



Procedure *a*: 44%. $^1\text{H-NMR}$ (CDCl_3 , 300 MHz, 20 °C): δ 1.52 (s, 9H, $\text{C}(\text{CH}_3)_3$), 3.96 (s, 3H, N- CH_3), 5.14 (s, 2H, N- CH_2), 6.98 (d, J = 2.1Hz, 1H, CH=), 7.11 (d, J = 2.1Hz, 1H, CH=), 7.32 (t, J = 6.7Hz, 2H, 2H_{Pyr}), 7.72 (t, J = 7.6, 1H, 1H_{Pyr}), 9.03 (m, 2H, 2H_{Pyr}). $^{13}\text{C-NMR}$ (CDCl_3 , 75 MHz, 20 °C): δ 28.3 (CH_3), 39.2 (N- CH_3), 53.0 (N- CH_2), 83.3 (O-C), 123.2 123.5 (CH=CH), 124.6 (C_{Pyr}), 137.8 (C_{Pyr}), 147.5 (C-Pd), 154.0 (C_{Pyr}), 165.9 (C=O).

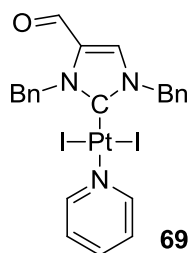


quant. $^1\text{H-NMR}$ (Acetone, 300 MHz, 20 °C): δ 3.95 (s, 3H, N- CH_3), 5.33 (s, 2H, N- CH_2), 7.32 (d, J = 2.1Hz, 1H, CH=), 7.39 (d, J = 2.1Hz, 1H, CH=), 7.49 (t, J = 6.8Hz, 2H, 2H_{Pyr}), 7.92 (t, J = 7.6, 1H, 1H_{Pyr}), 9.00 (m, 2H, 2H_{Pyr}). $^{13}\text{C-NMR}$ (Acetone, 75 MHz, 20 °C): δ 39.2 (N- CH_3), 52.6 (N- CH_2), 124.5 124.5 (CH=CH), 124.5 (C_{Pyr}), 139.0 (C_{Pyr}), 148.2 (C-Pd), 154.5 (C_{Pyr}), 168.4 (C=O).

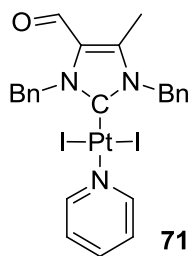


Procedure *b* was modified: CHA was used as solvent and the mixture stirred at room temperature for 1 hour: quant. $^1\text{H-NMR}$ (CDCl_3 , 300 MHz, 20 °C): δ 1.06-1.33 (m, 5H, 5H_{CHA}), 1.51 (s, 9H, $\text{C}(\text{CH}_3)_3$), 1.57-1.79 (m, 3H, 3H_{CHA}), 2.21-2.32 (m, 4H, Pt- NH_2 and 2H_{CHA}), 3.16 (m, 1H, CH_{CHA}), 3.87 (s, 3H, N- CH_3), 5.03 (s, 2H, N- CH_2), 6.92 (d, J = 2.1Hz, 1H, CH=), 7.06 (d, J = 2.1Hz, 1H, CH=). $^{13}\text{C-NMR}$ (CDCl_3 , 75 MHz, 20 °C): δ 25.1 (CH_2_{CHA}), 25.4 (CH_2_{CHA}), 28.3 (CH_3), 36.5 (CH_2_{CHA}), 38.9 (N- CH_3), 52.8 (N- CH_2), 53.9 (CH_{CHA}), 83.3 (O-C), 123.2 123.4 (CH=CH), 151.2 (C-Pd), 166 (C=O).

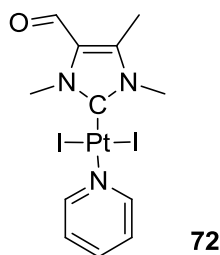
7.3.1.4 Synthesis of Pt-NHC complexes functionalized by aldehydes and acetals



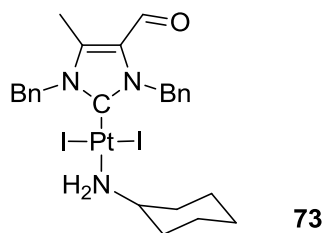
259



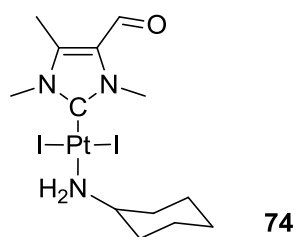
Procedure *a*: 89%. $^1\text{H-NMR}$ (CDCl_3 , 300 MHz, 20 °C): δ 2.24 (s, 3H, CH_3), 6.07 (s, 2H, N- CH_2), 6.27 (s, 2H, N- CH_2), 7.21-7.63 (m, 12H, 10 H_{ar} and 2 H_{Pyr}), 7.68 (tt, J = 7.6 and 1.5Hz, 1H, 1 H_{Pyr}), 8.93 (m, 2H, 2 H_{Pyr}), 9.47 (s, 1H, CH=O). $^{13}\text{C-NMR}$ (CDCl_3 , 75 MHz, 20 °C): δ 10.3 (CH_3), 53.7 (N- CH_2), 54.1 (N- CH_2), 124.9 (C_{Pyr}), 127.6 127.7 127.9 128.2 128.4 (CH_{ar}), 128.5 (C=), 128.9 (CH_{ar}), 134.4 (C_{ar}), 135.8 (C_{ar}), 137.7 (C_{Pyr}), 142.0 (C=), 147.1 (C-Pt), 153.5 (C_{Pyr}), 176.7 (CH=O). MS (positive ESI) [M_2+Na]: calculated for $\text{C}_{48}\text{H}_{46}\text{I}_4\text{N}_6\text{NaO}_2\text{Pt}_2$: 1658.9054, found 1658.9061, [$\text{M}+\text{Na}$]: calculated for $\text{C}_{24}\text{H}_{23}\text{I}_2\text{N}_3\text{NaOPt}$: 840.9473, found 840.9451, [$\text{M}+\text{H}$]: calculated for $\text{C}_{24}\text{H}_{23}\text{I}_2\text{N}_3\text{OPtH}$: 818.9653, found 818.9620, [$\text{M-I}+\text{CH}_3\text{CN}$]: calculated for $\text{C}_{26}\text{H}_{26}\text{IN}_4\text{OPt}$: 732.07996, found 732.0810, [M-I]: calculated for $\text{C}_{24}\text{H}_{23}\text{IN}_3\text{OPt}$: 691.0530, found 691.0540, [$\text{M-I}_2\text{-H}$]: calculated for $\text{C}_{24}\text{H}_{22}\text{N}_3\text{OPt}$: 563.1407, found 563.1443.



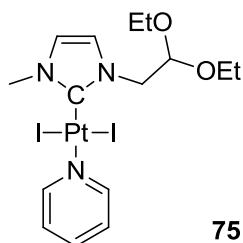
Procedure *a*: 72%. $^1\text{H-NMR}$ (CDCl_3 , 300 MHz, 20 °C): δ 2.49 (s, 3H, CH_3), 3.97 (s, 3H, N- CH_3), 4.26 (s, 3H, N- CH_3), 7.34 (ddd, J = 7.6, 5.1 and 1.6Hz, 2H, 2 H_{Pyr}), 7.75 (tt, J = 7.6 and 1.6Hz, 1H, 1 H_{Pyr}), 9.02 (m, 2H, 2 H_{Pyr}), 9.57 (s, 1H, CH=O). $^{13}\text{C-NMR}$ (CDCl_3 , 75 MHz, 20 °C): δ 9.3 (CH_3), 35.5 (N- CH_3), 37.7 (N- CH_3), 125.0 (C_{Pyr}), 128.3 (C=), 137.7 (C_{Pyr}), 141.6 (C=), 145.2 (C-Pt), 153.6 (C_{Pyr}), 176.6 (CH=O). MS (positive ESI) [$\text{M}_2\text{-I}$]: calculated for $\text{I}_3(\text{C}_{12}\text{H}_{15}\text{N}_3\text{Pt}_1\text{O}_1)_2$: 1204.8842, found 1204.8751.



Procedure *b* was modified: CH₂Cl₂ was used as a solvent and the solution was stirred at room temperature for one hour: 91%. ¹H-NMR (CDCl₃, 300 MHz, 20 °C): δ 1.02-1.74 (m, 8H, 8H_{CHA}), 2.14 (m, 2H, 2H_{CHA}), 2.22 (s, 3H, CH₃), 2.96 (m, 2H, Pt-NH₂), 3.20 (m, 1H, CH_{CHA}), 5.91 (s, 2H, N-CH₂), 6.10 (s, 2H, N-CH₂), 7.24-7.47 (m, 10H, 10H_{ar}), 9.43 (s, 1H, CH=O). ¹³C-NMR (CDCl₃, 75 MHz, 20 °C): δ 10.4 (CH₃), 24.9 (C_{CHA}), 25.4 (C_{CHA}), 35.9 (C_{CHA}), 53.6 (N-CH₂), 54.1 (N-CH₂), 55.1 (CH_{CHA}), 127.5 127.6 127.8 127.9 128.3 128.6 128.7 129.0 134.5 135.9 142.1 (CH_{ar}, C_{ar}, C=C and C-Pt), 176.9 (CH=O).

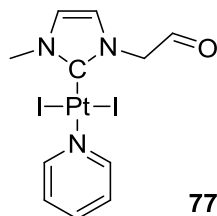


Procedure *b* was modified: CH₂Cl₂ was used as a solvent and the solution was stirred at room temperature for one hour: 92%. ¹H-NMR (CDCl₃, 300 MHz, 20 °C): δ 1.07-1.41 (m, 5H, 5H_{CHA}), 1.57-1.81 (m, 3H, 3H_{CHA}), 2.27 (m, 2H, 2H_{CHA}), 2.47 (s, 3H, CH₃), 2.96 (m, 2H, Pt-NH₂), 3.25 (m, 1H, CH_{CHA}), 3.87 (s, 3H, N-CH₃), 4.15 (s, 3H, N-CH₃), 9.55 (s, 1H, CH=O). ¹³C-NMR (CDCl₃, 75 MHz, 20 °C): δ 9.5 (CH₃), 25.0 (C_{CHA}), 25.4 (C_{CHA}), 35.4 (N-CH₃), 36.0 (C_{CHA}), 37.7 (N-CH₃), 55.1 (CH_{CHA}), 128.4 141.7 (C=C), 148.7 (C-Pt), 176.7 (CH=O).

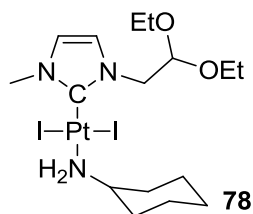


Procedure *a*: 56%. ¹H-NMR (CDCl₃, 300 MHz, 20 °C): δ 1.24 (t, J = 7.1Hz, 6H, 2 CH₃), 3.74 (m, 4H, 2 OCH₂), 3.96 (s, 3H, NCH₃), 4.53 (d, J = 5.5Hz, 2 H, N-CH₂), 5.29 (t, J = 5.5Hz, 1H, CH), 6.80 (d, J = 2.0Hz, 1H, C=CH), 7.01 (d, J = 2.0Hz, 1H, C=CH), 7.33 (ddd, J = 7.6Hz and 5.0Hz and 1.7Hz, 2H,

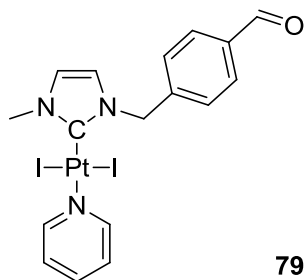
2 H_{pyr}), 7.73 (tq, J = 7.6Hz and 1.7Hz, 1H, 1 H_{pyr}), 9.01 (dt, J = 5.0Hz and 1.7Hz, 2H, 2 H_{pyr}). ¹³C-NMR (CDCl₃, 75 MHz, 20 °C): δ 15.5 (2 CH₃), 38.3 (NCH₃), 53.4 (NCH₂), 64.0 (2 OCH₂), 100.5 (CH), 121.5 (C=C), 122.6 (C=C), 125.0 (C_{pyr}), 136.0 (C-Pt), 137.6 (C_{pyr}), 153.6 (C_{pyr}).



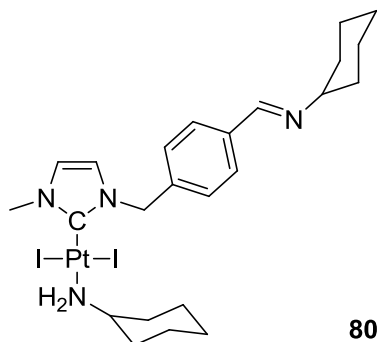
A solution of acetal complex **75** and iodine (excess) in acetone was stirred at 60 °C over one hour. The volatiles were removed under reduced pressure, CH₂Cl₂ was added and the solution washed three times with Na₂S₂O₃ (aq). Volatiles were removed under reduced pressure and crude product **76** dried overnight under reduced pressure at 40 °C to afford **77** (purity ~90%). <26%. ¹H-NMR (CDCl₃, 300 MHz, 20 °C): δ 4.01 (s, 3H, N-CH₃), 5.31 (s, 2H, N-CH₂), 6.96 (m, 2H, CH=CH), 7.30 (m, 2H, CH_{pyr}), 7.74 (m, 1H, CH_{pyr}), 8.98 (m, 2H, CH_{pyr}), 10.02 (s, 1H, CH=O). ¹³C-NMR (CDCl₃, 75 MHz, 20 °C): δ 38.5 (N-CH₃), 59.3 (N-CH₂), 121.5 (CH=), 122.9 (CH=), 125.0 (C_{pyr}), 137.6 (C_{pyr}), 139.0 (C-Pt), 195.5 (CH=O).



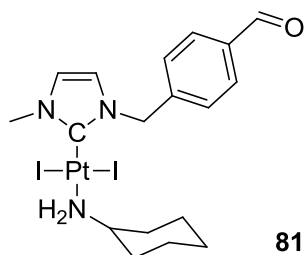
Procedure a: ¹H-NMR (CDCl₃, 300 MHz, 20 °C): δ 1.10-1.81 (m, 14H, 6H_{CH₃} and 8H_{CH₂}), 2.27 (m, 2H, 2H_{CH₂}), 2.90 (m, 2H, NH₂-Pt), 3.22 (m, 1H, CH_{CH₂}), 3.68 (m, 4H, 2 OCH₂), 3.83 (s, 3H, NCH₃), 4.40 (d, J = 5.4Hz, 2 H, N-CH₂), 5.16 (t, J = 5.4Hz, 1H, CH), 6.75 (d, J = 2.0Hz, 1H, CH=), 6.94 (d, J = 2.0Hz, 1H, CH=). ¹³C-NMR (CDCl₃, 75 MHz, 20 °C): δ 15.4 (CH₃, 24.8 CH₂), 25.3 (CH₂), 35.8 (CH₂), 38.0 (CH_{CH₂}), 53.2 (N-CH₃), 64.2 (O-CH₂), 100.7 (CH), 121.2 (CH=), 122.4 (CH=), 139.5 (C-Pt).



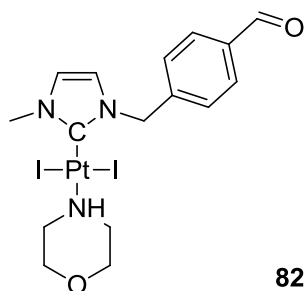
Procedure *a* was modified: $\text{PtCl}_2(\text{COD})$ was used as platinum precursor. 80%. ^1H -NMR (CDCl_3 , 300 MHz, 20 °C): δ 4.02 (s, 3H, N- CH_3), 5.83 (s, 2H, N- CH_2), 6.63 (d, $J = 2.1\text{ Hz}$, 1H, $\text{CH}=\text{}$), 6.88 (m, 1H, $\text{CH}=\text{}$), 7.33 (m, 2H, CH_{pyr}), 7.63 (m, 2H, 2H_{ar}), 7.73 (m, 1H, CH_{pyr}), 7.90 (m, 2H, 2H_{ar}), 9.02 (m, 2H, CH_{pyr}), 10.02 (s, 1H, $\text{CH}=\text{O}$). ^{13}C -NMR (CDCl_3 , 75 MHz, 20 °C): δ 38.5 (N- CH_3), 54.2 (N- CH_2), 119.9 ($\text{CH}=\text{}$), 122.8 ($\text{CH}=\text{}$), 125.0 (C_{pyr}), 129.4 (CH_{ar}), 130.2 (CH_{ar}), 136.3 (C_{ar}), 137.5 (C_{pyr}), 137.7 (C-Pt), 142.2 (C_{ar}), 153.7 (C_{pyr}), 191.7 ($\text{CH}=\text{O}$).



Purification by NEt_3 deactivated silica gel chromatography. Quant. ^1H -NMR (CDCl_3 , 300 MHz, 20 °C): δ 1.00-1.87 (m, 10H, CH_A), 2.24 (d, $J = 12.0\text{ Hz}$, 2H, CH_2), 2.48 (m, 2H, CH_2), 2.92 (m, 2H, NH_2), 3.18 (m, 2H, 2CH_{CHA}), 3.86 (s, 3H, N- CH_3), 5.59 (s, 2H, N- CH_2), 6.53 (d, $J = 2.1\text{ Hz}$, 1H, $\text{CH}=\text{}$), 6.77 (d, $J = 2.1\text{ Hz}$, 1H, $\text{CH}=\text{}$), 7.45 (d, $J = 8.1\text{ Hz}$, 2H, H_{ar}), 7.68 (d, $J = 8.1\text{ Hz}$, 2H, H_{ar}), 8.28 (s, 1H, $\text{CH}=\text{N}$). ^{13}C -NMR (CDCl_3 , 75 MHz, 20 °C): δ 24.8 25.3 25.7 34.3 36.6 (CH_A), 38.1 (N- CH_3), 50.5 (CH_A), 54.8 (N- CH_2), 69.9 (CH_A), 119.8 ($\text{CH}=\text{}$), 122.4 ($\text{CH}=\text{}$), 128.4 (CH_{Ar}), 129.1 (CH_{Ar}), 136.7 (C_{Ar}), 137.5 (C_{Ar}), 140.3 (C-Pt), 157.9 ($\text{CH}=\text{N}$).

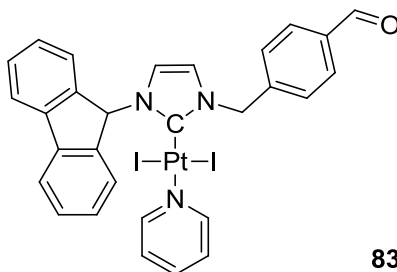


A mixture of 1-(4-formylbenzyl)-3-methyl-1H-imidazol-3-ium bromide (25 mg, 0.10 mmol), sodium iodide (149.3 mg, 1.0 mmol), platinum dichloride (26.5 mg, 0.10 mmol) and potassium carbonate (137.6 mg, 1.0 mmol) was suspended in cyclohexylamine (2mL). The mixture was sonicated, and then stirred at 100 °C overnight. The resulting suspension was concentrated under reduced pressure, then dissolved in dichloromethane, filtered through a celite plug and concentrated under reduced pressure. The residue was purified by silica gel chromatography with dichloromethane affording the complex as a yellow solid (29.3 mg, 44%). ¹H-NMR (CDCl₃, 300 MHz, 20 °C): δ 1.05-1.35 (m, 5H, CHA), 1.55-1.87 (m, 3H, CHA), 2.25 (d, J = 11.7 Hz, 2H, CH₂), 2.95 (m, 2H, NH₂), 3.27 (m, 1H, CH_{CHA}), 3.90 (s, 3H, N-CH₃), 5.70 (s, 2H, N-CH₂), 6.63 (s, 1H, CH=), 6.85 (s, 1H, CH=), 7.59 (d, J = 8.1 Hz, 2H, H_{ar}), 7.87 (d, J = 8.1 Hz, 2H, H_{ar}), 10.01 (s, 1H, CH=O). ¹³C-NMR (CDCl₃, 75 MHz, 20 °C): δ 24.8 (CHA), 25.3 (CHA), 35.9 (CHA), 38.3 (N-CH₃), 53.9 (CHA), 54.9 (N-CH₂), 120.0 (CH=), 122.6 (CH=), 129.3 (CH_{Ar}), 130.1 (CH_{Ar}), 136.2 (C_{Ar}), 141.1 (C-Pt), 142.2 (C_{Ar}), 191.7 (CH=O). ¹H-NMR (CD₂Cl₂, 300 MHz, 20 °C): δ 0.95-1.35 (m, 5H, CHA), 1.45-1.89 (m, 3H, CHA), 2.28 (d, J = 13.2 Hz, 2H, CH₂), 3.02 (m, 2H, NH₂), 3.23 (m, 1H, CH_{CHA}), 3.92 (s, 3H, N-CH₃), 5.74 (s, 2H, N-CH₂), 6.72 (d, J = 2.1 Hz, 1H, CH=), 6.93 (d, J = 2.1 Hz, 1H, CH=), 7.63 (d, J = 8.1 Hz, 2H, H_{ar}), 7.90 (d, J = 8.1 Hz, 2H, H_{ar}), 10.04 (s, 1H, CH=O). MS (positive ESI) [M-I]: calculated for C₁₈H₂₅I₁N₃O₁Pt₁ 621.069 found 621.072, [M-I+CH₃CN]: calculated for C₁₈H₂₅I₁N₃O₁Pt₁CH₃CN 662.095, found 662.096.

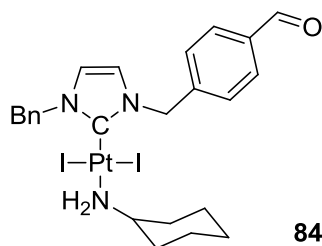


Procedure a: 49%. ¹H-NMR (CDCl₃, 300 MHz, 20 °C): 2.92 (d, J = 11.4 Hz, 2H, CH_{Mo}), 3.15-3.45 (m, 1H, NH), 3.46-3.71 (m, 4H, CH_{Mo}), 3.82 (d, J = 12.3 Hz, 2H, CH_{Mo}), 3.88 (s, 3H, N-CH₃), 5.67 (s, 2H, N-CH₂), 6.56 (s, 1H, CH=), 6.77 (s, 1H, CH=), 7.90 (m, 2H, 2H_{ar}), 7.55 (d, J = 8.1 Hz, 2H, H_{ar}), 7.90 (d, J = 8.1 Hz, 2H, H_{ar}), 10.02 (CH=O). ¹³C-NMR (CDCl₃, 75 MHz, 20 °C): δ 38.3 (N-CH₃), 50.6 (NH-

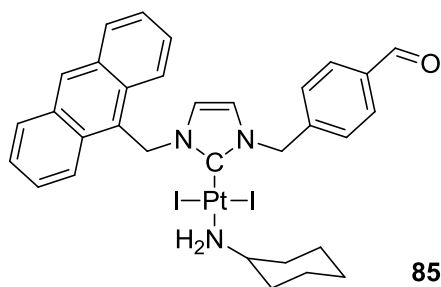
C_{Mo}), 54.0 (N-CH₂), 68.7 (O-C_{Mo}), 120.0 (CH=), 122.7 (CH=), 129.3 (CH_{ar}), 130.1 (CH_{ar}), 136.2 (C_{ar}), 137.5 (C-Pt), 142.0 (C_{ar}), 191.6 (CH=O).



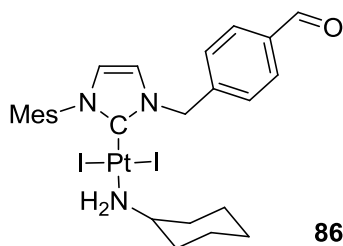
Procedure *a*: 2%. ¹H-NMR (CDCl₃, 300 MHz, 20 °C): δ 5.96 (s, 2H, N-CH₂), 6.22 (d, J= 2.1Hz, 1H, CH=), 6.56 (d, J= 2.1Hz, 1H, CH=), 7.27-7.97 (m, 14H, 11H_{ar} and 3H_{pyr}), 8.24 (d, J= 7.5Hz, 2H, 2H_{ar}), 9.06 (m, 2H, 2H_{pyr}) 10.05 (s, 1H, CH=O).



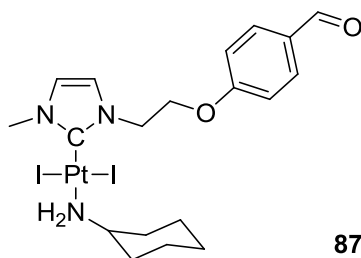
Procedure *a*: 42%. ¹H-NMR (CDCl₃, 300 MHz, 20 °C): 1.00-1.82 (m, 8H, 8H_{CHA}), 2.24 (m, 2H, 2H_{CHA}), 2.97 (m, 2H, NH₂-Pt), 3.24 (m, 1H, CH_{CHA}), 5.64 (s, 2H, N-CH₂), 5.74 (s, 2H, N-CH₂), 6.600 (s, 2H, CH=CH), 7.28-7.51 (m, 5H, 5H_{ar}), 7.62 (d, J= 8.1Hz, 2H, 2H_{ar}), 7.89 (d, J= 8.1Hz, 2H, 2H_{ar}), 10.01 (s, 1H, CH=O). ¹³C-NMR (CDCl₃, 75 MHz, 20 °C): δ 24.8 (CHA), 25.2 (CHA), 35.8 (CHA), 54.1 54.6 54.9 (2 N-CH₂ and CHA), 120.4 (CH=), 120.8 (CH=), 128.4 (CH_{ar}), 128.9 (CH_{ar}), 129.1 (CH_{ar}), 129.3 (CH_{ar}), 130.1 (CH_{ar}), 135.1 (C_{ar}), 136.2 (C_{ar}), 141.4 (C-Pt), 142.1 (C_{ar}), 191.7 (CH=O). MS (positive ESI) [M-I]: calculated for C₂₄H₂₉I₁N₃O₁Pt₁: 697.10 found 697.09.



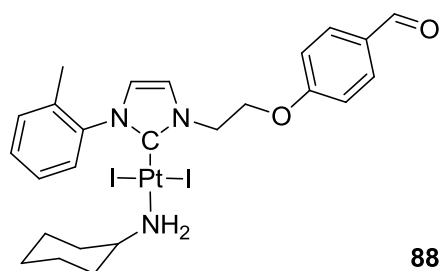
Procedure *a*: 42%. $^1\text{H-NMR}$ (CDCl_3 , 300 MHz, 20 °C): δ 1.01-1.83 (m, 8H, CH_A), 2.34 (m, 2H, CH_2), 3.09 (m, 2H, NH_2), 3.34 (m, 1H, CH_{CHA}), 5.77 (s, 2H, N-CH_2), 6.01 (d, $J = 2.1\text{Hz}$, 1H, CH=), 6.38 (d, $J = 2.1\text{Hz}$, 1H, CH=), 6.49 (s, 2H, N-CH_2), 7.44-7.64 (m, 6H, 6H_{ar}), 7.88 (d, $J = 8.1\text{Hz}$, 2H, 2H_{ar}), 8.06 (d, $J = 8.4\text{Hz}$, 2H, 2H_{ar}), 8.44 (d, $J = 9.0\text{Hz}$, 2H, 2H_{ar}), 8.57 (s, 1H, 1H_{antr}), 10.01 (s, 1H, CH=O). δ 24.8 (CH_A), 25.3 (CH_A), 35.9 (CH_A), 47.9 (N-CH_2 Antr), 54.3 (N-CH_2 Benzaldehyde), 55.0 (CH_{CHA}), 119.5 (CH=), 120.5 (CH=), 124.3 124.4 125.4 127.5 129.1 129.3 129.5 130.1 131.2 131.4 136.1 (C_{ar}), 140.5 (C-Pt), 142.1 (C_{ar}), 191.7 (CH=O).



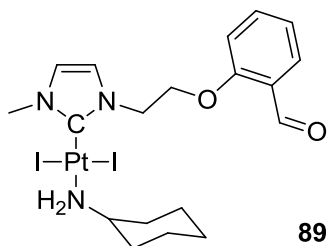
Procedure *a*: 84%. $^1\text{H-NMR}$ (CDCl_3 , 300 MHz, 20 °C): δ 0.95-1.17 (m, 5H, 5H_{CHA}), 1.51-1.66 (m, 3H, 3H_{CHA}), 1.95 (m, 2H, 2H_{CHA}), 2.29 (s, 6H, 2CH_3 Mes), 2.32 (s, 3H, CH_3 Mes), 2.82 (m, 2H, Pt-NH_2), 2.97 (m, 1H, CH_{CHA}), 5.83 (s, 2H, N-CH_2), 6.78 (d, $J = 1.9\text{Hz}$, 1H, CH=), 6.82 (d, $J = 1.9\text{Hz}$, 1H, CH=), 6.95 (s, 2H, 2H_{ar}), 7.65 (d, $J = 8.0\text{Hz}$, 2H, 2H_{ar}), 7.90 (d, $J = 8.0\text{Hz}$, 2H, 2H_{ar}), 10.01 (s, 1H, CH=O). $^{13}\text{C-NMR}$ (CDCl_3 , 75 MHz, 20 °C): δ 21.2 (CH_3 Mes), 21.3 (CH_3 Mes), 24.9 (CH_A), 25.3 (CH_A), 35.7 (CH_A), 54.9 (N-CH_2), 55.1 (CH_A), 120.0 (CH=), 124.3 (CH=), 129.2 129.3 130.2 (CH_{Ar}), 135.1 135.9 136.2 139.0 142.4 (C_{Ar}), 141.1 (C-Pt), 143.0 (C_{Ar}), 191.7 (CH=O).



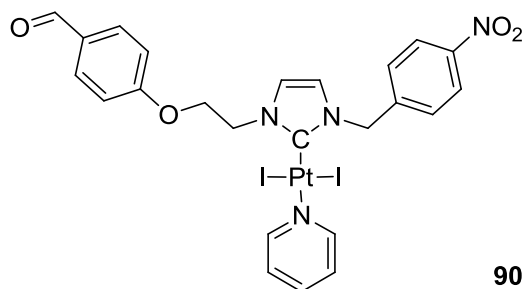
Procedure *a*: 46%. $^1\text{H-NMR}$ (CDCl_3 , 300 MHz, 20 °C): δ 1.00-1.85 (m, 8H, 8H_{CHA}), 2.25 (m, 2H, 2H_{CHA}), 2.93 (m, 2H, Pt-NH₂), 3.23 (m, 1H, CH_{CHA}), 3.84 (s, 3H, N-CH₃), 4.60 (t, $J = 5.1\text{Hz}$, 2H, CH₂), 4.79 (t, $J = 5.1\text{Hz}$, 2H, CH₂), 6.80 (d, $J = 1.9\text{Hz}$, 1H, CH=), 6.93-7.10 (m, 3H, 2H_{ar} +CH=), 7.80 (d, $J = 8.5\text{Hz}$, 2H, 2H_{ar}), 9.86 (s, 1H, CH=O). $^{13}\text{C-NMR}$ (CDCl_3 , 75 MHz, 20 °C): δ 24.9 (CH_2CHA), 25.3 (CH_2CHA), 35.9 (CH_2CHA), 38.1 (N-CH₃), 49.7 (N-CH₂), 54.9 (CH_{CHA}), 66.8 (O-CH₂), 115.0 (CH_{ar}), 121.9 122.0 (CH=CH), 130.4 (C_{ar}), 132.1 (CH_{ar}), 140.0 (C-Pt), 163.2 (C_{ar} -O), 190.8 (CH=O).



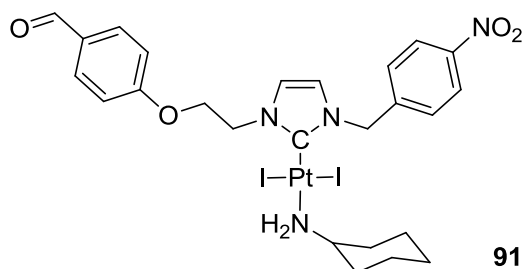
Procedure *a*: 66%. $^1\text{H-NMR}$ (CDCl_3 , 300 MHz, 20 °C): δ 0.94-1.26 (m, 5H, 5H_{CHA}), 1.54-1.67 (m, 3H, 3H_{CHA}), 1.95 (m, 2H, 2H_{CHA}), 2.25 (s, 3H, CH₃), 2.78 (m, 2H, Pt-NH₂), 2.99 (m, 1H, CH_{CHA}), 4.71 (t, $J = 5.0\text{Hz}$, 2H, CH₂), 4.93 (t, $J = 5.0\text{Hz}$, 2H, CH₂), 6.95 (d, $J = 2.0\text{Hz}$, 1H, CH=), 7.10 (d, $J = 8.6\text{Hz}$, 2H, 2H_{ar}), 7.23 (d, $J = 2.0\text{Hz}$, 1H, CH=), 7.27-7.39 (m, 3H, 3H_{ar}), 7.85 (d, $J = 8.6\text{Hz}$, 2H, 2H_{ar}), 7.93 (d, $J = 7.3\text{Hz}$, 1H, 1H_{ar}), 9.90 (s, 1H, CH=O). $^{13}\text{C-NMR}$ (CDCl_3 , 75 MHz, 20 °C): δ 19.6 (CH₃), 24.8 (CH_2CHA), 25.3 (CH_2CHA), 35.7 (CH_2CHA), 50.1 (N-CH₂), 55.1 (CH_{CHA}), 67.0 (O-CH₂), 115.1 (CH_{ar}), 122.0 123.0 (CH=CH), 125.8 129.1 130.4 (CH_{ar}), 130.5 (C_{ar}), 131.2 132.1 (CH_{ar}), 134.8 (C_{ar}), 138.3 (N- C_{ar}), 141.8 (C-Pt), 163.3 (C_{ar} -O), 190.8 (CH=O).



Procedure *a*: 45%. $^1\text{H-NMR}$ (CDCl_3 , 300 MHz, 20 °C): δ 1.05-1.90 (m, 8H, 8H_{CHA}), 2.26 (m, 2H, 2H_{CHA}), 2.93 (m, 2H, Pt-NH₂), 3.24 (m, 1H, CH_{CHA}), 3.86 (s, 3H, N-CH₃), 4.66 (t, $J = 5.0\text{Hz}$, 2H, CH₂), 4.84 (t, $J = 5.0\text{Hz}$, 2H, CH₂), 6.81 (d, $J = 2.0\text{Hz}$, 1H, CH=), 7.05 (t, $J = 8.5\text{Hz}$, 2H, 2H_{ar}), 7.11 (d, $J = 2.0\text{Hz}$, 1H, CH=), 7.53 (ddd, $J = 7.6, 8.3$ and 2.0Hz , 1H, 1H_{ar}), 7.80 (dd, $J = 7.6$ and 1.8Hz , 1H, 1H_{ar}), 10.41 (s, 1H, CH=O).

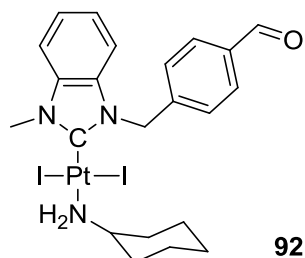


Procedure *a* was modified: $\text{PtCl}_2(\text{COD})$ was used as platinum precursor: 59%. $^1\text{H-NMR}$ (CDCl_3 , 300 MHz, 20 °C): δ 4.72 (t, $J = 4.9\text{Hz}$, 2H, CH₂), 5.00 (t, $J = 4.9\text{Hz}$, 2H, CH₂), 5.87 (s, 2H, N-CH₂), 6.70 (s, 1H, CH=), 7.08 (d, $J = 8.5\text{Hz}$, 2H, 2H_{ar}), 7.16 (s, 1H, CH=), 7.34 (t, $J = 6.6\text{Hz}$, 2H, 2H_{pyr}), 7.66 (d, $J = 8.5\text{Hz}$, 2H, 2H_{ar}), 7.75 (td, $J = 7.7$ and 1.2Hz , 1H, H_{pyr}), 7.84 (d, $J = 8.1\text{Hz}$, 2H, 2H_{ar}), 8.23 (d, $J = 8.1\text{Hz}$, 2H, 2H_{ar}), 9.00 (m, 2H, 2H_{pyr}), 9.89 (s, 1H, CH=O). $^{13}\text{C-NMR}$ (CDCl_3 , 75 MHz, 20 °C): δ 50.3 (N-CH₂), 54.0 (N-CH₂), 66.8 (O-CH₂), 115.1 (CH_{ar}), 120.4 (CH=), 123.4 (CH=), 124.1 (CH_{ar}), 125.2 (C_{pyr}), 129.7 (CH_{ar}), 130.6 (C_{ar}), 132.2 (CH_{ar}), 137.9 (C_{pyr}), 138.7 (C-Pt), 142.5 (C_{ar}), 148.0 ($\text{C}_{\text{ar-NO}_2}$), 153.8 (C_{pyr}), 163.1 ($\text{C}_{\text{ar-O}}$), 190.8 (CH=O). MS (positive ESI) $[\text{M}+\text{Na}]$: calculated for $\text{C}_{24}\text{H}_{22}\text{I}_2\text{N}_4\text{Pt}_1\text{O}_4\text{Na}$: 901.9272, found 902.9235, $[\text{M}-\text{I}]$: calculated for $\text{C}_{24}\text{H}_{22}\text{IN}_4\text{Pt}_1\text{O}_4$: 752.0330, found 752.0337.

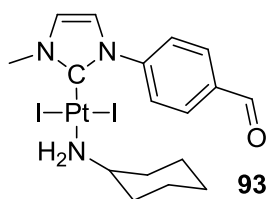


Procedure *b*: 96%. $^1\text{H-NMR}$ (CDCl_3 , 300 MHz, 20 °C): δ 1.13-1.78 (m, 8H, 8H_{CHA}), 2.21 (m, 2H, 2H_{CHA}), 2.96 (m, 2H, Pt-NH₂), 3.23 (m, 1H, CH_{CHA}), 4.65 (t, $J = 5.0\text{Hz}$, 2H, CH₂), 4.88 (t, $J = 5.0\text{Hz}$, 2H, CH₂), 5.74 (s, 2H, N-CH₂), 6.67 (d, $J = 2.1\text{Hz}$, 1H, CH=), 7.05 (d, $J = 8.7\text{Hz}$, 2H, 2H_{ar}), 7.11 (d, $J = 2.1\text{Hz}$, 1H, CH=), 7.59 (d, $J = 8.7\text{Hz}$, 2H, 2H_{ar}), 7.84 (d, $J = 8.7\text{Hz}$, 2H, 2H_{ar}), 8.22 (d, $J = 8.7\text{Hz}$, 2H, 2H_{ar}), 9.89 (s, 1H, CH=O). $^{13}\text{C-NMR}$ (CDCl_3 , 75 MHz, 20 °C): δ 24.7 (C_{CHA}), 25.2 (C_{CHA}), 35.8

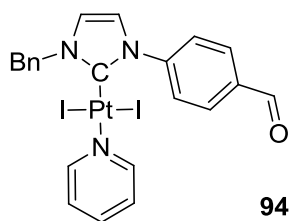
(C_{CHA}), 50.0 (N-CH₂), 53.6 (N-CH₂), 55.0 (CH_{CHA}), 66.6 (O-CH₂), 114.9 (CH_{ar}), 120.2 (CH=), 123.1 (CH=), 124.0 (CH_{ar}), 129.4 (CH_{ar}), 130.5 (C_{ar}), 132.0 (CH_{ar}), 142.0 (C-Pt), 142.4 (C_{ar}), 147.8 (C_{ar}-NO₂), 163.0 (C_{ar}-O), 190.6 (CH=O). MS (positive ESI) [M+Na]: calculated for C₂₅H₃₀I₂N₄Pt₁O₄Na: 921.9898, found 921.9967, [M₂+Na]: calculated for C₅₀H₆₀I₄N₈Pt₂O₈Na: 1820.9897, found 1820.9927.



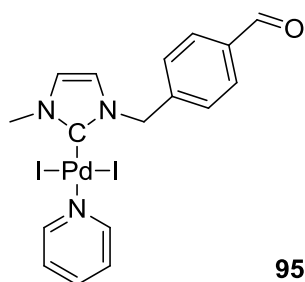
Procedure *a*: 60%. ¹H-NMR (CDCl₃, 300 MHz, 20 °C): δ 0.99-1.85 (m, 8H, 8H_{CHA}), 2.25 (m, 2H, 2H_{CHA}), 3.02 (m, 2H, Pt-NH₂), 3.26 (m, 1H, CH_{CHA}), 4.14 (s, 3H, N-CH₃), 6.06 (s, 2H, N-CH₂), 6.92 (d, J = 8.2Hz, 1H, 1H_{ar}), 7.07 (ddd, J = 8.3, 7.3 and 1.1Hz, 1H_{ar}), 7.21 (ddd, J = 8.3, 7.3 and 1.0Hz, 1H, CH_{ar}), 7.36 (d, J = 8.1Hz, 1H, 1H_{ar}), 7.60 (d, J = 8.2Hz, 2H, 2H_{ar}), 7.84 (dt, J = 8.2 and 1.8Hz, 2H, 2H_{ar}), 9.98 (s, 1H, CH=O). ¹³C-NMR (CDCl₃, 75 MHz, 20 °C): δ 24.8 25.2 (CH₂ CHA), 34.9 (N-CH₃), 35.8 (CH₂ CHA), 52.3 (N-CH₂), 54.9 (CH_{CHA}), 110.1 110.9 123.1 123.2 128.3 130.1 (CH_{ar}), 133.7 135.2 136.0 141.7 (C_{ar}), 154.9 (C-Pt), 191.7 (CH=O). MS (positive ESI) [M+Na]: calculated for C₂₂H₂₇I₂N₃O₁PtNa: 820.98, found 820.98, [M-I]: calculated for C₂₂H₂₇I₁N₃O₁Pt: 671.08, found 671.08.



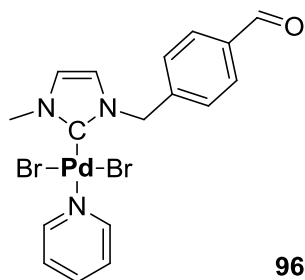
Procedure *a*: 44%. ¹H-NMR (CDCl₃, 300 MHz, 20 °C): δ 1.00-1.81 (m, 8H, 8H_{CHA}), 2.11 (m, 2H, 2H_{CHA}), 2.83 (m, 2H, NH₂-Pt), 3.08 (m, 1H, CH_{CHA}), 3.99 (s, 3H, N-CH₃), 7.03 (d, J = 2.1Hz, 1H, CH=), 7.12 (d, J = 2.1Hz, 1H, CH=), 8.00 (dt, J = 2.1Hz and 8.6Hz, 2H, 2H_{ar}), 8.12 (dt, J = 2.1Hz and 8.6Hz, 2H, 2H_{ar}), 10.08 (s, 1H, CH=O). ¹³C-NMR (CDCl₃, 75 MHz, 20 °C): δ 24.7 (CHA), 25.2 (CHA), 35.6 (CHA), 38.6 (N-CH₃), 54.9 (CH_{CHA}), 121.4 (CH=), 122.9 (CH=), 127.3 (CH_{ar}), 130.0 (CH_{ar}), 135.7 (C_{ar}), 141.6 (C-Pt), 144.6 (C_{ar}), 191.0 (CH=O). MS (positive ESI) [M+Na]: calculated for C₁₇H₂₃I₂N₃O₁PtNa: 756.95 found 756.94.



Procedure *a* was modified: $\text{PtI}_2(\text{pyr})_2$ was used as platinum precursor.: 41%. ^1H -NMR (CDCl_3 , 300 MHz, 20 °C): δ 5.87 (s, 2H, N- CH_2), 6.82 (d, J = 2.1Hz, 1H, CH=), 7.13 (d, J = 2.1Hz, 1H, CH=), 7.21-7.62 (m, 7H, 5H_{ar} + 2H_{pyr}), 7.69 (tt, J = 7.7 and 1.5Hz, 1H, 1H_{pyr}), 8.08 (d, J = 8.4Hz, 2H, 2H_{ar}), 8.29 (d, J = 8.4Hz, 2H, 2H_{ar}), 8.86 (m, 2H, 2H_{pyr}), 10.12 (s, 1H, CH=O). ^{13}C -NMR (CDCl_3 , 75 MHz, 20 °C): δ (N- CH_2), 121.2 (CH=), 122.0 (CH=), 125.0 (C_{pyr}), 127.1 128.6 129.0 129.4 130.2 (CH_{ar}), 134.8 (C_{ar}), 135.8 (C_{ar}), 137.5 (C_{pyr}), 138.4 (C-Pt), 144.9 (C_{ar}), 153.6 (C_{pyr}), 191.2 (CH=O). MS (TOF MS ES+) [M-I]: calculated for $\text{C}_{22}\text{H}_{19}\text{IN}_3\text{OPt}$: 663.02, found 663.04.

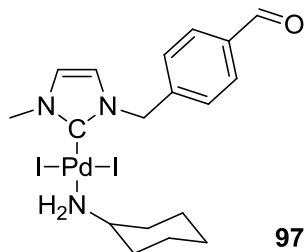


Procedure *a*: 14%. ^1H -NMR (CDCl_3 , 300 MHz, 20 °C): δ 4.03 (s, 3H, N- CH_3), 5.74 (s, 2H, N- CH_2), 6.70 (d, J = 2.0Hz, 1H, CH=), 6.97 (d, J = 2.0Hz, 1H, CH=), 7.33 (m, 2H, CH_{pyr}), 7.60-7.77 (m, 3H, 2H_{ar} and CH_{pyr}), 7.91 (d, J = 8.4Hz, 2H, 2H_{ar}), 9.02 (m, 2H, CH_{pyr}), 10.03 (s, 1H, CH=O).

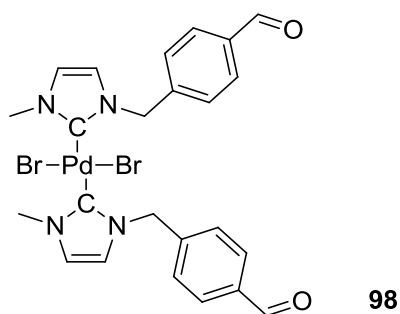


Procedure *a*: 24%. ^1H -NMR (CDCl_3 , 300 MHz, 20 °C): δ 4.15 (s, 3H, N- CH_3), 5.87 (s, 2H, N- CH_2), 6.74 (d, J = 2.1Hz, 1H, CH=), 6.96 (d, J = 2.1Hz, 1H, CH=), 7.33 (m, 2H, CH_{pyr}), 7.66 (d, J = 8.1Hz, 2H, 2H_{ar}), 7.75 (tt, J = 7.7 and 1.6Hz, 1H, CH_{pyr}), 7.90 (d, J = 8.1Hz, 2H, 2H_{ar}), 9.00 (m, 2H, CH_{pyr}), 10.02 (s, 1H, CH=O). ^{13}C -NMR (CDCl_3 , 75 MHz, 20 °C): δ 38.6 (N- CH_3), 54.5 (N- CH_2), 121.4

(CH=), 124.0 (CH=), 124.6 (C_{pyr}), 129.4 (CH_{ar}), 130.3 (CH_{ar}), 136.3 (C_{ar}), 138.0 (C_{pyr}), 142.0 (C_{ar}), 149.8 (C-Pt), 152.6 (C_{pyr}), 191.7 (CH=O). MS (positive ESI) [M+H]: calculated for C₁₇H₁₇Br₂N₃O₁Pd₁H: 547.88, found 547.89.



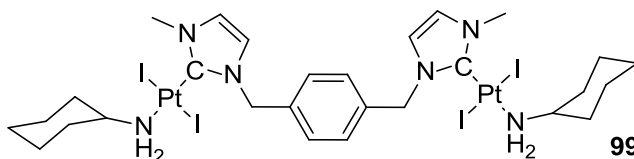
Procedure *b* was modified: cyclohexylamine was used as solvent and the solution was stirred overnight at room temperature: 33%. ¹H-NMR (CDCl₃, 300 MHz, 20 °C): δ 1.05-1.35 (m, 5H, CHA), 1.55-1.87 (m, 3H, CHA), 2.25 (m, 4H, CH₂ and NH₂), 3.15 (m, 1H, CH_{CHA}), 3.93 (s, 3H, N-CH₃), 5.62 (s, 2H, N-CH₂), 6.67 (d, J= 2.1Hz, 1H, CH=), 6.93 (d, J= 2.1Hz 1H, CH=), 7.62 (d, J= 8.1Hz, 2H, H_{ar}), 7.90 (d, J= 8.1Hz, 2H, H_{ar}), 10.02 (s, 1H, CH=O). ¹³C-NMR (CDCl₃, 75 MHz, 20 °C): δ 24.9 (CHA), 25.2 (CHA), 36.4 (CHA), 39.1 (N-CH₃), 53.8 (CHA), 54.7 (N-CH₂), 121.3 (CH=), 123.9 (CH=), 129.6 (CH_{Ar}), 130.2 (CH_{Ar}), 136.4 (C_{Ar}), 141.6 (C_{Ar}), 151.2 (C-Pd), 191.6 (CH=O). MS (positive ESI) [M-I]: calculated for C₁₈H₂₅I₁N₃O₁Pd: 532.01, found 532.01, [M+H]: calculated for C₁₈H₂₅I₂N₃O₁PdH: 659.92, found 659.92.



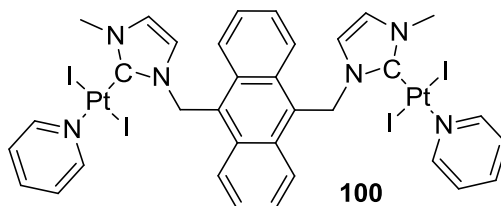
The product was synthesized using a reported procedure for bis-NHC Pd complexes.¹²⁷ <5%. ¹H-NMR (CDCl₃, 300 MHz, 20 °C): δ 4.15 (s, 3H, N-CH₃), 5.85 (s, 2H, N-CH₂), 6.77 (d, J= 2.1Hz, 1H, CH=), 6.96 (d, J= 2.1Hz, 1H, CH=), 7.59 (d, J= 7.7Hz, 2H, 2H_{ar}), 7.89 (d, J= 7.7Hz, 2H, 2H_{ar}), 10.0 (s, 1H, CH=O). ¹³C-NMR (CDCl₃, 75 MHz, 20 °C): δ 38.3 38.7 (N-CH₃), 54.1 54.6 (N-CH₂), 121.0 122.0 123.0 124.4 (CH=CH), 128.7 129.3 130.1 130.4 (CH_{ar}), 136.0 136.5 141.2 142.9 (C_{ar}), 146.4 (C-Pd), 191.7 191.8 (CH=O). MS (positive ESI) [M-Br]: calculated for C₂₄H₂₄BrN₄O₂Pd: 587.01, found 587.01.

7.3.1.5 Synthesis of Polynuclear platinum complexes

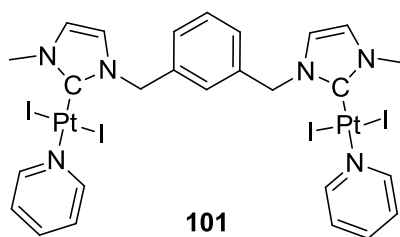
The general procedure *a* was changed for all polynuclear complexes: For platinum (II) source, 1.1 equivalents of $\text{PtI}_2(\text{Pyr})_2$ or $\text{PtCl}_2(\text{COD})$ were used / imidazolium moiety.



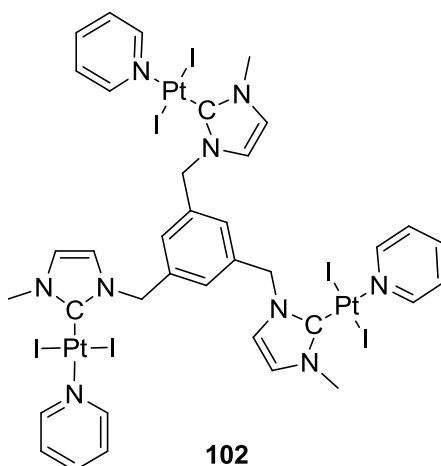
19%. $^1\text{H-NMR}$ (CDCl_3 , 300 MHz, 20°C): δ 0.96-1.78 (m, 20H, 16CH_{CHA}), 2.26 (m, 4H, 4CH_{CHA}), 2.90 (m, 4H, PtNH_2), 3.08-3.26 (m, 2H, 2CH_{CHA}), 3.89 (s, 6H, 2N-CH_3), 5.58 (s, 4H, 2N-CH_2), 6.62 (d, $J = 2.0$ Hz, 2H, 2CH=), 6.69 (d, $J = 2.0$ Hz, 2H, 2CH=), 7.44 (s, 4H, 4H_{Ar}).



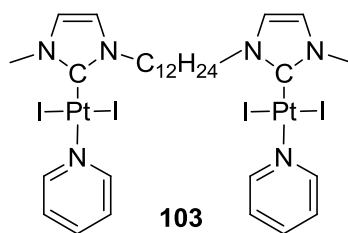
42%. $^1\text{H-NMR}$ (CDCl_3 , 300 MHz, 20°C): δ 4.05 (s, 6H, 2 N- CH_3), 6.06 (d, $J = 2.1$ Hz, 2H, CH=), 6.63 (s, 4H, 2 N- CH_2), 6.65 (d, $J = 2.1$ Hz, 2H, CH=), 7.83 (m, 4H, 4H_{pyr}), 7.65 (m, 4H, 4H_{ar}), 7.77 (m, 2H, 2H_{pyr}), 8.57 (m, 4H, 4H_{ar}), 9.14 (m, 4H, 4H_{pyr}). $^1\text{H-NMR}$ (Acetone, 300 MHz, 20°C): δ 4.02 (s, 6H, 2 N- CH_3), 6.29 (d, $J = 2.1$ Hz, 2H, CH=), 6.66 (s, 4H, 2 N- CH_2), 7.03 (d, $J = 2.1$ Hz, 2H, CH=), 7.59 (ddd, $J = 7.6$ Hz 5.2 Hz and 1.4 Hz, 4H, 4H_{pyr}), 7.71 (q, $J = 3.4$ Hz, 4H, 4H_{ar}), 7.97 (tt, $J = 7.7$ Hz and 1.4 Hz, 2H, 2H_{pyr}), 8.62 (q, $J = 3.4$ Hz, 4H, 4H_{ar}), 9.09 (dt, $J = 4.9$ Hz and 1.5 Hz, 4H, 4H_{pyr}). MS (positive ESI) $[\text{M-I}]$: calculated for $\text{C}_{34}\text{H}_{32}\text{I}_3\text{N}_6\text{Pt}_2$: 1294.91, found 1294.92, $[\text{M-I-C}_5\text{H}_5\text{N}]$: calculated for $\text{C}_{29}\text{H}_{27}\text{I}_3\text{N}_5\text{Pt}_2$: 1215.87, found 1215.87, $[\text{M-I}+\text{CH}_3\text{CN}]$: calculated for $\text{C}_{36}\text{H}_{35}\text{I}_3\text{N}_7\text{Pt}_2$: 1335.94, found 1335.94, $[\text{M}+\text{Na}]$: calculated for $\text{C}_{34}\text{H}_{32}\text{I}_4\text{N}_6\text{Pt}_2\text{Na}$: 1444.80, found 1444.81.



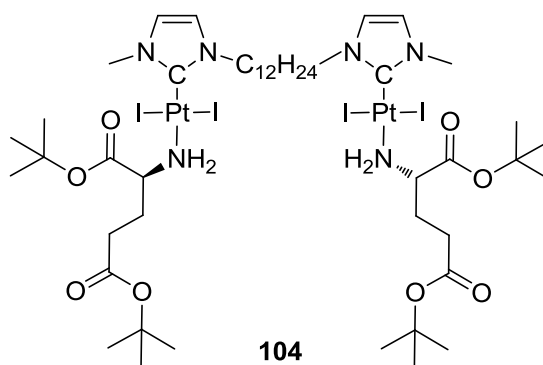
52%. $^1\text{H-NMR}$ (CDCl_3 , 300 MHz, 20 °C): δ 3.98 (s, 6H, 2N- CH_3), 5.74 (s, 4H, 2N- CH_2), 6.77 (s, 2H, 2CH=), 6.86 (s, 2H, 2CH=), 7.33 (t, J = 6.7Hz, 4H, 4H_{Pyr}), 7.41 (t, J = 7.7Hz, 1H, 1H_{ar}), 7.55 (d, J = 7.7Hz, 2H, 2H_{ar}), 7.64 (s, 1H, 1H_{ar}), 7.72 (td, J = 7.7 and 1.5Hz, 2H, 2H_{Pyr}), 9.03 (m, 4H, 4H_{Pyr}). $^{13}\text{C-NMR}$ (CDCl_3 , 75 MHz, 20 °C): δ 38.4 (N- CH_3), 54.1 (N- CH_2), 120.4 122.5 (CH=CH), 124.9 (CH_{Pyr}), 128.8 129.2 129.3 (CH_{ar}), 136.1 (C_{ar}), 136.3 (C-Pt), 137.5 (C_{Pyr}), 153.5 (C_{Pyr}). MS (positive ESI) [M+H]: calculated for $\text{C}_{26}\text{H}_{28}\text{I}_4\text{N}_6\text{Pt}_2$: 1322.7910, found 1322.7953, [M-I]: calculated for $\text{C}_{26}\text{H}_{28}\text{I}_3\text{N}_6\text{Pt}_2$: 1194.8787, found 1194.8878, [M-I-C₅H₅N]: calculated for $\text{C}_{21}\text{H}_{23}\text{I}_3\text{N}_5\text{Pt}_2$: 1115.8364, found 1115.8524, [M-I-2C₅H₅N]: calculated for $\text{C}_{16}\text{H}_{18}\text{I}_3\text{N}_4\text{Pt}_2$: 1036.7941, found 1036.8088, [M-I-HI-2C₅H₅N]: calculated for $\text{C}_{16}\text{H}_{17}\text{I}_2\text{N}_4\text{Pt}_2$: 908.8819, found 908.8875.



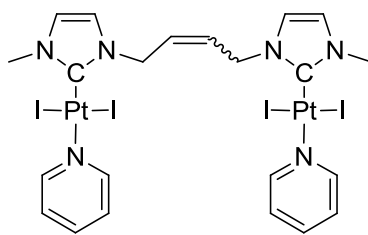
22%. $^1\text{H-NMR}$ (CDCl_3 , 300 MHz, 20 °C): δ 3.98 (s, 3H, N- CH_3), 5.71 (s, 2H, N- CH_2), 6.79 (s, 1H, CH=), 6.90 (s, 1H, CH=), 7.33 (t, J = 6.6Hz, 2H, 2H_{Pyr}), 7.71 (m, 2H, 1H_{Pyr}+1H_{ar}), 9.04 (m, 2H, 2H_{Pyr}). $^{13}\text{C-NMR}$ (CDCl_3 , 75 MHz, 20 °C): δ 38.5 (N- CH_3), 54.1 (N- CH_2), 121.2 122.7 (CH=CH), 125.1 (C_{Pyr}), 129.5 (CH_{ar}), 136.4 (C-Pt), 137.0 (C_{ar}), 137.6 (C_{Pyr}), 153.9 (C_{Pyr}). MS (positive ESI) [M-I]: calculated for $\text{C}_{36}\text{H}_{39}\text{I}_5\text{N}_9\text{Pt}_3$: 1816.7479, found 1816.7103, $\text{C}_{36}\text{H}_{39}\text{I}_6\text{N}_9\text{Pt}_3\text{Na}$: 11966.6422, found 1966.6052.



63%. $^1\text{H-NMR}$ (CDCl_3 , 300 MHz, 20 °C): δ 1.27-1.48 (m, 16H, 8CH₂), 2.04 (m, 4H, 2CH₂), 3.95 (s, 6H, 2N-CH₃), 4.42 (t, J = 7.5Hz, 4H, 2N-CH₂), 6.86 (s, 4H, 2CH=CH), 7.33 (ddd, J = 7.7, 5.0 and 1.4Hz, 4H, 4H_{Pyr}), 7.73 (tt, J = 7.7 and 1.6Hz, 2H, 2H_{Pyr}), 9.03 (m, 4H, 4H_{Pyr}). $^{13}\text{C-NMR}$ (CDCl_3 , 75 MHz, 20 °C): δ 26.7 29.1 29.4 29.5 (CH₂), 38.3 (N-CH₃), 50.8 (N-CH₂), 120.4 121.9 (CH=CH), 124.9 (C_{Pyr}), 134.9 (C-Pt), 137.5 (C_{Pyr}), 153.6 (C_{Pyr}).

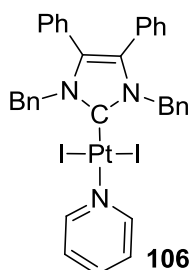


Procedure *b* was modified: two equivalents of aminium ester were used. 54%. $^1\text{H-NMR}$ (CDCl_3 , 300 MHz, 20 °C): δ 1.16-1.38 (m, 16H, 8CH₂), 1.46 (s, 18H, 2C(CH₃)₃), 1.49 (s, 18H, 2C(CH₃)₃), 1.94 (m, 4H, 2CH₂), 2.19-2.57 (m, 6H, 6H_{Glu}), 2.67-2.82 (m, 2H, 2H_{Glu}), 3.37 (m, 4H, 2Pt-NH₂), 3.84 (s, 6H, 2N-CH₃), 4.16 (m, 2H, 2CH_{Glu}), 4.29 (t, J = 7.5Hz, 4H, 2N-CH₂), 6.80 (s, 4H, CH=CH). $^{13}\text{C-NMR}$ (CDCl_3 , 75 MHz, 20 °C): δ 26.8 27.7 28.2 28.3 29.4 29.6 29.7 29.8 31.3 (CH₂ and OC(CH₃)₃), 38.3 (N-CH₃), 51.0 (N-CH₂), 57.9 (CH), 80.8 (OC(CH₃)₃), 83.1 (OC(CH₃)₃), 120.4 121.9 (CH=CH), 136.9 (C-Pt), 171.6 172.3 (2C=O). MS (positive ESI) [M+Na]: calculated for C₄₆H₈₄I₄N₆Pt₂O₈Na: 1769.1713, found 1769.1666, [M-I]: calculated for C₄₆H₈₄I₃N₆Pt₂O₈: 1619.2771, found 1619.2730.

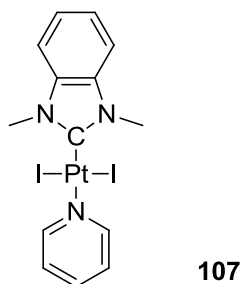
**105:** mixture E/Z 1.6/0.4

A solution of **42** and Grubbs catalyst (0.1 eq) in dichloromethane was stirred for two days at 25 °C. After filtration on celite plug, the crude product was purified over SiO₂ gel chromatography to yield **105** as a mixture E/Z 1.6/0.4. 38%. ¹H-NMR (CDCl₃, 300 MHz, 20 °C): δ 3.96 3.98 (s, 6H, 2N-CH₃), 5.18 (m, 3H), 5.48 (d, J= 4.3Hz, 0.8H), 6.06 (t, J= 4.7Hz, 0.4H), 6.20 (m, 1.8H), 6.83 (m, 2H, 2CH=), 6.95 (m, 2H, 2CH=), 7.32 (t, J= 6.7Hz, 4H, 4H_{pyr}), 7.72 7.32 (t, J= 6.9Hz, 2H, 2H_{pyr}), 9.04 (m, 4H, 4H_{pyr}).

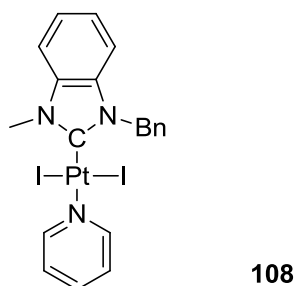
7.3.1.6 Synthesis of complexes with variations of the alkene substituents of the NHC-backbone

**106**

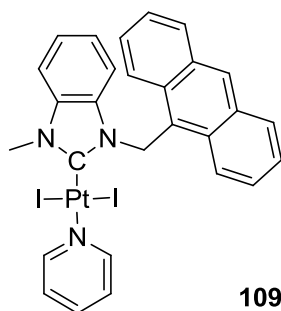
Procedure *a*: 74%. ¹H-NMR (CDCl₃, 300 MHz, 20 °C): δ 5.94 (s, 4H, 2N-CH₂), 6.93-7.02 (m, 4H, 4H_{ar}), 7.05-7.33 (m, 18H, 16H_{ar}+ 2H_{pyr}), 7.68 (tt, J= 7.7 and 1.6Hz, 1H, 1H_{pyr}), 8.94 (m, 2H, 2H_{pyr}). ¹³C-NMR (CDCl₃, 75 MHz, 20 °C): δ 53.8 (N-CH₂), 124.9 (C_{pyr}), 127.3 128.1 128.2 128.2 (CH_{ar}), 128.5 (C_{ar}), 128.6 130.8 (CH_{ar}), 132.5 136.3 (C_{ar}), 137.4 (C_{pyr}), 138.2 (C-Pt), 153.8 (C_{pyr}). MS (positive ESI) [M-I]: calculated for C₃₄H₂₉I₁N₃Pt₁: 801.1051, found 801.1014, [M-I+CH₃CN]: calculated for C₃₄H₂₉I₁N₃Pt₁CH₃CN: 842.1317, found 842.1240.



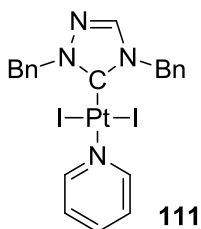
Procedure *a*: 73%. $^1\text{H-NMR}$ (CDCl_3 , 300 MHz, 20 °C): δ 4.17 (s, 6H, 2N- CH_3), 7.21-7.36 (m, 6H, 2H_{Pyr}+4H_{ar}), 7.7(t, J = 7.5Hz, 1H, 1H_{Pyr}), 9.07 (m, 2H, 2H_{Pyr}). $^{13}\text{C-NMR}$ (CDCl_3 , 75 MHz, 20 °C): δ 34.9 (N- CH_3), 109.9 (CH_{ar}), 122.9 (CH_{ar}), 125.1 (CH_{Pyr}), 134.7 (C_{ar}), 137.7 (CH_{Pyr}), 149.9 (C-Pt), 153.6 (CH_{Pyr}).



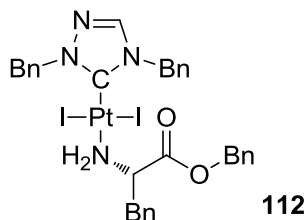
Procedure *a*: ~40%. $^1\text{H-NMR}$ (CDCl_3 , 300 MHz, 20 °C): δ 4.25 (s, 3H, N- CH_3), 6.13 (s, 2H, N- CH_2), 6.96 (d, J = 8.0Hz, 1H, 1H_{ar}), 7.06 (t, J = 7.6Hz, 1H, 1H_{ar}), 7.21 (t, J = 7.6Hz, 1H, 1H_{ar}), 7.26-7.44 (m, 6H, 6H_{ar}), 7.56 (d, J = 7.2Hz, 2H, 2H_{ar}), 7.72 (tt, J = 7.7 and 1.6Hz, 1H, 1H_{Pyr}), 9.05 (m, 2H, 2H_{Pyr}). $^{13}\text{C-NMR}$ (CDCl_3 , 75 MHz, 20 °C): δ 35.1 (N- CH_3), 53.3 (N- CH_2), 110.0 111.5 122.9 123.0 (C_{ar}), 125.0 (C_{Pyr}), 128.0 128.7 133.9 135.0 135.3 (C_{ar}), 137.7 (C_{Pyr}), 150.1 (C-Pt), 153.6 (C_{Pyr}). MS (positive ESI) [M+Na]: calculated for $\text{C}_{20}\text{H}_{19}\text{I}_2\text{N}_3\text{PtNa}$: 772.92, found 772.92, [M-I]: calculated for $\text{C}_{20}\text{H}_{19}\text{I}_1\text{N}_3\text{Pt}$: 623.03, found 623.02.



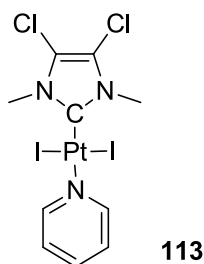
Procedure *a*: ~20%. $^1\text{H-NMR}$ (CDCl_3 , 300 MHz, 20 °C): 4.28 (s, 3H, N- CH_3), 5.83 (d, J = 8.2Hz, 1H, 1 H_{ar}), 6.54 (t, J = 7.8Hz, 1H, 1 H_{ar}), 7.00 (m, 3H, 1 H_{ar} +N- CH_2), 7.22 (d, J = 8.1Hz, 1H, 1 H_{ar}), 7.31 (t, J = 6.8Hz, 2 H_{Pyr}), 7.46-7.62 (m, 4H, 4 H_{ar}), 7.70 (t, J = 7.7Hz, 1H, 1 H_{Pyr}), 8.08 (d, J = 8.2Hz, 2H, 2 H_{ar}), 8.64 (t, J = 8.2, 3H, 3 H_{ar}), 9.01 (m, 2H, 2 H_{Pyr}). $^{13}\text{C-NMR}$ (CDCl_3 , 75 MHz, 20 °C): δ 35.4 (N- CH_3), 49.5 (N- CH_2), 109.9 114.4 122.4 122.8 124.9 125.1 125.5 127.3 129.3 129.6 131.4 131.7 134.5 (C_{ar} and C_{Pyr}), 137.7 (C_{Pyr}), 150.8 (C-Pt), 153.7 (C_{Pyr}).



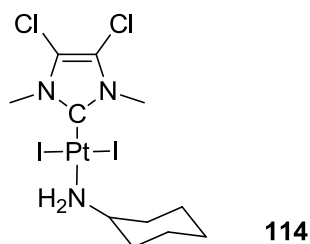
Procedure *a*: 46%. $^1\text{H-NMR}$ (CDCl_3 , 300 MHz, 20 °C): δ 5.72 (s, 2H, N- CH_2), 5.85 (s, 2H, N- CH_2), 7.20-7.80 (m, 14H, 10 H_{ar} + $\text{CH}=\text{N}$ + 3 H_{Pyr}), 9.03 (m, 2H, 2 H_{Pyr}). $^{13}\text{C-NMR}$ (CDCl_3 , 75 MHz, 20 °C): δ 53.0 (N- CH_2), 56.5 (N- CH_2), 125.1 128.4 128.6 129.0 129.2 129.3 129.4 133.6 134.5 137.8 142.2 (C_{ar} + $\text{CH}=\text{N}$ + C_{Pyr}), 143.7 (C-Pt), 153.7 (C_{Pyr}). RX: jlggd131105_02



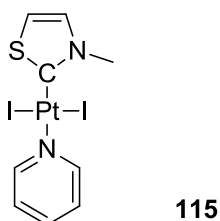
Procedure *b*: 58%. $^1\text{H-NMR}$ (CDCl_3 , 300 MHz, 20 °C): δ 3.21 (m, 1H, 1 H_{CH_2}), 3.44 (m, 1H, 1 H_{CH_2}), 4.23 (m, 2H, N- CH_2), 4.72 (m, 1H, 1 H_{CH}), 5.13 (s, 2H, CH_2), 5.54 (s, 2H, N- CH_2), 5.68 (s, 2H, N- CH_2), 6.53 (s, 1H, $\text{N}=\text{CH}$), 7.19-7.55 (20, 20H, 20 H_{ar}). $^{13}\text{C-NMR}$ (CDCl_3 , 75 MHz, 20 °C): δ 37.9 51.9 55.4 58.8 66.9 (4 CH_2 + CH), 126.6 127.5 127.8 127.9 128.0 128.2 128.4 128.8 132.6 133.5 133.6 133.8 141.3 (C_{ar}), 143.5 (C-Pt), 171.5 (C=O).



Procedure *a*: 74%. $^1\text{H-NMR}$ (CDCl_3 , 300 MHz, 20 °C): δ 3.97 (s, 6H, 2N-CH₃), 7.34 (ddd, J = 7.6, 5.0 and 1.3Hz, 2H, 2H_{Pyr}), 7.74 (tt, J = 7.7 and 1.5Hz, 1H, 1H_{Pyr}), 9.01 (m, 2H, 2H_{Pyr}). $^{13}\text{C-NMR}$ (CDCl_3 , 75 MHz, 20 °C): δ 36.5 (N-CH₃), 116.1 (CCl=CCl), 125.0 (C_{Pyr}), 137.7 (C_{Pyr}), 153.7 (C_{Pyr}). MS (positive ESI) [M-I]: calculated for C₁₀H₁₁Cl₂I₁N₃Pt₁: 565.9014, found 565.8937, [M-I+CH₃CN]: calculated for C₁₀H₁₁Cl₂I₁N₃Pt₁CH₃CN: 606.9280, found 606.9159.

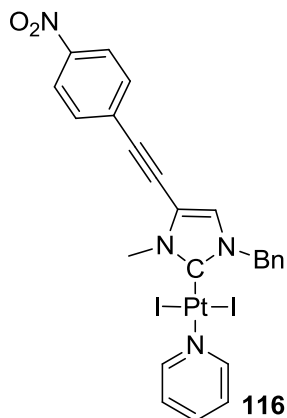


Procedure *b* was modified: cyclohexylamine was used as a solvent and the solution was stirred one hour at room temperature: 84%. $^1\text{H-NMR}$ (CDCl_3 , 300 MHz, 20 °C): δ 1.11-1.80 (m, 8H, 8H_{CHA}), 2.27 (m, 2H, 2H_{CHA}), 2.96 (m, 2H, Pt-NH₂), 3.24 (m, 1H, CH_{CHA}), 3.86 (s, 6H, 2N-CH₃). $^{13}\text{C-NMR}$ (CDCl_3 , 75 MHz, 20 °C): δ 25.0 (C_{CHA}), 25.4 (C_{CHA}), 36.0 (C_{CHA}), 36.4 (N-CH₂), 55.2 (CH_{CHA}), 116.1 (CCl=CCl), 141.3 (C-Pt).



Procedure *a*: 67 %. $^1\text{H-NMR}$ (CDCl_3 , 300 MHz, 20 °C): δ 4.17 (s, 3H, N-CH₃), 7.34 (ddd, J = 7.7, 5.0 and 1.6 Hz, 2H, 2H_{Pyr}), 7.43 (d, J = 3.9Hz, 1H, CH=), 7.50 (d, J = 3.9Hz, 1H, CH=), 7.74 (tt, J = 7.7 and 1.6Hz, 1H, 1H_{Pyr}), 9.00 (m, 2H, 2H_{Pyr}). MS (positive ESI) [M+Na]: calculated for C₉H₁₀I₂N₂PtSNa: 649.8195, found 649.8199, [M-I]: calculated for C₉H₁₀I₁N₂PtS: 499.9252, found 499.9234, [M-

I+CH₃CN]: calculated for C₉H₁₀I₁N₂PtS CH₃CN: 540.9518, found 540.9480. ¹³C-NMR (CDCl₃, 75 MHz, 20 °C): δ 44.5 (N-CH₃), 124.7 (C_{pyr}), 125.2 135.9 (CH=CH), 137.9 (C_{pyr}), 153.9 (C_{pyr}), 167.1 (C-Pt).

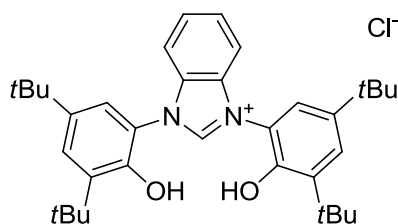


The complex was synthesized starting from alkyne platinum complex^{126,127} using standard Sonogashira conditions³⁰⁹ (CsCO₃ 10 eq, Pd(OAc)₂ 2%, DMF, 25 °C, overnight) and purified by silica gel chromatography (CH₂Cl₂/pentane-CH₂Cl₂): 37%. ¹H-NMR (CDCl₃, 300 MHz, 20 °C): δ 4.09 (s, 3H, N-CH₃), 5.74 (s, 2H, N-CH₂), 6.93 (s, 1H, CH=), 7.27-7.79 (m, 10H, 3H_{pyr} and 7 H_{ar}), 8.233 (d, J= 11.1Hz, 2H, 2H_{ar}), 9.05 (m, 2H, 2H_{pyr}). ¹³C-NMR (CDCl₃, 75 MHz, 20 °C): δ 36.5 (N-CH₃), 55.3 (CH₂), 80.4 (C_{alkyne}), 95.8 (C_{alkyne}), 117.4 (C=), 123.8 (C_{ar}), 124.8 (=CH), 125.1 (C_{pyr}), 128.3 128.7 129.1 129.4 132.1 134.6 (C_{ar}), 140.2 (C_{pyr}), 140.2 (C-Pt), 147.6 (C_{ar}-NO₂), 153.8 (C_{pyr}). MS (positive ESI): [M-I]: calculated for C₂₄H₂₀I₁N₄O₂Pt₁: 718.028 found 718.027.

7.3.2 Synthesis of complexes containing tridentate ligands

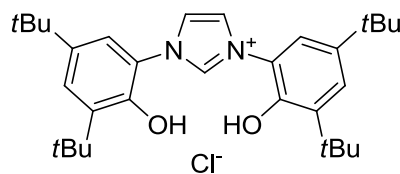
7.3.2.1 Synthesis of tridentate ($O^{\wedge}C^{\wedge}O$) ligand based complexes

The precursor **1,3-bis(3,5-di-*tert*-butyl-2-hydroxyphenyl)-1H-imidazol-3-ium chloride** and complexes **117-124** were reported by our group.³²⁴



1,3-bis(3,5-di-*tert*-butyl-2-hydroxyphenyl)-1H-benzo[d]imidazol-3-ium chloride

1,3-bis(3,5-di-*tert*-butyl-2-hydroxyphenyl)-1H-benzo[d]imidazol-3-ium chloride was synthesized following a literature procedure.⁵⁵⁶



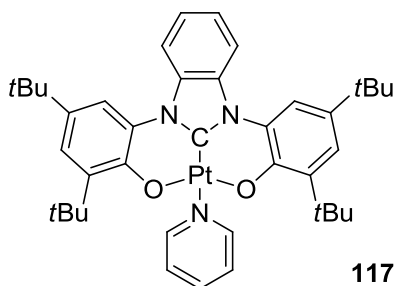
1,3-bis(3,5-di-*tert*-butyl-2-hydroxyphenyl)-1H-imidazol-3-ium chloride

2-Amino-4,6-di-*tert*-butylphenol (1.580 g, 7.14 mmol), glyoxal (518 mg, 3.57 mmol), and formic acid (4 drops) were stirred at room temperature for 12 h. The corresponding diimine was filtered off, washed with cold MeOH, and used without any further purification and characterization. The resulting yellow solid was then dissolved in AcOEt, and paraformaldehyde (114 mg, 3.79 mmol) and 4 N HCl/dioxane (1.166 mL, 4.67 mmol) were introduced to the reaction mixture. After 2 days of stirring, the volatiles were removed and the residue was purified on silica using $\text{CH}_2\text{Cl}_2/\text{MeOH}$ (from 1/0 to 95/5). A 526 mg portion of the ligand was obtained (30%, not optimized). $^1\text{H-NMR}$ (CDCl_3 , 300 MHz, 20 °C): δ 1.30 (s, 18H, $\text{C}(\text{CH}_3)_3$), 1.42 (s, 18H, $\text{C}(\text{CH}_3)_3$), 7.05 (d, $J = 2.3$, 2H, CH_{Ar}), 7.47 (d, $J = 2.3$, 2H, CH_{Ar}), 7.64 (s, 2H, CH), 8.40 (bs, 2H, OH), 8.83 (s, 1H, CH_{imid}). $^{13}\text{C-NMR}$ (CDCl_3 , 75 MHz, 20 °C): δ 29.6 (6C, $\text{C}(\text{CH}_3)_3$), 31.3 (6C, $\text{C}(\text{CH}_3)_3$), 34.4 (2C, $\text{C}(\text{CH}_3)_3$), 35.7 (2C, $\text{C}(\text{CH}_3)_3$),

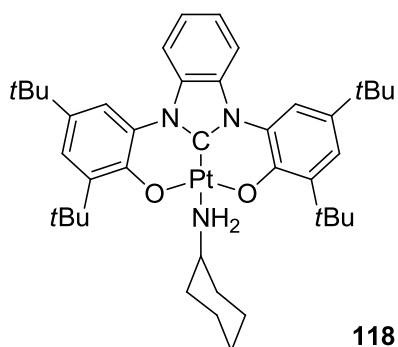
⁵⁵⁶ Bellemin-Lapponnaz, S.; Dagorne, S.; Romain, C.; Steffanut, P. PCT Int. Pat. Appl. WO 2012076140 (A1), 2012.

119.5 (2C, CH), 123.8 (2C, C_{Ar}), 124.5 (2C, CH_{Ar}), 126.5 (2C, CH_{Ar}), 136.7 (1C, CH_{carbene}), 141.7 (2C, CH_{Ar}), 143.2 (2C, CH_{Ar}), 148.1 (2C, CH_{Ar}). MS (positive ESI): [M – Cl]⁺ calculated for C₃₁H₄₅N₂O₂ 477.35, found 477.35.

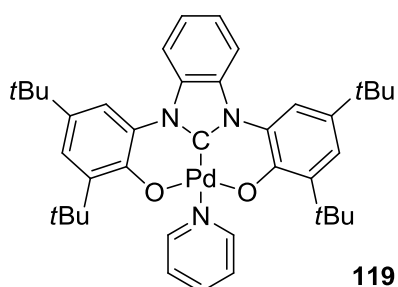
Unless mentioned, the following general procedure was used to afford [(O[^]C[^]O)M(L)] complexes (20-200 mg, 30-300 μmol scale): A suspension of tridentate ligand (O[^]C[^]O)H₂ (1 eq.), MCl₂ (M = Pt, Pd or Ni) (1 eq.), K₂CO₃ (30 eq.) in pyridine respectively cyclohexylamine were sonicated for 15 min then heated overnight at 100 °C. After evaporation of the volatiles under reduced pressure, CH₂Cl₂ was added and the suspension was filtrated over celite. Final product was obtained after silica gel chromatography (gradient cyclohexane/CH₂Cl₂ 1/1 to CH₂Cl₂) as a yellow solid.³²⁴



A mixture of 1,3-bis(3,5-di-tert-butyl-2-hydroxyphenyl)-1H-benzo[d]imidazol-3-ium chloride NHC (50 mg, 0.089 mmol), platinum dichloride (23.6 mg, 0.089 mmol) and potassium carbonate (368.1 mg, 2.663 mmol) was suspended in pyridine (5 mL). The mixture was sonicated for 10 minutes, stirred at 100°C during 10 minutes then 3 hours at 60°C. The resulting suspension was concentrated under reduced pressure, then dissolved in dichloromethane, filtered through a celite plug and concentrated under reduced pressure. The residue was purified by silica gel chromatography (dichloromethane/cyclohexane 1:1) affording the complex as a yellow solid (53.1 mg, 74%). ¹H-NMR (CDCl₃, 300 MHz, 20 °C): δ 1.35 (s, 18H, 2C(CH₃)₃), 1.36 (s, 18H, 2C(CH₃)₃), 7.15 (d, J = 1.2Hz, 2H, 2H_{ar}), 7.41-7.44 (m, H, 2H_{ar}), 7.54 (t, J = 7.6Hz, 2H, 2 H_{Pyr}), 7.76 (d, J = 1.2Hz, 2H, 2H_{ar}), 7.95 (tt, J = 7.7 and 1.6Hz, 1H, 1H_{Pyr}), 8.13-8.17 (m, 2H, 2H_{ar}), 8.99 (d, J = 4.8Hz, 2H, 2H_{Pyr}). ¹³C-NMR (CDCl₃, 75 MHz, 20 °C): δ 29.0 (C(CH₃)₃), 31.7 (C(CH₃)₃), 34.3 (C(CH₃)₃), 35.6 (C(CH₃)₃), 114.2 116.1 121.1 123.5 124.6 128.0 132.9 136.6 138.6 140.2 151.0 (C_{ar} and C_{Pyr}), 153.6 (C-Pt), 157.4 (C_{ar}). MS (positive ESI) [M-e⁻]: calculated for C₄₀H₄₉N₃O₂Pt: 798.35, found 798.35. Microanalysis: calculated for C₄₀H₄₉N₃O₂Pt: C, 60.13; H, 6.18; N, 5.26, found: C, 60.01; H, 6.12; N, 4.98.

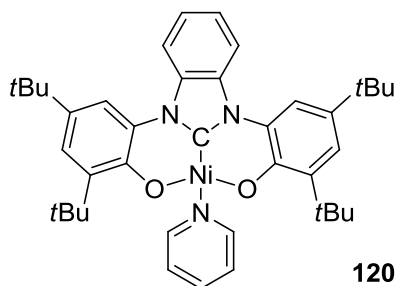


General procedure, or: Cyclohexylamine (1 mL) was added to **119** (25 mg, 0.032 mmol), then stirred 10 minutes at room temperature. The resulting product was concentrated under reduced pressure, the residue was purified by silica gel chromatography (dichloromethane/cyclohexane 1:1) affording the complex as a yellow solid (25.9 mg, 100%). $^1\text{H-NMR}$ (CDCl_3 , 300 MHz, 20 °C): δ 0.98-1.90 (m, 44H, $8\text{H}_{\text{CHA}}+36\text{H}_{\text{C}(\text{CH}_3)_3}$), 2.42 (m, 2H, 2H_{CHA}), 3.19 (m, 2H, Pt- NH_2), 3.34 (m, 1H, CH_{CHA}), 7.16 (d, $J=2.4\text{Hz}$, 2H, 2H_{ar}), 7.36-7.40 (m, 2H, 2H_{ar}), 7.70 (d, $J=2.4\text{Hz}$, 2H, 2H_{ar}), 8.06-8.10 (m, 2H, 2H_{ar}). MS (positive ESI) $[\text{M-e}^-]$: calculated for $\text{C}_{41}\text{H}_{57}\text{N}_3\text{O}_2\text{Pt}$: 818.41, found 818.42. Microanalysis: calculated for $\text{C}_{41}\text{H}_{57}\text{N}_3\text{O}_2\text{Pt}$: C, 60.13; H, 7.02; N, 5.13, found: C, 59.78; H, 6.80; N, 4.94.

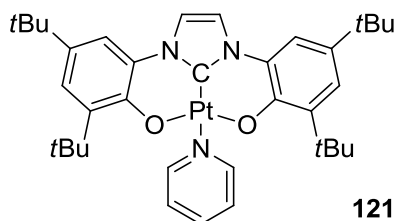


A mixture of 1,3-bis(3,5-di-tert-butyl-2-hydroxyphenyl)-1H-benzo[d]imidazol-3-ium chloride NHC (50 mg, 0.089 mmol), palladium dichloride (15.7 mg, 0.089 mmol) and potassium carbonate (368.1 mg, 2.663 mmol) was suspended in pyridine (5 mL). The mixture was sonicated 10 minutes, then stirred at 90°C during 3 hours. The resulting suspension was concentrated under reduced pressure, then dissolved in dichloromethane, filtered through a celite plug and concentrated under reduced pressure. The residue was purified by silica gel chromatography (dichloromethane/cyclohexane 1:1) affording the complex as a yellow-brown solid (63.1 mg, 66%). $^1\text{H-NMR}$ (CDCl_3 , 300 MHz, 20 °C): δ 1.31 (s, 18H, $2\text{C}(\text{CH}_3)_3$), 1.39 (s, 18H, $2\text{C}(\text{CH}_3)_3$), 7.20 (d, $J=2.4\text{Hz}$, 2H, 2H_{ar}), 7.40-7.51 (m, 4H, $2\text{H}_{\text{Pyr}}+2\text{H}_{\text{ar}}$), 7.73 (d, $J=2.4\text{Hz}$, 2H, 2H_{ar}), 7.88 (tt, $J=7.7$ and 1.6Hz , 1H, 1H_{Pyr}), 8.15-8.19 (m, 2H, 2H_{ar}), 8.89 (d, $J=4.8\text{Hz}$, 2H, 2H_{Pyr}). $^{13}\text{C-NMR}$ (CDCl_3 , 75 MHz, 20 °C): δ 29.5 ($\text{C}(\text{CH}_3)_3$), 31.8 ($\text{C}(\text{CH}_3)_3$), 34.3 ($\text{C}(\text{CH}_3)_3$), 35.6 ($\text{C}(\text{CH}_3)_3$), 114.1 116.2 121.5 123.7 124.2 128.5 133.2 135.7 138.4 140.5 150.6 157.1 (C_{ar} and C_{Pyr}), 165.3 (C-Pd). MS (positive ESI) $[\text{M-e}^-]$: calculated for

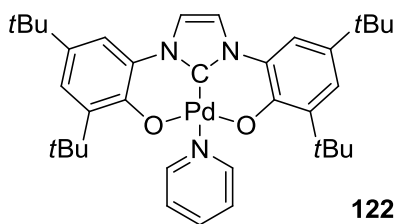
$C_{40}H_{49}N_3O_2Pd$: 709.29, found 709.29. Microanalysis: calculated for $C_{40}H_{49}N_3O_2Pd$: C, 67.64; H, 6.95; N, 5.92, found: C, 67.22; H, 6.66; N, 5.64.



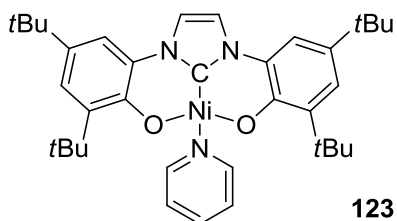
General procedure: 57 mg, 79%, green solid. 1H -NMR ($CDCl_3$, 300 MHz, 20 °C): δ 1.05 (s, 18H, $C(CH_3)_3$), 1.38 (s, 18H, $C(CH_3)_3$), 7.07 (d, $J = 2.5$ Hz, 2H, CH_{phenoxy}), 7.38–7.44 (m, 4H, CH_{Ar}), 7.76–7.80 (m, 3H, CH_{Ar}), 8.14–8.17 (m, 2H, $CH_{\text{benzimidazole}}$), 8.94 (d, $J = 5.0$ Hz, 2H, 2 NCH_{pyr}). ^{13}C -NMR ($CDCl_3$, 75 MHz, 20 °C): δ 29.1 (6C, $C(CH_3)_3$), 31.7 (6C, $C(CH_3)_3$), 34.3 (2C, $C(CH_3)_3$), 35.1 (2C, $C(CH_3)_3$), 113.7 (2C, CH_{Ar}), 114.6 (2C, CH_{Ar}), 120.7 (2C, CH_{Ar}), 123.3 (2C, CH_{Ar}), 123.6 (2C, CH_{Ar}), 127.6, 132.8, 135.3, 137.7, 140.4, 150.3, 154.1, 162.4 (1C, C_{carbene}). MS (positive ESI): $[M+H]^+$ calculated for $C_{40}H_{50}N_3NiO_2$ 662.33, found 662.32. Microanalysis: calculated for $C_{40}H_{49}N_3NiO_2$: C, 72.51; H, 7.45; N, 6.34, found: C, 72.69; H, 7.75; N, 5.94.



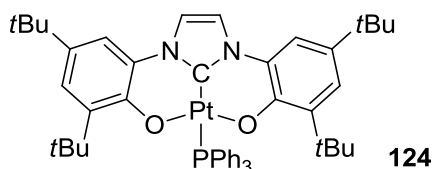
General procedure: 134 mg, 48%, yellow solid. 1H -NMR ($CDCl_3$, 300 MHz, 20 °C): δ 1.33 (s, 18H, $C(CH_3)_3$), 1.34 (s, 18H, $C(CH_3)_3$), 7.13 (d, $J = 2.4$, 2H, CH_{Phenoxy}), 7.23 (d, $J = 2.4$, 2H, CH_{Phenoxy}), 7.52 (td, $J = 6.5, 1.1$ Hz, 2H, CH_{pyr}), 7.67 (s, 2H, CH), 7.95 (tt, $J = 7.7, 1.1$ Hz, 1H, CH_{pyr}), 9.08 (d, $J = 6.5$ Hz, 2H, NCH_{pyr}). ^{13}C -NMR ($CDCl_3$, 75 MHz, 20 °C): δ 29.5 (6C, $C(CH_3)_3$), 31.6 (6C, $C(CH_3)_3$), 34.1 (2C, $C(CH_3)_3$), 35.8 (2C, $C(CH_3)_3$), 113.0 (2C, CH), 115.7 (2C, CH_{Ar}), 121.3 (2C, CH_{Ar}), 124.4 (2C, CH_{Ar}), 126.0 (2C, CH_{Ar}), 136.7 (2C, CH_{Ar}), 138.3 (1C, CH_{pyr}), 140.2 (2C, CH_{Ar}), 150.9 (2C, CH_{Ar}), 153.5 (1C, CH_{carbene}). MS (positive ESI): $[M]^+$ calculated for $C_{36}H_{47}N_3O_2Pt$ 748.33, found 748.33. Microanalysis: calculated for $C_{36}H_{47}N_3O_2Pt \cdot 0.33CH_2Cl_2$: C, 56.15; H, 6.18; N, 5.41, found: C, 55.97; H, 6.04; N, 5.37.



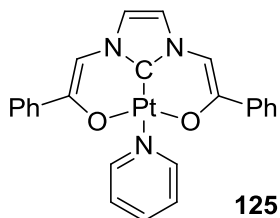
General procedure: 142 mg, 76%, yellow solid. $^1\text{H-NMR}$ (CDCl_3 , 300MHz, 20 °C): δ 1.38 (s, 18H, $\text{C}(\text{CH}_3)_3$), 1.39 (s, 18H, $\text{C}(\text{CH}_3)_3$), 7.20(d, $J = 2.3$, 2H, $\text{CH}_{\text{Phenoxy}}$), 7.27 (d, $J = 2.3$, 2H, $\text{CH}_{\text{Phenoxy}}$), 7.46–7.51(m, 2H, CH_{Pyr}), 7.75 (s, 2H, CH), 7.90 (tt, $J = 7.5$, 1.5 Hz, 1H, CH_{Pyr}), 9.08 (dd, $J = 6.4$, 1.5 Hz, 2H, NCH_{Pyr}). $^{13}\text{C-NMR}$ (CDCl_3 , 75MHz, 20 °C): δ 29.5 (6C, $\text{C}(\text{CH}_3)_3$), 31.7 (6C, $\text{C}(\text{CH}_3)_3$), 34.2 (2C, $\text{C}(\text{CH}_3)_3$), 35.7 (2C, $\text{C}(\text{CH}_3)_3$), 113.1 (2C, CH), 116.9 (2C, CH_{Ar}), 121.8 (2C, CH_{Ar}), 124.0 (2C, CH_{Ar}), 126.3 (2C, CH_{Ar}), 135.9 (2C, CH_{Ar}), 138.2 (1C, CH_{Pyr}), 140.3 (2C, CH_{Ar}), 149.8 (1C, $\text{CH}_{\text{carbene}}$), 150.5 (2C, CH_{Ar}), 154.3 (2C, CH_{Ar}). MS (positive ESI): $[\text{M} - \text{e}]^+$ calculated for $\text{C}_{36}\text{H}_{47}\text{N}_3\text{O}_2\text{Pd}$ 659.2711, found 659.2711. Microanalysis: calculated for $\text{C}_{36}\text{H}_{47}\text{N}_3\text{O}_2\text{Pd} \cdot \text{CH}_2\text{Cl}_2$: C, 59.64; H, 6.63; N, 5.64, found: C, 59.62; H, 6.50; N, 5.65.



General procedure: 102 mg, 83%, brown solid. $^1\text{H-NMR}$ (CDCl_3 , 300 MHz, 20 °C): δ 1.07 (s, 18H, $\text{C}(\text{CH}_3)_3$), 1.34 (s, 18H, $\text{C}(\text{CH}_3)_3$), 7.03 (d, $J = 2.3$ Hz, 2H, $\text{CH}_{\text{Phenoxy}}$), 7.19 (d, $J = 2.3$ Hz, 2H, $\text{CH}_{\text{Phenoxy}}$), 7.41 (t, $J = 6.4$ Hz, 2H, CH_{Pyr}), 7.69 (s, 2H, CH), 7.82 (t, $J = 7.7$ Hz, 1H, CH_{Pyr}), 9.07 (d, $J = 4.7$ Hz, 2H, NCH_{Pyr}). $^{13}\text{C-NMR}$ (CDCl_3 , 75MHz, 20 °C): δ 29.0 (6C, $\text{C}(\text{CH}_3)_3$), 31.7 (6C, $\text{C}(\text{CH}_3)_3$), 34.1 (2C, $\text{C}(\text{CH}_3)_3$), 35.2 (2C, $\text{C}(\text{CH}_3)_3$), 111.3 (2C, CH), 115.9 (2C, CH_{Ar}), 120.9 (2C, CH_{Ar}), 123.4 (2C, CH_{Ar}), 125.0 (2C, CH_{Ar}), 135.5 (2C, CH_{Ar}), 137.5 (1C, CH_{Ar}), 140.2 (2C, CH_{Ar}), 146.8 (1C, $\text{CH}_{\text{carbene}}$), 150.4 (2C, CH_{Ar}), 151.5 (2C, CH_{Ar}). MS (positive ESI): $[\text{M} - \text{e}]^+$ calculated for $\text{C}_{36}\text{H}_{47}\text{N}_3\text{NiO}_2$ 611.3016, found 611.2863. Microanalysis: calculated for $\text{C}_{36}\text{H}_{47}\text{N}_3\text{O}_2\text{Ni}$: C, 70.60; H, 7.73; N, 6.86, found: C, 70.27; H, 7.54; N, 6.65.



Complex **123** (80 mg, 0.11 mmol) and triphenylphosphine (140 mg, 0.53 mmol) were stirred in CH₃CN for 12 h. The volatiles were removed under reduced pressure, and the residue was purified by column chromatography (CH₂Cl₂/cyclohexane 5/5 to 8/2). A 79 mg portion of **7Pt** was obtained (80%, pale yellow solid). ¹H-NMR (CDCl₃, 300 MHz, 20 °C): δ 0.73 (s, 18H, C(CH₃)₃), 1.33 (s, 18H, C(CH₃)₃), 7.01 (d, J = 2.4 Hz, 2H, CH_{Phenoxy}), 7.21 (d, J = 2.4 Hz, 2H, CH_{Phenoxy}), 7.33–7.44 (m, 9H, CH_{PPh3}), 7.73 (d, J = 1.1 Hz, 2H, CH), 7.84–7.90 (m, 6H, CH_{PPh3}). ¹³C-NMR (CDCl₃, 75 MHz, 20 °C): δ 29.4 (6C, C(CH₃)₃), 31.6 (6C, C(CH₃)₃), 34.1 (2C, C(CH₃)₃), 35.1 (2C, C(CH₃)₃), 113.1 (2C, CH_{Ar}), 116.2 (2C, J_{C-P} = 4.9 Hz, C_{Ar}), 121.5 (2C, CH_{Ar}), 125.9 (2C, C_{Ar}), 128.3 (J_{C-P} = 10.3 Hz, C_{Ar}), 130.2 (J_{C-P} = 2.2 Hz, CH_{Ar}), 132.5 (J_{C-P} = 46.4 Hz, CH_{Ar}), 135.6 (J_{C-P} = 12.0 Hz, CH_{Ar}), 136.6 (2C, C_{Ar}), 141.0 (2C, CH_{Ar}), 149.9 (1C, J_{C-P} = 141 Hz, C_{Carbene}), 153.2 (2C, J_{C-P} = 1.6 Hz, C_{Ar}). ³¹P-NMR (CDCl₃, 121 MHz, 20 °C): δ 23.86 (J_{P-Pt} = 1411 Hz). MS (positive ESI): [M + H]⁺: calculated for C₄₉H₅₈N₂O₂Pt 932.39, found 932.38. Microanalysis: calculated for C₄₉H₅₇N₂O₂PPt·CH₂Cl₂: C, 59.05; H, 5.85; N, 2.75, found: C, 59.68; H, 5.92; N, 2.90.



46%. ¹H-NMR (CDCl₃, 300 MHz, 20 °C): δ 6.34 (s, 2H, 2CH=), 6.86 (s, 2H, CH=CH), 7.21–7.37 (m, 6H, 6H_{ar}), 7.53 (t, J = 7.6 Hz, 2H, 2H_{pyr}), 7.60–7.69 (m, 4H, 4H_{ar}), 7.89 (tt, J = 7.6 and 1.6 Hz, 1H, 1H_{pyr}), 9.19 (m, 2H, 2H_{pyr}). ¹³C-NMR (CDCl₃, 75 MHz, 20 °C): δ 99.5 (N-CH), 116.2 (CH=CH), 124.9 125.2 127.5 128.2 138.2 (CH_{ar} and CH_{pyr}), 139.1 (C_{ar}), 148.3 (C_{pyr}), 150.7 (C_{ar}).

7.3.2.2 Synthesis of tridentate (O[^]N[^]O) ligand based complexes

7.3.2.2.1 Synthesis of the (O[^]N[^]O)H₂ precursors

The (O[^]N[^]O)H₂ precursors were obtained³³⁰ by a two-step procedure from 2-(2-hydroxyphenyl)-4H-benzo[e][1,3]oxazin-4-one reported by Hegetschweiler and co-workers.³²⁹

2-(2-hydroxyphenyl)-4H-benzo[e][1,3]oxazin-4-one (precursor)

This compound was synthesized following a known procedure described by Steinhauser *et al.*:³²⁹ salicylamide (20 g, 146 mmol, 1 eq.), salicylic acid (24.3 g, 176 mmol, 1.21 eq.) and pyridine (12.1 mL, 11.9 g, 150 mmol, 1.03 eq.) were refluxed in xylenes (30 mL). Thionylchloride (35.7 g, 300 mmol, 2.05 eq.) was added drop wise over a period of 4 h. Stirring was continued for 30 min after the addition, and then the solvent was removed at reduced pressure. The solid residue was washed with a mixture of ethanol (60 mL) and acetic acid (1.5 mL) at 80 °C and then was allowed to cool down to room temperature. The precipitate was filtered, dried in vacuo, and then kept under an inert atmosphere of argon in a refrigerator. Yield: yellow needles (22.80 g, 95 mmol, 65%). ¹H NMR (DMSO-d₆, 300 MHz, 20 °C): δ = 7.06–7.11 (m, 2H_{ar}), 7.57–7.66 (m, 2H_{ar}), 7.77–7.80 (m, 1H_{ar}), 7.93 (ddd, J = 8.4, 7.3 and 1.1 Hz, 1H_{ar}), 8.50 (dd, J = 7.8 and 1.6 Hz, 1H_{ar}), 8.18–8.22 (m, 1H_{ar}), 8.75 (OH) ppm. ¹³C NMR (DMSO-d₆, 75 MHz, 20 °C): δ = 113.37, 119.39, 119.72, 119.87, 121.48, 128.66, 129.10, 130.90, 137.92, 138.62, 155.78, 163.73, 165.35, 166.71 ppm.

(O[^]N[^]O)H₂ ligands: (3,5-bis(2-hydroxyphenyl)-1-R-1,2,4-triazole

Ligands (O[^]N[^]O)H₂ ligands were synthesized according to a known procedure described by Steinhauser *et al.*:³²⁹ Precursor (1 eq.) and mono-substituted hydrazine chloride (1 eq.) were refluxed in ethanol for 2 h. The mixture was then allowed to cool down to room temperature, followed by the addition of 2M HCl aqueous solution until the formation of a white/pale yellow precipitate which was filtered and dried in vacuo.

R = H: precursor (1 g, 4.18 mmol) and hydrazine monohydrate (0.2 mL, 4.18 mmol) were refluxed in Et₂O for 12 h. The white precipitate was filtered and then washed with a small amount of Et₂O to yield 0.90 g (3.55 mmol, 85%) of the product. ¹H-NMR (DMSO-d₆, 300 MHz, 20 °C): δ 6.95–7.03 (m, 4H_{ar}), 7.33 (ddd, J = 8.6, 7.1 and 1.9 Hz, 2H_{ar}), 8.01 (dd, J = 7.8 and 1.6 Hz, 2H_{ar}) 11.81 (OH). ¹³C-

NMR (DMSO- d_6 , 75 MHz, 20 °C): δ 118.49, 121.40, 129.36, 129.40, 133.25, 157.79. MS (positive ESI) $[M+H]^+$: Calculated for $C_{14}H_{12}N_3O_2$: 254.09, found 254.09.

R = Me: (after recrystallization) 0.30 g, 1.12 mmol, 27%. 1H -NMR (DMSO- d_6 , 300 MHz, 20 °C): δ 3.83 (s, 3H_{Me}), 6.91–7.07 (m, 4H_{ar}), 7.30 (ddd, J = 8.5, 6.8 and 1.7 Hz, 1H_{ar}), 7.40–7.46 (m, 2H_{ar}), 7.94 (dd, J = 7.6 and 1.4 Hz), 10.43 (OH), 11.05 (OH). ^{13}C -NMR (CDCl₃, 75 MHz, 20 °C): δ 38.82 (Me), 110.60, 113.47, 116.99, 118.32, 119.33, 119.77, 126.77, 127.34, 131.41, 132.67, 152.09, 156.30, 157.71, 158.14.

R = Ph: 0.62 g, 1.98 mmol, 45%. 1H -NMR (DMSO- d_6 , 300 MHz, 20 °C): δ 6.84–7.01 (m, 4H_{ar}), 7.32–7.47 (m, 8H_{ar}), 8.02 (dd, J = 7.8 and 1.6 Hz, 1H_{ar}), 10.05 (s, OH), 10.88 (s, OH). ^{13}C -NMR (CDCl₃, 75 MHz, 20 °C): δ 110.06, 113.36, 117.14, 118.32, 118.85, 119.86, 126.38, 127.45, 127.61, 130.01, 130.26, 131.69, 132.79, 138.15, 151.99, 156.52, 158.61, 159.02. MS (positive ESI) $[M+H]^+$: Calculated for $C_{20}H_{16}N_3O_2$: 330.12, found 330.12, $[M+Na]^+$: Calculated for $C_{20}H_{15}N_3NaO_2$: 352.11, found 352.11.

R = *o*-tolyl: 1.03 g, 3.01 mmol, 72%. 1H -NMR (CDCl₃, 300 MHz, 20 °C): δ 2.09 (s, 3H_{Me}), 6.60 (ddd, J = 8.5, 6.8 and 1.7 Hz, 1H_{ar}), 6.77 (dd, J = 8.0 and 1.4 Hz, 1H_{ar}), 7.03–7.15 (m, 3H_{ar}), 7.29–7.48 (m, 5H_{ar}), 7.56 (ddd, J = 8.2, 6.3 and 2.1 Hz, 1H_{ar}), 8.16 (dd, J = 7.8 and 1.4 Hz, 1H_{ar}). ^{13}C -NMR (CDCl₃, 75 MHz, 20 °C): δ 18.38 (Me), 109.97, 113.33, 117.10, 118.28, 119.02, 119.83, 126.06, 127.52, 127.57, 127.66, 130.90, 131.63, 131.78, 132.80, 135.64, 137.33, 152.42, 156.48, 158.42, 158.78.

R = *m*-tolyl: 0.95 g, 2.80 mmol, 66%. 1H -NMR (CDCl₃, 300 MHz, 20 °C): δ 2.47 (s, 3H_{Me}), 6.65 (ddd, J = 7.1, 8.2 and 1.1 Hz, 1H_{ar}), 6.95 (dd, J = 7.9 and 1.7 Hz, 1H_{ar}), 7.02–7.16 (m, 3H_{ar}), 7.27–7.49 (m, 6H_{ar}), 8.15 (dd, J = 8.0 and 1.6 Hz, 1H_{ar}). ^{13}C -NMR (CDCl₃, 75 MHz, 20 °C): δ 21.31 (Me), 110.07, 113.37, 117.07, 118.22, 118.70, 118.75, 119.79, 123.37, 126.84, 127.41, 127.45, 127.54, 129.68, 129.73, 130.99, 131.58, 132.67, 138.02, 140.35, 151.90, 156.45, 158.19, 156.45, 158.20, 158.84.

R = *p*-tolyl: 0.90 g, 2.63 mmol, 63%. 1H -NMR (CDCl₃, 300 MHz, 20 °C): δ 2.51 (s, 3H_{Me}), 6.65 (ddd, J = 8.2, 7.2 and 1.0 Hz, 1H_{ar}), 6.97 (dd, J = 8.1 and 1.5 Hz, 1H_{ar}), 7.02–7.16 (m, 3H_{ar}), 7.30–7.40 (m, 6H_{ar}), 8.15 (dd, J = 7.8 and 1.5 Hz, 1H_{ar}). ^{13}C -NMR (CDCl₃, 75 MHz, 20 °C): δ 21.42 (Me), 110.13, 113.39, 117.11, 118.27, 118.81, 119.83, 126.15, 127.42, 127.57, 130.58, 131.63, 132.71, 135.62, 140.62, 151.91, 156.51, 158.24, 158.78.

R = 3,5-dimethylphenyl: 0.88 g, 2.47 mmol, 59%. 1H -NMR (CDCl₃, 300 MHz, 20 °C): δ 2.41 (s, 6H_{Me}), 6.65 (ddd, J = 8.2, 7.2 and 1.0 Hz, 1H_{ar}), 6.98 (dd, J = 8.1 and 1.5 Hz, 1H_{ar}), 7.01–7.15 (m, 5H_{ar}), 7.23 (s, 1H_{ar}), 7.30–7.41 (m, 2H_{ar}), 8.14 (dd, J = 7.8 and 1.8 Hz, 1H_{ar}). ^{13}C -NMR (CDCl₃, 75 MHz, 20 °C): δ 21.21 (Me), 110.11, 113.40, 117.06, 118.18, 118.72, 119.77, 123.90, 127.44, 127.52, 131.53, 131.87, 132.62, 137.94, 139.99, 151.81, 156.46, 158.22, 158.67.

R = 3,5-bis(trifluoromethyl)phenyl: 1.46 g, 3.17 mmol, 76%. $^1\text{H-NMR}$ (CDCl_3 , 300 MHz, 20 °C): δ 6.75 (ddd, $J = 8.1, 7.0$ and 1.1 Hz, 1H_{ar}), 6.89 (dd, $J = 8.1$ and 1.6 Hz, 1H_{ar}), 7.04-7.12 (m, 2H_{ar}), 7.19 (dd, $J = 8.4$ and 0.9 Hz, 1H_{ar}), 7.42 (ddd, $J = 8.4, 7.2$ and 1.2 Hz, 2H_{ar}), 8.03 (s, 1H_{ar}), 8.08 (s, 1H_{ar}), 8.15 (dd, $J = 7.9$ and 1.4 Hz, 1H_{ar}). $^{13}\text{C-NMR}$ (CDCl_3 , 75 MHz, 20 °C): δ 109.35, 112.76, 117.29, 118.82, 119.36, 120.08, 122.32 (q, $J = 273.5$ Hz), 123.49 (quin, $J = 3.7$ Hz), 126.17, 126.21, 127.26, 127.82, 132.27, 133.63 (q, $J = 34.6$ Hz), 133.73, 139.28, 152.45, 156.50, 157.86.

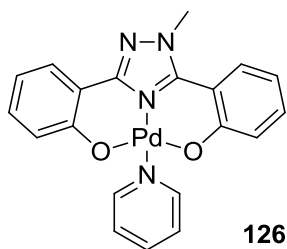
R = pentafluorophenyl: 318 mg, 0.76 mmol, 76%. $^1\text{H-NMR}$ (CDCl_3 , 300 MHz, 20 °C): δ : 6.8 (ddd, $^2J = 7.1\text{Hz}$, $^3J = 7.9\text{Hz}$, $^4J = 1.1\text{Hz}$, 1H , H_{ar}), 6.95 (d, $^2J = 7.9\text{Hz}$, 1H , H_{ar}), 7.06-7.1 (m, 2H , H_{ar}), 7.17 (d, $J = 7.8\text{Hz}$, 1H , H_{ar}), 7.4-7.44 (m, 2H , H_{ar}), 8.13 (dd, $^2J = 7.9\text{Hz}$, $^3J = 1.6\text{Hz}$, 1H , H_{ar}), 9.19 (s, 1H , H_{OH}), 11.33 (s, 1H , H_{OH}). $^{13}\text{C-NMR}$ (CDCl_3 , 75 MHz, 20 °C): δ 109.3, 112.82, 117.48, 119.08, 119.89, 120.23, 125.06, 128.06, 132.58, 134.07, 136.70, 140.16, 142.11, 145.58, 154.99, 156.77, 158.56, 161.18. $^{19}\text{F-NMR}$ (CDCl_3 , 300 MHz, 20 °C): δ -158.2, -142.92, -142.9. UV: $\epsilon = 3.4 \times 10^4 \text{ L} \cdot \text{mol}^{-1} \cdot \text{cm}^{-1}$ (251 nm).

R = *p* – carbonyl: 80%. NMR data are found in accordance with literature.³²⁹

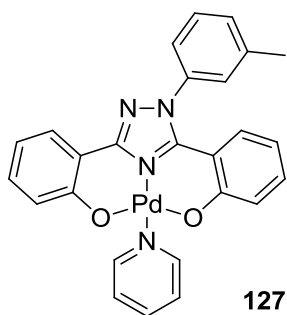
R = phenyl – *p*- carbamoyl: 25%. $^1\text{H-NMR}$ (CDCl_3 , 300 MHz, 20 °C): δ 0.88 (t, $J = 6.8$ Hz), 1.26-1.39 (m, $18\text{H}_{\text{alkyl}}$), 1.60 – 1.70, (m, CH_2), 3.5 (q, 6.7 Hz, NH-CH_2) 6.24 (t, $J = 5.7$, 1H_{ar}), 6.66 (ddd, $J = 7.0, 8.3$, and 1.2 Hz, 1H_{ar}), 6.93 (dd, $J = 7.7$ and 1.7 Hz, 1H_{ar}), 7.01-7.08 (m, 2H_{ar}), 7.14 (dd, $J = 8.4$ and 1.0 Hz, 1H_{ar}), 7.31-7.40 (m, 2H_{ar}), 7.95 (d, $J = 8.4$ Hz, 2H_{ar}), 8.13 (dd, $J = 7.6$ and 1.8 Hz, 1H_{ar})

7.3.2.2.2 Synthesis of the $[(\text{O}^{\wedge}\text{N}^{\wedge}\text{O})\text{M}(\text{L})]$ complexes

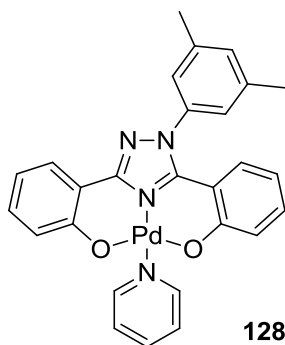
Unless mentioned, $[(\text{O}^{\wedge}\text{N}^{\wedge}\text{O})\text{M}(\text{L})]$ complexes are obtained using this general procedure: A suspension of tridentate precursor $(\text{O}^{\wedge}\text{N}^{\wedge}\text{O})\text{H}_2$ (1 eq.), MCl_2 ($\text{M} = \text{Pt}$ or Pd) (1 eq.), ligand (L) (1 eq), K_2CO_3 (30 eq.) in toluene (except when $\text{L} = \text{pyridine}$ or cyclohexylamine, pyridine respectively cyclohexylamine were used as solvent) were sonicated for 15 min then heated overnight at 100 °C. After evaporation of the volatiles under reduced pressure, CH_2Cl_2 was added and the suspension filtrated over celite. Final product was obtained after silica gel chromatography purification (gradient cyclohexane/ CH_2Cl_2 1/1 to CH_2Cl_2) as a green/yellow solid.



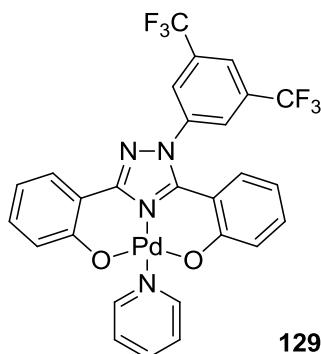
80 mg, 0.18 mmol, 63%. $^1\text{H-NMR}$ (CDCl_3 , 300 MHz, 20 °C): δ 4.20 (s, 3H_{Me}), 6.65-6.74 (m, 2H_{ar}), 6.97-7.25 (m, 4H_{ar}), 7.45-7.55 (m, 3H_{ar}), 7.87 (tt, J = 7.7 and 1.6 Hz, 1H_{ar}), 7.97 (dd, J = 7.9 and 1.8 Hz, 1H_{ar}), 8.95-8.97 (m, 2H_{ar}). $^{13}\text{C-NMR}$ (CDCl_3 , 75 MHz, 20 °C): δ 40.54 (Me), 111.27, 113.43, 115.22, 115.47, 120.79, 122.35, 124.49, 127.17, 127.26, 131.03, 131.89, 138.43, 147.50, 148.29, 152.22, 162.81, 166.03. MS (positive ESI) [M^+]: calculated for $\text{C}_{20}\text{H}_{16}\text{N}_4\text{O}_2\text{Pd}$: 450.03, found 450.04.



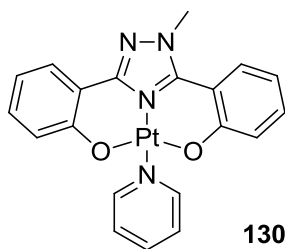
109 mg, 0.24 mmol, 86%. $^1\text{H-NMR}$ (CDCl_3 , 300 MHz, 20 °C): δ 2.46 (s, 3H_{Me}), 6.34 (ddd, J = 6.8, 8.1 and 1.4 Hz, 1H_{ar}), 6.67 (ddd, J = 7.9, 6.9 and 1.0 Hz, 1H_{ar}), 6.85 (dd, J = 8.3 and 1.3 Hz, 1H_{ar}), 7.01-7.07 (m, 2H_{ar}), 7.10-7.21 (m, 2H_{ar}), 7.30-7.46 (m, 4H_{ar}), 7.50-7.54 (m, 2H_{ar}), 7.91 (tdd, J = 7.6, 1.5 and 1.6 Hz, 1H_{ar}), 8.04 (dd, J = 8.1 and 1.8 Hz, 1H_{ar}), 9.02-9.04 (m, 2H_{ar}) ppm. $^{13}\text{C-NMR}$ (CDCl_3 , 75 MHz, 20 °C): δ 21.35 (Me), 110.58, 113.02, 114.87, 115.48, 120.80, 122.29, 123.21, 124.57, 126.61, 127.52, 128.29, 129.64, 130.68, 131.28, 132.00, 138.52, 139.12, 140.28, 147.02, 148.34, 153.01, 163.06, 166.02.

**128**

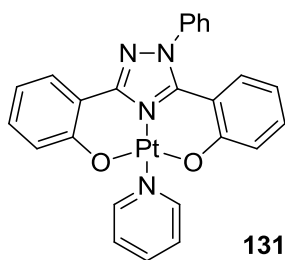
Quant. $^1\text{H-NMR}$ (CDCl_3 , 300 MHz, 20 °C): δ 2.40 (s, 6H_{Me}), 6.35 (ddd, J = 8.3, 6.7 and 1.4 Hz, 1H_{ar}), 6.66 (ddd, J = 7.7, 6.8 and 1.1 Hz, 1H_{ar}), 6.88 (dd, J = 8.3 and 1.6 Hz, 1H_{ar}), 7.02-7.20 (m, 7H_{ar}), 7.53 (td, J = 6.4 and 0.9 Hz, 2H_{ar}), 7.92 (tdd, J = 7.6, 1.5 and 1.5 Hz, 1H_{ar}), 8.04 (dd, J = 8.0 and 1.8 Hz, 1H_{ar}), 9.02-9.04 (m, 2H_{ar}). $^{13}\text{C-NMR}$ (CDCl_3 , 75 MHz, 20 °C): δ 21.23 (Me), 110.65, 113.08, 114.89, 115.50, 120.74, 122.20, 123.74, 124.57, 127.54, 128.30, 131.24, 131.60, 131.96, 13.51, 139.03, 139.95, 147.07, 148.40, 152.90, 162.99, 165.91. MS (positive ESI) [M^+]: calculated for $\text{C}_{27}\text{H}_{22}\text{N}_4\text{O}_2\text{Pd}$: 540.08, found 540.08, [$M+H$]: Calculated for $\text{C}_{27}\text{H}_{23}\text{N}_4\text{O}_2\text{Pd}$: 541.09, found 541.09.

**129**

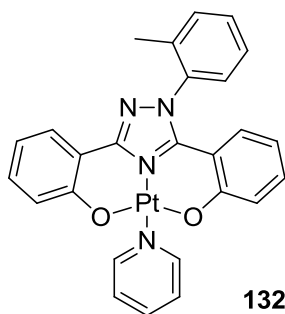
93 mg, 0.14 mmol, 50%. $^1\text{H-NMR}$ (CDCl_3 , 300 MHz, 20 °C): δ = 6.37-6.42 (m, 1H_{ar}), 6.64-6.73 (m, 2H_{ar}), 6.93-7.01 (m, 2H_{ar}), 7.13-7.18 (m, 2H_{ar}), 7.48 (t, J = 6.7 Hz), 7.87-8.05 (m, 5H_{ar}), 8.93 (d, J = 5.9 Hz). $^{13}\text{C-NMR}$ (CDCl_3 , 75 MHz, 20 °C): δ 109.38, 112.19, 115.17, 115.63, 121.01, 122.44 (q, J = 273.8 Hz, CF₃), 122.92 (t, J = 3.5 Hz), 123.03, 124.55, 126.06, 126.10, 127.47, 131.73, 132.94, 133.23 (q, J = 34.3 Hz, C-CF₃), 138.58, 140.34, 148.10, 148.17, 153.10, 163.25, 166.69.



80 mg, 0.17 mmol, 89%. $^1\text{H-NMR}$ (CDCl_3 , 300 MHz, 20 °C): δ 4.21 (s, 3H_{Me}), 6.68-6.76 (m, 2H_{ar}), 7.02 (dd, J = 8.5 and 1.0 Hz, 1H_{ar}), 7.08-7.24 (m, 3H_{ar}), 7.45-7.50 (m, 2H_{ar}), 7.6 (dd, J = 8.1 and 1.5 Hz, 1H_{ar}), 7.9 (tdd, J = 7.6, 1.6 and 1.3 Hz, 1H_{ar}), 8.01 (dd, J = 8.1 and 1.7 Hz, 1H_{ar}), 9.05 (dd, J = 6.7 and 1.4 Hz, 2H_{ar}). $^{13}\text{C-NMR}$ (CDCl_3 , 75 MHz, 20 °C): δ 40.77 (Me), 111.05, 113.15, 115.82, 116.01, 120.74, 122.43, 124.49, 126.77, 127.02, 130.74, 131.46, 137.94, 145.18, 148.67, 151.04, 162.33, 165.22.

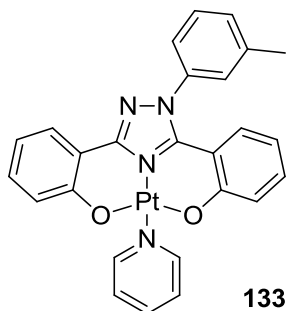


86%. $^1\text{H-NMR}$ (CDCl_3 , 300 MHz, 20 °C): δ 6.31 (ddd, J = 8.3, 6.7 and 1.6Hz, 1H, 1H_{ar}), 6.67 (ddd, J = 6.9, 8.0 and 1.3Hz, 1H, 1H_{ar}), 6.86 (dd, J = 8.3 and 1.6Hz, 1H, 1H_{ar}), 7.01-7.21 (m, 4H, 4H_{ar}), 7.51 (t, J = 6.8Hz, 2H, 2H_{Pyr}), 7.56 (s, 5H, 5H_{ar}), 7.93 (tt, J = 7.6 and 1.5Hz, 1H, 1H_{Pyr}), 8.06 (dd, J = 7.9 and 1.8Hz, 1H, 1H_{ar}), 9.13 (m, 2H, 2H_{Pyr}). $^{13}\text{C-NMR}$ (CDCl_3 , 75 MHz, 20 °C): δ 110.3 112.7 115.5 116.1 120.8 122.5 124.8 126.3 127.4 127.8 123.0 131.1 131.7 138.1 139.4 144.9 148.8 152.0 153.7 162.6 165.2 (18C_{ar} and 3C_{Pyr}).

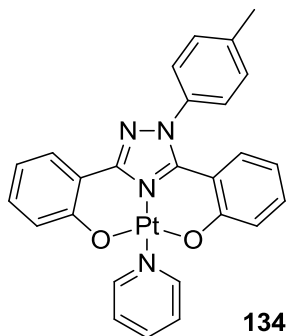


100 mg, 0.19 mmol, 68%. $^1\text{H-NMR}$ (CDCl_3 , 300 MHz, 20 °C): δ 2.167 (s, 3H_{Me}), 6.28 (ddd, J = 8.0, 6.6 and 1.4 Hz, 1H_{ar}), 6.68 (ddd, J = 8.2, 7.0 and 1.5 Hz, 1H_{ar}), 6.76 (dd, J = 8.3 and 1.3 Hz, 1H_{ar}),

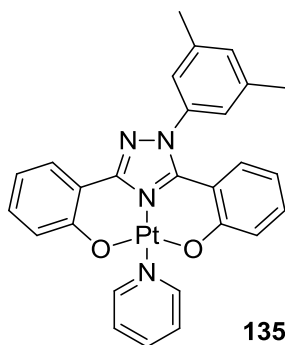
7.05-7.21 (m, 4H_{ar}), 7.44-7.54 (m, 6H_{ar}), 7.93 (tdd, J = 7.6, 1.2 and 1.6 Hz, 1H_{ar}), 8.07 (dd, J = 8.0 and 1.7 Hz, 1H_{ar}), 9.14 (dd, J = 6.4 and 1.3 Hz, 2H_{ar}). ¹³C-NMR (CDCl₃, 75 MHz, 20 °C): δ = 17.60 (Me), 110.37, 112.82, 115.79, 116.01, 120.75, 122.43, 124.79, 126.22, 127.42, 127.45, 127.74, 130.58, 131.01, 131.55, 131.78, 135.47, 138.11, 138.50, 144.94, 148.75, 151.98, 162.40, 164.40.



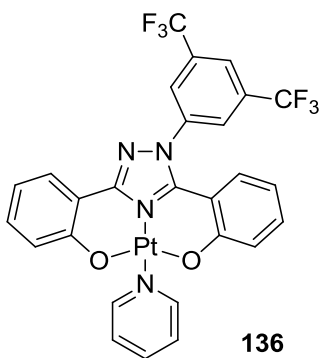
Quant. ¹H-NMR (CDCl₃, 300 MHz, 20 °C): δ 2.46 (s, 3H_{Me}), 6.33 (ddd, J = 8.1, 7.3 and 1.0 Hz, 1H_{ar}), 6.68 (t, J = 7.5 Hz, 1H_{ar}), 6.9 (dd, J = 8.3 and 1.0 Hz, 1H_{ar}), 7.03-7.20 (m, 4H_{ar}), 7.31-7.53 (m, 6H_{ar}), 7.92 (t, J = 7.4 Hz, 1H_{ar}), 8.07 (dd, J = 7.4 and 1.7 Hz, 1H_{ar}), 9.13 (d, J = 5.7 Hz, 2H_{ar}). ¹³C NMR (CDCl₃, 75 MHz, 20 °C): δ 21.35 (Me), 110.35, 112.74, 115.45, 115.99, 120.75, 122.83, 123.30, 124.76, 126.69, 127.37, 127.80, 129.70, 130.73, 130.97, 131.55, 138.06, 139.20, 140.34, 144.79, 148.74, 151.82, 162.54, 165.07.



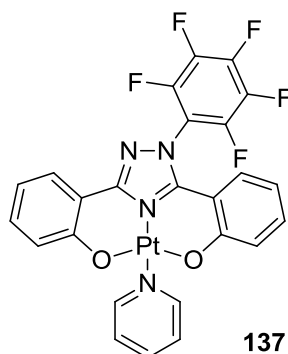
quant. ¹H-NMR (CDCl₃, 300 MHz, 20 °C): δ 2.481 (s, 3H_{Me}), 6.34 (ddd, J = 8.2, 6.6 and 1.6 Hz, 1H_{ar}), 6.68 (ddd, J = 7.8, 7.1 and 1.1 Hz, 1H_{ar}), 6.92 (dd, J = 8.6 and 1.4 Hz, 1H_{ar}), 7.03-7.20 (m, 4H_{ar}), 7.34-7.45 (m, 4H_{ar}), 7.50 (t, J = 7.1 Hz, 2H_{ar}), 7.92 (tdd, J = 7.7, 1.4 and 1.4 Hz, 1H_{ar}), 8.07 (dd, J = 7.8 and 1.8 Hz, 1H_{ar}), 9.12-9.14 (m, 2H_{ar}). ¹³C-NMR (CDCl₃, 75 MHz, 20 °C): δ = 21.36 (Me), 110.41, 112.79, 115.45, 115.98, 120.73, 122.83, 124.76, 125.98, 127.35, 127.74, 130.53, 130.94, 131.50, 136.80, 138.06, 140.17, 144.77, 148.73, 151.78.

**135**

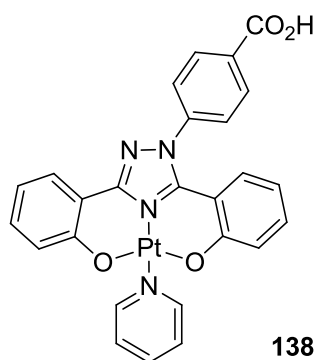
quant. $^1\text{H-NMR}$ (CDCl_3 , 300 MHz, 20 °C): δ = 2.40 (s, 6H_{Me}), 6.35 (ddd, J = 8.2, 6.2 and 1.6 Hz, 1H_{ar}), 6.68 (ddd, J = 8.0, 7.0 and 1.2 Hz, 1H_{ar}), 6.94 (dd, J = 8.2 and 1.4 Hz, 1H_{ar}), 7.03-7.19 (m, 7H_{ar}), 7.51 (td, J = 6.6 and 0.9 Hz, 2H_{ar}), 7.92 (tdd, J = 7.6, 1.9 and 1.6 Hz, 1H_{ar}), 8.08 (dd, J = 8.0 and 1.9 Hz, 1H_{ar}), 9.14 (dd, J = 6.6 and 1.4 Hz, 2H_{ar}). $^{13}\text{C-NMR}$ (CDCl_3 , 75 MHz, 20 °C): δ = 21.24 (Me), 110.41, 112.79, 115.43, 115.97, 120.73, 122.32, 123.82, 124.75, 127.37, 127.83, 130.93, 131.50, 131.66, 138.04, 139.12, 140.00, 144.68, 148.74, 151.71, 162.51, 164.96.

**136**

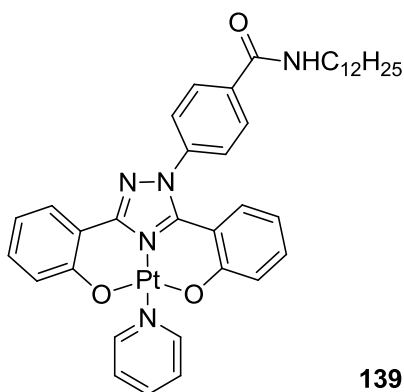
Quant. $^1\text{H-NMR}$ (CDCl_3 , 300 MHz, 20 °C): δ 6.37-6.42 (m, 1H_{ar}), 6.64-6.73 (m, 2H_{ar}), 6.93-7.01 (m, 2H_{ar}), 7.13-7.18 (m, 2H_{ar}), 7.48 (t, J = 6.7 Hz), 7.87-8.05 (m, 5H_{ar}), 8.93 (d, J = 5.9 Hz). $^{13}\text{C-NMR}$ (CDCl_3 , 75 MHz, 20 °C): δ 109.38, 112.19, 115.17, 115.63, 121.01, 122.44 (q, J = 273.8 Hz, CF₃), 122.92 (t, J = 3.5 Hz), 123.03, 124.55, 126.06, 126.10, 127.47, 131.73, 132.94, 133.23 (q, J = 34.3 Hz, C-CF₃), 138.58, 140.34, 148.10, 148.17, 153.10, 163.25, 166.69 ppm. $^{19}\text{F-NMR}$ (CDCl_3 , 300 MHz, 20 °C): δ = -63 ppm.



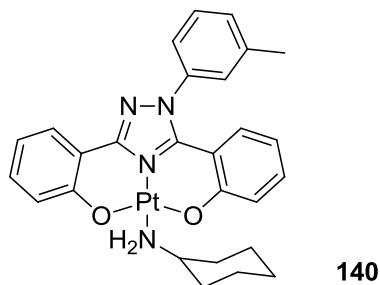
98 mg, 0,142 mmol, 82%. $^1\text{H-NMR}$ (CDCl_3 , 300 MHz, 20 °C): δ 5,26-5,30 (m, 1H_{ar}), 6,57-6,70 (m, 2H_{ar}), 6,93-7,25 (m, 4H_{ar}), 7,91-8,10 (m, 4H_{ar}), 9,07-9,08 (m, 2H_{ar}). $^{13}\text{C-NMR}$ (CDCl_3 , 75 MHz, 20 °C): δ 110.73, 111.93, 115.78, 116.16, 120.90, 122.42, 122.94, 123.15, 124.75, 126.13, 126.17, 127.26, 131.42, 132.39, 133.28, 138.17, 140.44, 145.42, 148.67, 152.77, 162.70, 165.71.



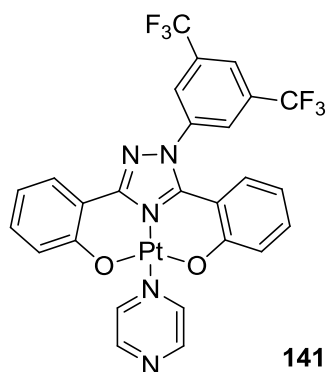
For silica gel chromatography purification, a gradient of CH_2Cl_2 to CH_2Cl_2 MeOH 10/1 was used. 81%. $^1\text{H-NMR}$ (CDCl_3 , 300 MHz, 20 °C): δ 6.36 (t, J = 7.5Hz, 1H), 6.68 (t, J = 7.5Hz, 1H), 6.88 (dd, J = 8.3 and 1.1Hz, 1H), 7.07 (t, J = 8.8Hz, 1H), 7.16 -7.25 (m, 2H), 7.53 (t, J = 6.9Hz, 2H), 7.71 (d, J = 8.4Hz, 2H), 7.95 (t, J = 7.6Hz, 1H), 8.05 (dd, J = 7.9 and 1.4Hz, 1H), 8.28 (d, J = 8.4Hz, 2H), 9.13 (m, 2H, 2H_{pyr}). MS (positive ESI) $[\text{M}+\text{H}]$: calculated for $\text{C}_{26}\text{H}_{18}\text{O}_4\text{N}_4\text{Pt}_1\text{H}$: 646.1051, found 646.1114.



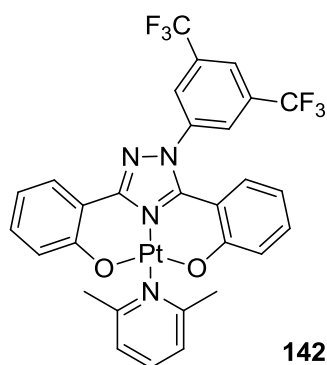
78%. $^1\text{H-NMR}$ (CDCl_3 , 300 MHz, 20 °C): δ 0.88 (t, J = 6.8 Hz, 1H), 1.26-1.36 (m, 18H_{alkyl}), 1.63-1.67 (m, 2H_{ar}), 3.49 (q, J = 6.5 Hz, NH-CH₂), 6.18 (t, J = 5.5 Hz, 1H_{ar}), 6.34 (ddd, J = 1.1, 8.1, and 7.1 Hz, 1H_{ar}), 6.68 (ddd, J = 7.0, 8.1, and 1.1, 1H_{ar}), 6.87 (dd, J = 8.2 and 1.6 Hz, 1H_{ar}), 7.06 (ddd, J = 8.3, 7.1, and 1.1 Hz, 2H_{ar}), 7.16 (dtd, J = 8.7, 6.7, and 1.9 Hz, 2H_{ar}), 7.53 (ddd, J = 7.3, 5.9, and 1.4 Hz, 2H_{ar}), 7.65 (d, J = 8.4 Hz, 2H_{ar}), 7.93-7.95 (m, 3H_{ar}), 8.04 (dd, J = 8.0 and 1.8 Hz), 9.12 (dd, J = 6.7 and 1.1 Hz, 2H_{ar}). $^{13}\text{C-NMR}$ (CDCl_3 , 75 MHz, 20 °C): δ = 14.26 (Me), 22.84, 27.18, 29.49, 29.71, 29.75, 29.78, 29.80, 29.85, 32.07, 40.54, 110.20, 112.64, 115.90, 116.29, 121.01, 122.84, 124.99, 126.39, 127.49, 127.96, 128.70, 131.36, 132.07, 136.23, 138.30, 141.71, 145.33, 148.96, 152.44



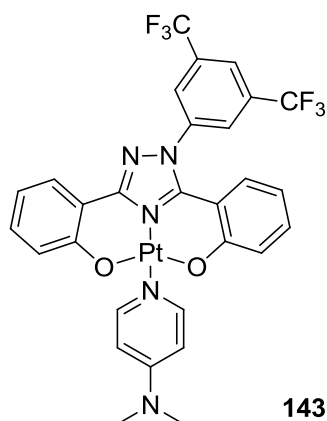
Quant. $^1\text{H-NMR}$ (CDCl_3 , 300 MHz, 20 °C): δ 1.21-1.40 (m, 5H, 5H_{CHA}), 1.56-1.84 (m, 3H, 3H_{CHA}), 2.38 (m, 2H, 2H_{CHA}), 2.44 (s, 3H, CH₃), 3.02 (m, 1H, CH_{CHA}), 4.08 (d, J = 6.4, 2H, NH₂), 6.27 (t, J = 7.5 Hz, 1H, 1H_{ar}), 6.66 (t, J = 7.4 Hz, 1H, 1H_{ar}), 6.77 (dd, J = 8.3 and 1.4 Hz, 1H, 1H_{ar}), 6.84 (d, J = 8.3 Hz, 1H, 1H_{ar}), 6.92 (d, J = 8.3 Hz, 1H, 1H_{ar}), 7.02-7.44 (m, 6H, 6H_{ar}), 8.03 (dd, J = 8.0 and 1.6 Hz, 1H, 1H_{ar}). $^{13}\text{C-NMR}$ (CDCl_3 , 75 MHz, 20 °C): δ 21.3 (CH₃), 24.8 (C_{CHA}), 25.4 (C_{CHA}), 34.2 (C_{CHA}), 53.6 (CH_{CHA}), 110.6 (C_{ar}), 113.2 (C_{ar}), 115.0, 115.8, 120.6, 122.1, 123.2, 126.6, 127.5, 127.9, 129.5, 130.5, 130.7, 131.2 (CH_{ar}), 139.3, 140.1, 144.1, 151.4, 162.1, 164.8 (C_{ar}). MS (positive ESI) [$\text{M}+\text{e}^-$]: calculated for C₂₇H₂₈N₄O₂Pt: 635.19, found 635.18.



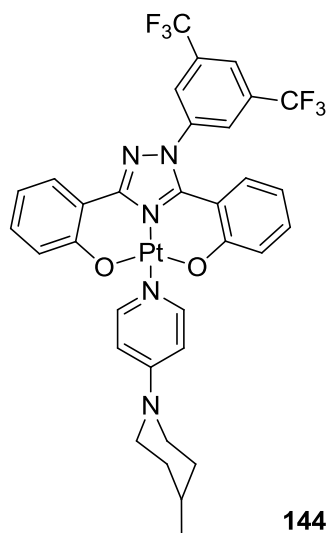
52%. $^1\text{H-NMR}$ (CDCl_3 , 300 MHz, 20 °C): 6.44 (t, $J = 7.6\text{Hz}$, 1H), 6.72 (t, $J = 7.3\text{Hz}$, 1H), (d, $J = 8.7\text{Hz}$, 1H), 7.06 (t, $J = 8.3\text{Hz}$, 1H), 7.12 (s, H), 7.21 (m, 2H), 8.05 (m, 4H), 8.85 (s, 2H), 9.23 (m, 2H). $^{19}\text{F-NMR}$ (CDCl_3 , 300 MHz, 20 °C): δ 63.01. MS (positive ESI) $[\text{M}+\text{H}]$: calculated for $\text{C}_{26}\text{H}_{15}\text{O}_2\text{F}_6\text{N}_5\text{Pt}_1\text{H}$: 739.0852, found 739.0823.



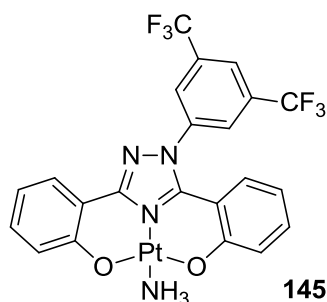
50%. $^1\text{H-NMR}$ (CDCl_3 , 300 MHz, 20 °C): δ = 1.26 (s, Me), 1.43 (s, Me), 6.36 (ddd, $J = 8.3$, 6.8, and 1.3Hz, 1H_{ar}), 6.58 (d, $J = 7.5\text{Hz}$, 2H_{ar}), 6.66 (ddd, $J = 8.0$, 6.7, and 1.2Hz, 1H_{ar}), 6.78 (dd, $J = 8.3$ and 1.6 Hz, 1H_{ar}), 7.01 (ddd, $J = 10$, 8.7, and 1.2 Hz, 2H_{ar}), 7.12-7.19 (m, 2H_{ar}), 8.00-8.03 (m, 2H_{ar}), 8.11 (s, 2H_{ar}), 8.52 (dd, $J = 6.1$ and 1.5 Hz, 2H_{ar}) ppm. $^{19}\text{F-NMR}$ (CDCl_3 , 272 MHz, 20 °C): δ = -62.95 ppm (s, CF_3).



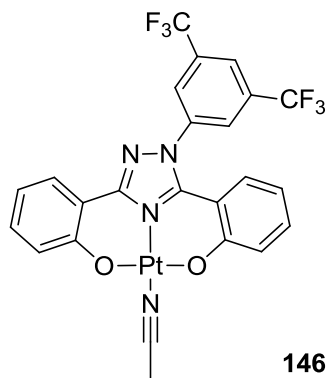
88%. $^1\text{H-NMR}$ (CDCl_3 , 300 MHz, 20 °C): δ 0.88 (t, J = 6.9 Hz, 2Me), 6.40 (ddd, J = 8.2, 7.0, and 1.3 Hz, 1H_{ar}), 6.67 (ddd, J = 8.2, 6.0, and 1.0 Hz, 1H_{ar}), 6.78-6.83 (m, 2H_{ar}), 6.86 (dd, J = 8.6, and 1.0 Hz, 1H_{ar}), 7.09-7.18 (m, 3H_{ar}), 7.23 (s, 1H_{ar}), 7.66 (t, J = 7.7 Hz, 1H_{ar}), 8.01-8.04 (m, 2H_{ar}), 8.11 (s, 2H_{ar}) ppm. $^{19}\text{F-NMR}$ (CDCl_3 , 272 MHz, 20 °C): δ = -63.00 (s, CF_3)



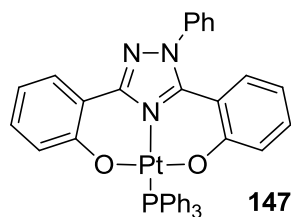
94%. $^1\text{H-NMR}$ (CDCl_3 , 300 MHz, 20 °C): δ 0.99 (d, J = 6.3 Hz, 3H, CH_3), 1.18-1.30 (m, 2H, 2H_{CH_2}), 1.66-1.79 (m, 3H, 2H_{CH_2} and CH), 2.99 (td, J = 12.9 and 2.1 Hz, 2H, 2H_{CH_2}), 3.95 (d, J = 13.2 Hz, 2H, 2H_{CH_2}), 6.35 (ddd, J = 8.2, 6.8 and 1.2 Hz, 1H, 1H_{ar}), 6.62-6.38 (m, 4H, 4H_{ar}), 7.00 (ddd, J = 9.9, 8.8 and 1.0 Hz, 2H, 2H_{ar}), 7.12-7.19 (m, 2H, 2H_{ar}), 7.98-8.02 (m, 2H, 2H_{ar}), 8.10 (s, 2H, 2H_{ar}), 8.48 (d, J = 7.4 Hz, 2H, 2H_{ar}). $^{19}\text{F-NMR}$ (CDCl_3 , 300 MHz, 20 °C): δ -62.96. $^{13}\text{C-NMR}$ (CDCl_3 , 75 MHz, 20 °C): δ 21.6 (CH_3), 30.8 (CH), 33.2 (CH_2), 46.5 (N- CH_2), 107.7 109.4 112.0 115.5 115.8 120.7 121.1 122.7 123.3 126.1 126.1 127.2 131.2 132.1 132.5 133.0 133.4 133.9 140.6 145.4 147.6 152.9 154.5 163.0 165.9 (C_{ar}).



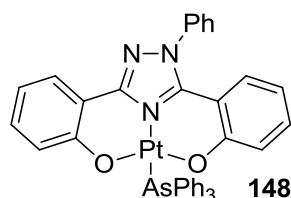
A suspension of ligand L (1 eq.), cisplatin (1 eq) and K_2CO_3 (30 eq.) in toluene was sonicated for 15 min then heated overnight at 100 °C. After evaporation of the volatiles under reduced pressure, CH_2Cl_2 was added and the suspension filtrated over celite plug. Final product was obtained after silica gel chromatography purifiaction (gradient cyclohexane/ CH_2Cl_2 1/1 to CH_2Cl_2) as a yellow solid. 92%. ^1H -NMR (CDCl_3 , 300 MHz, 20 °C): δ 3.60 (s, 3H, NH_3), 6.32 (t, J = 7.6Hz, 1H, 1H_{ar}), 6.63 (q, J = 8.2Hz, 2H, 2H_{ar}), 6.78 (t, J = 9.2Hz, 2H, 2H_{ar}), 7.11 (q, J = 7.5Hz, 2H, 2H_{ar}), 7.85-8.02 (m, 4H, 4H_{ar}). ^{19}F -NMR (CDCl_3 , 300 MHz, 20 °C): δ -63.0 (s, CF_3). ^{13}C -NMR (CDCl_3 , 75 MHz, 20 °C): δ 109.4 112.5 115.6 116.4 120.2 120.6 122.4 122.8 124.2 126.0 127.4 127.6 131.4 132.1 (C_{ar}), 133.1 (q, J = 34.0Hz, C_{ar}), 140.2 144.2 151.8 161.4 164.6 (C_{ar}). MS (positive ESI) $[\text{M}-\text{e}^-]$: calculated for $\text{C}_{22}\text{H}_{14}\text{N}_4\text{F}_6\text{O}_2\text{Pt}$: 675.07, found 675.07.



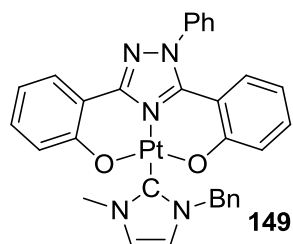
General procedure was changed: $\text{PtCl}_2(\text{CH}_3\text{CN})_2$ was used as platinum precursor. ~5%. ^1H -NMR (CDCl_3 , 300 MHz, 20 °C): δ 2.20 (s, 3H, NCCH_3), 6.44 (ddd, J = 8.3, 6.9 and 1.1Hz, 1H), 6.75 (m, 2H), 6.95 (m, 3H), 7.21 (ddd, J = 8.5, 6.9 and 1.8Hz, 2H), 8.05 (m, 4H), 13.75 (s, 1H). MS (positive ESI) $[\text{M}+\text{H}]$: calculated for $\text{C}_{24}\text{H}_{14}\text{O}_2\text{F}_6\text{N}_4\text{Pt}_1\text{H}$: 700.0743, found 700.0728; $[\text{M}+\text{H}_3\text{O}]$: calculated for $\text{C}_{24}\text{H}_{14}\text{O}_2\text{F}_6\text{N}_4\text{Pt}_1\text{H}_3\text{O}$: 718.0849, found 718.0898; $[\text{M}+\text{H}_3\text{O}+\text{CH}_3\text{CN}]$: calculated for $\text{C}_{24}\text{H}_{14}\text{O}_2\text{F}_6\text{N}_4\text{Pt}_1\text{H}_3\text{OCH}_3\text{CN}$: 759.1115, found 759.1162.



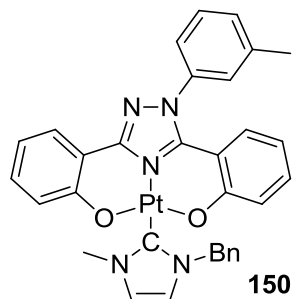
74%. $^1\text{H-NMR}$ (CDCl_3 , 300 MHz, 20 °C): δ 6.29 (ddd, J = 8.1, 6.8 and 1.2Hz, 1H, 1CH_{ar}), 6.48 (ddd, J = 15.0, 8.6 and 1.2Hz, 2H, 2CH_{ar}), 6.62 (ddd, J = 8.1, 6.7 and 1.7, 1H, CH_{ar}), 6.86 (dd, J = 8.1 and 1.7Hz, 1H, CH_{ar}), 6.90-7.06 (m, 2H, 2H_{ar}), 7.34- 7.61 (m, 14H, 14H_{ar}), 7.77-7.88 (m, 6H, 6H_{ar}), 8.07 (dd, J = 8.0 and 1.8Hz, 1H, 1H_{ar}). $^{13}\text{C-NMR}$ (CDCl_3 , 75 MHz, 20 °C): δ 110.9, 113.1 115.3 115.8 121.5 122.9 126.1 127.3 128.0 128.1 128.3 128.7 129.8 129.9 130.7 130.8 131.6 134.5 134.7 139.2 145.8 152.1 162.9 165.9 (C_{ar}). $^{31}\text{P-NMR}$ (CDCl_3 , 121 MHz, 20 °C): δ 9.18 (t, J = 2099.9Hz, $\text{P}(\text{Ph})_3$). MS (positive ESI) $[\text{M-e}^-]$: calculated for $\text{C}_{38}\text{H}_{28}\text{N}_3\text{O}_2\text{Pt}_1\text{P}_1$: 784.16, found 784.14.



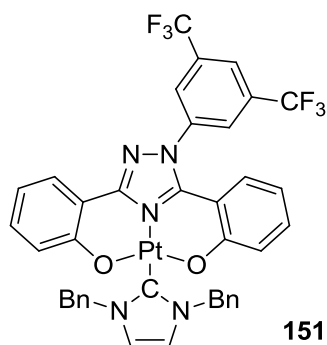
The product was obtained by stirring a solution of $[(\text{O}^-\text{N}^+\text{O})\text{Pt}(\text{Pyr})]$ **131** (1 eq) and AsPh_3 (10 eq) one week at room temperature. After evaporation of the volatiles, the crude product was purified over silica gel chromatography (gradient cyclohexane/ CH_2Cl_2 1/1 to CH_2Cl_2): 34%. $^1\text{H-NMR}$ (CDCl_3 , 300 MHz, 20 °C): δ 6.28 (t, J = 7.5Hz, 1H, 1CH_{ar}), 6.49-6.68 (m, 3H, 3CH_{ar}), 6.87 (dd, J = 8.3 and 1.1Hz, 1H, CH_{ar}), 6.91-7.06 (m, 2H, 2CH_{ar}), 7.34-7.61 (m, 14H, 14H_{ar}), 7.8 (dd, J = 7.8 and 1.4Hz, 6H, 6H_{ar}), 8.07 (dd, J = 7.9 and 1.7Hz, 1H, 1H_{ar}). $^{13}\text{C-NMR}$ (CDCl_3 , 75 MHz, 20 °C): δ 110.5 (C_{ar}), 112.7 (C_{ar}), 115.3 115.7 121.1 122.7 126.1 127.3 127.9 128.7 129.2 129.9 130.1 130.4 130.8 131.5 133.9 ($14\text{CH}_{\text{ar}}+1\text{C}_{\text{ar}}$), 139.3 145.1 151.5 162.4 165.5 (C_{ar}). MS (positive ESI) $[\text{M-e}^-]$: calculated for $\text{C}_{38}\text{H}_{28}\text{N}_3\text{O}_2\text{Pt}_1\text{As}_1$: 828.10, found 828.11.



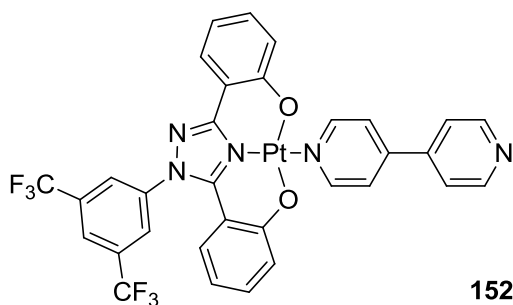
The complex was obtained by ligand exchange: A solution of [(NHC)PtCl₂(Pyr)] **234** (1 eq), K₂CO₃ (30 eq) and (O[−]N⁺O)H₂ ligand was stirred overnight in ethanol at 55 °C. After evaporation of the volatiles, CH₂Cl₂ was added and the suspension filtered over celite plug. The crude product was purified over silica gel chromatography (gradient cyclohexane/CH₂Cl₂ 1/1 to CH₂Cl₂). 59% ¹H-NMR (CDCl₃, 300 MHz, 20 °C): δ 4.14 (s, 3H, N-CH₃), 5.79 (s, 2H, N-CH₂), 6.29 (ddd, J= 8.2, 6.9 and 1.2Hz, 1H, 1H_{ar}), 6.63 (ddd, J= 7.9, 6.9 and 1.0Hz, 1H, 1H_{ar}), 6.74 (d, J= 2.1Hz, 1H, CH=), 6.91 (m, 1H, 1H_{ar}), 6.98-7.11 (m, 2H, 2H_{ar}), 7.28-7.64 (m, 10H, 10H_{ar}), 8.09 (dd, J= 8.0 and 1.8Hz, 1H, 1H_{ar}). ¹³C-NMR (CDCl₃, 75 MHz, 20 °C): δ 36.9 (N-CH₃), 53.2 (N-CH₂), 111.2 113.4 115.1 115.7 120.1 120.9 122.3 126.1 127.4 128.1 128.6 128.7 129.7 129.9 130.7 131.4 136.5 139.4 145.5 148.8 152.3 153.9 162.8 165.7 (CH=CH, C_{ar} and C-Pt). MS (positive ESI) [M-e[−]]: calculated for C₃₁H₂₅N₅O₂Pt: 694.17, found 694.16.



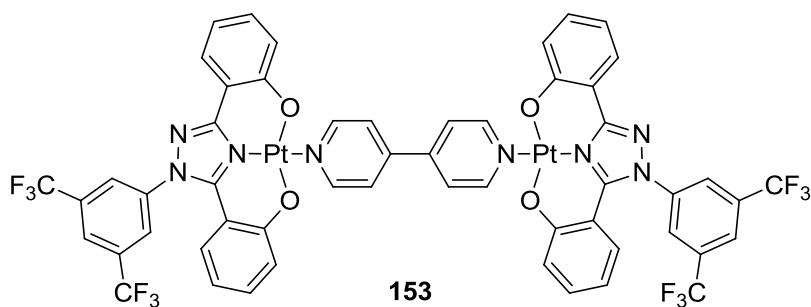
General procedure was changed: Pyridine was used as solvent and two equivalents of 1-benzyl-3-methyl-1H-imidazol-3-ium bromide added. 48%. ¹H-NMR (CDCl₃, 300 MHz, 20 °C): δ 2.43 (s, 3H, CH₃), 4.12 (s, 3H, N-CH₃), 5.78 (s, 2H, N-CH₂), 6.30 (t, J= 7.5Hz, 1H, 1H_{ar}), 6.63 (t, J= 7.5Hz, 1H, 1H_{ar}), 6.72 (t, J= 1.8Hz, 1H, 1H_{ar}), 6.75-6.83 (m, 2H, 2H_{ar}), 6.86-6.95 (m, 2H, 2H_{ar}), 6.99-7.12 (m, 2H, 2H_{ar}), 7.23-7.50 (m, 9H, 9H_{ar}), 8.10 (dt, J= 8.1 and 1.6Hz, 1H, 1H_{ar}). ¹³C-NMR (CDCl₃, 75 MHz, 20 °C): δ 21.4 (CH₃), 36.9 (N-CH₃), 53.2 (N-CH₂), 111.2 113.5 115.2 115.7 120.1 121.0 122.3 123.2 126.6 127.5 128.1 128.2 128.6 128.7 129.7 130.6 130.7 131.4 136.5 139.3 140.3 145.5 152.2 153.9 162.8 165.6 (CH=CH, C_{ar} and C-Pt). MS (positive ESI) [M-e[−]]: calculated for C₃₂H₂₇N₅O₂Pt: 708.18, found 708.18. RX: jlggd130626



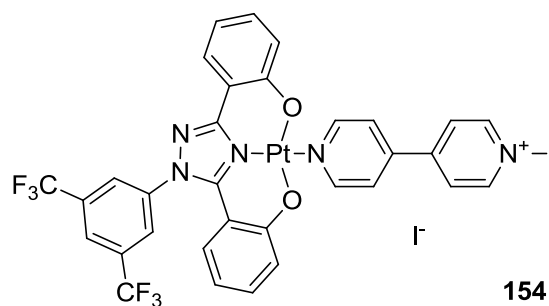
General procedure was changed: Pyridine was used as solvent and two equivalents of 1,3-dibenzyl-1H-imidazol-3-ium bromide added. 44%. $^1\text{H-NMR}$ (CDCl_3 , 300 MHz, 20 °C): δ 5.86 (s, 4H, 2N-CH₃), 6.35 (t, J = 7.7Hz, 1H, 1H_{ar}), 6.63 (t, J = 7.7Hz, 1H, 1H_{ar}), 6.70-6.83 (m, 5H, 5H_{ar}), 7.09 (ddd, J = 16.0, 7.5 and 1.5Hz, 2H, 2H_{ar}), 7.30-7.55 (m, 10H, 10H_{ar}), 8.00 (s, 1H, 1H_{ar}), 8.05 (dd, J = 8.0 and 1.7Hz, 1H, 1H_{ar}), 8.11 (s, 2H, 2H_{ar}). $^{19}\text{F-NMR}$ (CDCl_3 , 300 MHz, 20 °C): δ -63.0 (s, CF₃).



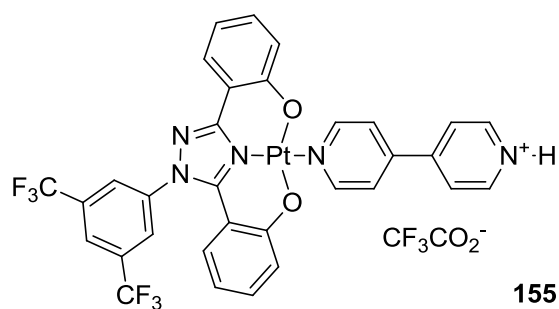
70%. $^1\text{H-NMR}$ (CDCl_3 , 300 MHz, 20 °C): δ 6.39 (t, J = 7.3Hz, 1H), 6.68 (t, J = 7.1Hz, 1H), 6.75 (d, 7.8Hz, 1H), 6.95-7.03 (m, 2H), 7.16 (m, 2H), 7.57 (d, J = 5.7Hz, 2H), 7.69 (d, J = 6.4Hz, 2H), 8.01 (m, 2H), 8.07 (s, 2H), 8.79 (d, J = 5.3Hz, 2H), 9.15 (d, J = 6.3Hz, 2H). $^{19}\text{F-NMR}$ (CDCl_3 , 300 MHz, 20 °C): δ -62.97. $^{13}\text{C-NMR}$ (CDCl_3 , 75 MHz, 20 °C): δ 109.2 111.9 115.8 116.2 117.0 120.6 120.9 121.1 122.4 122.9 123.1 124.3 126.2 127.3 131.5 132.4 133.1 133.5 140.4 143.7 145.4 147.5 149.0 151.0 152.7 162.6 165.6.



20%. ¹H-NMR (CDCl₃, 300 MHz, 20 °C): δ 6.39 (ddd, J= 7.0, 8.1 and 1.2Hz, 2H), 6.68 (ddd, J= 8.1, 6.8 and 1.1Hz, 2H), 6.77 (dd, 8.3 and 1.4Hz, 2H), 6.98-7.06 (m, 4H), 7.14-7.21 (m, 4H), 7.50 (ddd, J= 7.6, 5.4 and 1.2Hz, 4H), 7.93 (tt, J= 7.6 and 1.4Hz, 2H), 7.98-8.02 (m, 4H), 8.08 (s, 4H), 9.07 (m, 4H). ¹⁹F-NMR (CDCl₃, 300 MHz, 20 °C): δ -62.97. ¹³C-NMR (CDCl₃, 75 MHz, 20 °C): δ 109.4 112.1 116.0 116.3 120.8 121.1 123.1 123.4 124.4 124.9 126.4 127.5 131.6 132.6 132.8 133.3 133.7 134.2 138.4 140.7 145.6 148.9 153.0 162.9 165.9 (C_{ar}).



The complex was obtained by stirring complex **155** in MeI (1 mL) at room temperature for 1 hour. After evaporation of the volatiles, the complex was obtained. Quant. $^1\text{H-NMR}$ (DMSO, 300 MHz, 20 $^\circ\text{C}$): δ 4.04 (s, 3H, CH_3), 6.00 (t, $J = 7.5\text{Hz}$, 1H), 6.28 (m, 2H), 6.59 (dd, 12.7 and 8.7Hz, 2H), 6.79 (m, 2H), 7.29 (m, 1H), 7.49 (q, $J = 8.7\text{Hz}$, 1H), 7.99 (m, 2H), 8.07 (s, 1H), 8.20 (m, 2H), 8.34 (d, $J = 6.6\text{Hz}$, 2H), 8.85 (m, 3H). $^{19}\text{F-NMR}$ (DMSO, 300 MHz, 20 $^\circ\text{C}$): δ -60.92.



The complex was obtained by adding TFA to a solution of **155** in CH_2Cl_2 . After stirring at room temperature for 1 hour, evaporation of the volatiles, and drying under vacuum, the complex was obtained. Quant. ^1H -NMR (DMSO, 300 MHz, 20 °C): δ 6.38 (t, J = 7.5Hz, 1H), 6.64 (t, J = 7.3Hz, 1H), 6.72 (d, 8.2Hz, 1H), 6.9 (d, J = 8.2Hz, 1H), 7.00 (d, J = 8.2Hz, 1H), 7.18 (q, J = 8.1Hz, 2H), 7.90 (dd, J = 7.9 and 1.5Hz, 1H), 8.09 (d, J = 5.8Hz, 2H), 8.22 (d, J = 6.6Hz, 2H), 8.45 (s, 1H), 8.60 (s, 2H), 8.88 (d, J = 5.6Hz, 2H), 9.16 (d, J = 6.6Hz, 2H). ^{19}F -NMR (DMSO, 300 MHz, 20 °C): δ -74.46 (s, 3F, CF_3CO_2^-), -60.94 (s, 6F, 2 CF_3).

7.3.3 Post-functionalization of NHC complexes

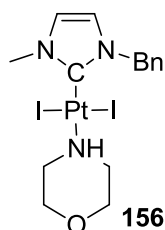
7.3.3.1 Ligand exchange with amines, hydroxylamines and polyamines

Unless mentioned, the following general procedures were used (20-75 mg, 30-100 μmol scale):

Procedure a: Synthesis from azolium precursor: (L = pyridine, cyclohexylamine or morpholine): Imidazolium halide (1.1 eq. 50-250 mg, 0.2-1 μmol), PtCl_2 (1 eq), NaI (10 eq.) and K_2CO_3 (10 eq) were suspended under argon in anhydrous solvent (pyridine, cyclohexylamine, morpholine 10 mL). The mixture was sonicated during 10 minutes, heated overnight at 100 $^\circ\text{C}$, then concentrated under reduced pressure, dissolved in CH_2Cl_2 and filtered through a celite plug. The residue was purified by a silica gel chromatography (gradient CH_2Cl_2 /pentane 1/1, CH_2Cl_2 , CH_2Cl_2 /MeOH 20/1) affording the complex as a yellow oil or powder.

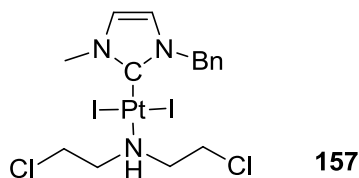
Procedure b: Synthesis by ligand exchange: (L = amine, amino acid, pnictogen ligand phosphine, arsine or stibine): the complex is obtained using reported procedures.^{124,125} A solution of platinum pyridine complex and the amine (1.1 eq) respectively the ammonium salt (1.1 eq) and triethylamine (10 eq) in ethanol (THF in case of hydroxylamine derivatives) was stirred at 55 $^\circ\text{C}$ overnight. The volatiles were removed and the crude product purified over silica gel chromatography (gradient CH_2Cl_2 /pentane 1/1, CH_2Cl_2 , CH_2Cl_2 /MeOH 20/1).

Complexes **156**, **164**, **165**, **166**, **171** and **172** were reported by our group.^{124,125}

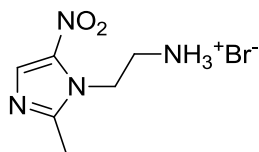


Morpholine (0.05 mL, 0.574 mmol) was added to **14** (22 mg, 0.031 mmol). The reaction was stirred for 20 h at room temperature, concentrated under reduced pressure and purified by silica gel chromatography with dichloromethane to afford the complex **158** as a yellow solid (13 mg, 58%). ^1H -NMR (CDCl_3 , 300 MHz, 20 $^\circ\text{C}$): δ 2.92 (d, J = 11.4 Hz, 2H, 2CH), 3.15-3.45 (m, 1H, NH), 3.46-3.71 (m, 4H, 4CH), 3.82 (d, J = 12.3 Hz, 2H, 2CH), 3.86 (s, 3H, NCH_3), 5.56 (s, 2H, NCH_2), 6.56 (s, 1H, CH), 6.77 (s, 1H, CH), 7.28-7.48 (m, 5H, 5Ar-H). ^{13}C -NMR (CDCl_3 , 75 MHz, 20 $^\circ\text{C}$): δ 38.2 (N-CH_3), 50.6 (CH_2), 54.5 (CH_2), 68.7 (CH_2), 120.0 (CH), 122.3 (CH), 128.3 ($\text{CH}_{\text{aromatic}}$), 128.8 ($\text{CH}_{\text{aromatic}}$), 129.1 ($\text{CH}_{\text{aromatic}}$), 135.3 ($\text{C}_{\text{aromatic}}$), 136.3 (C-Pt). HRMS (positive ESI) $[\text{M}+\text{Na}]$: Calculated for

$C_{15}H_{21}I_2N_3OPt.Na$ 730.932, found 730.929. Microanalysis: Calculated for $C_{15}H_{21}I_2N_3OPt.2H_2O$: C, 24.21; H, 3.39; N, 5.65. Found: C, 24.18; H, 3.03; N, 5.59.

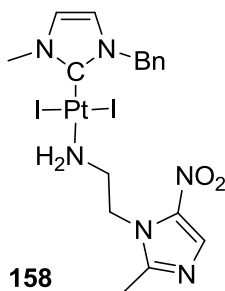


Procedure *b* was changed: The temperature was changed to 25 °C, and dichloromethane was used as solvent. Ten equivalents of bis(2-chloroethyl)ammonium chloride was used. 85%. 1H -NMR ($CDCl_3$, 300 MHz, 20 °C): δ 3.22 (m, 2H, CH_2), 3.77 (m, 2H, CH_2), 3.88 (s, 3H, N- CH_3), 3.96 (m, 2H, CH_2), 4.21 (m, 3H, CH_2 +NH-Pt), 5.54 (s, 2H, N- CH_2), 6.58 (d, J = 2.1Hz, 1H, CH=), 6.80 (d, J = 2.1Hz, 1H, CH=), 7.22-7.48 (m, 5H, $5H_{ar}$). ^{13}C -NMR ($CDCl_3$, 75 MHz, 20 °C): δ 38.2 (N- CH_3), 41.2 (2Cl- CH_2), 54.5 (N- CH_2), 55.4 (2NH- CH_2), 120.3 (CH=), 122.5 (CH=), 128.6 129.0 129.2 (CH_{ar}), 135.2 (C_{ar}), 136.3 (C-Pt).



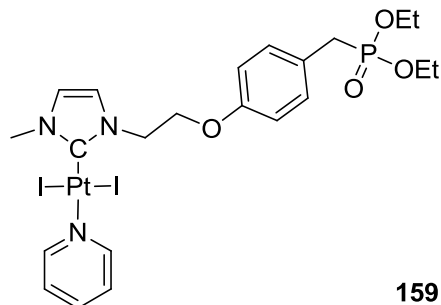
2-(2-methyl-5-nitro-1H-imidazol-1-yl)ethanaminium bromide

2-(2-methyl-5-nitro-1H-imidazol-1-yl)ethanaminium bromide was obtained from metronidazole according to literature.³⁴¹

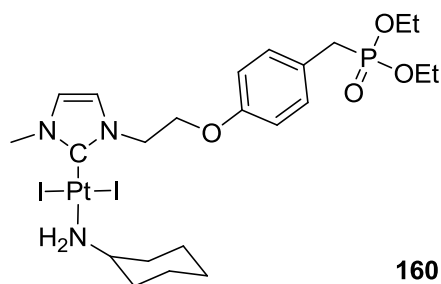


Procedure *b*: Quant, purity ~80%. 1H -NMR ($CDCl_3$, 300 MHz, 20 °C): 2.03 (s, 2H, NH_2), 2.92 (s, 3H, CH_3), 3.64 (t, J = 5.4Hz, 2H, CH_2), 3.98 (s, 3H, N- CH_3), 4.64 (t, J = 5.4Hz, 2H, CH_2), 5.69 (s, 2H, N- CH_2), 6.59 (d, J = 2.0Hz, 1H, CH=), 6.81 (d, J = 2.0Hz, 1H, CH=), 7.27-7.51 (m, 5H, $5H_{ar}$), 8.15 (s, 1H, CH=). MS (positive ESI) $[M+H]^+$: calculated for $C_{17}H_{22}I_2O_2N_6Pt_1H$: 791.9615, found 791.9678, $[M-I]^+$:

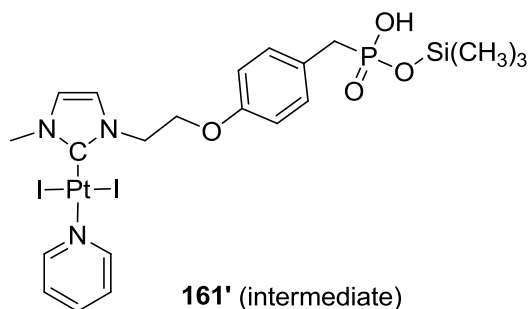
calculated for $C_{17}H_{22}I_1O_2N_6Pt_1$: 664.0492, found 664.0553, $[M-I+CH_3CN]$: calculated for $C_{17}H_{22}I_1O_2N_6Pt_1$ CH_3CN : 831.9802, found 831.9997.

**159**

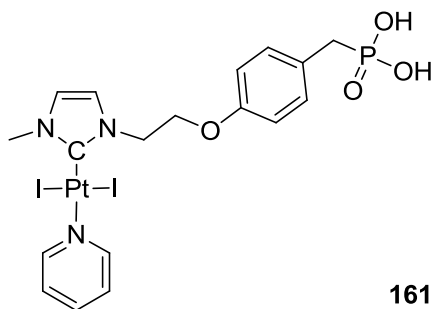
Procedure *a*: 55%. 1H -NMR ($CDCl_3$, 300 MHz, 20 °C): δ 1.23 (t, J = 7.1Hz, 6H, $2CH_3$), 3.07 (d, J_{PH} =21.1Hz, 2H, P- CH_2), 3.96 (m, 7H, N- CH_3 and 2O- CH_2), 4.52 (t, J = 4.9Hz, 2H, CH_2), 4.88 (t, J = 4.9Hz, 2H, CH_2), 6.83 (d, J = 1.8Hz, 1H, CH=), 6.89 (d, J = 8.4Hz, 2H, $2H_{ar}$), 7.09 (d, J = 1.8Hz, 1H, CH=), 7.18 (d, J = 8.4Hz, 2H, $2H_{ar}$), 7.32 (t, J = 6.8Hz, 2H, $2H_{Pyr}$), 7.72 (t, J = 7.5Hz, 1H, $1H_{Pyr}$), 9.03 (m, 2H, $2H_{Pyr}$). ^{31}P -NMR ($CDCl_3$, 121 MHz, 20 °C): δ 26.6. ^{13}C -NMR ($CDCl_3$, 75 MHz, 20 °C): δ 16.5 16.6 (CH_3), 32.0 33.8 (P- CH_2), 38.4 (N- CH_3), 50.1 (N- CH_2), 62.1 62.2 (2O- CH_2), 66.7 (O- CH_2), 114.9 114.9 (CH_{ar}), 122.1 (CH=), 122.2 (CH=), 124.2 124.3 (C_{ar}), 125.1 (C_{Pyr}), 130.9 131.0 (CH_{ar}), 136.0 (C-Pt), 137.6 (C_{Pyr}), 153.8 (C_{Pyr}), 157.2 157.3 (O- C_{ar}). MS (positive ESI) $[M+Na]$: calculated for $C_{22}H_{30}I_2N_3Pt_1O_4P_1Na$: 902.96, found 902.97.

**160**

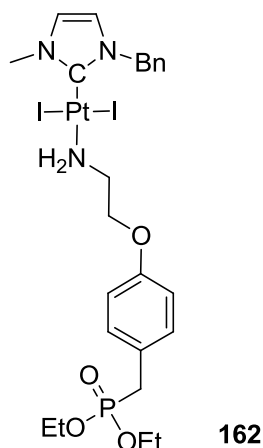
Procedure *b* was changed: cyclohexylamine was used as a solvent and the solution was stirred 15 min at 25 °C: 15%. 1H -NMR ($CDCl_3$, 300 MHz, 20 °C): δ 1.06-1.80 (m, 14H, $2CH_3$ +8 H_{CHA}), 2.28 (m, 2H, $2H_{CHA}$), 2.92 (m, 2H, Pt- NH_2), 3.08 (d, J_{PH} =21.1Hz, 2H, P- CH_2), 3.25 (m, 1H, CH_{CHA}), 3.86 (s, 3H, N- CH_3), 4.0 (t, J = 7.1Hz, 4H, 2O- CH_2), 4.46 (t, J = 5.1Hz, 2H, CH_2), 4.77 (t, J = 5.1Hz, 2H, CH_2), 6.79 (d, J = 2.1Hz, 1H, CH=), 6.86 (d, J = 8.1Hz, 2H, $2H_{ar}$), 7.06 (d, J = 2.1Hz, 1H, CH=), 7.20 (d, J = 8.1Hz, 2H, $2H_{ar}$). ^{31}P -NMR ($CDCl_3$, 121 MHz, 20 °C): δ 25.6.



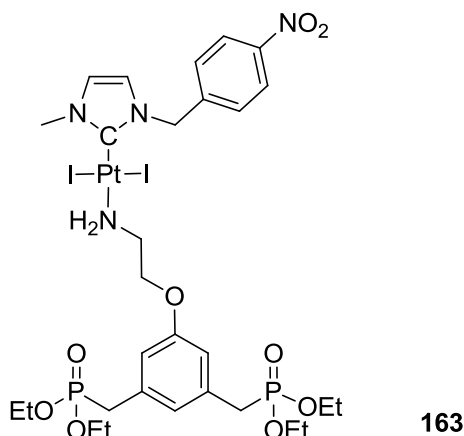
Quant. ¹H-NMR (CDCl₃, 300 MHz, 20 °C): δ 0.14 (s, 9H, 3Si-CH₃), 2.01 (s, 1H, OH), 2.94 (d, J_{PH}=21.1Hz, 2H, P-CH₂), 3.94 (s, 3H, N-CH₃), 4.49 (t, J= 5.0Hz, 2H, CH₂), 4.86 (t, J= 5.0Hz, 2H, CH₂), 6.77-7.37 (m, 8H, CH=CH, 4H_{ar} and 2H_{PyR}), 7.74 (t, J= 7.4Hz, 1H, 1H_{PyR}), 9.04 (m, 2H, 2H_{PyR}).
³¹P-NMR (CDCl₃, 121 MHz, 20 °C): δ 21.3.



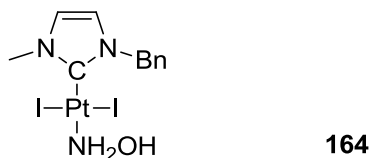
A solution of **165** and NaI (0.1 eq) in CH₂Cl₂ / TMSCl 1/1 was stirred at 25 °C. After disappearance of the starting complex, volatiles are removed under reduced pressure. CH₂Cl₂ was added, the solution filtered over celite plug and volatiles were removed under reduced pressure to afford **161'**. Methanol was added and evaporated after 15 min to afford **161** as yellow oil. Quant. ¹H-NMR (CDCl₃, 300 MHz, 20 °C): δ 3.00 (d, J_{PH}=21.4Hz, 2H, P-CH₂), 3.28 (s, 1H, OH), 3.94 (s, 3H, N-CH₃), 4.60 (t, J= 5.8Hz, 2H, CH₂), 4.84 (t, J= 5.8Hz, 2H, CH₂), 6.96-7.32 (m, 6H, CH=CH, 4H_{ar}), 7.53 (t, J= 6.7Hz, 2H, 2H_{PyR}), 7.93 (t, J= 7.6Hz, 1H, 1H_{PyR}), 9.00 (m, 2H, 2H_{PyR}). ³¹P-NMR (CDCl₃, 121 MHz, 20 °C): δ 27.1.



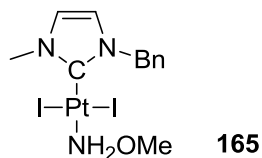
Procedure *b*. 73%. $^1\text{H-NMR}$ (CDCl_3 , 300 MHz, 20 °C): δ 1.23 (t, J = 7.1Hz, 6H, 2CH_3), 3.07 (d, J = 21.1Hz, 2H, $\text{CH}_2\text{-P}$), 3.18-3.51 (m, 4H, $\text{CH}_2\text{+NH}_2$), 3.86 (s, 3H, N- CH_3), 3.99 (t, J = 7.1Hz, 4H, 2O-CH_2), 4.11 (t, J = 4.8Hz, 2H, CH_2), 5.57 (s, 2H, N- CH_2), 6.56 (d, J = 2.1Hz, 1H, CH=), 6.77 (d, J = 2.1Hz, 1H, CH=), 6.86 (d, J = 8.6Hz, 2H, 2H_{ar}), 7.15-7.48 (m, 7H, 7H_{ar}). $^{31}\text{P-NMR}$ (CDCl_3 , 121 MHz, 20 °C): δ 36.6. $^{13}\text{C-NMR}$ (CDCl_3 , 75 MHz, 20 °C): δ 16.5 16.6 (CH_3), 32.0 33.9 (P-CH_2), 38.3 (N- CH_3), 44.9 ($\text{NH}_2\text{-CH}_2$), 54.5 (N- CH_2), 62.2 62.3 (2O-CH_2), 114.9 115.0 (C_{ar}), 120.0 (CH=), 122.4 (CH=), 124.3 124.4 (CH_{ar}), 128.4 (CH_{ar}), 128.9 (CH_{ar}), 129.1 (CH_{ar}), 130.9 131.0 (CH_{ar}), 135.5 (C_{ar}), 138.9 (C-Pt), 157.2 157.3 (O- C_{ar}). MS (positive ESI) $[\text{M}+\text{Na}]$: calculated for $\text{C}_{24}\text{H}_{34}\text{I}_2\text{N}_3\text{Pt}_1\text{O}_4\text{P}_1\text{Na}$: 930.99, found 931.02.



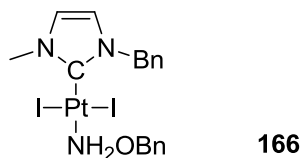
Procedure *b*. 71% Purification by SiO_2 gel chromatography ($\text{CH}_2\text{Cl}_2/\text{MeOH}$ 10/1) escorted by 5% of amino-phosphonate precursor. $^1\text{H-NMR}$ (CDCl_3 , 300 MHz, 20 °C): δ 1.25 (t, J = 7.2Hz, 12H, 4CH_3), 3.08 (d, 22.0Hz, 4H, $2\text{CH}_2\text{-P}$), 3.32 (m, 4H, $\text{CH}_2\text{-CH}_2$), 3.90 (s, 3H, N- CH_3), 4.02 (m, 8H, 4O-CH_2), 5.73 (s, 2H, N- CH_2), 6.64 (d, J = 2.1Hz, 1H, CH=), 6.77 (m, 3H, 3H_{ar}), 6.87 (d, J = 2.1Hz, 1H, CH=), 7.59 (d, J = 8.7Hz, 2H, 2H_{ar}), 8.21 (d, J = 8.7Hz, 2H, 2H_{ar}). $^{31}\text{P-NMR}$ (CDCl_3 , 121 MHz, 20 °C): δ 27.0.



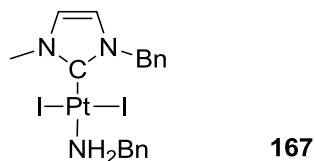
A mixture of trans-[(NHC)Pt^{II}I₂(pyridine)] (20 mg, 28.6 μmol), hydroxylammonium chloride (20 mg, 288 μmol), and triethylamine (77 μL, 571 μmol) in THF (3 mL) was stirred overnight at 55 °C. The mixture was concentrated under reduced pressure, filtered through celite plug with dichloromethane, concentrated under reduced pressure, washed with pentane and purified by chromatography on silica gel (cyclohexane/dichloromethane) to afford the complex as a yellow solid (9.3 mg, 49%). ¹H-NMR (CDCl₃, 300 MHz, 20 °C): δ 3.89 (s, 3H, N-CH₃), 5.56 (s, 2H, N-CH₂), 5.83 (t, J = 3.5, 1H, OH), 5.98 (m, 2H, NH₂), 6.62 (d, J = 2.1Hz, 1H, CH=), 6.83 (d, J = 2.1Hz, 1H, CH=), 7.27-7.48 (m, 5H, CH_{ar}). ¹³C-NMR (CDCl₃, 75 MHz, 20 °C): δ 38.3 (N-CH₃), 54.5 (N-CH₂), 120.3 (CH=), 122.6 (CH=), 128.4 128.8 128.9 (CH_{ar}), 135.0 (C_{ar}), 135.8 (C-Pt). MS (positive ESI) [M+Na]: calculated for C₁₁H₁₅I₂N₃O₁Pt₁Na₁: 676.88, found 676.89, [M-I+CH₃CN]: calculated for C₁₁H₁₅I₁N₃O₁Pt₁CH₃CN: 568.02, found 568.01, [M-I+]: calculated for C₁₁H₁₅I₁N₃O₁Pt₁: 526.99, found 526.99.



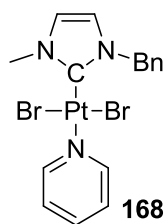
A mixture of 15 (20 mg, 28.6 μmol), O-methylhydroxylammonium chloride (24 mg, 287.4 μmol), and triethylamine (80 μL, 573 μmol) in THF (3 mL) were stirred overnight at 55 °C. The mixture was concentrated under reduced pressure, filtered through celite plug with dichloromethane, concentrated under reduced pressure, washed with pentane and purified by chromatography on silica gel (cyclohexane/dichloromethane) to afford the complex as a yellow solid (7.6 mg, 39%). ¹H-NMR (CDCl₃, 300 MHz, 20 °C): δ 3.90 (s, 3H, O-CH₃), 3.93 (s, 3H, N-CH₃), 5.58 (s, 2H, N-CH₂), 6.43 (m, 2H, NH₂), 6.59 (d, J = 2.2Hz, 1H, CH=), 6.81 (d, J = 2.2Hz, 1H, CH=), 7.27-7.49 (m, 5H, CH_{ar}). ¹³C-NMR (CDCl₃, 75 MHz, 20 °C): δ 38.2 (N-CH₃), 54.4 (N-CH₂), 63.8 (O-CH₃), 120.1 (CH=), 122.5 (CH=), 128.4 128.8 129.0 (CH_{ar}), 135.1 (C_{ar}), 137. (C-Pt). MS (positive ESI) [M+Na]: calculated for C₁₂H₁₇I₂N₃O₁Pt₁Na₁: 690.90, found 690.90, [M-I-NH₂OMe]: calculated for C₁₁H₁₂I₁N₂Pt₁: 493.97, found 493.97, [M-I]: calculated for C₁₂H₁₇I₁N₃O₁Pt₁: 541.01, found 541.00.



A mixture of **15** (30 mg, 42.8 μmol), O-benzylhydroxylammonium chloride (68.4 mg, 429 μmol), and triethylamine (120 μL , 889 μmol) in THF (3 mL) were stirred overnight at 55 $^{\circ}\text{C}$. The mixture was concentrated under reduced pressure, filtered through celite plug with dichloromethane, concentrated under reduced pressure, washed with pentane and purified by chromatography on silica gel (cyclohexane/dichloromethane) to afford the complex as a yellow solid (25.1 mg, 76%). ^1H -NMR (CDCl_3 , 300 MHz, 20 $^{\circ}\text{C}$): δ 3.90 (s, 3H, N- CH_3), 5.17 (s, 2H, O- CH_2), 5.59 (s, 2H, N- CH_2), 6.34 (m, 2H, NH_2), 6.59 (d, $J = 2.1\text{Hz}$, 1H, $\text{CH}=\text{}$), 6.81 (d, $J = 2.1\text{Hz}$, 1H, $\text{CH}=\text{}$), 7.27-7.52 (m, 10H, CH_{ar}). ^{13}C -NMR (CDCl_3 , 75 MHz, 20 $^{\circ}\text{C}$): δ 38.2 (N- CH_3), 54.5 (N- CH_2), 77.1 (O- CH_2), 120.1 ($\text{CH}=\text{}$) 122.4 ($\text{CH}=\text{}$), 128.3 128.4 128.6 128.9 129.1 129.3 133.8 135.2 (C_{ar}). MS (positive ESI) $[\text{M}-\text{I}]$: calculated for $\text{C}_{18}\text{H}_{21}\text{I}_2\text{N}_3\text{O}_1\text{Pt}_1$: 617.04, found 617.04, $[\text{M}-\text{I}+\text{CH}_3\text{CN}]$: calculated for $\text{C}_{18}\text{H}_{21}\text{I}_2\text{N}_3\text{O}_1\text{Pt}_1\text{CH}_3\text{CN}$: 658.06, found 658.07, $[\text{M}+\text{Na}]$: calculated for $\text{C}_{18}\text{H}_{21}\text{I}_2\text{N}_3\text{O}_1\text{Pt}_1\text{Na}_1$: 766.93, found 766.93.

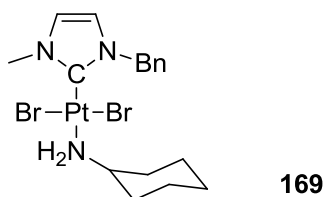


Procedure b. Quant. ^1H -NMR (CDCl_3 , 300 MHz, 20 $^{\circ}\text{C}$): δ 3.90 (s, 3H, N- CH_3), 4.11 (s, 2H, $\text{NH}_2\text{-CH}_2$), 5.59 (s, 2H, N- CH_2), 6.58 (d, $J = 2.1\text{Hz}$, 1H, $\text{CH}=\text{}$), 6.79 (d, $J = 2.1\text{Hz}$, 1H, $\text{CH}=\text{}$), 7.28-7.50 (m, 10H, 10H_{ar}). ^{13}C -NMR (CDCl_3 , 75 MHz, 20 $^{\circ}\text{C}$): δ 38.2 (N- CH_3), 49.1 ($\text{NH}_2\text{-CH}_2$), 54.4 (N- CH_2), 119.9 ($\text{CH}=\text{}$), 122.3 ($\text{CH}=\text{}$), 128.3 128.4 128.8 129.0 129.1 (CH_{ar}), 135.4 ($\text{C}_{\text{ar Ph}}$), 138.8 ($\text{C}_{\text{ar Benzylamine}}$), 139.0 (C-Pt). ^1H -NMR (MeOD, 300 MHz, 20 $^{\circ}\text{C}$): δ 3.83 (s, 3H, N- CH_3), 4.08 (s, 2H, $\text{NH}_2\text{-CH}_2$), 5.53 (s, 2H, N- CH_2), 6.76 (d, $J = 2.1\text{Hz}$, 1H, $\text{CH}=\text{}$), 7.03 (d, $J = 2.1\text{Hz}$, 1H, $\text{CH}=\text{}$), 7.20-7.54 (m, 10H, 10H_{ar}).

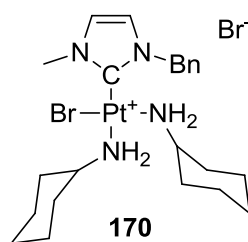


Procedure a was modified: NaI was replaced by NaBr. 55.9 mg, 52%: ^1H -NMR (CDCl_3 , 300 MHz, 20 $^{\circ}\text{C}$): δ 4.11 (s, 3H, N- CH_3), 5.83 (s, 2H, N- CH_2), 6.64 (d, $J = 2.1\text{Hz}$, 1H, $\text{CH}=\text{}$), 6.83 (d, $J = 2.1\text{Hz}$, 1H,

CH=), 7.27-7.53 (m, 7H, 5H_{ar} and 2H_{pyr}), 7.76 (tt, J= 7.6 and 1.6Hz, 1H, H_{pyr}), 9.04 (dt, J= 5.0 and 1.6Hz, 2H, 2H_{pyr}). ¹³C-NMR (CDCl₃, 75 MHz, 20 °C): δ 37.9 (N-CH₃), 54.2 (N-CH₂), 120.0 (CH=), 122.4 (CH=), 124.9 (C_{pyr}), 128.2 (CH_{ar}), 128.8 (CH_{ar}), 128.8 (CH_{ar}), 135.7 (C_{ar}), 137.7 (C_{pyr}), 138.2 (C-Pt), 152.6 (C_{pyr}). ¹³C-NMR (Acetone, 75 MHz, 20 °C): δ 37.1 (N-CH₃), 53.5 (N-CH₂), 120.3 (CH=), 123.0 (CH=), 125.1 (C_{pyr}), 127.9 (CH_{ar}), 128.5 (CH_{ar}), 128.8 (CH_{ar}), 136.8 (C_{ar}), 138.3 (C_{pyr}), 152.5 (C_{pyr}). ¹H-NMR (Acetone, 300 MHz, 20 °C): δ 4.08 (s, 3H, N-CH₃), 5.83 (s, 2H, N-CH₂), 6.99 (d, J= 2.1Hz, 1H, CH=), 7.21 (d, J= 2.1Hz, 1H, CH=), 7.20-7.67 (m, 7H, 5H_{ar} and 2H_{pyr}), 7.97 (tt, J= 7.7 and 1.7Hz, 1H, H_{pyr}), 9.02 (m, 2H, 2H_{pyr}).

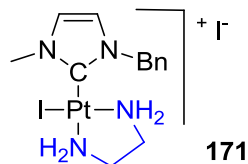


Procedure b was modified: CH₂Cl₂ was used as solvent in presence of 10 eq. of CHA and the solution was stirred at 25 °C for 10 minutes. Yellow solid. 96%: ¹H-NMR (CDCl₃, 300 MHz, 20 °C): δ 1.14-1.84 (m, 8H, H_{CHA}), 2.32 (m, 2H, H_{CHA}), 2.89 (m, 2H, NH₂), 3.17 (m, 1H, NH₂-CH_{CHA}), 4.02 (s, 3H, N-CH₃), 5.72 (s, 2H, N-CH₂), 6.60 (d, J= 2.0Hz, 1H, CH=), 6.78 (d, J= 2.0Hz, 1H, CH=), 7.30-7.45 (m, 5H, 5H_{ar}). ¹³C-NMR (CDCl₃, 75 MHz, 20 °C): δ 24.8 25.3 35.5 (C_{CHA}), 37.7 (N-CH₃), 53.5 (N-CH₂), 54.0 (NH₂-CH_{CHA}), 119.9 (CH=), 122.2 (CH=), 128.2 128.7 128.8 (CH_{ar}), 135.8 (C_{ar}), 141.9 (C-Pt). MS (positive ESI) [M-Br]: calculated for C₁₇H₂₅BrN₃Pt: 546.09, found 546.08.

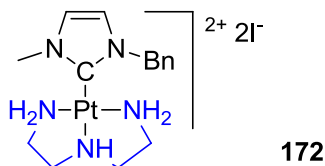


Procedure b was modified: CHA was used as solvent and the solution was stirred at 25 °C for one hour. White solid. 68%. ¹H-NMR (CDCl₃, 300 MHz, 20 °C): δ 0.93-1.74 (m, 16H, 16H_{CHA}), 2.06 (m, 1H, 1H_{CHA}), 2.26-2.39 (m, 3H, 3H_{CHA}), 3.13 (m, 1H, CH_{CHA}), 4.05 (s, 3H, N-CH₃), 4.13 (m, 2H, NH₂), 4.75 (m, 1H, NH_i), 5.51 (d, J= 14.8Hz, 1H, N-CH₂), 5.77 (m, 1H, NH₂), 5.98 (d, J= 14.8Hz, 1H, N-CH₂), 6.74 (d, J= 2.1Hz, 1H, CH=), 6.88 (d, J= 2.1Hz, 1H, CH=), 7.27-7.38 (m, 5H, 5H_{ar}). ¹³C-NMR (CDCl₃, 75 MHz, 20 °C): δ 24.9 25.1 25.3 33.9 34.1 34.8 (C_{CHA}), 38.0 (N-CH₃), 54.3 54.4 (C_{CHA} and N-CH₂), 58.6 (C_{CHA}), 121.0 122.7 (CH=CH), 128.4 128.6 129.1 (CH_{ar}), 135.5 (C_{ar}), 144.8 (C-Pt). MS

(positive ESI) $[M+H]^+$: calculated for $C_{23}H_{37}Br_1N_4Pt_1H$: 645.1887, found 645.1902, $[M_2+Br]^+$: calculated for $C_{46}H_{76}Br_3N_8Pt_2$: 1371.3002, found 1371.3050, $[M_3+H+2HBr]^+$: calculated for $C_{69}H_{114}Br_5N_{12}Pt_3$: 2096.4103, found 2096.3917.



(Ethylenediamine (10 μ L, 0.143 mmol) was added to a suspension of **14** (20 mg, 0.029 mmol) in ethanol (1.5 mL). The reaction was stirred for 20h at 55 $^{\circ}$ C, concentrated under reduced pressure, washed with dichloromethane and pentane to afford the complex as a white solid (10 mg, 50%). 1H -NMR CD_3OD , 300 MHz, 20 $^{\circ}$ C): δ 2.20-2.60 (m, 4H, 2CH₂), 3.94 (s, 3H, NCH₃), 5.36 and 5.84 (2d: AB system, J = 14.7 Hz, 2 x 1H, NCH₂), 7.04 (d, J = 2.1 Hz, 1H, CH), 7.20 (d, J = 2.1 Hz, 1H, CH), 7.37-7.47 (m, 5H, 5Ar-H).



Diethylenediamine (8 mL, 0.072 mmol) was added to a suspension of trans-[(NHC)PtI₂(pyridine)] **14** (10 mg, 0.014 mmol) in ethanol (2 mL). The solution was stirred for 3 h at 55 $^{\circ}$ C, concentrated under reduced pressure, and washed with CH_2Cl_2 and THF to afford the **174** as a white solid (6 mg, 60%). 1H NMR (CD_3CN , 300 MHz, 208 $^{\circ}$ C): δ =2.50–3.20 (m, 8H, 4CH₂), 3.55–3.86 (m, 2H, NH₂), 3.95 and 4.03 (s, 3H, NCH₃), 5.55 (s, 2H, NCH₂), 7.00–7.61 ppm (m, 7H, 5Ar-H and 2CH); ^{13}C -NMR ([D₆]DMSO, 75 MHz, 20 $^{\circ}$ C): δ =38.0 (NCH₃), 38.1 (NCH₃), 51.3 (NCH₂), 51.5 (NCH₂), 51.6 (NCH₂), 51.8 (NCH₂), 53.7 (NCH₂), 54.0 (NCH₂), 122.0 (CH), 124.0 (CH), 128.7 (CH_{ar}), 129.1 (CH_{ar}), 129.3 (CH_{ar}), 129.4 (CH_{ar}), 136.7 (C_{ar}), 137.1 (C_{ar}), 149.9 (C-Pt); HRMS (positive ESI, $[M-I]^+$: calculated for $C_{15}H_{25}N_5IPt$ 597.080, found 597.078.

General synthesis of [(NHC)PtI₂(PEI (M, n))] conjugates: Under argon, a solution of complex **14** (40 mg, 57.1 μ mol) and PEI_M ($n \times 2.46$ mg) in ethanol (10 mL) was stirred two days at 55 $^{\circ}$ C. The colour of the solution is turning from yellow to white-transparent. The solvent is removed under reduced

pressure, the solid obtained washed with pentane and dried under reduced pressure to afford $[(\text{NHC})\text{PtI}_2(\text{PEI}(\text{M}, \text{n}))]$ conjugates as a white-yellow solid

$[(\text{NHC})\text{PtI}_2(\text{PEI}(\text{M}, 10))]$: Under argon, a solution of complex **14** (40 mg, 57.1 μmol) and PEI (24.6 mg) in ethanol (10 mL, dried over molecular sieves) is stirred two days at 55 °C. The colour of the solution is turning from yellow to white-transparent. The solvent is removed under reduced pressure, the solid obtained washed with pentane and dried under reduced pressure to afford PEI 10 as a white-yellow solid (60.1 mg, quant.). $^1\text{H-NMR}$ ($\text{CD}_3\text{OD}/\text{CD}_3\text{CN}$, 300 MHz, 20°C): δ 2.2-3.1 (m, CH_2), 3.1-3.6 (m, NH_2 and NH masked partially by the H_2O and CD_3OD peaks), 4.0-4.5 (m, NCH_3), 5.9 (m, NCH_2), 7.1-8.0 (m, H_{ar} and 2CH). Elemental Analysis: Calculated for $\text{C}_{31}\text{H}_{62}\text{I}_2\text{N}_{12}\text{Pt}\cdot 6\text{H}_2\text{O}$ C, 32.10; H, 6.43; N, 14.49; found: C, 31.14; H, 5.08; N, 14.66.

$[(\text{NHC})\text{PtI}_2(\text{PEI}(\text{M}, 20))]$: Under argon, a solution of complex **14** (30 mg, 42.8 μmol) and PEI (36.9 mg) in ethanol (10 mL, dried over molecular sieves) is stirred two days at 55 °C. The colour of the solution is turning from yellow to white-transparent. The solvent is removed under reduced pressure, the solid obtained washed with pentane and dried under reduced pressure to afford PEI 10 as a white solid (63.5 mg, quant.). $^1\text{H-NMR}$ ($\text{CD}_3\text{OD}/\text{CD}_3\text{CN}$, 300 MHz, 20°C): δ 2.2-3.1 (m, CH_2), 3.1-3.6 (m, NH_2 and NH masked partially by the H_2O and CD_3OD peaks), 4.0-4.5 (m, NCH_3), 5.9 (m, NCH_2), 7.1-8.0 (m, H_{ar} and 2CH). Elemental Analysis: Calculated for $\text{C}_{51}\text{H}_{112}\text{I}_2\text{N}_{22}\text{Pt}\cdot 14\text{H}_2\text{O}$ C, 35.31; H, 8.13; N, 17.76, found C, 35.22; H, 6.20; N, 14.85.

$[(\text{NHC})\text{PtI}_2(\text{PEI}(\text{M}, 30))]$: Under argon, a solution of complex **14** (20 mg, 28.6 μmol) and PEI (36.9 mg) in ethanol (10 mL, dried over molecular sieves) is stirred two days at 55 °C. The colour of the solution is turning from yellow to white-transparent. The solvent is removed under reduced pressure, the solid obtained washed with pentane and dried under reduced pressure to afford PEI 10 as a white solid (54.6 mg, quant.). $^1\text{H-NMR}$ ($\text{CD}_3\text{OD}/\text{CD}_3\text{CN}$, 300 MHz, 20°C): δ 2.2-3.1 (m, CH_2), 3.1-3.6 (m, NH_2 and NH masked partially by the H_2O and CD_3OD peaks), 4.0-4.5 (m, NCH_3), 5.9 (m, NCH_2), 7.1-8.0 (m, H_{ar} and 2CH). Elemental Analysis: Calculated for $\text{C}_{71}\text{H}_{162}\text{I}_2\text{N}_{32}\text{Pt}\cdot 25\text{H}_2\text{O}$: C, 36.08; H, 9.04; N, 18.96; found C, 38.09; H, 7.60; N, 16.24.

$[\text{PtCl}_2(\text{PEI}(25000, 20))]$: Under argon, a solution of $\text{PtCl}_2(\text{NH}_3)_2$ (10 mg, 33.3 μmol) and PEI (28.7 mg) in ethanol (5 mL, dried over molecular sieves) is stirred two days at 55 °C. The colour of the solution is turning from yellow to white-yellow. The solvent is removed under reduced pressure, the

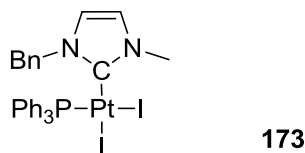
solid obtained washed with pentane and dried under reduced pressure to afford PEI - Platinum as a white-yellow solid (42.4 mg, quant.). $^1\text{H-NMR}$ ($\text{CD}_3\text{OD}/\text{CD}_3\text{CN}$, 300 MHz, 20°C): δ 2.0-3.3 (m, CH_2), 3.0-3.5 (m, NH_2 and NH masked partially by the H_2O and CD_3OD peaks).

7.3.3.2 Introduction of phosphines, arsines, stibines

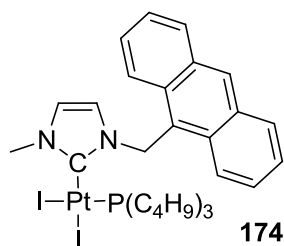
Unless mentioned, following general procedures were used for pnictogen ligand introduction:

Neutral complexes: A solution of the corresponding *trans*-NHC- PtI_2 -pyridine (1 eq) and the Pnictogen ligand (1.2 eq) under argon in ethanol was stirred overnight at 55°C , then concentrated under reduced pressure and purified by silica gel chromatography (gradient CH_2Cl_2 /pentane 1/1, CH_2Cl_2 , CH_2Cl_2) to afford the complex as a yellow solid.

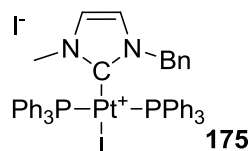
Cationic complex: A solution of the corresponding *trans*-NHC- PtI_2 -pyridine (1 eq) and the Pnictogen ligand (2.2 eq) under argon in ethanol was stirred overnight at 55°C , then concentrated under reduced pressure and purified by silica gel chromatography (gradient CH_2Cl_2 /pentane 1/1, CH_2Cl_2 , $\text{CH}_2\text{Cl}_2/\text{MeOH}$ 20/1) to afford the complex as a white solid.



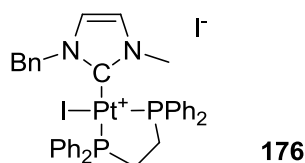
71.7 mg, 51%: $^1\text{H-NMR}$ (CDCl_3 , 300 MHz, 20°C): δ 3.53 (s, 3H, N-CH_3), 4.32 (d, $J = 14.0\text{Hz}$, 1H, N-CH_2), 5.84 (d, $J = 14.0\text{Hz}$, 1H, N-CH_2), 6.25 (d, $J = 2.1\text{Hz}$, 1H, CH=), 6.54 (d, $J = 2.1\text{Hz}$, 2H, 2H_{ar}), 7.15-7.64 (m, 20H, 20H_{ar}). $^{31}\text{P-NMR}$ (CDCl_3 , 121 MHz, 20°C): δ 8.46 (t, $J = 3684\text{Hz}$, PPh_3). $^{13}\text{C-NMR}$ (CDCl_3 , 75 MHz, 20°C): δ 37.7 (N-CH_3), 53.8 (N-CH_2), 119.8 (CH=), 122.7 (CH=), 128.2, 128.7, 129.6, 130.2, 131.0, 133.8, 134.0, 134.5 (C_{ar}), 154.0 (C-Pt).



General procedure was modified: A solution of pyridine precursor **30**, [H-PnBu₃].BF₄ (1 eq) and DIPEA (1 eq) was stirred in ethanol at 55 °C: 92%. ¹H-NMR (300 MHz, CDCl₃, 25 °C) δ: 1.20-1.54 (m, 27H, nBu), 3.98 (s, 3H, N-CH₃), 5.91 (s, 2H, N-CH₂), 6.04 (s, 1H, CH=), 7.43 (s, 1H, CH=), 7.52 (dd, 4H, H_{ar}), 7.85 (d, 2H, H_{ar}), 8.16 (d, 2H, H_{ar}), 8.71 (s, 1H, H_{ar}). ³¹P-NMR (121 MHz, CDCl₃, 25 °C) δ: 4.55 (t, J = 2197 Hz). Crystal data for Anthracene-NHC-PtI₂-P(C₄H₉)₃: C₃₁H₄₃I₂N₂Ppt, yellow, M = 923.53, Monoclinic, P 21/c, a = 13.2867(4), b = 15.1211(7), c = 16.3833(8) Å, α = 90, β = 96.133(3), γ = 90 °, U = 3272.7(2) Å³, Z = 4, D_c = 1.874 g cm⁻³, μ 6.245 mm⁻¹, F(000) = 1768, number of data meas.: 25653 (1.541 < 2θ < 27.487 °) at 173(2) K, radiation: MoKα graphite monochromated, number of data with I > 3σ(I): 5285, number of variables: 338, R = 0.0620, R_w = 0.1137, GOF = 1.212. Crystals have been obtained by slow vapour diffusion of pentane into a solution of the complex in dichloromethane.

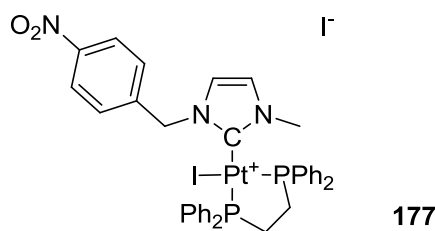


18.9 mg, quant: ¹H-NMR (CDCl₃, 300 MHz, 20 °C): δ 3.31 (s, 3H, N-CH₃), 4.71 (s, 2H, N-CH₂), 6.32 (d, J = 2.1 Hz, 1H, CH=), 6.65 (d, J = 2.1 Hz, 2H, 2H_{ar}), 7.08-7.59 (m, 36H, 35H_{ar}+CH=). ³¹P-NMR (CDCl₃, 121 MHz, 20 °C): δ 13.01 (t, J = 2448 Hz). ¹³C-NMR (CDCl₃, 75 MHz, 20 °C): δ 38.0 (N-CH₃), 54.0 (N-CH₂), 121.0 (CH=), 125.2 (CH=), 129.0 129.1 129.3 129.4 129.6 131.0 132.2 134.3 (C_{ar}), 150.1 (C-Pt). MS (positive ESI) [M-I]: calculated for C₄₇H₄₂IN₂P₂Pt: 1018.15 found 1018.15.

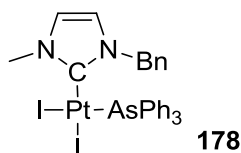


General procedure was adapted: one equivalent of dppe was used: 62.7 mg, 86%. ¹H-NMR (MeOD, 300 MHz, 20 °C): δ 2.38-2.86 (m, 4H, CH₂CH₂), 3.37 (s, 3H, N-CH₃), 4.18 (d, J = 14.6 Hz, 1H, N-CH₂), 5.24 (d, J = 14.6 Hz, 1H, N-CH₂), 6.83 (s, 1H, CH=), 7.12 (m, 6H, 6H_{ar}), 7.44-7.64 (m, 16H,

16H_{ar}), 7.83-7.94 (m, 4H, 4H_{ar}). ³¹P-NMR (MeOD, 121 MHz, 20 °C): δ 26.4 (d, J= 14.7Hz, 1P), 31.8 (d, J= 14.7Hz, 1P), 40.0 (d, J= 12.9Hz, 4P), 41.0 (d, J= 12.9Hz, 4P), 50.1 (d, J= 12.9Hz, 1P), 53.6 (d, J= 14.7Hz, 1P). ¹³C-NMR (MeOD, 75 MHz, 20 °C): δ 26.8 (dd, J= 37.1 and 8.7Hz, CH₂-P), 29.9 (dd, J= 39.7 and 10.2Hz, CH₂-P), 38.4 (N-CH₃), 54.5 (N-CH₂), 123.3 125.8 (CH=CH), 127.6 128.3 128.3 129.1 129.2 129.5 129.6 129.8 130.0 130.2 130.3 130.6 130.7 130.8 133.1 133.5 133.7 133.8 134.0 134.1 134.9 135.0 135.1 135.2 135.4 135.8 165.5 (dd, J= 138.3 and 7.8Hz, C-Pt). MS (positive ESI) [M-I]: calculated for C₃₇H₃₆I₁N₂P₂Pt₁: 892.1044, found 892.0957.

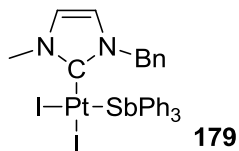


General procedure was adapted: one equivalent of dppe was used: ~70%. ¹H-NMR (300MHz, CDCl₃, 25°C) δ: 2.64-3.09 (m, 4H, CH₂CH₂), 3.41 (s, 3H, N-CH₃), 4.59 (d, J= 14.6Hz, 1H, N-CH₂), 5.11 (d, J= 14.6Hz, 1H, N-CH₂), 7.30 – 7.61 (m, 18H, H_{ar}), 7.55-7.79 (m, 4H, H_{ar}), 8.044 -8.08 (m, 4H, 4H_{ar}). ³¹P-NMR (121 MHz, CDCl₃, 25°C) δ: 27.9 (d, J= 4.4Hz), 32.3 (d, J= 4.4Hz), 41.6 (d, J= 5.4Hz), 50.6 (d, J= 5.1Hz), 55.3 (d, J= 12.9Hz).

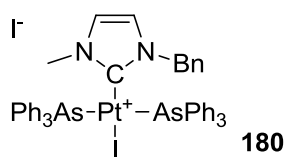


27.3 mg, 82%: ¹H-NMR (CDCl₃, 300 MHz, 20 °C): δ 3.56 (s, 3H, N-CH₃), 4.57 (d, J= 14.1Hz, 1H, 1H_{N-CH2}), 5.77 (d, J= 14.1Hz, 1H, 1H_{N-CH2}), 6.32 (d, J= 2.1Hz, 1H, CH=), 6.51 (d, J= 2.1Hz, 1H, CH=), 7.12-7.55 (m, 20H, 20H_{ar}). ¹³C-NMR (CDCl₃, 75 MHz, 20 °C): δ 37.6 (N-CH₃), 54.0 (N-CH₂), 120.1(CH=), 122.2 (CH=), 128.6 128.9 129.5 130.6 131.8 133.2 133.4 133.9 (C_{ar}), 151.5 (C-Pt). MS (positive ESI) [M-I]: calculated for C₂₉H₂₇I₂N₂AsPt: 800.01 found 800.00, MS (positive ESI) [M-I+CH₃CN]: calculated for C₂₉H₂₇I₂N₂AsPtCH₃CN: 841.03 found 841.03. Crystal data for *cis*-NHC-Pt(I)₂AsPh₃: C₂₉H₂₇I₂N₂AsPtCHCl₃, yellow, M = 1046.70, Triclinic, P ₋₁ a = 10.0662(2), b = 13.1123(5), c =14.3293(5) Å, α =62.8920(10), β =83.365(2), γ =89.873(2) °, U = 1669.58(9) Å³, Z = 2, D_c = 2.082 g cm⁻³, μ 7.297 mm⁻¹, F(000) = 980, number of data meas.: 18806 (1.61 < O < 27.45°) at 173(2) K, radiation: MoKα graphite monochromated, number of data with I > 3σ(I): 6532, number

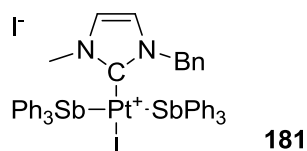
of variables: 353, $R = 0.0411$, $R_w = 0.1112$, $GOF = 1.103$. Crystals have been obtained by slow vapour diffusion of pentane into a solution of the complex in $CDCl_3$.



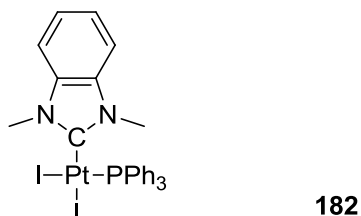
71.7 mg, 92%: 1H -NMR ($CDCl_3$, 300 MHz, 50 °C): δ 3.62 (s, 3H, N-CH₃), 5.11 (d, $J = 14.2$ Hz, 1H, N-CH₂), 5.56 (d, $J = 14.2$ Hz, 1H, N-CH₂), 6.50 (d, $J = 1.9$ Hz, 1H, CH=), 6.56 (d, $J = 1.9$ Hz, 1H, CH=), 7.00-7.72 (m, 20H, 20H_{ar}). 1H -NMR ($CDCl_3$, 300 MHz, 20 °C): δ 3.58 (s, 3H, N-CH₃), 5.11 (d, $J = 14.2$ Hz, 1H, N-CH₂), 5.50 (d, $J = 14.2$ Hz, 1H, N-CH₂), 6.52 (d, $J = 2.1$ Hz, 1H, CH=), 6.55 (d, $J = 2.1$ Hz, 1H, CH=), 7.00-7.71 (m, 20H, 20H_{ar}). ^{13}C -NMR ($CDCl_3$, 75 MHz, 20 °C): δ 37.8 (N-CH₃), 54.4 (N-CH₂), 120.9 122.8 (CH=CH), 128.7 128.9 129.1 129.5 130.8 (CH_{ar}), 134.3 (C_{ar}), 135.5 (CH_{ar}), 136.3 (C_{ar}), 150.1 (C-Pt). MS (positive ESI) [M-I]: calculated for C₂₉H₂₇SbI₁N₂Pt₁: 846.99, found 846.98, [M-I+CH₃CN]: calculated for C₂₉H₂₇SbI₁N₂Pt₁CH₃CN: 888.02, found 888.00, [M+Na]: calculated for C₂₉H₂₇SbI₂N₂Pt₁Na: 996.88, found 996.9. Crystal data for *cis*-NHC-Pt(I)₂SbPh₃: C₂₉H₂₇SbI₂N₂Pt₁, yellow, $M = 974.16$, orthorhombic, $P b c a$, $a = 7.6160(2)$, $b = 17.1007(4)$, $c = 46.5050(13)$ Å, $\alpha = 90$, $\beta = 90$, $\gamma = 90$ °, $U = 6056.8(3)$ Å³, $Z = 8$, $D_c = 2.137$ g cm⁻³, μ 7.564 mm⁻¹, $F(000) = 3600$, number of data meas.: 34749 ($1.752 < \theta < 27.489^\circ$) at 173(2) K, radiation: MoK α graphite monochromated, number of data with $I > 3\sigma(I)$: 4424, number of variables: 317, $R = 0.0466$, $R_w =$ refine_ls_wR_factor_gt, $GOF = 0.1047$. Crystals have been obtained by slow vapour diffusion of pentane into a solution of the complex in dichloromethane.



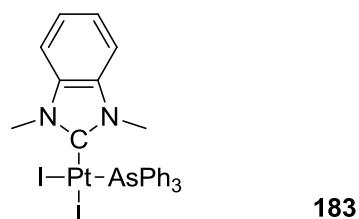
45.8 mg, Quant: 1H -NMR ($CDCl_3$, 300 MHz, 20 °C): δ 3.49 (s, 3H, N-CH₃), 4.50 (d, $J = 14.0$ H, N-CH₂), 5.70 (d, $J = 14.0$ H, N-CH₂), 6.25 (s, 1H, CH=), 6.44 (s, 1H, CH=), 7.07-7.47 (m, 35H, 35H_{ar}).



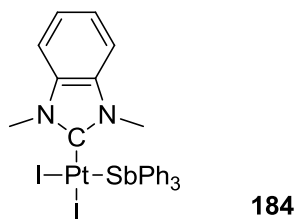
29.3 mg, quant: $^1\text{H-NMR}$ (CDCl_3 , 300 MHz, 20 °C): δ 3.58 (s, 3H, N-CH₃), 5.12 (d, J = 14.2Hz, 1H, N-CH₂), 5.50 (d, J = 14.2Hz, 1H, N-CH₂), 6.52 (d, J = 2.0Hz, 1H, CH=), 6.55 (d, J = 2.0Hz, 1H, CH=), 7.04-7.72 (m, 35H, 35H_{ar}). $^{13}\text{C-NMR}$ (CDCl_3 , 75 MHz, 20 °C): δ 37.8 (N-CH₃), 54.5 (N-CH₂), 120.9 122.7 (CH=CH), 128.7 129.0 129.1 129.5 130.8 (CH_{ar}), 134.4 (C_{ar}), 135.7 136.4 (CH_{ar}), 137.0 (C_{ar}), 138.5 (C_{ar}), 150.7 (C-Pt). MS (positive ESI) [M-I]: calculated for C₄₇H₄₂Sb₂I₁N₂Pt₁: 1198.0112, found 1198.0082.



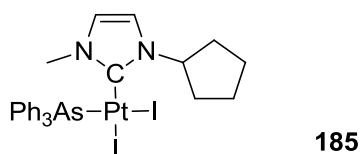
39.1 mg, 69%: $^1\text{H-NMR}$ (CDCl_3 , 300 MHz, 20 °C): δ 3.75 (s, 6H, 2N-CH₃), 7.06-7.35 (m, 13H, 13H_{ar}), 7.61 (m, 6H, 6H_{ar}). $^{31}\text{P-NMR}$ (CDCl_3 , 121 MHz, 20 °C): δ 8.36 (t, J = 1832.3Hz). $^{13}\text{C-NMR}$ (CDCl_3 , 75 MHz, 20 °C): δ 34.1 (N-CH₃), 109.8 (CH_{ar}), 123.1 127.9 128.1 (CH_{ar}), 129.7 130.5 (C_{ar}), 130.5 130.9 134.0 134.2 134.3 (CH_{ar}), 166.3 (C-Pt). MS (positive ESI) [M-I]: calculated for C₂₇H₂₅P₁I₁N₂Pt₁: 730.0445, found 730.0388, [M-I-HI]: calculated for C₂₇H₂₄P₁N₂Pt₁: 602.1322, found 602.1041.



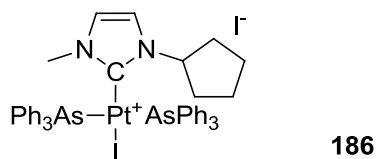
36.1 mg, 50%: $^1\text{H-NMR}$ (CDCl_3 , 300 MHz, 20 °C): δ 3.78 (s, 6H, 2N-CH₃), 7.05-7.31 (m, 13H, 13H_{ar}), 7.53 (m, 6H, 6H_{ar}). $^{13}\text{C-NMR}$ (CDCl_3 , 75 MHz, 20 °C): δ 34.1 (N-CH₃), 109.8 (CH_{ar}), 123.2 128.8 130.6 (CH_{ar}), 131.5 130.5 (C_{ar}), 133.3 (CH_{ar}), 134.6 (C_{ar}), 163.9 (C-Pt). MS (positive ESI) [M+Na]: calculated for C₂₇H₂₅As₁I₂N₂Pt₁Na: 923.8866, found 923.8794, [M-I]: calculated for C₂₇H₂₅As₁I₁N₂Pt₁: 773.9923, found 773.9850.



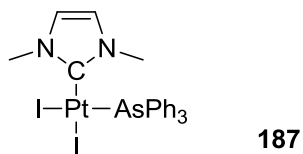
48.6 mg, 69%: $^1\text{H-NMR}$ (CDCl_3 , 300 MHz, 20 °C): δ 3.82 (s, 6H, 2N-CH₃), 7.04-7.32 (m, 13H, 13H_{ar}), 7.52 (m, 6H, 6H_{ar}). $^{13}\text{C-NMR}$ (CDCl_3 , 75 MHz, 20 °C): 34.2 (N-CH₃), 109.8 123.2 128.6 129.4 129.7 130.9 134.3 134.9 135.4 (C_{ar}), 163.2 (C-Pt). MS (positive ESI) [M+Na]: calculated for C₂₇H₂₅SbI₂N₂PtNa: 970.8687, found 970.8620. [M-I+CH₃CN]: calculated for C₂₇H₂₅SbI₁N₂Pt₁CH₃CN: 862.0010, found 861.9932.



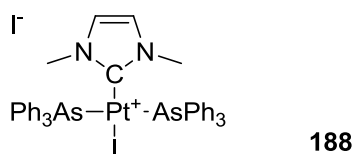
21.6 mg, 77%: $^1\text{H-NMR}$ (CDCl_3 , 300 MHz, 20 °C): δ 1.05-1.78 (m, 9H, 9H_{CH2}), 2.55 (m, 1H, 1H_{CH2}), 3.42 (s, 3H, N-CH₃), 5.55 (q, J= 8.1Hz, 1H, N-CH), 6.56 (d, J= 2.1Hz, 1H, CH=), 6.68 (d, J= 2.1Hz, 1H, CH=), 7.25-7.56 (15H, 15H_{Ph-As}). MS (positive ESI) [M-I+CH₃CN]: calculated for C₂₇H₂₉AsIN₂PtCH₃CN: 819.05, found 819.04, [M-I]: calculated for C₂₇H₂₉AsIN₂Pt: 778.02, found 778.02, [M+Na]: calculated for C₂₇H₂₉AsI₂N₂PtNa: 927.92, found 927.92. $^{13}\text{C-NMR}$ (CDCl_3 , 75 MHz, 20 °C): δ 23.9 24.5 32.1 33.7 (4CH₂), 37.3 (N-CH₃), 60.9 (N-CH), 117.1 122.9 (CH=CH), 128.8 130.5 131.7 (CH_{ar}), 133.4 (C_{ar}), 150.1 (C-Pt).



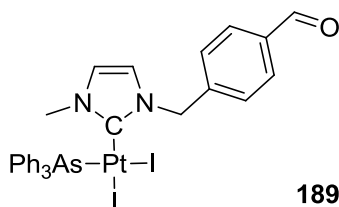
7.1 mg, 19%: $^1\text{H-NMR}$ (CDCl_3 , 300 MHz, 20 °C): δ 0.95-1.78 (m, 9H, CH_{alkane}), 2.53 (m, 1H, CH_{alkane}), 3.42 (s, 3H, N-CH₃), 5.54 (q, J= 8.2Hz, 1H, N-CH), 6.58 (d, J= 2.1Hz, 1H, CH=), 6.69 (d, J= 2.1Hz, 1H, CH=), 7.25-7.49 (m, 30H, 30H_{ar}). MS (positive ESI) [M-I]: calculated for C₄₅H₄₄As₂IN₂Pt: 1084.06, found 1084.06.



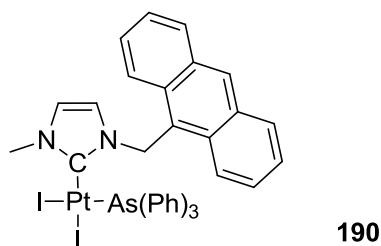
~80%. ^1H -NMR (CDCl_3 , 300 MHz, 20 °C): δ 3.52 (s, 6H, 2N- CH_3), 6.53 (s, 2H, $\text{CH}=\text{CH}$), 7.27-7.56 (m, 15H, 15H_{ar}). ^{13}C -NMR (CDCl_3 , 75 MHz, 20 °C): δ 37.5 (N- CH_3), 122.2 ($\text{CH}=\text{CH}$), 129.0 (CH_{ar}), 130.7 (CH_{ar}), 131.9 (C_{ar}), 133.4 (CH_{ar}), 151.5 (C-Pt). MS (positive ESI) $[\text{M}-\text{I}]$: calculated for $\text{C}_{23}\text{H}_{23}\text{I}_1\text{N}_2\text{Pt}_1\text{As}$: 723.98, found 723.97, $[\text{M}+\text{Na}]$: calculated for $\text{C}_{23}\text{H}_{23}\text{I}_2\text{N}_2\text{Pt}_1\text{AsNa}$: 874.87, found 874.86.



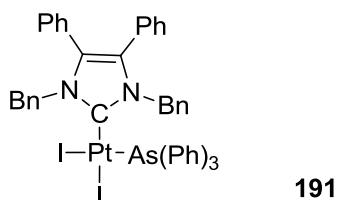
Quant. ^1H -NMR (CDCl_3 , 300 MHz, 20 °C): δ 3.55 (s, 6H, 2N- CH_3), 6.51 (s, 2H, $\text{CH}=\text{CH}$), 7.29-7.58 (m, 30H, 30H_{ar}). ^{13}C -NMR (CDCl_3 , 75 MHz, 20 °C): δ 29.8 (N- CH_3), 37.5 (N- CH_3), 122.0 ($\text{CH}=\text{CH}$), 128.6 (CH_{ar}), 128.8 129.0 129.8 130.7 132.1 133.5 133.9 139.7 (C_{ar}). MS (positive ESI) $[\text{M}-\text{I}]$: calculated for $\text{C}_{41}\text{H}_{38}\text{I}_1\text{N}_2\text{Pt}_1\text{As}_2$: 1030.02, found 1030.01.



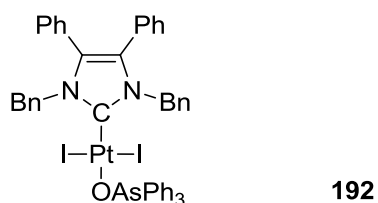
27.3 mg, 88%: ^1H -NMR (CDCl_3 , 300 MHz, 20 °C): δ 3.58 (s, 3H, N- CH_3), 4.62 (d, $J = 14.6\text{Hz}$, 1H, $1\text{H}_{\text{N-CH}_2}$), 5.92 (d, $J = 14.6\text{Hz}$, 1H, $1\text{H}_{\text{N-CH}_2}$), 6.36 (t, $J = 1.8\text{Hz}$, 1H, $\text{CH}=\text{CH}$), 6.59 (t, $J = 1.8\text{Hz}$, 1H, $\text{CH}=\text{CH}$), 7.28-7.81 (m, 19H, 19H_{ar}), 9.95 (s, 1H, $\text{CH}=\text{O}$). ^{13}C -NMR (CDCl_3 , 75 MHz, 20 °C): δ 37.7 (N- CH_3), 53.4 (N- CH_2), 120.2 ($\text{CH}=\text{CH}$), 122.8 ($\text{CH}=\text{CH}$), 128.2 129.1 130.1 130.7 133.1 134.7 136.3 140.5 (C_{ar}), 152.6 (C-Pt), 191.5 ($\text{CH}=\text{O}$). MS (positive ESI) $[\text{M}-2\text{I}-\text{H}]$: calculated for $\text{C}_{30}\text{H}_{26}\text{N}_2\text{Pt}_1\text{O}_1\text{As}_1$: 700.09, found 700.08, $[\text{M}+\text{Na}]$: calculated for $\text{C}_{30}\text{H}_{27}\text{N}_2\text{Pt}_1\text{O}_1\text{As}_1\text{I}_2\text{Na}$: 977.90, found 977.89, $[\text{M}-\text{I}]$: calculated for $\text{C}_{30}\text{H}_{27}\text{N}_2\text{Pt}_1\text{O}_1\text{As}_1\text{I}_1$: 828.00, found 827.99.



Crystal data for Anthracene-NHC-PtI₂-AsPh₃: C₃₇H₃₁AsI₂N₂ Pt, yellow, M = 1027.45, monoclinic, P 2₁/c, a = 12.8029(5), b = 19.9263(8), c = 18.7923(6) Å, α = 90°, β = 118.125(2)°, γ = 90°, U = 4228.1(3) Å³, Z = 4, D_c = 1.614 g cm⁻³, μ = 5.578 mm⁻¹, F(000) = 1936, number of data meas.: 31068 (1.598 < 2θ < 28.029 °) at 173(2) K, radiation: MoKα graphite monochromated, number of data with I > 3σ(I): 7402, number of variables: 371, R = 0.0395, R_w = 0.0920, GOF = 1.043. Crystals have been obtained by slow vapour diffusion of pentane into a solution of the complex in dichloromethane.

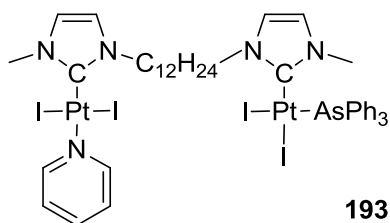


30.6 mg, 60%: ¹H-NMR (CDCl₃, 300 MHz, 20 °C): δ 5.12 (d, J = 14.6 Hz, 2H, N-CH₂), 6.05 (d, J = 14.6 Hz, 2H, N-CH₂), 6.62 (d, J = 7.0 Hz, 4H, 4H_{ar}), 6.79 (d, J = 7.6 Hz, 4H, 4H_{ar}), 6.95 (t, J = 7.3 Hz, 2H, 2H_{ar}), 6.92-7.19 (m, 11H, 11H_{ar}), 7.31-7.52 (m, 11H, 11H_{ar}). ¹³C-NMR (CDCl₃, 75 MHz, 20 °C): δ 52.9 (N-CH₂), 127.7 128.1 128.3 128.8 128.9 129.2 130.7 130.8 132.7 132.9 134.1 134.9 (C_{ar}), 152.3 (C-Pt). MS (positive ESI) [M-I]: calculated for C₄₇H₃₉AsI₁N₂Pt₁: 1028.1020, found 1028.0552.



4.6 mg, 9%: ¹H-NMR (CDCl₃, 300 MHz, 20 °C): δ 5.83 (s, 4H, 2N-CH₂), 6.93-7.44 (m, 29H, 29H_{ar}), 7.60 (m, 6H, 6H_{ar}). ¹³C-NMR (CDCl₃, 75 MHz, 20 °C): δ 53.7 (N-CH₂), 127.3 128.2 128.3 128.4 128.5 128.7 129.9 130.9 131.0 133.6 134.9 136.2 (C_{ar}), 155.3 (C-Pt). Crystal data for *trans*-NHC-Pt(I₂)-OAsPh₃: 3(C₄₇H₃₉AsI₂N₂OPt), C₁₈H₁₅AsO, yellow, M = 3837.05, trigonal, R 3 c, a = 48.1461(11), b = 48.1461(11), c = 10.89710(10) Å, α = 90°, β = 90°, γ = 120°, U = 21875.8(12) Å³, Z = 6, D_c = 1.748 g cm⁻³, μ = 5.097 mm⁻¹, F(000) = 11064, number of data meas.: 41937 (1.465 < 2θ <

27.491 °) at 173(2) K, radiation: MoK α graphite monochromated, number of data with $I > 3\sigma(I)$: 8952, number of variables: 523, $R = 0.0472$, $R_w = 0.0987$, $GOF = 1.176$. Crystals have been obtained by slow vapour diffusion of pentane into a solution of the complex in dichloromethane.

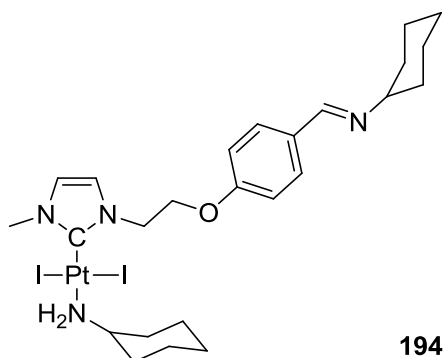


General procedure was adapted: 0.9 equivalents of AsPh_3 were used. 23.9 mg, 64%: $^1\text{H-NMR}$ (CDCl_3 , 300 MHz, 20 °C): δ 1.11-1.55 (m, 17H, 17H_{alkane}), 1.75 (m, 1H, 1H_{alkane}), 2.03 (t, $J = 6.8\text{Hz}$, 2H, 2H_{alkane}), 3.5 (s, 3H, N-CH₃), 3.68 (m, 1H, 1H_{N-CH2}), 3.94 (s, 3H, N-CH₃), 4.18 (m, 1H, 1H_{N-CH2}), 4.41 (t, $J = 7.7\text{Hz}$, 2H, N-CH₂), 6.55 (s, 2H, CH=CH), 6.85 (d, $J = 2.2\text{Hz}$, 2H, CH=CH), 7.26-7.50 (m, 17H, 2H_{Pyr}+15H_{Ph}), 7.72 (tt, $J = 7.7$ and 1.6Hz , 1H, 1H_{Pyr}), 9.02 (m, 2H, 2H_{Pyr}). $^{13}\text{C-NMR}$ (CDCl_3 , 75 MHz, 20 °C): δ 26.8 26.8 29.1 29.3 29.5 29.6 (CH₂), 37.6 38.4 (N-CH₃), 50.4 51.0 (N-CH₂), 120.3 120.5 122.0 122.3 (2CH=CH), 125.0 (C_{Pyr}), 128.9 130.7 (CH_{ar}), 131.9 (C_{ar}), 134.0 (CH_{ar}), 135.1 (C-Pt), 137.6 (C_{Pyr}), 150.5 (C-Pt-As), 153.8 (C_{Pyr}). MS (positive ESI) [M-I]: calculated for $\text{C}_{47}\text{H}_{54}\text{I}_3\text{N}_5\text{Pt}_2\text{As}_1$: 1486.06, found 1486.02.

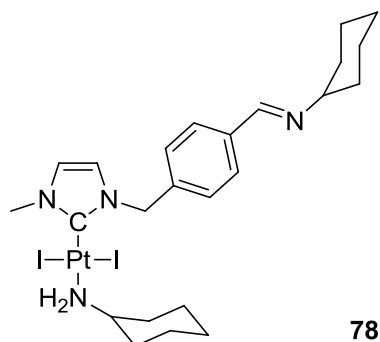
7.3.3.3 Condensation reactions with Pt complexes featured with benzaldehyde

7.3.3.3.1 Imine formation

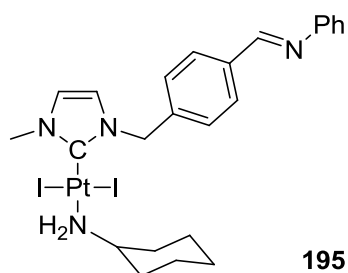
General procedure: To a mixture of benzaldehyde complex (1 eq.), oven-dried Na_2SO_4 (excess) and amine (1 eq.) respectively ammonium halide (1 eq.) with triethylamine (10 eq.) was added anhydrous dichloromethane. The solution was stirred overnight at 25 °C. The solution was filtered over celite plug and volatiles removed under reduced pressure. The crude product was purified by chromatography (SiO_2 deactivated by NEt_3 , gradient CH_2Cl_2 /pentane 1/1 to CH_2Cl_2).



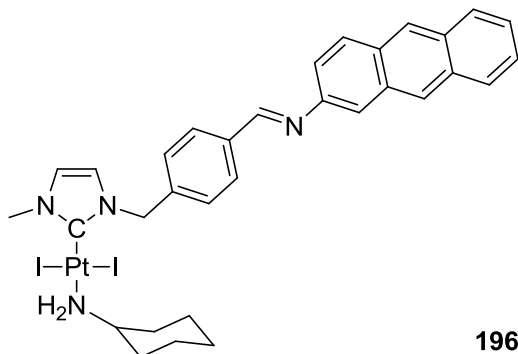
Quant. $^1\text{H-NMR}$ (CDCl_3 , 300 MHz, 20 °C): δ 1.00-1.85 (m, 18H, 18H_{CHA}), 2.27 (m, 2H, 2H_{CHA}), 2.94 (m, 2H, Pt-NH₂), 3.15 (m, 1H, CH_{CHA}), 3.27 (m, 1H, CH_{CHA}), 3.86 (s, 3H, N-CH₃), 4.54 (t, $J = 5.1\text{Hz}$, 2H, CH₂), 4.79 (t, $J = 5.1\text{Hz}$, 2H, CH₂), 6.79 (d, $J = 2.1\text{Hz}$, 1H, CH=), 6.94 (d, $J = 8.7\text{Hz}$, 2H, 2H_{ar}), 7.04 (d, $J = 2.1\text{Hz}$, 1H, CH=), 7.66 (d, $J = 8.7\text{Hz}$, 2H, 2H_{ar}), 8.23 (s, 1H, CH=N). MS (positive ESI) [M+H]: calculated for $\text{C}_{25}\text{H}_{38}\text{I}_2\text{N}_4\text{Pt}_1\text{O}_1\text{H}$: 860.09, found 860.09.



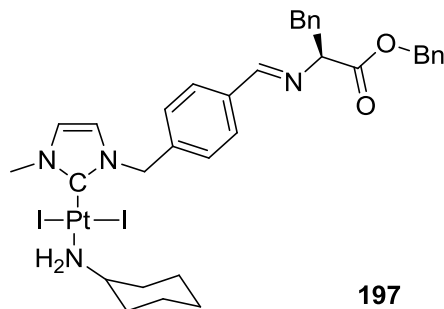
Quant. $^1\text{H-NMR}$ (CDCl_3 , 300 MHz, 20 °C): δ 1.00-1.87 (m, 10H, CHA), 2.24 (d, $J = 12.0\text{Hz}$, 2H, CH₂), 2.48 (m, 2H, CH₂), 2.92 (m, 2H, NH₂), 3.18 (m, 2H, 2CH_{CHA}), 3.86 (s, 3H, N-CH₃), 5.59 (s, 2H, N-CH₂), 6.53 (d, $J = 2.1\text{Hz}$, 1H, CH=), 6.77 (d, $J = 2.1\text{Hz}$, 1H, CH=), 7.45 (d, $J = 8.1\text{Hz}$, 2H, H_{ar}), 7.68 (d, $J = 8.1\text{Hz}$, 2H, H_{ar}), 8.28 (s, 1H, CH=N). $^{13}\text{C-NMR}$ (CDCl_3 , 75 MHz, 20 °C): δ 24.8 25.3 25.7 34.3 36.6 (CHA), 38.1 (N-CH₃), 50.5 (CHA), 54.8 (N-CH₂), 69.9 (CHA), 119.8 (CH=), 122.4 (CH=), 128.4 (CH_{Ar}), 129.1 (CH_{Ar}), 136.7 (C_{Ar}), 137.5 (C_{Ar}), 140.3 (C-Pt), 157.9 (CH=N).



44%. $^1\text{H-NMR}$ (CDCl_3 , 300 MHz, 20 °C): δ 1.00-1.95 (m, 8H, 8H_{CHA}), 2.24 (m, 2H, 2H_{CHA}), 2.94 (m, 2H, $\text{NH}_2\text{-Pt}$), 3.26 (m, 1H, CH_{CHA}), 3.91 (s, 3H, N-CH_3), 5.67 (s, 2H, N-CH_2), 6.61 (d, $J = 2.1\text{Hz}$, 1H, CH=), 6.82 (d, $J = 2.1\text{Hz}$, 1H, CH=), 7.17-7.42 (m, 5H, 5H_{ar}), 7.55 (d, $J = 8.1\text{Hz}$, 2H, 2H_{ar}), 7.91 (d, $J = 8.1\text{Hz}$, 2H), 8.46 (s, 1H, CH=N). MS (positive ESI) $[\text{M}+\text{H}]$: calculated for $\text{C}_{24}\text{H}_{30}\text{I}_2\text{N}_4\text{Pt}_1\text{H}$: 824.03 found 824.02, $[\text{M-I}]$: calculated for $\text{C}_{24}\text{H}_{30}\text{I}_1\text{N}_4\text{Pt}_1$: 696.12 found 696.11, $[\text{M-I-NH}_2\text{-C}_6\text{H}_{11}]$: calculated for $\text{C}_{18}\text{H}_{17}\text{I}_1\text{N}_3\text{Pt}_1$: 597.01 found 597.01.

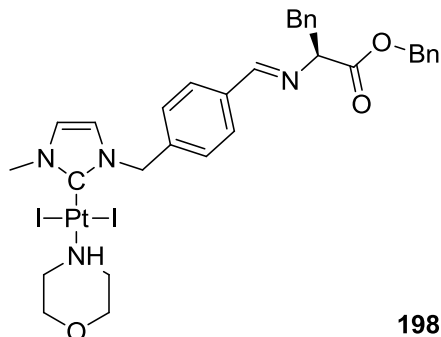


25%. $^1\text{H-NMR}$ (CDCl_3 , 300 MHz, 20 °C): δ 1.00-1.95 (m, 8H, 8H_{CHA}), 2.23 (m, 2H, 2H_{CHA}), 2.96 (m, 2H, $\text{NH}_2\text{-Pt}$), 3.25 (m, 1H, CH_{CHA}), 3.92 (s, 3H, N-CH_3), 5.69 (s, 2H, N-CH_2), 6.62 (s, 1H, CH=), 6.84 (s, 1H, CH=), 7.19-8.06 (m, 11H, 4H_{ar} and 7H_{antr}), 8.43 (s, 2H, 2H_{antr}), 8.68 (s, 1H, CH=N).

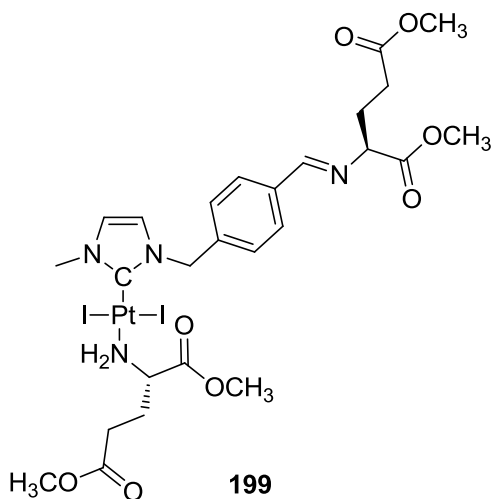


70%. $^1\text{H-NMR}$ (CDCl_3 , 300 MHz, 20 °C): δ 1.02-1.42 (m, 5H, CHA), 1.55-1.87 (m, 3H, CHA), 2.26 (m, 2H, CH_2), 2.65 (m, 2H, NH_2), 3.15-3.45 (m, 3H, $\text{CH}_{\text{CHA}} + \text{CH-CH}_2$), 3.90 (s, 3H, N-CH_3), 4.22 (m, 1H, CH^*), 5.17 (s, 2H, O-CH_2), 5.62 (s, 2H, N-CH_2), 5.57 (d, $J = 2.1\text{Hz}$, 1H, CH=), 5.80 (d, $J = 2.1\text{Hz}$, 1H, CH=), 7.01 (m, 10H, 2Ph), 7.46 (d, $J = 8.1\text{Hz}$, 2H, 2H_{ar}), 7.68 (d, $J = 8.1\text{Hz}$, 2H, 2H_{ar}), 7.93 (s, 1H, CH=N). $^{13}\text{C-NMR}$ (CDCl_3 , 75 MHz, 20 °C): 24.8 (CHA), 25.3 (CHA), 35.9 (CHA), 38.2 (CH^*-CH_2 and N-CH_3), 54.1 (CHA), 54.9 (N-CH_2), 66.8 (O-CH_2), 74.8 (CH^*), 120.0 (CH=), 122.4 (CH=), 126.6 127.4 128.2 128.5 128.7 128.9 129.1 129.3 129.7 134.8 135.7 137.3 (12 C_{ar}), 138.4 (C-Pt), 163.1 (CH=N), 171.3 (O-C=O). MS (positive ESI): $[\text{M}+\text{H}]$: calculated for $\text{C}_{34}\text{H}_{40}\text{I}_2\text{N}_4\text{O}_2\text{Pt}_1\text{H}$: 986.10

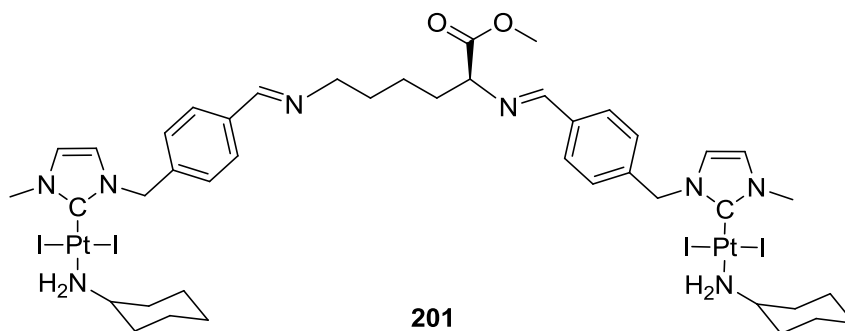
found 986.10, [M-I]: calculated for $C_{34}H_{40}N_4O_2PtI$: 858.18, found 858.18, [M-I+CH₃CN]: calculated for $C_{34}H_{40}N_4O_2PtI_1CH_3CN$: 899.21, found 899.21.



83%. ¹H-NMR (CDCl₃, 300 MHz, 20 °C): δ 2.80-3.83 (m, 11H, CH*-CH₂ and 9H_{Mo}), 3.872 (s, 3H, N-CH₃), 4.22 (dd, J= 8.5 and 5.3Hz, CH*), 5.18 (s, 2H, O-CH₂), 5.59 (s, 2H, N-CH₂), 6.57 (d, J= 2.1Hz, 1H, CH=), 6.80 (d, J= 2.1Hz, 1H, CH=), 7.11-7.33 (m, 10H, 10H_{ar}), 7.44 (d, J= 8.1Hz, 2H, 2H_{ar}), 7.68 (d, J= 8.1Hz, 2H, 2H_{ar}), 7.92 (s, 1H, CH=N). ¹³C-NMR (CDCl₃, 75 MHz, 20 °C): 38.2 (N-CH₃), 39.7 (C*-CH₂), 50.6 (NH-CH₂ Mo), 54.2 (N-CH₂), 66.8 (CH₂-O), 68.7 (O-CH₂ Mo), 74.7 (CH*), 120 (CH=), 122.5 (CH=), 126.6 128.2 128.3 128.9 129.1 129.7 (CH_{ar}), 135.7 137.3 138.3 (C_{ar}), 136.8 (C-Pt), 163.1 (CH=N), 171.3 (C=O). MS (positive ESI): [M+H]: calculated for C₃₂H₃₆I₂N₄O₃Pt₁H 974.06, found 974.06.



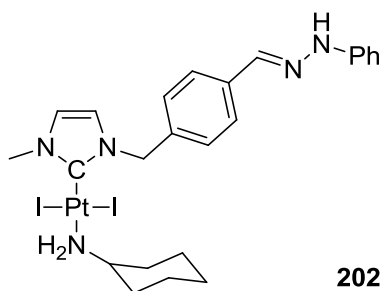
82%. ¹H-NMR (CDCl₃, 300 MHz, 20 °C): δ 2.10-2.95 (m, 8H, CH₂ Glu), 3.54 (m, 2H, NH₂), 3.63 (s, 6H, 2O-CH₃), 3.73 (s, 6H, 2O-CH₃), 3.88 (s, 3H, N-CH₃), 4.07 (m, 1H, CH_{Glu}), 4.33 (m, 1H, CH_{Glu}), 5.63 (s, 2H, N-CH₂), 6.59 (d, J= 2.1Hz, 2H, CH=), 6.83 (d, J= 2.1Hz, 2H, CH=), 7.49 (d, J= 8.1Hz, 2H, CH_{ar}), 7.77(d, J= 8.1Hz, 2H, CH_{ar}), 8.28 (s, 1H, CH=N).



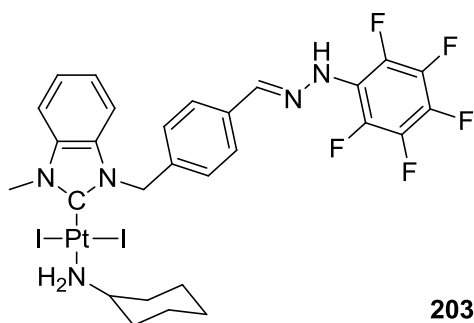
General procedure was adapted: 2.2 equivalents of platinum complexes were used for one equivalent of lysine salt. 42%. $^1\text{H-NMR}$ (CDCl_3 , 300 MHz, 20 °C): δ 0.99-2.14 (m, 22H, 16H_{CHA} and 6 H_{Lys}), 2.26 (m, 4H, 4H_{CHA}), 2.93 (m, 4H, 2NH₂-Pt), 3.23 (m, 2H, 2H_{CHA}), 3.58 (m, 2H, N-CH₂ Lys), 3.72 (s, 3H, O-CH₃), 3.89 (s, 6H, 2N-CH₃), 3.98 (m, 1H, CH_{Lys}), 5.62 (s, 2H, N-CH₂), 5.63 (s, 2H, N-CH₂), 6.56 (s, 2H, 2 CH=), 6.80 (s, 2H, 2 CH=), 7.47 (m, 4H, 4H_{ar}), 7.68 (d, J= 7.8Hz, 2H, 2H_{ar}), 7.76 7.68 (d, J= 7.8Hz, 2H, 2H_{ar}), 8.24 (s, 1H, CH=N), 8.26 (s, 1H, CH=N). $^{13}\text{C-NMR}$ (CDCl_3 , 75 MHz, 20 °C): 21.0 (C_{Lys}), 24.8 25.3 (C_{CHA}), 30.4 (C_{Lys}), 33.0 (C_{Lys}), 35.9 (C_{CHA}), 38.1 (N-CH₃), 52.2 (O-CH₃), 54.0 (C_{CHA}), 54.8 (N-CH₂), 61.2 (C_{Lys}), 73.3 (CH_{Lys}), 119.8 (CH=), 119.9 (CH=), 122.4 (CH=), 128.4 128.9 129.1 130.1 (CH_{ar}), 135.6 136.2 137.7 138.4 (C_{ar}), 140.2 140.4 (C-Pt), 160.3 162.7 (CH=N), 172.5 (C=O). MS (positive ESI) [M+H]: calculated for C₄₃H₆₂I₄N₈O₂Pt₂H: 161.05, found 1621.06, [M-I]: calculated for C₄₃H₆₂I₃N₈O₂Pt₂: 1493.14, found 1493.17.

7.3.3.3.2 Hydrazine formation

General procedure: To a mixture of benzaldehyde complex (1 eq.) and hydrazine (1 eq.) respectively hydrazinium halide (1 eq.) with triethylamine (10 eq.) was added anhydrous dichloromethane. The solution was stirred overnight at 25 °C. The solution was filtered off over celite plug and volatiles removed under reduced pressure. The crude product was purified by chromatography (SiO_2 deactivated by NEt_3 , gradient CH_2Cl_2 /pentane to CH_2Cl_2).



Quant. %. $^1\text{H-NMR}$ (CDCl_3 , 300 MHz, 20 $^\circ\text{C}$): δ 1.01-1.86 (m, 8H, 8H_{CHA}), 2.21 (m, 2H, 2H_{CHA}), 2.94 (m, 2H, $\text{NH}_2\text{-Pt}$), 3.25 (m, 1H, CH_{CHA}), 3.89 (s, 3H, N-CH_3), 5.60 (s, 2H, N-CH_2), 6.58 (d, $J = 2.1\text{Hz}$, 1H, CH=), 6.78 (d, $J = 2.1\text{Hz}$, 1H, CH=), 6.78-7.76 (m, 11H, 9H_{ar} , NH , CH=N). MS (positive ESI) $[\text{M}+\text{Na}]$: calculated for $\text{C}_{24}\text{H}_{31}\text{I}_2\text{N}_5\text{PtNa}$ 861.02, found 861.02.

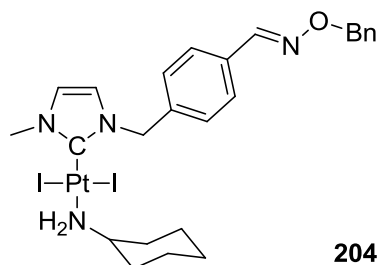


~80%. $^1\text{H-NMR}$ (CDCl_3 , 300 MHz, 20 $^\circ\text{C}$): δ 1.11-1.83 (m, 8H, 8H_{CHA}), 2.31 (m, 2H, 2H_{CHA}), 3.01 (m, 2H, Pt-NH_2), 3.28 (m, 1H, CH_{CHA}), 4.14 (s, 3H, N-CH_3), 6.00 (s, 2H, N-CH_2), 6.94 (d, $J = 8.2\text{Hz}$, 1H, 1H_{ar}), 7.05 (ddd, $J = 8.2$, 7.2 and 0.9Hz, 1H_{ar}), 7.20 (ddd, $J = 8.0$, 7.0 and 0.9Hz, 1H, CH_{ar}), 7.29 (t, $J = 2.8\text{Hz}$, 1H, NH), 7.34 (d, $J = 8.2\text{Hz}$, 1H, 1H_{ar}), 7.19 (d, $J = 8.1\text{Hz}$, 2H, 2H_{ar}), 7.60 (d, $J = 8.1\text{Hz}$, 2H, 2H_{ar}), 7.80 (s, 1H, CH=N). $^{19}\text{F-NMR}$ (CDCl_3 , 75 MHz, 20 $^\circ\text{C}$): δ -166.8 (tt, $J = 21.7$ and 4.4Hz, 1F), -163.3 (m, 2F), -156.0 (m, 2F). $^{13}\text{C-NMR}$ (CDCl_3 , 75 MHz, 20 $^\circ\text{C}$): δ 24.9 25.4 (CH_2_{CHA}), 35.0 (N-CH_3), 36.0 (CH_2_{CHA}), 52.7 (N-CH_2), 55.1 (CH_{CHA}), 110.1 110.4 (CH_{ar}), 120.5 (CF_{ar}), 123.0 123.1 127.1 128.4 (CH_{ar}), 133.8 134.0 135.4 136.6 (C_{ar} and CF_{ar}), 140.0 (CF_{ar}), 142.6 (CH=N), 154.5 (C-Pt). MS (positive ESI) $[\text{M}+\text{Na}]$: calculated for $\text{C}_{28}\text{H}_{28}\text{F}_5\text{I}_2\text{N}_5\text{PtNa}$: 1000.99, found 1000.99, $[\text{M-I}]$: calculated for $\text{C}_{28}\text{H}_{28}\text{F}_5\text{I}_1\text{N}_5\text{PtI}$: 851.10, found 851.10.

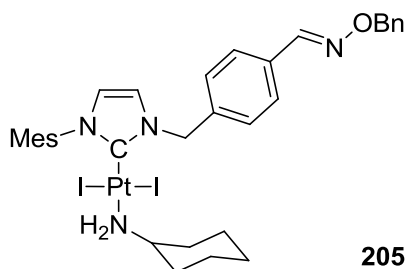
7.3.3.3 Oxime formation

General procedure: To a mixture of benzaldehyde complex (1 eq.) and hydroxylamine (1 eq.) respectively hydroxylammonium halide (1 eq.) with triethylamine (10 eq.) was added anhydrous

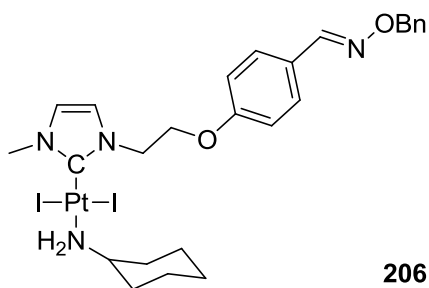
dichloromethane. The solution was stirred overnight at 25 °C. The solution was filtered off over celite plug and volatiles removed under reduced pressure. The crude product was purified by chromatography (SiO₂, CH₂Cl₂/pentane).



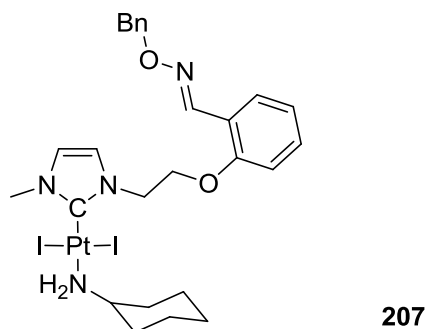
92%. ¹H-NMR (CDCl₃, 300 MHz, 20 °C): δ 1.05-1.35 (m, 5H, CHA), 1.55-1.87 (m, 3H, CHA), 2.22 (d, J= 11.7Hz, 2H, CH₂), 2.85 (m, 2H, NH₂), 3.27 (m, 1H, CH_{CHA}), 3.89 (s, 3H, N-CH₃), 5.21 (s, 2H, O-CH₂), 5.61 (s, 2H, N-CH₂), 6.56 (d, J= 2.4Hz, 1H, CH=), 6.79 (d, J= 2.4Hz, 1H, CH=), 7.26-7.64 (m, 9H, H_{ar}), 8.12 (s, 1H, CH=N). ¹³C-NMR (CDCl₃, 75 MHz, 20 °C): δ 24.8 (CHA), 25.3 (CHA), 26.9 (CHA), 35.9 (N-CH₃), 54.0 (CHA), 54.9 (N-CH₂), 77.2 (O-CH₂), 119.8 (CH=), 122.4 (CH=), 127.5 (C_{Ar}), 127.9 (C_{Ar}), 127.9 (C_{Ar}), 128.0 (C_{Ar}), 128.3 (C_{Ar}), 128.4 (C_{Ar}), 128.4 (C_{Ar}), 129.3 (C_{Ar}), 132.3 (C_{Ar}), 137.1 (C_{Ar}), 137.5 (C_{Ar}), 140.3 (C-Pt), 148.4 (CH=N). ¹H-NMR (Acetone, 300 MHz, 20 °C): δ 1.15-1.35 (m, 3H, CHA), 1.55-1.87 (m, 2H, CHA), 2.31 (m, 2H, CHA), 2.90 (m, 2H, CH₂), 3.28 (m, 1H, CH_{CHA}), 3.45 (m, 2H, NH₂), 3.86 (s, 3H, N-CH₃), 5.18 (s, 2H, O-CH₂), 5.64 (s, 2H, N-CH₂), 6.93 (d, J= 2.4Hz, 1H, CH=), 7.16 (d, J= 2.4Hz, 1H, CH=), 7.26-7.45 (m, 5H, H_{ar}), 7.59 (m, 4H, H_{ar}), 8.21 (s, 1H, CH=N). ¹³C-NMR (Acetone, 75 MHz, 20 °C): δ 24.7 (CHA), 25.3 (CHA), 29.0 (CHA hide by solvent), 35.2 (N-CH₃), 53.3 (CHA), 54.7 (N-CH₂), 76.0 (O-CH₂), 120.2 (CH=), 122.9 (CH=), 127.0 (C_{Ar}), 127.7 (C_{Ar}), 128.3 (C_{Ar}), 129.2 (C_{Ar}), 132.2 (C_{Ar}), 138.0 (C_{Ar}), 140.0 (C-Pt), 148.4 (CH=N). MS (positive ESI) [M-I]: calculated for C₂₅H₃₂I₁N₄O₁Pt₁ 726.127, found 726.130, [M-I+CH₃CN]: calculated for C₂₅H₃₂I₁N₄O₁Pt₁CH₃CN 767.153, found 767.153, [M+Na]: calculated for C₂₅H₃₂I₂N₄O₁Pt₁Na 876.021 found 876.023. RX: mdgd120509



%. $^1\text{H-NMR}$ (CDCl_3 , 300 MHz, 20 °C): δ 0.96-1.19 (m, 5H, 5H_{CHA}), 1.52-1.67 (m, 3H, 3H_{CHA}), 1.98 (m, 2H, 2H_{CHA}), 2.29 (s, 6H, $2\text{CH}_3_{\text{Mes}}$), 2.33 (s, 3H, CH_3_{Mes}), 2.83 (m, 2H, Pt-NH_2), 3.00 (m, 1H, CH_{CHA}), 5.22 (s, 2H, O-CH_2), 5.76 (s, 2H, N-CH_2), 6.73 (d, $J = 2.1\text{Hz}$, 1H, CH=), 6.78 (d, $J = 2.1\text{Hz}$, 1H, CH=), 6.97 (s, 2H, 2H_{ar}), 7.27-7.45 (m, 5H, 5H_{ar}), 7.51 (d, $J = 8.2\text{Hz}$, 2H, 2H_{ar}), 7.62 (d, $J = 8.2\text{Hz}$, 2H, 2H_{ar}), 8.15 (s, 1H, CH=N). $^{13}\text{C-NMR}$ (CDCl_3 , 75 MHz, 20 °C): δ 21.1 (CH_3_{Mes}), 21.2 (CH_3_{Mes}), 24.8 (CHA), 25.2 (CHA), 35.7 (CHA), 54.9 (N-CH_2), 55.0 (CHA), 76.5 (O-CH_2), 119.7 (CH=), 123.9 (CH=), 127.5 128.0 128.3 128.4 129.0 129.2 132.2 135.1 135.9 137.3 137.4 138.8 (C_{Ar}), 142.1 (C-Pt), 148.4 (CH=N). $[\text{M}+\text{H}]$: calculated for $\text{C}_{33}\text{H}_{40}\text{O}_1\text{I}_2\text{N}_4\text{Pt}_1\text{H}$: 958.1015, found 958.1108.

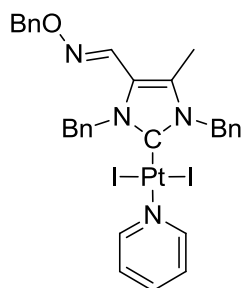


73%. $^1\text{H-NMR}$ (CDCl_3 , 300 MHz, 20 °C): δ 1.01-1.83 (m, 8H, 8H_{CHA}), 2.25 (m, 2H, 2H_{CHA}), 2.94 (m, 2H, Pt-NH_2), 3.24 (m, 1H, CH_{CHA}), 3.86 (s, 3H, N-CH_3), 4.52 (t, $J = 5.1\text{Hz}$, 2H, CH_2), 4.78 (t, $J = 5.1\text{Hz}$, 2H, CH_2), 5.18 (s, 2H, O-CH_2), 6.79 (d, $J = 1.9\text{Hz}$, 1H, CH=), 6.91 (d, $J = 8.7\text{Hz}$, 2H, 2H_{ar}), 7.03 (d, $J = 1.9\text{Hz}$, 1H, CH=), 7.28-7.48 (m, 5H, 5H_{ar}), 7.50 (d, $J = 8.7\text{Hz}$, 2H, 2H_{ar}), 8.07 (s, 1H, CH=N). $^{13}\text{C-NMR}$ (CDCl_3 , 75 MHz, 20 °C): δ 24.8 (CH_2_{CHA}), 25.2 (CH_2_{CHA}), 35.9 (CH_2_{CHA}), 38.0 (N-CH_3), 49.7 (N-CH_2), 54.8 (CH_{CHA}), 66.5 (O-CH_2), 76.2 ($\text{CH}_2\text{-ON}$), 114.8 (CH_{ar}), 121.8 121.9 (CH=CH), 125.4 (C_{ar}), 127.9 128.3 128.4 128.6 (CH_{ar}), 137.6 (C_{ar}), 139.6 (C-Pt), 148.5 (CH=N), 159.5 ($\text{C}_{\text{ar-O}}$). MS (positive ESI) $[\text{M}+\text{Na}]$: calculated for $\text{C}_{26}\text{H}_{34}\text{I}_2\text{N}_4\text{Pt}_1\text{O}_2\text{Na}$: 906.03, found 906.03, $[\text{M-I}]$: calculated for $\text{C}_{26}\text{H}_{34}\text{I}_1\text{N}_4\text{Pt}_1\text{O}_2$: 756.14, found 756.13.

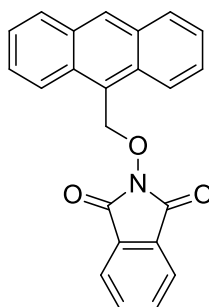


72%. $^1\text{H-NMR}$ (CDCl_3 , 300 MHz, 20 °C): δ 1.03-1.87 (m, 8H, 8H_{CHA}), 2.27 (m, 2H, 2H_{CHA}), 2.92 (m, 2H, Pt-NH_2), 3.25 (m, 1H, CH_{CHA}), 3.85 (s, 3H, N-CH_3), 4.54 (t, $J = 5.1\text{Hz}$, 2H, CH_2), 4.77 (t, $J =$

5.1Hz, 2H, CH₂), 5.22 (s, 2H, O-CH₂), 6.74 (d, J= 2.0Hz, 1H, CH=), 6.92-7.01 (m, 3H, 3H_{ar}), 7.26-7.45 (m, 7H, 7H_{ar}), 7.74 (dd, J= 7.6 and 2.0Hz, 1H, 1H_{ar}), 8.47 (s, 1H, CH=N). ¹³C-NMR (CDCl₃, 75 MHz, 20 °C): δ 24.9 (C_{CHA}), 25.4 (C_{CHA}), 36.0 (C_{CHA}), 38.2 (N-CH₃), 50.0 (N-CH₂), 55.0 (CH_{CHA}), 67.1 (O-CH₂), 76.4 (CH₂-ON), 112.7 (CH_{ar}), 120.9 (C_{ar}), 121.5 122.0 122.2 128.1 128.5 128.6 131.4 (CH_{ar} and CH=CH), 137.8 (C_{ar}), 139.7 (C-Pt), 145.3 (CH=N), 156.3 (C_{ar}-O). MS (positive ESI) [M+H]⁺: calculated for C₂₆H₃₄I₂N₄Pt₁O₂H₁: 884.049, found 884.046, [M+Na]⁺: calculated for C₂₆H₃₄I₂N₄Pt₁O₂Na₁: 906.031, found 906.027, [M-I]⁺: calculated for C₂₆H₃₄I₁N₄Pt₁O₂: 756.137, found 756.133.

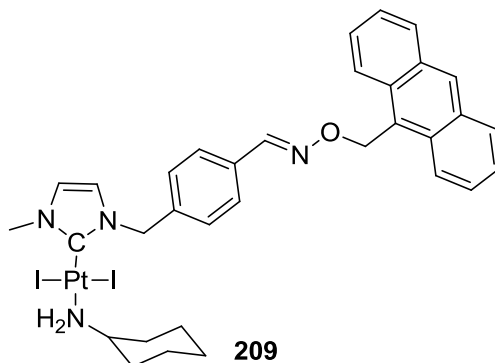
**208**

21%. ¹H-NMR (CDCl₃, 300 MHz, 20 °C): δ 2.01 (s, 3H, CH₃), 4.98 (s, 2H, O-CH₂), 5.95 (s, 2H, N-CH₂), 6.07 (s, 2H, N-CH₂), 7.10-7.50 (m, 17H, 15H_{ar} and 2H_{pyr}), 7.67 (tt, J= 7.7 and 1.6Hz, 1H, 1H_{pyr}), 7.75 (s, 1H, CH=N), 8.92 (m, 2H, 2H_{pyr}). ¹³C-NMR (CDCl₃, 75 MHz, 20 °C): δ 10.7 (CH₃), 53.8 (N-CH₂), 54.4 (N-CH₂), 123.5 125.0 127.6 127.7 127.8 128.0 128.2 128.5 128.6 128.9 132.4 135.5 136.1 137.2 137.6 137.8 141.7 (CH_{ar}, C_{ar}, C=C, C_{pyr} and C-Pt), 153.9 (C_{pyr}). MS (positive ESI) [M-I]⁺: calculated for C₃₁H₃₀I₁N₄Pt₁O₁: 796.1109, found 796.0995.

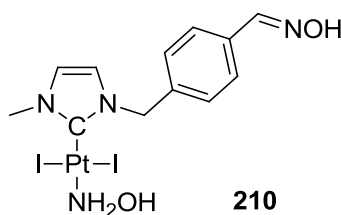


The compound was obtained from 9-(chloromethyl)anthracene 2-hydroxyisindoline-1,3-dione adopting reported procedure. O-(anthracen-9-ylmethyl)hydroxylamine was obtained by hydrazine deprotection and used without any isolation. ¹H-NMR (CDCl₃, 300 MHz, 20 °C): δ 6.21 (s, 2H, CH₂-O), 7.51 (t, J= 7.5Hz, 2H, 2H_{ar}), 7.68 (t, J= 7.6, 2H, 2H_{ar}), 7.72-7.92 (m, 4H, 4H_{ar}), 8.04 (d, J= 8.4Hz, 2H, 2H_{ar}), 8.56 (s, 1H, H_{ar}), 8.73 (d, J= 9.0Hz, 2H, 2H_{ar}). ¹³C-NMR (CDCl₃, 75 MHz, 20 °C): δ 72.1

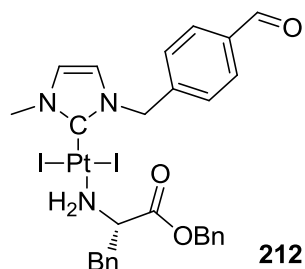
(CH₂-O), 123.6 (CH_{ar}), 123.8 (C_{ar}), 124.1 (CH_{ar}), 125.2 (CH_{ar}), 127.2 (CH_{ar}), 129.0 (CH_{ar}), 129.1 (C_{ar}), 130.2 (CH_{ar}), 131.3 (C_{ar}), 132.0 (C_{ar}), 134.5 (CH_{ar}), 163.7 (C=O).



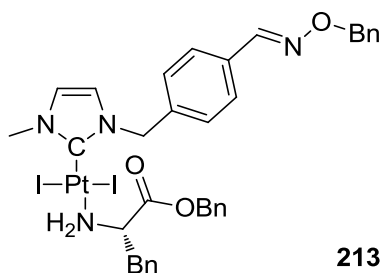
98%. ¹H-NMR (CDCl₃, 300 MHz, 20 °C): δ 1.05-1.35 (m, 5H, CHA), 1.55-1.84 (m, 3H, CHA), 2.27 (m, 2H, CHA), 2.94 (m, 2H, NH₂-Pt), 3.24 (m, 1H, CH_{CHA}), 3.90 (s, 3H, N-CH₃), 5.60 (s, 2H, N-CH₂), 6.22 (s, 2H, O-CH₂), 6.55 (d, J= 2.1Hz, 1H, CH=), 6.79 (d, J= 2.1Hz, 1H, CH=), 7.40-7.62 (m, 8H, 2H_{ar}+ 6H_{antr}), 8.02 (d, J= 8.1Hz, 2H, 2H_{ar}), 8.08 (s, 1H, CH=N or 1H_{antr}), 8.74 (s, 1H, CH=N or 1H_{antr}), 8.50 (s, 2H, 2H_{antr}). ¹³C-NMR (CDCl₃, 75 MHz, 20 °C): δ 24.8 (CHA), 25.5 (CHA), 35.9 (CHA), 38.1 (N-CH₃), 54.0 and 54.8 (CH_{CHA} and N-CH₂), 68.7 (O-CH₂), 119.8 (CH=), 122.4 (CH=), 124.4 125.0 126.4 127.3 127.4 128.9 129.0 129.3 131.2 131.4 132.2 137.0 (C_{ar}), 140.2 (C-Pt), 148.4 (CH=N). UV/Vis (CH₂Cl₂) λ_{max} (nm) (ε, M⁻¹ cm⁻¹): 273 (7833), 367 (6812), 392 (6788); luminescent properties: λ_{exc}=368 nm; λ_{em}= 400-470 nm.



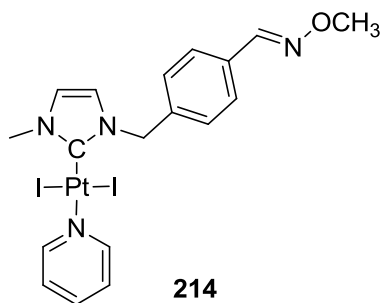
The product was eluted by a mixture of CH₂Cl₂/MeOH 10/1. 39%. ¹H-NMR (CDCl₃, 300 MHz, 20 °C): δ 3.89 (s, 3H, N-CH₃), 5.59 (s, 2H, N-CH₂), 5.83 (t, J= 3.5Hz, 1H, OH), 5.97 (m, 2H, NH₂), 6.64 (d, J= 1.2Hz, 1H, CH=), 6.85 (d, J= 1.2Hz, 1H, CH=), 7.23 (s, 1H, OH), 7.43 (d, J= 8.1Hz, 2H, H_{ar}), 7.59 (d, J= 8.1Hz, 2H, H_{ar}), 8.13 (s, 1H, CH=N). MS (positive ESI): [M-I]: calculated for C₁₂H₁₆I₁N₄O₂Pt₁: 570.00, found 570.00, [M+Na]: calculated for C₁₂H₁₆I₂N₄O₂Pt₁Na 719.89, found 719.89.



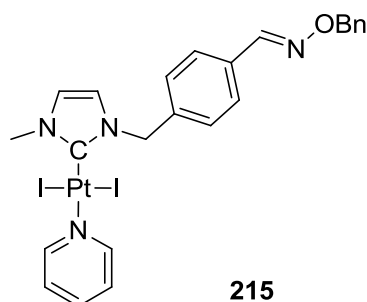
The product was synthesized by ligand exchange from **79** using 5 eq. of ammonium ester salt. Purification was undertaken by SiO₂ gel chromatography. 82%. ¹H-NMR (CDCl₃, 300 MHz, 20 °C): δ 3.10-3.51 (m, 4H, CH₂ and NH₂), 3.69 (s, 2H, O-CH₂), 3.89 (s, 3H, N-CH₃), 4.63 (m, 1H, CH), 5.67 (s, 2H, N-CH₂), 6.63 (d, J= 2.1Hz, 1H, CH=), 6.85 (d, J= 2.1Hz, 1H, CH=), 7.19-7.39 (m, 10H, 10H_{ar}), 7.58 (d, J= 8.1Hz, 2H, H_{ar}), 7.87 (d, J= 8.1Hz, 2H, H_{ar}), 10.00 (s, 1H, CH=O). ¹³C-NMR (CDCl₃, 75 MHz, 20 °C): δ 38.3 (N-CH₃), 38.8 (CH₂), 52.5 (N-CH₂), 59.5 (CH), 65.4 (O-CH₂), 120.1 (CH=), 122.8 (CH=), 127.0 127.5 127.6 128.6 128.9 129.3 129.6 130.2 134.8 136.2 (C_{ar}), 138.5 (C-Pt), 140.9 (C_{ar}), 142.1 (C_{ar}), 172.9 (C=O), 191.7 (CH=O). MS (positive ESI): [M+Na]: calculated for C₂₈H₂₉I₂N₃O₃Pt₁Na 926.98, found 926.98.



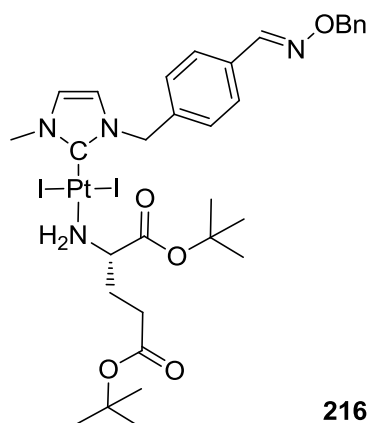
The product was synthesized by oxime condensation from **215**. 75%. ¹H-NMR (CDCl₃, 300 MHz, 20 °C): δ 3.15-3.50 (m, 4H, CH₂ and NH₂), 3.70 (s, 2H, O-CH₂), 3.87 (s, 3H, N-CH₃), 4.64 (m, 1H, CH), 5.20 (s, 2H, NO-CH₂), 5.57 (s, 2H, N-CH₂), 6.57 (d, J= 2.1Hz, 1H, CH=), 6.80 (d, J= 2.1Hz, 1H, CH=), 7.19-7.50 (m, 17H, 17H_{ar}), 7.58 (d, J= 8.1Hz, 2H, H_{ar}), 8.12 (s, 1H, CH=N). ¹³C-NMR (CDCl₃, 75 MHz, 20 °C): δ 38.2 (N-CH₃), 38.8 (CH₂), 54.1 (N-CH₂), 59.5 (CH), 65.4 (O-CH₂), 76.5 (NO-CH₂ hide by solvent, visible by DEPT135), 120.0 (CH=), 122.5 (CH=), 127.0 127.5 127.7 128.0 128.4 128.5 128.6 128.7 128.9 129.3 129.7 (CH_{ar}), 132.3 134.8 136.9 137.4 (C_{ar}), 137.7 (C-Pt), 148.4 (CH=N), 172.9 (O-C=O). MS (positive ESI): [M+Na]: calculated for C₃₅H₃₆I₂N₄O₃Pt₁Na 1032.04 found 1032.05.



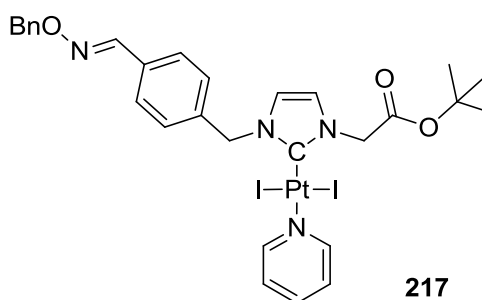
The oxime condensation was carried out without the presence of NEt_3 . 52%. $^1\text{H-NMR}$ (CDCl_3 , 300 MHz, 20 °C): δ 3.99 (s, 3H, N- CH_3), 4.58 (s, 3H, O- CH_3), 5.72 (s, 2H, N- CH_2), 6.58 (s, 1H, CH=), 6.84 (d, J = 1.8Hz, 1H, CH=), 7.32 (ddd, J = 7.5, 4.8 and 1.6Hz, 2H, 2H_{Pyr}), 7.43 (d, J = 8.1Hz, 2H, 2H_{ar}), 7.58 (d, J = 8.1Hz, 2H, 2H_{ar}), 7.72 (tt, J = 7.6 and 1.5Hz, 1H, 1H_{Pyr}), 8.20 (s, 1H, CH=N), 9.02 (m, 2H, 2H_{Pyr}).



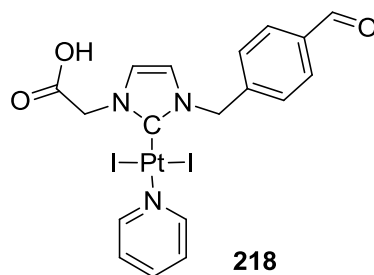
The oxime condensation was carried out without the presence of NEt_3 . 40%. $^1\text{H-NMR}$ (CDCl_3 , 300 MHz, 20 °C): δ 4.00 (s, 3H, N- CH_3), 5.21 (s, 2H, N- CH_2), 5.74 (s, 2H, O- CH_2), 6.60 (d, J = 2.1Hz, 1H, CH=), 6.83 (d, J = 2.1Hz, 1H, CH=), 7.29-7.44 (m, 7H, $5\text{H}_{\text{ar}}+2\text{H}_{\text{Pyr}}$), 7.50 (d, J = 8.1Hz, 2H, 2H_{ar}), 7.60 (d, J = 8.1Hz, 2H, 2H_{ar}), 7.72 (tt, J = 7.7 and 1.5Hz, 1H, 1H_{Pyr}), 8.13 (s, 1H, CH=N), 9.04 (m, 2H, 2H_{Pyr}). $^{13}\text{C-NMR}$ (CDCl_3 , 75 MHz, 20 °C): δ 38.3 (N- CH_3), 54.2 (N- CH_2), 76.5 (O- CH_2), 119.9 122.5 (CH=CH), 124.9 (C_{Pyr}), 127.5 128.0 128.4 129.3 (CH_{ar}), 132.3 (C_{ar}), 136.8 (C-Pt), 137.0 137.4 (C_{ar}), 137.4 (C_{Pyr}), 148.4 (CH=N), 1537 (C_{Pyr}).



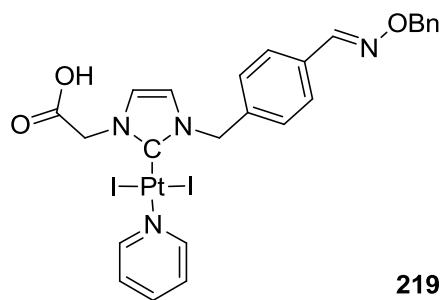
The product was obtained from **215** by ligand exchange. 54%. $^1\text{H-NMR}$ (CDCl_3 , 300 MHz, 20 °C): δ 1.41 (s, 9H, $\text{O-C(CH}_3)_3$), 1.47 (s, 9H, $\text{O-C(CH}_3)_3$), 2.27-2.69 (m, 2H, 2H_{Glu}), 3.29-3.53 (m, 4H, $2\text{H}_{\text{Glu}}+\text{NH}_2$), 3.99 (m, 1H, 1H_{Glu}), 4.06 (s, 3H, N- CH_3), 5.20 (s, 2H, N- CH_2), 5.74 (s, 2H, O- CH_2), 6.63 (d, $J = 2.1\text{Hz}$, 1H, CH=), 6.80 (d, $J = 2.1\text{Hz}$, 1H, CH=), 7.30-7.44 (m, 7H, 7H_{ar}), 7.57 (d, $J = 8.2\text{Hz}$, 2H, 2H_{ar}), 8.11 (s, 1H, CH=N). $^{13}\text{C-NMR}$ (CDCl_3 , 75 MHz, 20 °C): δ 27.9 (CH_2), 28.1 28.2 ($\text{OC(CH}_3)_3$), 31.3 (CH_2), 37.6 (N- CH_3), 53.7 (CH), 55.5 (N- CH_2), 80.9 (O- CH_2), 83.1 83.2 ($\text{OC(CH}_3)_3$), 120.1 122.6 (CH=CH), 127.6 128.1 128.6 128.9 129.2 (CH_{ar}), 132.4 (C_{ar}), 137.4 (C-Pt), 137.6 137.7 (C_{ar}), 148.6 (CH=N), 171.8 171.9 (2C=O). MS (positive ESI) $[\text{M-I}]$: calculated for $\text{C}_{32}\text{H}_{44}\text{I}_1\text{N}_4\text{O}_5\text{Pt}_1$: 886.2001, found 886.2091.



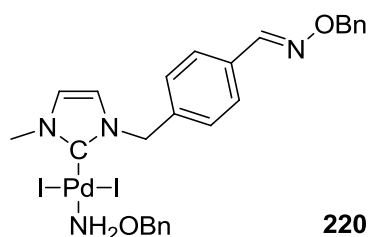
quant. $^1\text{H-NMR}$ (CDCl_3 , 300 MHz, 20 °C): δ 1.54 (s, 9H, $\text{C(CH}_3)_3$), 5.21 (s, 2H, CH_2), 5.28 (s, 2H, CH_2), 5.74 (s, 2H, CH_2), 6.64 (d, $J = 2.1\text{Hz}$, 1H, CH=), 7.01 (d, $J = 2.1\text{Hz}$, 1H, CH=), 7.28-7.44 (m, 7H, 5H_{ar} and 2H_{Pyr}), 7.50 (d, $J = 8.1\text{Hz}$, 2H, 2H_{ar}), 7.60 (d, $J = 8.1\text{Hz}$, 2H, 2H_{ar}), 7.72 (tt, $J = 5.1$ and 1.6Hz , 1H, 1H_{pyr}), 8.13 (s, 1H, CH=N), 9.03 (m, 2H, 2H_{pyr}). $^{13}\text{C-NMR}$ (CDCl_3 , 75 MHz, 20 °C): δ 28.4 (3CH_3), 53.4 (N- CH_2), 54.6 (N- CH_2), 76.7 (O- CH_2), 83.2 (O-C), 120.3 122.6 (CH=CH), 125.1 (C_{Pyr}), 127.6 128.1 128.6 129.5 129.5 (CH_{ar}), 132.5 (C_{ar}), 137.0 (C_{ar}), 137.6 (C_{Pyr}), 138.7 (C-Pt), 148.6 (C=N), 153.9 (C_{Pyr}), 166.3 (C=O).



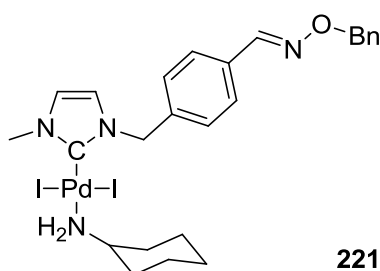
Quant. $^1\text{H-NMR}$ (Acetone, 300 MHz, 20 °C): δ 5.48 (s, 2H, N-CH₂), 5.89 (s, 2H, N-CH₂), 7.14 (d, J= 2.1Hz, 1H, CH=), 7.38 (d, J= 2.1Hz, 1H, CH=), 7.51 (t, J= 7.1, 2H, 2H_{pyr}), 7.78-7.99 (m, 5H, 4H_{ar}+1H_{pyr}), 8.99 (m, 2H, 2H_{pyr}), 10.07 (s, 1H, CH=O). $^{13}\text{C-NMR}$ (CDCl₃, 75 MHz, 20 °C): δ 52.0 (N-CH₂), 54.6 (N-CH₂), 121.8 124.3 (CH=CH), 126.0 (C_{pyr}), 130.4 (2CH_{ar}), 137.3 (C_{ar}), 139.0 (C_{pyr}), 139.7 (C-Pt), 143.7 (C_{ar}), 154.4 (C_{pyr}), 168.6 (C=O), 192.6 (CH=O).



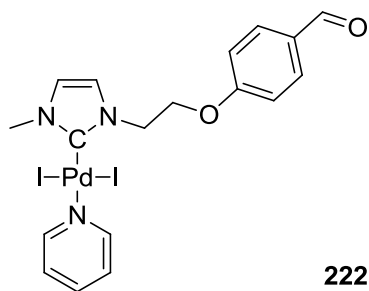
The product was obtained from **217** by ester deprotection (HCO₂H/CH₂Cl₂, 25 °C) 89% or from **79** by ester deprotection (HCO₂H/CH₂Cl₂, 25 °C) followed by oxime condensation (1 week). 52%. $^1\text{H-NMR}$ (CDCl₃, 300 MHz, 20 °C): δ 5.21 (s, 2H, O-CH₂), 5.43 (s, 2H, N-CH₂), 5.73 (s, 2H, N-CH₂), 6.66 (d, J= 2.1Hz, 1H, CH=), 7.01 (d, J= 2.1Hz, 1H, CH=), 7.26-7.72 (m, 12H, 9H_{ar} and 3H_{pyr}), 8.13 (s, 1H, CH=N), 9.00 (m, 2H, 2H_{pyr}). $^{13}\text{C-NMR}$ (CDCl₃, 75 MHz, 20 °C): δ 53.5 (N-CH₂), 54.3 (N-CH₂), 75.4 (O-CH₂), 120.6 123.8 (CH=CH), 125.2 (C_{pyr}), 127.6 128.1 128.5 128.6 129.5 132.3 (C_{ar}), 137.2 (C-Pt), 137.6 (C_{pyr}), 148.6 (C=N), 153.8 (C_{pyr}), 192.6 (CH=O). MS (negative ESI) [M-H]: calculated for C₂₅H₂₃I₂N₄PtO₂: 875.95, found 875.95, [M-H-pyr]: calculated for C₂₀H₁₈I₂N₃PtO₃: 796.91, found 796.92, [M+I]: calculated for C₂₅H₂₄I₃N₄PtO₂: 1009.86, found 1009.87, [M+Cl]: calculated for C₂₅H₂₄I₂N₄PtO₂Cl₁: 911.93, found 911.93.



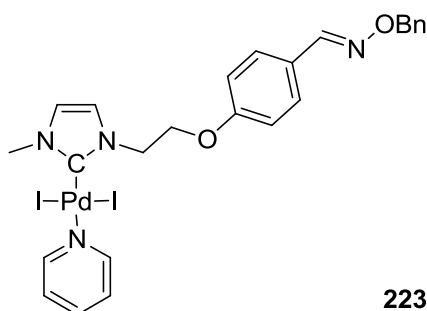
Instable at room temperature. $^1\text{H-NMR}$ (CDCl_3 , 300 MHz, 20 °C): δ 3.91 (s, 3H, N- CH_3), 4.70 (s, 2H, O- CH_2), 5.21 (s, 2H, O- CH_2), 5.80 (s, 2H, N- CH_2), 6.64 (d, J = 2.0Hz, 1H, CH=), 6.90 (d, J = 2.0Hz, 1H, CH=), 7.26-7.51 (m, 12H, H_{ar}), 7.59 (d, J = 8.1Hz, 2H, H_{ar}), 8.12 (s, 1H, CH=N).



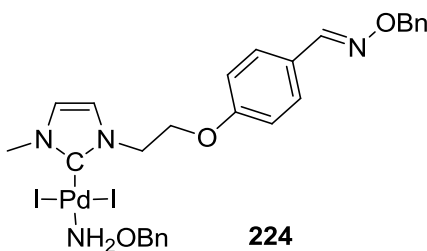
Instable at room temperature. MS (positive ESI) $[\text{M-I}]$: calculated for $\text{C}_{25}\text{H}_{32}\text{I}_2\text{N}_4\text{O}_1\text{Pd}_1$ 637.07, found 637.07, $[\text{M+H}]$: calculated for $\text{C}_{25}\text{H}_{32}\text{I}_2\text{N}_4\text{O}_1\text{Pd}_1\text{H}$ 764.98 found 764.99.



Procedure *a* from PdCl_2 in pyridine: 37%. $^1\text{H-NMR}$ (CDCl_3 , 300 MHz, 20 °C): δ 3.94 (s, 3H, N- CH_3), 4.66 (t, J = 5.1Hz, 2H, CH_2), 4.85 (t, J = 5.1Hz, 2H, CH_2), 6.93 (d, J = 2.0Hz, 1H, CH=), 7.04 (d, J = 8.8Hz, 2H, 2H_{ar}), 7.15 (d, J = 2.0Hz, 1H, CH=), 7.15 (m, 2H, 2H_{Pyr}), 7.71 (tt, J = 7.7 and 1.6Hz, 1H, 1H_{Pyr}), 7.80 (d, J = 8.8Hz, 2H, 2H_{ar}), 9.00 (m, 2H, 2H_{Pyr}), 9.85 (s, 1H, CH=O). $^{13}\text{C-NMR}$ (CDCl_3 , 75 MHz, 20 °C): δ 39.1 (N- CH_3), 50.4.7 (N- CH_2), 66.5 (O- CH_2), 115.0 (CH_{ar}), 123.3 123.5 (CH=CH), 124.5 (C_{Pyr}), 130.4 (C_{ar}), 132.0 (CH_{ar}), 137.8 (C_{Pyr}), 146.1 (C-Pd), 153.8 (C_{Pyr}), 163.0 ($\text{C}_{\text{ar-O}}$), 190.7 (CH=O). MS (positive ESI) $[\text{M+H}]$: calculated for $\text{C}_{18}\text{H}_{19}\text{I}_2\text{N}_3\text{Pd}_1\text{O}_2\text{H}_1$: 669.8681, found 669.8527.



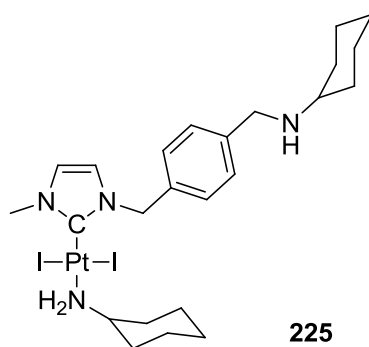
The product was obtained by oxime condensation without the presence of NEt_3 . 54%. $^1\text{H-NMR}$ (CDCl_3 , 300 MHz, 20 °C): δ 3.98 (s, 3H, N- CH_3), 4.60 (t, J = 5.0Hz, 2H, CH_2), 4.86 (t, J = 5.0Hz, 2H, CH_2), 5.18 (s, 2H, O- CH_2), 6.93 (m, 2H, 2H_{ar}), 6.96 (d, J = 2.0Hz, 1H, CH=), 7.18 (d, J = 2.0Hz, 1H, CH=), 7.26-7.56 (m, 9H, $7\text{H}_{\text{ar}}+2\text{H}_{\text{pyr}}$), 7.74 (tt, J = 7.7 and 1.6Hz, 1H, 1H_{pyr}), 8.08 (s, 1H, CH=N), 9.04 (m, 2H, 2H_{pyr}). $^{13}\text{C-NMR}$ (CDCl_3 , 75 MHz, 20 °C): δ 39.0 (N- CH_3), 50.6 (N- CH_2), 66.3 (O- CH_2), 76.2 ($\text{CH}_2\text{-ON}$), 114.9 (CH_{ar}), 123.3 123.3 (CH=CH), 124.5 (C_{pyr}), 125.5 (C_{ar}), 127.9 128.3 128.4 128.6 (CH_{ar}), 137.6 (C_{ar}), 137.7 (C_{pyr}), 146.0 (C-Pd), 148.5 (CH=N), 153.9 (C_{pyr}), 159.4 ($\text{C}_{\text{ar-O}}$).



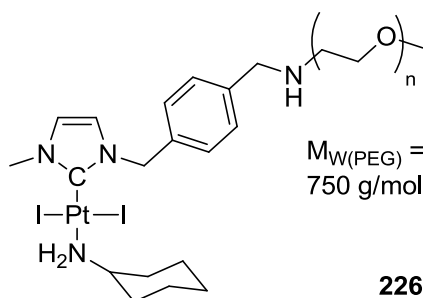
Instable at room temperature. $^1\text{H-NMR}$ (CDCl_3 , 300 MHz, 20 °C): δ 3.87 (s, 3H, N- CH_3), 4.51 (t, J = 4.9Hz, 2H, CH_2), 4.73 (t, J = 4.9Hz, 2H, CH_2), 5.09 (s, 2H, O- CH_2), 5.19 (s, 2H, O- CH_2), 6.90 (m, 2H, 2H_{ar}), 6.92 (s, 1H, CH=), 7.16 (d, J = 1.8Hz, 1H, CH=), 7.26-7.53 (m, 12H, 12H_{ar}), 8.08 (s, 1H, CH=N). $^{13}\text{C-NMR}$ (CDCl_3 , 75 MHz, 20 °C): δ 39.0 (N- CH_3), 50.6 (N- CH_2), 66.3 (O- CH_2), 76.2 ($\text{CH}_2\text{-ON}$), 78.5 ($\text{CH}_2\text{-ON}$), 114.8 (CH_{ar}), 123.4 (CH=CH), 125.5 (C_{ar}), 127.9 128.3 128.4 128.6 128.9 (CH_{ar}), 133.9 (C_{ar}), 137.6 (C_{ar}), 146.9 (C-Pd), 148.5 (CH=N), 159.3 ($\text{C}_{\text{ar-O}}$).

7.3.3.4 Imine hydrogenation

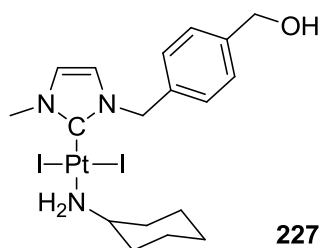
General procedure: A solution of the imine precursor (1 eq) and sodium triacetoxyborohydride (3 eq) in CH_2Cl_2 was stirred overnight at 25 °C. After filtration over celite plug, evaporation of volatiles, and silica gel chromatography (SiO_2 deactivated by NEt_3 , gradient CH_2Cl_2 /pentane to CH_2Cl_2) the product is obtained as a yellow powder.



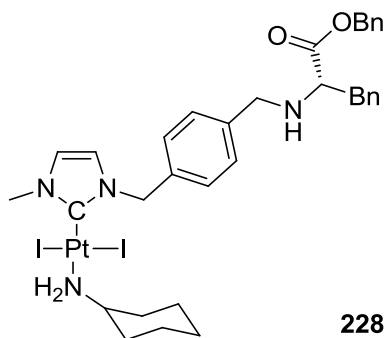
48%. $^1\text{H-NMR}$ (CDCl_3 , 300 MHz, 20 °C): δ 1.00-2.07 (m, 18H, CHA), 2.27 (m, 2H, CHA), 2.72 (m, 1H, CH_{CHA}), 2.92 (m, 2H, $\text{NH}_2\text{-Pt}$), 3.23 (m, 1H, CH_{CHA}), 3.87 (s, 3H, N- CH_3), 3.96 (s, 2H, Ph- CH_2), 5.54 (s, 2H, N- CH_2), 6.41 (m, 1H, NH), 6.57 (d, $J = 1.8\text{Hz}$, 1H, CH=), 7.78 (d, $J = 1.8\text{Hz}$, 1H, CH=), 7.42 (d, $J = 8.1\text{Hz}$, 2H, H_{ar}), 7.47 (d, $J = 8.1\text{Hz}$, 2H, H_{ar}). $^{13}\text{C-NMR}$ (CDCl_3 , 75 MHz, 20 °C): δ 24.6 24.8 25.2 25.3 30.1 35.8 (CHA), 38.1 (N- CH_3), 47.6 (CH_{CHA}), 53.8 ($\text{CH}_2\text{-NH}$), 54.8 (N- CH_2), 55.2 (CH_{CHA}), 120.0 (CH=), 122.3 (CH=), 129.4 (CH_{Ar}), 130.0 (CH_{Ar}), 133.6 (C_{Ar}), 135.9 (C_{Ar}), 140.1 (C-Pt). MS (positive ESI): $[\text{M}+\text{H}]$: calculated for $\text{C}_{24}\text{H}_{38}\text{I}_2\text{N}_4\text{PtH}$: 832.09, found 832.08.



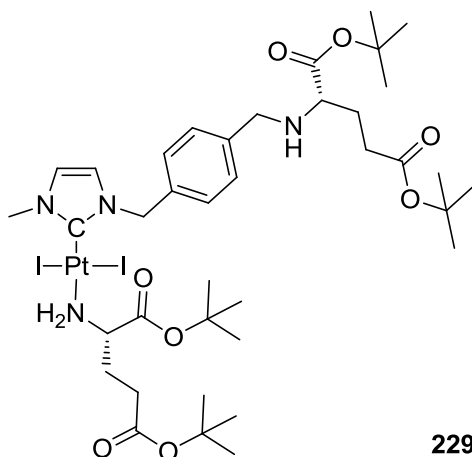
24%. $^{13}\text{C-NMR}$ (CDCl_3 , 75 MHz, 20 °C): δ 24.9 25.3 35.9 (CHA), 38.2 (N- CH_3), 50.4 (CHA), 53.8 (NH- $\text{CH}_2\text{-Ph}$) 54.9 57.2 (CH_{CHA} and N- CH_2), 59.1(O- CH_3), 70.2 70.6 71.9 ($\text{CH}_2\text{ PEG}$), 120.5 (CH=), 122.4 (CH=), 128.8 129.7 132.2 137.6 (C_{ar}), 140.6 (C-Pt).



95%. $^1\text{H-NMR}$ (CDCl_3 , 300 MHz, 20 °C): δ 1.00-1.38 (m, 5H, CHA), 1.55-1.82 (m, 3H, CHA), 2.28 (m, 2H, CHA), 2.93 (m, 2H, NH_2), 3.25 (m, 1H, CH_{CHA}), 3.89 (s, 3H, N- CH_3), 4.70 (s, 2H, CH_2OH), 5.59 (s, 2H, N- CH_2), 6.56 (d, $J = 2.1\text{Hz}$, 1H, $\text{CH}=\text{}$), 6.78 (d, $J = 2.1\text{Hz}$, 1H, $\text{CH}=\text{}$), 7.37 (d, $J = 8.1\text{Hz}$, 2H, H_{ar}), 7.45 (d, $J = 8.1\text{Hz}$, 2H, H_{ar}). $^{13}\text{C-NMR}$ (CDCl_3 , 75 MHz, 20 °C): δ 24.8 (CHA), 25.3 (CHA), 35.9 (CHA), 38.1 (N- CH_3), 54.0 (N- CH_2), 54.8 (CHA), 65.0 (CH_2OH), 119.8 ($\text{CH}=\text{}$), 122.2 ($\text{CH}=\text{}$), 127.4 (CH_{Ar}), 129.2 (CH_{Ar}), 134.8 (C_{Ar}), 139.9 (C-Pt), 140.9 (C_{Ar}). MS (positive ESI): $[\text{M}+\text{Na}]$: calculated for $\text{C}_{18}\text{H}_{27}\text{I}_2\text{N}_3\text{O}_1\text{Pt}_1\text{Na}$: 772.98, found 772.98, $[\text{M}-\text{I}]$: calculated for $\text{C}_{18}\text{H}_{27}\text{N}_3\text{O}_1\text{Pt}_1\text{I}_1$: 623.08, found 623.09.

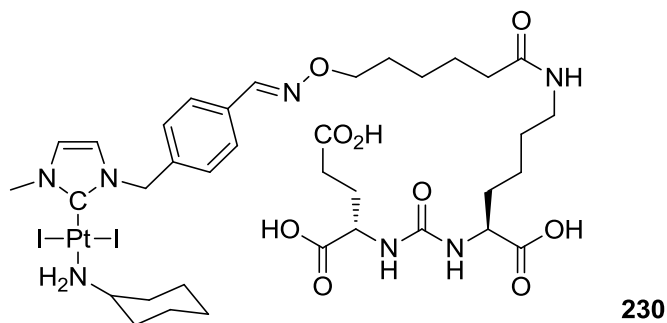


%. $^1\text{H-NMR}$ (CDCl_3 , 300 MHz, 20 °C): δ 1.04-1.42 (m, 5H, CHA), 1.57-1.85 (m, 3H, CHA), 2.28 (m, 2H, CH_2), 2.96 (m, 3H, $\text{NH}_2\text{-Pt}$ and NH), 3.26 (CH_{CHA}), 3.55-3.85 (m, 3H, CH^* and $\text{CH}^*\text{-CH}_2$), 3.88 (s, 3H, N- CH_3), 5.08 (s, 2H, OCH_2), 5.55 (s, 2H, N- CH_2), 6.53 (d, $J = 2.1\text{Hz}$, 1H, $\text{CH}=\text{}$), 6.76 (d, $J = 2.1\text{Hz}$, 1H, $\text{CH}=\text{}$), 7.10-7.43 (m, 14H, 14H_{ar}). $^{13}\text{C-NMR}$ (CDCl_3 , 75 MHz, 20 °C): 24.9 25.3 35.9 (C_{CHA}), 38.1 (N- CH_3), 39.7 (CH_2), 51.6 (CH_{CHA}), 54.0 (N- CH_2), 54.9 (NH-CH_2), 62.1 (CH), 66.6 (O-CH_2), 119.8 ($\text{CH}=\text{}$), 122.2 ($\text{CH}=\text{}$), 126.7 128.5 128.6 129.1 129.3 (CH_{ar}), 134.2 135.6 137.1 139.7 (C_{ar}), 174.4 (C=O). MS (positive ESI): $[\text{M}+\text{H}]$: calculated for $\text{C}_{34}\text{H}_{42}\text{I}_2\text{N}_4\text{O}_2\text{Pt}_1\text{H}$: 988.11 found 988.11, $[\text{M}-\text{I}]$: calculated for $\text{C}_{34}\text{H}_{42}\text{I}_1\text{N}_4\text{O}_2\text{Pt}_1$: 860.20 found 860.20, $[\text{M}-\text{I}+\text{CH}_3\text{CN}]$: calculated for $\text{C}_{34}\text{H}_{42}\text{I}_1\text{N}_4\text{O}_2\text{Pt}_1\text{CH}_3\text{CN}$: 901.23 found 901.23, $[\text{M}-2\text{I}-\text{H}]$: calculated for $\text{C}_{34}\text{H}_{41}\text{N}_4\text{O}_2\text{Pt}_1$: 732.29 found 732.28.



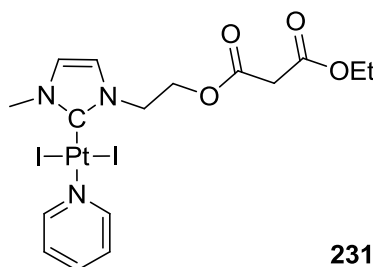
75%. $^1\text{H-NMR}$ (CDCl_3 , 300 MHz, 20 °C): δ 1.40 (s, 18H, 6CH_3 $t\text{Bu}$), 1.45 (s, 18H, 6CH_3 $t\text{Bu}$), 1.62-1.98 (m, 4H, 4H_{Glu}), 2.15-2.56 (m, 5H, 5H_{Glu}), 2.65-2.80 (m, 1H, 1H_{Glu}), 3.08 (m, 1H, 1H_{Glu}), 3.42 (m, 2H, $\text{NH}_2\text{-Pt}$), 3.49-3.84 (m, 3H, 3H_{Glu}), 3.85 (s, 3H, N- CH_3), 4.14 (m, 1H, 1H_{Glu}), 5.53 (s, 2H, N- CH_2), 6.52 (d, $J = 2.1\text{Hz}$, 1H, $\text{CH}=\text{}$), 6.76 (d, $J = 2.1\text{Hz}$, 1H, $\text{CH}=\text{}$), 7.30 (d, $J = 8.1\text{Hz}$, 2H, 2CH_{ar}), 7.37 (d, $J = 8.1\text{Hz}$, 2H, 2CH_{ar}). $^{13}\text{C-NMR}$ (CDCl_3 , 75 MHz, 20 °C): 27.6 (CH_2), 28.0 (CH_3 $t\text{Bu}$), 28.5 (CH_2), 31.2 (CH_2), 32.0 (CH_2), 38.1 (N- CH_3), 51.6 (NH- CH_2), 54.0 (N- CH_2), 57.7 (CH), 60.6 (CH), 80.2 80.6 81.3 ($\text{O-C } t\text{Bu}$), 119.8 ($\text{CH}=\text{}$), 122.2 ($\text{CH}=\text{}$), 128.6 (CH_{ar}), 129.1 (CH_{ar}), 133.9 (C_{ar}), 137.7 (C-Pt), 140.2 (C_{ar}), 171.4 172.0 172.5 174.3 (C=O). MS (positive ESI): $[\text{M}+\text{H}]$: calculated for $\text{C}_{38}\text{H}_{62}\text{I}_2\text{N}_4\text{O}_8\text{Pt}_1\text{H}$: 1152.25, found 1152.23.

7.3.3.5 PSMA targeting urea platinum conjugate



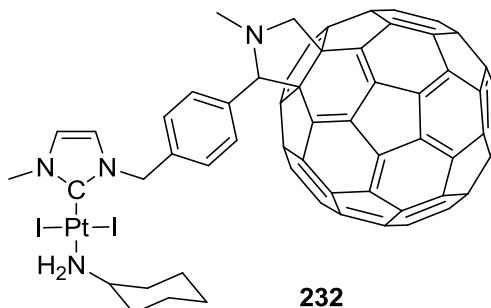
Synthesis by Dr. Etienne Borré. A solution of **81** (49 mg, 1.1 eq) and the urea derivative (45mg, 1.0 eq) in a H₂O/MeOH/CH₂Cl₂ solution was stirred overnight at room temperature. The volatiles were removed under reduced pressure and the crude product purified by SiO₂ gel chromatography (gradient CH₂Cl₂ to CH₂Cl₂/MeOH 8/2). 30%: ¹H-NMR (CDCl₃, 300 MHz, 20 °C): δ 0.88 (t, J= 6.9Hz, 2H, 2H_{urea}) 1.05-2.38 (m, 29H, H_{CHA}+H_{urea}), 2.94 (m, 2H, Pt-NH₂), 3.24 (m, 3H, CH_{CHA}+2H_{urea}), 3.89 (s, 3H, N-CH₃), 4.15 (t, J= 6.6Hz, 2H, 2H_{urea}), 4.30 (m, 2H, 2H_{urea}), 5.29 (m, 2H, 2H_{urea}), 5.60 (s, 2H, N-CH₂), 6.04 (m, 1H, 1H_{urea}), 6.57 (d, J= 2.1Hz, 1H, CH=), 6.79 (d, J= 2.1Hz, 1H, CH=), 7.44 (d, J= 8.1Hz, 2H, H_{ar}), 7.57 (d, J= 8.1Hz, 2H, H_{ar}), 8.05 (s, 1H, CH=N). ¹³C-NMR (CDCl₃, 75 MHz, 20 °C): δ 22.5 22.5 25.0 25.4 25.7 25.8 31.8 32.7 36.0 36.7 38.3 39.1 53.4 54.1 55.0 74.4 (C_{CHA}, C_{NHC} and C_{urea}), 120.0 (CH=), 122.5 (CH=), 127.5 (CH_{Ar}), 129.4 (CH_{Ar}), 132.1 (C_{Ar}), 137.1 (C_{Ar}), 140.4 (C-Pt), 147.9 (CH=N). 157.2 (NCON), 172.5 173.4 (C=O).

7.3.3.6 Synthesis of platinum NHC- C_{60} conjugate



Procedure a: 57%. ¹H-NMR (CDCl₃, 300 MHz, 20 °C): δ 1.25 (t, J= 7.1Hz, 3H, CH₃), 3.41 (s, 2H, COCH₂CO), 3.93 (s, 3H, N-CH₃), 4.17 (q, J= 7.1Hz, 2H, O-CH₂), 4.75 (s, 4H, N-CH₂ and CH₂), 6.85 (s, 1H, CH=), 7.00 (s, 1H, CH=), 7.30 (t, J= 6.5Hz, 2H, 2H_{PyT}), 7.70 (t, J= 7.7Hz, 1H, 1H_{PyT}), 8.99 (m, 2H, 2H_{PyT}). ¹³C-NMR (CDCl₃, 75 MHz, 20 °C): δ 14.2 (CH₃), 38.3 (N-CH₃), 41.6 (CH₂), 49.2 (N-

CH₂), 61.7 (O-CH₂), 63.6 (O-CH₂), 121.6 (CH=), 122.2 (CH=), 125.0 (C_{Pyr}), 136.6 (C-Pt), 137.6 (C_{Pyr}), 153.6 (C_{Pyr}), 166.1 (C=O), 166.4 (C=O).

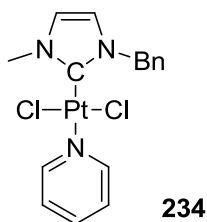


A solution of **81** (1.0 eq), sarcosine (1.1 eq) and fullerene C₆₀ (1.5 eq) in toluene were refluxed over 6 hours. The volatiles were removed under reduced pressure and the crude product purified by SiO₂ gel chromatography (gradient pentane to CH₂Cl₂/pentane 1/1 to CH₂Cl₂). 37%. ¹H-NMR (CDCl₃, 300 MHz, 20 °C): δ 1.13-1.33 (m, 5H, 5H_{CHA}), 1.72 (m, 2H, 2H_{CHA}), 2.25 (m, 3H, 3H_{CHA}), 2.81 (s, 3H, CH₃), 2.90 (m, 2H, Pt-NH₂), 3.22 (m, 1H, CH_{CHA}), 3.87 (s, 3H, N-CH₃), 4.27 (d, J= 9.3Hz, 1H), 4.94 (s, 1H), 4.99 (d, J= 9.3Hz, 1H), 5.57 (d, J= 4.2Hz, 2H, N-CH₂), 6.50 (d, J= 2.1Hz, 1H, CH=), 6.76 (d, J= 2.1Hz, 1H, CH=), 7.49 (d, J= 8.2Hz, 2H, 2H_{ar}), 7.82 (m, 2H, 2H_{ar}). MS (positive ESI) [M+H]: calculated for C₈₀H₃₀I₂N₄Pt₁H: 1497.03, found 1497.05; [M-I+CH₃CN]: calculated for C₈₂H₃₃I₁N₅Pt₁: 1410,1454, found 1410.1515.

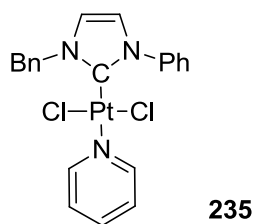
7.3.3.7 Halogen exchange reaction on NHC Pt complexes

7.3.3.7.1 Synthesis of the NHC-PtX₂-L precursors (X = Cl or Br)General synthesis of NHC-PtCl₂-pyridine or NHC-PtBr₂-pyridine- from corresponding imidazolium:

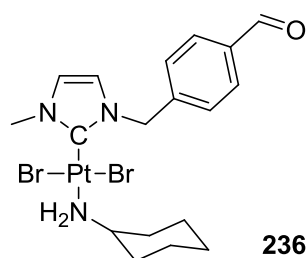
A mixture of corresponding imidazolium chloride respectively bromide (1 eq), sodium chloride respectively bromide (10 eq), platinum dichloride (9.3 mg, 0.035 mmol) and potassium carbonate (10 eq) was suspended in pyridine (5 mL). The mixture was sonicated 10 minutes then stirred at 100 °C overnight. The resulting suspension was concentrated under reduced pressure, dissolved in dichloromethane, filtered through a celite plug and concentrated under reduced pressure. The residue was purified by silica gel chromatography (Dichloromethane/Cyclohexane 1/1, then Dichloromethane) affording the desired complex as a yellow solid.



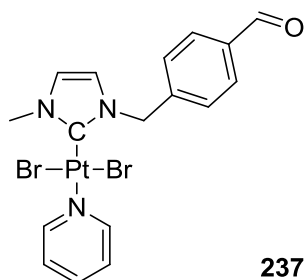
Yellow solid, 11.3 mg, 24%: ¹H-NMR (CDCl₃, 300 MHz, 20 °C): δ 4.14 (s, 3H, N-CH₃), 5.84 (s, 2H, N-CH₂), 6.68 (d, J= 1.8Hz, 1H, CH=), 6.84 (d, J= 1.8Hz, 1H, CH=), 7.25-7.52 (m, 7H, 5H_{ar} and 2H_{Pyr}), 7.80 (t, J= 7.6Hz, 1H, H_{Pyr}), 9.03 (d, J= 5.2Hz, 2H, 2H_{Pyr}). ¹H-NMR (CD₃CN, 300 MHz, 20 °C): δ 4.06 (s, 3H, N-CH₃), 5.78 (s, 2H, N-CH₂), 6.93 (s, 1H, CH=), 7.05 (s, 1H, CH=), 7.25-7.62 (m, 7H, 5H_{ar} and 2H_{Pyr}), 7.92 (m, 1H, H_{Pyr}), 8.92 (m, 2H, 2H_{Pyr}). ¹H-NMR (Acetone, 300 MHz, 20 °C): δ 4.09 (s, 3H, N-CH₃), 5.83 (s, 2H, N-CH₂), 7.04 (s, 1H, CH=), 7.21 (s, 1H, CH=), 7.25-7.69 (m, 7H, 5H_{ar} and 2H_{Pyr}), 8.01 (tt, J= 7.5Hz and 1.5Hz, 1H, H_{Pyr}), 9.00 (m, 2H, 2H_{Pyr}). ¹³C-NMR (CDCl₃, 75 MHz, 20 °C): δ 37.5 (N-CH₃), 54.0 (N-CH₂), 120.1 (CH=), 122.4 (CH=), 124.8 (C_{Pyr}), 128 (CH_{ar}), 128.6 (CH_{ar}), 128.8 (CH_{ar}), 135.9 (C_{ar}), 137.9 (C_{Pyr}), 139.8 (C-Pt), 151.3 (C_{Pyr}). MS (positive ESI) [M-Cl]: calculated for C₁₆H₁₇Cl₁N₃Pt₁: 481.08 found 481.07, [M+Na]: calculated for C₁₆H₁₇Cl₂N₃Pt₁Na: 540.03 found 540.03, [M-2Cl-H]: calculated for C₁₆H₁₆N₃Pt₁: 445.10 found 445.09, [M-Cl+CH₃CN]: calculated for C₁₆H₁₇Cl₁N₃Pt₁CH₃CN: 523.10 found 523.10.



Yellow solid. 21.3 mg, 36%: $^1\text{H-NMR}$ (CDCl_3 , 300 MHz, 20 °C): δ 6.03 (s, 2H, N- CH_2), 6.86 (d, J = 2.1Hz, 1H, CH=), 7.11 (d, J = 2.1Hz, 1H, CH=), 7.25-7.65 (m, 10H, $8\text{H}_{\text{ar}}+2\text{H}_{\text{pyr}}$), 7.74 (tt, J = 7.6 and 1.6Hz, 1H, 1H_{pyr}), 8.05 (dt, J = 7.0 and 1.6Hz, 2H, 2H_{ar}), 8.89 (m, 2H, 2H_{pyr}). $^{13}\text{C-NMR}$ (ACETONE, 75 MHz, 20 °C): δ 54.4 (N- CH_2), 120.6 (CH=), 122.6 (CH=), 124.8 (CH_{pyr}), 126.2 128.4 128.9 129.0 (CH_{ar}), 135.5 (C_{ar}), 137.9 (CH_{pyr}), 139.7 (N- C_{ar}), 140.3 (C-Pt), 151.3 (CH_{pyr}). MS (positive ESI) [$\text{M}-\text{Cl}+\text{CH}_3\text{CN}$]: calculated for $\text{C}_{21}\text{H}_{19}\text{ClN}_3\text{PtCH}_3\text{CN}$: 584.12, found 584.12, [$\text{M}+\text{Na}$]: calculated for $\text{C}_{21}\text{H}_{19}\text{Cl}_2\text{N}_3\text{PtNa}$: 602.05, found 602.05.



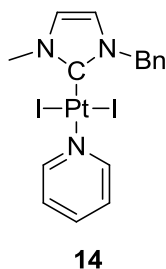
To a solution of $(\text{NHC})\text{PtBr}_2(\text{pyr})$ **237** (1 eq) in dichloromethane (1 mL) is added cyclohexylamine (1 mL). After stirring ten minutes at room temperature, the solution is concentrated under reduced pressure at room temperature, residual cyclohexylamine is removed by silica gel chromatography (dichloromethane) to afford the complex as a yellow solid. 4.7 mg, 18%: $^1\text{H-NMR}$ (CDCl_3 , 300 MHz, 20 °C): δ 1.05-1.35 (m, 8H, CH_2), 2.27 (m, 2H, CH_2), 2.99 (m, 2H, Pt- NH_2), 3.15 (m, 1H, CH_{CHA}), 4.05 (s, 3H, N- CH_3), 5.82 (s, 2H, N- CH_2), 6.67 (d, J = 2.0Hz, 1H, CH=), 6.85 (d, J = 2.0Hz, 1H, CH=), 7.58 (d, J = 8.0Hz, 2H, H_{ar}), 7.88 (d, J = 8.0Hz, 2H, H_{ar}), 10.01 (s, 1H, CH=O).



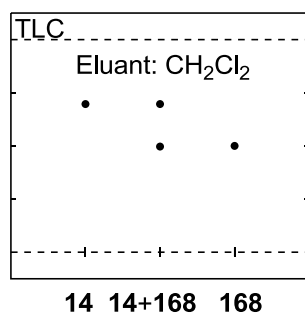
Yellow solid. 129.6 mg, 72%: ^1H -NMR (CDCl_3 , 300 MHz, 20 °C): δ 4.06 (s, 3H, N-CH₃), 5.87 (s, 2H, N-CH₂), 6.68 (d, J = 2.0Hz, 1H, CH=), 6.87 (d, J = 2.0Hz, 1H, CH=), 7.30 (t, J = 7.0Hz, 2H, CH_{pyr}), 7.59 (d, J = 8.0Hz, 2H, 2H_{ar}), 7.72 (tt, J = 7.6 and 1.7Hz, 1H, CH_{pyr}), 7.83 (d, J = 8.0Hz, 2H, 2H_{ar}), 9.95 (m, 2H, CH_{pyr}), 9.96 (s, 1H, CH=O). ^{13}C -NMR (CDCl_3 , 75 MHz, 20 °C): δ 38.0 (N-CH₃), 53.8 (N-CH₂), 120.2 (CH=), 122.9 (CH=), 125.0 (C_{pyr}), 129.1 (CH_{ar}), 130.2 (CH_{ar}), 136.2 (C_{ar}), 137.9 (C_{pyr}), 139.3 (C-Pt), 142.6 (C_{ar}), 152.5 (C_{pyr}), 191.8 (CH=O).

7.3.3.7.2 Optimized halogen ligand exchange reactions:

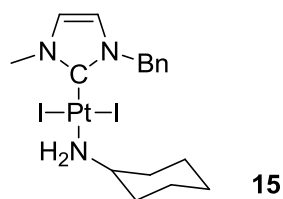
The reactions were performed in air and in non-dried solvents. ^1H and ^{13}C -NMR of both complexes are corresponding to data previously described.



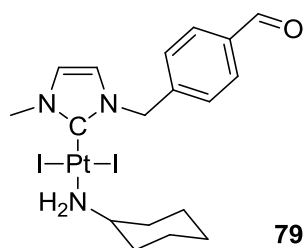
Method I: NaI solid: NaI was grounded in a mortar. NaI (16.3 mg, 2.2 eq, 0.109 mmol) was added to a solution of (NHC)PtBr₂(pyr) **168** (30 mg, 1 eq, 0.049 mmol) in acetone (2 mL). The mixture was heated at reflux during 1h under vigorous stirring. The solvent was evaporated. CH₂Cl₂ (2 × 5 mL) was added and the mixture was filtered through cotton. The CH₂Cl₂ was evaporated to afford **14** quantitatively. Total time: 70 min.



Method II: NaI in H₂O: A solution of NaI (19.8 mg, 4 eq, 0.132 mmol) in H₂O (1 mL) was added to a solution of (NHC)PtBr₂(pyr) **168** (20 mg, 1 eq, 0.033 mmol) in acetone (1 mL). The mixture was heated at 55 °C during 1 h under vigorous stirring. The acetone was evaporated; the complex was extracted by CH₂Cl₂ and dried under reduced pressure to afford **14** quantitatively. Total time: 70 min.



Method I: NaI solid: NaI was grounded in a mortar. NaI (5.3 mg, 2.2 eq, 0.035 mmol) was added to a solution of (NHC)PtBr₂(cyclohexylamine) **169** (10 mg, 1 eq, 0.016 mmol) in acetone (2 mL). The mixture was heated at 56 °C during 1h under vigorous stirring. The solvent was evaporated. CH₂Cl₂ (2 × 5 mL) was added and the mixture was filtered through cotton. The CH₂Cl₂ was evaporated to afford **15** quantitatively. Total time: 70 min.



Method I: KI solid: Grounded KI (2.6 mg, 2.2 eq, 0.016 mmol) was added to a solution of (benzaldehyde-NHC)PtBr₂(cyclohexylamine) **237** (4.7 mg, 1 eq, 0.007 mmol) in acetone (2 mL). The mixture was heated at reflux during 1h under vigorous stirring. The solvent was evaporated. CH₂Cl₂ (2 × 5 mL) was added and the mixture was filtered through cotton. The CH₂Cl₂ was evaporated to afford **79** quantitatively. Total time: 70 min.

¹²³I experiments: 23 mg de [(NHC)PtBr₂(pyr)] **168** were dissolved in 1 mL of acetone. 50 MBq of ¹²³I (NaI) in 1 mL of aqueous solution was added (NaCl, NaHCO₃). The solution was heated 70 minutes at 56°C. The solvents were removed under air by heating at 103 °C during (30 minutes). ¹²³I introduction was proven by Whatman (dichloromethane). The stability of the product was ascertained by measure of radioactivity by Whatman (dichloromethane) after 22, 24 and 26 hours showing no release of radioactive iodide from the complex.

7.4 Biological studies: General descriptions

General description of *in vitro* tests: Cells were grown in Dulbecco's modified Eagle's medium supplemented with 25 mM glucose, 10% (v/v) foetal calf serum, 100 UI penicillin, 100µg/ml streptomycin and 1.5 µg/ml fungizone and kept under 5%CO₂ at 37 °C. 96 well plates were seeded with 600 cells per well in 200 µl medium. Twenty-four hours later, chemicals dissolved in DMSO were added for 72h at a final concentration (10⁻⁵M) in a fixed volume of DMSO. (1% final concentration). Controls received an equal volume of DMSO. The number of viable cells measured at 490 nm with the MTS reagent (Promega, Madison, WI) and IC₅₀ was calculated as the concentration of compound eliciting a 50% inhibition of cell proliferation.

For PEI conjugates, following procedure was employed: Cells were treated with various concentrations of Pt complexes dissolved in EtOH. After 24h of treatment, cell death was evaluated using MTS Assay. Results are expressed as the mean of 3 experiments ± SEM. The statistical significance was calculated by a non-parametric ANOVA 2 way test plus a Bonferonni correction. Results with a p-value less than 0.05 were considered significant. Each experiment was made in triplicate. The IC₅₀ was determined using the software Prims Prism Graph Pad 5.0

In vivo tests: Into 5-week-old athymic female nude mice were injected 5.10⁶ dissociated HCT116 cells in the right flank and tumor were allowed to growth until reaching the mean volume of 25mm³. Injections of NHC-PEI 30 (10 mg/kg), oxaliplatin (2 mg/kg, 10 mg/kg) or vehicles (0.9% NaCl / EtOH 10% or 0.9% NaCl) were administered in i.p route over 48h, during 13 days. Tumor volume was determined by caliper measurement and normalized toward the tumor volume observed at the beginning of the treatment. Results are expressed as the mean of 2 experiments ± SEM (n= 18). Results with a p-value less than 0.05 were considered significant.

8 Résumé détaillée en français

8.1 I Introduction

La chimiothérapie, avec la chirurgie et la radiothérapie, sont aujourd'hui les outils principaux pour la lutte contre le cancer. Depuis sa découverte dans les années 1960 par Barnett Rosenberg⁵⁵⁷ le cisplatine $cis\text{-PtCl}_2(\text{NH}_3)_2$ est l'un des anticancéreux les plus utilisés en chimiothérapie. Cependant malgré son succès, il présente des effets secondaires importants tels que la néphrotoxicité, l'ototoxicité, la neurotoxicité et son efficacité thérapeutique reste limitée par des mécanismes de résistance intrinsèques et acquis. Pour ces raisons, de nouveaux dérivés de platine présentant potentiellement des effets secondaires amoindris sont toujours à l'étude. Récemment, les équipes de Ghosh⁵⁵⁸ et de Marinetti⁵⁵⁹ ont montré que des dérivés de Carbènes *N*-HétéroCycliques (NHC)⁵⁶⁰ de palladium et de platine présentent des activités cytotoxiques supérieures au cisplatine et sont des composés prometteurs pour remplacer le cisplatine (**Figure 201**).

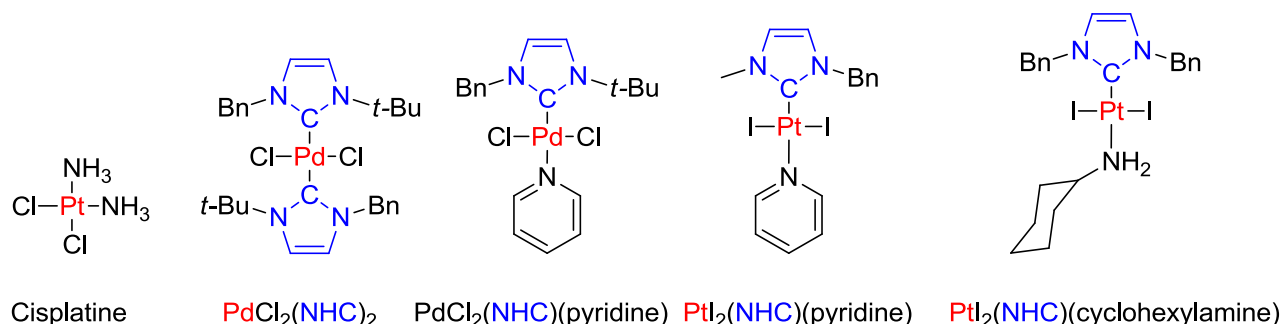


Figure 201: Cisplatine et exemples de dérivés NHC de platine et de palladium cytotoxiques

Les carbènes *N*-hétérocycliques, utilisés comme ligands dans ces complexes, sont des composés cycliques contenant un carbone singulet divalent à six électrons de valence lié à deux atomes d'azote. Stabilisés de manière stérique par les groupements substituants des azotes et de manière électronique par les doublets libres des azotes sur l'orbitale *p* vide du carbone carbénique, les NHCs constituent de bons ligands riches en électrons et fortement σ -donneurs. Ils se laissent facilement moduler en variant

⁵⁵⁷ Rosenberg, B.; VanCamp, L.; Trosko, J. E.; Mansour, V. H. *Nature* **1969**, 222, 385-387.

⁵⁵⁸ Ray, S.; Mohan, R.; Singh, J. K.; Samantaray, M. K.; Shaikh, M. M.; Panda, D.; Ghosh, P. *J. Am. Chem. Soc.* **2007**, 129, 15042-15053

⁵⁵⁹ (a) Skander, M.; Retailleau, P.; Bourrie, B.; Schio, L.; Mailliet, P.; Marinetti, A. *J. Med. Chem.* **2010**, 53, 2146-2154
2154 (b) Mailliet, P.; Marinetti, A.; Skander, M. *WO2009/118475*. **2009**

⁵⁶⁰ Métallob carbènes comme agents anticancéreux: a) Gautier, A.; Cisnetti, F. *Metallomics*, **2012**, 4, 23-32, b) Oehninger, L.; Rubbiani, R.; Ott, I. *Dalton Trans.*, **2013**, 42, 3269-3284

les substituants portés par les atomes d'azote pour introduire de la diversité structurale ou électronique (**Figure 202**).⁵⁶¹

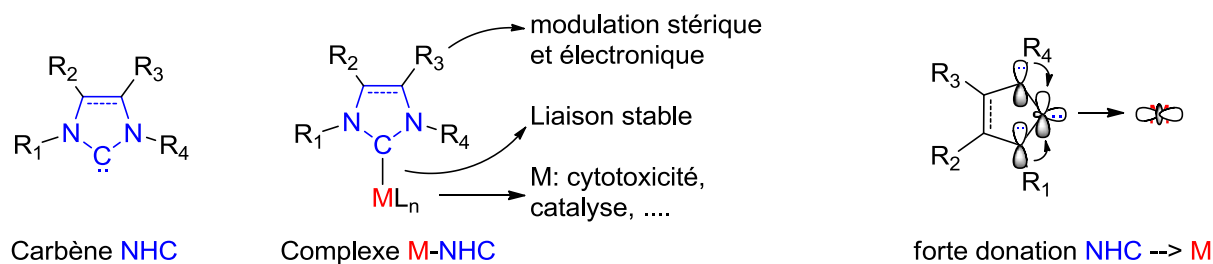


Figure 202: Carbène NHC et sa liaison avec les métaux de transition

Afin de diminuer les effets secondaires des médicaments anti-tumoraux, les agents cytotoxiques doivent avoir une sélectivité élevée pour les cellules cancéreuses vis-à-vis des cellules saines. Ceci pourrait être obtenu en liant chimiquement l'agent toxique à un agent de ciblage, par exemple des dérivés d'œstrogène (ciblage de cancers hormonodépendants)⁵⁶² ou des dérivés d'urée (ciblant le Prostate-specific membrane antigen PSMA surexprimé par les cellules cancéreuses de la prostate)⁵⁶³.

La stratégie classique en synthèse organométallique consiste à synthétiser un ligand plus ou moins sophistiqué, et ensuite le complexer lors d'une dernière étape sur le métal. Cette stratégie linéaire comporte un certain nombre d'inconvénients : incompatibilité avec diverses fonctions chimiques, rendement souvent faible de l'étape de complexation, besoin de recommencer tout au début lorsqu'on veut moduler le ligand afin de l'optimiser (**Figure 203**).

⁵⁶¹ César, V.; Bellemín-Laponnaz, S. *Actualité Chimique* **2009**, 326, 10-16

⁵⁶² (a) Descoteaux, C.; Provencher - Mandeville, J.; Mathieu I.; Perron, V.; Manal, S. K.; Asselin, E.; Berube, G. *Bioorg. Med. Chem. Lett.* **2003**, 13, 3927-3931 (b) Gagnon, V.; St-Germain, M.-E.; Descoteaux, C.; Provencher-Mandeville, J.; Parent, S.; Mandal, S. K.; Asselina E.; Berube, G. *Bioorg. Med. Chem. Lett.* **2004**, 14, 5919-5924 (c) Provencher-Mandeville, J.; Descoteaux, C.; Mandal, S. K.; Leblanc, V.; Asselina, E.; Berube, G. *Bioorg. Med. Chem. Lett.* **2008**, 18, 2282-2287 (d) Descoteaux, C.; Leblanc, V.; Belanger, G.; Parent, S.; Asselin E.; Berube, G. *Steroids* **2008**, 73, 1077-1089

⁵⁶³ Kozikowski, A. P.; Nan, F.; Conti, P.; Zhang, J.; Ramadan, E.; Bzdega, T.; Wroblewska, B.; Neale, J. H.; Pshenichkin, S.; Wroblewski, J. T. *J. Med. Chem.* **2001**, 44, 298

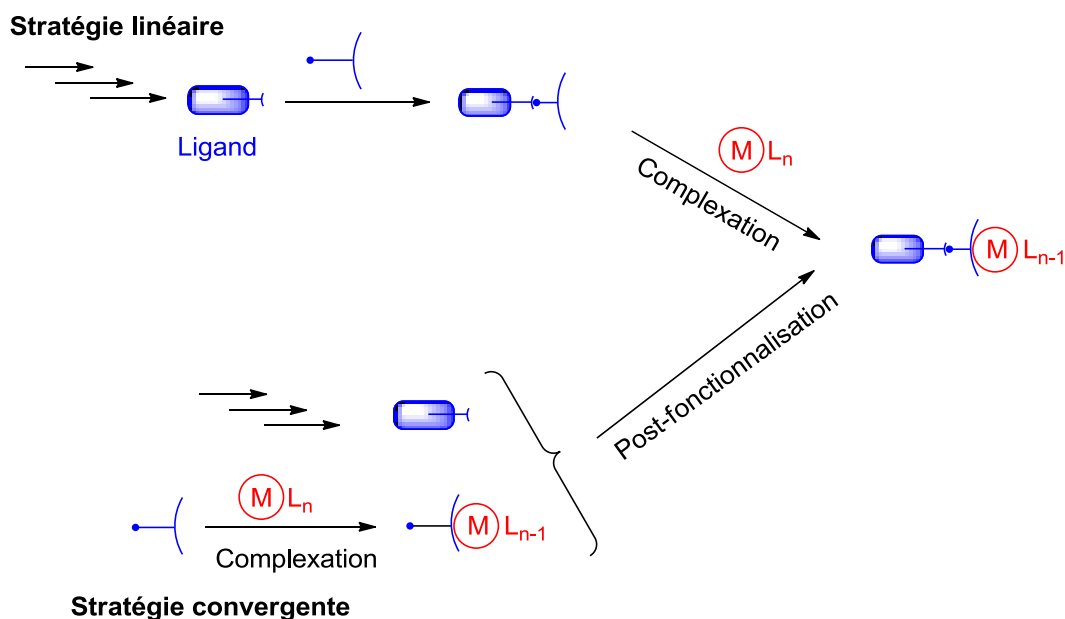


Figure 203: Les deux stratégies de fonctionnalisation

Au laboratoire, des méthodes de post-fonctionnalisation de complexes NHC de platine "simples" par Ruthenium catalysed 1,3-dipolar Azide-Alkyne Cycloaddition (RuAAC)⁵⁶⁴ ou par échange de ligands (

Figure 204) ont été développées.⁵⁶⁵

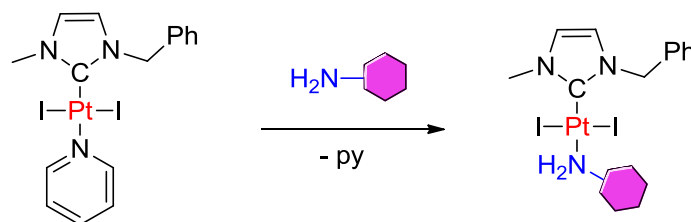


Figure 204: Fonctionnalisation de complexes NHC par échange de ligands⁹

Dans la continuité de ces travaux, une nouvelle voie de post-fonctionnalisation de complexes NHC de platine a été développée durant cette thèse. Des complexes portant des fonctions aldéhydes sont condensés avec des amines pour donner les imines correspondantes (

Figure 205). Les amines utilisés seront des entités ayant un intérêt biologique tels que des acides aminés, des peptides, urées, ... Il sera montré qu'il est possible de combiner la méthode de

⁵⁶⁴ Chardon, E.; Puleo, G. L.; Dahm, G.; Guichard, G.; Bellemin-Lapponnaz, S. *Chem. Commun.*, **2011**, *47*, 5864-5866.

⁵⁶⁵ Exemples de post-fonctionnalisation de complexes: (a) Hospital, A.; Gibard, C.; Gaulier, C.; Nauton, L.; Théry, V.; El-Ghozzi, M.; Avignant, D.; Cisnetti, F.; Gautier, A. *Dalton Trans.*, **2012**, *41*, 6803-6812 (b) Raszeja, L. Maghnouj, A. Hahn S.; Metzler-Nolte, N. *ChemBioChem*, **2011**, *12*, 1 ; (c) Noor, F.; Kinscherf, R.; Bonaterra, G. A.; Walczak, S.; Wölfl S.; Metzler-Nolte, N. *ChemBioChem*, **2009**, *10*, 493 (d) Benhamou, L.; Vujkovic, N.; César, V.; Gornitzka, H.; Lugan, N.; Lavigne, G.; *Organometallics*, **2010**, *29*, 2616

fonctionnalisation par échange de ligand avec la nouvelle voie de condensation d'amine pour former des complexes bi-fonctionnalisés.

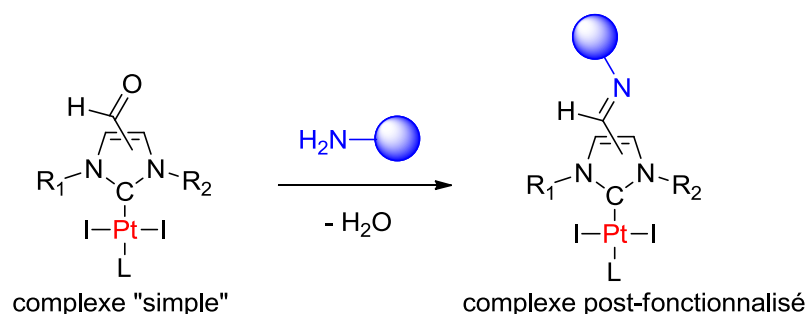


Figure 205: Post-fonctionnalisation de complexes NHC par condensation aldéhyde-amine

En parallèle, toute une série de complexes fonctionnalisés avec différents groupements chimiques a été testé *in vitro* pour évaluer leurs propriétés biologiques, ainsi que des ligands tridentés pour des applications en fluorescence.

8.2 Complexes NHC de platine synthétisés et étudiés

Plusieurs complexes de platine portant des fonctions chimiques divers (alcènes, alcènes, alcools, nitriles, aldéhydes, acétals, éther, esters, phosphonates) ou di-nucléaires ont été synthétisés par la voie de Ghosh *et al.*⁵⁶⁶ à partir des sels d'imidazolium correspondants. Des acides carboxyliques libres sont obtenus par déprotection d'esters *tert*-butyliques en milieu acide. Par déprotonation, des complexes carboxylates hydrosolubles ont pu être obtenus.

Quelques exemples sont représentés sur la **Figure 206**. Dans une seconde étape, ces composés seront les précurseurs pour des réactions de postmodification.

⁵⁶⁶ Ray, S.; Mohan, R.; Singh, J. K.; Samantaray, M. K.; Shaikh, M. M.; Panda, D.; Ghosh, P. *J. Am. Chem. Soc.*, 2007, 129, 15042–15053

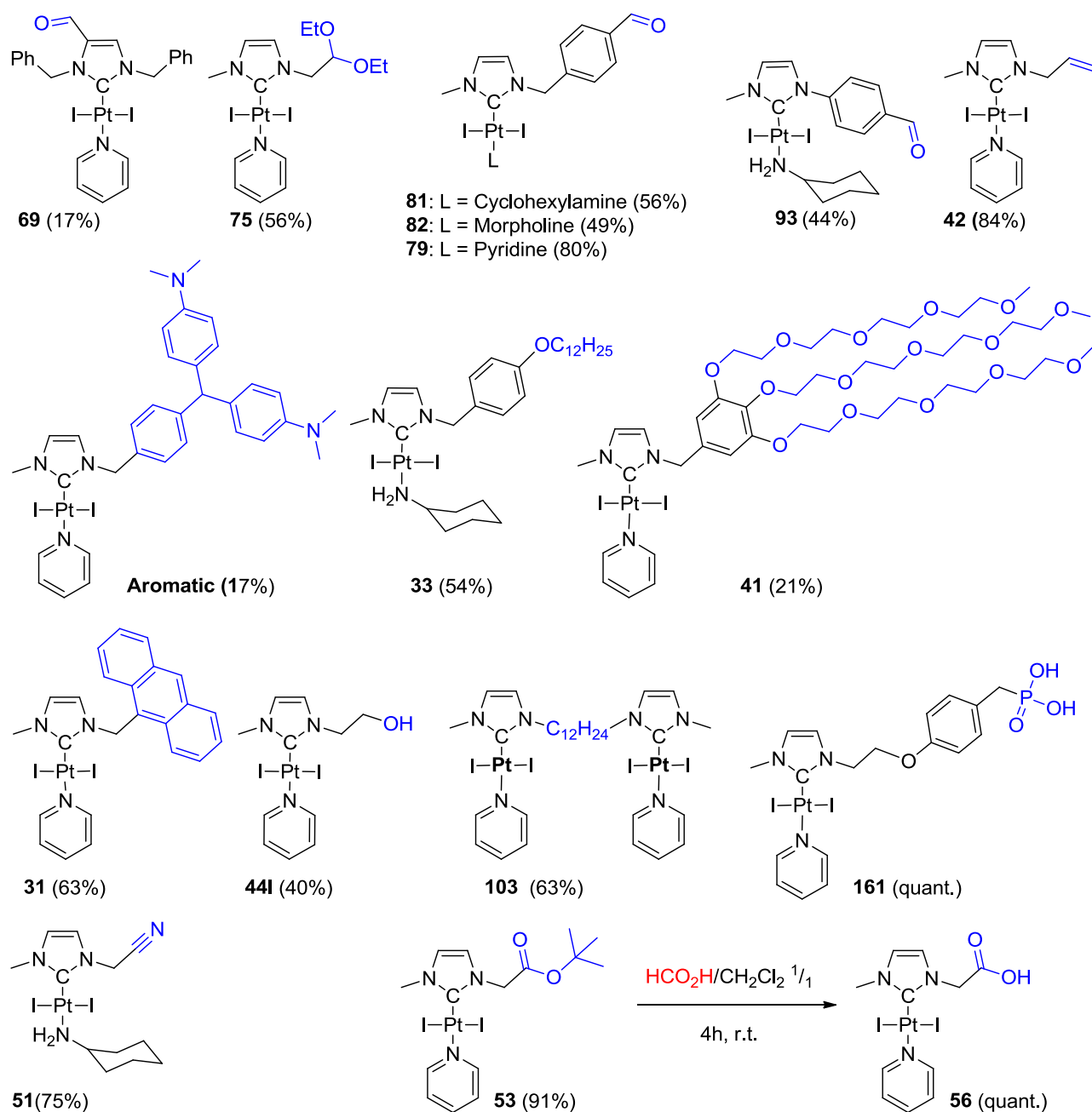


Figure 206: Exemples de complexes fonctionnalisés avec différentes fonctions chimiques

1.1 Fonctionnalisation des complexes NHC

8.2.1 Fonctionnalisation par condensation d'hydroxylamines, hydrazines ou amines

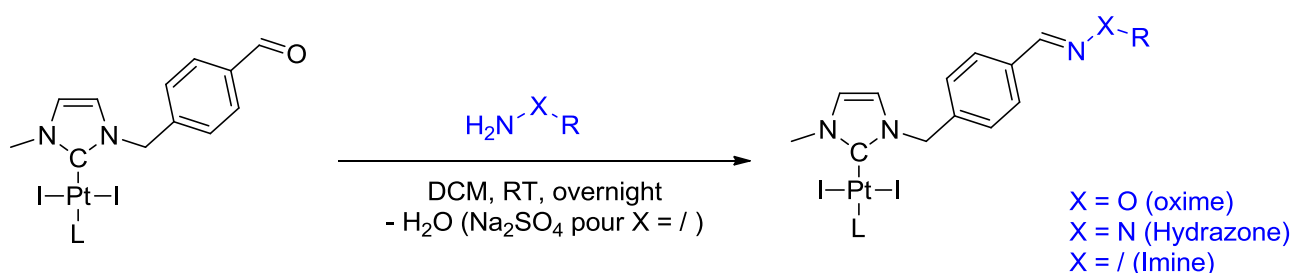


Figure 207: Fonctionnalisation par des hydroxylamines/hydrazines

La réaction de condensation entre un dérivé benzaldéhyde et une hydroxylamine pour former une oxime est une réaction permettant de fonctionnaliser des complexes simples.⁵⁶⁷ Elle permet d'introduire des hydroxylamines ou des hydrazines modèles telles que la benzyle-hydroxylamine ou la phenylhydrazine, mais aussi des composés fluorescents ou des dérivés d'intérêt biologique (**Figure 207**).

De façon analogue, des imines peuvent être formées par réaction entre une amine et notre complexe, permettant d'introduire des dérivés tels que des acides aminés. La réaction nécessite cependant la présence d'un desséchant (Na_2SO_4 anhydre) pour pousser l'équilibre vers la formation d'imine.

Toute une série de produits a ainsi pu être obtenu (**Figure 208** et **Figure 209**).

⁵⁶⁷ Voir par exemple : Tan, Y.; Dyson, P.; Ang, W. *Organometallics*, **2011**, 30, 5965–5971
 Dirksen, A.; Dawson, P. *Bioconjugate Chem.*, **2008**, 19, 2543–2548

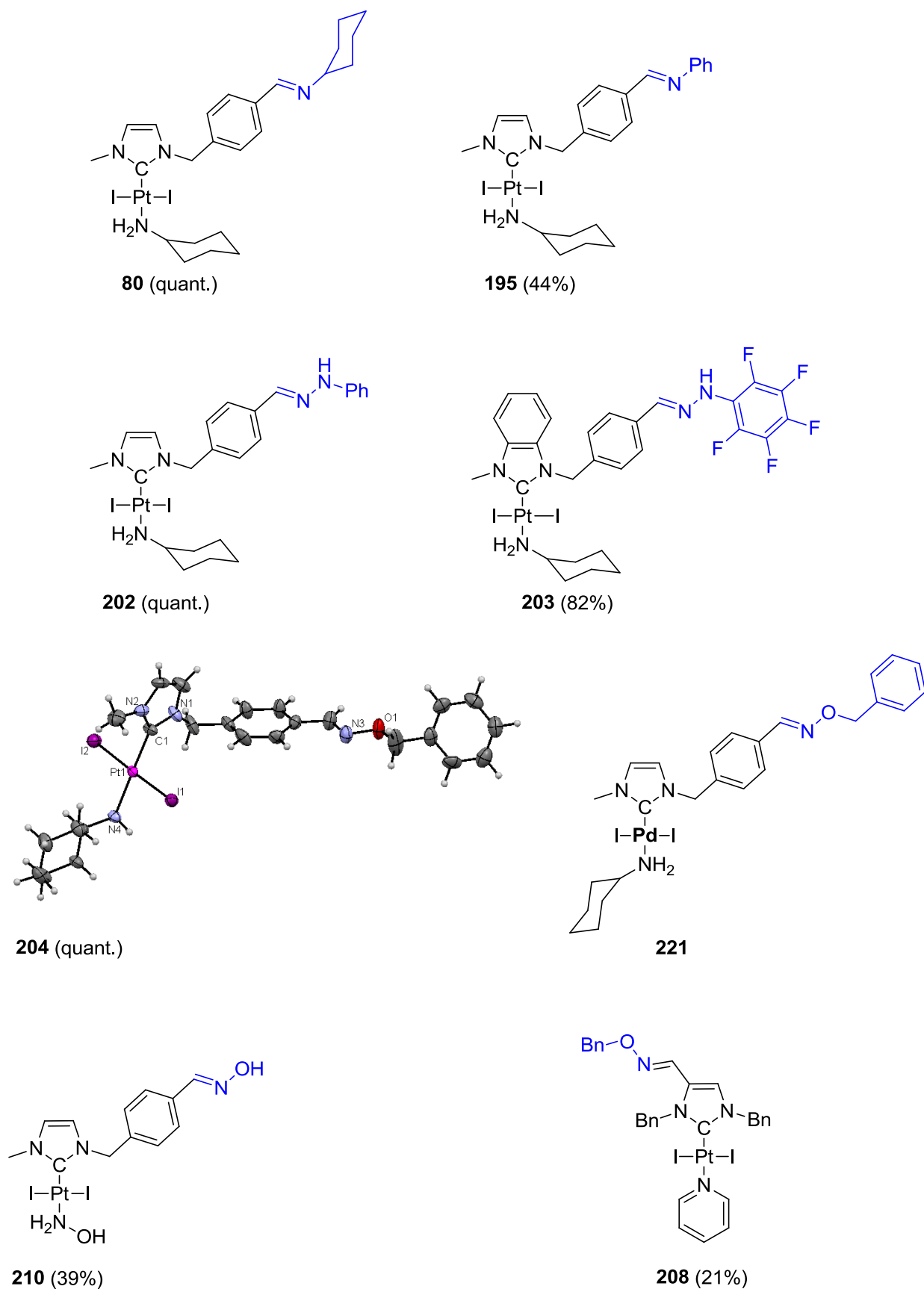


Figure 208: Produits modèles obtenus avec des amines, hydrazines et des hydroxylamines simples

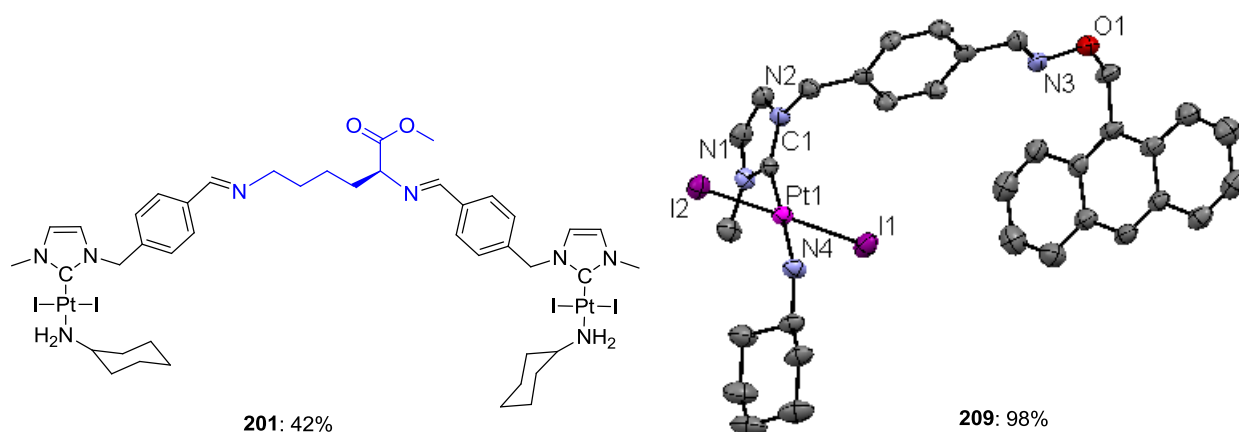


Figure 209 : Produits modèles obtenus avec des hydroxylamines fluorescentes et des acides aminés

La caractérisation des imines, hydrazones, ou hydroxyimines est facilité par les pics caractéristiques des produits en RMN (^1H NMR: $\text{CH}=\text{O}$: 10ppm, $\text{CH}=\text{N}$: 8 ppm ; ^{13}C NMR: $\text{CH}=\text{O}$: 190 ppm, $\text{CH}=\text{N}$: 160 ppm). Des structures obtenues par diffraction des rayons RX des oximes permet de confirmer la configuration E de la nouvelle double $\text{C}=\text{N}$.

La stabilité de la liaison s'avère suivre cet ordre: imine < hydrazone < hydroxyimine. Pendant que les imines s'hydrolysent sur colonne de gel de silice non basifié avec de la triéthylamine, les hydrazones et hydroxyimines sont stables dans ces conditions.

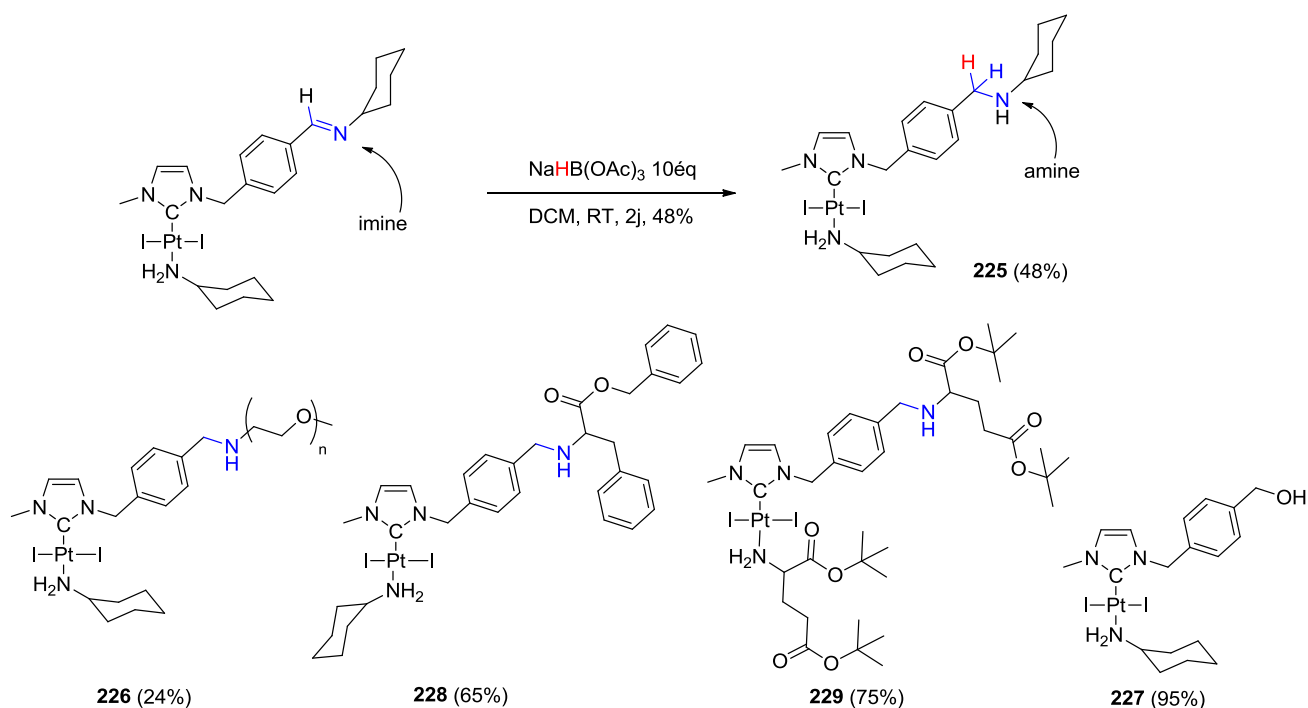


Figure 210: Réduction des imines et produits obtenus

La fonction imine moins stable que l'oxime peut être réduite en amine en utilisant le réducteur doux $\text{NaBH}(\text{OAc})_3$.⁵⁶⁸ De même, il est aussi possible de former l'alcool en réduisant le complexe benzaldéhyde (**Figure 210**).

Au laboratoire, l'étude de la condensation d'hydroxylamines portant un groupement ciblant l'antigène PSMA (Prostate Specific Membrane Antigen) exprimé fortement et uniquement par les cellules cancéreuses de la prostate et la neovascularisation de la majorité des cancers solides⁵⁶⁹ a également été entrepris avec succès (**Figure 211**).

⁵⁶⁸ Abdel-Magid, A. F.; Carson, K. G.; Harris, B. D.; Maryanoff, C. A.; Shah, R. D. *J. Org. Chem.*, **1996**, *61*, 3849–3862

⁵⁶⁹ a) Schülke, N.; Varlamova, O.; Donovan, G.; Ma, D.; Gardner, J.; Morrissey, D.; Arrigale, R.; Zhan, C.; Chodera, A.; Surowitz, K.; Maddon, P.; Heston, W.; Olson, W. *PNAS*, **2003**, *100*, 12590–12595, b) Nakajima, T.; Mitsunaga, M.; Bander, Heston, W.; Choyke, P.; Kobayashi, H. *Bioconjugate Chem.*, **2011**, *22*, 1700–1705

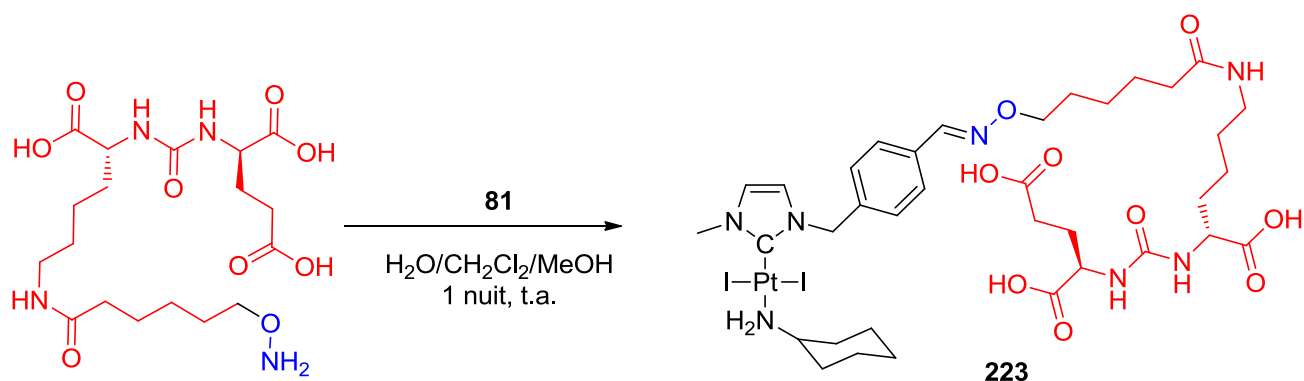


Figure 211: Fonctionnalisation avec une fonction de ciblage du PMSA

Une méthode de bis-post-modification de complexes NHC a été développée (**Figure 212**) réunissant la post-modification par condensation d'amine et celle par échange de ligands. Partant du complexe NHC-benzaldehyde Pt(II)-pyridine, soit la pyridine peut être échangée par une amine et ensuite un autre groupement fixé par condensation d'oxime en milieu acide, soit d'abord la condensation d'oxime sur le benzaldehyde suivi de l'échange de la pyridine en milieu neutre ou basique pour aboutir dans les deux cas à un complexe bis-fonctionnalisé.

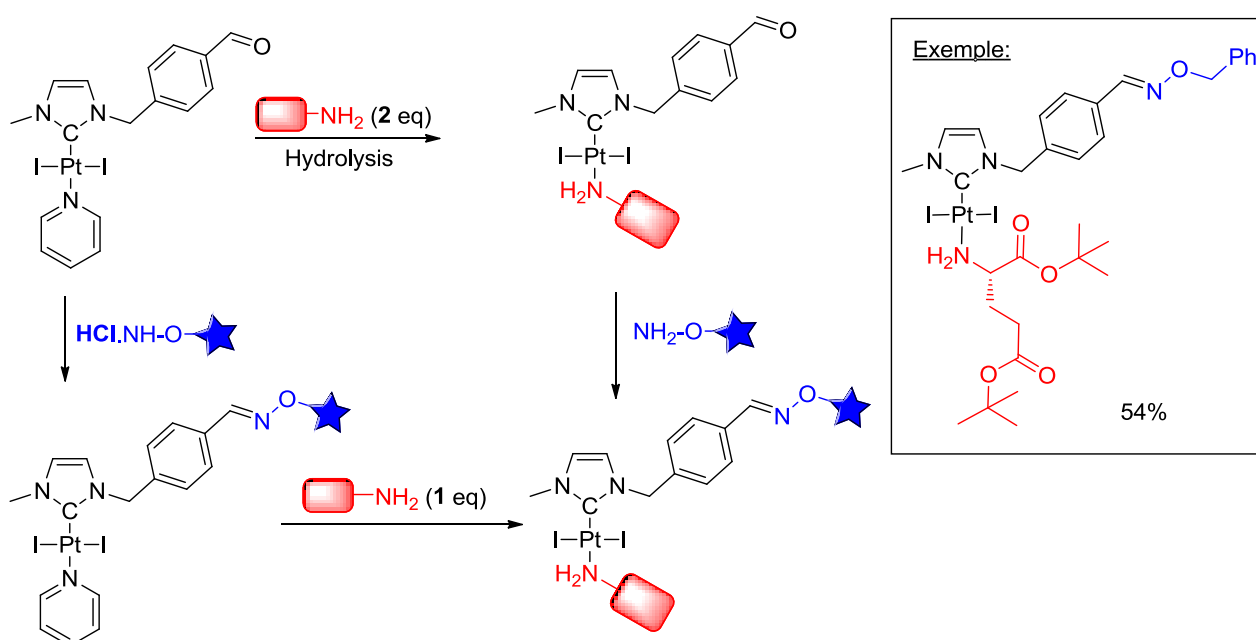


Figure 212: Double fonctionnalisation par condensation et échange de ligand

8.2.2 Introduction de ligands pnictogènes (phosphine, arsine, stibine)

Après les bons résultats obtenus par échange de ligand avec des dérivés azotés, nous avons continués avec des ligands pnictogènes. Des essais d'échange de ligand avec des phosphines, arsines ou stibines ont donné un mono-échange du ligand (en cas d'utilisation d'un équivalent), soit un double échange en cas d'excès donnant des composés cationiques (**Figure 213**). Les analyses RMN, confirmés par diffraction des rayons X, montrent clairement la configuration *cis* des ligands L par rapport au NHC de ces complexes.

L'avantage de notre voie de synthèse est clairement la facilité de mise en œuvre et la modularité élevée donnant lieu à tout un ensemble de composés avec des rendements élevés.

L'étude biologique de cette toute nouvelle classe de complexes de type NHC-Pt(II)-L et NHC-Pt(II)-L₂ avec L = AsR₃ et SbR₃ a montré des activités modérés.

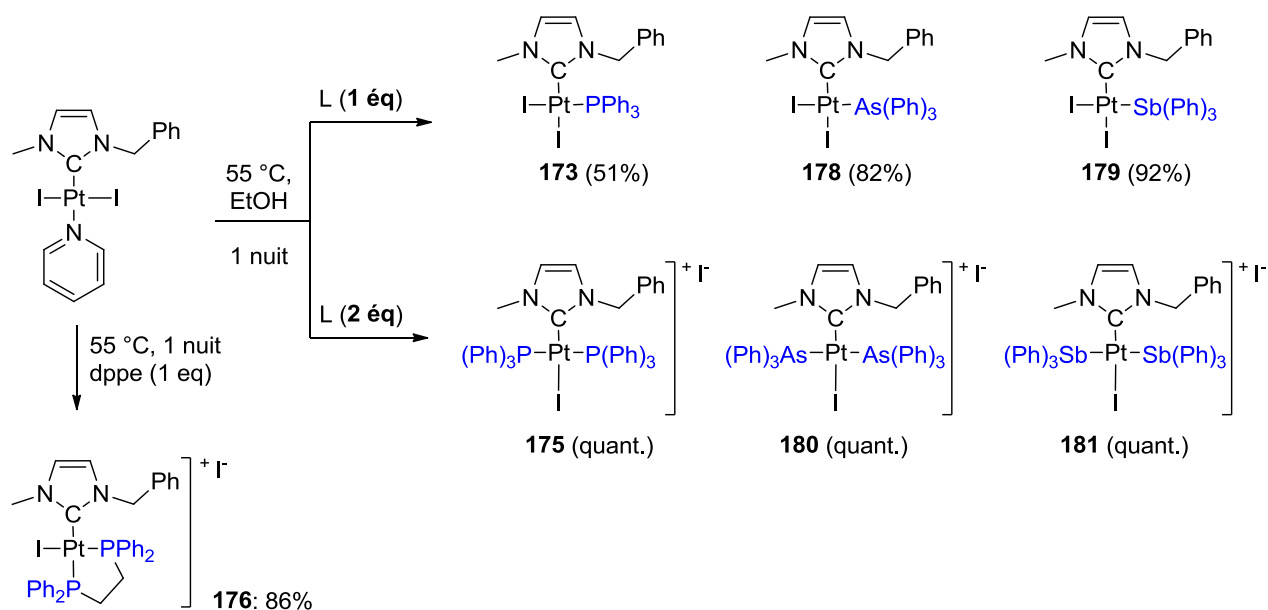


Figure 213: Fonctionnalisation avec des pnictogènes: exemples de composés obtenus

8.2.3 Introduction de PEI (polyéthylène imine)

Les PEI linéaires sont une classe de polymères organiques de la forme $-\text{CH}_2\text{CH}_2\text{NH}-$. En milieu physiologique, ces composés seront protonés et ainsi chargés positivement ce qui leur affecte une forte affinité pour l'ADN, propriété d'ailleurs exploitée pour s'en servir comme agent de transfection.⁵⁷⁰ Nous avons introduit sur un tel polymère des complexes de platine (Figure 214) en espérant profiter de l'effet EPR (Enhanced permeability and retention effect)⁵⁷¹ d'une telle macromolécule. Toute une panoplie de composés a été produit en variant 1. la masse molaire du PEI et 2. le rapport monomères/platine.

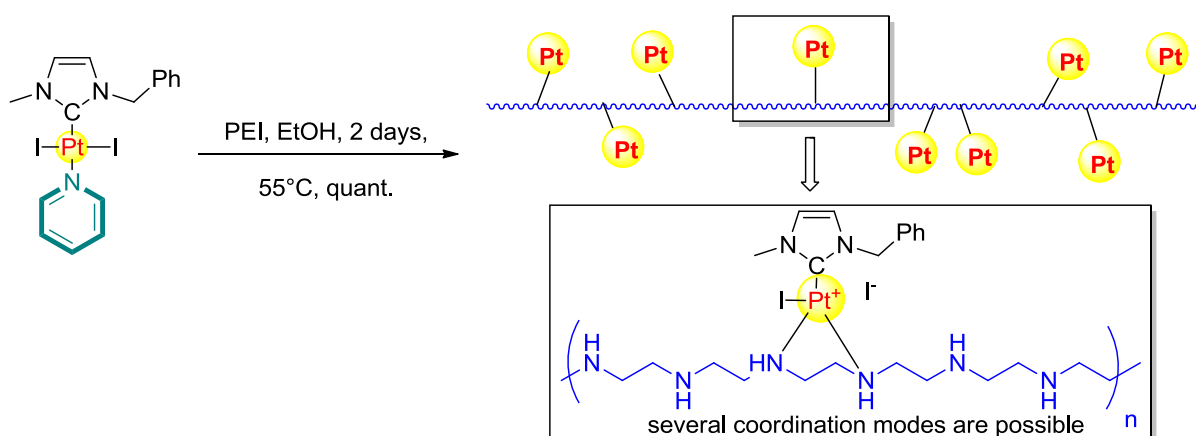


Figure 214: Greffage de complexes NHC de platine sur des PEI

⁵⁷⁰ Godbey, W. T.; Wu, K. K.; Mikos, A. M. *J. Control. Release* **1999**, *60*, 149; Lungwitz, U.; Breunig, M.; Blunk, T.; Göpferich, A. *Eur. J. Pharm. Biopharm.* **2005**, *60*, 247; Nguyen, D. N.; Green, J. J.; Chan, J. M.; Langer, R.; Anderson, D. G. *Adv. Mater.* **2008**, *20*, 1; Amiji, M. M.; Ogris, M. *Polymeric Gene Delivery: Principles and Applications*, Part II. A. Chapter 7, CRC Press **2010**

⁵⁷¹ Iyer, A. K.; Khaled, G.; Fang, J.; Maeda, H. *Drug Discovery Today*, **2006**, *11*, 812; Maeda, H.; Bharate, G. Y.; Daruwalla, J. *Eur. J. Pharma. Biopharma* **2009**, *71*, 409; Greish, K. *Methods Mol. Biol.* **2010**, *624*, 25; Fang, J.; Nakamura, H.; Maeda, J. *Advanced Drug Delivery Reviews* **2011**, *63*, 136; Maeda, H. *J. Control. Release* **2012**, *164*, 138; Prabhakar, U.; Maeda, H.; Jain, R. K.; Sevik-Muraca, E. M.; Zamboni, W.; Farokhzad, O. C.; Barry, S. T.; Gabizon, A.; Grodzinski, P.; Blakey, D. C. *Cancer Res.* **2013**, *73*, 2412;

8.3 Etude de la chimie de coordination avec des ligands de type (O[^]C[^]O)Pt(L) et (O[^]N[^]O)Pt(L)

La synthèse de complexes NHC a été étendue à des composés portant des ligands tridentates⁵⁷² de structure générale (O[^]C[^]O)Pt(L) (Figure 215), puis à des complexes (O[^]N[^]O)Pt(L) portant des ligands tridentates dérivés du défasirox⁵⁷³. La plupart de ces complexes sont fluorescentes sous lampe UV (245 ou 365 nm).

L'étude de leurs propriétés fluorescentes a été entreprise en collaboration avec le Dr. Matteo Mauro de l'ISIS. La propriété de fluorescence est intéressante du point de vue marquage en biologie.

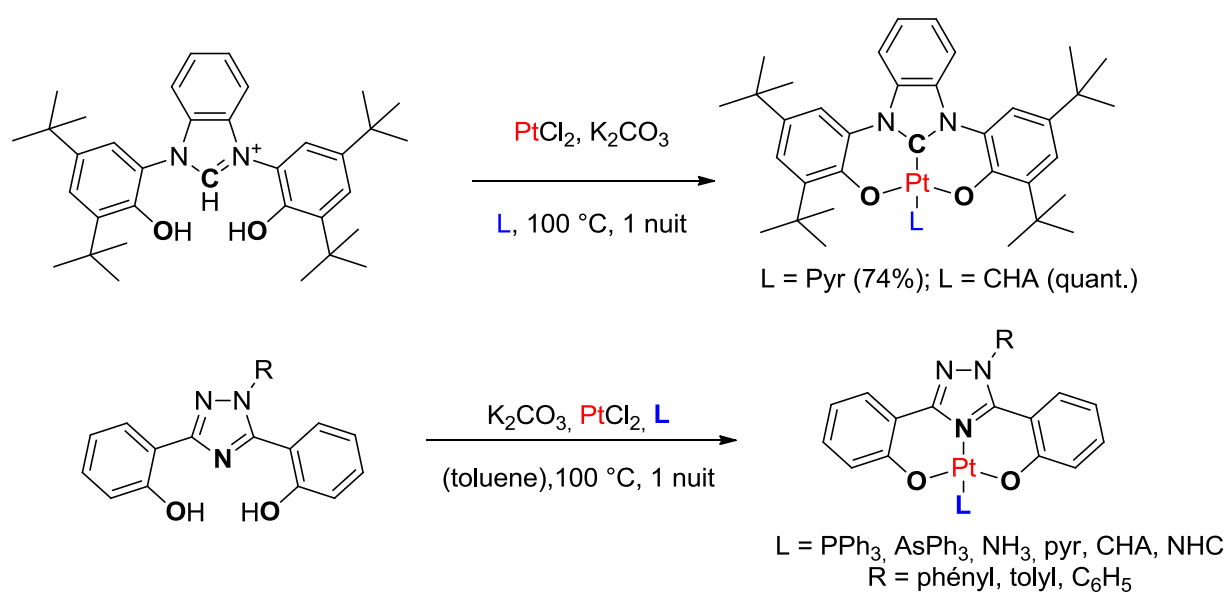


Figure 215: Exemples de complexes de type (O[^]C[^]O)Pt(L) et (O[^]N[^]O)Pt(L)

⁵⁷² a) Romain, C.; Brelot, L.; Bellemin-Laponnaz, S.; Dagorne, S. *Organometallics*, **2010**, 29, 1191–1198, b) Sun, R.; Chow, A.; Li, X.; Yan, J.; Chui, S.; Che, C. *Chem. Sci.*, 2011, **2**, 728–736.

⁵⁷³ Steinhauser, S.; Heinz, U.; Bartholomä, M.; Weyhermüller, T.; Nick, H.; Hegetschweiler K. *Eur. J. Inorg. Chem.*, **2004**, 2004, 4177–4192.

8.4 Introduction d'isotopes radioactives de iode

Une autre voie de post-fonctionnalisation a été envisagée.

Partant d'un complexe bis-chlorure respectivement bis-bromure, des ligands iode peuvent facilement et rapidement être introduits par simple échange de ligands X (théorie HSAB) en chauffant le complexe en présence de deux équivalents d'iodure de sodium (**Figure 194**).

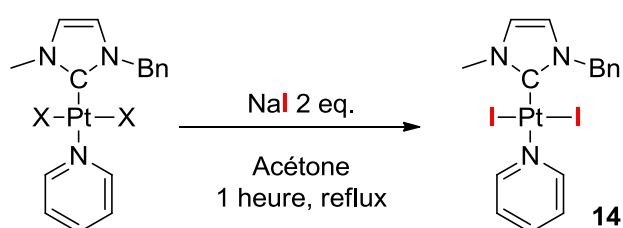


Figure 216: Introduction de ligands iode par échange de ligand X

Ces résultats ont pu être appliqués avec succès à du iode ^{123}I radioactif en collaboration avec C. Darcissac et A. Clotagatide de la Radiopharmacie CHU de Saint Etienne. La réaction a été validée par suivi par HPLC.

Le groupe du Pr. C. Billotey à Saint Etienne a lancé des essais *in vivo* (modèle souris) avec des complexes NHC de platine portant du ^{123}I Pt NHC afin d'élucider les mécanismes d'action et la biodistribution des complexes.

8.5 Résultats biologiques

La cytotoxicité de la plupart de ces complexes a été mesurée sur plusieurs lignées de cellules (mesure du pourcentage d'inhibition à une concentration fixée ou mesure de l'IC₅₀ en collaboration avec le Prof. Fournel. Par exemple, le complexe non fonctionnalisé **3_{pyr}** a un IC₅₀ de 0.49 μ M pour les cellules du cancer du sein MCF7, 0.93 μ M pour les cellules de la prostate PC3 et 1.50 μ M pour les cellules du cancer des ovaires OV3. Une fonctionnalisation par une hydroxylamine, une amine ou des acides aminés O-protégés permet de garder ou même d'augmenter l'activité cytotoxique.

Nous avons étudié en détail les complexes PEI-platine. Les résultats encourageants *in vitro* nous ont poussés à des études *in vivo* sur des souris nues et immunodéficientes auxquelles sont injectés des cellules humaines cancéreuses. L'inhibition de la croissance de la tumeur engendrée est comparée à des souris contrôles non traitées ou traitées avec un anticancéreux bien établie (oxaliplatine).

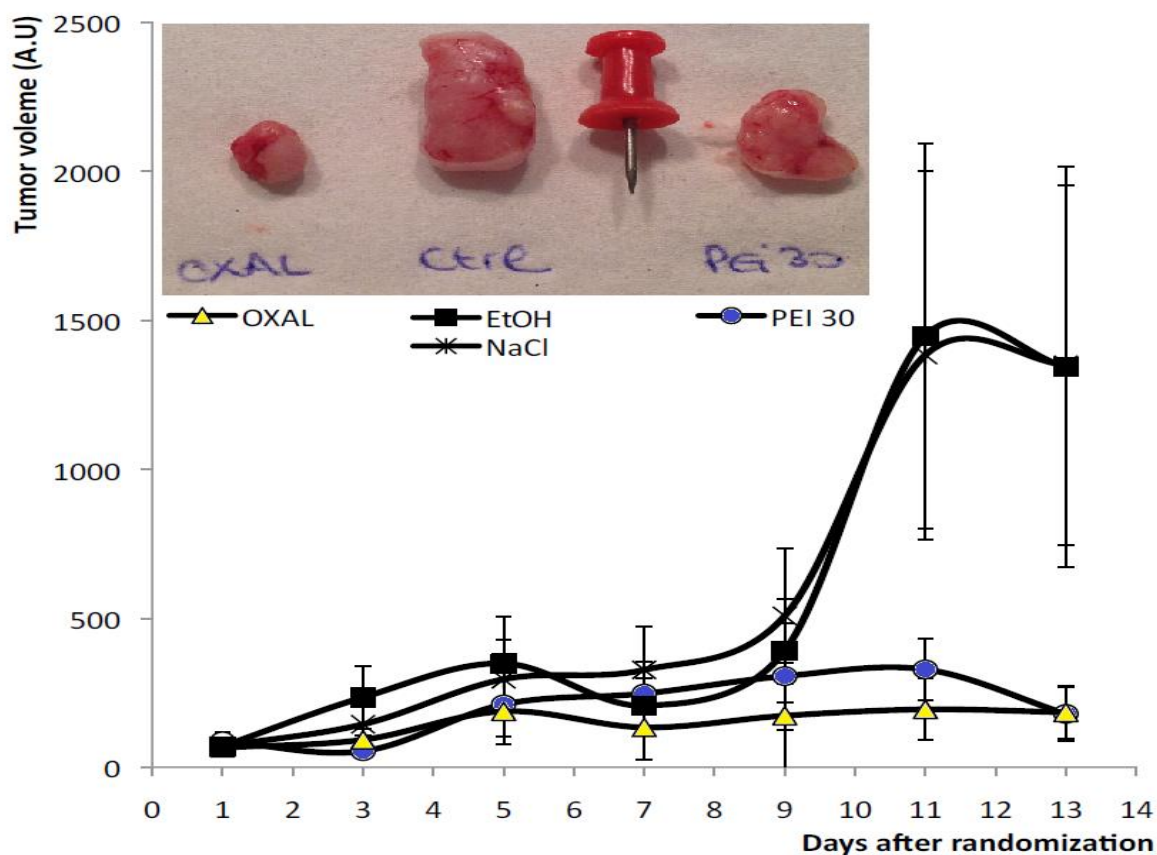


Figure 217: Expériences *in vivo* : Mesures d'inhibition de la croissance tumorale par nos complexes PEI-Platine

La Figure 217 montre une inhibition comparable de la croissance tumorale à l'oxaliplatine. Comparé au dernier, nos composés sont fortement prometteurs car n'engendrent pas d'effets secondaires tels que des hémorragies mortels pour les souris causés par l'oxaliplatine.

8.6 Conclusions

Plusieurs complexes NHC de platine fonctionnalisés avec des groupements chimiques diverses ont été obtenus avec de bons rendements. Des complexes portant un NHC fonctionnalisé avec un bras benzaldéhyde ont été synthétisés et post-fonctionnalisés avec différentes amines, hydrazines ou hydroxyamines par des réactions de condensation. Ceci permet de conjuguer chimiquement les complexes de platine avec des acides aminés ou des dérivés fluorescents dans des conditions douces. Les résultats de cytotoxicité montrent qu'une large majorité des composés sont cytotoxiques.

La méthodologie développée a été appliquée pour introduire un groupement urée ciblant l'antigène PSMA.

Elle permettrait de conjuguer d'autres agents de ciblage au platine pour synthétiser une bibliothèque de composés afin de trouver le meilleur candidat du point de vue cytotoxicité et sélectivité entre cellules saines et tumorales.

Par voie d'échange de ligand, une nouvelle classe complexes platine-NHC avec des ligands pnictogènes (phosphines, arsines, stibines) a été obtenu. La géométrie *cis* au niveau du platine laisse à attendre un mécanisme d'action en biologie différent des complexes *trans*-NHC-platine-amine. Des cytotoxicités modérées ont été mesurées pour ces complexes

Des dérivés PEI-platine ont prouvé une activité anti-tumorale prometteuse sur le modèle animal. Notamment, une inhibition de la croissance tumorale plus élevée que pour le cisplatine a été mesurée. Aucun effet secondaire visible n'a été constaté pour nos composés.

Finalement, la synthèse de composés fluorescents de type $(O^{\wedge}C^{\wedge}O)Pt(L)$ et $(O^{\wedge}N^{\wedge}O)Pt(L)$ a été effectuée et leurs propriétés de luminescence étudiées. Des mesures photophysiques ainsi que des calculs DFT ont été entrepris sur plusieurs complexes afin d'évaluer l'influence des substituants portés par le ligand $(O^{\wedge}N^{\wedge}O)$. Les complexes de type $(O^{\wedge}C^{\wedge}O)Pt(L)$ montrent une luminescence faible à basse température.

Métallocarbènes pour des applications thérapeutiques

Metal *N*-Heterocyclic Carbene (NHC) complexes are of great potential for cancer therapy. In particular, *in vitro* studies confirmed their significantly higher cytotoxicity than cisplatin.

In this work, we introduced molecular diversity on new NHC-Pt complexes by coordination of various NHC precursors to platinum. As a second strategy, post-synthetic functionalization of Pt complexes has been fully investigated by:

- oxime formation, e.g. with a PSMA targeting urea derivative
- ligand exchange reaction with hydrosoluble polyamines (PEI) and pnictogen-based ligands (phosphines, arsines, stibines)
- halogen exchange with iodide isotopes

Cytotoxic properties of these new compounds were evaluated *in vitro*. Best candidate was selected for *in vivo* evaluation on mice model showing for PEI-Pt similar tumour inhibition as oxaliplatin. Besides, no “visual” side effects were detected in contrast to oxaliplatin (hematomas). These outstanding results opened up new perspectives in the field of platinum-based drugs.

Les complexes métalliques des carbènes *N*-hétérocycliques (NHC) présentent un grand potentiel comme anticancéreux. En particulier, des études *in vitro* ont confirmés une cytotoxicité supérieure au cisplatine.

Dans ce travail, nous avons introduit de la diversité moléculaire à de nouveaux complexes NHC-Pt par coordination de différents ligands NHC. Une deuxième stratégie, la post-fonctionnalisation de complexes de Pt a été étudié par :

- formation d'oxime, notamment avec une urée ciblant le PSMA
- échange de ligand avec des polyamines hydrosolubles (PEI) ou des pnictogènes (phosphines, arsines, stibines)
- échange d'halogène avec des isotopes de l'iode

Les propriétés cytotoxiques de ces composés ont été évaluées *in vitro*. *In vivo* (souris), un complexe PEI-Pt montre une inhibition tumorale similaire à l'oxaliplatine. Néanmoins, aucun effet secondaire n'a été détecté contrairement à l'oxaliplatine (hématomes). Ces résultats ouvrent de nouvelles perspectives dans le domaine des anticancéreux sur la base de platine.